PO Box 2345, Beijing 100023, China
www.wjgnet.com
wjg@wjgnet.com

ELSEVIER

World J Gastroenterol 2005;11(39):6079-6084
World Journal of Gastroenterology ISSN 1007-9327

• *REVIEW* •

Research progress of vasculopathy in portal hypertension

Tao Li, Zhen Yang

Tao Li, Zhen Yang, Department of General Surgery, Tongji Medical College, Huazhong University of Science and Technology, Wuhan 430030, Hubei Province, China
Supported by the National Natural Science Foundation of China, No. A30170920
Correspondence to: Professor Zhen Yang, Department of General Surgery, Tongji Medical College, Huazhong University of Science and Technology, Wuhan 430030, Hubei Province, China. litaoforgood@tom.com
Telephone: +86-27-83663502 Fax: +86-27-83622624
Received: 2004-09-06 Accepted: 2004-12-26

Abstract

Portal hypertension, one of the vascular diseases, not only has lesions in liver, but also changes in vascular structures and functions of extrahepatic portal system, systemic system and pulmonary circulation. The pathological changes of vasculopathy in portal hypertension include remodeling of arterialized visceral veins, intimal injury of visceral veins and destruction of contractile structure in visceral arterial wall. The mechanisms of vasculopathy in portal hypertension may be attributed to the changes of hemodynamics in portal system, immune response, gene modulation, vasoactive substances, and intrahepatic blood flow resistance. Portal hypertension can cause visceral hyperdynamic circulation, and the development and progression of visceral vasculopathy, while visceral vasculopathy can promote the development and progression of portal hypertension and visceral hyperdynamic circulation in turn. The aforementioned three factors interact in the pathogenesis of hepatic cirrhosis-induced portal hypertension and are involved in hemorrhage due to varicose vein rupture.

Key words: Portal hypertension; Visceral vasculopathy; Visceral hyperdynamic circulation

Li T, Yang Z. Research progress of vasculopathy in portal hypertension. *World J Gastroenterol* 2005; 11(39): 6079-6084
http://www.wjgnet.com/1007-9327/11/6079.asp

INTRODUCTION

Portal hypertension is characterized not only by lesions in liver, but also by the changes in vascular structures and functions of extrahepatic portal system, systemic system and pulmonary circulation. During a long-term animal experiment as well as in clinical practice, Yang *et al*.[1], discovered that obvious pathological changes occurred in visceral vessels with the increment of the portal pressure, such as formation of extensive portal-systemic communicating branches, the changes in modeling of visceral veins and arteries, etc., which were named vasculopathy in portal hypertension. Generally, vascular lesions also include microvascular lesions in viscera, especially in stomach and intestine, named as portal hypertensive gastropathy and portal hypertensive intestinal vasculopathy, respectively, which can cause hematochezia, occult blood in stool or hemorrhage of digestive tract. Portal hypertension can also be complicated with pulmonary vascular lesions, leading to pulmonary hypertension and elevation of pulmonary venous pressure, the former might contribute to the inevitable injury of pulmonary arterioles and arteries due to the passage of vasoactive substances into lung through collateral circulation, as well as the synthesis of vasoactive substances produced by lung itself, while the latter can result in varicose vein in lung, trachea and bronchi, and hemorrhage following the disruption of the varicose veins[2,3]. Perforating vein is the special vascular structure of gastric wall in portal hypertension[4], and is considered as a vascular lesion. The connection of varicose vessels outside gastric tunica serosa with the perforating vein leads to the abnormal flow into the submucous layer of the gastric wall to form the varicose vein. In this paper, we have briefly reviewed the research progress in the pathology and pathogenesis of vasculopathy in portal hypertension.

Pathology of vascular lesions in portal hypertension-induced remodeling of arterialized visceral veins

The changes in visceral venous structures, such as collagen, elastic fibers, and smooth muscles, are involved in the vein lesions. Under light microscope, the smooth muscle cells in portal wall display hypertrophy and hyperplasia. Under electron microscope, the traverse areas of the smooth muscle cells have onefold increase as compared with the normal one and that of vascular media is increased subsequently. The rat model of partial portal ligation revealed the changes in vascular structure, contractility, contractile components and structural proteins, and the proportion of desmin and actin was found to be increased. The thickened vascular intima contained hyperplastic collagenous fibers and large numbers of disordered smooth muscles. The interstitial was also obviously thickened with thickened and condensed muscle fibers. In the adventitial layers, there was infiltration of inflammatory cells and onefold increase in the active contractility[5].

The arterialized remodeling exists in both splenic veins and coronary vein of stomach in the patients with portal hypertension[6], which includes: (1) Obviously thickened intima, showing diffuse thickening and locally thickened areas, forming neointima containing hyperplastic collagenous fibers and large numbers of disordered smooth muscle cells.

The hillock-shaped hyperplastic spots extrude towards the vascular cavity, also containing large numbers of collagenous fibers and disordered smooth muscle cells. Platelet aggregation and blood cell attachment to the surface of injured endothelial cells gradually lead to the formation of microthrombi, similar to the plaque of atherosclerosis. The vascular intima is widely injured with infiltration of inflammatory cells; (2) The interstitial layer is significantly thickened, internal circular muscles are arranged lengthwise and breadthwise, and longitudinal muscles undergo up-growth with thickened and condensed muscle fibers; (3) There is infiltration of inflammatory cells in the adventitial layer and few lymphatic nodes are complicated with inflammation. The feeding vessels are squeezed with the formation of thrombi; (4) The phenotypes of part muscle cells convert from contractile type to synthetic type, that is, many rough reticulum and ribosomes and decreased myofilaments exist in the cytoplasm, and migrate from interstitia to intima.

Intimal injury of visceral veins

Vascular endothelial cell, attaching to the surface of vascular intima, is a semi-transparent barrier membrane and possesses complicated metabolic and endocrine functions simultaneously. Researchers are paying attention to the importance of endothelial cells in cardiovascular diseases increasingly, but the correlation between endothelial cells and portal hypertension has not been elucidated clearly. It has been confirmed that the vascular intima in the patients with non-hepatic cirrhosis is intact, there is a thin layer of smooth muscle in subintima, and the feeding vessels are intact and open. While in the patients with hepatic cirrhosis, the vascular intima is severely injured, endothelial cells are detached, the subintima is nude and edematous, and there are large numbers of inflammatory cells and fibroblasts in the vascular cavity, many blood cells adhere to the nude subintima, and mural thrombi form in the vascular cavity. In the vascular adventitia, the feeding vessels become flat by extrusion and thrombi formation also takes place. McCarthy *et al*.[7], found that when the vascular endothelial cells and basement membrane were injured, the sensitivity of vessels to angiotensin-II (AngII) was increased, suggesting that the damage to the intima could influence the contractile function of the vessels.

Destruction of contractile structure in visceral arterial wall

The patients with portal hypertension are in a state of high flow and low resistance in systemic circulation (i.e., the cardiac output and arterial pressure are decreased). Moreover, they are commonly associated with splenomegaly and hypersplenism. The splenic artery has obvious histopathological changes, i.e., destruction of contractile structure in arterial wall[8] as follows: (1) Damage of arterial endothelial cells. Partial endothelial cells detach, platelets attach to intima, which is thickened and the smooth muscles in interstitia migrate to it; (2) Weigert staining certifies that the folded ripples from elastic membrane in arterial wall become flat or completely disappear. The elastic membrane is split into multiple layers. Some parts are ruptured completely. The elastic fibers in arterial wall are also diffusely ruptured and degenerated. Under an electron microscope, split, even partly ruptured elastic membrane, is clearly seen; (3) Under light microscope, the smooth muscles in interstitia can be seen to be migrated to intima. Some medial smooth muscle cells are atrophic and anatrophic, others are hypertrophic and hyperplastic. The smooth muscle cells are separated by collagenous fibers, and arranged disorderly. Under electron microscope, the size and morphology of the smooth muscle cells are uneven, i.e., some are atrophic and anatrophic, vacuoles form in the necrotized local cytoplasm, and even whole muscle cell is lysed, while others are compensatively hypertrophic and hyperplastic. In some muscle cells, cytoplasmic cellular organs are obviously increased, mitochondria are increased and swollen, and their cristae disappear with the formation of vacuoles. In others, there exist many rough reticulum, ribosomes and Golgi bodies in cytoplasm, while the filaments are decreased, indicating that the phenotypes of muscle cells convert from contractile type to synthetic type. The cytoplasm and nuclei in some muscle cells display the characteristics of cell apoptosis; (4) Under light microscope, collagenous fibers and extracellular matrix in whole vascular wall are increased, leading to collagenization of vascular wall, and its thickening and rigidness, and decreased elasticity. Under electron microscope, the extracellular matrix in arterial wall is obviously increased, but the elastic fibers are degenerated and ruptured.

Mechanism of vasculopathy in portal hypertension

The mechanism of vasculopathy in portal hypertension is not clear. The changes in hemodynamics of portal system, immune responses, gene regulation, and vasoactive substances might contribute to the process of vasculopathy in portal hypertension.

Changes in portal hemodynamics

Vascular wall, composed of different biomaterials, possesses multiple layers of compound structure. Within a certain pressure range, vascular tension, transmural blood pressure, and the geometrical parameters follow the Laplace's law of biomechanics: $T = P(R/W)$. The vascular tension (T) has its regulatory limitation. Within an elastic range, when the transmural blood pressure (P) is increased, compensation can be achieved by increasing the vascular width (W) and decreasing vascular radius (R). So, the high pressure of portal vein can thicken the vascular wall.

The increase of vascular resistance in portal system at any part can result in portal hypertension. Neurohumoral factors and vasoactive substances can actively regulate the contractility of vascular smooth muscles. The active changes in vascular resistance can happen in hepatic microcirculation, also in prehepatic portal-systemic communicating vessels, portal vein and their branches. Effect on vascular resistance can be expressed by Poiseuille law: $r = 8\,\mu L/\pi r^4$, in which μ represents the viscosity coefficient of blood, L the length of vessel and r the radius. It can be seen that the changes in vascular radius of extrahepatic portal system are the main factors influencing the resistance of portal resistance. Intimal hyperplasia, spot formation, internal wall roughness, decreased elasticity and contractility in visceral veins can limit the vascular diastolization, promote the mural thrombosis, occlude vessels and narrow vascular cavity, leading to hypostasis, even obstruction, and finally increasing the blood

flow resistance. When visceral veins and portal-systemic communicating vessels are contracted, the portal resistance is obviously increased. The collateral vessels are flexural and tortuous, so their increases in length can also significantly increase the blood flow resistance. The changes of hemoglobin and plasma protein concentration in portal blood, especially the increased blood viscosity following gastrointestinal hemorrhage, can also increase the blood flow resistance in portal veins.

Hypertrophy and hyperplasia of vascular smooth muscle cells are the important features of vasculopathy in portal hypertension. Krieger and Dzau[9] found that the increase in mechanical load of vessels could directly induce the expression of myosin gene, increase the expression of RNA and protein, and finally induce the growth of muscle cells. It is suggested that the hyperplasia and hypertrophy of vascular smooth muscle cells may be one of the adaptive compensatory responses of vessels to increased pressure.

Persistent stimulation of high pressure and blood flow of portal veins may be the main factors responsible for the vascular intimal injury of the patients with portal hypertension. Compression of feeding vessels can decrease the supply of blood to vascular wall and partial pressure of oxygen, causing ischemic damage and nutrient disturbance of vascular intima. In hepatic cirrhosis, dysfunction of liver and kidney, decreased clearance of oxygen-free radical, and increased injurants and oxygen-free radicals in portal blood can directly injure the vascular intima.

Immune response

Researchers pay increasingly more attention to the roles that vascular endothelial cells play in the pathogenesis of cardiovascular diseases. The damages to endothelial cells in portal hypertension can destroy the structure of vascular wall, cause dysfunction, influence substance exchange and result in inflammation and immune response. In the patients with hepatic cirrhosis, the cells are markedly increased in the peripheral tissue around vessels, mainly lymphocytes and inflammatory cells, associated with the proliferation of lymph follicles. Immunohistochemistry reveals that there exists strong expressions of platelet-derived growth factor, basic fibroblastic growth factor, epidermal growth factor, transforming growth factor-α (TGF-α), etc., on the vascular wall of gastric coronary vein in the patients with portal hypertension[10], indicating that the elevated pressure in gastric coronary vein can activate the smooth muscle cells of vascular wall to release many kinds of vasoactive substances. These growth factors can stimulate the proliferation, differentiation, and migration of vascular smooth muscle cells in turn, resulting in abnormal metabolism of collagenous fibers and elastic fibers. The phenotypic shift of smooth muscle cells is a chronic response to mechanical stimulation, which can induce not only cell migration, but also the synthesis of collagen and elastin, leading to the thickening of venous wall, decreased elasticity and compliance, and finally causing the increase in blood flow resistance.

Studies have also confirmed that the levels of inflammatory factors (e.g., C3, C4, IgG, IgE, IgA) in visceral venous wall in portal hypertension are significantly higher than that in the normal controls[11], suggesting that there are obvious immune inflammations in the vessels of portal system in the patients with portal hypertension, and the immune complex deposit and immune response may participate in the process of vasculopathy in portal hypertension.

In some studies, immunohistochemistry and double labeling immunofluorescence combined with laser scanning confocal microscopy are applied to detect the expressions of eNOS, ET-1, PKC, NF-κB in splenic vein of the patients with portal hypertension and portal endothelial cells of mouse portal hypertension model in order to investigate the relationship between the changes in the expression of eNOS and ET-1 in vascular endothelial cells in portal hypertension and signaling molecules PKC and NF-κB. The results showed that in the splenic vein of patients with portal hypertension and portal endothelial cells of mouse portal hypertension model, the expression of PKC was positive or strong positive, while in the controls, the expression of PKC was negative or weak positive[12]. Double labeling immunofluorescence combined with laser scanning confocal microscopy revealed that eNOS, ET-1, and NF-κB were mainly expressed in vascular endothelia and the fluorescent signaling intensity of them in the splenic vein of patients with portal hypertension and portal endothelial cells of mouse portal hypertension model was stronger than controls, suggesting that the increases of ET-1 and NO in venous blood was attributed to the increased synthesis from endothelial cells in portal system. The increased NO production in endothelial cells is related to the upregulation of eNOS expression. In portal hypertension, the mechanical stress signaling pathway in vascular endothelial cells is activated, which is responsible for the upregulation of ET-1 and eNOS expression in endothelial cells.

Recent studies showed that during the development of vasculopathy, endothelial cells and vascular smooth muscle cells are major effector cells. Various traumatic factors, such as shear stress, hydrostatic pressure, endotoxin, cytokines, growth factors, and inflammatory mediators, can result in injury and detachment of endothelial cells, leading to the bareness of collagenous fibers and aggregation of platelets. Endothelial cells express adhesion molecules (e.g., ICAM-1), release chemotactic factors (e.g., MCP-1)[13] and complement fragment C5a after complement activation[14]. As chemotactic factors, they can promote the mononuclear cells to bind to endothelial cells, translocating through endothelial cells to subintima, also enhance the migration of vascular smooth muscle cells to subintima and the phenotypic shift. The migration to subintima and proliferation of vascular smooth muscle cells and synthesized large quantities of extracellular matrix depositing in vascular wall to form neointima can induce remodeling of vessels before vasculopathy occurs. During this process, the interactive regulation between endothelial cells and vascular smooth muscle cells runs through the development of vasculopathy. Endothelial cells are the permissive cells to various stimulators, while vascular smooth muscle cells are the effector cells. This is a repair response of vessels to varied injures, at the same time, a pathological process of vasculopathy.

Gene regulation

c-fos is a message transferring factor. Dzau *et al*.[15], have

found that after vascular smooth muscle cells receive message, nuclear c-fos is expressed, the synthesis of DNA and mRNA is increased and cells proliferate. In the patients with hepatic cirrhosis, the expression of c-fos in splenic vein is increased, indicating that the proliferation, migration, and phenotypic shift of smooth muscle cells are related to the activation of oncogenes. The signaling pathway of c-fos that connects the mechanical signaling with the expression of proliferating gene is the biological basis of vascular remodelization.

Some suppressive oncogenes, such as p53, the effective regulatory factor for apoptosis, can promote the apoptosis of vascular smooth muscle cells, while prokaryotic genes, such as *c-myc* and *bcl-2*, can inhibit the apoptosis of these cells[16,17]. In patients with portal hypertension, the bax gene is strongly expressed and takes part in the regulation of apoptosis of smooth muscle cells in portal hypertension, indicating that the process of vasculopathy in portal hypertension involves gene modulation.

MAPK pathway is one of the important signaling conductive pathways modulating cellular proliferation, differentiation, and apoptosis[18,19]. Many extracellular stimulators, such as ultraviolet radiation[20], oxygen stress[21,22], cytokines[23,24], inflammatory mediators[25-27], can stimulate the cells to upregulate the expression and activation of MAPK. In an experiment using the specific antibody directed against Tyr-phosphorylated site at $ERK_{1/2}$204, the results revealed that in portal hypertension, the expressions of phosphorylated $ERK_{1/2}$ and its downstream factor c-fos were increased in vascular wall of splenic vein, indicating that the activation of $ERK_{1/2}$/c-fos signaling transduction pathway might contribute to the development of vasculopathy in portal hypertension.

Collagen, an important vascular extracellular matrix protein, can retain the flexibility and intensity of vascular wall. In normal human vascular wall, the predominant collagen subtypes are types I, III, and V[28]. When vascular endothelia are damaged, collagenous fibers, as a strong promoter factor, can promote the aggregation of platelets. During the process of intervention-induced vascular injury and atherogenesis[29,30], the synthesis of vascular wall types I and III collagen and procollagen is increased. Types I and III collagen and procollagen are all the components of extracellular matrix, synthesized and secreted mainly by vascular smooth muscle cells in vasculopathy. A study has shown that a slight change in the constitutional ratio of types I and III collagen can trigger atherogenesis[12]. In the study on vasculopathy in portal hypertension, it was found that in the gastric coronary venous wall, the synthesis of connectin and laminin was increased, suggesting that extracellular matrix might play an important role in the pathogenesis of vasculopathy in portal hypertension. In several studies, RT-PCR was used to detect the expression of types I and III procollagen in portal hypertensive vasculopathy to investigate the mechanism of vasculopathy. The results showed that in portal hypertension, the expression of type III procollagen mRNA in splenic venous wall was 5-6 times higher than that in the patients with non-portal hypertension ($P<0.01$), while there was no significant difference in the expression of type I procollagen mRNA between them. It demonstrated that in the development of vasculopathy in portal hypertension, type III procollagen, depositing in vascular wall when extracellular matrical components are greatly expressed, is one of the important factors promoting the remodelization of splenic veins.

Vasoactive substances

Vasoactive substances act on vascular smooth muscle cells through paracrine and autocrine system. Immunohistochemistry confirmed that in portal hypertension, the activities of iNOS, P substance, and VIP in visceral arterial wall were increased[8]. Among them, the expression of iNOS in vascular smooth muscle cells of splenic vein was increased, indicating that the production of NO was increased correspondingly. NO, a stronger vascular diastolic factor, can attenuate the response of vessels to endogenous systolic active substances, which is contributed to the activation of soluble guanylate cyclase in vascular smooth muscle cells by NO, leading to the increased production of cGMP, and intracellular Ca^{2+}, diastolization of smooth muscles, dilation of vessels, and decreased resistance. However, in hepatic cirrhosis-induced portal hypertension, the expression and activity of eNOS is reduced[31]. Transfection of eNOS[32] or heterogenic nNOS[33] genes by genetic techniques[3] could significantly reduce the animal portal pressure. By using PCR assay, Morales-Ruiz *et al*.[34], confirmed the expression of iNOS mRNA in thoracic aorta, abdominal aorta, and mesenteric arteries. The studies by Suga *et al*.[35], proved that the diastolic effect of mesenteric arteries to vasodilators in response was stronger than that of portal system. It is suggested that the over-release of NO may play an important role in the pathogenesis of visceral vascular low systolization and diastolization in portal hypertension[36].

Endothelin (ET) is the strongest vasoconstrictive polypeptide, crucially regulating the hepatic microcirculation and portal pressure. By using RT-PCR and RIA assays, Tieche *et al*., reported that in the mouse model of hepatic cirrhosis caused by bile duct ligation, the expression of ET gene was increased 6 times at 3 d after ligation and 30 times at 28 d after ligation. Moreover, it was directly correlated with the activation of hepatic stellate cells (HSCs) and the increased portal pressure. The increased expression and activity of ET gene were more obvious in portal vein and hepatic microcirculation than that in visceral arteries, and its systolic effect on veins was significantly stronger than that on arteries[37], suggesting that ET and NO are two important antagonists against portal hypertension.

AngII is an endogenous eight peptide and induces the increase in the targeting cellular Ca^{2+} concentration by binding to the specific receptor on the membrane of targeting cells to form a receptor-ligand compound. The increased Ca^{2+}, as a second messenger, can produce the intensive effects of vasoconstriction and promote smooth muscle cell proliferation by different cascade reactions. In hepatic cirrhosis-induced portal hypertension, the vasodilator substances, such as NO and PGT2, can directly or indirectly reduce the expression of AngII receptors (AT1 and AT2) in vascular endothelial cells and decrease their affinity to AngII on the surface of smooth muscle cells. Both receptors in combination with the phenotypic changes of obviously

hypertrophic or hyperplastic vascular smooth muscle cells can influence the responses of vessels to AngII[38].

TGF-β plays a crucial role in regulating the deposition of external vascular matrix[39], promotes the transcription of types I and III procollagen, and contributes to fibrosis in liver and other organs noticeably. In animal models of hepatic cirrhosis and patients with chronic hepatitis, the increased TGF-β concentration was associated with the deposition of internal vascular matrix in the targeting organs. In HSCs, TGF-β could promote the synthesis of collagen[40]. Administration of TGF-β antibody or antagonists of TGF-β receptors can inhibit the synthesis of collagen. In contrast, the addition of exogenous TGF-β can increase the synthesis of collagen in smooth muscle cells[41,42]. TGF-β has many functions and exerts its biological effects via TGF-β receptors. TGF-β binds with its receptors before phosphorylation of the Smad protein and then enters into nuclei to regulate the transcription of proteins[43]. Also, TGF-β can increase the synthesis of extracellular matrix by activating Ras, Raf-1, and MEK in sequence[44,45].

NF-κB, as an important transcriptional regulatory factor, plays a key role in vasculopathy in portal hypertension[46]. After activation, the inhibition subunit I-κB of NF-κB is released into the nuclei to promote the transcription of fibrosis-associated genes via the JNK, AP-1 pathway. NK-κB is also the transcription of intercellular adhesion molecule-1 and vascular cell adhesion molecule-1[47]. It is known that besides the increased deposition of external vascular collagen for the vascular remodeling, the main factors for angiosclerosis are extracellular matrix and the binding sites of smooth muscle cells. During this process, adhesion molecules take part in regulating the binding of smooth muscles with extracellular matrix, promoting the development of vasculopathy.

Activator protein-1 (AP-1) binds with the AP-1 binding sites at the VEGF gene promoter that can promote transcription of VEGF[48]. VEGF acts through various pathways. Firstly, VEGF, the known strongest factor enhancing the vascular permeability, can increase the permeability of vascular wall[49]. VEGF functions through its receptors FLt-1 and FLk-1. In hepatic fibrosis, visceral vessels mainly express FLt-1, by which VEGF can promote the cell proliferation and collagen synthesis[50]. Secondly, VEGF possesses the chemotaxis to mononuclear macrophages and increases the adhesion of macrophages. The increased vascular permeability and the entry of mononuclear cells and macrophages into vascular intima result in the release of inflammatory factors, which can promote the smooth muscle cells proliferation and increase the synthesis of collagen[51]. VEGF can interact with basic cellular growth factor, TGF-β and hyaluronic acid to coordinately promote the proliferation of smooth muscle cells and collagen synthesis.

To sum up, the pathological changes of vasculopathy in portal hypertension include arterialized remodeling of visceral veins, the intimal injury of visceral veins and the destruction of contractile structure in visceral arterial wall. The mechanism of vasculopathy in portal hypertension may be attributed to the changes of hemodynamics in portal system, immune response, gene modulation, vasoactive substances, and intrahepatic blood flow resistance. On the one hand, portal hypertension can cause visceral hyperdynamic circulation and the development and progression of visceral vasculopathy. The visceral vasculopathy includes the destruction of contractile structure in visceral arterial wall and the remodelization of visceral veins. Vasculopathy results from the increased portal pressure and blood flow. On the other hand, visceral vasculopathy can promote the development and progression of portal hypertension and visceral hyperdynamic circulation in turn. The aforementioned three factors interact in the pathogenesis of hepatic cirrhosis-induced portal hypertension and are involved in hemorrhage of varicose vein rupture. The interaction between them is demonstrated as follows[6]:

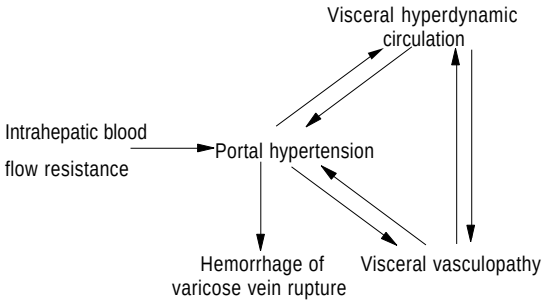

REFERENCES

1 **Yang Z**, Liu R, Yang R. Pathology of endothelium, extracellular matrix and smooth muscle in gastric coronary vein of cirrhotic patients. *Zhonghua Waike Zazhi* 1996; **34**: 138-140
2 **Lebrec D**. Pharmacological treatment of portal hypertension: hemodynamic effects and prevention of bleeding. *Pharmacol Ther* 1994; **61**: 65-107
3 **Youssef AI**, Escalante-Glorsky S, Bonnet RB, Chen YK. Hemoptysis secondary to bronchial varices associated with alcoholic liver cirrhosis and portal hypertension. *Am J Gastroenterol* 1994; **89**: 1562-1563
4 **Burtin P**, Cales P, Oberti F, Joundy N, Person B, Carpentier S, Boyer J. Endoscopic ultrasonographic signs of portal hypertension in cirrhosis. *Gastrointesit Endosc* 1996; **44**: 257-261
5 **Malmqvist U**. Effect of long-term portal hypertension on structure, active force and content of contractile and structural proteins in smooth muscle of the rat portal vein. *Acta Physiol Scand* 1994; **150**: 171-179
6 **Yang Z**, Zhang L, Li D, Qiu F. Pathological morphology alteration of the splanchic vascular wall in portal hypertensive patients. *Chin Med J* 2002; **115**: 559-562
7 **McCarthy AL**, Woolfson RG, Raju SK, Posten L. Abnormal endothelial cell fuction of resistance arteries from women with preclampsia. *Am J Obstet Gynecol* 1993; **168**: 1323-1330
8 **Yang Z**, Ren D, Li D, Qiu F. Portal hypertensive vasculopathy of splenic artery. *Zhonghua Waike Zazhi* 1999; **37**: 412-414
9 **Krieger JE**, Dzau VJ. Molecular biology of hypertension. *Hypertension* 1991; **18**(3 Suppl): 13-17
10 **Yang Z**, Lei T, Lin P, Qiu F. Immunohistochemical analysis of growth factor expression and localization in gastric coronary vein of cirrhotic patients. *J Tongji Med Univ* 1996; **16**: 229-233
11 **Mba Mba C**, Yang Z. Role of injury of gastric parietal vessels by im-munocomplexes in the mechanism of gastric mucosal lesion in portal hypertension with cirrhosis. *J Tongji Med Univ* 1997; **17**: 44-48
12 **Li T**, Li HY, Zhang T, Ni JY, Yang Z. Splenic angiopathy in portal hypertension. *Shjie Huaren Xiaohua Zazhi* 2004; **12**: 1616-1622
13 **Watanabe T**, Pakala R, Katagiri T, Benedict CR. Monocyte chemotactic protein 1 amplifies serotonin-induced vascular smooth muscle cell proliferation. *J Vasc Res* 2001; **38**: 341-349
14 **Niculescu F**, Rus H. Complement activation and atherosclerosis.

Mol Immunol 1999; **36**: 949-955
15 **Dzau VJ**, Gibbons GH, Morishita R, Pratt RE. New perspectives in hypertension research. Potentials of vascular biology. *Hypertension* 1994; **23**: 1132-1140
16 **Bennett MR**, Evan GI, Schwartz SM. Apoptosis of rat vascular smooth muscle cells is regulated by p53-dependent and -independent pathways. *Cir Res* 1995; **77**: 266-273
17 **Chen HW**, Huang HC. Effect of curcumin on cell cycle progression and apoptosis in vascular smooth muscle cells. *Br J Pharmacol* 1998; **124**: 1029-1040
18 **Johnson GL**, Lapadat R. Mitogen-activated protein kinase pathways mediated by ERK, JNK and p38 protein kinases. *Science* 2002; **298**: 1911-1912
19 **Agell N**, Bachs O, Rocamora N, Villalonga P. Modulation of the Ras/Raf/MEK/ERK passway by Ca^{2+}, and calmodulin. *Cell Signal* 2002; **14**: 649-654
20 **Sasu S**, LaVerda D, Qureshi N, Golenbock DT, Beasley D. Chlamydia pneumoniae and chlamydial heat shock protein 60 stimulate proliferation of human vascular smooth muscle cells via toll-like receptor 4 and p44/p42 mitogen-activated protein kinase activation. *Circ Res* 2001; **89**: 244-250
21 **Blaschke F,** Stawowy P, Goetze S, Hintz O, Grafe M, Kintscher U, Fleck E, Graf K. Hypoxia activates beta(1)-intergrin via ERK1/2 and p38 MAP kinase in human vascular smooth muscle cells. *Biochem Biophys Res Commun* 2002; **296**: 890-896
22 **Komai N**, Morishita R, Yamada S, Oishi M, Iguchi S, Aoki M, Sasaki M, Sakurabayashi I, Higaki J, Ogihara T. Mitogenic activity of oxidized lipoprotein (a) on human vascular smooth muscle cells. *Hypertension* 2002; **40**: 310-314
23 **Goetze S**, Xi XP, Kawano Y, Kawano H, Fleck E, Hsueh WA, Law RE. TNF-alpha-induced migration of vascular smooth muscle cells is MAPK dependent. *Hypertension* 1999; **33** (1Pt 2): 183-189
24 **Jiang B**, Xu S, Brecher P, Cohen RA. Growth factors enhance interleukin-1 beta-induced persistent activation of nuclear factor-kappa B in rat vascular smooth muscle cells. *Arterioscler Thromb Vasc Biol* 2002; **22**: 1811-1816
25 **Christopher J**, Velarde V, Jaffa AA. Induction of B (1)-kinin receptors in vascular smooth muscle cells: cellular mechanisms of map kinase activation. *Hypertension* 2001; **38**(3Pt 2): 602-605
26 **Douillet CD**, Velarde V, Christopher JT, Mayfield RK, Trojanowska ME, Jaffa AA. Mechanisms by which bradykinin promotes fibrosis in vascular smooth muscle cells: role of TGF-beta and MAPK. *Am J Physiol Heart Circ Physiol* 2000; **279**: H2829-2837
27 **Agata J**, Miao RQ, Yayama K, Chao L, Chao J. Bradykinin B (1) recepter mediates inhibition of neointima formation in rat artery after balloon angioplasty. *Hypertension* 2000; **36**: 364-370
28 **Karim MA**, Miller DD, Farrar MA, Eleftheriades E, Reddy BH, Breland CM, Samarel AM. Histomorphometric and biochemical correlates of arterial procollagen gene expression during vascular repair after experimental angioplasty. *Circulation* 1995; **91**: 2049-2057
29 **Shi Y**, O'Brien JE Jr, Ala-Kokko L, Chung W, Mannion JD, Zalewski A. Origin of extracellular matrix synthsis during coronary repair. *Circulation* 1997; **95**: 997-1006
30 **Bahadori L**, Milder J, Gold L, Botney M. Active macrophage-associated TGF-beta β co-localizes with type I procollagen gene expression in atherosclerotic human pulmonary arteries. *Am J Pathol* 1995; **146**: 1140-1149
31 **Rockey DC**, Chung JJ. Reduced nitric oxide production by endothelial cells in cirrhotic rat liver: endothelial dysfunction in portal hypertension. *Gastroenterology* 1998; **114**: 344–351
32 **Van de Casteele M**, Omasta A, Janssens S, Roskams T, Desmet V, Nevens F, Fevery J. *In vivo* gene transfer of endothelial nitric oxide synthase decreases portal pressure in anaesthetised carbon tetrachloride cirrhotic rats. *Gut* 2002; **51**: 440-445
33 **Yu Q**, Shao R, Qian HS, George SE, Rockey DC. Gene transfer of the neuronal NO synthase isoform to cirrhotic rat liver ameliorates portal hypertension. *J Clin Invest* 2000; **105**: 741-748
34 **Morales-Ruiz M**, Jimenez W, Perez-Sala D, Ros J, Leivas A, Lamas S, Rivera F, Arroyo V. Increased nitric oxide synthase expression in arterial vessels of cirrhotic rats with ascites. *Hepatology* 1996; **24**: 1481-1486
35 **Suga T**, Itoh H, Shimomura A, Kusagawa M, Zto M, Takase K, Konishi T, Nakano T. Comparison of the effects of various vasodilators on the rat portal vein and mesenteric artery. *Eur J Pharmacol* 1993; **242**: 129-136
36 **Hartleb M**, Michielsen PP, Dziurkowska-Marek A. The role of nitric oxide in portal hypertensive systemic and portal vascular pathology. *Acta Gastroenterol Belg* 1997; **60**: 222-232
37 **Luscher TF**, Yang Z, Tschudi M, von Segesser L, Stulz P, Boulanger C, Siebenmann R, Turina M, Buhler FR. Interaction between endothelin-1 and endothelium-derived relaxing factor in human arteries and veins. *Circ Res* 1990; **66**: 1088-1094
38 **Cahill PA**, Redmond EM, Sitzmann JV. Endothelial dysfunction in cirrhosis and portal hypertension. *Pharmacol Ther* 2001; **89**: 273-293
39 **George J**, Roulot D, Koteliansky VE, Bissell DM. *In vivo* inhibition of rat stellate cell activation by soluble transforming growth factor beta type? receptor: a potential new therapy for hepatic fibrosis. *Proc Natl Acad Sci USA* 1999; **96**: 12719-12724
40 **Schlumberger W**, Thiem M, Rauterberg J, Robenek H. Collagen synthesis in cultured aortic smooth muscle cells. Modulation by collagen lattice culture transforming growth factor-beta 1 and epidermal growth factor. *Arterioscler Thromb* 1991; **11**: 1660-1666
41 **O'Callaghan CJ**, Williams B. Mechanical strain-induced extracellular matrix production by human vascular smooth muscle cells: role of TGF-beta(1). *Hypertension* 2000; **36**: 319-324
42 **Simonson MS**. Endothelins: multifunctional renal peptides. *Physiol Rev* 1993; **73**: 375-411
43 **Reimann T**, Hempel U, Krautwald S, Axmann A, Scheibe R, Seidel D, Wenzel KW. Transforming growth factor-beta1 induces activation of Ras, Raf-1, MEK and MAPK in rat hepatic stellate cells. *FEBS Lett* 1997; **403**: 57-60
44 **Davis BH,** Chen AP, Beno DW. Raf and mitogen-activated protein kinase regulate stellate cell collagen gene expression. *J Biol Chem* 1996; **271**: 11039-11042
45 **Gomez-Garre D**, Largo R, Tejera N, Fortes J, Manzarbeitia F, Egido J. Activation of NF-KappaB in tubular epithelial cells of rats with intense proteinuria: role of angiotensin II and endothelin-1. *Hypertension* 2001; **37**: 1171-1178
46 **Liu H**, Lo CR, Czaja MJ. NF-KappaB inhibition sensitizes hepatocytes to TNF-induced apoptosis through a sustained activation of JNK and c-Jun. *Hepatology* 2002; **33**: 772-778
47 **Tomita N**, Morishita R, Tomita S, Kaneda Y, Higaki J, Ogihara T, Horiuchi M. Inhibition of TNF-alphainduced cytokine and adhesion molecule. Expression in glomerular cells *in vitro* and *in vivo* by transcription factor decoy for NFkappaB. *Exp Nephrol* 2001; **9**: 181-190
48 **Tischer E**, Mitchell R, Hartman T, Silva M, Gospodarowicz D, Fiddes JC, Abraham JA. The human gene for vascular endothelial growth factor. Multiple protein forms are encoded through alternative exon splicing. *J Biol Chem* 1991; **266**: 11947-11954
49 **Keck PJ**, Hauseris D, Krivi G, Sanzo K, Warren T, Feder J, Connolly DT. Vascular permeability factor an endothelial cell mitogen related to PDGF. *Science* 1989; **246**: 1309-1312
50 **Corpechot C**, Barbu V, Wendum D, Kinnman N, Rey C, Poupon R, Housset C, Rosmorduc O. Hypoxia-induced VEGF and collagen I expressions are associated with angiogenesis and fibrogenesis in experimental cirrhosis. *Hepatology* 2002; **35**: 1010-1021
51 **Barleon B**, Sozzani S, Zhou D, Weich HA, Mantovani A, Marme D. Migration of human monocytes in response to vascular endothelial growth factor (VEGF) is mediated via the receptor flt-1. *Blood* 1996; **87**: 3336-3343

Science Editor Zhu LH and Kumar M, Guo SY **Language Editor** Elsevier HK

PO Box 2345, Beijing 100023, China
www.wjgnet.com
wjg@wjgnet.com

ELSEVIER

World J Gastroenterol 2005;11(39):6085-6089
World Journal of Gastroenterology ISSN 1007-9327

• *REVIEW* •

Chronic hepatitis C virus infection and post-liver transplantation diabetes mellitus

Yun Ma, Wen-Wei Yan

Yun Ma, Basement 3 The Marco Polo Hotel, 6 Xuanwumen Nei Avenue, Xicheng District, Beijing 10003, China
Wen-Wei Yan, Department of Organ Transplantation, Tianjin First Central Hospital, Tianjin 300192, China
Correspondence to: Wen-Wei Yan, MD, Department of Organ Transplantation, Tianjin First Central Hospital, Tianjin 300192, China. wenweiyanboy@yahoo.com
Telephone: +86-22-23626549 Fax: +86-22-23682662
Received: 2005-03-01 Accepted: 2005-04-11

Abstract

Patients with chronic hepatitis C virus (HCV) infection have a significantly increased prevalence of type 2 diabetes mellitus compared to controls or HBV-infected patients. Moreover, the incidence rate of post-liver transplantation diabetes mellitus (PTDM) also appears to be higher among patients with HCV infection. PTDM is often associated with direct viral infection, autoimmune disorders, and immunosuppressive regimen. Activation of tumor necrosis factor-α may be the link between HCV infection and diabetes. In this article, we reviewed the epidemiologic association between HCV infection and PTDM, highlighting the most recent pathophysiologic insights into the mechanisms underlying this association.

Key words: Hepatitis C virus; Post-liver transplantation diabetes mellitus; Tumor necrosis factor; Immunosuppressive therapy

Ma Y, Yan WW. Chronic hepatitis C virus infection and post-liver transplantation diabetes mellitus. *World J Gastroenterol* 2005; 11(39): 6085-6089
http://www.wjgnet.com/1007-9327/11/6085.asp

INTRODUCTION

The last two decades have seen an increase in various types of organ transplantation for the treatment of end stage organ diseases. Prevention of organ rejection requires long-term immunosuppressive therapy, which places recipients at the increasing risk of infection and metabolic disorders, such as recurrent hepatitis C virus (HCV) infection and post-liver transplantation diabetes mellitus (PTDM). Recipients with HCV infection have a higher incidence of PTDM, which depends on the degree and duration of immunosuppressant[1]. On the other hand, the occurrence of PTDM is associated with direct viral infection, autoimmune disorders[3], and immunosuppressive regimen, notably tacrolimus[4]. PTDM characteristically shows insidious onset and aggressive behavior thereafter. PTDM in HCV-infected patients might be partially or completely recovered after reduction or switching of immunosuppressive therapy[5].

PTDM AND HCV ASSOCIATION: RISK FACTORS

The high prevalence of diabetes mellitus, especially type 2 diabetes mellitus (type 2 DM) in HCV-infected patients comes from epidemiologic studies (Table 1), most of which are case control studies,[6,7,9,10-12,14] in addition to two multicenters and cohort[8,13]. Risk factors resulting in the increasing prevalence of type 2 DM in HCV-infected patients include positive family history of diabetes and black ethnicity[15]. Thus, it is conceivable that HCV leads to type 2 DM in susceptible hosts. Immunogenetic studies suggest that an infectious process coexists in patients with type 2 DM and chronic liver disease and HLA-DR2, -DR51, -DQB6 haplotypes provide a two- and three-fold relative risk for the development of diabetes[16].

It is reported that liver transplantation recipients with HCV infection have a four- to eight-fold prevalence of diabetes compared with recipients with other viral or cholestatic liver diseases 1 year after liver transplantation. A recent study of 260 HCV-infected patients has confirmed that insulin resistance is an independent predictor of the degree of fibrosis, and that insulin sensitivity has a significant correlation with serum aspartate aminotransferase, histological activity index and degree of fibrosis[18] in non-diabetic HCV-infected patients. Gray *et al*.[17], observed that abnormal liver function tests are found in 72.3% of HCV-positive diabetic patients and in only 24.7% of HCV-negative diabetic patients ($P<0.001$). In summary, the occurrence of PTDM seems to be associated with HCV infection.

PATHOPHYSIOLOGY

The pathophysiologic mechanism underlying the development of PTDM in patients with HCV infection has not been clearly illustrated. Possible mechanisms are shown in Figure 1.

Tumor necrosis factor-alpha (TNF-α)

A study of liver biopsy specimens from non-diabetic HCV-infected patients has revealed significant impairments in the insulin-signaling pathway[19], which is strikingly similar to the known effect of tumor necrosis factor-α (TNF-α) on insulin resistance[20]. The role of TNF-α in the pathogenesis of this HCV-associated insulin resistance state is strongly

Table 1 Studies of PTDM in patients with chronic HCV infection

PTDM (%)		RR (95%CI)	Study description	Reference
HCV+	HCV-			
33	12	3 (0.98-9.6)[b]	Case control	Zein *et al.*, 2000
34	9.8	0.95 (0.2-3.9)[a]	Case control	Bigam *et al.*, 2000
20.9	-	1.9 (0.4-14.2)	Multicenter	Khalili *et al.*, 2004
43	13	1.9 (1-2.6)[b]	Case control	AlDosary *et al.*, 2002
64	28	2 (0.9-4.6)[b]	Case control	Baid *et al.*, 2002
29	10	2 (0.96-4.3)[b]	Case control	Bigam *et al.*, 2000
72	37	4.8 (0.8-30)[d]	Case control	Yildiz *et al.*, 2002
62	8	11.6 (1.7-79)[b]	Cohort	Delgado-Borrego *et al.*, 2004
18.29	-	-	Case control	Parolin *et al.*, 2004

[a]$P<0.05$, [b]$P<0.01$, [d]$P<0.001$ *vs* control.

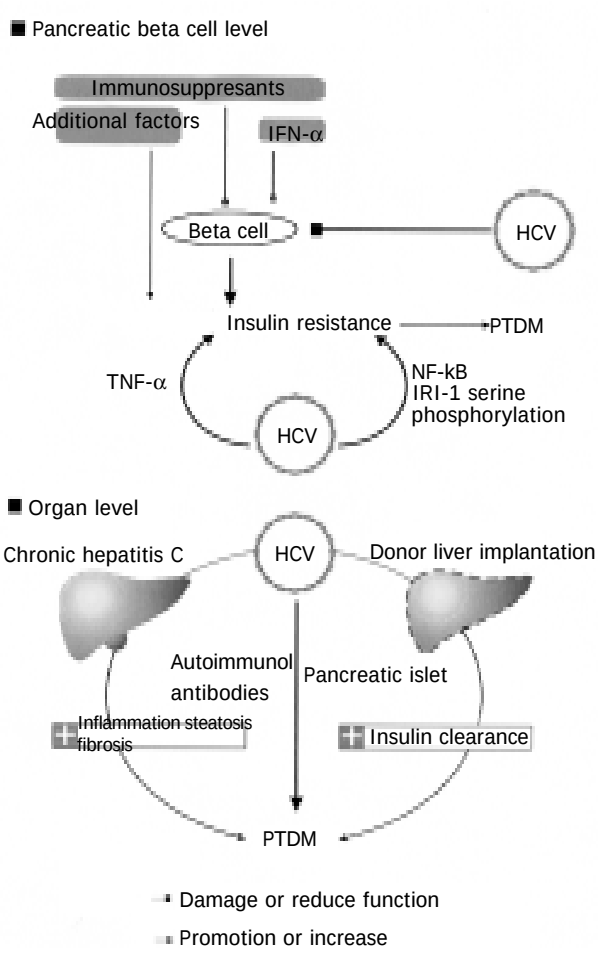

Figure 1 Possible mechanism underlying the development of PTDM in HCV infection (at least four mechanisms contribute to exacerbation of insulin resistance). (1) Chronic activation of TNF-α, which plays a key role not only in the production of and response to HCV itself, but also in the development of insulin resistance. Additional factors for developing PTDM in HCV-infected patients, including obesity, black ethnicity, and aging, are known to be associated with increased TNF-α independent mechanisms; (2) the increased clearance of insulin that occurs in post-transplant recipients thus creates a reactive hyperinsulinemic medium, and that in turn might enhance insulin resistance; (3) a bi-directional relationship between liver disease and diabetes is possible, as both insulin resistance and PTDM can adversely affect HCV liver disease; (4) directly diabetogenic effect of immunosuppressive therapy on pancreatic β cell.

supported by findings of elevated intra-hepatic TNF-α and amelioration of the metabolic abnormalities after TNF-α antibodies are administered[2]. The interrelationship between HCV and other predisposing conditions of PTDM could partly be mediated by TNF-α and most of the established risk factors for PTDM, such as obesity, aging[21], black ethnicity[22], and a family history of type 2 DM[23].

HCV per se

HCV replicates in hepatocytes, but its genome has been identified in a number of other tissues, including pancreatic acinar cells and epithelial cells of the pancreatic duct[24]. The destruction of pancreatic β cells could be mediated either directly by HCV or by HCV-induced immune responses, but evidence is scanty[3]. More recently, a transgenic mouse model that specifically expresses the HCV core protein in hepatocytes has been studied[2]. These animals had insulin resistance at an early age, and when challenged by a high fat diet, they developed glucose intolerance. Further characterization of the metabolic defects in these animals revealed that insulin resistance was caused mainly by failure of insulin to suppress hepatic glucose production. Piquer *et al.*[25], assessed the prevalence of islet cell autoantibodies in 303 non-selected HCV-infected patients (277 non-diabetic and 26 type 2 DM patients) and 273 sex- and age-matched control subjects, and found that patients with HCV have no significantly higher pancreatic autoantibodies compared with controls. However, it was reported that type 1 DM occurs more frequently in HCV patients treated with interferon (IFN) as a result of amplification of previously existing autoimmunity against pancreatic β cells, and that treatment of healthy volunteers with IFN can stimulate counter-regulatory hormone secretion, impair glucose tolerance and insulin sensitivity and induce insulin clearance, suggesting that HCV-induced immune response might be involved in the development of insulin resistance[26].

Immunosuppressive therapy

The overall effects of immunosuppression may potentiate the diabetogenic effects of HCV infection by enhancing the level of viral replication. A study on the effects of corticosteroids on post-transplant levels of viremia and PTDM showed that pulsed intravenous methylprednisolone therapy is associated with transient 4- to 100-fold rise in HCV RNA levels and the reduced translocation of glucose transporter 4 from cytosol into membrane, and that higher HCV RNA level is correlated with increased severity of graft and islet injury[30,45,46]. Immunosuppressive agents, especially steroids and calcineurin

inhibitors, are diabetogenic. The direct and indirect effects of corticosteroids, CyA on pancreatic β cells are well documented. With regard to FK506, the available data are not as extensive as for CyA, and its role in low blood insulin levels *vs* insulin resistance has not been fully evaluated. Human pancreatic allograft biopsies demonstrating both FK506 and CyA can induce structural damage of the graft islets, for example, cytoplasmic swelling, vacuolization, apoptosis, and abnormal immunostaining for insulin and the absent or reduced dense core secretory granules in the β cells. These changes are related to the doses of FK506 and/or CyA used. Although CyA and FK506 bind to different target molecules, both drugs inhibit or perturb the intermediate molecular events of insulin signal transduction (serine phosphorylations/dephosphorylations) in the same fashion. As a result, insulin signal fails to dephosphorylate the cytoplasmic component of the nuclear factor of activated signal transduction and transcription of insulin-sensitive gene, thus incorporating insulin resistance[27,28].

Organ level

Nonalcoholic fatty liver disease is associated with type 2 DM and the metabolic syndrome in patients with HCV[29]. However, the role of HCV as a risk factor for fatty liver has been questioned. It was reported that obesity and hyperlipidemia have a confounding effect on the association between HCV and steatosis[30]. In one study, serum ferritin levels were determined in 123 HCV-infected patients (55 diabetic and 68 non-diabetic patients)[32]. Increased iron store, which occurs in up to 40% of patients with chronic HCV infection[31], has been linked to the pathogenesis of diabetes development in those patients. The hepatic parasympathetic nerves are mediated by the activation of the Ach/NO/cGMP pathway involved in the secretion of a hepatic insulin sensitizing substance to mediate peripheral insulin sensitivity[41,42]. Schneiter *et al.*[33], found that liver transplantation recipients have severe insulinopenia as a result of the increased insulin clearance[33].

CLINICAL FEATURES

PTDM shares many similarities with type 2 DM in that the onset can be insidious, and individuals may experience glucose intolerance and may be asymptomatic for years[5]. The development of PTDM involves two distinct phases: (a) patients are initially at the greatest risk during the first 6 mo post-transplantation, and (b) the number of patients developing diabetes increases progressively thereafter. This has been illustrated by a study of 618 liver allograft recipients in which 7.2% of patients developed diabetes in the first 6 mo after transplantation, but then the percentage of cases increased linearly, leading to cumulative percentages of 7.1%, 10.4%, 13.2%, 20.5%, and 29.8%, respectively after 1, 3, 5, 10, and 15 years[34]. In a recent study, unadjusted cumulative incidences of diabetes 3, 12, and 36 mo after kidney transplantation were 15.6%, 25.6%, and 35.4% compared to 8.8%, 15.4%, and 23.4% in patients who were HCV negative at transplantation ($P<0.0001$)[35]. The potentially asymptomatic and/or transient nature of diabetes after transplantation makes the condition difficult to diagnose, thus underlining the importance of establishing a precise definition. It is recommended that the definition and diagnosis of PTDM should be based on the currently accepted definition of diabetes mellitus by the American Diabetes Association[5]. Diabetes mellitus is diagnosed by three fasting glucose measurements in the plasma above 7.0 mmol/L and/or antidiabetic medication (oral antidiabetic drugs or insulin), excluding periods requiring total parenteral nutrition or high steroid dosages for treatment of acute rejection, which may transiently impair glucose tolerance. After liver transplantation, patients with diabetes mellitus are classified either as non-insulin-requiring PTDM when taking only oral antidiabetic drugs or diet or as insulin-requiring PTDM when they require insulin injections. This classification of the patients should be done more than 1 year after liver transplantation[36]. Some preliminary reports suggest that pre-emptive therapy with IFN or a combination of IFN plus ribavirin may lead to less severe HCV infection recurrence after liver transplantation[43,44]. However, there are no controlled studies evaluating the prophylaxis of IFN in PTDM with HCV infection.

IMPLICATIONS

The HCV-diabetes association represents a major public health problem. Hundreds and thousands of patients in the USA alone are probably affected, and many more may have impaired glucose tolerance. Diabetes-related micro- and macrovascular complications are likely to occur, and the ongoing hepatic inflammatory response may contribute to atherogenesis. Furthermore, a putative bi-directional relationship between HCV-induced liver disease and diabetes may occur. Both insulin resistance and diabetes can adversely affect the course of chronic hepatitis C, and lead to enhanced steatosis, steatohepatitis, and liver fibrosis[37,38]. Moreover, recent evidence strongly suggests that steatosis and diabetes may also significantly enhance the risk of hepatocellular cancer[39,40].

FUTURE DIRECTIONS

There is evidence that HCV infection is related with the presence of PTDM. However, several questions remain to be answered. Firstly, randomized trials aimed to evaluate interactions of immunosuppressive regimens for the prophylaxis and treatment of PTDM are scarce. Secondly, the antiviral therapy for intervention remains to be determined. Finally, information is needed to clarify and diminish the effect of PTDM on quality of life and long-term outcomes. Further studies are necessary to evaluate the prognostic meaning of PTDM and the predictive factors for PTDM and to elucidate the pathophysiologic mechanisms.

REFERENCES

1 **Mathew JT**, Rao M, Job V, Ratnaswamy S, Jacob CK. Post-transplant hyper- glycaemia: a study of risk factors. *Nephrol Dial Transplant* 2003; **18**: 164-171
2 **Shintani Y**, Fujie H, Miyoshi H, Tsutsumi T, Tsukamoto K, Kimura S, Moriya K, Koike K. Hepatitis C virus infection and diabetes: direct involvement of the virus in the development of insulin resistance. *Gastroenterology* 2004; **26**: 840-848
3 **Hadziyannis SJ**. The spectrum of extrahepatic manifestations in hepatitis C virus infection. *J Viral Hepat* 1997; **4**: 9-28
4 **Kreis H**, Oberbauer R, Campistol JM, Mathew T, Daloze P,

Schena FP, Burke JT, Brault Y, Gioud-Paquet M, Scarola JA, Neylan JF. Rapamune Maintenance Regimen trial. Long-term benefits with sirolimus-based therapy after early cyclosporine withdrawal. *J Am Soc Nephrol* 2004; **15**: 809-817

5 **Davidson J**, Wilkinson A, Dantal J, Dotta F, Haller H, Hernandez D, Kasiske BL, Kiberd B, Krentz A, Legendre C, Marchetti P, Markell M, van der Woude FJ, Wheeler DC. International Expert Panel. New-onset diabetes after transplantation: 2003 International consensus guidelines. Proceedings of an international expert panel meeting. Barcelona, Spain, 19 February 2003. *Transplantation* 2003; **75**(10 Suppl): SS3-24

6 **Zein NN**, Abdulkarim AS, Wiesner RH, Egan KS, Persing DH. Prevalence of diabetes mellitus in patients with end-stage liver cirrhosis due to hepatitis C, alcohol, or cholestatic disease. *J Hepatol* 2000; **32**: 209-217

7 **Bigam DL**, Pennington JJ, Carpentier A, Wanless IR, Hemming AW, Croxford R, Greig PD, Lilly LB, Heathcote JE, Levy GA, Cattral MS. Hepatitis C-related cirrhosis: a predictor of diabetes after liver transplantation. *Hepatology* 2000; **32**: 87-90

8 **Khalili M**, Lim JW, Bass N, Ascher NL, Roberts JP, Terrault NA. New onset diabetes mellitus after liver transplantation: the critical role of hepatitis C infection. *Liver Transpl* 2004; **10**: 349-355

9 **AlDosary AA**, Ramji AS, Elliott TG, Sirrs SM, Thompson DM, Erb SR, Steinbrecher UP, Yoshida EM. Post-liver transplantation diabetes mellitus: an association with hepatitis C. *Liver Transpl* 2002; **8**: 356-361

10 **Baid S**, Tolkoff-Rubin N, Farrell ML, Delmonico F, Williams WW, Hayden D, Ko D, Cosimi AB, Pascual M. Tacrolimus-associated posttransplant diabetes mellitus in renal transplant recipients: role of hepatitis C infection. *Transplant Proc* 2002; **34**: 1771-1773

11 **Bigam DL**, Pennington JJ, Carpentier A, Wanless IR, Hemming AW, Croxford R, Greig PD, Lilly LB, Heathcote JE, Levy GA, Cattral MS. Hepatitis C-related cirrhosis: a predictor of diabetes after liver transplantation. *Hepatology* 2000; **32**: 87-90

12 **Yildiz A**, Tutuncu Y, Yazici H, Akkaya V, Kayacan SM, Sever MS, Carin M, Karsidag K. Association between hepatitis C virus infection and development of post-transplantation diabetes mellitus in renal transplant recipients. *Transplantation* 2002; **74**: 1109-1113

13 **Delgado-Borrego A**, Casson D, Schoenfeld D, Somsouk M, Terella A, Jordan SH, Bhan A, Baid S, Cosimi AB, Pascual M, Chung RT. Hepatitis C virus is independently associated with increased insulin resistance after liver transplantation. *Transplantation* 2004; **77**: 703-710

14 **Parolin MB**, Zaina FE, Araujo MV, Kupka E, Coelho JC. Prevalence of new-onset diabetes mellitus in Brazilian liver transplant recipients: association with HCV infection. *Transplant Proc* 2004; **36**: 2776-2777

15 **Mehta SH**, Brancati FL, Strathdee SA, Pankow JS, Netski D, Coresh J, Szklo M, Thomas DL. Hepatitis C virus infection and incident type 2 diabetes. *Hepatology* 2003; **38**: 50-56

16 **Bosi E**, Minelli R, Bazzigaluppi E, Salvi M. Fulminant autoimmune Type 1 diabetes during interferon-alpha therapy: a case of Th1-mediated disease? *Diabet Med* 2001; **18**: 329-332

17 **Gray H**, Wreghitt T, Stratton IM, Alexander GJ, Turner RC, O'Rahilly S. High prevalence of hepatitis C infection in Afro-Caribbean patients with type 2 diabetes and abnormal liver function tests. *Diabet Med* 1995; **12**: 244-249

18 **Hui JM**, Kench JG, Chitturi S, Sud A, Farrell GC, Byth K, Hall P, Khan M, George J. Long-term outcomes of cirrhosis in nonalcoholic steatohepatitis compared with hepatitis C. *Hepatology* 2003; **38**: 420-427

19 **Aytug S**, Reich D, Sapiro LE, Bernstein D, Begum N. Impaired IRS-1/PI3-kinase signaling in patients with HCV: a mechanism for increased prevalence of type 2 diabetes. *Hepatology* 2003; **38**: 1384-1392

20 **Ruan H**, Lodish HF. Insulin resistance in adipose tissue: direct and indirect effects of tumor necrosis factor-alpha. *Cytokine Growth Factor Rev* 2003; **14**: 447-455

21 **Ersoy C**, Imamoglu S, Budak F, Tuncel E, Erturk E, Oral B. Effect of amlodipine on insulin resistance & tumor necrosis factor-alpha levels in hypertensive obese type 2 diabetic patients. *Indian J Med Res* 2004; **120**: 481-488

22 **Kimball P**, Elswick RK, Shiffman M. Ethnicity and cytokine production gauge response of patients with hepatitis C to interferon-alpha therapy. *J Med Virol* 2001; **65**: 510-516

23 **Kobayashi S**, Suzuki M, Tsuneki H, Nagai R, Horiuchi S, Hagino N. Overproduction of N(epsilon)-(carboxymethyl) lysine-induced neovascularization in cultured choroidal explant of streptozotocin diabetic rat. *Biol Pharm Bull* 2004; **27**: 1565-1571

24 **Gowans EJ**, Jones KL, Bharadwaj M, Jackson DC. Prospects for dendritic cell vaccination in persistent infection with hepatitis C virus. *J Clin Virol* 2004; **30**: 283-290

25 **Piquer S**, Hernandez C, Enriquez J, Ross A, Esteban JI, Genesca J, Bonifacio E, Puig-Domingo M, Simo R. Islet cell and thyroid antibody prevalence in patients with hepatitis C virus infection: effect of treatment with interferon. *J Lab Clin Med* 2001; **137**: 38-42

26 **Weir MR**, Fink JC. Risk for posttransplant Diabetes mellitus with current immuno- suppressive medications. *Am J Kidney Dis* 1999; **34**: 1-13

27 **Drachenberg CB**, Klassen DK, Weir MR, Wiland A, Fink JC, Bartlett ST, Cangro CB, Blahut S, Papadimitriou JC. Islet cell damage associated with tacrolimus and cyclosporine: morphologicalfeatures in pancreas allograft biopsies and clinical correlation. *Transplantation* 1999; **68**: 396-402

28 **Aytug S**, Reich D, Sapiro LE, Bernstein D, Begum N. Impaired IRS-1/PI3-kinase signaling in patients with HCV: a mechanism for increased prevalence of type 2 diabetes. *Hepatology* 2003; **38**: 1384-1392

29 **Sanyal AJ**, Contos MJ, Sterling RK, Luketic VA, Shiffman ML, Stravitz RT, Mills AS. Nonalcoholic fatty liver disease in patients with hepatitis C is associated with features of the metabolic syndrome. *Am J Gastroenterol* 2003; **98**: 2064-2071

30 **Monto A**, Alonzo J, Watson JJ, Grunfeld C, Wright TL. Steatosis in chronic hepatitis C: relative contributions of obesity, diabetes mellitus, and alcohol. *Hepatology* 2002; **36**: 729-736

31 **Riggio O**, Montagnese F, Fiore P, Folino S, Giambartolomei S, Gandin C, Merli M, Quinti I, Violante N, Caroli S, Senofonte O, Capoccaccia L. Iron overload in patients with chronic viral hepatitis: how common is it? *Am J Gastroenterol* 1997; **92**: 1298-1301

32 **Furutani M**, Nakashima T, Sumida Y, Hirohama A, Yoh T, Kakisaka Y, Mitsuyoshi H, Senmaru H, Okanoue T. Insulin resistance/beta-cell function and serum ferritin level in non-diabetic patients with hepatitis C virus infection. *Liver Int* 2003; **23**: 294-299

33 **Schneiter P**, Gillet M, Chiolero R, Jequier E, Mosimann F, Temler E, Teta D, Matter M, Wauters JP, Tappy L. Mechanisms of postprandial hyperglycemia in liver transplant recipients:comparison of liver transplant patients with kidney transplant patients and healthy controls. *Diabetes Metab* 2000; **26**: 51-56

34 **Huo TI**, Yang WC, Wu JC, King KL, Lin CY, Loong CC, Lui WY, Chang FY, Lee SD. Long-term outcome of kidney transplantation in patients with hepatitis C virus infection. *Hepatogastroenterology* 2001; **48**: 169-173

35 **Duijnhoven EM**, Boots JM, Christiaans MH, Wolffenbuttel BH, Van Hooff JP. Influence of tacrolimus on glucose metabolism before and after renal transplant- tation: a prospective study. *J Am Soc Nephrol* 2001; **12**: 583-588

36 **Stockmann M**, Steinmuller T, Nolting S, Neuhaus P. Posttransplant diabetes mellitus after orthotopic liver transplantation. *Transplant Proc* 2002; **34**: 1571-1572

37 **Adinolfi LE**, Gambardella M, Andreana A, Tripodi MF, Utili R, Ruggiero G. Steatosis accelerates the progression of liver damage of chronic hepatitis C patients and correlates with specific HCV genotype and visceral obesity. *Hepatology* 2001; **33**: 1358-1364

38 **Castera L**, Hezode C, Roudot-Thoraval F, Bastie A, Zafrani

ES, Pawlotsky JM, Dhumeaux D. Worsening of steatosis is an independent factor of fibrosis progression in untreated patients with chronic hepatitis C and paired liver biopsies. *Gut* 2003; **52**: 288-292

39 **Tazawa J**, Maeda M, Nakagawa M, Ohbayashi H, Kusano F, Yamane M, Sakai Y, Suzuki K. Diabetes mellitus may be associated with hepatocarcinogenesis in patients with chronic hepatitis C. *Dig Dis Sci* 2002; **47**: 710-715

40 **Ohata K**, Hamasaki K, Toriyama K, Matsumoto K, Saeki A, Yanagi K, Abiru S, Nakagawa Y, Shigeno M, Miyazoe S, Ichikawa T, Ishikawa H, Nakao K, Eguchi K. Hepatic steatosis is a risk factor for hepatocellular carcinoma in patients with chronic hepatitis C virus infection. *Cancer* 2003; **97**: 3036-3043

41 **Lautt WW**, Macedo MP, Sadri P, Takayama S, Duarte Ramos F, Legare DJ. Hepatic parasympathetic (HISS) control of insulin sensitivity determined by feeding and fasting. *Am J Physiol Gastrointest Liver Physiol* 2001; **281**: 29-36

42 **Guarino MP**, Afonso RA, Raimundo N, Raposo JF, Macedo MP. Hepatic glutathione and nitric oxide are critical for hepatic insulin-sensitizing substance action. *Am J Physiol Gastrointest Liver Physiol* 2003; **284**: G588-G594

43 **Sheiner PA**, Boros P, Klion FM, Thung SN, Schluger LK, Lau JY, Mor E, Bodian C, Guy SR, Schwartz ME, Emre S, Bodenheimer HC Jr, Miller CM. The efficacy of prophylactic interferon alfa-2b in preventing recurrent hepatitis C after liver transplantation. *Hepatology* 1998; **28**: 831-838

44 **Singh N**, Gayowski T, Wannstedt CF, Shakil AO, Wagener MM, Fung JJ, Marino IR. Interferon- alpha for prophylaxis of recurrent viral hepatitis C in liver transplant recipients: a prospective, randomized, controlled trial. *Transplantation* 1998; **65**: 82-86

45 **Charlton M**. Liver biopsy, viral kinetics, and the impact of viremia on severity of hepatitis C virus recurrence. *Liver Transpl* 2003; **9**: S58-S62

46 **Konrad T**, Zeuzem S, Toffolo G, Vicini P, Teuber G, Briem D, Lormann J, Lenz T, Herrmann G, Berger A, Cobelli C, Usadel K. Severity of HCV-induced liver damage alters glucose homeostasis in noncirrhotic patients with chronic HCV infection. *Digestion* 2000; **62**: 52-59

Science Editor Wang XL and Guo SY **Language Editor** Elsevier HK

PO Box 2345, Beijing 100023, China
www.wjgnet.com
wjg@wjgnet.com

ELSEVIER

World J Gastroenterol 2005;11(39):6090-6095
World Journal of Gastroenterology ISSN 1007-9327

Value of endoscopic methylene blue and Lugol's iodine double staining and detection of GST-π and telomerase in the early diagnosis of esophageal carcinoma

Xuan Zhu, Shuang-Hong Zhang, Kun-He Zhang, Bi-Ming Li, Jiang Chen

Xuan Zhu, Shuang-Hong Zhang, Bi-Ming Li, Department of Gastroenterology, the First Affiliated Hospital, Jiangxi Medical College, Nanchang 330006, Jiangxi Province, China
Kun-He Zhang, Jiang Chen, Department of Digestive Institution, the First Affiliated Hospital, Jiangxi Medical College, Nanchang 330006, Jiangxi Province, China
Supported by the Scientific and Technological Foundation of the Education Department of Jiangxi Province
Co-first-authors: Xuan Zhu and Shuang-Hong Zhang
Co-correspondents: Xuan Zhu
Correspondence to: Dr. Xuan Zhu, Department of Gastroenterology, the First Affiliated Hospital, Jiangxi Medical College, Nanchang 330006, Jiangxi Province, China. jyyfyzx@163.com
Telephone: +86-791-8692505
Received: 2004-12-30 Accepted: 2005-02-28

Abstract

AIM: To explore the expressions of GST-π and telomerase activity in esophageal carcinoma and premalignant lesions and to investigate the value of endoscopic methylene blue (MB) and Lugol's iodine double staining.

METHODS: Seventy-two patients with esophagopathy were sprayed endoscopically with MB and Lugol's iodine in proper order and the areas stained blue and brown, and the area between the blue and brown stains were obtained. Depending on the pattern of mucosal staining, biopsy specimen was obtained. GST-π and telomerase activity in specimens were examined by immunohistochemistry and PCR-based silver staining telomeric repeat amplification protocol, respectively.

RESULTS: After MB and Lugol's iodine staining, the area between both the colors was obtained in 64 of the 72 patients and the areas were stained blue and brown in all of the 72 patients. Association test of two simultaneous ordinal categorical data showed a correlation between the esophageal mucosal staining and the esophageal histology (P<0.005). The expression of GST-π and telomerase activity in esophageal carcinoma and premalignant lesions increased. The expression of GST-π and telomerase activity in dysplasia and carcinoma was significantly higher than that in normal epithelium (P<0.005). The expression in hyperplasia was slightly higher than that in normal epithelium. With the lesions progressing from low- to moderate- to high-grade dysplasia, the positive rate increased (P<0.025). Expression of GST-π was correlated with that of telomerase activity in dysplasia and carcinoma (φ = 0.4831, P<0.005; φ = 0.3031, P<0.025, respectively); but there was no correlation between them in normal epithelium and hyperplasia.

CONCLUSION: The expression of GST-π and telomerase may be an early event in the carcinogenesis of esophagus. They may play an induced and synergistic role with each other in the carcinogenesis of esophagus. Endoscopic MB and Lugol's iodine double staining and detection of GST-π and telomerase activity may contribute to the early diagnosis of esophageal carcinoma.

Key words: Esophageal carcinoma; Endoscopy; Glutathione *S*-transferases; Telomerase

Zhu X, Zhang SH, Zhang KH, Li BM, Chen J. Value of endoscopic methylene blue and Lugol's iodine double staining and detection of GST-π and telomerase in the early diagnosis of esophageal carcinoma. *World J Gastroenterol* 2005; 11 (39): 6090-6095
http://www.wjgnet.com/1007-9327/11/6090.asp

INTRODUCTION

The early diagnosis of esophageal carcinoma correlates closely to improvement in prognosis. Much dependent on endoscopy, esophageal carcinoma is clinically diagnosed till now, but the choice of biopsy site, partly, has a limitation. The esophageal mucosal staining technique not only obtains the characteristic of the morphology of the lesions, but also helps to direct its biopsy in esophageal carcinoma. Carcinogen is one of the induced etiological factors. The glutathione *S*-transferases (GSTs) are a family of enzymes, which participate in metabolic detoxication and play important roles in the prevention of carcinogenesis by detoxifying numerous potentially carcinogenic compounds[1]. The present studies showed that telomerase activity had a close correlation with cell immortalization and carcinogenesis. The length of telomerase extends to maintain a proportional balance because telomerase is activated[2,3], therefore, the cells may unlimitedly proliferate to induce carcinogenesis. The aim of this study was to examine the expressions of GST-π and telomerase in esophageal carcinoma and premalignant lesions using immunohistochemistry and telomeric repeat amplification protocol (TRAP)-silver staining assay, respectively, and to investigate the value of endoscopic methylene blue (MB) and Lugol's iodine double

staining and detection of GST-π and telomerase in the early diagnosis of esophageal carcinoma.

MATERIALS AND METHODS

Specimen collection and processing

Tissue specimens were obtained endoscopically from in- and outpatients with abnormal findings, such as mucosal congestion, erosions, swelling or masses in the esophagus in the Affiliated Hospital of Jiangxi Medical College from 2002 to 2003. A total of 72 patients were included in this study, aged between 27 and 78 years, composed of 49 men and 23 women. All 72 patients underwent upper endoscopy and MB and Lugol's iodine staining with biopsy. After the endoscopic examination, the esophageal lumen was washed with 50 mL of distilled water. At first, 5 g/L MB solution was sprayed on the esophageal lesion. After 1 min, approximately 120-200 mL of distilled water was sprayed on the esophageal mucosa to wash off excess dye. Then 30 mL/L Lugol's iodine solution was sprayed on the esophageal lesion. After MB and Lugol's iodine staining, the pattern of mucosal staining was classified as blue, brown and the areas between both the colors. Depending on the color, two to four biopsy specimens of positive staining were obtained using the large cup biopsy forceps. Endoscopic specimens were immediately placed in the Eppendorf tube and a 10% buffered formalin solution, but immediately these specimens in the Eppendorf tube were kept in liquid nitrogen, and after 24 h, were stored at -80 ℃ until extraction for telomerase.

GST-π determination

Expression of GST-π was examined using indirect immunohistochemical staining accompanied by positive and negative controls. The key steps in the staining procedure were as follows: 4-μm-thick sections cut from each formalin-fixed and paraffin-embedded tissue specimen; deparaffinized in xylene, dehydrated through graded alcohol and washed thrice with distilled water; incubated for 5 min with 30 mL/L hydrogen peroxide to block endogenous peroxidase activity; again incubated with citrate buffer (pH 6.0) for 3 min using a household microwave oven at 800 W, followed by incubation for 1 h at 37 ℃ with the primary GST-π antibody at a dilution of 1∶100, and then washed thrice with PBS. After a second incubation with the GST-π anti-rabbit antibody HRP, 3, 3'-diaminobenzidine tetrachloride was used for color development and finally counterstained with hematoxylin. The immunohistochemical expression of GST-π was examined by means of light microscopy. The staining results were assigned to one of the following groups: (-), less than 25% of cells stained or the cells staining intensity being consistent with that of the background; (+), 25-50% of cells stained with light yellow fine granule showing in cells; (++), 50-70% of cells stained with dark brown granule showing in cells; (+++), more than 70% of cells stained with a great amount of dark brown granule showing in cells. Positive staining provided an internal positive control for GST-π staining. The primary antibody was replaced by PBS for the negative control.

Telomerase activity assay

Expression of telomerase activity was measured using TRAP-silver staining assay. Frozen specimens were homogenized and incubated with 20 μL of ice-cold lyses buffer (10 mmol/L Tris-HCl, pH 7.5, 1 mmol/L EGTA, 0.1 mmol/L benzamidine, 5 mmol/L β-mercaptoethanol, 5 g/L CHAPS, 100 mL/L glycerol). After 30 min of incubation on ice, the lysate was centrifuged at 14 500 *g* for 30 min at 2-8 ℃, and the supernatant was frozen and stored at -80 ℃. A total volume of PCR reactions was 25 μL. TRAP reaction was performed using 2 μL extracts, 2.5 μL 10× TRAP buffer (200 mmol/L Tris-HCl, pH 8.3, 15 mmol/L $MgCl_2$, 630 mmol/L KCl, 5 g/L Tween 20, 10 mmol/L EGTA, 1 g/L BSA), 1 μL of 4 mmol/L dNTP, 0.5 μL TS primer, and 18 μL double-distilled water. After 10 min incubation at 23 ℃ for telomerase-mediated extension of the TS primer, the reaction mixture was heated for 5 min at 94 ℃ to inactivate the telomerase, then added 2 U of Taq, 0.5 μL CX primer and finally 30 μL wax barrier. All the above steps were performed on ice. PCR reactions were performed for 27 amplification cycles, each cycle consisting of denaturation at 94 ℃ for 30 s, primers annealing at 50 ℃ for 30 s and extension at 72 ℃ for 90 s, followed by an extra incubation at 72 ℃ for 10 min to ensure full extension of the products. The PCR products were electrophoresed on a 120 g/L gel polyacrylamide for 2-3 h and then gel was stained using $AgNO_3$ and was photographed. The extract, which showed a ladder of products with 6-bp increments after being stained on the gel, was considered telomerase positive. For the negative controls of telomerase, the extract was heat-treated by incubation at 65 ℃ for 10 min prior to TRAP assay to inactivate the telomerase, and no PCR product was observed in the negative controls of telomerase.

Criteria of pathological histology

This was performed by evaluating the H&E-stained tissue sections under a microscope according to the criteria described previously by Qiu and Yang[4]. We classified the tissue sections into eight groups: normal epithelium; pure hyperplasia; low-grade dysplasia; moderate-grade dysplasia; high-grade dysplasia; carcinoma *in situ*; squamous cell carcinoma; and adenocarcinoma.

Statistical analysis

Proportion (relative number, %) was used for result analysis, and statistical significance was tested using χ^2 test, exact method analysis, rank sum test or association test of categorical data. A P value less than 0.05 was considered statistically significant.

RESULTS

Endoscopic methylene blue and Lugol's iodine double staining

After staining with MB and Lugol's iodine, the area between both the colors was obtained in 64 of the 72 patients. We observed areas stained blue and brown in all the 72 patients. Association test of two simultaneous ordinal categorical data showed a significant correlation between the esophageal mucosal staining and the esophageal histology (P<0.005, Table 1, Figure 1).

Table 1 Endoscopic MB and Lugol's iodine double staining (*n*, %)

Histology	*n*	Areas stained blue (%)	Areas between both the colors (%)	Areas stained brown (%)
Normal epithelium	53	49 (92.5)	4 (7.5)	0
Hyperplasia	21	13 (61.9)	6 (28.6)	2 (9.5)
Dysplasia	79	10 (12.6)	45 (57.0)	24 (30.4)
Low-grade	17	7 (41.2)	7 (41.2)	3 (17.6)
Moderate-grade	21	3 (14.3)	13 (61.9)	5 (29.4)
High-grade	41	0	25 (61.0)	16 (39.0)
Carcinoma	55	0	9 (16.4)	46 (83.6)
Carcinoma *in situ*	1	0	1 (100)	0
Squamous cell carcinoma	51	0	8 (15.7)	43 (84.3)
Adenocarcinoma	3	0	0	3 (100)
Total	208	72	64	72

$\chi^2 = 170.58$, $P<0.005$.

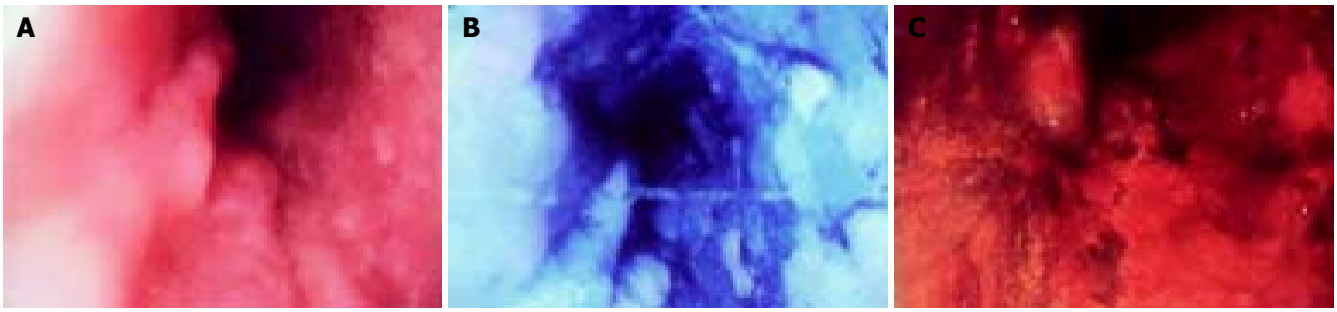

Figure 1 Endoscopic view of esophageal wall after MB and Lugol's iodine double staining. A: Before staining, a large broad-based erosion was observed on esophageal wall and the outlines of erosion were unclearly discernible; B: after MB staining, the same lesion stained more deeper blue than surrounding mucosa; C: after Lugol's iodine double staining, the normal mucosa appeared brown, the same lesion stained more deeper blue than surrounding mucosa and the areas between both the colors were not stained.

Expression of GST-π in esophageal carcinoma and premalignant lesions

GST-π was expressed in 5.7% normal epithelium (3/53), 62.0% dysplasia (49/79) and 83.6% carcinoma (46/55, $P<0.005$); the positive rate of hyperplasia was slightly higher than that of normal epithelium. With the lesions progressing from low- to moderate- to high-grade dysplasia, the positive rate increased ($P<0.025$, Tables 2 and 3, Figure 2).

Table 2 GST-π protein expression in esophageal carcinogenesis (*n*, %)

Histology	*n*	GST-π expression				Positive rate (%)
		–	+	++	++	
Normal epithelium	53	50	3	0	0	5.7
Hyperplasia	21	19	2	0	0	9.5[1]
Dysplasia	79	30	34	12	3	62.0[b]
Carcinoma	55	9	30	13	3	83.6[b]

[1]$P>0.9$, [b]$P<0.001$ *vs* normal epithelium.

Table 3 GST-π protein expression in various histology mucosa of esophagus (*n*, %)

Histology	*n*	GST-π expression				Positive rate (%)
		–	+	++	++	
Low-grade dysplasia	17	11	5	1	0	35.3
Moderate-grade dysplasia	21	9	8	3	1	57.1
High-grade dysplasia	41	10	21	8	2	75.6

$P<0.025$.

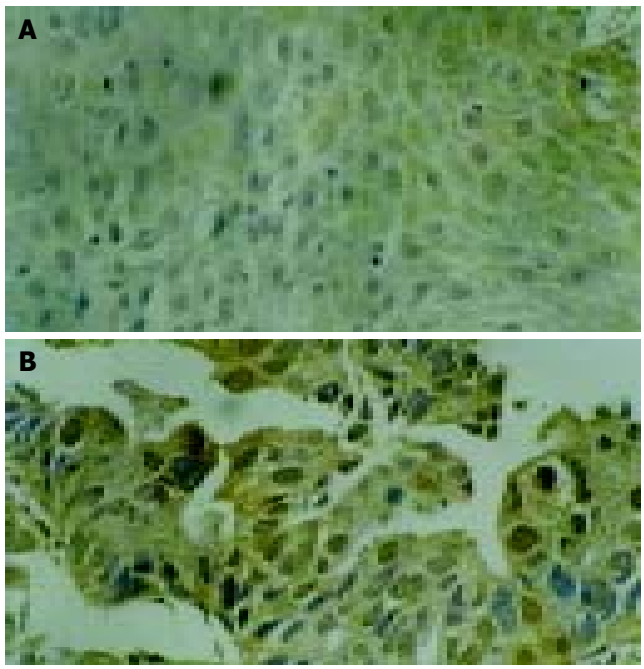

Figure 2 Expression of GST-π in histological esophageal tissues (×400). A: Esophageal dysplasia showing yellow or brown granule in cell substance and nucleus; B: esophageal carcinoma showing yellow or brown granules in cell substance and nucleus.

Expression of telomerase in esophageal carcinoma and premalignant lesions

Telomerase activity was expressed in 3.8% normal epithelium

(2/53), 51.9% dysplasia (41/79), and 89.1% carcinoma (49/55, $P<0.005$); the positive rate of hyperplasia was slightly higher than that of normal epithelium. With the lesions progressing from low-to moderate-to high-grade dysplasia, the positive rate increased ($P<0.005$, Tables 3 and 4, Figure 3).

Table 4 Telomerase activity expression in esophageal carcinogenesis (*n*, %)

Histology	*n*	Telomerase activity expression		Positive number of telomerase (%)
		+	–	
Normal epithelium	53	25	1	2 (3.8)
Hyperplasia	21	1	20	1 (4.8)[1]
Dysplasia	79	41	28	41 (51.9)[a]
Carcinoma	55	49	6	49 (89.1)[c]

[1]$P = 0.998$, hyperplasia *vs* normal epithelium; [a]$P<0.005$, $\chi^2 = 33.45$, dysplasia *vs* normal epithelium; [c]$P<0.005$, $\chi^2 = 78.83$, carcinoma *vs* normal epithelium.

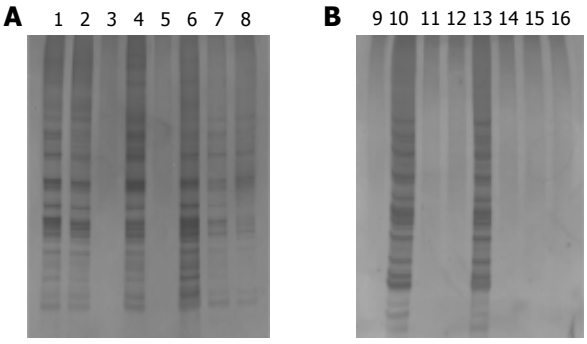

Figure 3 Analysis of telomerase activity of esophageal wall tissues using TRAP-silver staining assay. A: Esophageal carcinoma showing telomerase positivity (lanes 1, 2, 4, 6-8) and telomerase negativity (lanes 3 and 5); B: esophageal dysplasia showing telomerase positivity (lanes 10 and 13), and telomerase negativity (lanes 9, 11, 12, 14, and 15), and negative control (lane 16).

There was a positive correlation between the expression of GST-π and telomerase activity in esophageal carcinoma and premalignant lesions ($r = 0.9687$, $P<0.001$, Table 5). Expression of GST-π correlated to that of telomerase activity in dysplasia and carcinoma ($\varphi = 0.4831$, $P<0.005$; $\varphi = 0.3031$, $P<0.025$, respectively); but there was no correlation between the expression of GST-π and telomerase activity in normal epithelium and hyperplasia. Expression of GST-π was higher than that of telomerase activity in low- and moderate-grade dysplasia (Table 6).

DISCUSSION

In recent years, most scholars have advocated that the esophageal mucosal staining technique can be used for diagnosis of esophageal carcinoma to increase the sensitivity of the detection. Endoscopic MB and Lugol's iodine staining is one of the mucosal staining technique. The basis of the mucosal double staining technique is that MB stains lesion blue and Lugol's iodine reversibly stains glycogen brown. Normal squamous epithelium appears unstained because it does not absorb MB, but in abnormal mucosa, including intestinal metaplasia cells, columnar cells, erosions, ulcers and squamous carcinoma, the superficial epithelium is often stained blue because it absorbs MB. In normal squamous esophageal mucosa, the superficial epithelium contains large glycogen, so the mucosa stains dark brown, but in abnormal mucosa, the superficial epithelium often loses much of its glycogen, and remains partially or totally unstained. Therefore, the area stained blue indicates the existence of carcinoma; the area stained brown belongs to normal squamous esophageal mucosa and the area between both the colors clarifies the invasive lesion of carcinoma. Canto[5] reported that the diagnostic yield in 43 patients with Barrett's esophagus using MB-directed biopsies were compared with surveillance using a random biopsy technique in a controlled trial and the result indicated MB-directed biopsy was a more accurate technique than random biopsy for diagnosing specialized columnar epithelium and dysplasia and cancer. By means of the analysis of comparing the routine endoscopy to the endoscopy with 12 mL/L Lugol's iodine solution, Dawsey *et al*.[6], found that mucosal iodine solution improved endoscopic detection and this simple technique was highly sensitive in identifying these precursors and invasive squamous carcinoma. Our findings showed a correlation between the esophageal mucosal staining and esophageal histology ($P<0.005$), i.e. the areas between both the colors was a majority of dysplasia, especially moderate- and high-grade dysplasia, and the area stained blue was mostly carcinoma, and the area stained brown was mainly normal epithelium and hyperplasia. Overall,

Table 5 Telomerase activity expression in various histological mucosa of esophagus (*n*, %)

Histology	*n*	Telomerase activity expression		Positive number of telomerase (%)
		+	–	
Low-grade dysplasia	17	2	15	2 (11.8)
Moderate-grade dysplasia	21	7	14	7 (33.3)
High-grade dysplasia	41	32	9	32 (78.0)

Comparing among dysplasias $\chi^2 = 25.10$, $P<0.005$; there was significant difference between high- and low- or moderate-grade dysplasia ($\chi^2 = 21.77$, $P<0.005$; $\chi^2 = 11.90$, $P<0.005$, respectively), but no obvious difference between low- and moderate-grade dysplasia ($\chi^2 = 1.37$, $P>0.1$).

Table 6 Expressions of GST-π and telomerase activity in esophageal carcinoma and premalignant lesions

	Normal epithelium		Hyperplasia		Dysplasia		Carcinoma	
	GST-π (+)	GST-π (–)	GST-π (+)	GST- π(–)	GST- π(+)	GST-π (–)	GST-π (+)	GST-π (–)
TA (+)	0	2	0	1	36	5	43	6
TA (–)	3	48	2	18	13	25	3	3

TA: telomerase activity. Expression of GST-π correlated to that of telomerase activity in dysplasia and carcinoma ($\varphi = 0.4831$, $P<0.00$; $\varphi = 0.3031$, $P<0.025$ respectively); but there was no correlation between the expression of GST-π and telomerase activity in normal epithelium and hyperplasia ($P>0.05$).

endoscopic MB and Lugol's iodine double staining improves our ability to see the true size and borders of these esophageal lesions and to take biopsy accurately, which contributes to the early diagnosis of the high risk population and patients with esophageal carcinoma and premalignant lesion, thereby preventing the carcinogenesis of esophagus and reducing the mortality of the esophageal carcinoma.

In 1984, Sato *et al*.[7] firstly reported high level expression of GST-π protein in preneoplastic foci of rat liver, and subsequently the evidence suggested GST-π as an important marker of rat hepatocarcinogenesis. With a close crossing-immunity between GST-π in human tissues and GST-π in rat tissues, GST-π was regarded as a major research focus on the study of human carcinogenesis. A recent study has suggested that GST-π closely correlates with human alimentary carcinoma and is overexpressed in carcinoma and premalignant lesions. Ishioka *et al*.[8], showed that the RNA transcript levels of GST-π in tumor tissues were obviously higher than those in normal tissues in 80% cases (20/25), but no correlation between GST-π mRNA level and clinical stage or histologic characteristics was apparent. Li *et al*.[9], reported that the expression of GST-π increased in esophageal carcinoma and premalignant lesions and was associated with tumor differentiation, but no correlation between GST-π expression and clinical stage or lymphatic metastasis, while found that the mean serum GST-π levels in esophageal squamous cell carcinoma patients were significantly higher than those in normal subjects ($P<0.05$). Our data showed increased expression of GST-π in esophageal carcinoma and premalignant lesions, and with the lesions progressing from low- to moderate- to high-grade dysplasia, the positive rate obviously increased ($P<0.005$). In conclusion, when the cells are in the course of premalignancy, it is possible that some preneoplastic changes in metabolic enzyme have taken place, which are undetectable by using routinely stained sections and it is consistent with the fact of their increased GST-π expression level. Therefore, increased GST-π levels may be recognized as a useful marker of esophageal carcinogenesis.

Telomerase is a ribonuclear protein complex, which contains human telomerase RNA component and binding protein. Telomerase binding protein controls cell senescence, immortalization, and carcinogenesis by means of regulating telomerase activity and changing telomere length[10,11]. Normal somatic cells express undetectable levels of telomerase activity, whereas malignant cells express high levels[12]. Telomerase activity is strongly expressed in most human carcinomas, such as thyroid, breast, esophageal, gastric, lung, pancreatic, hepatocellular, and colorectal carcinoma[13-20]. Lord *et al*.[21], demonstrated that telomerase activation was an important early event in the development of Barrett's esophagus and esophageal adenocarcinoma, suggesting that very high telomerase levels might be a clinically useful biomarker for the detection of occult adenocarcinoma. Using microdissection-TRAP-silver staining assay, Li *et al*.[22], reported telomerase activity was high in both esophageal squamous cell carcinoma and preneoplastic lesions and was related to lymphatic metastasis, but not to cancer differentiation. The data from our studies showed that the positive rates of telomerase activity in low-, moderate-, high-grade dysplasia and carcinoma were 11.8%, 33.3%, 78.0% and 89.1%, respectively, but the positive rates of that in normal epithelium and hyperplasia were 3.8% and 4.8%. These observations reveal a crucial role for telomerase in the esophageal carcinogenesis. High expression levels in dysplasia show that telomerase may be activated in the early stage of esophageal carcinogenesis, indicating that telomerase activation is an early event in the carcinogenesis of the esophagus. It is, therefore, concluded that esophageal premalignant lesion may be effectively prevented from the progression to invasive malignancy in the light of irregularly surveying the variations of expression levels of telomerase activity in esophageal dysplasia patients and the prognosis of early esophageal carcinoma and premalignant lesion will improve significantly.

Our study provided evidence that expression of GST-π was higher than that of telomerase in low-moderate dysplasia. We infer that GST-π may be an early event in the carcinogenesis of esophagus in comparison with telomerase, but the relationship between GST-π and telomerase activity was not statistically significant. With the lesion progressing from dysplasia to carcinoma, expression level of GST-π showed an increased trend in degrees, whereas telomerase activity remained unchanged. We found that expression of GST-π was correlated to that of telomerase activity in dysplasia and carcinoma; but there was no correlation between the expression of GST-π and telomerase activity in normal epithelium and hyperplasia. Consequently, the results suggest that GST-π and telomerase may play an induced and synergistic role with each other in the carcinogenesis of esophageal carcinoma, but we do not know at present the mechanism to correlate GST-π with telomerase.

At present, many methods are widely used for the early diagnosis of esophageal carcinoma, but the sensitivity and specificity of a single method make it difficult to clinically diagnose an esophageal carcinoma. So, several authors have been exploring whether the combined method may improve the early diagnosis of esophageal carcinoma. Koyanagi *et al*.[23], reported that 10 of 18 iodine-nonreactive samples obtained from surgically resected specimens showed telomerase activity and in all 10 telomerase-positive samples, carcinoma *in situ* were observed in iodine-nonreactive mucosa by light microscopy and in 8 telomerase-negative samples, no tumor tissue were observed in iodine-nonreactive lesions. Inai *et al*.[24], also reported similar findings. Our study demonstrated that the expression levels of GST-π and telomerase were high in areas stained blue which was mostly carcinoma and the area between both the colors which was a majority of moderate- and high-grade dysplasia, and with the lesions progressing from low- to moderate- to high-grade dysplasia, the positive rate increased. In summary, the combined method of endoscopic MB and Lugol's iodine double staining and the detection of GST-π and telomerase activity are helpful to the early diagnosis of esophageal carcinoma and provide the chosen method for the physician.

REFERENCES

1 **Coles B,** Ketterer B. The role of glutathione and glutathione transferases in chemical carcinogenesis. *Crit Rev Biochem Mol*

Biol 1990; **25**: 47-70
2 **Colgin LM,** Reddel RR. Telomerase maintenance mechanisms and cellular immortalization. *Curr Opin Genet Dev* 1999; **9**: 97-103
3 **Meyerson M.** Role of telomerase in normal and cancer cells. *J Clin Oncol* 2000; **18**: 2626-2634
4 **Qiu SL,** Yang GR. Precursor lesions of esophageal cancer in high-risk populations in Henan Province, China. *Cancer* 1988; **62**: 551-557
5 **Canto MI.** Methylene blue-directed biopsies improve detection of intestinal metaplasis and dysplasia in Barrett's esophagus. *Gastrointest Endosc* 2000; **51**: 560-568
6 **Dawsey SM,** Fleischer DE, Wang GQ, Zhou B, Kidwell JA, Lu N, Lewin KJ, Roth MJ, Tio TL, Taylor PR. Mucosal lodine staining improves endoscopic visualization of squamous dysplasia and squamous cell carcinoma of the esophagus in Linxian, China. *Cancer* 1998; **83**: 220-230
7 **Sato K,** Kitahara A, Sathoh Kl. The placental form of glutathione S-transferase as a new marker protein for preneoplasia in rat chemical hepatocarcinogenesis. *Jpn J Cancer Res* 1984; **75**: 199-202
8 **Ishioka C,** Kanamaru R, Shibata H, Konishi Y, Ishikawa A, Wakui A, Sato T, Nishihira T. Expression of glutathione S-transferase-π messenger RNA in human esophageal cancers. *Cancer* 1991; **67**: 2560-2564
9 **Li Z,** Zhang R, Luo X. Expression of glutatgione S-transferase-π in human esophageal squamous cell carcinoma. *Chin J Oncol* 2001; **23**: 39-42
10 **Van SB,** Lang TD. Control of telomere length by the human telomeric protein TRF1. *Nature* 1997; **385**: 740-743
11 **Grieder CW.** Telomerase activation: one step on the road to cancer? *Trends Genetics* 1999; **15**: 109-112
12 **Chiu CP,** Harley CB. Replicative senescence and cell immortality: the role of telomeres and telomerase. *Proc Soc Exp Biol Med* 1997; **214**: 99-106
13 **Suzuki S,** Fukushima T, Ami H, Onogi H, Nakamura I, Takenoshita S. New attempt of preoperative differential diagnosis of thyroid neoplasms by telomerase activity measurement. *Oncol Rep* 2002; **9**: 539-544
14 **Shah NG,** Choksi TJ, Patel DD, Vora HH, Ghosh N, Trivedi TI, Trivedi KA. Telomerase activity in breast cancer in Western India (Gujarat). *Int J Biol Markers* 2002; **17**: 49-55
15 **Tominaga T,** Kashimura H, Suzuki K, Nakahara A, Tanaka N, Noguchi M, Itabashi M, Ohkawa J. Telomerase activity and expression of human telomerase catalytic subunit gene in esophageal tissues. *J Gastroenterol* 2002; **37**: 418-427
16 **Suzuki K,** Kashimura H, Ohkawa J, Itabashi M, Watanabe T, Sawahata T, Nakahara A, Muto H, Tanaka N. Expression of human telomerase catalytic subunit gene in cancerous and precancerous gastric conditions. *J Gastroenterol Hepatol* 2000; **15**: 744-751
17 **Fujita Y,** Fujikane T, Fujiuchi S, Nishigaki Y, Yamazaki Y, Nagase A, Shimizu T, Ohsaki Y, Kikuchi K. The diagnostic and prognostic relevance of human telomerase reverse transcriptase mRNA expression detected *in situ* in patients with nonsmall cell lung carcinoma. *Cancer* 2003; **98**: 1008-1013
18 **Zhou JH,** Zhang HM, Chen Q, Han DD, Pei F, Zhang LS, Yang DT. Relationship between telomerase activity and its subunit expression and inhibitory effect of antisense hTR on pancreatic carcinoma. *World J Gastroenterol* 2003; **9**: 1808-1814
19 **Miura N,** Shiota G, Nakagawa T, Maeda Y, Sano A, Marumoto A, Kishimoto Y, Murawaki Y, Hasegawa J. Sensitive detection of human telomerase reverse transcriptase mRNA in the serum of patients with hepatocellular carcinoma. *Oncology* 2003; **64**: 430-434
20 **Abe N,** Watanabe T, Nakashima M, Masaki T, Mori T, Sugiyama M, Atomi Y. Quantitative analysis of telomerase activity: a potential diagnostic tool for colorectal carcinoma. *Hepatogastroenterology* 2001; **48**: 692-695
21 **Lord RV,** Salonga D, Danenberg KD, Peters JH, DeMeester TR, Park JM, Johansson J, Skinner KA, Chandrasoma P, DeMeester SR, Bremner CG, Tsai PI, Danenberg PV. Telomerase reverse transcriptase expression is increased early in the Barrett's metaplasia, dysplasia, adenocarcinoma sequence. *J Gastrointest Surg* 2000; **4**: 135-142
22 **Li C,** Liang Y, Wu M, Xu L, Cai W. Telomerase activity analysis of esophageal carcinoma using microdissection-TRAP assay. *Chin Med J* 2002; **115**: 1405-1408
23 **Koyanagi K,** Ozawa S, Ando N, Mukai M, Kitagawa Y, Ueda M, Kitajima M. Telomerase activity as an indicator of malignant potential in iodine-nonreactive Lesions of the esophagus. *Cancer* 2000; **88**: 1524-1529
24 **Inai M,** Kano M, Shimada Y, Sakurai T, Chiba T, Imamura M. Telomerase activity of the Lugol-stained and -unstained squamous epithelia in the process of oesophageal carcinogenesis. *Br J Cancer* 2001; **85**: 1006-1013

Science Editor Kumar M and Guo SY **Language Editor** Elsevier HK

PO Box 2345, Beijing 100023, China
www.wjgnet.com
wjg@wjgnet.com

ELSEVIER

World J Gastroenterol 2005;11(39):6096-6103
World Journal of Gastroenterology ISSN 1007-9327

• *GASTRIC CANCER* •

Epstein-Barr virus-associated gastric carcinoma: Evidence of age-dependence among a Mexican population

Roberto Herrera-Goepfert, Suminori Akiba, Chihaya Koriyama, Shan Ding, Edgardo Reyes, Tetsuhiko Itoh, Yoshie Minakami, Yoshito Eizuru

Roberto Herrera-Goepfert, Department of Pathology, Instituto Nacional de Cancerologia, Mexico City, Mexico
Suminori Akiba, Chihaya Koriyama, Shan Ding, Department of Epidemiology and Preventive Medicine, Kagoshima University Graduate School of Medical and Dental Sciences, Kagoshima, Japan
Edgardo Reyes, Department of Pathology, Instituto Nacional de Ciencias Médicas y de la Nutrición "Salvador Zubirán", Mexico City, Mexico
Tetsuhiko Itoh, Department of Pathology, Kagoshima Institute of Preventive Medicine, Kagoshima, Japan
Yoshie Minakami, Yoshito Eizuru, Division of Oncogenic and Persistent Viruses, Center for Chronic Viral Diseases, Kagoshima University Graduate School of Medical and Dental Sciences, Kagoshima, Japan
Supported by a Grant No. 12218231 from Grants-in-Aid for Scientific Research of the Ministry of Education, Science, Sports, and Culture of Japan
Correspondence to: Roberto Herrera-Goepfert, MD, Departamento de Patología Instituto Nacional de Cancerología, Av. San Fernando #22, Colonia Sección XVI, Tlalpan, México DF 14080, Mexico. rhgoepfert@yahoo.com.mx
Telephone: +52-55-5628-0466 Fax: +52-55-5573-4662
Received: 2005-04-13 Accepted: 2005-05-24

Abstract

AIM: To investigate features of Epstein-Barr virus (EBV)-associated gastric carcinoma (EBVaGC) among a Mexican population.

METHODS: Cases of primary gastric adenocarcinoma were retrieved from the files of the Departments of Pathology at the Instituto Nacional de Cancerología and the Instituto Nacional de la Nutrición in Mexico City. The anatomic site of the gastric neoplasia was identified, and carcinomas were histologically classified as intestinal and diffuse types and subclassified as proposed by the Japanese Research Society for Gastric Cancer. EBV-encoded small non-polyadenylated RNA-1 (EBER-1) *in situ* hybridization was conducted to determine the presence of EBV in neoplastic cells.

RESULTS: We studied 330 consecutive, non-selected, primary gastric carcinomas. Among these, there were 173 male and 157 female patients (male/female ratio 1.1/1). EBER-1 was detected in 24 (7.3%) cases (male/female ratio: 1.2/1). The mean age for the entire group was 58.1 years (range: 20-88 years), whereas the mean age for patients harboring EBER-1-positive gastric carcinomas was 65.3 years (range: 50-84 years). Age and histological type showed statistically significant differences, when EBER-1-positive and -negative gastric carcinomas were compared. EBER-1 was detected in hyperplastic- and dysplastic-gastric mucosa surrounding two EBER-1-negative carcinomas, respectively.

CONCLUSION: Among Latin-American countries, Mexico has the lowest frequency of EBVaGC. Indeed, the Mexican population >50 years of age was selectively affected. Ethnic variations are responsible for the epidemiologic behavior of EBVaGC among the worldwide population.

Key words: Epstein-Barr virus; Stomach; Lymphoepithelioma-like carcinoma; Gastric carcinoma; EBV-A; EBER-1; LMP-1

Herrera-Goepfert R, Akiba S, Koriyama C, Ding S, Reyes E, Itoh T, Minakami Y, Eizuru Y. Epstein-Barr virus-associated gastric carcinoma: Evidence of age-dependence among a Mexican population. *World J Gastroenterol* 2005; 11(39): 6096-6103
http://www.wjgnet.com/1007-9327/11/6096.asp

INTRODUCTION

Gastric cancer (GC) is the second leading cause among cancer deaths in the world[1] and is one of the most frequent malignant neoplasms in Mexico[2]. Although the etiology of gastric carcinoma is now accepted as multifactorial, infectious agents play a central role in the mechanism of neoplastic transformation. The bacterium *Helicobacter pylori* (*H pylori*) has been implicated in a high percentage of gastric adenocarcinomas[3], in intestinal- as well as diffuse-type adenocarcinomas, according to the Lauren histoepidemiologic classification[4]. Another infectious agent, Epstein-Barr virus (EBV) or gamma type 4 herpes virus, has also been proved to be associated with gastric carcinoma in approximately 10% of cases[5]. This association has been reported in intestinal- and diffuse-type adenocarcinomas, as well as in nearly 100% of cases labeled lymphoid stroma-rich, lymphoepithelioma-like (LEL) carcinomas. The etiological role of EBV in GC development has been suspected on the basis of the uniform expression of Epstein-Barr nuclear antigen (EBNA)-1 protein, and EBV-encoded small non-polyadenylated RNA (EBER)-1 in all GC cells, the episomal monoclonality of the EBV genome, the elevated serum antibodies against EBV-related antigens among EBV-GC patients, and the unique 'lace pattern' morphology in some

early-stage EBV-GCs.

EBV-associated gastric carcinoma (EBVaGC) accounts for 1.7-16% of gastric carcinomas throughout the world, excluding LEL carcinomas[6]. The lowest frequency has been recorded in the UK, whereas the highest was in the USA. The definitive explanation for this figure remains unclear, but is probably related with genetic variations among different populations, as well as cultural and environmental influences among different geographic regions. Among Latin Americans, Mexican individuals are less likely to develop GC in association with EBV infection; in a previous study, we reported a prevalence of 8.15%[7]. In these series, diffuse-type EBV-GCs were seen exclusively, and EBER-1 was demonstrated in 100% of LEL carcinomas. In the present study, we expanded the number of cases under scrutiny and provided evidence that the risk for EBVaGC was significantly increased among patients >50 years of age in Mexico.

MATERIALS AND METHODS

Patient population

We retrieved cases of gastric adenocarcinoma from the files of the Departments of Pathology at the Instituto Nacional de Cancerología (1983-2000) and the Instituto Nacional de la Nutrición (1980-1995) in Mexico City. The results of a partial analysis of 135 cases were published previously elsewhere[7]. Eligible cases were included whenever they possessed complete demographic and pathologic information, as well as paraffin blocks with appropriate and well-preserved neoplastic tissue for molecular analysis. The age and gender of patients, and anatomic site, histological type, and depth of invasion of gastric carcinomas were obtained from records at the corresponding Department of Pathology.

Pathologic features

The anatomic site of gastric neoplasia was identified as upper (proximal) third, middle third, or lower (distal) third[8]. On the basis of predominant histological pattern, carcinomas were classified as intestinal- or diffuse-type according to the Lauren criteria[4] and subclassified as proposed by the Japanese Research Society for Gastric Cancer as follows[9]: intestinal types tub1 (well-differentiated adenocarcinoma with distinct glandular pattern and columnar epithelium throughout, moderate or small amount of stroma); tub2 (moderately differentiated adenocarcinoma with small or incomplete tubular structures with cubical or flat epithelium, amount of stroma variable from case to case), and muc (mucinous carcinoma); diffuse types, including por1 (poorly differentiated adenocarcinoma with solid, sheet-like proliferation with an alveolar pattern and indistinct tubular differentiation), por2 (poorly differentiated adenocarcinoma with acinar and trabecular pattern, usually showing diffuse infiltration with abundant fibrous stroma), and sig (signet-ring cell carcinoma). A special category, LEL carcinoma, similar to por1 adenocarcinoma but with dense lymphoid infiltrate exceeding total mass of carcinoma cells, was included. The depth of invasion was specified as mucosa; submucosa; or muscularis propria, subserosa, or serosa.

In situ hybridization

Molecular analysis was conducted as previously described[10]. Briefly, we retrieved one representative formalin-fixed, paraffin-embedded tissue sample from each carcinoma containing the neighboring non-neoplastic gastric mucosa. Two slides with 5 μm sections were prepared from each paraffin block. A set of slides were conventionally stained with hematoxylin and eosin, whereas the remainder were enhanced for EBER-1 *in situ* hybridization. The remaining paraffin-block sections were deparaffinized, rehydrated, predigested with pronase, prehybridized, and hybridized overnight at 37 ℃ with a concentration of 0.5 ng of digoxigenin-labeled probe. After sections were washed with 0.5×saline sodium citrate, hybridization was detected by anti-digoxigenin, antibody-alkaline phosphatase conjugate. Sections from a patient with known EBV-positive gastric carcinoma were used for a positive control, and sense probe to EBER-1 was used for a negative control for each procedure.

EBV genotyping

Preparation of DNA Each formalin-fixed and paraffin-embedded specimen was cut into 10-μm-thick slices, and a DNA sample was prepared following the method reported previously[11]. Each deparaffinized sample was treated with proteinase K (200 μg/mL) at 37 ℃ overnight followed by phenol/chloroform extraction and ethanol precipitation. Finally, the extracted DNA sample was dissolved in 50 μL of TE buffer.

Genotype-specific primer sets and probes Four different regions, the EBNA-3C, *Bam*HI-F, *Bam*HI-I, and *Xho*I sites in LMP-1, were used to determine viral genotypes. Types A and B can be determined by using the EBNA-2, -3A, -3B, or -3C gene[12-14]. In the present study, we chose EBNA-3C for genotyping because we experienced a higher detection rate of the primer set than those of the EBNA-2 region found in previous studies[15,16]. Types A and B, identified by PCR amplification of EBNA-3C region, corresponded to a 153- and a 246-bp band, respectively, and were confirmed by Southern blot hybridization with type-specific internal probes [14]. Wild-type F and f variant were identified by the presence of a 186-bp fragment in amplification of the *Bam*HI F region; after *Bam*HI cleavage, a 186-bp fragment could be identified in the case of wild-type F, and a 127-bp fragment could be identified in the case of the f variant. Wild-type F and f variants were confirmed by Southern blot hybridization with the internal probe as described previously[15].

For the *Bam*HI-I region, a 205-bp fragment was amplified by using primer sets as described previously[17], and types C and D were distinguished after cleavage by *Bam*HI-restriction enzyme. Type C had a 205-bp fragment, and type D had cleaved fragments with 130 and 75 bp. Types C and D were also confirmed by Southern blot hybridization with a cloned *Bam*HI-I DNA fragment probe.

To detect the *Xho*I polymorphism in exon 1 of the LMP-1 gene, we amplified a 497-bp DNA fragment with a primer set as previously described[18]. When two fragments, 340- and 157-bp long, were observed after *Xho*I digestion of the PCR product, the case was considered to contain the *Xho*I cleavage site. The 497-bp fragment of the PCR product of the B95-8 cell line was used as a probe to confirm the *Xho*I

cleavage site of LMP-1 by Southern blot hybridization[19].

PCR and Southern blot hybridization The PCR template contained the appropriate primer pair (1 μmol/L each), deoxyribonucleotide triphosphates (200 μmol/L each), and *Taq* polymerase (Takara Shuzo, Kyoto, Japan) in a total of 100 μL of PCR buffer. PCR products or PCR products digested with *Bam*HI and *Xho*I were confirmed by electrophoresis in 2% agarose gel and by staining with 0.5 μg/mL of ethidium bromide. Then, electrophoretic pattern was photographed under ultraviolet light. Electrophoretic DNA was transferred onto a Hybond N^+ nylon membrane (Amersham Pharmacia Biotech, UK) by capillary blotting using 0.4 N NaOH solution. Membranes were prehybridized with hybridization buffer for 0.5-1 h at 42 ℃. After the probe was added, hybridization was carried out overnight at 42 ℃. Probes of types A and B, and *Bam*HI-F were labeled with Dig oligonucleotide 3'-end labeling kit and detected using a Dig luminescent detection kit (Boehringer Mannheim, Germany). For detecting the *Bam*HI-I fragment and *Xho*I polymorphism in LMP-1, hybridization was carried out using the ECL direct labeling and detection kit (Amersham Pharmacia Biotech, UK) according to the manufacturer's instructions.

Statistical analysis

Odds ratios (ORs) and 95% confidence intervals (95%CIs) were obtained from logistic regression analysis, making comparisons between EBER-1-positive and EBER-1-negative gastric carcinomas with regard to age, gender, decade, anatomic site, histologic type, and depth of invasion.

RESULTS

Patient characteristics

We studied 330 consecutive, non-selected cases of gastrectomies due to primary gastric carcinoma. Among the 330 cases, there were 173 male and 157 female patients. The mean age was 58.1 years (range: 20-88 years) for all the patients, 59.9 years (range: 22-88 years) for male patients, and 56.1 years (range 20-88 years) for female patients. EBER-1 was detected in 24 (7.3%) of the 330 cases, 13 in men (7.5%) and 11 in women (7.0%). The mean age for patients harboring EBER-1-positive gastric carcinomas was 65.3 years: male patients 66.2 years (range: 51-74 years) and female patients 64.4 years (range: 50-84 years). The male/female ratio was 1.1/1 for the entire group and 1.2/1 for those with EBER-1-positive carcinomas.

Pathologic findings

With regard to the anatomic site of the primary neoplasia, 44 (13.3%) carcinomas were localized in the upper-third, 128 (38.8%) were in the middle portion, and 156 (47.3%) were in the lower-third of the stomach. In two cases (one male and one female), the anatomic location could not be determined; the entire stomach showed neoplastic infiltration in the male patient, and information on the original location of primary neoplasia was not available in the female patient. Both cases were EBER-1-negative. The distribution of carcinomas according to anatomic site and histological type, and the anatomic site and histological type of EBER-1-positive carcinomas are shown in Tables 1 and 2, respectively. Fourteen cases corresponded to early carcinomas, and only 4 were confined to mucosa; 10 cases invaded the submucosal layer. The remaining 316 cases were advanced carcinomas affecting muscular, subserosal, and serosal layers, as well as adjacent organs. EBER-1 was positive in all LEL carcinomas, in 4 out of 141 intestinal-type adenocarcinomas and in 11 out of 180 diffuse-type adenocarcinomas. The EBER-1 *in situ* hybridization signal was uniformly distributed in the nuclei of all 24 positive cases (Figures 1-6). A characteristic

Table 1 Distribution of EBER-1-positive gastric carcinomas by anatomic site[1] and gender

	Total (EBER-1+/total) %		Males (EBER-1+/total) %		Females (EBER-1+/total) %	
Total	24/330	7.3	13/173	7.5	11/157	7.0
Upper	3/44	6.8	3/31	9.7	0/13	0
Middle	13/128	10.2	7/67	10.4	6/61	9.8
Lower	8/156	5.1	3/74	4.1	5/82	6.1

[1]In two cases, anatomic location could not be determined. All (one male and one female) were EBER-1-negative.

Table 2 Distribution of EBER-1-positive gastric carcinomas by histologic type and gender

	Total (EBER-1+/total) %		Males (EBER-1+/total) %		Females (EBER-1+/total) %	
I-type	4/141	2.8	3/87	3.5	1/54	1.9
Tub1	0/42	0	0/28	0	0/14	0
Tub2	4/80	5.0	3/47	6.4	1/33	3.0
Muc	0/19	0	0/12	0	0/7	0
D-type	20/189	10.6	10/86	11.6	10/103	9.7
Por1	8/64	12.5	3/31	9.7	5/33	15.2
Por2	2/45	4.4	2/19	10.5	0/26	0
Sig	1/71	1.4	1/32	3.1	0/39	0
LEL	9/9	100	4/4	100	5/5	100

I-type: Intestinal-type adenocarcinoma; *D-type*: Diffuse-type adenocarcinoma.

lace pattern was evident in the intramucosal component of three EBER-1-positive carcinomas, two por1 plus tub2 and one tub2 plus por1 adenocarcinomas. Twenty-two of twenty-four EBER-1-positive cases extended beyond the submucosa, whereas two carcinomas, one from a female and one from a male patient, did not exceed the submucosal layer.

There were two EBER-1-negative carcinomas accompanied by EBER-1-positive gastric lesions. The first case, a 52-year-old male patient (Figures 7 and 8), had EBER-1 expression in regenerative epithelium of gastric mucosa adjacent to an EBER-1-negative primary adenocarcinoma (por1). The second case was a 46-year-old female patient whose EBER-1-negative adenocarcinoma (por1) was in the immediate vicinity of dysplastic gastric glands with EBER-1 expression (Figures 9 and 10).

Among the demographic and pathologic variables analyzed, age and histologic type had statistically significant differences, when EBER-1-positive and EBER-1 negative gastric carcinomas were compared (Table 3). In addition, comparison among patients more or less than 60 years of age showed significant differences ($P = 0.008$).

EBV genotype

We examined the genotype of seven EBV strains detected from

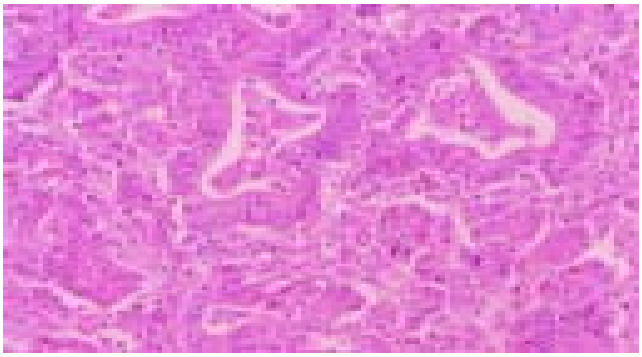

Figure 1 Moderately differentiated, intestinal-type (tub2) adenocarcinoma. Irregular neoplastic tubular structures are seen throughout the field (hematoxylin and eosin stain).

Figure 4 Same case as in Figure 3. A uniform nuclear signal of EBER-1 is seen in neoplastic cells (*in situ* hybridization).

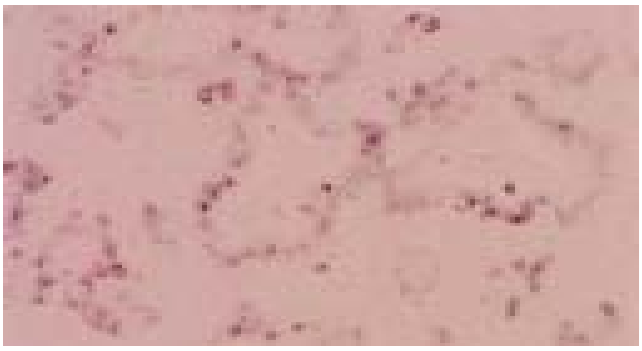

Figure 2 Same case as in Figure 1. EBER-1 nuclear positivity is limited to neoplastic cells lining the tubular structures (*in situ* hybridization).

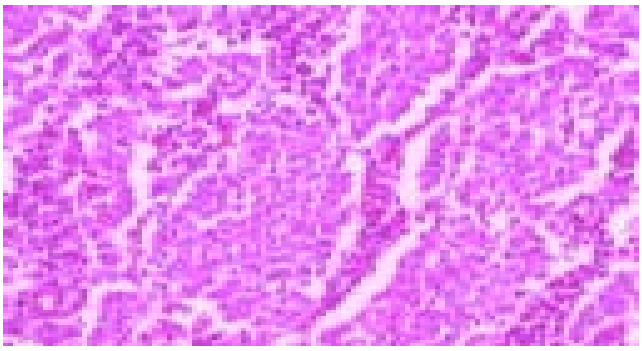

Figure 5 Poorly differentiated, LEL carcinoma. Clusters of neoplastic cells are separated by lymphoplasmacytic infiltrate.

Figure 3 Diffuse-type (por1) adenocarcinoma. Sheets of neoplastic cells are distributed in an indistinct pattern (hematoxylin and eosin stain).

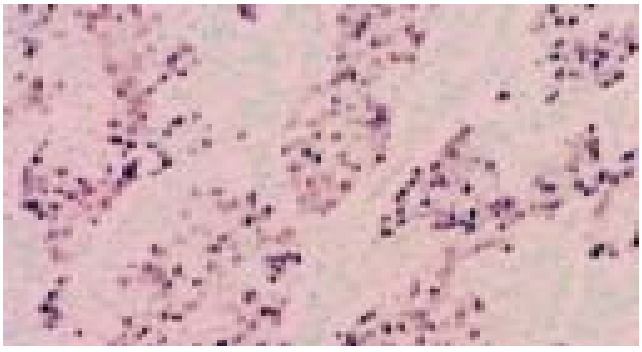

Figure 6 Same case as in Figure 5. An EBER-1-positive signal is detected in the nuclei of neoplastic cells (*in situ* hybridization).

EBER-1-positive cases; genotype could be determined in five of them. All were type A, wild-type F, and type D. In analysis of the *Xba*I cleavage site in LMP-1, we found that the cleavage site was lost in four cases and was maintained in one case.

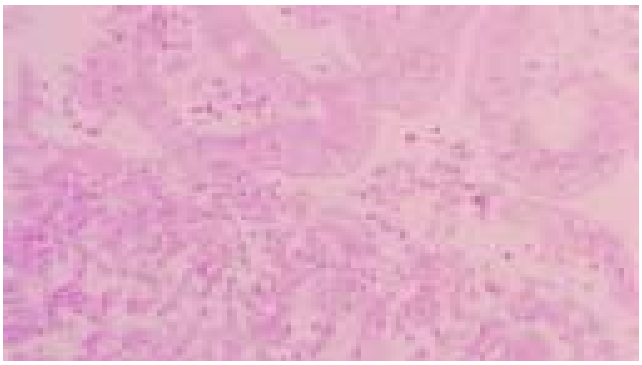

Figure 7 Lining gastric epithelium shows regenerative changes characterized by nuclear growth without atypia. There are few neoplastic cells in the underlying lamina propria (hematoxylin and eosin stain).

Figure 8 Same case as in Figure 7. The EBER-1-positive nuclear signal is restricted to regenerative epithelium. Note the EBER-1 nuclear negativity of neoplastic cells infiltrating the lamina propria (*in situ* hybridization).

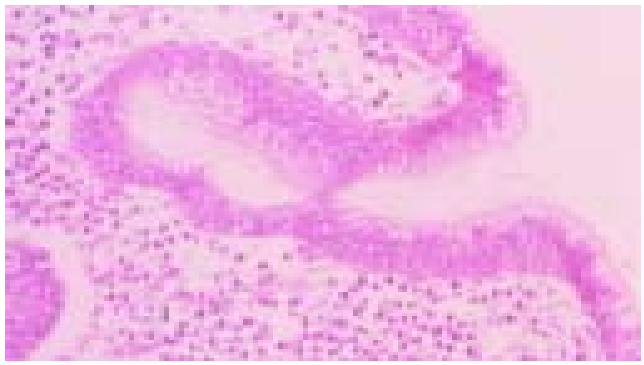

Figure 9 Lining gastric epithelium shows high-grade dysplasia, characterized by cell stratification and crowding, increased nuclear/cytoplasm ratio, nuclear atypia, and prominent eosinophilic nucleoli (hematoxylin and eosin stain).

Figure 10 Same case as in Figure 9. Dysplastic epithelium is intensely positive for the EBER-1 nuclear signal (*in situ* hybridization).

Table 3 Comparison of demographic and pathologic variables between EBER-1-positive and EBER-1-negative gastric carcinomas[1]

	EBER-1+/total	OR	95%CI	*P*
Gender				0.859
Female	11/157	1	Reference	
Male	13/173	0.9	0.4-2.2	
Age (yr)				0.013
20-49	0/87	<0.1		
50-69	14/170	0.6	0.2-1.3	
70-88	10/73	1	Reference	
Decade				0.787
1980-1989	11/130	1	Reference	
1990-2000	13/200	0.9	0.4-2.1	
Tumor site				0.229
Cardia	3/35	1.9	0.5-7.5	
Middle	13/137	2.2	0.9-5.5	
Antrum	8/156	1	Reference	
Lauren classification				0.005
Intestinal	4/141	1	Reference	
Diffuse	20/189	4.9	1.6-14.8	
Depth				0.273
Early	2/14	2.4	0.5-11.8	
Advanced	22/316	1	Reference	

[1]Odds ratios and 95% confidence intervals were obtained from logistic analysis. Age was adjusted in the analysis of variables other than age.

DISCUSSION

In this study, we found a 7.3% prevalence of EBVaGC in Mexico. In Latin America, this frequency is in contrast with that reported by Koriyama *et al*., (11.2%)[20] and Lopes *et al*., (11.3%)[21] in Brazil, Carrascal *et al*., in Colombia (13%)[22], and Corvalan *et al*., in Chile (16.8%)[23]. Excluding LEL carcinomas, the prevalence of EBVaGC in Mexico was 4.7%, whereas in Chile it was 15.8%. In a Brazilian study by Koriyama *et al*.[20], and a Colombian study by Carrascal *et al*.[22], there were no LEL carcinomas. Nonetheless, in the study by Lopes *et al*.[21], a high prevalence of LEL carcinomas (66.7%) among EBVaGC patients was found in a Brazilian population; thus, the prevalence of EBVaGC excluding LEL carcinomas is the lowest (3.8%). Conversely, the prevalence of LEL carcinoma was 7.6% in Brazil, 2.7% in Mexico, and 1.1% in Chile. The male/female ratio (1.2/1) was, as previously noted[7], the lowest among the series reported worldwide. Moreover, after excluding LEL carcinomas, Mexico remains among countries with the low prevalence of EBVaGC worldwide[6].

The frequency of EBVaGC among GC patients of Mexican ancestry in the USA ranged from 10.2%[24] to 12%[25], which is higher than the frequency (7.3%) reported by us. This peculiar migratory phenomenon has also been seen in other countries such as Japan and China. In Japan, the mean frequency of EBVaGC is 6.2%, but among patients of Japanese descent, those who are living in Hawaii, the frequency is 10.2%. In Taiwan, the frequency of EBVaGC among patients of Chinese descent is 11.2%, in comparison to 6.8% in China[26]. This figure probably indicates that besides ethnic and genetic backgrounds, environmental factors are involved in the development of EBVaGC.

A high frequency of EBVaGC at older ages is evident in our Mexican study. Not a single case of EBVaGC was observed among patients aged <50 years. This feature was previously highlighted by Gulley *et al*.[25], who examined American patients of Mexican descent in the USA and found EBVaGC cases only among those aged 56 years or older. Age dependence of EBVaGC frequency was statistically significant in their study ($P = 0.04$). The absence of EBVaGC in a set of patients of Mexican ancestry aged <56 years was also reported by Vo *et al*.[24], although the age difference they reported was not statistically significant. A similar age dependence was reported in China[26], where EBVaGC frequency was higher among those aged 60 years or older than those aged <60 years ($P = 0.03$); interestingly, the frequency of EBVaGC (7.8%) in their study is quite similar to that reported by us (7.3%).

In Brazil, Lopes *et al*.[21], also did not find any patient less than 52 years of age, although other Latin-American studies such as those of Koriyama *et al*.[20], and Corvalan *et al*.[23], did not show any age dependence, reporting EBVaGC cases in patients <50 years. Contrary to the age dependence observed in the present study, a large-scale Japanese study reported a high prevalence of EBVaGC in young men[27]. Furthermore, the same authors showed a significant decreasing trend in EBV prevalence with increasing age for males ($P = 0.04$). Carrascal *et al*.[22], also reported an age-dependent decrease of EBVaGC frequency among Colombian individuals with GC (P for trend = 0.022).

The fact that EBV-associated cancer cannot be detected in other digestive tract organs including the colon and esophagus indicates the importance of epithelial change(s) specific to the stomach[28]. EBV-latent infection products were reported to be expressed in predisposing conditions for gastric carcinoma[29,30]. Our observation showing that EBVaGC could not be found among patients <50 years of age supports the involvement of gastric-mucosal changes occurring late in human life in Mexico, as well as in Brazil and China, and relatively early in Japan and Colombia.

EBVaGC has been related to atrophic gastritis, and EBV DNA has been isolated from epithelial cells in gastric mucosa carrying chronic atrophic gastritis[29-31]. Indeed, intestinal metaplasia may enhance EBV entrance into epithelial cells via adherence of the virus to the secretory component of polymeric immunoglobulin A[32]. Our finding of two cases of EBV non-associated gastric carcinoma, one positive for EBER-1 in adjacent hyperplastic mucosa -a finding not previously described -and the other with an EBER-1-positive signal in dysplastic mucosa -a finding originally reported by Shibata and Weiss[33] -also suggests that the most plausible mechanisms for EBV entry into gastric epithelial cells are those related to previous mucosal damage and cooperation with some unknown promoter factors. In the present study, we did not observe any EBER-1 expression in normal gastric mucosa, even surrounding LEL-EBVaGC or infiltrating lymphocytes. Furthermore, we analyzed endoscopic gastric biopsies from 116 Mexican individuals >40 years of age carrying gastritis with mild atypia, and we did not find any EBER-1-positive case (unpublished data).

In addition to the age dependence of EBVaGC, the present study shows other characteristics of EBVaGC such as distal presentation among female patients and no male preponderance, altogether supporting that ethnicity and genetic backgrounds may address this particular outcome of EBV infection in the Mexican population. Among genetic backgrounds, an immunogenetic constitution may influence the outcome of EBV infection. Human leukocyte antigens (HLA) of the major histocompatibility complex have been implicated in susceptibility to develop EBV-related malignancies[34]. Very recently, we reported an association between the *HLA-DQB1**0501 allele and GC, predominantly in those labeled as diffuse-type carcinomas[35]; unfortunately, EBV status could not be assessed.

In Mexico, EBV antibody prevalence at 4-6 years of age is about 75%[36]. All EBV strains detected in EBVaGC and subjected to EBV genotyping were type A. Previous molecular studies on nasal T-lymphocyte/natural killer-cell lymphomas (nT/NKL) in Mexico[37] documented that EBV type A (EBV-1) is more frequent than EBV type B (EBV-2), as in nT/NKL and sino-nasal-B-cell lymphomas, and as in reactive tonsils from healthy individuals, thus suggesting that viral infection with EBV-1 strain is highly predominant among the Mexican population. In addition, the same authors[37] found a similar incidence of EBV LMP-1 deletions in Mexican individuals harboring nT/NKL as compared with normal subjects. Mori *et al*.[38], found no significant differences in DNA sequences of the LMP-1 region of EBV strains isolated from EBVaGC patients and throat washing samples of healthy individuals. So far no studies

have revealed differences in the genotype of EBV detected in EBVaGC *vs* that found in healthy individuals.

In conclusion, EBVaGC occurs less in Mexico than among other Latin-American populations, but it is as frequent in male as it is in female patients >50 years. In Mexican women, EBVaGC affects the middle and distal portions of the stomach but not the proximal portion. Finally, the participation of sequential steps in the mechanism of neoplastic transformation in EBVaGC, in a similar manner to the cascade of events described by Correa[39] in gastric carcinogenesis, cannot be ruled out.

REFERENCES

1 **Fuchs CS**, Mayer RJ. Gastric carcinoma. *N Engl J Med* 1995; **333**: 32–41
2 **Oñate-Ocaña LF**. Gastric Cancer in Mexico. *Gastric Cancer* 2001; **4**: 162–164
3 **Uemura N**, Okamoto S, Yamamoto S, Matsumura N, Yamaguchi S, Yamakido M, Taniyama K, Sasaki N, Schlemper RJ. *Helicobacter pylori* infection and the development of gastric cancer. *N Engl J Med* 2001; **345**: 784–789
4 **Laurén P**. The two histological main types of gastric carcinoma: diffuse and so-called intestinal type carcinoma. An attempt at a histo-clinical classification. *Acta Pathol Microbiol Scand* 1965; **64**: 31-49
5 **Takada K**. Epstein-Barr virus and gastric carcinoma. *J Clin Pathol* 2000; **53**: 255-261
6 **Burgess DE**, Woodman CB, Flavell KJ, Rowlands DC, Crocker J, Scott K, Biddulph JP, Young LS, Murray PG. Low prevalence of Epstein-Barr virus in incident gastric adenocarcinomas from the United Kingdom. *Br J Cancer* 2002; **86**: 702-704
7 **Herrera-Goepfert R**, Reyes E, Hernández-Avila M, Mohar A, Shinkura R, Fujiyama C, Akiba S, Eizuru Y, Harada Y, Tokunaga M. Epstein-Barr virus-associated gastric carcinoma in Mexico: analysis of 135 consecutive gastrectomies in two hospitals. *Mod Pathol* 1999; **12**: 873-878
8 Japanese Research Society for Gastric Cancer. Japanese Classification of Gastric Carcinoma. 1st english ed. *Tokyo Kanehara & Co Ltd* 1995: 3
9 Japanese Research Society for Gastric Cancer. Japanese Classification of Gastric Carcinoma. 1st english ed. *Tokyo Kanehara & Co Ltd* 1995: 39–43
10 **Chang KL**, Chen YY, Shibata D, Weiss LM. Description of an *in situ* hybridization methodology for detection of Epstein-Barr virus RNA in paraffin-embedded tissues, with a survey of normal and neoplastic tissues. *Diagn Mol Pathol* 1992; **1**: 246-255
11 **Greer CE**, Wheeler CM, Manos MM. PCR amplification from paraffin-embedded tissues: sample preparation and the effects of fixation In: Carl WD, and Gabriela SD, eds. PCR primer: a laboratory manual. *New York Cold Spring Harbor Laboratory Press* 1995: 99-112
12 **Adldinger HK**, Delius H, Freese UK, Clarke J, Bornkamm GW. A putative transforming gene Jijoye virus differs from that of Epstein-Barr virus prototypes. *J Virol* 1985; **14**: 221-234
13 **Rowe M**, Young L, Cadwallader K, Petti L, Kieff E, Rickinson A. Distinction between Epstein- Barr virus type-A (EBNA-2A) and type-B (EBNA-2B) isolates extends to the EBNA-3 family of nuclear proteins. *J Virol* 1989; **63**: 1031–1039
14 **Sample J**, Young L, Martin B, Chatman T, Kieff E, Rickinson A, Kieff E l. Epstein-Barr virus types 1 and 2 differ in their EBNA 3A, EBNA 3B, and ENBA 3C genes. *J Virol* 1990; **64**: 4084-4092
15 **Sidagis J**, Ueno K, Tokunaga M, Ohyama M, Eizuru Y. Molecular epidemiology of Epstein-Barr virus (EBV) in EBV-related malignancies. *Int J Cancer* 1997; **72**: 72–76
16 **Kunimoto M**, Tamura S, Tabata T, Yoshie O. One step typing of Epstein- Barr virus by polymerase chain reaction: Predominance of type 1 virus in Japan. *J Gen Virol* 1992; **73**: 455-461
17 **Lung ML**, Chang GC, Miller TR, Wara WM, Phillips TL. Genotypic analysis of Epstein-Barr virus isolates associated with nasopharyngeal carcinoma in Chinese immigrants to the United States. *Int J Cancer* 1994; **59**: 743-746
18 **Chen ML**, Tsai CN, Liang CL, Shu CH, Huang CR, Sulitzeanu D, Liu ST, Chang YS. Cloning and characterization of the latent membrane protein (LMP) of a specific Epstein-Barr virus variant derived from the nasopharyngeal carcinoma in the Taiwanese population. *Oncogene* 1992; **7**: 2131-2140
19 **Wu SJ**, Lay JD, Chen CL, Chen JY, Liu MY, Su IJ. Genomic analysis of Epstein-Barr virus in Nasal and Peripheral T-cell Lymphoma: a comparison with nasopharyngeal carcinoma in an endemic area. *J Med Virol* 1996; **50**: 314–321
20 **Koriyama C**, Akiba S, Iriya K, Yamaguti T, Hamada GS, Itoh T, Eizuru Y, Aikou T, Watanabe S, Tsugane S, Tokunaga M. Epstein-Barr virus-associated gastric carcinoma in Japanese Brazilians and non-Japanese Brazilians in Sao Paulo. *Jpn J Cancer Res* 2001; **92**: 911–917
21 **Lopes LF**, Bacchi MM, Elgui-de-Oliveira D, Zanati SG, Alvarenga M, Bacchi CE. Epstein-Barr virus infection and gastric carcinoma in Sao Paolo State, Brazil. *Braz J Med Biol Res* 2004; **37**: 1707-1712
22 **Carrascal E**, Koriyama C, Akiba S, Tamayo O, Itoh T, Eizuru Y, Garcia F, Sera M, Carrasquilla G, Piazuelo MB, Florez L, Bravo JC. Epstein-Barr virus-associated gastric carcinoma in Cali, Colombia. *Oncol Rep* 2003; **10**: 1059-1062
23 **Corvalan A**, Koriyama C, Akiba S, Eizuru Y, Backhouse C, Palma M, Argandoña J, Tokunaga M. Epstein-Barr virus in gastric carcinoma is associated with location in the cardia with a diffuse histology. A study in one area of Chile. *Int J Cancer* 2001; **94**: 527-530
24 **Vo QN**, Geradts J, Gulley ML, Boudreau DA, Bravo JC, Schneider BG. Epstein-Barr virus in gastric adenocarcinomas: association with ethnicity and CDKN2A promoter methylation. *J Clin Pathol* 2002; **55**: 669-675
25 **Gulley ML**, Pulitzer DR. Eagan PA, Schneider BG. Epstein-Barr virus infection is an early event in gastric carcinogenesis and is independent of *bcl*-2 expression and *p*53 accumulation. *Hum Pathol* 1996; **27**: 20-27
26 **Qiu K**, Tomita Y, Hashimoto M, Ohsawa M, Kawano K, Wu DM, Aozasa K. Epstein-Barr virus in gastric carcinoma in Suzhuo, China and Osaka, Japan: association with clinicopathologic factors and HLA-subtype. *Int J Cancer* 1997; **71**: 155-158
27 **Tokunaga M**, Uemura Y, Tokudome T, Ishidate T, Masuda H, Okazaki E, Kaneko K, Naoe S, Ito M, Okamura A, Shimada A, Sato E, Land CE. Epstein-Barr virus related gastric cancer in Japan: a molecular patho-epidemiological study. *Acta Pathol Japonica* 1993; **43**: 574-581
28 **Kijima Y**, Hokita S, Takao S, Baba M, Natsugoe S, Yoshinaka H, Aridome K, Otsuji T, Itoh T, Tokunaga M, Eizuru Y, Aikou T. Epstein-Barr virus involvement is mainly restricted to lymphoepithelial type of gastric carcinoma among various epithelial neoplasms. *J Med Virol* 2001; **64**: 513-518
29 **Kaizaki Y**, Sakurai S, Chong JM, Fukayama M. Atrophic gastritis, Epstein-Barr virus infection, and Epstein-Barr virus-associated gastric carcinoma. *Gastric Cancer* 1999; **2**: 101-108
30 **Yanai H**, Takada K, Shimizu N, Mizugaki Y, Tada M, Okita K. Epstein-Barr virus infection in non-carcinomatous gastric epithelium. *J Pathol* 1997; **183**: 293-298
31 **Hirano A**, Yanai H, Shimizu N, Okamoto T, Matsubara Y, Yamamoto K, Okita K. Evaluation of Epstein-Barr virus DNA load in gastric mucosa with chronic atrophic gastritis using a real-time quantitative PCR assay. *Int J Gastrointest Cancer* 2003; **34**: 87-94
32 **Sixbey JW**, Yao QY. Immunoglobulin A-induced shift of Epstein-Barr virus tissue tropism. *Science* 1992; **255**: 1578-1580

33 **Shibata D**, Weiss LM. Epstein-Barr Virus-associated Gastric Adenocarcinoma. *Am J Pathol* 1992; **140**: 769–774
34 **Koriyama C**, Shinkura R, Hamasaki Y, Fujiyoshi T, Eizuru Y, Tokunaga M. Human leukocyte antigens related to Epstein-Barr virus-associated gastric carcinoma in Japanese patients. *Eur J Cancer Prev* 2001; **10**: 69-75
35 **Herrera-Goepfert R**, Zúñiga J, Hernández-Guerrero A, Rodriguez-Reyna T, Osnaya N, Ruiz-Morales J, Vargas-Alarcón G, Yamamoto-Furusho JK, Mohar-Betancourt A, Granados J. Asociación del alelo HLA-DQB1*0501 del complejo principal de histocompatibilidad con cáncer gástrico en México. *Gac Med Mex* 2004; **140**: 299-303
36 **Niederman JC**, Evans AS. Epstein-Barr virus In: Evans AS, Kaslow RA eds. Viral Infections of Humans: Epidemiology and Control. 4th edition. *New York Plenum Medical Book Company* 1997: 253-283
37 **Elenitoba-Johnson KS**, Zarate-Osorno A, Meneses A, Krenacs L, Kingma DW, Raffeld M, Jaffe ES. Cytotoxic granular protein expression, EBV strain type and latent membrane protein-1 oncogene deletions in nasal T-lymphocyte/natural killer cell lymphomas from Mexico. *Mod Pathol* 1998; **11**: 754-761
38 **Mori S**, Itoh T, Tokunaga M, Eizuru Y. Deletions and single-base mutations within the carboxy-terminal region of the latent membrane protein 1 oncogene in Epstein-Barr virus-related gastric cancers of southern Japan. *J Med Virol* 1999; **57**: 152-158
39 **Correa P**. Human gastric carcinogenesis: A multistep and multifactorial process. First American Cancer Society Award Lecture on Cancer Epidemiology and Prevention. *Cancer Res* 1992; **52**: 6735-6740

Science Editor Guo SY **Language Editor** Elsevier HK

PO Box 2345, Beijing 100023, China
www.wjgnet.com
wjg@wjgnet.com

ELSEVIER

World J Gastroenterol 2005;11(39):6104-6109
World Journal of Gastroenterology ISSN 1007-9327

Combined TACE and PEI for palliative treatment of unresectable hepatocellular carcinoma

Gerhild Becker, Tarik Soezgen, Manfred Olschewski, Joerg Laubenberger, Hubert Erich Blum, Hans-Peter Allgaier

Gerhild Becker, Tarik Soezgen, Manfred Olschewski, Joerg Laubenberger, Hubert Erich Blum, Hans-Peter Allgaier, for the Hcc Study Group, Department of Medicine II, Department of Medical Biometry and Statistics and Department of Radiology, University Hospital Freiburg, Germany
Correspondence to: Professor. Dr. Drs. h.c. Hubert Erich Blum, Abteilung Innere Medizin II, Medizinische Universitätsklinik, Hugstetter Str. 55, D-79106 Freiburg, Germany. hubert.blum@uniklinik-freiburg.de
Telephone: +49-761-270-3403 Fax: +49-761-270-3610
Received: 2005-01-19 Accepted: 2005-05-20

Abstract

AIM: To assess whether the effectiveness of a combination of transarterial chemoembolization (TACE) and percutaneous ethanol injection (PEI) in the treatment of unresectable hepatocellular carcinoma (HCC) is superior to TACE alone a randomized controlled trial was performed.

METHODS: The effect of combination therapy on long-term survival rates and duration of hospitalization was evaluated in 52 previously untreated HCCs, randomly allocated to TACE-PEI (27 pts) or TACE alone (25 pts).

RESULTS: The cumulative survival rate of the TACE group was 75.8% at 6 mo, 62.9% at 12 mo, and 18.0% at 24 mo and of the TACE-PEI group 76.9%, 61.5%, and 38.7%, respectively. Comparison of overall survival in both groups showed no statistically significant difference. Regarding the patients with HCCs Okuda stage I (n = 26), the median survival of the TACE-PEI group was significantly longer (>24 mo, median not yet reached in the study period) compared to the TACE group (18.4 mo [range 11.6-21.7 mo]; P = 0.04). TACE-PEI reduced the relative risk for mortality to 0.4 (95%CI 0.15-0.96) compared to patients who received TACE alone. Median survival in patients with HCCs Okuda stage II or III was 5.0 mo in the TACE group (1.7 mo-not defined) compared to 10.4 mo in the TACE-PEI group.

CONCLUSION: The combination TACE-PEI improved survival time compared to TACE alone. Our study revealed a statistically significant improved survival in HCCs Okuda stage I. Side effects were minor and the combination therapy did not prolong duration of hospitalization considerably.

Key words: Hepatocellular carcinoma; Chemoembolization; Ethanol injection; Combination therapy

Becker G, Soezgen T, Olschewski M, Laubenberger J, Blum HE, Allgaier HP. Combined TACE and PEI for palliative treatment of unresectable hepatocellular carcinoma. *World J Gastroenterol* 2005; 11(39): 6104-6109
http://www.wjgnet.com/1007-9327/11/6104.asp

INTRODUCTION

Hepatocellular carcinoma (HCC) is one of the major malignancies worldwide with the highest incidence in Asia and sub-Saharan Africa[1]. Potentially curative therapeutic strategies such as orthotopic liver transplantation and hepatic resection are possible only in a minority of patients[2-7]. Due to tumor size and multicentricity, comorbidity and advanced or decompensated liver cirrhosis 70-80% of HCCs are inoperable at the time of diagnosis[8]. Because HCCs are chemo- and radio-resistant, systemic chemotherapy and radiation therapy are not options for the treatment[9]. Therefore, in most HCC patients, percutaneous ethanol injection (PEI) or thermal ablation, e.g., radiofrequency thermal ablation, and transarterial chemoembolization (TACE) are palliative treatment options[5,10-14].

Ultrasound guided PEI has been shown to be highly effective in the treatment of small HCCs[15-17]. However, PEI treatment was shown to be of limited efficacy in patients with large HCC (>5 cm) because ethanol diffusion within the tumor mass is incomplete and residual viable neoplastic tissue often persists in the periphery of the tumor lesion.

Advanced HCCs have been widely treated with TACE, using various combinations of chemotherapeutic drugs and embolic agents. The standard protocol adopted in many institutions includes repeated intra-arterial injections of a chemotherapeutic agent such as cisplatin, doxorubicin, or mitomycin C mixed with lipiodol. Lipiodol is added because of its relative selective uptake in HCCs and its antitumor effect[18]. The injection of chemotherapeutic oil emulsion is followed by embolization of feeding arteries with small gelatin-sponge particles.

A potential benefit of combining TACE with PEI in the treatment of HCC was first suggested by Tanaka *et al*.[19]. Adding PEI after TACE has been expected to achieve complete necrosis of the main tumors and to alter the texture of the tumor parenchyma, so that a large volume of ethanol can be administered to penetrate entire tumor lesions resulting in a complete necrosis[20]. In a previous study, we prospectively analyzed the clinical factors determining the prognosis of 132 inoperable HCC patients treated at our institution. Multivariate analysis revealed that patients treated with TACE-PEI had a significantly longer survival than patients treated with PEI or TACE alone[15]. These observations

prompted us to do a multicenter randomized controlled trial evaluating the effect of combination therapy with TACE-PEI *vs* TACE on long-term survival rates, duration of hospitalization and quality of life.

MATERIALS AND METHODS

Patient characteristics and study design

The study was performed as a multicenter randomized controlled trial comparing treatment with TACE and TACE-PEI. The mean 3-year-survival rate in patients treated with TACE is about 30%[18,21-24]. To demonstrate an improvement of the 3-year-survival from 30% to 40% with a statistical power of 80%, it was calculated that 308 patients in each group were needed (group 1 = TACE treatment, group 2 = treatment with TACE in combination with PEI). As a period of recruitment, 36 mo were calculated, and 24 mo were planned as follow-up period.

Participants for the trial were recruited from five centers listed in the Appendix. Patients included in the study fulfilled the following criteria: Untreated patients with HCC, confirmed histologically or diagnosed by significantly elevated α-fetoprotein (AFP) levels (>250 ng/mL) and imaging by CT, MRI, ultrasound, or angiography. No indication for surgery or any local treatment, no evidence for extrahepatic metastases, assessed by clinical and chest X-ray examinations. In patients with clinically suspected bone metastases, a bone scan was performed. There was no age limit. Exclusion criteria were: Second malignancy, any local, or systemic pretreatment, extrahepatic metastases, Child-Pugh C score, complete portal vein thrombosis (main trunk or both branches), serum creatinine >1.5 mg/dL, severe- and therapy-resistant hepatic encephalopathy, contraindications for peripheral artery catheterization. The study protocol conformed to the ethical guidelines of the 1975 Declaration of Helsinki and was approved by the ethics committee of the University Hospital Freiburg. All participants provided written informed consent. By external blockwise randomization centrally performed by fax, patients were assigned to treatment with TACE only or treatment with TACE-PEI.

Therapeutic procedures

TACE A diagnostic angiography was performed in all patients. For TACE, the tip of the catheter was placed in the left or right hepatic artery. Under fluoroscopic guidance, 5-10 mL of a solution containing 10 mg mitomycin C (Medac, Hamburg, Germany) in 10 mL iodized oil was injected into the artery feeding the lesion(s). The mitomycin/oil mixture was prepared immediately before injection by vigorous mixing for a few minutes. Embolization was performed with gelatin-sponge particles (Gelfoam; Upjohn, Kalamazoo, MI, USA). In case of unilateral portal vein thrombosis and contralateral localization of the HCC(s), chemoperfusion without embolization (TAC) of the corresponding lobe was performed. At the end of the procedure, the extent of vascular occlusion was demonstrated angiographically. The patients stayed in general, 1 d in the hospital for observation. Two weeks after TACE, a CT scan was performed. The results were interpreted as follows: (1) tumor necrosis: hypo-attenuated and contrast medium-non-enhanced lesion(s) in the early arterial phase; (2) residual tumor: contrast medium-enhanced lesion(s).

The procedure was repeated every 6-10 wk until one of the following end points was reached: (1) no viable tumor cells detectable by CT or biopsy; (2) contraindications for the procedure developed; (3) patient's death. In patients who developed thrombosis of the main portal trunk, TACE was performed only in cases of compensated cirrhosis Child-Pugh A score and adequate collateral circulation around the thrombosis (cavernous transformation with prograde intrahepatic portal perfusion on ultrasound Doppler flow examination). Patients not qualifying for TACE received best supportive care, including treatment of complications of liver cirrhosis and pain relief.

Combination of TACE-PEI Patients assigned to TACE-PEI additionally received PEI treatment for all visible lesions, 10 d after TACE. PEI was performed under real-time ultrasound guidance. A 3-MHz convex probe (Ultramark 4; ATL, Solingen, Germany) with a lateral guide attachment or a 3.5-MHz convex probe (EUB 525; Hitachi, Wiesbaden, Germany) with an incorporated guide was used. Two needle types were used: a 15-cm, 20-gauge spinal needle (Becton Dickinson, Franklin Lakes, NJ, USA) or a 20-cm, 20-gauge needle with a closed conical tip and side holes at the tip over a length of 1 or 2 cm (Pflugbeil, Ottobrunn, Germany). Ethanol (96%, 1-10 mL) was slowly injected. The PEI result was photodocumented. In general, PEI treatment involved 6-12 injections per lesion 1-6 d apart. After PEI treatment, patients regularly stayed in general 1 day in the hospital for observation. The procedure was repeated after every TACE, until one of the end points described above was reached.

Follow up

As primary end point of the study, death of any cause was chosen. Secondary end points were tumor response, quality of life, side effects, and duration of hospitalization because of treatment or side effects.

Follow-up period was 24 mo. Patients were seen on an outpatient basis 1 mo after initiation of the therapy, later on for every 3 mo. Routine follow-up included clinical examination, determination of AFP, and abdominal ultrasound. Abdominal CT or MRI was performed after 1, 3, and 6 mo, and then for every 6 mo. If HCC recurrence was suspected based on ultrasonography or AFP elevation, CT or MRI was performed earlier. Chest X-rays were done after 6, 12, and 24 mo. Quality of life evaluation (EORTC QLQ 30) was performed at inclusion in the study and then after 6, 12, and 24 mo. The therapeutic effect was assessed by CT or MRI every 3 mo according to WHO criteria[25]. A complete response was defined as disappearance of all HCC lesions documented by imaging analyses (ultrasound, CT, or MRI), and confirmation 4 or more weeks later. A partial response was defined as more than 50% reduction of the tumor size based on the measurement of the two longest perpendicular diameters of the tumor.

Statistical analyses

Study design was a multicenter randomized controlled trial to compare therapeutic effect of TACE and TACE-PEI.

Between January 1997 and August 2001, 58 patients

were recruited for the study. Recruitment was stopped after 56 mo. Follow-up period of 24 mo was planned.

Comparison between groups was made on an intention-to-treat basis. Survival time for the TACE- and TACE-PEI group was assessed by the Kaplan-Maier method and log-rank test for univariate analysis. Therapeutic effect was estimated by Cox's proportional hazards regression model for multivariate analysis. All significance tests were two-sided and $P<0.05$ was considered statistically significant. Data processing and analysis were performed using the statistical analysis system (SAS Institute, Cary, NC, USA).

RESULTS

From January 1997 to August 2001, 58 patients were enrolled in the study and were randomly assigned to TACE (n = 29) or to TACE-PEI (n = 29). Five patients were excluded because of complete portal vein thrombosis (1 patient), operability (1 patient), death (1 patient) or retraction of consent (2 patients). The remaining 53 patients (26 TACE and 27 TACE-PEI) received allocated intervention. One patient in the TACE group was lost to follow-up after moving. Thus, the data of 52 patients could be analyzed (Figure 1).

Patient characteristics showed no statistically significant differences between the two treatment groups (Table 1).

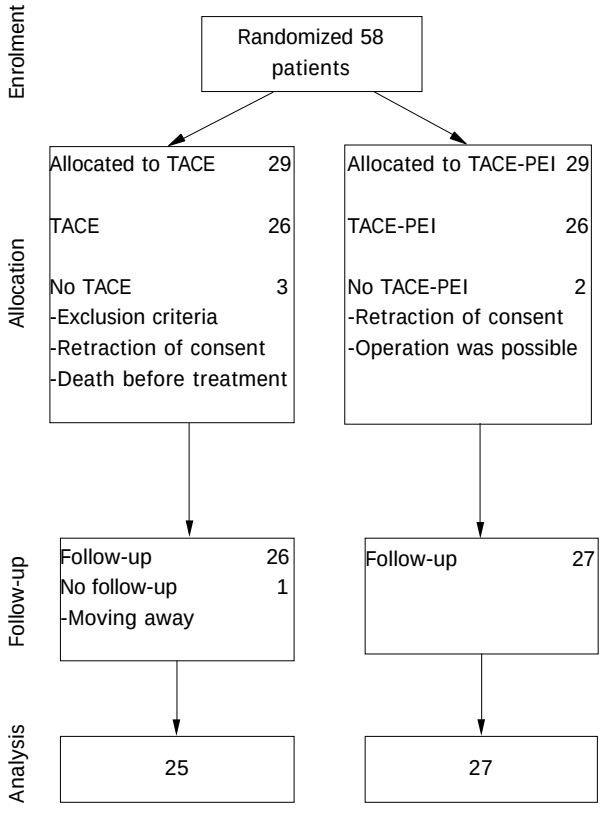

Figure 1 Flowchart of study patients.

Survival

At the time of final analysis (median follow-up time 32 mo [range 5-57 mo]), 18 patients of the TACE group and 17 patients of the TACE-PEI group had died. Median survival time was 18.4 mo (range 5.8-22.0 mo) of the TACE group as compared to 15.3 mo (range 9.2-49.0 mo) of the TACE-PEI group.

The cumulative survival rate of the TACE group was 75.8% at 6 mo, 62.9% at 12 mo and 18.0% at 24 mo and of the TACE-PEI group 76.9%, 61.5%, and 38.7%, respectively (Figure 2A). Comparison of overall survival in both groups showed no statistically significant difference.

Subgroup analysis of patients with HCC Okuda stage I (n = 26) showed a significant longer survival of the TACE-PEI group (>24 mo, median not yet reached in the study period) as compared to the TACE group (18.4 mo [range 11.6-21.7 mo]; P = 0.04; Figure 2B). TACE-PEI treatment reduced the relative risk for mortality to 0.4 (95%CI 0.15-0.96) compared to patients receiving TACE only.

Median survival of patients with HCCs Okuda stage II or III was 5.0 mo in the TACE group (1.7 mo-not defined) compared to 10.4 mo in the TACE-PEI group (Figure 2C). This difference was not statistically significant (P = 0.39).

Table 1 Patients' characteristics according to treatment

	TACE	TACE-PEI
Patients (n)	25	27
ean age yr (range)	63.6 (48-79)	64 (47-76)
M:F (%)	84:16	74.1:25.9
Cirrhosis/no cirrhosis	22/3	23/4
Etiology of cirrhosis (n/%)		
Alcohol	12 (55)	13 (57)
Hepatitis B or C	7 (32)	7 (30)
Hemochromatosis	2 (9)	1 (4)
Unknown	1 (4)	2 (9)
Liver function (n/%)		
Child Pugh A	22 (88)	17 (63)
Child Pugh B	3 (12)	10 (37)
Child Pugh C	0	0
Tumor stage (n)		
Okuda I	19	17
Okuda II	6	9
Okuda III	0	1
AFP		
<100 ng/mL	14	15
⩾100 ng/mL	11	12
Portal vein thrombosis (partial or complete)	8	6
Number of tumor lesions		
1	9	13
2	6	5
3	5	2
>3	4	5
Diffuse	0	2
Not documented	1	0
Largest diameter >5 cm (US)	17	17

Tumor response and side effects

Four patients in the TACE and five patients in the TACE-PEI group showed stable disease, respectively. The remaining 18 patients in the TACE and 20 patients in the combination group had a progressive disease, respectively (Table 2). In both groups, no major treatment-related complication occurred. The most common side effects of TACE were fever, abdominal pain, and elevation of total bilirubin levels. These side effects were transient and disappeared within a week. Side effects of PEI were spontaneously remitting mild local pain in all patients and mild transient fever in most patients.

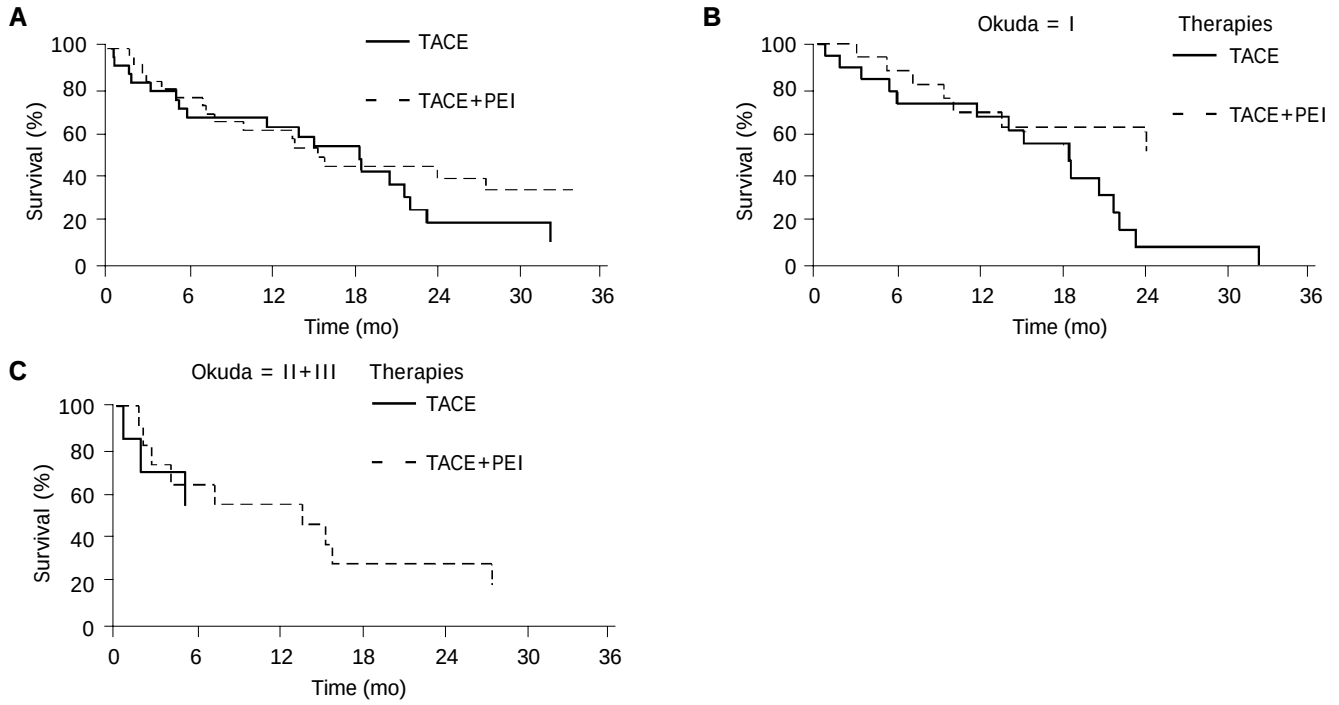

Figure 2 A: Overall survival according to treatment; B: Survival of patients with HCCs Okuda stage I according to treatment; C: Survival of patients with HCCs Okuda stage II or III according to treatment.

Table 2 Tumor response according to treatment

	TACE	TACE+PEI	*P* (χ^2-test)
Patients (*n*)	22	25	
Complete response	-	-	-
Partial response	-	-	-
Stable disease	4	5	NS
Progressive disease	18	20	NS

Duration of hospitalization

For all the 52 study patients, we recorded in-patient stays and out-patient visits during follow-up and discriminated between (1) treatment-related hospital stays/visits including adverse effects or complications and (2) hospital stays/visits because of other reasons (Table 3). As expected, patients treated with TACE-PEI had on average slightly longer hospital stays. Overall, however, there was no statistically significant difference between both treatment groups with respect to in-patient days and out-patient visits, respectively.

Table 3 Hospitalization or out-patient visits according to treatment

	TACE	TACE-PEI	*P* (Wilcoxon rank test)
IST (d)	33	44.67	0.46
OST (d)	2.72	3.07	0.75
ISO (d)	9.16	5.74	0.91

IST = average inpatient hospitalization because of treatment or complications; OST = average outpatient visits because of treatment or complications; ISO = average inpatient hospitalization for other reasons.

Quality of life

To evaluate quality of life, we used a validated self-rating questionnaire (EORTC QLQ 30). According to the design of the study, patients were expected to complete the questionnaire at enrolment into the study and at mo 6, 12, and 24. Unfortunately, only 17 completely filled out questionnaires were obtained. Most patients suffered from poor and worsening physical condition, including hepatic encephalopathy, so that only a minority of patients was able to complete the self-rating questionnaire. Therefore, we could not statistically analyze quality of life.

DISCUSSION

In a previous study, we prospectively analyzed the clinical factors determining the prognosis of 132 patients with inoperable HCCs who were treated with TACE, PEI, the combination of both, or best supportive care[15]. Multivariate analysis revealed that patients treated with a combination of TACE and PEI had a significantly better survival than patients receiving either PEI or TACE only. These observations prompted us to undertake a multicenter randomized controlled trial evaluating the effect of combination therapy with TACE-PEI on long-term survival.

The purpose of the combination is to overcome the shortcomings of both therapies and to get improved therapeutic results by combined effects. TACE is one of the most common therapies in patients with unresectable HCC. This regional therapy combines targeted chemotherapy and arterial embolization in order to induce both selective ischemic and chemotherapeutic effects on HCC. Although survival benefit has been reported after TACE[5], it is difficult to achieve complete necrosis of the target tumor by TACE alone, because HCC often has intercapsular or extracapsular invasion and viable tumor cells remain after TACE[26]. PEI is also widely used and is an effective means of treating

Table 4 Patients' characteristics and survival according to treatment

	Becker *et al.*,	Kamada [26]	Bartolozzi [27]	Tanaka [28]	Koda [29]	Yamamoto [20]
Number of patients						
	52	69	53	43	36	100
Cause of cirrhosis						
Hepatitis:alcohol	14:25	65	5:48	No data	No data	100
1-yr survival in % of patients						
TACE+PEI	62	90	100	100	100[1]	95
TACE	63	86	92.6	68	75[1]	92.5
2-yr survival in % of patients						
TACE+PEI	39	3-yr:65	86.7	85	82[2]	72.5
TACE	18	3-yr:44	69.7	37	50[2]	57.5
P	NS (0.371)	NS	NS	<0.001	<0.05	<0.05

[1]Observation period only 10 mo. [2]Observation period only 20 mo.

unresectable HCC. The method is effective in cases of capsular invasion. The injection of absolute alcohol causes cellular dehydration, coagulation necrosis, and vascular thrombosis within the treated tumor[27]. But several factors limit the therapeutic effect of PEI, such as tumor consistency, intratumoral septa, tumoral capsule, and tumor vascularization[28]. The rationale for combination of TACE and PEI relies on the fact that after TACE tumor consistency is markedly decreased and intratumoral septa are usually disrupted providing enhanced ethanol diffusion within the tumor. Therefore, combined therapy with TACE-PEI has been expected to improve survival rates of patients with advanced HCC.

In our randomized controlled multicenter trial comparing TACE and TACE-PEI, we observed no difference in overall survival. However, subgroup analysis based on HCC Okuda stage revealed that TACE-PEI results in statistically significant improved survival in patients with HCC Okuda stage I.

Similar to our findings, a recently published retrospective analysis based on medical records showed that patients receiving TACE alone had a median survival rate of 16 mo, whereas the median survival rate in patients receiving TACE followed by PEI was 24 mo[29].

The prospective randomized trials by Kamada *et al.*[30], and by Bartolozzi *et al.*[31], also showed improved survival for patients treated with TACE-PEI compared to TACE alone. Because of the small number of patients included in these studies, the difference did not reach statistical significance. Further, Tanaka *et al.*[32], Koda *et al.*[33], and Yamamoto *et al.*[20], showed a significant improved survival for patients treated with TACE-PEI as compared to TACE alone (Table 4).

Even though these studies included patients with Child-Pugh C score liver cirrhosis[20,32,33], mean survival time in our study, which excluded Child-Pugh C score patients, was shorter. This may be due to the following facts: (1) We only excluded patients with complete portal vein thrombosis (main trunk or both branches) whereas others excluded patients with any evidence of (partial) thrombosis[30-33]; that is predicting poor survival[15,20]. (2) Liver disease in our study was caused in about 50% by alcohol, whereas in all other studies most patients had chronic hepatitis B or C (Table 4). Our findings, therefore, may suggest that combination therapy with TACE-PEI may be less effective in patients with alcohol-induced than in patients with HBV- or HCV-induced cirrhosis. (3) Tanaka *et al.*[32], Koda *et al.*[33], and Yamamoto *et al.*[20], used doxorubicin, whereas in our study mitomycin C was used. Advantages for anthracyclin-based regimes were advocated in one randomized controlled trial[34], but a recently published meta-analysis showed no good evidence for best chemotherapeutic agent[5].

The primary end point of our study was survival time. Secondary end point was the duration of hospitalization and/or the number of out-patient visits. As expected, patients treated with TACE-PEI had on average slightly longer hospital stays than patients with TACE only. There was no statistically significant difference between both treatment groups, however. This aspect is important not only with respect to financial costs, but also with respect to patient's quality of life.

In conclusion, the combination of TACE-PEI compared with TACE alone prolongs survival in patients at Okuda stage I. Side effects were mild and combined therapy with TACE-PEI did not prolong duration of hospitalization or the number of out-patient visits considerably.

REFERENCES

1 **Wanebo HJ**, Falkson G, Order SE. Cancer of the hepatobiliary system. In: Devita VT Jr, Hellman S and Rosenberg SA (Eds.): Cancer Principles and Practice of Oncology *(*3rd ed.), *Philadelphia Lippincott* 1989: 836-874

2 **Andriulli A**, de Sio I, Solmi L, de Carlis L, Troisi R, Grasso A, Festa V, Caturelli E, Giacomoni A, de Veccio Blanco C, de Hemptinne B, Burroughs A, Perri F. Survival of Cirrhotic Patients With Early Hepatocellular Carcinoma Treated by Percutaneous Ethanol Injection or Liver Transplantation. *Liver Transplantation* 2004; **10**: 1355-1363

3 **Bruix J**. Treatment of hepatocellular carcinoma. *Hepatology* 1997; **25**: 259-262

4 **Kulik** L, Abecassis M. Living Donor Liver Transplantation for Hepatocellular Carcinoma. *Gastroenterology* 2004; **127**: S277-S282

5 **Llovet JM**, Burroughs A, Bruix J. Hepatocellular carcinoma. *Lancet* 2003; **362**: 1907-1917

6 **Schafer DF**, Sorrell MF. Hepatocellular carcinoma. *Lancet* 1999; **353**: 1253-1257

7 **Wiesner RH**, Freeman RB, Mulligan DC. Liver Transplantation for hepatocellular carcinoma: the impact of the meld allocation policy. *Gastroenterology* 2004; **127**: S261-S267

8 **Llovet JM**, Real MI, Montana X, Planas R, Coll S, Aponte J, Ayuso C, Sala M, Muchart J, Sola R, Rodes J, Bruix J. Arterial embolisation or chemoembolisation versus symptomatic treatment in patients with unresectable hepatocellular

carcinoma: a randomised controlled trial. *Lancet* 2002; **359**: 1734-1739
9 **Trevisani F**, De Notariis S, Rossi C, Bernardi M. Randomized control Trials on Chemoembolization for Hepatocellular Carcinoma. *J Clin Gastroenterol* 2001; **32**: 383-389
10 **Bruix J**, Sala M, Llovet JM. Chemoembolization for Hepatocellular Carcinoma. *Gastroenterology* 2004; **127**: S179-S188
11 **Llovet JM**, Bustamante J, Castells A, Villana R, Ayuso Mdel C, Sala M, Bru C, Rodes J, Bruix J. Natural history of untreated nonsurgical hepatocellular carcinoma: rationale for the design and evaluation of therapeutic trials. *Hepatology* 1999; **29**: 62-67
12 **Omata M**, Tateishi R, Haruhiko Y, Shiina S. Treatment of hepatocellular carcinoma by percutaneous tumor ablation methods: ethanol injection therapy and radiofrequency ablation. *Gastroenterology* 2004; **127**: S159-S166s•
13 **Lencioni R**, Allgaier HP, Cioni D, Olschewski M, Deibert P, Crocetti L, Frings H, Laubenberger J, Zuber I, Blum HE, Bartolozzi C. Small hepatocellular carcinoma in cirrhosis: randomized comparison of radio-frequency thermal ablation versus percutaneous ethanol injection. *Radiology* 2003; **228**: 235-240
14 **Tanaka K**, Nakamura S, Numata K, Kondo M, Morita K, Kitamura T, Saito S, Kiba T, Okazaki H, Sekihara H. The long term efficacy of combined transcatheter arterial embolization and percutaneous ethanol injection in the treatment of patients with large hepatocellular carcinoma and cirrhosis. *Cancer* 1998; **82**: 78-85
15 **Allgaier HP**, Deibert P, Olschewski M, Spamer C, Blum U, Gerok W, Blum HE. Survival benefit of patients with inoperable hepatocellular carcinoma treated by a combination of transarterial chemoembolization and percutaneous ethanol injection - a single center analysis including 132 patients. *Int J Cancer* 1998; **79**: 601-605
16 **Seki T**, Nonaka T, Kubota Y, Mizuno T, Sameshima Y. Ultrasonically guided percutaneous ethanol injection therapy for hoepatocellular carcinoma. *Am J Gastroenterol* 1989; **84**: 1400-1407
17 **Shiina S**, Tagawa K, Unuma T, Fujino H, Uta Y, Niwa Y, Hata Y, Komatsu Y, Shiratori Y, Terano A. Percutaneous ethanol injection therapy of hepatocellular carcinoma: analysis of 77 patients. *Am J Roentgenol* 1990; **155**: 1221-1226
18 **Mondazzi L**, Bottelli R, Brambilla G, Rampoldi A, Rezakovic I, Zavaglia C, Alberti A, Ideo G. Transarterial oily chemoembolization for the treatment of hepatocellular carcinoma: a multivariate analysis of prognostic factors. *Hepatology* 1994; **19**: 1115-1123
19 **Tanaka K**, Okazaki H, Nakamura S, Endo O, Inoue S, Takamura Y, Sugiyama M, Ohaki Y. Hepatocellular carcinoma: treatment with a combination therapy of transcatheter arterial embolization and percutaneous ethanol injection. *Radiology* 1991; **179**: 713-717
20 **Yamamoto K**, Masuzawa M, Kato M, Kurosawa K, Kaneko A, Ishida H, Imamura E, Park NJ, Shirai Y, Fujimoto K, Michida T, Hayashi N, Ikeda M. Evaluation of combined therapy with chemoembolization and ethanol injection for advanced hepatocellular carcinmoa. *Sem Oncol* 1997; **24**: 6 (Suppl): 50-55
21 **Bronowicki JP**, Vetter D, Dumas F, Boudjema K, Bader R, Weiss AM, Wenger JJ, Boissel P, Bigard MA, Doffoel M. Transcatheter oily chemoembolization for hepatocellular carcinoma. *Cancer* 1994; **74**: 16-24
22 **Chang JM**, Tzeng WS, Pan HB, Yang CF, Lai KH. Transcatheter arterial embolization with or without cisplatin treatment of hepatocellular carcinoma. *Cancer* 1994; **74**: 2449-2453
23 **Lencioni R**, Paolicchi A, Moretti M, Pinto F, Armillotta N, Di Giulio M, Cicorelli A, Donati F, Cioni D, Bartolozzi C. Combined transcatheter arterial chemoembolization and percutaneous ethanol injection for the treatment of large hepatocellular carcinoma: local therapeutic effect and long-term survival rate. *Eur Radiol* 1998; **8**: 439-444
24 **Stefanini GF**, Amorati P, Biselli M, Mucci F, Celi A, Arienti V, Roversi R, Rossi C, Re G, Gasbarrini G. Efficacy of transarterial targeted treatments on survival of patients with hepatocelllular carcinoma. *Cancer* 1995; **75**: 2427-2434
25 **Miller AB**, Hoogstraten B, Staquet M, Winkler A. Reporting results of cancer treatment. *Cancer* 1981; **47**: 207-214
26 **Jansen MC**, van Hillegersberg R, Chamuleau RA, van Delden OM, Gouma DJ, van Gulik TM. Outcome of regional and local ablative therapies for hepatocellular carcinoma: a collective review. *EJSO* 2005; **31**: 331-347
27 **Guan YS**, Sun L, Zhou XP, Li X, Zheng XH. Hepatocellular carcinoma treated with interventional procedures: CT and MRI follow-up. *World J Gastroenterol* 2004; **15**: 3543-3548
28 **Koda M**, Murawaki Y, Oyama K, Okamoto K, Idobe Y, Suou T, Kawasaki H. Combination therapy with transcatheter arterial chemoembolization and percutaneous ethanol injection compared with percutaneous ethanol injection alone for patients with small hepatocellular carcinoma. *Cancer* 2001; **92**: 1516-1524
29 **Greten TF**, Papendorf F, Bleck JS, Kirchhoff T, Wohlberedt T, Kubicka S, Klempnauer J, Galanski M, Manns MP. Survival rate in patients with hepatocellular carcinoma: a retrospective analysis of 389 patients. *Br J Cancer* 2005; **92**: 1862-1868
30 **Kamada K**, Kitamoto M, Aikata H, Kawakami Y, Kono H, Imamura M, Nakanishi T, Chayama K. Combination of transcatheter arterial chemoembolization using cisplatin-lipiodol suspension and percutaneous ethanol injection for treatment of advanced small hepatocellular carcinoma. *Am J Surg* 2002; **184**: 284-290
31 **Bartolozzi C**, Lencioni R, Caramella D, Vignali C, Cioni R, Mazzeo S, Carrai M, Maltinti G, Capria A, Conte PF. Treatment of large HCC: transcatheter arterial chemoembolization combined with percutaneous ethanol injection versus repeated transcatheter arterial chemoembolization. *Radiology* 1995; **197**: 812-818
32 **Tanaka K**, Nakamura S, Numata K, Okazaki H, Endo O, Inoue S, Takamura Y, Sugiyama M, Ohaki Y. Hepatocellular carcinoma: treatment with percutaneous ethanol injection and transcatheter arterial embolization. *Radiology* 1992; **185**: 457-460
33 **Koda M**, Okamoto K, Miyoshi Y, Kato S, Murawaki Y, Horie Y, Suou T, Kawasaki H. Combination therapy with transcatheter arterial embolization and percutaneous ethanol injection for advanced hepatocellular carcinoma. *Hepatogastroenterology* 1994; **41**: 25-29
34 **Kawai S**, Tani M, Okamura J, Ogawa M, Ohashi Y, Monden M, Hayashi S, Inoue J, Kawarada Y, Kusano M. Prospective and randomized clinical trial for the treatment of hepatocellular carcinoma -a comparison of L-TAE with farmorubicin and L-TAE with adriamycin (second cooperative study). *Cancer Chemother Pharmacol* 1994; **33**: S97-102

Science Editor Guo SY **Language Editor** Elsevier HK

PO Box 2345, Beijing 100023, China
www.wjgnet.com
wjg@wjgnet.com

ELSEVIER

World J Gastroenterol 2005;11(39):6110-6114
World Journal of Gastroenterology ISSN 1007-9327

Effects of adenovirus-mediated human cyclooxygenase-2 antisense RNA on the growth of hepatocellular carcinoma

Xiao-Hu Wang, Sheng-Bao Li, Qiang Tong, Guo-Jian Xie, Qing-Ming Wu

Xiao-Hu Wang, Sheng-Bao Li, Qiang Tong, Guo-Jian Xie, Qing-Ming Wu, Department of Gastroenterology, Taihe Hospital, Yunyang Medical College, Shiyan 442000, Hubei Province, China
Supported by the Bureau of Science and Technology of Shiyan City
Correspondence to: Sheng-Bao Li, Department of Gastroenterology, Taihe Hospital, Yunyang Medical College, Shiyan 442000, Hubei Province, China. libao@sycatv.net
Telephone: +86-719-8801431
Received: 2004-07-30 Accepted: 2004-12-29

Abstract

AIM: To investigate the relation between the expression of cyclooxygenase-2 (COX-2) and liver cancer, to construct the recombinant adenovirus encoding human COX-2 antisense RNA, and to explore its effects on liver cancer cell proliferation.

METHODS: We studied the expression of COX-2 in 34 cases of hepatocellular carcinoma (HCC) and SMMC7402 and SMMC7721 by immunohistochemical technique. Recombinant adenovirus Ad-AShcox-2 was constructed and transfected into human HCC cell lines SMMC7402 and SMMC7721, and its effects on COX-2 expression, cell apoptosis and cell cycle were analyzed by flow cytometry. Cell proliferation was determined by colony-forming efficiency.

RESULTS: We observed COX-2 expression in 82.4% of HCC and SMMC7402 cells, but no COX-2 expression in SMMC7721 cells. In addition, recombinant adenovirus encoding antisense COX-2 fragment Ad-AShcox-2 was obtained with the titer of 1.06×10^{12} PFU/mL. Ad-AShcox-2 could reduce the expression of COX-2 and enhance the percentage of cells in G_1/G_0 phase in SMMC7402 cell line. The difference of apoptotic index between the Ad-AShcox-2 group and control group was statistically significant ($t_{control\ group}$ = 32.62 and $t_{Ad\text{-}LacZ}$ = 10.93, $P<0.001$) in SMMC7402 but not in SMMC7721. Similarly, colony-forming rates of SMMC7402 and SMMC7721 cell lines, after the transfer of Ad-AShcox-2, were (2.7±0.94)% and (33.6±4.24)%, respectively.

CONCLUSION: Reduction in the expression of COX-2 can inhibit COX-2 expressing HCC cells.

Key words: Adenovirus; Cyclooxygenase-2; Antisense RNA; Hepatocellular carcinoma

Wang XH, Li SB, Tong Q, Xie GJ, Wu QM. Effects of adenovirus-mediated human cyclooxygenase-2 antisense RNA on the growth of hepatocellular carcinoma. *World J Gastroenterol* 2005; 11(39): 6110-6114
http://www.wjgnet.com/1007-9327/11/6110.asp

INTRODUCTION

Liver cancer is a kind of malignant tumor with a high mortality at present. Its morbidity is rather high in our country. Although a great number of researches on liver cancer as well as many achievements have been made, the exact molecular pathogenesis of liver cancer is not clear. Cyclooxygenase-2 (COX-2) has a high expression in quite a few tumors such as colorectal cancer[1,2], esophageal cancer[3], and other cancers[4]. It is likely to be related to the genesis and development of tumor, but the causing-carcinoma effect can be resisted by COX-2 selective inhibitors[5-7]. Our prophase researches showed that COX-2 antisense RNA obviously inhibits the growth of carcinoma of esophagus with a high expression of COX-2[8,9]. COX-2 is likely to become a new target of treating tumor. The present study aimed to investigate the relationship between the expression of COX-2 and liver cancer, to the construction of the recombinant adenovirus encoding human COX-2 anti-sense RNA, and to treat hepatocellular carcinoma (HCC) with or without the expression of COX-2 and to explore its mechanism.

MATERIALS AND METHODS

Intraremovelase

*Bam*HI, *Xba*I, and T_4 DNA ligase were purchased from Huamei Biological Engineering Company. RPMI 1640 and Lipofectamine were provided by GIBCO/BRL. CsCl was from Sigma Company. COX-2 cDNA and primer of adenovirus PCR were designed and synthesized by Saibaisheng Biology Company.

Plasmid, adenovirus, and cell line

Ad-LacZ was a gift from Dr. Jia-Ning Wang in our Molecular Biological Laboratory. COX-2 plasmid PCR™II vector was supplied by Dr. You-Fei Guan in Vanderbilt University, USA. pHCMVSP1A and pJM17 were donated by academician Wu Zuze in the Second Institute of Academy of Military Medical Sciences. DH_{5a} was donated by Dr. Peng Xu in Cardiology Internal Medicine Department of No. 1 Hospital Peking University. 293 cells and HCC cell lines SMMC7721 and SMMC7402 were purchased from Shanghai Cell Bank

of Chinese Academy of Medical Sciences.

Equipments

High-speed refrigerated centrifuge (Jouan, Italy), carbon dioxide incubator (Sany D, Japan), ultrahigh refrigerated centrifuge (Hitachi, Japan), inversion difference microscope (Olympus IX-To, Japan), PCR amplifier (Amplitron II, USA), flow cytometer (EPICS XL, Beckman Coulter Company, USA), ultraviolet spectrophotometer (752, Shanghai), air bath, and water bath cradle were used in our study.

Expression of COX-2 in HCC tissue

Immunohistochemical transfection was conducted by streptomy-glair-in-biotin-horseradish peroxidase (SP) compound method. The tissue was fixed with paraffin and cut into 5-μm-thick sections. HCC tissue slides were fixed in 4% PFA in PBS for 10 min, washed twice with PBS, and incubated in 3% H_2O_2 to eliminate the endogenous peroxidase activities. The tissues were then incubated either at room temperature for 1 h or at 4 ℃ overnight with 1% goat serum in PBS to block the nonspecific binding of antibodies. The slides were further incubated sequentially with rabbit anti-man COX-2 polyclonal antibody. PBS was used as a control. Color development was performed by incubation with 3,3-diaminobenzidine tetrahydrochloride in 0.03% H_2O_2 and 50 mmol/L Tris-HCl, pH 7.4. The percentage of positive tumor cells was determined semiquantitatively by assessing the whole tumor section, and each sample was assigned to one of the following categories: 0 (0-4%), 1 (5-24%), 2 (25-49%), 3 (50-74%), 4 (75-100%). Transfection strength was indicated with 0 (negative), 1 (weak positive), and 2 (positive). The expression levels were indicated with positive rate of tumor cells of one tumor tissue showing the different transfection strength. Its expression level was the transfection strength fraction by positive rate fraction. For example, if 50 tumor cells of one tumor tissue showed positive staining, we could mark 3 by 2 equaling 6; if 25 showed weak positive staining, we could mark 2 by 1 equaling 2; if 25% showed negative staining, we could mark 2 by 0 equaling 0. Thus the total was 6 plus 2 plus 0 equaling 8. The specific result statistics were carried out as previously described[10].

Construction, identification, amplification, purification, and titer assay

First, we obtained a COX-2 cDNA fragment using *Xba*I and *Bam*HI to bi-mold-cut the plasmid PCR™IICOX-2, and cloned the COX-2 cDNA fragment in the reverse direction onto two spots of *Xba*I and *Bam*HI of the pHCMUSP1A, the connection product was pAd-Ashcox-2. Then the latter was plasmid-amplified by transformed bacillus coli DH_{5a} and identified as positive plasmid by mold-cutting. The shuttle plasmid pAd-Ashcox-2 mediated Lipofectamine and pJM17 were co-transferred into 293 cells. When 293 cells had pathologic lesions and exfoliative cells made up 20%, we collected the upper clear liquid. Then we extracted viral DNA from the upper clear liquid and identified it by PCR. COX-2 primer's upstream sequences are 5'-TTG GCT TCA AGA CTG AGA TA-3' and 5'-AGC CCA AAT TAT TGG TTC-3'. Adenovirus primer's upstream sequence is 5'-TCG TTT CTC AGC AGC TGT TG-3', downstream sequence is 5'-CAT CTG AAC TCA AAG CGT GG-3'. PCR reaction system contained 10 μL viral DNA, 10 μL 20 μmol/L primer respectively (5 μL adenovirus), 5 μL 10× PCR buffer, 2 μL $MgCl_2$, 5 μL 2 mmol/L dNTP and 1 μL Taq enzyme. Water was added until the final volume of PCR reaction was 50 μL. Thirty cycles of PCR were carried out, each consisting of 30 s at 94 ℃, 30 s at 56 ℃, 1 min at 72 ℃, then a final extension at 72 ℃ for 10 min. Electrophoresis in 1.0% agarose gel was performed to amplify cDNA and adenovirus fragments as positive reconstructive cloning. Without adding mould, PCR amplification was used as a negative control. After positive reconstructive adenovirus was identified, we transferred 293 cells again. 293 cells were collected, refrigerated, melted, fragmented and ultracentrifuged twice with CsCl, viruses were collected and purified. At last the virus titer was assayed.

Efficiency of virus transfection

The recombinant adenovirus Ad-LacZ with genes encoding LacZ was used to infect liver cancer cell lines SMMC7721 and SMMC7402 according to multiplicity of infection-MOI 25, 50, 100, and 200. After 48 h, the cells were fixed and stained with X-gal. The number of cells stained blue was recorded under microscope. Then the percentage of cells with blue staining was calculated.

Transfection of recombinant adenovirus and expression of COX-2

Human liver cancer cell lines SMMC7721 and SMMC7402 were incubated in a 50 mL/L CO_2 at 37 ℃. When the density reached 40-50%, the medium was replaced by serum-free RPMI 1640 and incubated for 24 h. The experimental group infected the two cell lines with 100MOI, and was incubated for 2 h with serum. During the process, the culture fluid was shaken every 15 min. Two hours later, the medium was replaced by 10% FCS RPMI 1640. The control groups were Ad-LacZ group and non-virus group. Carcinoma cells were incubated for 24, 48, 72, 96 h respectively, fixed for 10 min in 4 ℃ cold acetone, and dried for 10 min at room temperature. Then the cells were stored at -85 ℃. The experiment was carried out with SP immunohistochemical method.

Flow cytometry

When the density of the two cell lines reached 40-50%, the medium was replaced by RPMI 1640 containing serum and incubated for 24 h. Forty-eight hours after the experimental group and control group finished virus transfection, the cells were collected (using trypsin digestion method) and centrifuged (1 000 r/min, 5 min). The upper clear fluid was discarded, PBS was added to adjust cell density to 10^6/mL. One hundred microliters of cell suspension was put into the tube, 200 μL DNA-PREP™I-PR was added to it and mixed. Two microliters DNA-PREP™ stain reagent (PI stain) was added and mixed after 30 s. After 30 min, the cell cycle and apoptosis was detected with flow cytometry (FCM).

Colony-forming experiment

The two cell lines was digested into single-cell suspension

respectively, and inoculated into a six-well board. Each well was inoculated with 500 cells. Each group had three pang-punches. After being treated with culture fluid Ad-AShcox-2, they were incubated for 10 d and fixed with 1:3 acetic acid:methanol, stained with Rui stain fluid. Then the number of colonies with more than 50 cells was recorded.

Statistical analysis

Expression level of COX-2 in liver cancer tissue was expressed as mean±SD. *t*-Test was used to show the cell apoptosis rate and cell cycle distribution rate.

RESULTS

Expression of COX-2 in liver cancer tissue

COX-2 was positive in 28 of 34 cases of liver cancers and was negative in 6 of 34 cases of liver cancer. Positive rate was 82.4%. The positive staining of COX-2 was mainly in cytoplasm. High expression of COX-2 was correlated with clinical pathological features of liver cancer (Figure 1). COX-2 expression level was high, if the cancer cells were well differentiated. COX-2 expression was not related to AFP levels, source cells and transference in liver (Table 1).

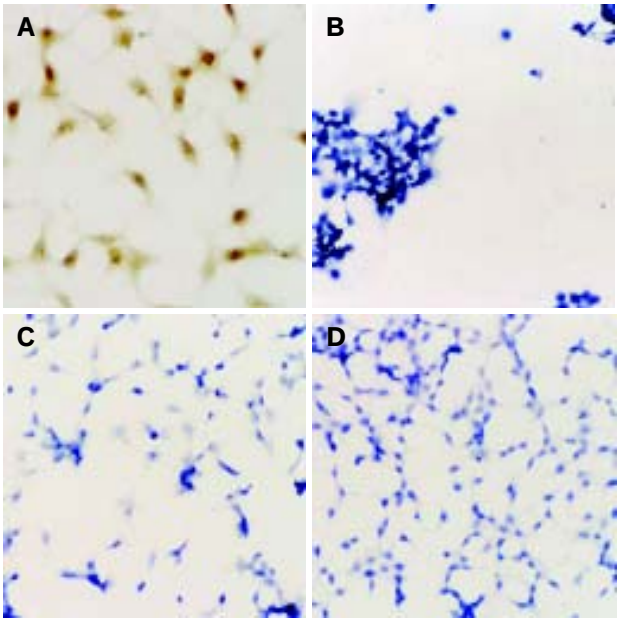

Figure 1 Expression of COX-2 in SMMC7402 and SMMC7721 before (A and B) and after (C and D) the transfer of Ad-AShcox-2.

Identification of recombinant adenovirus by PCR co-amplification method

DNA was extracted and precipitated, then PCR amplification was performed on this DNA model. The product of PCR amplification was evaluated with 0.8% agarose electrophoresis, and 277-bp COX-2 cDNA fragments and 860-bp virus gene frame fragments were obtained. After pAd-AShcox-2 and pJM17 were co-transferred to 293 cells, we produced anti-sense RNA recombinant adenovirus which could express COX-2.

Table 1 Relationship between high expression of COX-2 and clinical pathological features of liver cancer (mean±SD)

Clinical pathological features	*n*	Stain fraction	*t*	*P*
AFP (ng/mL)				
<20	4	6.48±1.46	0.74	>0.05
⩾20	24	6.36±1.15		
Cell category				
Liver cell category	27	6.79±1.60		
Bile duct cell category	1	6.26±1.25		
Transference in liver				
Yes	3	6.43±1.42	1.08	<0.05
No	25	7.15±1.80		
Pathological differentiation				
High	22	8.25±0.86	5.23	<0.05
Middle and low	6	6.11±1.02		

Titer and transfection rate of Ad-AShcox-2

After Ad-AShcox-2 was amplified, extracted, purified, and assayed with ultraviolet spectrophotometer, the virus titer was 1.06×10^{12} PFU/mL. When the MOI was 50 or greater, the transfection rate of SMMC7721 and SMMC7402 reached 100%.

Expression of COX-2 in HCC cell lines

Immunohistochemistry showed that SMMC7402 had a high expression of COX-2. But after Ad-AShcox-2 was transferred, the expression of COX-2 decreased obviously. Before and after Ad-AShcox-2 was transferred, SMMC7721 did not express COX-2 (Figures 1A-D).

Apoptosis of liver cancer cells

Forty-eight hours after SMMC7402 cells were treated with Ad-AShcox-2, FCM showed that apoptotic cells reached apoptosis peak prior to G_0/G_1 peak. The apoptosis rates of Ad-AShcox-2, Ad-LacZ, and the control group were (33.3±3.02)%, (0.42±0.14)%, and (0.25±0.08)%, respectively. The apoptosis rate of the experimental group increased obviously in comparison to the control group. However, after SMMC7721 was treated with Ad-AShcox-2, we could not detect the apoptosis peak with FCM. The apoptosis rates were (0.61±0.25)%, (0.48±0.09)%, and (0.56±0.11)%, respectively. The apoptosis rates of these two liver cancer cell lines, induced by Ad-AShcox-2, differed sharply when compared to each other (t = 32.05, P<0.001).

Effect of Ad-AShcox-2 on cell cycle

Cell cycle from FCM is listed in Table 2. After SMMC7402 cells were treated with Ad-LacZ and non-virus culture fluid, the cell proliferation rate decreased in G_0/G_1 phase, but it was high in S phase indicating that the proliferation of cells was active. After they were treated with Ad-AShcox-2, the number of cells in G_0/G_1 phase increased obviously, while in S phase, the number of cells decreased, suggesting that there was a significant difference compared to control group (P<0.05). The cells were blocked in G_1 phase. But after SMMC7721 was treated with Ad-AShcox-2, the cell proliferation rates in G_1/G_0 phase were low both in experimental group and in control group (Table 3); yet they were high in

Table 2 Cell apoptosis rate and cell cycle after SMMC7402 was treated in experimental group and control group (n = 9, mean±SD)

Groups	Apoptosis rate	Cell cycle (%)		
	(%)	G_0/G_1	S	G_2/M
Control group	0.25	40.39±3.86	49.61±4.27	13.10±1.03
Ad-LacZ	0.42	40.17±4.03	50.18±3.66	12.57±2.85
Ad-ASHcox-2	33.3	66.52±5.48	22.15±3.26	10.33±1.12

Table 3 Cell apoptosis rate and cell cycle after SMMC7721 was treated in experimental group and control group (mean±SD)

Groups	Apoptosis rate	Cell cycle (%)		
	(%)	G_0/G_1	S	G_2/M
Control group	0.56	40.39±3.86	49.61±4.27	13.10±1.03
Ad-LacZ	0.48	42.17±2.63	50.26±2.85	12.27±2.72
Ad-ASHcox-2	0.91	39.92±4.11	49.28±4.13	12.64±1.25

S phase. There was no difference (P>0.05) when compared to each other.

Effect of Ad-AShcox-2 on colony-forming ability of liver cancer cells

After Ad-AShcox-2 infected SMMC7721 and SMMC7402, the colony-forming rates were (2.7±0.94)% and (33.6±4.24)%. There were significant differences between the two groups (P<0.05, n = 6).

DISCUSSION

Cyclooxygenase is a kind of a rate-limiting enzyme, which catalyzes and synthesizes prostaglandin. It has two isomers -COX-1 and COX-2. COX-1 is constitutively expressed in most mammalian tissues and is thought to carry out "housekeeping" functions such as cytoprotection of the gastric mucosa, regulation of renal blood flow, and control of platelet aggregation. In contrast, COX-2 mRNA and protein are normally undetectable in most tissues, but can be rapidly induced by proinflammatory or mitogenic stimuli including cytokines, endotoxins, interleukins, and phorbolester. It has high expression levels in many cancer tissues. Researches showed that COX-2 can promote the formation and opening of tumor vessels[11,12], inhibit tumor immunity[13,14], stimulate transference of tumors and inhibit apoptosis[15-18].

Studies indicate that COX-2 selective inhibitor can inhibit proliferation of colon cancer cells[19,20], and induce their apoptosis[21,22]. In our prophase researches, by using the carrier of COX-2 antisense RNA adenovirus-transferred esophageal carcinoma cells, we successfully inhibited the expression of COX-2 in esophageal carcinoma cells[8,9]. The growth and proliferation of esophageal carcinoma cells were obviously inhibited, showing that reducing the expression of COX-2 or inhibiting the activity of COX-2 is likely to become a new way to treat tumors.

COX-2 is strongly positive in 28 of 34 cases of HCC. The positive rate reached 82.4%, suggesting that the high expression of COX-2 is related to the carcinogenesis and development of HCC. We also found that most HCCs with positive expression of COX-2 were well differentiated, but poorly differentiated HCC had a low expression of COX-2, indicating that COX-2 can promote the proliferation and differentiation of liver cancer cells, which is in line with the report of Koga *et al*.[23]. We can infer that HCC is related to COX-2 inhibiting cell apoptosis and increasing cytoplasmic matrix protein.

We successfully constructed the recombinant adenovirus expressing COX-2 anti-sense RNA. When the two liver cancer cells were treated with it, the expression of COX-2 decreased obviously. Meanwhile, the growth of cells was inhibited and the colony-forming rates of cells decreased apparently as well. But the colony-forming rates of SMMC7721 did not decrease, indicating that inhibiting the expression of COX-2 could inhibit the growth of liver cancer cells with positive expression of COX-2. However, cells with negative expression of COX-2 could not be inhibited. We further confirmed that the feasibility of COX-2 independent way in which NSAIDs could inhibit the colon cancer cells without the expression of COX-2[24].

After SMMC7402 was transferred in Ad-AShcox-2, the rate of cell apoptosis increased notably. There was a significant difference when control group, Ad-LacZ treatment group, and blank group were compared to each other (P<0.001), but the apoptosis rate of SMMC7721 did not increase, showing that by reducing the expression of COX-2, we can increase the apoptosis of cancer cells. This is in line with the result of a previous study[17].

Cell cycle test showed that Ad-AShcox-2 could reduce the expression of COX-2 in SMMC7402, the cell number increased evidently in G_0/G_1 phase. It could prevent cells passing from G_1 to S phase. It is likely to be linked with the expression of raised P_{27} and the inhibition of cyclin/CDK activity[25,26].

In conclusion, the adenovirus carrier with the expression of COX-2 anti-sense RNA is able to inhibit SMMC7402 and induce apoptosis.

REFERENCES

1 **Giardiello FM**, Spannhake EW, DuBois RN, Hylind LM, Robinson CR, Hubbard WC, Hamilton SR, Yang VW. Prostaglandin levels in human colorectal mucosa: effects of sulindac in patients with familial adenomatous polyposis. *Dig Dis Sci* 1998; **43**: 311-316

2 **Zhan J**, Liu JP, Zhu ZH, Yao HR, Chen CY. Relationship between COX-2 expression and clinicopathological features of colorectal cancers. *Chin Med J* 2004; **117**: 1151-1154

3 **Wu QM**, Li SB, Wang Q, Wang DH, Li XB, Liu CZ. The expression of cox-2 in esophageal carcinoma and its realation to clinicopathologic characteristic. *Shijie Huaren Xiahua Zazhi* 2001; **1**: 11-14

4 **Takahashi T**, Kozaki K, Yatabe Y, Achiwa H, Hida T. Increased expression of COX-2 in the development of human lung cancers. *J Environ Pathol Toxicol Oncol* 2002; **21**: 177-181

5 **Dang CT**, Shapiro CL, Hudis CA. Potential role of selective COX-2 inhibitors in cancer management. *Oncology* 2002; **16** (5 Suppl 4): 30-36

6 **Howe LR**, Dannenberg AJ. A role for cyclooxygenase-2 inhibitors in the prevention and treatment of cancer. *Semin Oncol* 2002; **29**(3 Suppl 11): 111-119

7 **Minter HA**, Eveson JW, Huntley S, Elder DJ, Hague A. The cyclooxygenase 2-selective inhibitor NS398 inhibits proliferation of oral carcinoma cell lines by mechanisms dependent and independent of reduces prostaglandin E2 synthesis. *Clin Cancer*

Res 2003; **9**: 1885-1897
8 **Wu QM**, Li SB, Liu CZ, Wang XH, Xie GJ, Yu JP. The effects of adenovirus-mediated human COX-2 antisense RNA on growth of esophageal carcinoma cells. *Zhongguo Zhongliu Shengwu Zhiliao Zazhi* 2001; **8**: 285-289
9 **Li SB**, Wu QM, Wang Q, Wang XH, Xie GJ. Effects of adenovirus-mediated human cox-2 antisense RNA on synthesis of DNA and proteins in esophageal carcinoma cell line. *Shijie Huaren Xiahua Zazhi* 2003; **5**: 517-521
10 **Krajewska M**, Krijewski S, Epstein JL, Shabaik A, Sauvageot J, Song K, Kitada S, Reed JC. Immunohistochemical analysis of bcl-2, bax, bcl-x and mcl-1expression in prostate cancers. *Am J Pathol* 1996; **148**: 1567-1576
11 **Leung WK**, To KF, Go MY, Chan FK, Ng EK, Chung SC, Sung JJ. Cyclooxygenase-2 upregulates vascular endothelial growth factor expression and angiogenesis in human gastric carcinoma. *Int J Oncol* 2003; **23**: 1317-1322
12 **Tsujii M**, Kawano S, Tsuji S, Sawaoka H, Hori M, DuBois RN. Cyclooxygenase regulates angiogenesis induced by colon cancer cells. *Cell* 1998; **93**: 705-716
13 **Kusumoto H**, Machara Y, Anai H, Kusumoto T, Sugimachi K. Potentiation of adriamycin cytotoxicity by dipyridamole against HeLa cells *in vitro* and sarcoma 180 cells *in vivo*. *Cancer Res* 1988; **48**: 1208-1212
14 **Kakiuchi Y**, Tsuji S, Tsujii M, Murata H, Kawai N, Yasumaru M, Kimura A, Komori M, Irie T, Miyoshi E, Sasaki Y, Hayashi N, Kawano S, Hori M. Cyclooxygenase-2 activity altered the cell surface carbohydrate antigens on colon cancer cells and enhanced liver metastasis. *Cancer Res* 2002; **62**: 1567-1572
15 **Hamasaki Y**, Kitzler J, Hardman R, Nettesheim P, Eling TE. Phorbol ester and epidermal growth factor enhance the expression of two inducible prostaglandin H synthase genes in rat tracheal epithelial cells. *Arch Biochem Bioghys* 1993; **304**: 226-234
16 **Jones DA**, Carlton DP, McIntyre TM, Zimmerman GA, Prescott SM. Molecular cloning of human prostaglandin endoperoxide synthase type II and demonstration of expression in response to cytokines. *J Biol Chem* 1993; **268**: 9049-9055
17 **Tsujii M**, DuBois RN. Alterations in cellular adhesion and apoptosis in epithelial cells overexpressing prostahlandin endoperoxide synthase 2. *Cell* 1995; **83**: 493-450
18 **Aoki T**, Tsukinoki K, Karakida K, Ota Y, Otsuru M, Kaneko A. Expression of cyclooxygenase-2, Bcl-2 and Ki-67 in pleomorphic adenoma with special reference to tumor proliferation and apoptosis. *Oral Onco* 2004; **40**: 954-959
19 **Kawamori T**, Rao CV, Seibert K, Reddy BS. Chemopreventive activity of celecoxib, a specific cyclooxygenase-2 inhibitor, against colon carcinogenesis. *Cancer Res* 1998; **58**: 409-412
20 **Minter HA**, Eveson JW, Huntley S, Elder DJ, Hague A. The cyclooxygenase 2-selective inhibitor NS398 inhibits proliferation of oral carcinoma cell lines by mechanisms dependent and independent of reduced prostaglandin E2 synthesis. *Clin Cancer Res* 2003; **9**: 1885-1897
21 **Grosch S**, Tegeder I, Niederberger E, Brautigam L, Geisslinger G. COX-2 independent induction of cell cycle arrest and apoptosis in colon cancer cells by the selective COX-2 inhibitor celecoxib. *FASEB J* 2001; **15**: 2742-2744
22 **Richter M**, Weiss M, Weinberger I, Furstenberger G, Marian B. Growth inhibition and induction of apoptosis in colorectal tumor cells by cyclooxygenase inhibitors. *Carcinogenesis* 2001; **22**: 17-25
23 **Koga H**, Sakisaka S, Ohishi M, Kawaguchi T, Taniguchi E, Sasatomi K, Harada M, Kusaba T, Tanaka M, Kimura R, Nakashima Y, Nakashima O, Kojiro M, Kurohiji T, Sata M. Expression of cyclocygenase-2 in human hepatocellular carcinoma: relevance to tumor differentiation. *Hepatology* 1999; **29**: 688-696
24 **Tsujii M**, Kawano S, DuBois RN. Cyclooxygenase-2 expression in human colon cancer cells increases metastatic potential. *Proc Natl Acad Sci USA* 1997; **94**: 3336-3340
25 **DuBois RN**, Shao J, Tsujii M, Sheng H, Beauchamp RD. G1 delay in cells overexpressing prostaglandin endoperoxide synthase-2. *Cancer Res* 1996; **56**: 733-737
26 **Hung WC**, Chang HC, Pan MR, Lee TH, Chuang LY. Induction of p27(KIP1) as a mechanism underlying NS398-induced growth inhibition in human lung cancer cells. *Mol Pharmacol* 2000; **58**: 1398-1403

Science Editor Wang XL and Zhu LH **Language Editor** Elsevier HK

PO Box 2345, Beijing 100023, China
www.wjgnet.com
wjg@wjgnet.com

ELSEVIER

World J Gastroenterol 2005;11(39):6115-6119
World Journal of Gastroenterology ISSN 1007-9327

• *LIVER CANCER* •

Usefulness of serum des-γ-carboxy prothrombin in detection of hepatocellular carcinoma

Chaur-Shine Wang, Chih-Lin Lin, Hsi-Chang Lee, Kuan-Yang Chen, Ming-Feng Chiang, Hung-Sheng Chen, Tsung-Jung Lin, Li-Ying Liao

Chaur-Shine Wang, Chih-Lin Lin, Hsi-Chang Lee, Kuan-Yang Chen, Ming-Feng Chiang, Hung-Sheng Chen, Tsung-Jung Lin, Li-Ying Liao, Department of Gastroenterology, Ren-Ai Branch, Taipei City Hospital, Taipei, Taiwan, China
Supported by the Taipei Institute of Pathology, Taipei, Taiwan and Eisai Co., Tokyo, Japan
Correspondence to: Dr. Chaur-Shine Wang, Department of Gastroenterology, Ren-Ai Branch, Taipei City Hospital, No. 10, Sec. 4, Ren-ai Road, Da-an District Taipei City 106, Taiwan, China. lcl@tpech.gov.tw
Telephone: +886-2-27093600-1157 Fax: +886-2-27047859
Received: 2005-01-24 Accepted: 2005-04-09

Abstract

AIM: To evaluate whether DCP is better than AFP for differentiating HCC from nonmalignant liver disease and further evaluate the usefulness of DCP in early diagnosis of small HCC.

METHODS: Serum DCP and AFP levels were determined in 127 patients. Among these patients, 32 were with non-cirrhotic chronic hepatitis, 34 were with compensated cirrhosis, and 61 were with HCC. The cut-off value for the DCP and AFP were set as 40 mAU/mL and 20 ng/mL, respectively. To compare the diagnostic value of DCP and AFP in distinguishing HCC from nonmalignant chronic liver disease, receiver operating characteristic (ROC) curves were constructed for each assay.

RESULTS: The accuracy, sensitivity, and specificity of DCP were higher than AFP in detecting HCC (81.9%, 77%, and 86.4% *vs* 68.5%, 59%, and 77.3%, respectively). The area under the ROC (AUROC) curves revealed that DCP had a better accuracy than AFP in diagnosis of HCC (0.85 [95%CI, 0.78-0.91] *vs* 0.73 [95%CI, 0.65-0.81], $P = 0.013$). In 39 patients with solitary HCC, the positive rates of DCP were 100% in patients with tumor size larger than 3 cm, 66.7% in patients with tumor size 2-3 cm and 50% in patients with tumor size less than 2 cm. The positive rates of AFP in patients with tumor size larger than 3 cm, 2-3 cm and less than 2 cm were 55.6%, 50%, and 33.3%, respectively. The median level of DCP in HCC patients with tumor size larger than 3 cm was significantly higher than those with tumor size 2-3 cm and those with the size of less than 2 cm.

CONCLUSION: Our study indicates that DCP has a better diagnostic value than AFP in differentiating HCC from nonmalignant chronic liver disease. DCP has not only a stronger correlation with HCC than AFP in tumor size but also more effectiveness than AFP in detecting small size of HCC.

Key words: Des-γ-carboxy prothrombin; α-Fetoprotein; Hepatocellular carcinoma

Wang CS, Lin CL, Lee HC, Chen KY, Chiang MF, Chen HS, Lin TJ, Liao LY. Usefulness of serum des-γ-carboxy prothrombin in detection of hepatocellular carcinoma. *World J Gastroenterol* 2005; 11(39): 6115-6119
http://www.wjgnet.com/1007-9327/11/6115.asp

INTRODUCTION

Hepatocellular carcinoma (HCC) is one of the most common cancers in the world[1]. The major causes of HCC are through chronic infection with HBV or hepatitis C virus (HCV)[2], cirrhosis and finally culminating into HCC[3,4]. HCC tends to occur in a definable population, so-called high risk population. Periodic screening among the high risk population would benefit in detecting HCC in an early curable stage and yield a long-term survival[5,6]. However, the worldwide 5-year survival rate of HCC only slightly increased from 2% to 5% over the past two decades[7]. This is partially due to the poor performance of currently available tumor markers, including α-fetoprotein (AFP), which cause the delay in diagnosis[8]. There is a need to develop an additional sensitive serum marker to improve the early detection of small HCC.

In 1984, Liebman *et al*., firstly reported the increasing levels of DCP in patients with HCC[9]. Since then, numerous studies indicated that DCP would be a useful marker in detecting HCC[10-14]. The conventional enzyme immunoassay (EIA) for DCP can detect advanced HCC with a high specificity. But the conventional EIA was limited in detecting small HCC[14-17]. A new method, revised EIA (Eitest PIVKA-II, Eisai, Tokyo, Japan), had been developed in recent years. The new sensitive DCP kit can measure the low concentration of serum DCP in normal persons. Thereafter, the diagnostic sensitivity of DCP for HCC had been much improved. It had been reported to be more sensitive and specific than AFP for the diagnosis of HCC[18,19]. However, the efficacy of DCP in diagnosis of small HCC still remains unclear.

Thus, we conducted a cross-sectional case control study to evaluate whether DCP is better than AFP for differentiating HCC from nonmalignant liver disease and further evaluate the usefulness of DCP in early diagnosis of small HCC.

MATERIALS AND METHODS

Patients

A total of 127 patients who were regularly followed up at Ren-Ai Branch, Taipei City Hospital were consecutively enrolled. Among the 127 patients, 32 had chronic hepatitis with higher serum alanine aminotransferase (ALT) levels than normal (upper limit of normal: 40 U/L) for at least 6 mo before enrollment, 34 had compensated cirrhosis (Child-Pugh score < 7) (20) and 61 had HCC. Cirrhosis was defined by clinical development of esophageal varices, thrombocytopenia (platelet count less than 100 000/mm^3), splenomegaly or small liver size with irregular liver surface to be noted by imaging studies at enrollment. Among all patients with chronic hepatitis and cirrhosis, HCC must be ruled out on the basis of imaging examinations including sonography and/or computed tomography (CT) performed on a regular examination. Also, cirrhotic patients who developed HCC within 6 mo after getting serum were excluded. The diagnosis of HCC was made on 47 (77%) histologically confirmed patients. The remaining 14 (23%) patients, who had advanced HCC with tumor size larger than 3 cm or patients with portal vein invasion, were confirmed by various combination of imaging studies, such as ultrasonography, enhanced CT, magnetic resonance imaging and/or angiography. Tumor size was estimated by using ultrasonography. Blood samples from HCC patients were drawn before initial treatment. The rest of the data obtained at enrollment included hepatitis B surface antigen (HBsAg), antibody to HCV (anti-HCV), ALT, albumin, total bilirubin, platelet count, prothrombin time, and serum level of tumor markers, AFP and DCP. Patients who had a history of alcohol consumption in excess of 80 g/ethanol per day for more than 5 years, serum total bilirubin level of more than 20 mg/L or under vitamin K medication were excluded. All subjects had given informed consent for the participation in the study. Serum samples were collected and stored at -70 ℃ until examined.

Biochemical and serological testing

The biochemical tests were measured by using routine automated methods. The HBsAg, anti-HCV were assayed by commercial kits (General Biological HBsAg RIA, General Biological Cooperation, Taiwan; HCV EIA II, Abbott Laboratories, North Chicago, IL, USA).

AFP assay

AFP was tested by using commercially available immunometric assay (Architect AFP assay, Abbott Laboratories, North Chicago, IL, USA). The cut-off value of AFP for HCC was set at 20 ng/mL, the most commonly set value[21-24].

DCP assay

DCP level was measured by using an ELISA (Eitest PIVKA-II, Eisai Co., Tokyo, Japan), according to the manufacturer's instructions. The detection limit is 10 mAU/mL. The cut-off value is determined as 40 mAU/mL for differentiation of HCC and nonmalignant liver disease based on previous studies[19].

Histological grading of HCC

Based on the criteria proposed by the Liver Cancer Study Group of Japan[25], each HCC was histologically graded into well differentiated, moderately differentiated, or poorly differentiated. Patients with multiple tumors consisted of more than two grades of histological differentiation; therefore, the most dedifferentiated grade was used.

Statistical analysis

Values were presented as mean ± SD and median:range. Data were analyzed by χ^2 test, Fisher's exact test, Student's *t*-test, Kruskal-Wallis ANOVA median test, and Pearson correlation where appropriate. All of the tests of significance were two-tailed and a *P* value of less than 0.05 was considered statistically significant. To compare the accuracy of DCP and AFP in the diagnosis of HCC, receiver operating characteristic (ROC) curves were constructed by using all possible cut-offs for each assay. The area under the ROC (AUROC) curves were calculated and compared by using a computer program of the MedCalc software version 7.5 (Mariakerke, Belgium).

RESULTS

Patient characteristics

Serum DCP and AFP levels were determined in 32 patients with chronic hepatitis, 34 patients with cirrhosis and 61 patients with HCC (their clinical characteristics were summarized in Table 1). The three groups were comparable in terms of gender, prevalence of HBsAg and anti-HCV. The mean age of HCC patients was significantly higher than those of chronic hepatitis patients and cirrhotic patients (63 ± 13 years *vs* 52 ± 10 years and 57 ± 12 years respectively, $P < 0.001$).

DCP and AFP in patients with chronic hepatitis, cirrhosis, and HCC

Both DCP and AFP levels increased progressively from nonmalignant chronic liver disease to HCC (Table 1). The mean values of DCP in patients with HCC was significantly higher than patients with chronic hepatitis and cirrhosis (2 808 ± 6 216 *vs* 21 ± 9 and 33 ± 14 mAU/mL, respectively, $P < 0.001$). In all, 2 of 32 (6.3%) patients with chronic hepatitis, 7 of 34 (20.6%) patients with cirrhosis, and 47 of 61 (77%) with HCC had DCP levels above the cut-off value of 40 mAU/mL.

The mean values of AFP were comparable among the three groups of patients (54 174 ± 296 329 *vs* 15 ± 24 and 13 ± 14 ng/mL, respectively $P > 0.05$). The AFP level above 20 ng/mL was found in 36 of 61 (59%) HCC, in 9 of 34 (26.5%) cirrhosis and in 6 of 32 (18.8%) chronic hepatitis patients. The overall accuracy, sensitivity, specificity, and positive and negative predictive values for the usefulness in the diagnosis of patients with HCC are shown in Table 2. ROC curves were plotted to compare the accuracy of DCP and AFP in the diagnosis of HCC, AUROC curves indicated

a better accuracy for DCP than AFP in diagnosis of HCC (0.85 [95%CI, 0.78-0.91] *vs* 0.73 [95%CI, 0.65-0.81], $P = 0.013$, Figure 1).

Relation between serum levels of AFP and DCP

Both DCP and AFP levels above cut-off value were found in 32 (52.5%) of 61 patients with HCC. Fifteen (60%) of twenty-five patients with AFP level less than 20 ng/mL had elevated concentrations of DCP. We failed to find any correlation between serum levels of AFP and DCP in 61 HCC patients (Figure 2, $r = 0.12$, $P = 0.36$).

Positive rates of DCP and AFP in patients with HCC

The positive rates of DCP and AFP in patients with HCC were detailed as follows: (1) When the largest size of HCC was more than 3 cm ($n = 22$), between 2 and 3 cm ($n = 16$) and less than 2 cm ($n = 23$), the rates were 100%, 75%, and 56.5% for DCP, 77.3%, 56.3%, and 43.5% for AFP; (2) When HCC was moderately to poorly differentiated ($n = 39$) and well differentiated ($n = 8$), the rates were 76.9% and 37.5% for DCP, 53.8% and 12.5% for AFP; (3) When the number of HCC were more than 2 ($n = 22$) and single ($n = 39$), the rates were 95.5% and 66.7% for DCP, 86.4% and 43.6% for AFP (Table 3).

The relation between the tumor size of HCC and levels of DCP and AFP were further analyzed. In the 39 patients with solitary HCC, 9 more than 3 cm, 12 between 2 and 3 cm, and 18 less than 2 cm, the positive rates were 100%, 66.7%, and 50% for DCP, 55.6%, 50%, and 33.3% for AFP respectively. DCP also had a better correlation with tumor size in comparison with AFP. The median (range) levels of DCP in patients with a size of HCC more than 3 cm was significantly higher than those with 2-3 cm and less than 2 cm [6 729 (40.4-20 000) *vs* 159 (12-655) and 89 (7-348) mAU/mL, respectively, $P = 0.01$] (Figure 3).

Table 1 Clinical characteristics of 127 patients with different stages of liver disease

	Chronic hepatitis ($n = 32$)	Cirrhosis ($n = 34$)	HCC ($n = 61$)	*P*
Age (yr/o)	52±10	57±12	63±13	<0.001[a]
Male/female	2.2	2.8	3.4	NS
Positive for HBsAg	17	18	28	NS
Positive for anti-HCV	15	13	24	NS
Positive for both HBsAg and anti-HCV	0	1	4	
Negative for both HBsAg and anti-HCV	0	2	4	
DCP level (mAu/mL), mean±SD	21±9	33±14	2 808±6 216	<0.001[a]
AFP level (ng/mL), mean±SD	15±24	13±14	54 174±296 329	NS

[a]$P<0.05$, HCC *vs* chronic hepatitis and cirrhosis. HBsAg: hepatitis B surface antigen; anti-HCV: antibody to hepatitis C virus; DCP: des-γ-carboxy prothrombin; AFP: α-fetoprotein.

Table 2 Diagnostic values of DCP and AFP for the detection of HCC

Groups	Case number	DCP		AFP		DCP/AFP	
		40 mAU/mL		20 ng/mL		DCP 40 mAU/mL or AFP 20 ng/mL	
		Positive	Negative	Positive	Negative	Positive	Negative
Nonmalignant liver disease							
Chronic hepatitis	32	2	30	6	26	8	24
Cirrhosis	34	7	27	9	25	13	21
HCC	61	47	14	36	25	51	10
Overall accuracy (%)		81.9		68.5		75.6	
Sensitivity		77.0		59.0		83.6	
Specificity		86.4		77.3		68.2	
Positive prediction rate		83.9		70.6		70.8	
Negative prediction rate		80.3		67.1		81.8	

DCP: des-γ-carboxy prothrombin; AFP: α-fetoprotein; HCC: hepatocellular carcinoma.

Table 3 Positive rates for serum concentrations of DCP and AFP in relation to largest size, histologic differentiation, and number of HCC

	Total HCC	Largest size of HCC			Histologic differentiation of HCCz		Number of HCC	
		2 cm	Between 2 and 3 cm	⩾3 cm	Well	Moderately and poorly	1	⩾2
2Case number	61	23	16	22	8	39	39	22
DCP (%)	77.0	56.5	75.0	100	37.5	76.9	66.7	95.5
AFP (%)	59.0	43.5	56.3	77.3	12.5	53.8	43.6	86.4

DCP: des-γ-carboxy prothrombin; AFP: α-fetoprotein; HCC: hepatocellular carcinoma.

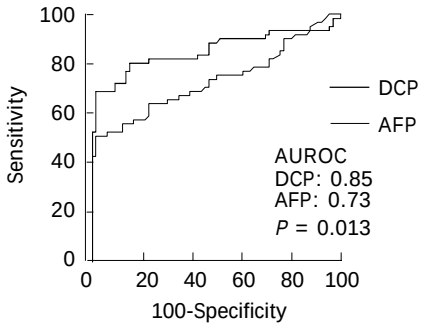

Figure 1 AUROC curves comparing DCP and AFP in patients with HCC and those with nonmalignant liver disease.

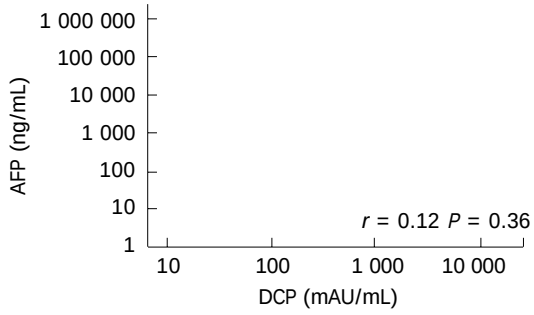

Figure 2 Relationship between DCP and AFP levels in 61 patients with HCC.

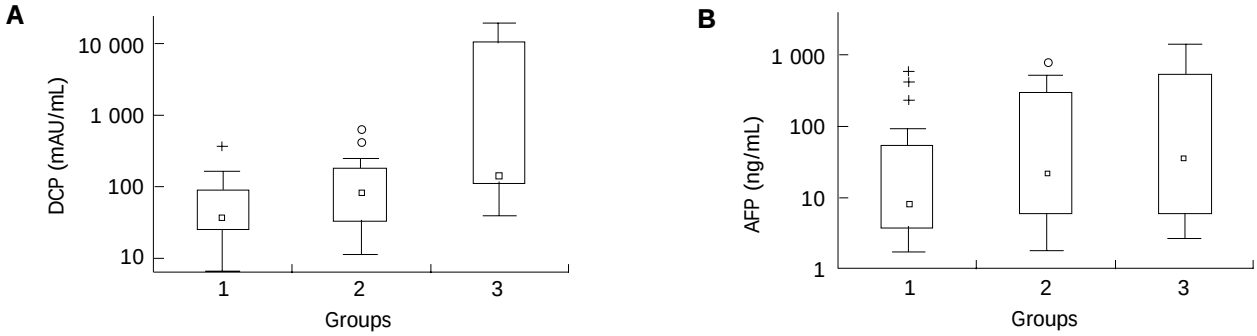

Figure 3 Box plot for DCP and AFP values in relation to size of tumor in 39 patients with solitary HCC (group 1, tumor less than 2 cm; group 2, tumor between 2 and 3 cm; and group 3, tumor more than 3 cm). The data were presented as the median and the range from the 25th-75th percentile(A and B).

DISCUSSION

Almost no symptoms would be noticed in patients with small HCC. The symptomatic HCC was usually incurable and lethal, and most previous studies reported that the median survival was only 3-6 mo after the onset of symptoms[26-28]. Early diagnosis is the most important issue in improving the long-term survival rate of HCC. Up to now, periodic screening among high risk population of HCC is the only way to detect the small HCC[5,6]. AFP is the most commonly used marker in diagnosing HCC. However, in 35-45% of HCC patients, the AFP level may be normal[21-24]; particularly in patients with small HCC[29]. On the other hand, patients with cirrhosis or chronic hepatitis, the elevated AFP level may be observed as well[30]. The dilemma is the reason why some cases of HCC could not be correctly diagnosed by AFP alone.

Based on our results, AUROC curves indicated a better accuracy for DCP than AFP in diagnosis of HCC (0.85 [95%CI, 0.78-0.91] *vs* 0.73 [95%CI, 0.65-0.81], $P = 0.013$). The cut-off value of DCP and AFP for HCC was set at 40 mAU/mL and 20 ng/mL, respectively. These values yielded a sensitivity and specificity for DCP of 77% and 86.4%, and for AFP of 59% and 77.3%, respectively. The sensitivity, specificity, and accuracy of DCP were significantly higher than APP in diagnosis of HCC (Table 2). Meanwhile, 25 of 61 (41%) patients with HCC had AFP level lower than 20 ng/mL. On the other hand, 15 of 66 (22.7%) patients with nonmalignant chronic liver disease had serum AFP level higher than 20 ng/mL. Taken together, DCP would be a better marker than AFP for HCC. Our results are also in accordance with recent studies that showed the unsatisfactory performance of AFP in diagnosis of HCC[8].

We did not find any correlation between the DCP and AFP in HCC patients (Figure 2). AFP secretion in HCC resulted from re-expression in the tumor of fetal origin[31]. DCP was produced by the malignant hepatocyte that resulted from an acquired post-translational defect in the vitamin K-dependent carboxylase system[32]. Because no correlation was observed between DCP and AFP, the simultaneous determination of both markers might be more effective in the diagnosis of HCC[33]. In our data, the increase in sensitivity from 77% to 83.6% (Table 2) in detecting HCC was found by the complementary use of the two markers.

We further analyzed 39 patients with solitary HCC in our study. We found that DCP levels had a better correlation with tumor size when compared with AFP levels (Figure 3). DCP also had a higher diagnostic sensitivity than AFP in patients with tumor size less than 2 cm in diameter. Particularly, for five patients with well-differentiated HCC less than 2 cm, the positive detection rate of DCP was 40%, which was much higher than 0% of AFP. It seems that DCP might be a better marker than AFP in detecting early-stage HCC. Because of the limited number of early-stage HCC in our report, further study is necessary to determine whether DCP plays an important role in early diagnosis of HCC.

In conclusion, our study indicates that DCP has a better diagnostic value than AFP in differentiating HCC from

nonmalignant chronic liver disease. DCP has not only a stronger correlation with HCC than AFP in tumor size but also more effectiveness than AFP in detecting small size of HCC.

REFERENCES

1 **Bosch FX,** Ribes J, Diaz M, Cleries R. Primary liver cancer: worldwide incidence and trends. *Gastroenterology* 2004; **127**: S5-16
2 **Bosch FX,** Ribes J, Borras J. Epidemiology of primary liver cancer. *Semin Liver Dis* 1999; **19**: 271-285
3 **Zaman SN,** Melia WM, Johnson RD, Portmann BC, Johnson PJ, Williams R. Risk factors in development of hepatocellular carcinoma in cirrhosis: prospective study of 613 patients. *Lancet* 1985; **1**: 1357-1360
4 **Benvegnu L,** Gios M, Boccato S, Alberti A. Natural history of compensated viral cirrhosis: a prospective study on the incidence and hierarchy of major complications. *Gut* 2004; **53**: 744-749
5 **Liaw YF,** Tai DI, Chu CM, Lin DY, Sheen IS, Chen TJ, Pao CC. Early detection of hepatocellular carcinoma in patients with chronic type B hepatitis. A prospective study. *Gastroenterology* 1986; **90**: 263-267
6 **Zhang BH,** Yang BH, Tang ZY. Randomized controlled trial of screening for hepatocellular carcinoma. *J Cancer Res Clin Oncol* 2004; **130**: 417-421
7 **El-Serag HB,** Mason AC, Key C. Trends in survival of patients with hepatocellular carcinoma between 1977 and 1996 in the United States. *Hepatology* 2001; **33**: 62-65
8 **Bruix J,** Sherman M, Llovet JM, Beaugrand M, Lencioni R, Burroughs AK, Christensen E, Pagliaro L, Colombo M, Rodes J. EASL panel of rxperts on HCC. Clinical management of hepatocellular carcinoma. Conclusions of the barcelona-2000 EASL conference. European sssociation for the dtudy of the liver. *J Hepatol* 2001; **35**: 421-430
9 **Liebman HA,** Furie BC, Tong MJ, Blanchard RA, Lo KJ, Lee SD, Coleman MS, Furie B. Des-gamma-carboxy (abnormal) prothrombin as a serum marker of primary hepatocellular carcinoma. *N Engl J Med* 1984; **310**: 1427-1431
10 **Soulier JP,** Gozin D, Lefrere JJ. A new method to assay des-gamma-carboxyprothrombin. Results obtained in 75 cases of hepatocellular carcinoma. *Gastroenterology* 1986; **91**: 1258-1262
11 **Okuda H,** Obata H, Nakanishi T, Furukawa R, Hashimoto E. Production of abnormal prothrombin (des-gamma-carboxy prothrombin) by hepatocellular carcinoma. A clinical and experimental study. *J Hepatol* 1987; **4**: 357-363
12 **Nakao A,** Suzuki Y, Isshiki K, Kimura Y, Takeda S, Kishimoto W, Nonami T, Harada A, Takagi H. Clinical evaluation of plasma abnormal prothrombin (des-gamma-carboxy prothrombin) in hepatobiliary malignancies and other diseases. *Am J Gastroenterol* 1991; **86**: 62-66
13 **Marrero JA,** Su GL, Wei W, Emick D, Conjeevaram HS, Fontana RJ, Lok AS. Des-gamma carboxyprothrombin can differentiate hepatocellular carcinoma from nonmalignant chronic liver disease in american patients. *Hepatology* 2003; **37**: 1114-1121
14 **Tsai SL,** Huang GT, Yang PM, Sheu JC, Sung JL, Chen DS. Plasma des-gamma-carboxyprothrombin in the early stage of hepatocellular carcinoma. *Hepatology* 1990; **11**: 481-488
15 **Chan CY,** Lee SD, Wu JC, Lin HC, Huang YS, Lo GH, Lee FY, Tsai YT, Lo KJ. The diagnostic value of the assay of des-gamma-carboxy prothrombin in the detection of small hepatocellular carcinoma. *J Hepatol* 1991; **13**: 21-24
16 **Kuromatsu R,** Tanaka M, Shimauchi Y, Shimada M, Tanikawa K, Watanabe K, Yokoo T. Usefulness of ED036 kit for measuring serum PIVKA-II levels in small hepatocellular carcinoma. *J Gastroenterol* 1997; **32**: 507-512
17 **Nomura F,** Ishijima M, Kuwa K, Tanaka N, Nakai T, Ohnishi K. Serum des-gamma-carboxy prothrombin levels determined by a new generation of sensitive immunoassays in patients with small-sized hepatocellular carcinoma. *Am J Gastroenterol* 1999; **94**: 650-654
18 **Mita Y,** Aoyagi Y, Yanagi M, Suda T, Suzuki Y, Asakura H. The usefulness of determining des-gamma-carboxy prothrombin by sensitive enzyme immunoassay in the early diagnosis of patients with hepatocellular carcinoma. *Cancer* 1998; **82**: 1643-1648
19 **Okuda H,** Nakanishi T, Takatsu K, Saito A, Hayashi N, Watanabe K. Measurement of serum levels of des-gcarboxy prothrombin in patients with hepatocellular carcinoma by a revised enzyme immunoassay kit with increased sensitivity. *Cancer* 1999; **85**: 812-818
20 **Pugh RNH,** Muray-Lyon IM, Dawson JL. Transection of the esophagus in the bleeding esophageal varices. *Br J Surg* 1973; **60**: 648-652
21 **Cedrone A,** Covino M, Caturelli E, Pompili M, Lorenzelli G, Villani MR. Utility of alpha-fetoprotein (AFP) in the screening of patients with virus-related chronic liver disease: does different viral etiology influence AFP levels in HCC? A study in 350 western patients. *Hepatogastroenterology* 2000; **47**: 1654-1658
22 **Nguyen MH,** Garcia RT, Simpson PW, Wright TL, Keeffe EB. Racial differences in effectiveness of alpha-fetoprotein for diagnosis of hepatocellular carcinoma in hepatitis C virus cirrhosis. *Hepatology* 2002; **36**: 410-417
23 **Peng YC,** Chan CS, Chen GH. The effectiveness of serum alpha-fetoprotein level in anti-HCV positive patients for screening hepatocellular carcinoma. *Hepatogastroenterology* 1999; **46**: 3208-3211
24 **Trevisani F,** D'Intino PE, Morselli-Labate AM, Mazzella G, Accogli E, Caraceni P. Serum alpha-fetoprotein for diagnosis of hepatocellular carcinoma in patients with chronic liver disease: influence of HBsAg and anti-HCV status. *J Hepatol* 2001; **34**: 570-575
25 Liver Cancer Study Group of Japan. Primary liver cancer in Japan: clinicopathologic features and results of surgical treatment. *Ann Surg* 1990; **211**: 277-287
26 **Naofumi N,** Hirofumi Y, Tadao H. The natural history of hepatocellular carcinoma: a study of 100 untreated cases. *Cancer* 1984; **54**: 1461-1465
27 **Wood WJ,** Rawlings M, Evans H, Lim CNH. Hepatocellular carcinoma: importance of histological classification as a prognostic factor. *Am J Surg* 1988; **155**: 663-666
28 **Douglas GF,** Michael HR, Abraham S, Ronald WB. Current treatment modalities for hepatocellular carcinoma. *Ann Surg* 1994; **219**: 236-247
29 **Chen DS,** Sung JL, Sheu JC, Lai MY, How SW, Hsu HC, Lee CS, Wei TC. Serum alpha-fetoprotein in the early stage of human hepatocellular carcinoma. *Gastroenterology* 1984; **86**: 1404-1409
30 **Di Bisceglie AM,** Hoofnagle JH. Elevations in serum alpha-fetoprotein levels in patients with chronic hepatitis B. *Cancer* 1989; **64**: 2117-2120
31 **Abelev GI.** Production of embryonal serum alpha-globulin by hepatomas: review of experimental and clinical data. *Cancer Res* 1968; **28**: 1344-1350
32 **Weitz IC,** Liebman HA. Des-gamma-carboxy (abnormal) prothrombin and hepatocellular carcinoma: a critical review. *Hepatology* 1993; **18**: 990-997
33 **Ishii M,** Gama H, Chida N, Ueno Y, Shinzawa H, Takagi T, Toyota T, Takahashi T, Kasukawa R. Simultaneous measurements of serum alpha-fetoprotein and protein induced by vitamin K absence for detecting hepatocellular carcinoma. South Tohoku District Study Group. *Am J Gastroenterol* 2000; **95**: 1036-1040

Science Editor Guo SY **Language Editor** Elsevier HK

PO Box 2345, Beijing 100023, China
www.wjgnet.com
wjg@wjgnet.com

ELSEVIER

World J Gastroenterol 2005;11(39):6120-6124
World Journal of Gastroenterology ISSN 1007-9327

• *COLORECTAL CANCER* •

Genetic alterations and expression of inhibitor of growth 1 in human sporadic colorectal cancer

Li-Sheng Chen, Jian-Bao Wei, Yong-Chun Zhou, Sen Zhang, Jun-Lin Liang, Yun-Fei Cao, Zong-Jiang Tang, Xiao-Long Zhang, Feng Gao

Li-Sheng Chen, Jian-Bao Wei, Yong-Chun Zhou, Sen Zhang, Jun-Lin Liang, Yun-Fei Cao, Zong-Jiang Tang, Xiao-Long Zhang, Feng Gao, Department of Coloproctological Surgery, the First Affiliated Hospital, Guangxi Medical University, Nanning 530021, Guangxi Province, China
Supported by the Guangxi Provincial Scientific Fund for the Returned Overseas Chinese Scholars, No. 0342018 and Key Research Fund from Public Health Bureau of Guangxi, No. 200206
Correspondence to: Dr. Li-Sheng Chen, Department of Coloproctological Surgery, the First Affiliated Hospital, Guangxi Medical University, Nanning 530021, Guangxi Province, China. clisheng@vip.sina.com
Telephone: +86-771-5356529 Fax: +86-771-5358968
Received: 2005-03-31 Accepted: 2005-04-18

Abstract

AIM: To explore the effect and significance of inhibitor of growth 1 (ING1) gene in carcinogenesis and progression of human sporadic colorectal cancer.

METHODS: mRNA expression, mutation, and loss of heterozygosity (LOH) of ING1 gene in 35 specimens of sporadic colorectal cancer tissues and the matched normal mucous membrane tissues were detected by semi-quantitative reverse transcriptase-polymerase chain reaction (RT-PCR), PCR-single strain conformation polymorphism (PCR-SSCP) and PCR-simple sequence length polymorphism (PCR-SSLP) using microsatellite markers, respectively.

RESULTS: The average ratios of light intensities of $p33^{ING1b}$ and $p47^{ING1a}$ mRNA expression in the cancerous tissues were significantly lower than those in normal tissues. The difference between the two mRNA splices was not significant in the matched tissues. In addition, the ratios of light intensities of $p33^{ING1b}$ and $p47^{ING1a}$ mRNA expression in the cancerous tissues of Dukes' stages C and D were significantly lower than those in cancerous tissues of Dukes' stages A and B. However, no mutation of ING1 gene was detected in all 35 cases; only 4 cases of LOH (11.4%) were found.

CONCLUSION: $p33^{ING1b}$ and $p47^{ING1a}$ mRNA expressions are closely related with the carcinogenesis and progression of human sporadic colorectal cancer. No mutation of ING1 gene is found, and there are only few LOH in sporadic colorectal cancers. These might not be the main reasons for the down regulation of ING1 expression. Its low expression may happen in transcription or post-transcription.

Key words: Colorectal cancer; Inhibitor of growth 1 (ING1); Expression; Mutation; Loss of heterozygosity

Chen LS, Wei JB, Zhou YC, Zhang S, Liang JL, Cao YF, Tang ZJ, Zhang XL, Gao F. Genetic alterations and expression of inhibitor of growth 1 in human sporadic colorectal cancer. *World J Gastroenterol* 2005; 11(39): 6120-6124
http://www.wjgnet.com/1007-9327/11/6120.asp

INTRODUCTION

A candidate tumor suppressor gene, inhibitor of growth 1 (ING1), has recently been cloned and mapped on human chromosome $13q^{33-34}$[1-3]. It has at least three exons and two introns. Its three alternative spliced transcripts encode $p47^{ING1a}$, $p33^{ING1b}$, and $p24^{ING1c}$ protein, respectively[4]. $p33^{ING1b}$ is a nuclear protein, which physically interacts with p53, and cooperates with it in many ways[2,5]. Overexpression of $p33^{ING1b}$ could efficiently block the growth of cells and induce apoptosis[6-8]. Conversely, inhibition of its expression by antisense constructs could promote cells growth and protect cells from apoptosis[7]. Downregulation of $p33^{ING1b}$ has been reported to be closely related with occurrence of various cancers, such as head and neck[4], esophageal[9], lung[10], gastric[11,12], bladder[13], ovary[14], breast[14,15], liver cell cancer[16,17], and so on. Genetic alterations, such as mutation or allelic imbalance, have been found in some cancers listed above. To the author's knowledge, only a few studies of ING1 gene on colorectal cancer have been reported as yet, and the results are different from each other[18]. Moreover, there is some lack of knowledge about $p47^{ING1a}$ expression in colorectal cancer till now. Accordingly, in order to evaluate the effect and significance of ING1 gene in carcinogenesis and progression of human sporadic colorectal cancer, we examined mRNA expression, mutation, and LOH of ING1 gene by using RT-PCR, PCR-SSCP, and PCR-RFLP.

MATERIALS AND METHODS

Patients and tissues

The tumor and matched normal mucosal tissues (at least 10 cm away from tumor margin) were obtained from 35 patients with sporadic colorectal cancer, who underwent surgical resection in our hospital, from December 2002 to March 2003. The patients consisted of 20 males and 15 females with the mean age of 59 years (range, 25-79 years). All the diagnoses were verified by pathological diagnosis.

Sixteen were colon and 19 were rectal carcinomas with Dukes' stages as follows: stage A (2 cases); stage B (15 cases); stage C (13 cases); and stage D (5 cases). All the specimens were frozen in liquid nitrogen after removal, followed by storage at -80 ℃.

RNA and DNA extraction

Total RNA and genomic DNA were isolated from the specimens using TRIzol reagent (Invitrogen, USA) and spin column genomic DNA isolation kit (BBI, Canada) according to the manufacturer's instructions. The integrity of total RNA and genomic DNA were checked on 10 g/L agarose gel.

RT-PCR

ING1 mRNA expression in tumor and matched normal tissues was examined using RT-PCR. RNase-free DNase I was used to remove DNA contamination at first. Then, cDNA was synthesized using first strand cDNA synthesis kit, following the manufacturer's instructions. At last, PCR was performed in 20 μL reaction mixtures comprising 2 μL of cDNA, 2.5 μL of 10×buffer, 1.5 μL of 2.5 mol/L deoxynucleotide triphosphate mixture (dNTP mixture), 2 U of Taq DNA polymerase (TaKaRa, Dalian, China), 0.5 μL of 10 mol/L each primer of ING1, 0.5 μL of 10 mol/L primer of GAPDH, and 12 μL of sterilized ddH_2O. Intron-spanning primers were: for $p47^{ING1a}$, 5'-CCGCATCTTT-GCTGACCCGA-3' and 5'-GCCTTCTTCTCCTTG-GGTGT-3' (444 bp); and for $p33^{ING1b}$, 5'-CTCCATCGAG-TCCCTGCCTT-3' and 5'-GCCTTCTTCTCCTTGG-GTGT-3' (480 bp). Primers for GAPDH were 5'-CGG-AGTCAACGGATTTGGTGCGTAT-3' and 5'-AGCCTT-CTCCATGGTGGYGAAGAC-3' (306 bp). The samples were amplified through 32 cycles, each amplification consisting of denaturation at 94 ℃ for 1 min, primer annealing at 62 ℃ for 1 min and extension at 72 ℃ for 1 min. Cycles were preceded by incubation at 94 ℃ for 5 min to ensure full denaturation of the target gene, followed by an extra incubation at 72 ℃ for 10 min to ensure full extension of the products. Primers for GAPDH were added to PCR tubes at the end of the 10^{th} cycle. Products of RT-PCR were electrophoresed on 20 g/L agarose gel. The light intensities of DNA bands were scanned by electrophoretic image analysis system (Bio-Rad Gel DOC 2000, USA). Reproducibility was confirmed by processing all samples at least twice.

PCR-SSCP

PCR reactions were carried out in a volume of 20 μL containing 100 ng of genomic DNA, 2.5 μL of 10× buffer, 1.5 μL of 2.5 mol/L dNTP mixture, 2 U of Taq DNA polymerase (TaKaRa, Dalian, China), 0.5 μL of 10 mol/L each primer, and 14 μL of sterilized ddH_2O. The samples were amplified through 32 cycles, each amplification consisting of denaturation at 94 ¡æ for 30 s, primer annealing at 62 ¡æ or 64 ¡æ for 30 s and extension at 72 ¡æ for 1 min. Finally, the samples underwent an extra incubation at 72 ¡æ for 10 min. The sequences of ING1 primers used for PCR-SSCP: exon 1, 5'-TGCAGTGCTATTTTT-TGAGGGG-3' and 5'-CGCCCCCGCCCATCCATCA-3' (248 bp); exon 2a, 5'-ACGCCTGTCCTTCTTGCCCC-3' and 5'-CTTGCCGCTGTTGCCCGCTG-3' (272 bp); exon 2b, 5'-TTCGAGGCGCAGCAGGAGCT-3' and 5'-CTTGGCCTTCTTCTCCTTGGG-3' (210 bp); exon 2c, 5'-TGAGCCCCACGCACGAGAAG-3' and 5'-CAGCA-ACCACGACCACGACG-3' (242 bp); exon 2d, 5'-CCTCC-CCATCGACCCCAACG-3' and 5'-ACATTTTACACT-CCTTGCACCTCA-3' (327 bp). Ten microliters of PCR products was mixed with 10 μL of loading dye (950 mL/L formamide, 20 mol/L EDTA, 0.5 g/L bromophenol blue, and 0.5 g/L xylene cyanol), heat denatured at 98 ¡æ for 10 min, chilled on ice, put onto 120 g/L polyacrylamide gel, and run at a constant rate of 12 V/cm for 10-14 h at variable temperatures. The DNA bands were detected by silver staining as previously described[19]. Reproducibility was confirmed by processing all samples at least twice.

LOH analysis

We examined genomic DNA for LOH by PCR-SSCP using five microsatellite markers (D13S158, D13S278, D13S285, D13S779, and D13S796), which are located in the ING1 locus. The primer pairs were available through the internet genome database (http://www.gdb.org). PCR was performed in 20 μL of reaction mixture comprising 100 ng of genomic DNA, 2.5 μL of 10× buffer, 1.5 μL of 2.5 mol/L dNTP mixture, 2 U of Taq DNA polymerase (TaKaRa, Dalian, China), 0.5 μL of 10 mol/L each primer, and 14 μL of sterilized ddH_2O. The samples were amplified through 32 cycles, each amplification consisting of denaturation at 62 ℃ for 30 s, primer annealing at 52 ℃ or 54 ℃ for 30 s and extension at 72 ℃ for 1 min. Finally, the samples underwent an extra incubation at 72 ℃ for 5 min. Ten microliters of PCR products was mixed with 10 μL of loading dye as described above, heat denatured for 10 min at 98 ℃, chilled on ice, put onto 120 g/L polyacrylamide gel containing 8 mol/L urea, and run at a constant rate of 25 V/cm for 3-4 h at room temperature. The DNA bands were visualized by silver staining. Reproducibility was confirmed by processing all samples at least twice. LOH was scored, if the heterozygous alleles showed at least 50% reduced intensity in tumor DNA bands as compared with the corresponding normal ones.

Statistical analysis

The SPSS 10.0 software package was used for all statistical analyses. Differences in expression of ING1 mRNA between the different groups were compared by using independent *t*-test. A *P* value less than 0.05 was considered statistically significant.

RESULTS

ING1 mRNA expression detected by RT-PCR

All the samples of tumor tissues and normal tissues showed ING1 mRNA expression. Moreover, the average ratios of light intensities of $p33^{ING1b}$ mRNA and $p47^{ING1a}$ mRNA expression in the cancerous tissues were significantly lower than those in normal tissues (0.52 *vs* 1.28, $P<0.01$; 0.51 *vs* 1.21, $P<0.01$, respectively; Figure 1); difference between the two mRNA splices was not significant in the matched tissues.

The average ratios of light intensities of $p33^{ING1b}$ mRNA and $p47^{ING1a}$ mRNA expression in the cancerous tissues of Dukes' stages C and D were significantly lower than those in cancerous tissues of Dukes' stages A and B (0.38 *vs* 0.65, $P<0.01$; 0.40 *vs* 0.63, $P<0.01$, respectively).

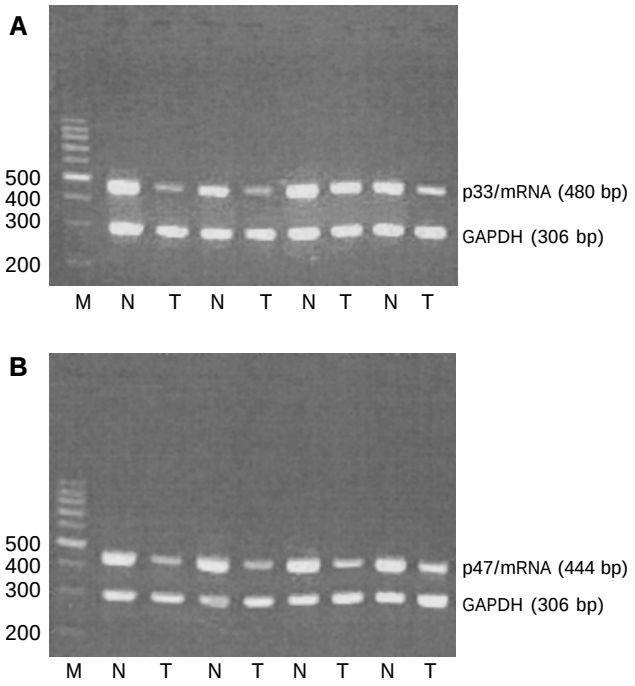

Figure 1 RT-PCR analysis of p33/ING1 and p47/ING1 mRNA expressions. N: normal tissue; T: tumor tissue (A and B).

Detection of ING1 gene mutation

To investigate whether the ING1 gene is the target of functional loss in tumors, we searched for mutation in the encoding regions of the gene in all 35 samples of colorectal cancer by using PCR-SSCP. However, no mutation was found (Figure 2).

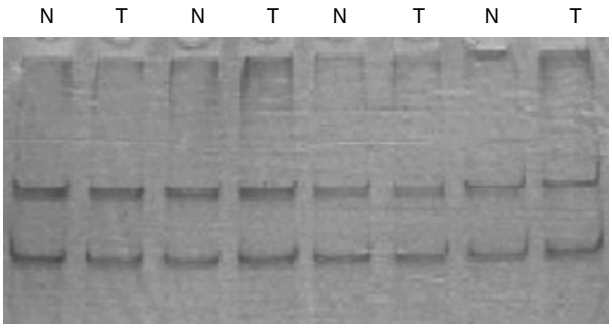

Figure 2 No mutation of ING1 gene was detected by PCR-SSCP (fragment exon 2a).

LOH analysis

To investigate whether allelic imbalance of terminal regions of chromosome 13q is reserved, we examined DNA from 35 pairs of matched tumor tissues and normal tissues for losses at five microsatellite markers (D13S158, D13S278, D13S285, D13S779, and D13S796). But only four cases of LOH (11.4%) were observed, two in D13S158, one in D13S278 and one in D13S285 (Figure 3).

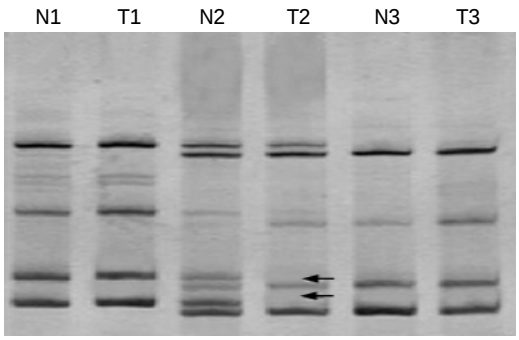

Figure 3 Electrophoretic picture of LOH analysis (LOH is seen in T2).

DISCUSSION

In this study, we found downregulation of $p33^{ING1}$ mRNA, and $p47^{ING1}$ mRNA expressions in the cancerous tissues of sporadic colorectal cancer, and the later Dukes' stage they were in, the less mRNA expression they presented. Our results are consistent with the previous data on head and neck[4], esophageal[9], lung[10], gastric[11,12], breast[14,15], and liver cell[16,17] cancers, neuroblastomas[20], and astrocytoma[21], but not with the other studies on colorectal cancer[18]. The precise mechanisms of tumor suppression by $p33^{ING1}$ and $p47^{ING1}$ remain unclear. Previous several reports thought that $p33^{ING1}$ might inhibit cells growth and promote apoptosis through both p53-dependent[5,8,17,21] and -independent pathways[21-24]. One is: $p33^{ING1}$ could stabilize p53 via disrupting the regulation of p53 by MDM2[23], and promote acetylation of p53 through inhibition of hSIR2[21,24]. Another one is: $p33^{ING1}$ and $p47^{ING1}$ could directly repress transcription promoters, and upregulate $p21^{WAF1}$ promoter activity[21]. Moreover, $p33^{ING1}$ could cooperate with p53. We, therefore, think that reduced expressions of $p33^{ING1}$ and $p47^{ING1}$ may lead to decreased inhibition of cell cycle and apoptosis, and strongly associated with the carcinogenesis and progression of human sporadic colorectal cancer.

Some previous studies have reported about several mis-sense mutations and silent changes in esophageal[9], head and neck[4], esophagogastric junction[25], gastric[11], skin[26], pancreatic[27], and breast[14] cancers. These mutations were all located in PDH finger and/or nuclear localization signal in the COOH-terminal half of ING1, and might lead to loss of the functions of ING1. But the rate of mutations was rare or no mis-sense mutation was found in oral squamous cell carcinoma[28], lymphoid malignancies[29], colorectal carcinoma[18], and hematological malignancies[30]. In our study, we could not detect mis-sense mutation of ING1 gene. Although PCR-SSCP analysis was reported to be less than 100% sensitive for mutation detection, this result suggests that mutation of ING1 occur with a very

low frequency in sporadic colorectal cancer. We, hereby, propose that gene mutation is not the main reason for the downregulation of ING1 expression.

Loss of heterozygosity (LOH), i.e., loss of one allele at a constitutional heterozygous locus, indicates the probability of loss of a tumor suppressor gene, which might promote neoplastic progression and metastasis. LOH is a critical event in the development of human cancers. It is thought to have resulted from either a large deletion or recombination between homologous alleles during repair of DNA double-strand breaks. These types of genetic alterations may produce mutations in some gene mutation assay. Previous studies demonstrated that high rates of LOH were found in human chromosome $13q^{33\text{-}34}$ region[4,9,31], such as the rates in esophageal/head and neck squamous cell cancers were 58.9% (20/34) and 68% (23/34), respectively[4,9]. Because the gene encoding ING1 is located in $13q^{33\text{-}34}$ region, we detected for LOH in this region using five microsatellite markers (D13S158, D13S278, D13S285, D13S779, and D13S796), which are at different locations on chromosome $13q^{33\text{-}34}$. In our study, the rate of LOH was only 11.4% (4/35), which is obviously lower than those in the previous reports. LOH at ING1 locus and the vicinity may affect the function of ING1, but these might not be the main reason for the downregulation of ING1 expression as well.

In conclusion, downregulation of $p33^{ING1}$ and $p47^{ING1}$ mRNA expressions in human sporadic colorectal cancer is substantial, relating with the carcinogenesis and progression, but mutation and LOH of gene might not be the main reason for the downregulation of ING1 expression. The reason for loss of function of ING1 gene is very complex. We speculate that the alterations at transcriptional or post-transcriptional levels, such as acetylation, methylation, ubiquitination, or phosphorylation, might be involved in the downregulation of ING1 gene. Further studies are needed to elucidate the possibility.

REFERENCES

1 **Garkavtsev I**, Kazarov A, Gudkov A, Riabowol K. Suppression of the novel growth inhibitor p33ING1 promotes neoplastic transformation. *Nat Genet* 1996; **14**: 415-420
2 **Garkavtsev I**, Demetrick D, Riabowol K. Cellular localization and chromosome mapping of a novel candidate tumor suppressor gene (ING1). *Cytogenet Cell Genet* 1997; **76**: 176-178
3 **Zeremski M**, Horrigan SK, Grigorian IA, Westbrook CA, Gudkov AV. Localization of the candidate tumor suppressor gene ING1 to human chromosome 13q34. *Somat Cell Mol Genet* 1997; **23**: 233-236
4 **Gunduz M**, Ouchida M, Fukushima K, Hanafusa H, Etani T, Nishioka S, Nishizaki K, Shimizu K. Genomic structure of the human ING1 gene and tumor-specific mutations detected in head and neck squamous cell carcinomas. *Cancer Res* 2000; **60**: 3143-3146
5 **Garkavtsev I**, Grigorian LA, Ossovskaya VS, Chernov MV, Chumakov PM, Gudkov AV. The candidate tumor suppression p33/ING1 cooperates with p53 in cell growth control. *Nature* 1998; **391**: 295-298
6 **Garkavtsev I**, Riabowol K. Extension of the replicative life span of human diploid fibroblasts by inhibition of the p33ING1 candidate tumor suppressor. *Mol Cell Biol* 1997; **17**: 2014-2019
7 **Helbing CC**, Veillette C, Riabowol K, Johnston RN, Garkavtsev I. A novel candidate tumor suppression. ING1, is involved in the regulation of apoptosis. *Gancer Res* 1997; **57**: 1255-1258
8 **Shinoura N**, Muramatsu Y, Nishimura M, Yoshida Y, Saito A, Yokoyama T, Furukawa T, Horii A, Hashimoto M, Asai A, Kirino T, Hamada H. Adenovirus-mediated transfer of p33ING1 with p53 drastically augments apoptosis in glionas. *Cancer Res* 1999; **59**: 5521-5528
9 **Chen LS**, Matsubara N, Yoshino T, Nagasaka T, Hoshizima N, Shirakawa Y, Naomoto Y, Isozaki H, Riabowol K, Tanaka N. Genetic alterations of candidate tumor suppressor ING1 in human esophageal squamous cell cancer. *Cancer Res* 2001; **61**: 4345-4349
10 **Kameyama K**, Huang CL, Liu D, Masuya D, Masuya D, Nakashima T, Sumitomo S, Takami Y, Kinoshita M, Yokomise H. Reduced ING1b gene expression plays an important role in carcinogenesis of non-small cell lung cancer patients. *Clin Cancer Res* 2003; **9**: 4926-4934
11 **Oki E**, Maehara Y, Tokunaga E, Kakeji Y, Sugimachi K. Reduced expression of p33(ING1) and the relationship with p53 expression in human gastric cancer. *Cancer Res* 1999; **147**: 157-162
12 **Ding HZ**, Yang D, Wu FR, Li H, Feng K, Zheng SJ, Ni CR, Yu GZ. p33(ING1) gene expression and mutation in stomach cancer tissues and precarcinomatous tissues. *Zhonghua Yixue Zazhi* 2003; **83**: 320-323
13 **Sanchez-Carbayo M**, Socci ND, Lozano JJ, Li W, Charytonowicz E, Belbin TJ, Prystowsky MB, Ortiz AR, Childs G, Cordon-Cardo C. Gene discovery in bladder cancer progression using cDNA microarrays. *Am J Pathol* 2003; **163**: 505-516
14 **Toyama T**, Iwase H, Wastson P, Muzik H, Saettler E, Magliocco A, DiFrancesco L, Forsyth P, Garkavtsev I, Kobayashi S, Riabowol K. Suppression of ING1 expression in sporadic breast cancer. *Oncogene* 1999; **18**: 5187-5193
15 **Nouman GS**, Anderson JJ, Crosier S, Shrimankar J, Lunec J, Angus B. Downregulation of nuclear expression of the p33 (ING1b) inhibitor of growth protein in invasive carcinoma of the breast. *J Clin Pathol* 2003; **56**: 507-511
16 **Ohgi T**, Masaki T, Nakai S, Morishita A, Yukimasa S, Nagai M, Miyauchi Y, Funaki T, Kurokohchi K, Watanabe S, Kuriyama S. Expression of p33(ING1) in hepatocellular carcinoma: relationships to tumour differentiation and cyclin E kinase activity. *Scand J Gastroenterol* 2002; **37**: 1440-1448
17 **Zhu Z**, Zhu M, Ni C. Significance of p33(ING1b) and p53 gene expression in hepatocellular carcinoma. *Zhonghua Yizxue Zazhi* 2002; **82**: 1332-1336
18 **Sarela AI**, Farmery SM, Markham AF, Guillou PJ. The candidate tumour suppressor gene, ING1, is retained in colorectal carcinomas. *Eur J Cancer* 1999; **35**: 1264-1267
19 **Bassam BJ**, Caetano-Anolles G, Gresshoff PM. Fast and sensitive silver straining of DNA in polyacrylamide gels. *Anal Biochem* 1991; **196**: 80-83
20 **Takahashi M**, Ozaki T, Todo S, Nakagawara A. Decreased expression of the candidate tumor suppressor gene ING1 is associated with poor prognosis in advanced neuroblastomas. *Oncol Rep* 2004; **12**: 811-816
21 **Tallwn G**, Riabowol K, Wolff JE. Expression of p33ING1 mRNA and chemosensitivity in brain tumor cells. *Anticancer Res* 2003; **23**: 1631-1635
22 **Kataoka H**, Bonnefin P, Vieyra D, Feng X, Hara Y, Miura Y, Joh T, Nakabayashi H, Vaziri H, Harris CC, Riabowol K. ING1 represses transcription by direct DNA binding and through effects on p53. *Cancer Res* 2003; **63**: 5785-5792
23 **Leung KM**, Po LS, Tsang FC, Siu WY, Lau A, Ho HT, Poon RY. The candidate tumor suppressor ING1b can stabilize p53 by disrupting the regulation of p53 by MDM2. *Cancer Res* 2002; **62**: 4890-4893
24 **Vieyra D**, Loewith R, Scott M, Bonnefin P, Boisvert FM, Cheema P, Pastyryeva S, Meijer M, Johnston RN, Bazett-Jones DP, McMahon S, Cole MD, Young D, Riabowol K. Human ING1 proteins differentially regulate histone acetylation. *J Biol Chem* 2002; **277**: 29832-29839
25 **Hara Y**, Zheng Z, Evans SC, Malatjalian D, Riddell DC, Guernsey DL, Wang LD, Riabowol K, Casson AG. ING1 and p53

tumor suppressor gene alterations in adenocarcinomas of the esophagogastric junction. *Cancer Lett* 2003; **192**: 109-116

26 **Chen B**, Campos EI, Crawford R, Martinka M, Li G. Analyses of the tumour suppressor ING1 expression and gene mutation in human basal cell carcinoma. *Int J Oncol* 2003; **22**: 927-931

27 **Yu GZ**, Zhu MH, Zhu Z, Ni CR, Zheng JM, Li FM. Genetic alterations and reduced expression of tumor suppressor p33 (ING1b) in human exocrine pancreatic carcinoma. *World J Gastroenterol* 2004; **10**: 3597-3601

28 **Krishnamurthy J**, Kannan K, Feng J, Mohanprasad BK, Tsuchida N, Shanmugam G. Mutational analysis of the candidate tumor suppressor gene ING1 in Indian oral squamous cell carcinoma. *Oral Oncol* 2001; **37**: 222-224

29 **Ohmori M**, Nagai M, Tasaka T, Koeffler HP, Toyama T, Riabowol K, Takahara J. Decreased expression of p33ING1 mRNA in lymphoid malignancies. *Am J Hematol* 1999; **62**: 118-119

30 **Bromidge T**, Lynas C. Relative levels of alternative transcripts of the ING1 gene and lack of mutations of p33/ING1 in haematological malignancies. *Leuk Res* 2002; **26**: 631-635

31 **Sanchez-Cespedes M**, Okami K, Cairns P, Sidransky D. Molecular analysis of the candidate tumor suppressor gene ING1 in human head and neck tumors with 13q deletions. *Genes Chromosomes Cancer* 2000; **27**: 319-322

Science Editor Kumar M and Guo SY **Language Editor** Elsevier HK

PO Box 2345, Beijing 100023, China
www.wjgnet.com
wjg@wjgnet.com

ELSEVIER

World J Gastroenterol 2005;11(39):6125-6129
World Journal of Gastroenterology ISSN 1007-9327

Mechanism of counterattack of colorectal cancer cell by Fas/Fas ligand system

Qiang Zhu, Ji-Yong Liu, Hong-Wei Xu, Chong-Mei Yang, An-Zhong Zhang, Yi Cui, Hong-Bo Wang

Qiang Zhu, Ji-Yong Liu, Hong-Wei Xu, Chong-Mei Yang, An-Zhong Zhang, Yi Cui, Hong-Bo Wang, Department of Gastroenterology, Shandong Provincial Hospital, Jing 5 Wei 7 Road, 324#, Jinan 250021, Shandong Province, China
Correspondence to: Qiang Zhu, Department of Gastroenterology, Shandong Provincial Hospital, Jing 5 Wei 7 Road, 324#, Jinan 250021, Shandong Province, China. zhuqiang@medmail.com.cn
Telephone: +86-531-5186355 Fax: +86-531-7904002
Received: 2004-12-24 Accepted: 2005-01-26

Abstract

AIM: To determine the role of Fas/Fas ligand (FasL) in the immune escape of colon cancer cells.

METHODS: Immunohistochemistry was used to observe the expression of Fas and FasL in the tissues of colon cancer patients. *In situ* hybridization was used to detect the localization of FasL mRNA expression in cancer tissues. Terminal deoxynucleotide transferase-mediated dUTP nick end labeling (TUNEL) assay and CD45 staining were performed to detect the apoptosis of tumor-infiltrating lymphocytes (TILs). Co-culture assays of colon cancer cells (SW480) and Jurkat cells (Fas-sensitive cells) were performed to observe the counterattack of colon cancer cells to lymphocytes.

RESULTS: Of 53 cases of colon carcinomas, 23 cases (43.4%) expressed Fas which was significantly lower as compared to the normal colonic mucosa (73.3%, $P<0.01$), and 45 cases (84.9%) of colon carcinomas expressed FasL, whereas only two cases (3.75%) in normal mucosa expressed FasL. FasL expression in the colon cancer cells was found to be associated with increased cell death of TILs. The apoptotic rate of TIL in the FasL-positive staining regions of tumor cells was significantly higher than that in the FasL-negative staining region (54.84±2.79% *vs* 25.73±1.98%, $P<0.01$). The co-culture of SW480 cells and Jurkat cells confirmed the function of FasL on the SW480 cells. The apoptotic rates of Jurkat cells were found to be related with the amount of SW480 cells.

CONCLUSION: Colon cancer cells can escape the immune surveillance and killing via decreasing Fas expression, and can counterattack the immune system via increasing FasL expression. Fas/FasL can serve as potential targets for effective antitumor therapy.

Key words: Colon neoplasm; Fas system; Immune counterattack

Zhu Q, Liu JY, Xu HW, Yang CM, Zhang AZ, Cui Y, Wang HB. Mechanism of counterattack of colorectal cancer cell by Fas/Fas ligand system. *World J Gastroenterol* 2005; 11(39): 6125-6129
http://www.wjgnet.com/1007-9327/11/6125.asp

INTRODUCTION

Fas (Apo-1/CD95) is a 45-ku type I membrane protein, and Fas ligand (FasL) is a 37-40-ku type II membrane protein, which belong to the tumor necrosis factor receptor and ligand families. Activation of Fas by certain anti-Fas antibodies or by FasL results in apoptotic cell death in susceptible cells. Fas/FasL interaction constitutes one of the main systems mediating the cytotoxicity of T cells and regulating immune responses, tissue development, and homeostasis[1,2].

Fas system is one of the killing pathways by cytotoxic T lymphocytes (CTL) to tumor cells in human body; however, in recent reports, the most enticing interpretation of FasL expression by tumor cells is that it offers a further novel mechanism of immune evasion. Tumor cells could counterattack the immune system of human body by inducing apoptosis of immune effector cells through Fas/FasL system[3]. We used *in vivo* and *in vitro* methods to determine the role of Fas/FasL in the immune escape of colon cancer cells.

MATERIALS AND METHODS

Immunohistochemical detection of Fas/FasL protein

Fifty-three colon carcinomas were collected after surgical resection performed at Shandong Provincial Hospital. None of the patients had received chemo-, radio- or immuno-therapy before resection. Paraffin wax-embedded surgically resected tumor sections were deparaffinized in xylene and rehydrated before analysis. The primary antibodies were purified rabbit polyclonal anti-human Fas and FasL-specific IgG (Santa Cruz Biotechnology, Santa Cruz, CA, USA) at 0.1 μg/mL in a wash buffer. Antibody binding was localized using a biotinylated secondary antibody, avidin conjugated horseradish peroxidase, and diamiobenzidine substrate, contained within the ABC detection kit. The immunizing peptide (Santa Cruz Biotechnology), to which the antibody was raised, was included at 1 μg/mL during primary antibody incubation as a direct internal competitive control for antibody specificity.

Localization of FasL mRNA expression by in situ hybridization

In situ hybridization was performed on paraffin-embedded human colonic tumor sections (4 μm thick), mounted on aminopropylethoxysilane-treated slides. A digoxigenin-labeled RNA hybridization probe (344 bp) was used, corresponding to codons 96-210 of the human FasL cDNA sequence. The nucleotide sequence of the FasL probe showed insignificant homology to any other sequence in the EMBL DNA sequence database. Prehybridization and hybridization were performed as previously described[3]. In order to confirm the specificity of hybridization, a 10-fold excess of unlabeled riboprobe was added to the digoxigenin-labeled probe prior to hybridization.

In situ apoptosis assessment of tumor-infiltrating lymphocyte

To identify tumor-infiltrating lymphocytes (TILs), CD45 staining was performed on consecutive sections with a mouse anti-human CD45 monoclonal IgG (clone 2B11+PD7/26, Dako Corp., Carpinteria, CA, USA, dilution 1/70) according to the standard immunohistochemical methods as described above. Alkaline phosphatase conjugated anti-alkaline phosphatase complex (DO651, Dako Corp.) was used to display the color of CD45 staining. The membrane of the CD45-positive cells was red. Apoptosis of TILs was detected *in situ* in frozen sections of resected tissues using Terminal deoxynucleotide transferase-mediated dUTP nick end labeling (TUNEL) assay (Boehringer Mannheim GmbH, Mannheim, Germany) applied to the histological sections. Visualization of the final reaction product was achieved by diaminobenzidine. TUNEL-positive TILs (with red membrane and brown nucleus) were counted at high power (×400) from fields of view chosen according to a systematic random sampling method. Approximately 1 000 TILs were counted and a TUNEL index (TI) was expressed as the percentage of TUNEL lymphocytes.

Cell culture and growth assay

Colon cancer SW480 cells were grown in RPMI medium supplemented with penicillin G (100 U/mL), streptomycin (100 μg/mL) and 100 mL/L fetal bovine serum at 37 ℃ in humidified atmosphere containing 50 mL/L CO_2 in air. Cell growth was determined by the 3-(4,5-methylthiazol-2yl)-2, 5-diaphenyl-tertrazolium bromide (MTT) colorimetric assay. The assay was initiated by adding MTT solution to each well at a final concentration of 0.625 μg MTT/mL medium. After 4 h, the optical density was determined with an ELISA plate reader after removal of the medium and dissolving of the dye crystals in acidified isopropylalcohol.

Co-culture assays of colon cancer and Jurkat cells

Different concentrations of SW480 cells (0, 1×10^5/mL, 2×10^5/mL, 4×10^5/mL) were plated in triplicate on 24-multiwell tissue culture dishes. After 24 h, 2×10^4/mL Jurkat cells were seeded onto the plates. The wells with colon cancer cells alone (without overlying Jurkat cells) were maintained as additional controls. After 48 h, the non-adherent phase of the mixed culture was aspirated and assayed for viability using MTT assay. In experiments using recombinant FasFc (ZB4) as a competitor, similar experimental conditions were used with the following exception. MTT assay was used to evaluate the amount of Jurkat cells at the co-culture time of 24, 48, 72, and 96 h.

Detection of apoptosis of Jurkat cells

After being co-cultured with SW480 for 48 h, the Jurkat cells were collected and added with Hoechst 33258 (Sigma) on a slide glass. The specimens were examined under a Nikon fluorescence microscope with B2-type filter (magnification ×200). When apoptotic bodies or chromatin condensations were observed, the observation was defined as apoptosis. Apoptotic cells were assessed morphologically by staining with Hoechst 33258 using cells fixed with Clarke fixative (ethanol:acetic acid = 3:1). Apoptotic index (AI) was defined as follows: AI = 100×apoptotic cells/200 cells.

Statistical analysis

All experiments for cell cultures were performed at least in triplicate. Data were expressed as mean±SD. Statistical analysis was performed by one-way variance (ANOVA), and the comparisons between groups were performed by independent sample *t*-test. The regressive relation between two variables was performed by linear regression. A two-tailed *P* value less than 0.05 was considered statistically significant.

RESULTS

Decrease of Fas expression and increase of FasL expression in colon cancer tissues

Of 53 cases of colon carcinomas, 23 cases (43.4%) expressed Fas which was significantly lower as compared to that in normal colonic mucosa (73.3%) ($P<0.01$), and 45 cases (84.9%) of colon carcinomas expressed FasL, whereas only 2 cases (3.75%) in normal mucosa expressed FasL. Intensity and extent of positive staining varied within individual tumors. Neoplastic areas with positive and negative staining for FasL frequently co-existed within the same tumor. The extent of FasL expression varied significantly between different cancer stages and differentiations (data not shown, Figures 1A and B). FasL expression also existed on TILs in all cases. TILs were smaller in volume than cancer cells, which could distinguish the two kinds of FasL-expressing cells.

In situ hybridization was performed on paraffin-embedded human colonic tumor sections in order to detect the localization of FasL mRNA expression. FasL mRNA was detected in the colon cancer cells and in TILs (Figure 2). The location of FasL mRNA and expression of FasL protein coincided.

To further study the role of FasL expressed in cancer cells in tissues, 23 cases of lymph node metastases from colorectal carcinomas were obtained to detect the expression of FasL immunohistochemically. All cases of lymph node metastases showed FasL immunoreactivity in greater than 60% of the metastatic cells (Figure 1C).

Apoptosis of tumor-infiltrating lymphocytes induced by FasL on colon cancer

To evaluate apoptosis of TILs, we detected the presence of apoptotic cells in tissue sections using CD45 staining

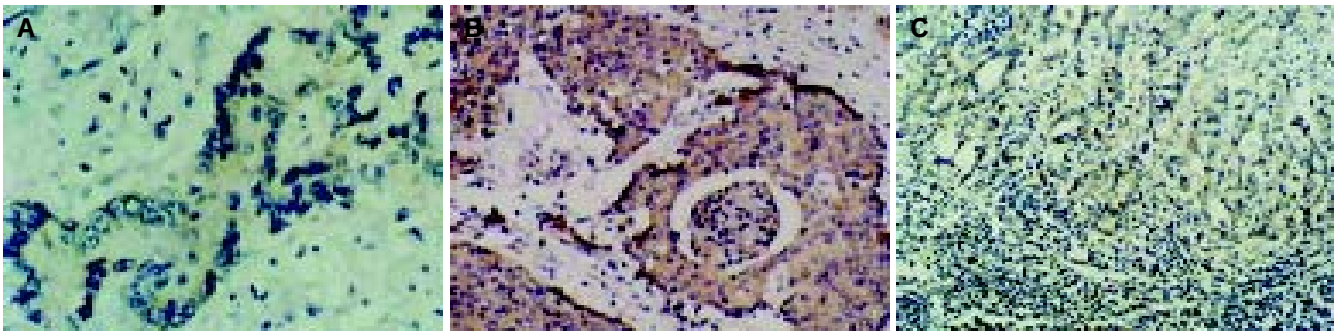

Figure 1 Immunohistochemical staining of Fas and FasL expression in colon cancer cells. A: Low expression of Fas in colon cancer cells; B: high expression of FasL in colon cancer cells; and C: high expression of FasL in lymph node metastases from colon cancer cells.

(WBC common antigen) and TUNEL techniques. Tonsil sections were included as positive controls, stained strongly, and omission of the primary antibody abolished staining. To quantify the extent of apoptosis of TILs, the percentage of TUNEL-positive and CD45-positive cells was calculated. The apoptotic rate of TILs in FasL-positive staining regions of tumor cells was significantly higher than that in FasL-negative region of tumor cells (54.84±2.79% *vs* 25.73±1.98%, $P<0.01$, Figure 3). *In vivo* FasL expression in colon cancer cells was found to be associated with increased cell death of TILs.

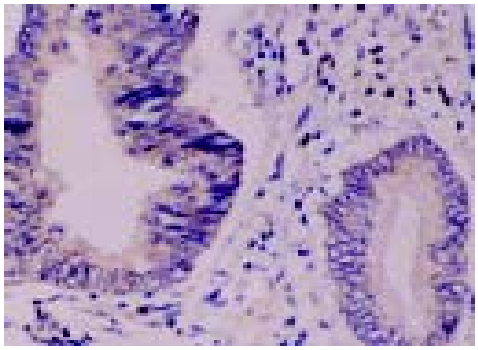

Figure 2 Localization of FasL mRNA by *in situ* hybridization.

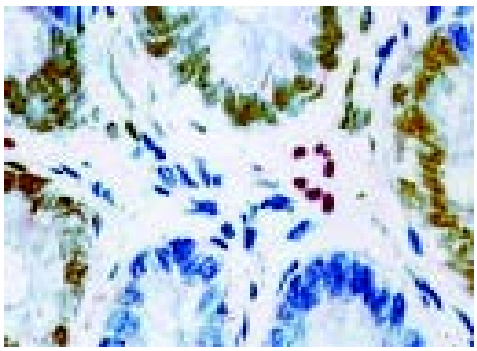

Figure 3 Detection of TILs. They were displayed by double staining (CD45 staining and TUNEL).

Colon cancer cell-mediated killing of Jurkat cells

Jurkat cells grown in the absence of human colon cancer cells showed a marked proliferation after 48 h. However, when co-cultured over a mono-layer of the FasL-expressing colon cancer cell line SW480, we observed a marked decrease in Jurkat cells while using MTT assay (Figure 4). The Jurkat cell killing was largely inhibited by pre-incubating the colon cancer mono-layer with a low concentration of recombinant Fas neutral antibody ZB4, which is capable of binding to FasL and blocking Fas/FasL interaction.

We used fluorescence microscopy to observe the shape of apoptotic Jurkat cells by the untreated SW480 cells. Condensation of chromatin, nuclear fragmentation and typical apoptotic bodies were observed in the tested group (Figure 5). The fluorescence microscopy results revealed that the apoptotic rates of Jurkat cells induced by SW480 cells after being co-cultured had a significant difference with the natural apoptotic rate of Jurkat cells (Table 1).

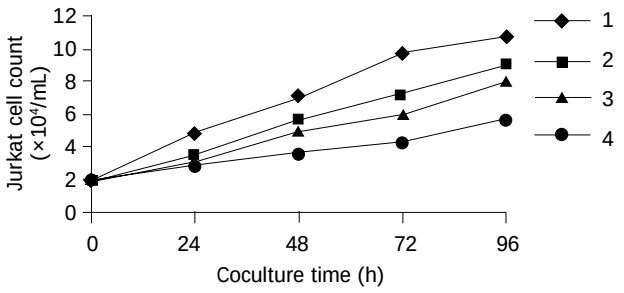

Figure 4 Jurkat cells growth curve after being co-cultured with SW480. 1: Control group; 2: 0.5×10^5/mL SW480 planting group; 3: 1×10^5/mL SW480 planting group; and 4: 2×10^5/mL SW480 planting group.

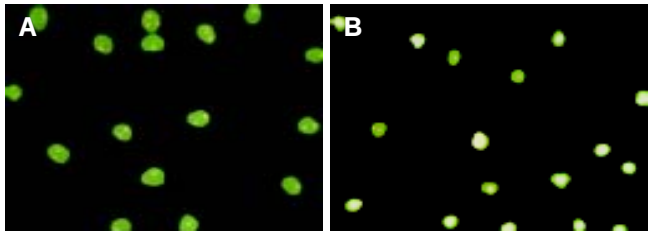

Figure 5 Detection of apoptotic Jurkat cells by fluorescence microscopy. A: Negative control of Jurkat cells; B: apoptotic Jurkat cells after being co-cultured with SW480 cells.

Table 1 Apoptotic rates of Jurkat cells detected by fluorescence microscopy

Planting concentration of SW480	Apoptotic rate of Jurkat cell (%)
0 (controls)	1.58±0.12
0.5×10^5/mL	5.22±0.13[b]
1×10^5/mL	9.74±0.21[b]
2×10^5/mL	19.33±0.18[b]

[b]$P<0.01$ *vs* controls.

DISCUSSION

Fas molecule was identified for the first time in 1989 by two research groups of Germany and Japanese separately[4,5]. In the beginning days of the twentieth century, researchers worldwide paid attention to the role of Fas system in the process of CTL killing cancer cells. It has been concluded that CTL-induced apoptosis of cancer cells via Fas system is one of the two main ways of CTL killing cancer cells, namely, Fas-based cytotoxicity is one of the two molecular mechanisms of T cell-mediated cytotoxicity, the other is perforin-based[1].

In recent years, some reports found that caner cells could decrease Fas expression which could escape the immune surveillance and killing, but could express FasL which could induce apoptosis of CTL, especially TILs[3,6,7]. In these cases, Fas and FasL may contribute to tumor immune privilege by inducing FasL-mediated apoptosis of host CTL and NK cells. We found that Fas expression on the colon cancer cells decreased significantly compared to the normal colonic epithelial cells ($P<0.05$), which was in agreement with the previous reports by Houston *et al.*[8], and Okada *et al.*[9]. Colon cancer could escape the immune surveillance and killing by decreasing Fas expression.

In addition to decrease in Fas expression, functional FasL expression by certain cancer cell types has been implicated in tumor escape via destruction of infiltrating Fas-bearing lymphocytes. In this study, we also found that FasL expression was absent in normal colonic epithelial cells, whereas markedly increased in colon carcinomas ($P<0.05$), and it was obviously correlated with apoptosis of TILs in colon cancer tissues. To evaluate the functional significance of FasL expression in colon cancer cells, we performed co-culture experiments using the Fas-sensitive Jurkat cell line (of human T-cell origin) as a target cell. These cells have been demonstrated to be capable of apoptosis following exposure to FasL. *In vitro*, colon cancer cells without any treatment could mediate apoptosis of Jurkat cells by Fas and FasL. Expression of FasL potentially enables colon cancer cells to counterattack Fas-sensitive anti-tumor immune effector cells by delivering a Fas-mediated apoptotic death signal. Ohta *et al.*[10], reported that 37 (82%) of the primary pancreatic cancers and both of the hepatic metastases expressed FasL, and the patients with FasL-positive tumor had significantly shorter survival times as compared with the FasL-negative, suggesting FasL as a significant prognostic factor of pancreatic cancer.

FasL expression may have effects on the immune system beyond the tumor site, and soluble FasL has been identified in certain types of FasL-positive leukemias and lymphomas[11]. Circulating forms of FasL (soluble FasL) were also found in blood from cancer patients, this could contribute to the generalized depression of cellular immunity. Thus, FasL expression might facilitate tumor invasion by inducing apoptosis in surrounding Fas-positive tissue, allowing the tumor to grow into the resulting space.

We found that large areas of most colonic tumors co-expressed FasL and Fas, indicating that these cells must have disabled the intracellular Fas apoptotic pathway due to intracellular defects in Fas signal transduction. Strand *et al.*[12], reported that MMP-7 cleavage of Fas resulted in reduced Fas surface expression and decreased Fas-mediated apoptosis sensitivity of tumor cells. Moreover, overexpression of inhibitors of apoptosis or intracellular apoptotic signal transduction may further contribute to the observed resistance to Fas-dependent apoptosis in colon cancer[13]. Several additional mechanisms of the Fas resistance have been described. Expression of soluble Fas by liver cancer cells may be involved in the Fas resistance of liver cancer *in vivo*[14].

A "Fas counterattack" model of colon cancer immune escape can be proposed, in which colon cancer cells, by expressing FasL, may remove Fas-sensitive immune effector cells by apoptosis. Increased expression of FasL is associated with decreased Fas levels in colon cancer cells that can escape immune surveillance and facilitate tumor progression and metastasis. Fas/FasL can serve as potential targets for effective antitumor therapy[15].

REFERENCES

1 **Nagata S,** Golstein P. The Fas death factor. *Science* 1995; **267**: 1449-1456

2 **Maher S,** Toomey D, Condron C, Bouchier-Hayes D. Activation-induced cell death: the controversial role of Fas and Fas ligand in immune privilege and tumour counterattack. *Immunol Cell Biol* 2002; **80**: 131-137

3 **Perabo FG,** Kamp S, Schmidt D, Lindner H, Steiner G, Mattes RH, Wirger A, Pegelow K, Albers P, Kohn EC, von Ruecker A, Mueller SC. Bladder cancer cells acquire competent mechanisms to escape Fas-mediated apoptosis and immune surveillance in the course of malignant transformation. *Br J Cancer* 2001; **84**: 1330-1338

4 **Trauth BC,** Klas C, Peters AM, Matzku S, Moller P, Falk W, Debatin KM, Krammer PH. Monoclonal antibody-mediated tumor regression by induction of apoptosis. *Science* 1989; **245**: 301-305

5 **Yonehara S,** Ishii A, Yonehara M. A cell-killing monoclonal antibody (anti-Fas) to a cell surface antigen co-downregulated with the receptor of tumor necrosis factor. *J Exp Med* 1989; **169**: 1747-1756

6 **Krishnakumar S,** Kandalam M, Mohan A, Iyer A, Venkatesan N, Biswas J, Shanmugam MP. Expression of Fas ligand in retinoblastoma. *Cancer* 2004; **101**: 1672-1676

7 **Abrams SI.** Positive and negative consequences of Fas/Fas ligand interactions in the antitumor response. *Front Biosci* 2005; **10**: 809-821

8 **Houston A,** Bennett MW, O'Sullivan GC, Shanahan F, O'Connell J. Fas ligand mediates immune privilege and not inflammation in human colon cancer, irrespective of TGF-beta expression. *Br J Cancer* 2003; **89**: 1345-1351

9 **Okada K,** Komuta K, Hashimoto S, Matsuzaki S, Kanematsu T, Koji T. Frequency of apoptosis of tumor-infiltrating lymphocytes induced by fas counterattack in human colorectal carcinoma and its correlation with prognosis. *Clin Cancer Res* 2000; **6**: 3560-3564

10 **Ohta T,** Elnemr A, Kitagawa H, Kayahara M, Takamura H, Fujimura T, Nishimura G, Shimizu K, Yi SQ, Miwa K. Fas ligand expression in human pancreatic cancer. *Oncol Rep* 2004; **12**: 749-754
11 **Hallermalm K,** De Geer A, Kiessling R, Levitsky V, Levitskaya J. Autocrine secretion of Fas ligand shields tumor cells from Fas-mediated killing by cytotoxic lymphocytes. *Cancer Res* 2004; **64**: 6775-6782
12 **Strand S,** Vollmer P, van den Abeelen L, Gottfried D, Alla V, Heid H, Kuball J, Theobald M, Galle PR, Strand D. Cleavage of CD95 by matrix metalloproteinase-7 induces apoptosis resistance in tumour cells. *Oncogene* 2004; **23**: 3732-3736
13 **Kase S,** Osaki M, Adachi H, Kaibara N, Ito H. Expression of Fas and Fas ligand in esophageal tissue mucosa and carcinomas. *Int J Oncol* 2002; **20**: 291-297
14 **Lee SH,** Shin MS, Lee HS, Bae JH, Lee HK, Kim HS, Kim SY, Jang JJ, Joo M, Kang YK, Park WS, Park JY, Oh RR, Han SY, Lee JH, Kim SH, Lee JY, Yoo NJ. Expression of Fas and Fas-related molecules in human hepatocellular carcinoma. *Hum Pathol* 2001; **32**: 250-256
15 **Kim R,** Emi M, Tanabe K, Uchida Y, Toge T. The role of Fas ligand and transforming growth factor beta in tumor progression: molecular mechanisms of immune privilege via Fas-mediated apoptosis and potential targets for cancer therapy. *Cancer* 2004; **100**: 2281-22891

Science Editor Kumar M and Guo SY **Language Editor** Elsevier HK

PO Box 2345, Beijing 100023, China
www.wjgnet.com
wjg@wjgnet.com

ELSEVIER

World J Gastroenterol 2005;11(39):6130-6133
World Journal of Gastroenterology ISSN 1007-9327

Specific ssDNA concentration in liver tissue as an index of apoptosis in hepatitis C virus-infected patients

Tadeusz Wojciech Lapiński, Anatol Panasiuk, Jerzy Jaroszewicz, Oksana Kowalczuk, Robert Flisiak, Magdalena Rogalska

Tadeusz Wojciech Lapiński, Anatol Panasiuk, Jerzy Jaroszewicz, Robert Flisiak, Magdalena Rogalska, Department of Infectious Diseases, Medical University of Bialystok, Poland
Oksana Kowalczuk, Institute of Molecular Biology, Medical University of Bialystok, Poland
Correspondence to: Tadeusz Wojciech Lapiński, MD, Department of Infectious Diseases, Medical University of Bialystok, Bialystok 15-540, Żurawia str, 14, Poland. twlapinski@wp.pl
Telephone: +48-85-741-69-21
Received: 2005-01-19 Accepted: 2005-02-18

Abstract

AIM: To evaluate the activity of apoptosis in liver tissue and explore its possible association with hepatic necroinflammation and fibrosis as well as serum hepatitis C virus (HCV) load.

METHODS: The studied population included 50 chronic hepatitis C patients (20 women and 30 men, aged 18-66 years). HCV-RNA quantification was performed by two-step real-time quantitative RT-PCR method using the TaqMan technology (reagents of Applera Corporation firm, USA). The morphology of liver tissue was assessed descriptively and scored (necroinflammatory activity and fibrosis). The early apoptosis activity in liver tissue was examined by ssDNA apoptosis ELISA kit, (Chemicon, Germany).

RESULTS: The correlation between apoptosis and fibrosis in liver tissue was observed. High intensification of apoptosis was proportional to the increase of fibrosis (ssDNA: 16.65×10^{-5} μg/g; 12.71×10^{-5} μg/g), however, this difference was not statistically significant ($P>0.05$). Activity of apoptosis in the liver tissue, expressed by ssDNA concentration did not depend on hepatic necroinflammatory changes, HCV-RNA viral load, ALT, and AST activity as well as prothrombin time and INR index.

CONCLUSION: Fibrosis in the tissue is closely associated with early apoptosis in HCV-infected patients.

Key words: Apoptosis; Hepatitis C virus; ssDNA; Fibrosis

Lapiński TW, Panasiuk A, Jaroszewicz J, Kowalczuk O, Flisiak R, Rogalska M. Specific ssDNA concentration in liver tissue as an index of apoptosis in hepatitis C virus-infected patients. *World J Gastroenterol* 2005; 11(39): 6130-6133
http://www.wjgnet.com/1007-9327/11/6130.asp

INTRODUCTION

Activity of apoptosis during hepatitis C virus (HCV) infection is a result of inhibitory and stimulatory effects of viral proteins. Apoptosis of HCV-infected hepatocytes influences the elimination of viruses. Insufficient activity of this process can lead to persistent liver inflammation[1]. On the contrary, excessive activity of apoptosis causes uncontrolled damage to liver cells. Moreover, there is evidence that apoptosis influences fibrosis progression.

This study was to evaluate the activity of apoptosis in liver tissue and explore its possible association with hepatic necroinflammation and fibrosis activity as well as serum HCV viral load.

MATERIALS AND METHODS

Patients

The study included 50 chronic hepatitis C patients (20 women and 30 men, aged 18-66 years). Their HCV infection did not exceed 5 years. Inclusion criteria were the following: no focal changes in ultrasonography investigation of liver, absence of drugs or alcohol abuse, autoimmune disease, HIV and hepatitis B co-infection as well as neoplasmatic and other serious diseases, which might alter apoptosis activity. Informed consent was obtained from each patient and the Bioethics Committee at the Medical University of Bialystok approved the study protocol.

The presence of anti-HCV antibodies in serum was detected by MEIA (Abbott, USA). Test was based on recombinant core proteins for HCr43, structural proteins for c200 (NS3 and NS4) and unstructured proteins for c100-3 (NS4) and NS5.

HCV-RNA quantification methods

Blood samples were obtained from 47 patients with known chronic hepatitis C. All blood samples were collected to Vacutainer tubes with no additives and centrifuged within 2 h of collection. The serum was aliquoted and kept at -80 ℃ until further use.

RNA was extracted from 280 μL of each serum sample using Qiagen (Hilden, Germany) QIAamp viral RNA mini kit according to the manufacturer's protocol and dissolved in 50 μL of RNase-free water. This resulted in nearly sixfold concentration of the original output material. RNA was stored at -80 ℃ until further testing. Each isolation was carried out in duplicate.

HCV-RNA quantification was performed by two-step real-time quantitative RT-PCR method using the TaqMan technology[2]. First, 3.5 μL of total RNA was subjected to reverse transcription in 10 μL of reaction mixture using the Applied Biosystems (Applera Corporation, USA) TaqMan

reverse transcription reagents and random hexamers $(dN)_6$. RNA was previously denatured at 70 ℃ for 10 min. The reaction mixture was prepared as follows: 1×reverse transcription buffer, 5.5 mmol/L $MgCl_2$, 0.5 mmol/L of each dNTPs, 2.5 mmol/L of primer $(dN)_6$, 0.4 U of RNase inhibitor per μL and 1.25 U of MultiScribe transcriptase per μL. The reaction was carried out at 48 ℃ for 30 min preceded by the incubation at 25 ℃ for 10 min. Incubation at 95 ℃ for 5 min terminated the reaction. The resulting cDNA was used as a template for PCR amplification.

cDNA amplification was performed by the Applied Biosystem (Applera Corporation, USA) ABI Prism 7 900HT sequence detection system in TaqMan universal PCR master mix, which is optimized for TaqMan reactions and contains Applied Biosystems (Applera Corporation, USA) AmpliTaq gold DNA polymerase, AmpErase UNG, dNTPs with UTP, passive reference ROX and optimized buffer components. For each PCR reaction, 4 μL of cDNA was added to 16 μL of PCR mix containing 450 nmoL each of HCV-specific forward and reverse primers and 300 nmoL of HCV-specific FAM-MGB probe. The primers and probe were designed and manufactured by Applied Biosystems (Applera Corporation, USA) and optimized for HCV genotype RNA detection. Thermal cycling conditions were designed as follows: inactivation of possible contaminating amplicons by AmpErase UNG at 50 ℃ for 2 min, initial cDNA denaturation at 95 ℃ for 10 min, followed by 40 cycles at 95 ℃ for 15 s and at 60 ℃ for 60 s. All amplification reactions were carried out in triplicate.

Fluorescent measurements were recorded during the annealing step of each cycle. At the end of each PCR run, data were automatically analyzed by the system to generate the amplification plots and the threshold cycle (Ct) for each sample was calculated. Sample RNA concentrations were then automatically calculated by interpolation of the experimentally determined standard curve.

An external standard curve was generated with each run by amplification of 10-fold serial dilutions of RNA isolated from the viral quality control serum (PeliSpy, Sanguin), containing 38 000 geq/mL HCV. RNA isolation and cDNA synthesis were carried out as described for unknown samples. All amplification reactions were carried out in duplicate. The standard curve was created automatically by the ABI Prism 7 900HT detection system by plotting the Ct values against each standard dilution of known concentration.

Precautions were undertaken to minimize the risk of PCR contamination during analysis.

Liver morphology

Liver tissue was obtained from the right lobe of the liver (with 1.6-1.8 mm needles from Hypafix packs by Braun, Germany). A part of the liver tissue was subjected to morphologic examination. The morphology of liver tissue was assessed descriptively and scored (necroinflammatory activity and fibrosis) according to Scheuer[3].

Another part of the liver tissue was transferred to 0.9% NaCl buffer and then subjected to apoptosis activity measurement.

Apoptosis in liver tissue

The early apoptosis activity in liver tissue was measured by ssDNA apoptosis ELISA kit, (Chemicon, Germany) based on the mAb to single-stranded DNA (ssDNA). The intensity of the reaction between ssDNA and mAb was evaluated. The amount of ssDNA was calculated with reference to absorbance line of positive and negative control.

The liver tissue was homogenized in 0.9% NaCl buffer. The concentrations of ssDNA and total proteins in the homogenized liver tissue were analyzed in duplicate. The homogenates of liver tissue were transferred to wells 24 h prior to the succeeding steps of the procedure to allow cell attachment. Then formamide was added to denature DNA in apoptotic cells, but not in necrotic cells or in cells with DNA damage in the absence of apoptosis. This process enabled specific receptors of apoptotic ssDNA binding to mAb. Following this reaction, 3-ethylbenziazoline-6-sulfonic acid was added to color the products of this reaction[4].

Absorbance was defined at 405 nm. The concentration of ssDNA was calculated from a prepared standard curve of absorbance (basis of different increasing positive and negative control). The results of ssDNA were referred to 1.0 g of proteins in the liver tissue sample.

Statistical analysis

Statistical analysis was performed by non-parametric Mann-Whitney *U*, Wilcoxon rank, and Pearson tests. $P<0.05$ was considered statistically significant.

RESULTS

Diagnostic biopsy was obtained from 47 patients. In three of the remaining cases, the liver biopsy sample did not contain five portobiliary areas, therefore it was impossible to obtain reliable histology results.

The activity of apoptosis in liver tissue of the studied group was independent of sex and age. ssDNA concentration in liver tissue did not correlate with ALT, AST activity, prothrombin time, and INR index. Moreover, apoptosis was independent of necroinflammatory changes in liver tissue (Table 1).

Table 1 Correlation between ALT, AST activity, prothrombin time, and INR index in chronic hepatitis C patients

	ALT	AST	Prothrombin time	INR index
Pearson test	0.08	0.14	-0.01	0.03

The correlation between fibrosis and apoptosis was observed. Concentration of ssDNA was higher (16.65×10^{-5} μg/g) in patients with more intensified fibrosis of liver tissue than in those with fibrosis (12.71×10^{-5} μg/g). However, this difference was not statistically significant ($P>0.05$). (Figures 1 and 2)

The serum HCV-RNA concentration did not correlate with ALT, AST activity, prothrombin time, and INR index. Moreover, no correlation between serum HCV-RNA and ssDNA concentrations in liver tissue was observed (Table 2).

DISCUSSION

Table 2 Concentration of apoptosis ssDNA in respect to serum HCV-RNA concentration, necroinflammatory changes (G) and fibrosis (S) in liver tissue

n	G1+G2	Concentration of ssDNA (μg/g)	Concentration of HCV-RNA (geq/mL)	Pearson test	*n*	*S*	Concentration of ssDNA (μg/g)	Concentration of HCV-RNA (geq/mL)	Pearson test
16	0-3	13.16×10^{-5} 3.95×10^{-5} SD±	$4.96\text{-}54.2\times10^{3}$	-0.11	39	0-1	12.71×10^{-5} $4.85\text{-}10^{-5}$ SD±	$4.96\text{-}227\times10^{3}$	0.01
13	4	13.41×10^{-5} 6.0×10^{-5} SD±	$2.48\times10^{2}\text{-}227\times10^{3}$	-0.14	8	2-3	16.65×10^{-5} 5.98×10^{-5} SD±	$14.7\text{-}266\times10^{3}$	0.01
18	5-7	13.56×10^{-5} 5.85×10^{-5} SD±	$14.7\text{-}266\times10^{3}$	-0.13					

Necroinflammatory activity: G1 = 0-4; G2 = 0-4; G1/2 = 0-8; *S* = 0-4.

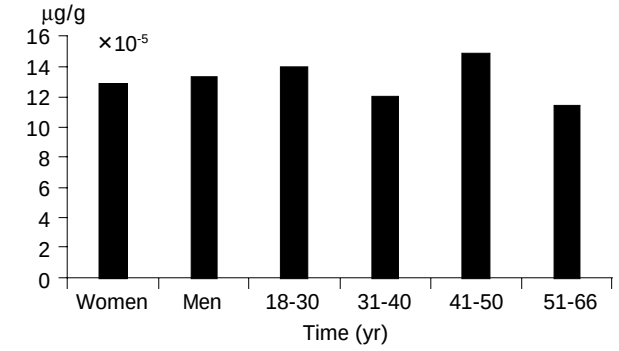

Figure 1 Concentration of ssDNA in HCV-infected patients with respect to age and sex.

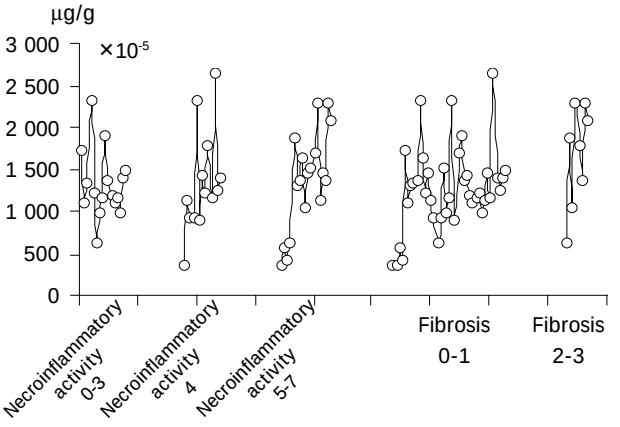

Figure 2 Concentration of ssDNA in liver tissue stratified according to liver morphology changes. Necroinflammatory activity: G1 = 0-4; G2 = 0-4; G1/2 = 0-8; *S* = 0-4.

Apoptosis is one of the factors regulating the course of chronic viral hepatitis. Since this process runs gradually, modification of its course is possible. Different HCV proteins can accelerate or suppress apoptosis.

HCV core proteins overactivate Fas particles expressed on hepatocytes, leading to degradation of cell DNA[5,6]. The Fas particles are "death domains" and indicators of apoptosis. Higher Fas concentration in patients with HCV infection can increase the activity of apoptosis.

HCV non-structural proteins (NS5A) are able to suppress apoptosis by diminishing synthesis of caspase 3, protein kinase A and suppressing TNF-α stimulating polymerase[7,8]. Insufficient activity of apoptosis can influence the persistence of chronic inflammation related to HCV infection[1].

Di Martino *et al*.[9], showed that activity of apoptosis in chronic hepatitis C patients is proportional to HCV-RNA levels. Caronia *et al*.[10], have shown that HCV strongly inhibits apoptosis. In previous investigations, the concentration of ssDNA, as an early indicator of apoptosis was not correlated with HCV viral load, functional state of the liver and necroinflammatory changes in liver tissue samples.

Tsamandas *et al*.[11], evaluated the location and concentration of Bcl-2 and Bax protein, markers of apoptosis activity, in patents with HBV and HCV infection, and found that Bcl-2 and Bax concentrations are enhanced in the regions of intense fibrosis. Takehara *et al*.[12], have shown the linear dependence between the concentration of Bcl-2 family members and activity of fibrosis in the liver. Our results are in accordance with their observations.

Bcl-2 and Bax proteins can mark the late period of apoptosis. Correlation between apoptosis and fibrosis in liver tissue seems unquestionable. However, whether cells with high activity of apoptosis are molecular inductors of fibrosis in HCV-infected patients remains to be solved.

In conclusion, fibrosis of liver tissue is associated with HCV-infection, but apoptosis is not associated with necroinflammatory changes in chronic hepatitis C patients.

REFERENCES

1 **Zuckerman E**, Zuckerman T, Sahar D, Streichman S, Attias D, Sabo E, Yeshurun D, Rowe J. bcl-2 and immunoglobulin gene rearrangement in patients with hepatitis C virus infection. *Br J Haematol* 2001; **112**: 364-369

2 **Castelain S**, Descamps V, Thibault V, Francois C, Bonte D, Morel V, Izopet J, Capron D, Zawadzki P, Duverlie G. TaqMan amplification system with an internal positive control for HCV RNA quantitation. *J Clin Virol* 2004; **31**: 227-234

3 **Scheuer PJ**. Classification of chronic viral hepatitis: A need for reassessment. *J Hepatol* 1991; **13**: 372-374

4 **Frankfurt OS**, Krishan A. Apoptosis enzyme-linked immunosorbent assay distinguishes anticancer drugs from toxic chemicals and predicts drug synergism. *Chem Biol Interact* 2003; **145**: 89-99

5 **Hahn CS**, Cho YG, Kang BS, Lester IM, Hahn YS. The HCV core protein acts as a positive regulator of fas-mediated apoptosis in a human lymphoblastoid T cell line. *Virology* 2000; **276**: 127-137

6 **Zhu N**, Ware CF, Lai MM. Hepatitis C virus core protein enhances FADD-mediated apoptosis and suppresses TRADD signaling of tumor necrosis factor receptor. *Virology* 2001; **283**: 178-187

7 **Ghosh AK**, Majumder M, Steele R, Meyer K, Ray R, Ray RB. Hepatitis C virus NS5A protein protects against TNF-alpha

mediated apoptotic cell death. *Virus Res* 2000; **67**: 173-178
8 **Ezelle HJ**, Balachandran S, Sicheri F, Polyak SJ, Barber GN. Analyzing the mechanisms of interferon-induced apoptosis using CrmA and hepatitis C virus NS5A. *Virology* 2001; **281**: 124-137
9 **Di Martino V**, Brenot C, Samuel D, Saurini F, Paradis V, Reynes M, Bismuth H, Feray C. Influence of liver hepatitis C virus RNA and hepatitis C virus genotype on Fas-mediated apoptosis after liver transplantation for hepatitis C. *Transplantation* 2000; **15**: 1390-1396
10 **Caronia S**, McGarvey MJ, Goldin RD, Foster GR. Negative correlation between intrahepatic expression of hepatitis C antigens and apoptosis despite high-level expression of Fas and HLA antigens. *J Viral Hepatol* 2004; **11**: 511-518
11 **Tsamandas AC**, Thomopoulos K, Zolota V, Kourelis T, Karatzas T, Ravazoula P, Tepetes K, Petsas T, Karavias D, Karatza C, Bonikos DS, Gogos C. Potential role of bcl-2 and bax mRNA and protein expression in chronic hepatitis type B and C: a clinicopathologic study. *Mod Pathol* 2003; **16**: 1273-1288
12 **Takehara T**, Tatsumi T, Suzuki T, Rucker EB 3rd, Hennighausen L, Jinushi M, Miyagi T, Kanazawa Y, Hayashi N. Hepatocyte-specific disruption of Bcl-xL leads to continuous hepatocyte apoptosis and liver fibrotic responses. *Gastroenterology* 2004; **127**: 1189-1197

Science Editor Wang XL and Guo SY **Language Editor** Elsevier HK

PO Box 2345, Beijing 100023, China
www.wjgnet.com
wjg@wjgnet.com

ELSEVIER

World J Gastroenterol 2005;11(39):6134-6143
World Journal of Gastroenterology ISSN 1007-9327

NF-κB and ERK-signaling pathways contribute to the gene expression induced by *cag* PAI-positive-*Helicobacter pylori* infection

Wataru Shibata, Yoshihiro Hirata, Haruhiko Yoshida, Motoyuki Otsuka, Yujin Hoshida, Keiji Ogura, Shin Maeda, Tomoya Ohmae, Ayako Yanai, Yuzo Mitsuno, Naohiko Seki, Takao Kawabe, Masao Omata

Wataru Shibata, Yoshihiro Hirata, Haruhiko Yoshida, Motoyuki Otsuka, Yujin Hoshida, Keiji Ogura, Shin Maeda, Tomoya Ohmae, Ayako Yanai, Yuzo Mitsuno, Takao Kawabe, Masao Omata, Department of Gastroenterology, Graduate School of Medicine, University of Tokyo, Japan
Naohiko Seki, Department of Functional Genomics, Graduate School of Medicine, University of Chiba, Japan
Supported by a Grant-in-Aid for Scientific Research from the Ministry of Education, Science, Sport, and Culture of Japan
Correspondence to: Wataru Shibata, MD, PhD, Department of Gastroenterology, Graduate School of Medicine, University of Tokyo, 7-3-1 Hongo, Bunkyo-ku, Tokyo 113-8655, Japan. wshibata-tky@umin.ac.jp
Telephone: +81-3-3815-5411-33070 Fax: +81-3-3814-0021
Received: 2005-03-24 Accepted: 2005-04-26

Abstract

AIM: To elucidate the sequential gene expression profile in AGS cells co-cultured with wild-type *Helicobacter pylori* (*H pylori*) as a model of *H pylori*-infected gastric epithelium, and to further examine the contribution of *cag*-pathogenicity islands (*cag*PAI)-coding type IV secretion system and the two pathways, nuclear factor kappa B (NF-κB) and extracellular signal-regulated kinases (ERK) on wild-type *H pylori*-induced gene expression.

METHODS: Gene expression profiles induced by *H pylori* were evaluated in AGS gastric epithelial cells using cDNA microarray, which were present in the 4 600 independent clones picked up from the human gastric tissue. We also analyzed the contribution of NF-κB and ERK signaling on *H pylori*-induced gene expression by using inhibitors of specific signal pathways. The isogenic mutant with disrupted *cag*E (△*cag*E) was used to elucidate the role of *cag*PAI-encoding type IV secretion system in the gene expression profile.

RESULTS: According to the expression profile, the genes were classified into four clusters. Among them, the clusters characterized by continuous upregulation were most conspicuous, and it contained many signal transducer activity-associated genes. The role of *cag*PAI on cultured cells was also investigated using isogenic mutant *cag*E, which carries non-functional *cag*PAI. Then the upregulation of more than 80% of the induced genes (476/566) was found to depend on *cag*PAI. Signal transducer pathway through NF-κB or ERK are the major pathways which are known to be activated by *cag*PAI-positive *H pylori*. The role of these pathways in the whole signal activation by *cag*PAI-positive *H pylori* was analyzed. The specific inhibitors against NF-κB or ERK pathway blocked the activation of gene expression in 65% (367/566) or 76% (429/566) of the genes whose activation appealed to depend on *cag*PAI.

CONCLUSION: These results suggest that more than half of the genes induced by *cag*PAI-positive *H pylori* depend on NF-κB and ERK signaling activation, and these pathways may play a role in the gene expression induced by host-bacterial interaction which may associate with *H pylori*-related gastro-duodenal diseases.

Key words: *Helicobacter pylori*; *Cag*-pathogenicity islands; cDNA microarray, Cluster analysis; Signal transduction

Shibata W, Hirata Y, Yoshida H, Otsuka M, Hoshida Y, Ogura K, Maeda S, Ohmae T, Yanai A, Mitsuno Y, Seki N, Kawabe T, Omata M. NF-κB and ERK-signaling pathways contribute to the gene expression induced by *cag* PAI-positive-*Helicobacter pylori* infection. *World J Gastroenterol* 2005; 11(39): 6134-6143
http://www.wjgnet.com/1007-9327/11/6134.asp

INTRODUCTION

Helicobacter pylori (*H pylori*) is the causative agent for various gastro-duodenal diseases[1] and has been classified as a definite carcinogen by the International Agency for Research on Cancer[2]. Previous studies have shown that the eradication of *H pylori* virtually eliminates the recurrence of peptic ulcer diseases, suppresses the recurrence of gastric cancer after mucosal resection, and cures mucosa-associated lymphoid tissue lymphoma[3-10]. The molecular mechanisms underlying these *H pylori*-related diseases have been extensively studied.

The *cag*-pathogenicity island (*cag*PAI), a cluster of about 28 genes, is one of the best known virulence factors; it encodes a type IV secretion system that transports CagA protein, peptidoglycan and possibly other molecules into host epithelial cells[11-16]. Transported CagA binds to molecules such as SH2 domain-containing protein-tyrosine phosphatase-2 (SHP-2), growth factor receptor bound 2 (Grb2), and cortactin[17-19]. Then it induces epithelial disruption as well as cytoskeletal changes[20], which might result in inducing ulcer diseases and gastric cancer[21,22].

The *cag*PAI is also associated with activation of the transcription factors nuclear factor kappa B (NF-κB) and

activator protein-1 (AP-1)[23-26], two key regulators of the expression of various inflammatory genes. NF-κB acts as a transcriptional modulator in the host response to bacterial invasion[27-33]. Its activation may in turn increase inflammation by inducing cytokines similar to the stimulation of interleukin-1 (IL-1) and tumor necrotizing factor-alpha (TNF-α)[34], and induce cell proliferation via activating anti-apoptotic effect[35]. The attachment of *H pylori* to gastric epithelial cells also induces the rapid activation of p38, c-Jun NH2-terminal kinase, and mitogen-activated protein kinase (MAPK)[36]; the downstream effectors of these signals include oncogene c-*fos* and its promoter element serum response element (SRE)[37,38]. These are possibly involved in cellular proliferation and survival[39-41], which might be associated with gastric carcinogenesis.

Some of the host cell responses to infection with *H pylori* induce many gene expressions and appear to function in contradictory directions, such as inflammation and cell proliferation, or apoptosis and anti-apoptosis[35]; the relative importance of each response is thus not immediately obvious. Recently, cDNA microarray analysis has been used to comprehensively characterize the individual responses in host cells[42,43]. The authors and coworkers have previously profiled *H pylori*-induced gene expression *in vitro*[44-51] and *in vivo*[52-54]. However, the contribution of the *cag*PAI-encoding type IV secretion system and the importance of intracellular signaling activation have not been fully elucidated.

In this study, we analyzed sequential gene expression profile in AGS cells co-cultured with wild-type *H pylori* as a model of *H pylori*-infected gastric epithelium. Furthermore, we examined the contribution of *cag*PAI-coding type IV secretion system and the two pathways, NF-κB and extracellular signal-regulated kinases (ERK) on wild-type *H pylori*-induced gene expression.

MATERIALS AND METHODS

Bacterial strains and cell culture

The *H pylori* TN2 strain, which is positive for entire *cag*PAI, and *vacA*, was generously denoted by Dr. M. Nakao (Takeda Chemical Industries, Ltd, Osaka, Japan). The isogenic *cagE* mutant TN2-△*cagE* was prepared by insertion of a kanamycin-resistant gene into the *cagE* gene locus of TN2, as described previously[55]. These strains were cultured on Columbia agar with 50 mL/L horse blood and Dent's selective antibiotic supplement (Oxoid, Basingstoke, UK) at 37 ℃ for 3 d under microaerobic conditions (Campy-Pak Systems; BBL, Cockeysville, MD, USA). The bacterial stocks were stored at -80 ℃ in Brucella broth with 50 mL/L fetal bovine serum (FBS) containing 160 mL/L glycerol. For co-culture experiments, *H pylori* was cultured in Brucella broth containing 7.5% FBS for 24 h, pelleted, resuspended in cell culture medium without FBS, and used to inoculate the host cells at a multiplicity of infection of 50 to 100:1 according to the previous reports[56,57]. At each time point, the AGS cells were collected by scraping, isolated by centrifugation, and stored at -80 ℃ for subsequent isolation of total RNA. Human gastric cancer cells (AGS; ATCC CRL 1739), established from poorly differentiated gastric adenocarcinoma, were maintained in Ham's F12 supplemented with 10% FBS. The medium was replaced with serum-free Ham's F12 at 24 h before the inoculation of the AGS cells with *H pylori*.

Treatment of AGS cells with specific NF-κB and ERK inhibitors

AGS cells were treated with ammonium pyrolidinedithiocarbamate (APDC; 400 μmol/L), which inhibits NF-κB activation, or with the ERK inhibitor PD98059 (25 μmol/L; Calbiochem, San Diego, CA, USA)[58] for 60 min before infection with *H pylori*, as described above. Total RNA was extracted from the AGS cells at 1.5, 3, 6, and 12 h of the co-culture period, as described above.

RNA extraction

Total cellular RNA was extracted using an acid guanidium thiocyanate-phenol-chloroform method, according to the manufacturer's instructions (ISOGEN Reagents; Nippon Gene, Tokyo, Japan), and column chromatography (RNeasy; Qiagen, Tokyo, Japan). The poly(A) mRNA was isolated from the total RNA using the Oligotex-dT30 mRNA purification kit (Takara Shuzo Co., Tokyo, Japan). The integrity of the purified mRNA was confirmed by agarose gel electrophoresis with ethidium bromide staining.

cDNA microarray

A cDNA microarray containing 4 600 cDNAs was made as previously described[44,59-61]. Briefly, human cDNAs were purchased from Research Genetics (Invitrogen Japan K. K., Tokyo, Japan). PCR-amplified cDNA products were mixed with nitrocellulose in dimethyl sulfoxide just before printing and were then spotted onto carbodiimide-coated glass slides using a robotics system (SPBIO-2000, Hitachi Software Engineering, Yokohama, Japan). In this study, we spotted 4 600 sequence-validated cDNAs on the array, including glyceraldehyde-3-phosphate dehydrogenase (GAPDH) and beta-actin to serve as an internal standard and the luciferase gene of *Photinus pyralis* as a negative control.

Sequential changes in gene expression in vitro

For the analysis of the time course of infection-induced gene expression in AGS cells, Cy5-labeled fluorescent cDNAs were prepared from 2 μg mRNA isolated from the infected AGS cells after 1.5, 3, 6, and 12 h of co-culture. The Cy5-labeled sample probes were then applied to the microarray slides for analysis. The Cy3-labeled control probes were similarly prepared from mRNA isolated from uninfected AGS cells. Two independent experiments were performed, and the array data were subject to a simple algorithm (see Data analysis) to set a lower bound threshold and to normalize for unequal incorporation label. Then average ratio was calculated and they were used for the following analysis.

Data analysis

The fluorescence signals from the microarrays were quantified with IMAGENE ver. 4.01 (Biodiscovery, Los Angeles, CA, USA) and analyzed with GENESIGHT LIGHT (Biodiscovery). Briefly, a cDNA spot was included in the analysis only if the raw fluorescence signal intensity was at least 1.5 times that of the local background. The signals were normalized between the arrays using a correction factor calculated from the sum

intensity of all spots. To control the uneven incorporation of the fluorescent dyes, the Cy5 and Cy3 fluorescence intensities for each spot were adjusted so that the mean Cy3:Cy5 ratio was equal to 1.0. We adjusted the raw fluorescence ratios by log transformation, median centering, and normalization to a mean of zero and a variance of one. Changes in expression (Cy3:Cy5 fluorescence ratio) with a factor of 3 or greater in either direction were considered significant, and if the maximum minus minimum values of the log-transformed fluorescence ratios were greater than 1. 0. (Full microarray data are deposited in the Gene Expression Omnibus at NCBI. The platform ID numbers are GPL 1303, and the sample ID numbers are GSM 25915-20). We performed cluster analysis using the average linkage method with uncentered correlation as the distance function by using the Cluster program (ver. 2.11) with TreeView (ver. 1.50) (http://rana.stanford.edu/software)[62]. The Onto-Express program (http://vortex.cs.wayne.edu/Projects.html) was used to perform functional characterization accompanied by the computation of significance values for each functional category, allowing significant biological processes to be distinguished from random events[63-65].

Reverse transcriptase-polymerase chain reaction (RT-PCR)

To validate the results obtained in the microarray experiments, first-strand cDNA was synthesized using 1 μg of total RNA, 1 mmol/L of oligo-dT primer, and reverse transcriptase (Superscript II; Invitrogen, Carlsbad, CA, USA). Each cDNA sample was amplified by PCR using specific primers, as the following, for 10 min at 95 ℃ for initial denaturing, followed by 35-40 cycles of 95 ℃ for 30 s, 52-54 ℃ for 30 s and 72 ℃ for 30 s, yielding products of approximately 300-500 bp. The PCR products were examined, with appropriate molecular size markers, by agarose gel electrophoresis and ethidium bromide staining. The primer pairs used for PCR analysis are listed in Table 1.

RESULTS

Sequential changes in gene expression in AGS cells co-cultured with cagPAI-positive H pylori

We used microarray technology to characterize the time course of changes in gene expression induced by wild-type *H pylori* in AGS cells infected *in vitro* and obtained 3 228 genes that were valid for the analysis. Changes in expression with a factor of 3 or greater in either direction were considered significant. Of the 3 228 genes, about 20% (641 genes) were altered significantly (Figure 1A). The percentage of the significantly altered genes at each time point is shown in Figure 1B. The number of upregulated genes reached their peak at 3 h after infection, while the downregulated genes peaked at 6 h after infection. It implicates that *H pylori*-associated phenomena like inflammatory changes following the induction of IL-8 or *c fos* might occur as the early event *in vitro*. Hierarchical clustering was used to classify the genes into upregulated and downregulated groups (Figure 1C). Each group was further divided into two minor clusters, resulting in a total of four clusters, designated as C-1 to C-4, based on the time course of expression induced by *H pylori*. Genes in both C-1 and C-2 were upregulated during the early phase (1.5-3 h); however, the genes in C-1 were downregulated in the late phase (6-12 h), while those in C-2 remained upregulated. The C-1 cluster contained 764 genes which include *c fos*, DSS1 (DELETED IN SPLIT-HAND/SPLIT-FOOT 1 REGION), NF-κB p65 subunit, Rac1 (Rho family small GTP-binding protein), and MAP2K1 (mitogen-activated protein kinase kinase 1). The C-2 cluster contained 943 genes which include Interleukin-8, NFKBIA (factor of kappa light polypeptide gene enhancer in B-cells inhibitor, alpha), VCL (vincullin), DUSP1 (dual specificity phosphatase 1), and NDRG1 (N-myc downstream regulated gene 1). The sequential changes in the expression of 2 of C-1 genes and 4 of C-2 genes were confirmed by RT-PCR (Figure 1D). In contrast, the expression of the genes in clusters C-3 (950 genes) showed downregulation at early-phase of infection, and C-4 (651 genes) were downregulated at late phase of infection. At late phase of infection, other functional events were modulated by response to these early events. We next performed to characterize the clusters to identify their function.

Gene expression profile and annotated function

The functional profiles of the *H pylori*-induced changes in gene expression *in vitro* are shown in Table 2. The Onto-Express program was used for functional profiling as described in Materials and Methods, using hypergeometric distribution to determine the significance of differences ($n \geqslant 5$, $P<0.05$). This result indicated that the transiently upregulated C-1 cluster included genes that participate in transcription regulator activity, such as Smad4, *c fos*, and RelA, and others involved in chaperon activity, such as DNAJB1 (DnaJ (Hsp40) homolog, subfamily B, member 1) and CD74 antigen (invariant polypeptide of major histocompatibility complex, class II antigen-associated), more frequently than did the other clusters. The C-2 cluster, the members of which were upregulated during both the early and late phases,

Table 1 Primer sequences for RT-PCR

Genes	Forward	Reverse
IL-8	5′-GCT TTC TGA TGG AAG AGA GC-3′	5′-GGC ACA GTG GAA CAA GGA CT-3′
c-fos	5′-GTC AAG AGC ATC AGC AGCA T-3′	5′-TCG GGG TAG GTG AAG ACG AA-3′
HNRPDL	5′-GTT TCA GAG GAC CTG GAA TA-3′	5′-TCA CTA CCC TAG ACA CCG CA3′
Vinculin	5′-CAA GTG TGA CCG AGT GGA CC-3′	5′-TTG GTA TCA ATG GCT TCG TC-3′
DSS1	5′-CAA GTC TCT ATG GTA GCG TCA GC-3′	5′-ACC ATG TTT CTC TAG TTC AG-3′
NDRG1	5′-GGC GCG ACC TGG AGA TGAG-3′	5′-CTA GCA GGA GAC CTC CAT GG-3′
EMK-1	5′-GAG ATG GAG GTG TGC AAA CT-3′	5′-TGG TTT AGG CGA AAT ACT CT-3′
GAPDH	5′-ACC ACA GTC CAT GCC ATC AC-3′	5′-TCC ACC ACC CTG TTG CTG TA-3′

contained genes related to signal transduction activity, such as TNF receptor-associated factor 4, and those related to structural molecular activity, such as VCL and ARPS2. The genes in the C-3 and C-4 clusters were downregulated by *H pylori*. The C-3 cluster contained genes related to antioxidant activity, such as TXNRD1 (thioredoxin reductase 1) and GPX (glutathione peroxidase) 1/2, and the C-4 cluster contained genes encoding lyase activity, such as GLO1 and

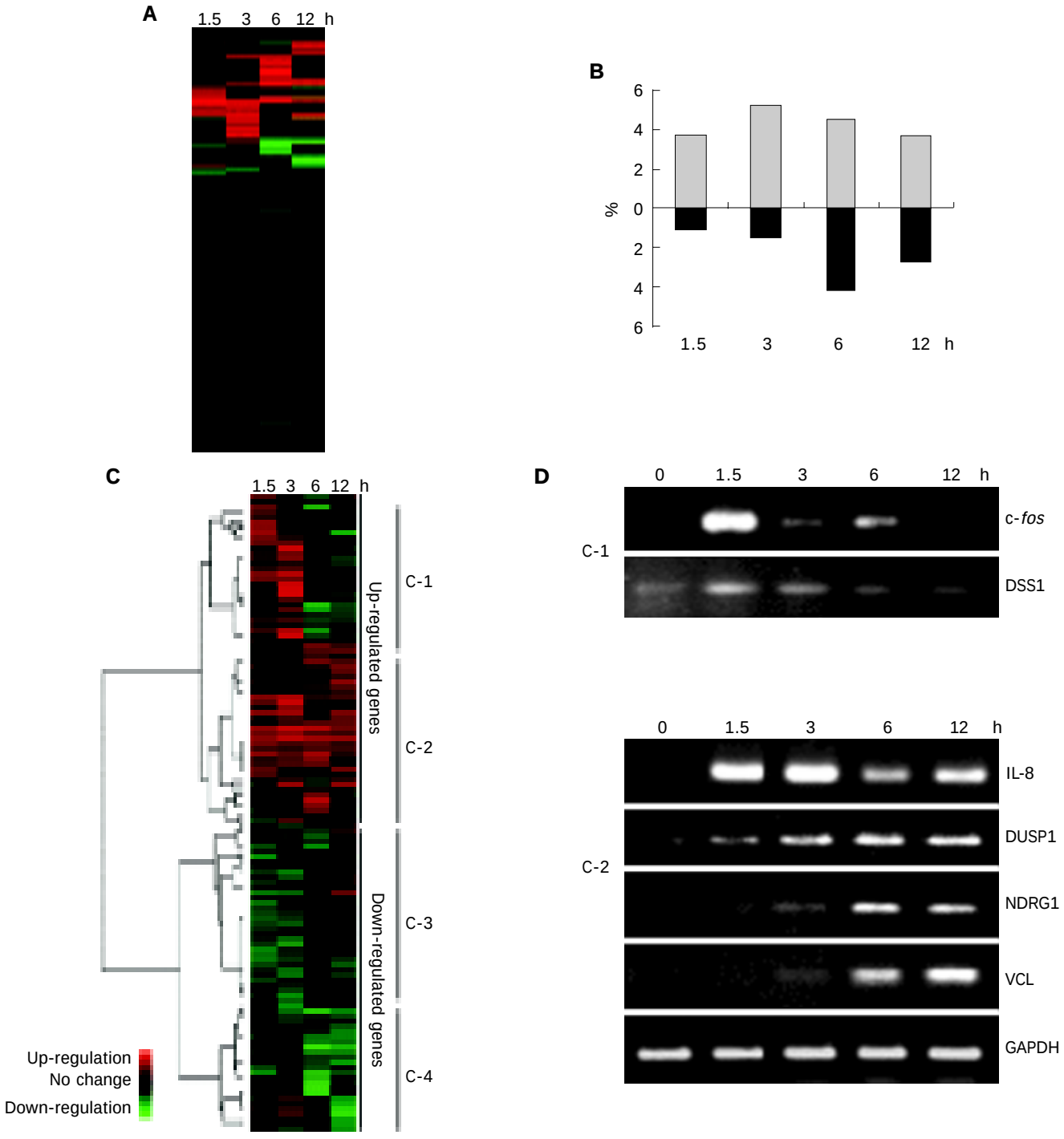

Figure 1 A: Schematic representation of the genes affected by wild-type *H pylori*-infection during 12 h in AGS cells. Red or green indicates up- or downregulation, respectively. About 20% of all the analyzed genes were significantly altered during infection experiments *in vitro*. Changes in expression with a factor of 3 or greater in either direction were considered significant; B: The percentage of the altered genes at each time point. The upregulated genes reached maximum number at 3 h after wild-type *H pylori*-infection, but the downregulated genes peaked at 6 h after infection; C: Cluster diagram of gene expression in AGS cells. The rows correspond to 3 228 genes for which the level of expression in AGS was changed by infection with wild-type *H pylori*, and the columns represent the various time points (1.5, 3, 6, and 12 h after wild-type *H pylori*-infection from left to right, respectively). Red or green indicates up- or downregulation, respectively, compared with the expression level in uninfected AGS cells. The dendrogram on the left and the horizontal distances between the nodes represent the statistical similarities between the neighboring genes and clusters. The genes were divided into two large clusters, comprising upregulated or downregulated genes. Each of the large clusters contained two smaller clusters, resulting in four clusters (C-1 to C-4; see Results for description); D: Validation of the microarray results by RT-PCR. Total RNAs from wild-type *H pylori*-infected AGS cells were isolated at the indicated times and subjected to reverse transcription and PCR with specific primers. The bands of the size corresponding to the expected length of the amplified fragment for each specific transcript were analyzed by agarose gel electrophoresis, along with GAPDH as a loading control.

Table 2 The functional profiles of the *H pylori*-induced changes in gene expression *in vitro*. Cluster represents the assigned cluster numbers in Figure 1C. Functions were defined by using the Onto-Express program, using hypergeometric distribution to determine the significance of differences ($n \geqslant 5$, $P<0.05$, see Materials and methods)

Cluster	Function	No. of the genes (total)	*P*
C-1	Chaperon activity	12 (31)	0.019
	Transcription regulator activity	29 (92)	0.033
C-2	Apoptosis regulator activity	7 (9)	<0.01
	Cell adhesion molecule activity	18 (39)	<0.01
	Signal transducer activity	47 (132)	0.034
	Transcription regulator activity	9 (20)	0.037
	Structural molecular activity	40 (113)	0.049
C-3	Antioxidant activity	6 (8)	<0.01
C-4	Lyase activity	8 (10)	0.011
	Chaperon activity	10 (31)	0.037

ENO1, and chaperone proteins. The genes undergoing most striking upregulation during *H pylori* infection *in vitro* are listed in Table 3.

Contribution of cagPAI-coding type IV secretion system in host gene expression

The contribution of *cag*PAI-coding type IV secretion system in host gene expression was examined by comparing the pattern of expression induced by the wild-type *H pylori vs* the isogenic *cag*E mutant strain. We tried to compare the gene expression profile 3 h post-infection when the number of the upregulated genes were most frequent, and when interleukin-8 (IL-8) which is the gene induced by the functional type IV secretion system was upregulated. Five hundred and sixty-six genes on the microarray were upregulated at least threefold by the wild-type *H pylori* infection 3 h post-infection. Four hundred and seventy-six out of five hundred and sixty-six genes (86%) required *cag*PAI-coding type IV secretion system for their upregulation, whereas only 90 out of 566 genes (14%) were upregulated without functional type IV secretion system (Figure 2A). For example, IL-8, RelA, VCL, and Rac1 were upregulated 3- to 15-fold by infection with the wild-type *H pylori*, while the *cagE* mutant induced only one to threefold increases from the control level. On the other hand, some signal transduction-associated genes were significantly upregulated by the *cag*E mutant infection such as STC2, HKR3, and LZTR1. These genes might be induced by the *cag*-independent virulence factor.

Contribution of NF-κB and ERK pathways in H pylori-induced gene expression

It has been reported that wild-type *H pylori* activates NF-κB and ERK pathways; however, the contribution of these signaling pathways on gene expression profiles has not been investigated. Our analysis of the sequential changes in the gene expression profile revealed that signal transducer activity-associated genes show the continuous expression infected with wild-type *H pylori*. We thus analyzed the contribution of NF-κB and ERK signaling on *H pylori*-induced gene expression by using specific inhibitors as previously described[23,36]. As a control sample, we used AGS cells without adding inhibitor reagents because it could avoid the downregulation of the gene expression of nontreated AGS cells by the inhibitors. Among the 566 genes upregulated by wild-type *H pylori*, the expression of 367 genes (65%) was suppressed by pre-incubation with APDC, an inhibitor of NF-κB (Figure 2B).

Table 3 Genes undergoing most striking upregulation during *H pylori*-infection *in vitro*. Values show the mean change in gene expression from two separate microarray experiments *in vitro* (shown at "1.5, 3, 6, and 12 h"). Significantly upregulated values are shown in bold (above threefold)

Acc. Number	Gene Symbol	Name	Function	1.5 h	3 h	6 h	12 h
U79243	LZTR1	Leucine-zipper-like transcriptional regulator 1	Transcription	5.08	3.08	0.95	2.30
X61118	LMO2	LIM domain only 2 (rhombotin-like 1)	Tumor associated	2.53	16.24	0.28	1.04
BC004247	RAC1	Ras-related C3 botulinum toxin substrate 1 (rho family small GTP binding protein Rac1)	Adhesion/cytoskeleton	1.13	4.78	0.89	1.29
AF005043	PARG	Poly (ADP-ribose) glycohydrolase	Metabolism	0.58	0.62	14.72	0.53
U86782	POH1	26S proteasome-associated pad1 homolog	RNA/Protein processing	2.55	3.59	7.24	3.56
M62839	APOH	Apolipoprotein H (beta-2-glycoprotein I)	Immunity	0.49	3.49	0.65	1.47
BC004980	SLC25A1	Solute carrier family 25 (mitochondrial carrier; citrate transporter) member 1	Metabolism	4.07	0.81	0.95	1.54
Z26649	PLCB3	Phospholipase C beta 3 (phosphatidylinositol-specific)	Tumor associated	2.49	3.32	0.75	2.52
M62399	RELA	V-rel reticuloendotheliosis viral oncogene homolog A nuclear factor of kappa light polypeptide gene enhancer in B-cells 3 p65 (avian)	Apoptosis	2.84	3.24	1.43	1.13
BC000665	TCP1	T-complex 1	RNA/Protein processing	1.73	3.21	1.05	1.41
V01512	c-fos	V01512|HSCFOS Human cellular oncogene c-fos (complete sequence).	Tumor associated	37.81	2.48	0.57	0.91
BC000117	GMDS	GDP-mannose 46-dehydratase	Metabolism	2.63	4.37	2.28	3.75
L29218	CLK2	CDC-like kinase 2	Growth/maintenance	1.46	4.03	1.96	0.60
BC000771	NTRK1	Neurotrophic tyrosine kinase receptor type 1	Tumor associated	3.33	3.47	1.42	3.59
X68836	MAT2A	Methionine adenosyltransferase II alpha	Metabolism	3.14	2.95	0.85	1.28
X94232	MAPRE2	Microtubule-associated protein RP/EB family member 2	Growth/maintenance	0.58	3.23	0.69	0.29
X80200	TRAF4	TNF receptor-associated factor 4	Signal transduction	3.20	3.02	3.67	1.08
D76444	ZFP103	Zinc finger protein 103 homolog (mouse)	Growth/maintenance	1.38	2.63	3.99	1.78

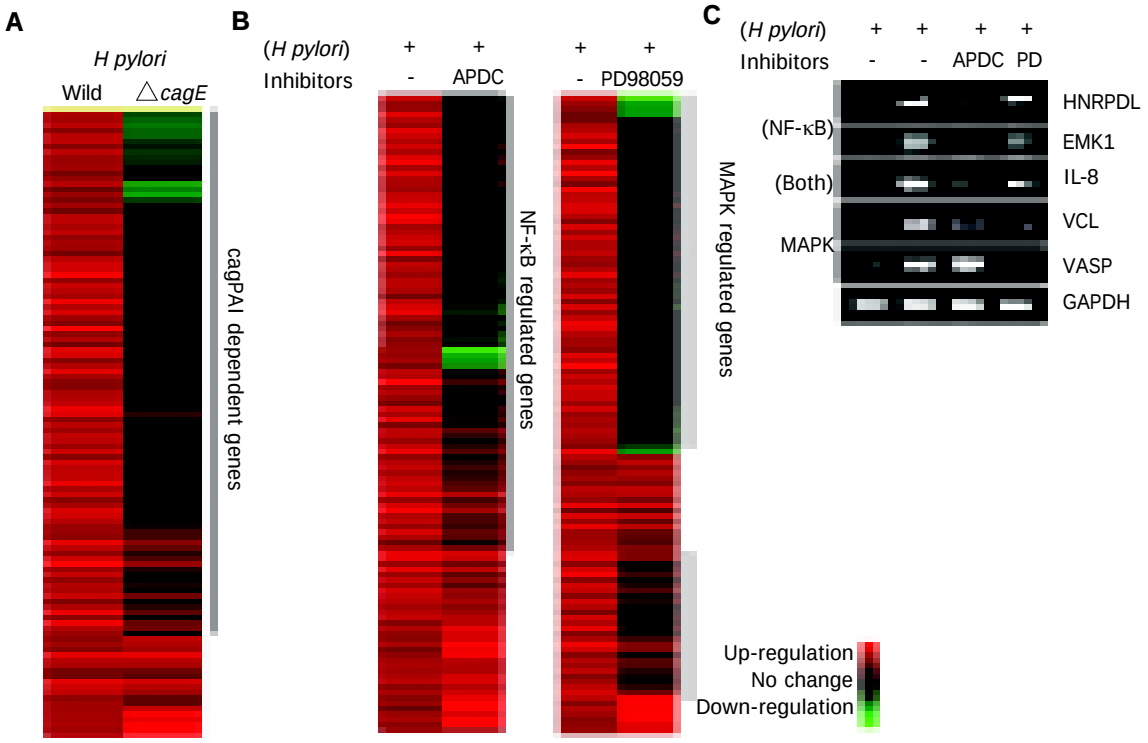

Figure 2 A: The contribution of the *cag*PAI-coded type IV secretion system to the gene expression profile in AGS cells. Hierarchical clustering of genes induced by *H pylori* with or without a functional type IV secretion system (wild type or *cag*E mutant, respectively). Left lane; gene expression profile of AGS cells co-cultured with wild-type *H pylori* relative to control. Right lane; gene expression profile of AGS cells co-cultured with the isogenic mutant *cag*E. Only the 566 significantly upregulated genes at 3 h are shown. About 84% of the genes were induced only by the wild-type *H pylori* infection. These genes were supposed to be induced by the presence of *cag*PAI-coded type IV secretion system. B: The contribution of NF-κB or ERK pathways to the gene expression profile. Inhibitors specific for NF-κB or ERK were added to AGS cells co-cultured with *H pylori*. The gene expression profiles in the presence or absence of the inhibitors were compared. C: The changes in the expression of some representative genes were confirmed by RT-PCR. All genes were induced by wild-type *H pylori* infection, and suppressed by the incubation with inhibitors of specific signal pathways.

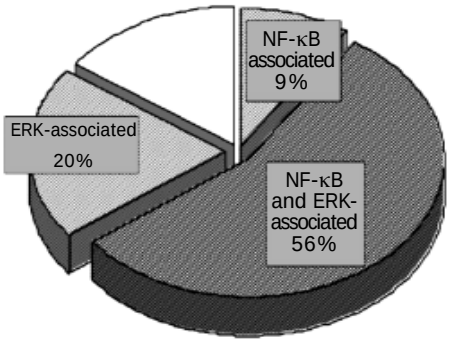

Figure 3 Schematic representation of the distribution of genes affected by wild-type *H pylori* infection. The complete upregulated genes at 3 h after infection is represented by the circle as a whole. The expression of 367 genes (65%) of the 566 genes upregulated by wild type *H pylori* was suppressed by pre-incubation with APDC, an inhibitor of NF-κB. On the other hand, pre-incubation with PD98059, an inhibitor of ERK, suppressed the expression of 429 genes (76%) of the 566 genes upregulated by wild type *H pylori*. Expression of 475 of the 566 genes (84%) was induced under NF-κB and/or ERK signaling activation, whereas changes in the remaining 16% are NF-κB or ERK signaling independent.

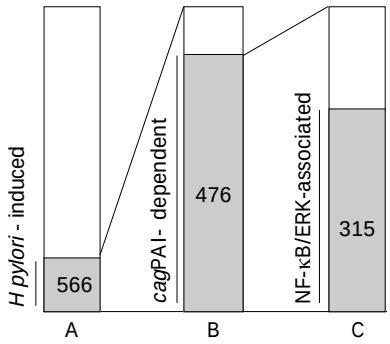

Figure 4 Characterization of the upregulated genes co-cultured with *H pylori* for 3 h (n = 566). A: The bar represents the number of 566 upregulated genes among 3 228 analyzed genes (566 genes). B: The genes induced by *cag*PAI-positive *H pylori* infection among the 566-*H pylori*-induced genes (476 genes). C: The contribution of NF-κB or ERK signaling pathway among the *cag*PAI-dependent gene expression. Among the 476-*cag*PAI-dependent genes, 66% (315 genes) were also involved in the NF-κB- and/or ERK-signaling activation, whereas 34% (161 genes) of 476 genes were dependent on *cag*PAI but not involved in either NF-κB or ERK signaling activation.

The suppressed genes included IL-8, NFKB1A, HNRPDL (heterogeneous nuclear ribonucleoprotein D-like protein) and EMK1 (ELKL motif kinase). On the other hand, pre-incubation with PD98059, an inhibitor of ERK, suppressed the expression of 429 genes (76%). The effects of the inhibitors on several genes were confirmed by RT-PCR (Figure 2C). Among the 566 upregulated genes, 315 genes (56%) were upregulated under NF-κB and ERK signaling activation, and 481 genes (85%) were upregulated under NF-κB and/or ERK signaling activation (Figure 3). HNRPDL was induced at 3.5-fold by wild-type *H pylori* infection, 1.2-fold with APDC, and 2.2-fold with PD98059, and the same

suppression was confirmed by RT-PCR.

It was reported that the activation of NF-κB and ERK by *H pylori* is dependent on the presence of *cag*PAI. Thus, we compared the gene expression profiles under the presence or absence of *cag*PAI-coding type IV secretion system, and we analyzed the contribution of NF-κB or ERK on their gene expression (Figure 4). About 66% (315 genes) of the 476 upregulated genes were induced under NF-κB and/or ERK activation, while 34% (161 genes) of the 476 upregulated genes were dependent on *cag*PAI but not on either NF-κB or ERK.

DISCUSSION

H pylori is now recognized as a definite exogenous carcinogen; hence intensive research effort is currently devoted to investigations of the molecular mechanism of *H pylori*-related gastric pathogenesis. In particular, recent reports have shown the importance of *cag*PAI as a potent bacterial virulence factor and the activation of NF-κB and MAPK signaling as the corresponding host responses[23,36]. However, the relative importance of these factors in gastric pathogenesis among all the events that are raised under *H pylori* infection has not been well established. In the present study, we showed that the genes upregulated by wild-type *H pylori* infection were mostly induced under the presence of *cag*PAI-coding type IV secretion system and that the expression of these genes mostly occurred via NF-κB and/or ERK activation *in vitro*.

Firstly, we analyzed the sequential gene expression changes in cultured cells. The experiments *in vitro* are supposed to simulate the environment in the acute phase of infection and cannot necessarily represent the conditions *in vivo* of chronic infection in which atrophic gastritis and/or gastric cancer actually develops. Therefore we analyzed the sequential changes of gene expression *in vitro* to seek the time-dependent characters of gene function. The genes in the C-1 cluster, which were upregulated during the early phase of infection, included interesting genes which might affect the pathogenesis of *H pylori* infection. *c fos* and DSS1 were included in this cluster. The expression of *c fos* is regulated by ERK (MAPK) signaling and *H pylori* activates the proto-oncogene *c fos* through SRE transactivation[38,66]. DSS1 has not previously been reported to be associated with *H pylori* infection. It has been shown to directly interact with BRCA2 and may play a role in the completion of the cell cycle[67]. The genes in C-2, which were persistently upregulated *in vitro*, contained the genes associated with intracellular signal transduction or cytoskeletal change, including Rho-family GTPases *rac1* and *cdc42*. The activation of them are known to be dependent on *cag*PAI[68]; Rac1 in turn regulates the vacuolation caused by the *vacA* virulence factor of *H pylori*[69]. NDRG1 was upregulated during the late phase of infection as shown in Figure 1D; the protein encoded by this gene is a cytoplasmic protein involved in stress responses, hormone responses, cell growth, and differentiation[70].

We show here that the upregulation of a large part of the genes depends on the presence of functional type IV secretion system. *Cag*PAI codes a type IV secretion system which transports CagA inside the host cells[11-15]; the transported CagA activates SRE[37]. Guilemin *et al*., reported that *cag*A gene, which encodes an effector molecule secreted by the type IV secretion system, induced the expression of many of the cytoskeletal genes. Recently, it has been reported that one of the effectors for NF-κB activation is peptidoglycan[16], and CagA is probably not involved[37,71,72]. In addition, *cag*E, which codes a structural component of the type IV secretion system, is required for the expression of many immune responsive genes. These results suggest that several distinct molecules are involved in *cag*PAI-dependent upregulation. Moreover, the interaction of some molecules of the secretion system with the molecules of the host cell might directly activate some intracellular signaling cascades.

The microarray analysis is useful to identify the downstream genes in the specific intracellular signaling pathway because it could detect a large number of the gene expression at a time. Then we analyzed the alteration of the gene expression by the inhibitor reagents against the signaling molecules to identify the genes which are induced through NF-κB or ERK signaling pathway. In this study, we have shown that the majority of the *H pylori*-induced gene were upregulated under NF-κB and/or ERK activation[23,36] NF-κB activation *in vivo* is associated with gastric inflammation via the production of cytokines, IL-8[24] and is associated with cell survival induced by c-IAP-2 mediated anti-apoptosis[35]. Among the genes affected by NF-κB activation, HNRPDL and EMK1 were identified in the current microarray analysis and were confirmed by RT-PCR to be suppressed by NF-κB inhibition. HNRPDL is reported to be a member of the family of heterogeneous nuclear ribonucleoproteins (hnRNPs) that function in mRNA biogenesis and mRNA metabolism[73]. EMK (ELKL motif kinase) belongs to a small family of serine/threonine protein kinases involved in the control of cell polarity, microtubule stability, and cancer[74].

ERK signaling is activated by *H pylori* infection and leads to the expression of some oncogenes, such as *c fos* and cyclin-D1[75,76]. The upregulated genes under ERK-signaling activation included VCL and VASP, which are involved in integrin-mediated cell adhesion. Jawhari *et al*., reported that E-cadherin contributes to the development and progression of the neoplastic phenotype in gastric carcinoma[77]. Kuroda *et al*., reported that the activation of Rho-Ras signaling induces the dissociation of cell-cell adhesion and it is associated with the cell migration and metastasis of carcinoma cells[78]. Recently, Cottet *et al*., identified that *H pylori*-induced Rho-Ras signaling proteins[79].

In conclusion, we characterized the gene expression induced by *H pylori* using cDNA microarray, and we determined the contribution of *cag*PAI-coding type IV secretion system and NF-κB/ERK signaling pathways on the most part of the gene expression induced by *H pylori*. In the future, we should elucidate how the NF-κB and/or ERK contribute to the development of gastric inflammation *in vivo* and characterize the gastric mucosal gene expression in human beings which may help us to understand the gastric pathogenesis induced by *H pylori* infection.

ACKNOWLEDGMENTS

We thank Mitsuko Tsubouchi for her excellent technical assistance.

REFERENCES

1 **Marshall BJ**, Warren JR. Unidentified curved bacilli in the stomach of patients with gastritis and peptic ulceration. *Lancet* 1984; **1**: 1311-1315
2 Schistosomes, liver flukes and *Helicobacter pylori*. IARC Working Group on the Evaluation of Carcinogenic Risks to Humans. Lyon, 7-14 June 1994. *IARC Monogr Eval Carcinog Risks Hum* 1994; **61**: 1-241
3 **Parsonnet J**, Friedman GD, Vandersteen DP, Chang Y, Vogelman JH, Orentreich N, Sibley RK. *Helicobacter pylori* infection and the risk of gastric carcinoma. *N Engl J Med* 1991; **325**: 1127-1131
4 **Nomura A**, Stemmermann GN, Chyou PH, Kato I, Perez-Perez GI, Blaser MJ. *Helicobacter pylori* infection and gastric carcinoma among Japanese Americans in Hawaii. *N Engl J Med* 1991; **325**: 1132-1136
5 **Graham DY**, Lew GM, Klein PD, Evans DG, Evans DJ Jr, Saeed ZA, Malaty HM. Effect of treatment of *Helicobacter pylori* infection on the long-term recurrence of gastric or duodenal ulcer. A randomized, controlled study. *Ann Intern Med* 1992; **116**: 705-708
6 **Wotherspoon AC**, Doglioni C, Diss TC, Pan L, Moschini A, de Boni M, Isaacson PG. Regression of primary low-grade B-cell gastric lymphoma of mucosa-associated lymphoid tissue type after eradication of *Helicobacter pylori*. *Lancet* 1993; **342**: 575-577
7 **Forbes GM**, Glaser ME, Cullen DJ, Warren JR, Christiansen KJ, Marshall BJ, Collins BJ. Duodenal ulcer treated with *Helicobacter pylori* eradication: seven-year follow-up. *Lancet* 1994; **343**: 258-260
8 **Sung JJ**, Lin SR, Ching JY, Zhou LY, To KF, Wang RT, Leung WK, Ng EK, Lau JY, Lee YT, Yeung CK, Chao W, Chung SC. Atrophy and intestinal metaplasia one year after cure of *H pylori* infection: a prospective, randomized study. *Gastroenterology* 2000; **119**: 7-14
9 **Uemura N**, Okamoto S, Yamamoto S, Matsumura N, Yamaguchi S, Yamakido M, Taniyama K, Sasaki N, Schlemper RJ. *Helicobacter pylori* infection and the development of gastric cancer. *N Engl J Med* 2001; **345**: 784-789
10 **Peek RM Jr**, Blaser MJ. *Helicobacter pylori* and gastrointestinal tract adenocarcinomas. *Nat Rev Cancer* 2002; **2**: 28-37
11 **Backert S**, Ziska E, Brinkmann V, Zimny-Arndt U, Fauconnier A, Jungblut PR, Naumann M, Meyer TF. Translocation of the *Helicobacter pylori* CagA protein in gastric epithelial cells by a type IV secretion apparatus. *Cell Microbiol* 2000; **2**: 155-164
12 **Odenbreit S**, Puls J, Sedlmaier B, Gerland E, Fischer W, Haas R. Translocation of *Helicobacter pylori* CagA into gastric epithelial cells by type IV secretion. *Science* 2000; **287**: 1497-1500
13 **Segal ED**, Cha J, Lo J, Falkow S, Tompkins LS. Altered states: involvement of phosphorylated CagA in the induction of host cellular growth changes by *Helicobacter pylori*. *Proc Natl Acad Sci USA* 1999; **96**: 14559-14564
14 **Stein M**, Rappuoli R, Covacci A. Tyrosine phosphorylation of the *Helicobacter pylori* CagA antigen after cag-driven host cell translocation. *Proc Natl Acad Sci USA* 2000; **97**: 1263-1268
15 **Asahi M**, Azuma T, Ito S, Ito Y, Suto H, Nagai Y, Tsubokawa M, Tohyama Y, Maeda S, Omata M, Suzuki T, Sasakawa C. *Helicobacter pylori* CagA protein can be tyrosine phosphorylated in gastric epithelial cells. *J Exp Med* 2000; **191**: 593-602
16 **Viala J**, Chaput C, Boneca IG, Cardona A, Girardin SE, Moran AP, Athman R, Memet S, Huerre MR, Coyle AJ, DiStefano PS, Sansonetti PJ, Labigne A, Bertin J, Philpott DJ, Ferrero RL. Nod1 responds to peptidoglycan delivered by the *Helicobacter pylori* cag pathogenicity island. *Nat Immunol* 2004; **5**: 1166-1174
17 **Mimuro H**, Suzuki T, Tanaka J, Asahi M, Haas R, Sasakawa C. Grb2 is a key mediator of *helicobacter pylori* CagA protein activities. *Molecular Cell* 2002; **10**: 745-755
18 **Higashi H**, Tsutsumi R, Muto S, Sugiyama T, Azuma T, Asaka M, Hatakeyama M. SHP-2 tyrosine phosphatase as an intracellular target of *Helicobacter pylori* CagA protein. *Science* 2002; **295**: 683-686
19 **Churin Y**, Al-Ghoul L, Kepp O, Meyer TF, Birchmeier W, Naumann M. *Helicobacter pylori* CagA protein targets the c-Met receptor and enhances the motogenic response. *J Cell Biol* 2003; **161**: 249-255
20 **Amieva MR**, Vogelmann R, Covacci A, Tompkins LS, Nelson WJ, Falkow S. Disruption of the epithelial apical-junctional complex by *Helicobacter pylori* CagA. *Science* 2003; **300**: 1430-1434
21 **Peek RM Jr**, Moss SF, Tham KT, Perez-Perez GI, Wang S, Miller GG, Atherton JC, Holt PR, Blaser MJ. *Helicobacter pylori* cagA+strains and dissociation of gastric epithelial cell proliferation from apoptosis. *J Natl Cancer Inst* 1997; **89**: 863-868
22 **Argent RH**, Kidd M, Owen RJ, Thomas RJ, Limb MC, Atherton JC. Determinants and consequences of different levels of CagA phosphorylation for clinical isolates of *Helicobacter pylori*. *Gastroenterology* 2004; **127**: 514-523
23 **Keates S**, Hitti YS, Upton M, Kelly CP. *Helicobacter pylori* infection activates NF-kappa B in gastric epithelial cells. *Gastroenterology* 1997; **113**: 1099-1109
24 **Sharma SA**, Tummuru MK, Blaser MJ, Kerr LD. Activation of IL-8 gene expression by *Helicobacter pylori* is regulated by transcription factor nuclear factor-kappa B in gastric epithelial cells. *J Immunol* 1998; **160**: 2401-2407
25 **Aihara M**, Tsuchimoto D, Takizawa H, Azuma A, Wakebe H, Ohmoto Y, Imagawa K, Kikuchi M, Mukaida N, Matsushima K. Mechanisms involved in *Helicobacter pylori*-induced interleukin-8 production by a gastric cancer cell line, MKN45. *Infect Immun* 1997; **65**: 3218-3224
26 **Meyer-ter-Vehn T**, Covacci A, Kist M, Pahl HL. *Helicobacter pylori* activates mitogen-activated protein kinase cascades and induces expression of the proto-oncogenes c-fos and c-jun. *J Biol Chem* 2000; **275**: 16064-16072
27 **Barnes PJ**, Karin M. Nuclear factor-kappaB: a pivotal transcription factor in chronic inflammatory diseases. *N Engl J Med* 1997; **336**: 1066-1071
28 **Baeuerle PA**. IkappaB-NF-kappaB structures: at the interface of inflammation control. *Cell* 1998; **95**: 729-731
29 **Ghosh S**, May MJ, Kopp EB. NF-kappa B and Rel proteins: evolutionarily conserved mediators of immune responses. *Annu Rev Immunol* 1998; **16**: 225-260
30 **Sha WC**. Regulation of immune responses by NF-kappa B/Rel transcription factor. *J Exp Med* 1998; **187**: 143-146
31 **Neurath MF**, Becker C, Barbulescu K. Role of NF-kappaB in immune and inflammatory responses in the gut. *Gut* 1998; **43**: 856-860
32 **Munzenmaier A**, Lange C, Glocker E, Covacci A, Moran A, Bereswill S, Baeuerle PA, Kist M, Pahl HL. A secreted/shed product of *Helicobacter pylori* activates transcription factor nuclear factor-kappa B. *J Immunol* 1997; **159**: 6140-6147
33 **Eckmann L**, Smith JR, Housley MP, Dwinell MB, Kagnoff MF. Analysis by high density cDNA arrays of altered gene expression in human intestinal epithelial cells in response to infection with the invasive enteric bacteria Salmonella. *J Biol Chem* 2000; **275**: 14084-14094
34 **Noach LA**, Bosma NB, Jansen J, Hoek FJ, van Deventer SJ, Tytgat GN. Mucosal tumor necrosis factor-alpha, interleukin-1 beta, and interleukin-8 production in patients with *Helicobacter pylori* infection. *Scand J Gastroenterol* 1994; **29**: 425-429
35 **Yanai A**, Hirata Y, Mitsuno Y, Maeda S, Shibata W, Akanuma M, Yoshida H, Kawabe T, Omata M. *Helicobacter pylori* induces antiapoptosis through buclear factor-kappaB activation. *J Infect Dis* 2003; **188**: 1741-1751
36 **Keates S**, Keates AC, Warny M, Peek RM Jr, Murray PG, Kelly CP. Differential activation of mitogen-activated protein kinases in AGS gastric epithelial cells by cag+ and cag- *Helicobacter pylori*. *J Immunol* 1998; **66**: 5552-5559

37 **Hirata Y**, Maeda S, Mitsuno Y, Tateishi K, Yanai A, Akanuma M, Yoshida H, Kawabe T, Shiratori Y, Omata M. *Helicobacter pylori* CagA protein activates serum response element-driven transcription independently of tyrosine phosphorylation. *Gastroenterology* 2002; **123**: 1962-1971

38 **Mitsuno Y**, Maeda S, Yoshida H, Hirata Y, Ogura K, Akanuma M, Kawabe T, Shiratori Y, Omata M. *Helicobacter pylori* activates the proto-oncogene c-fos through SRE transactivation. *Biochem Biophys Res Commun* 2002; **291**: 868-874

39 **Han J**, Lee JD, Bibbs L, Ulevitch RJ. A MAP kinase targeted by endotoxin and hyperosmolarity in mammalian cells. *Science* 1994; **265**: 808-811

40 **Kyriakis JM**, Banerjee P, Nikolakaki E, Dai T, Rubie EA, Ahmad MF, Avruch J, Woodgett JR. The stress-activated protein kinase subfamily of c-Jun kinases. *Nature* 1994; **369**: 156-160

41 **Lee JC**, Laydon JT, McDonnell PC, Gallagher TF, Kumar S, Green D, McNulty D, Blumenthal MJ, Heys JR, Landvatter SW. A protein kinase involved in the regulation of inflammatory cytokine biosynthesis. *Nature* 1994; **372**: 739-746

42 **Schena M**, Shalon D, Davis RW, Brown PO. Quantitative monitoring of gene expression patterns with a complementary DNA microarray. *Science* 1995; **270**: 467-470

43 **Schena M**, Shalon D, Heller R, Chai A, Brown PO, Davis RW. Parallel human genome analysis: microarray-based expression monitoring of 1000 genes. *Proc Natl Acad Sci USA* 1996; **93**: 10614-10619

44 **Maeda S**, Otsuka M, Hirata Y, Mitsuno Y, Yoshida H, Shiratori Y, Masuho Y, Muramatsu M, Seki N, Omata M. cDNA microarray analysis of *Helicobacter pylori*-mediated alteration of gene expression in gastric cancer cells. *Biochem Biophys Res Commun* 2001; **284**: 443-449

45 **Cox JM**, Clayton CL, Tomita T, Wallace DM, Robinson PA, Crabtree JE. cDNA array analysis of cag pathogenicity island-associated *Helicobacter pylori* epithelial cell response genes. *Infect Immun* 2001; **69**: 6970-6980

46 **Guillemin K**, Salama NR, Tompkins LS, Falkow S. Cag pathogenicity island-specific responses of gastric epithelial cells to *Helicobacter pylori* infection. *Proc Natl Acad Sci USA* 2002; **99**: 15136-15141

47 **Bach S,** Makristathis A, Rotter M, Hirschl AM. Gene expression profiling in AGS cells stimulated with *Helicobacter pylori* isogenic strains (cagA positive or cagA negative). *Infect Immun* 2002; **70**: 988-992

48 **Lim JW**, Kim H, Kim KH. Cell adhesion-related gene expression by *Helicobacter pylori* in gastric epithelial AGS cells. *Int J Biochem Cell Biol* 2003; **35**: 1284-1296

49 **Sepulveda AR**, Tao H, Carloni E, Sepulveda J, Graham DY, Peterson LE. Screening of gene expression profiles in gastric epithelial cells induced by *Helicobacter pylori* using microarray analysis. *Aliment Pharmacol Ther* 2002; **16**(Suppl 2): 145-157

50 **Wang HT**, Li ZH, Yuan JP, Zhao W, Shi XD, Tong SQ, Guo XK. Effect of *Helicobacter pylori* VacA on gene expression of gastric cancer cells. *World J Gastroenterol* 2004; **10**: 109-113

51 **Yuan JP**, Li T, Li ZH, Yang GZ, Hu BY, Shi XD, Shi TL, Tong SQ, Guo XK. mRNA expression profiling reveals a role of *Helicobacter pylori* vacuolating toxin in escaping host defense. *World J Gastroenterol* 2004; **10**: 1528-1532

52 **Wen S**, Felley CP, Bouzourene H, Reimers M, Michetti P, Pan-Hammarstrom Q. Inflammatory gene profiles in gastric mucosa during *Helicobacter pylori* infection in humans. *J Immunol* 2004; **172**: 2595-2606

53 **Mills JC**, Syder AJ, Hong CV, Guruge JL, Raaii F, Gordon JI. A molecular profile of the mouse gastric parietal cell with and without exposure to *Helicobacter pylori*. *Proc Natl Acad Sci USA* 2001; **98**: 13687-13692

54 **Mueller A**, O'Rourke J, Grimm J, Guillemin K, Dixon MF, Lee A, Falkow S. Distinct gene expression profiles characterize the histopathological stages of disease in Helicobacter-induced mucosa-associated lymphoid tissue lymphoma. *Proc Natl Acad Sci USA* 2003; **100**: 1292-1297

55 **Ogura K**, Maeda S, Nakao M, Watanabe T, Tada M, Kyutoku T, Yoshida H, Shiratori Y, Omata M. Virulence factors of *Helicobacter pylori* responsible for gastric diseases in Mongolian gerbil. *J Exp Med* 2000; **192**: 1601-1610

56 **Maeda S**, Yoshida H, Ogura K, Mitsuno Y, Hirata Y, Yamaji Y, Akanuma M, Shiratori Y, Omata M. *H pylori* activates NF-kappaB through a signaling pathway involving IkappaB kinases, NF-kappaB-inducing kinase, TRAF2, and TRAF6 in gastric cancer cells. *Gastroenterology* 2000; **119**: 97-108

57 **Maeda S**, Akanuma M, Mitsuno Y, Hirata Y, Ogura K, Yoshida H, Shiratori Y, Omata M. Distinct mechanism of *Helicobacter pylori*-mediated NF-kappa B activation between gastric cancer cells and monocytic cells. *J Biol Chem* 2001; **276**: 44856-44864

58 **Dudley DT**, Pang L, Decker SJ, Bridges AJ, Saltiel AR. A synthetic inhibitor of the mitogen-activated protein kinase cascade. *Proc Natl Acad Sci USA* 1995; **92**: 7686-7689

59 **Otsuka M**, Kato M, Yoshikawa T, Chen H, Brown EJ, Masuho Y, Omata M, Seki N. Differential expression of the L-plastin gene in human colorectal cancer progression and metastasis. *Biochem Biophys Res Commun* 2001; **289**: 876-881

60 **Otsuka M**, Aizaki H, Kato N, Suzuki T, Miyamura T, Omata M, Seki N. Differential cellular gene expression induced by hepatitis B and C viruses. *Biochem Biophys Res Commun* 2003; **300**: 443-447

61 **Mori M**, Shimada H, Gunji Y, Matsubara H, Hayashi H, Nimura Y, Kato M, Takiguchi M, Ochiai T, Seki N. S100A11 gene identified by in-house cDNA microarray as an accurate predictor of lymph node metastases of gastric cancer. *Oncology Reports* 2004; **11**: 1287-1293

62 **Eisen MB**, Spellman PT, Brown PO, Botstein D. Cluster analysis and display of genome-wide expression patterns. *Proc Natl Acad Sci USA* 1998; **95**: 14863-14868

63 **Draghici S**, Khatri P, Bhavsar P, Shah A, Krawetz SA, Tainsky MA. Onto-Tools, the toolkit of the modern biologist: Onto-Express, Onto-Compare, Onto-Design and Onto-Translate. *Nucleic Acids Res* 2002; **79**: 3775-3781

64 **Khatri P**, Draghici S, Ostermeier GC, Krawetz SA. Profiling gene expression using onto-express. *Genomics* 2002; **79**: 266-270

65 **Draghici S**, Khatri P, Martins RP, Ostermeier GC, Krawetz SA. Global functional profiling of gene expression. *Genomics* 2003; **81**: 98-104

66 **Yang YL**, Xu B, Song YG, Zhang WD. Overexpression of c-fos in *Helicobacter pylori*-induced gastric precancerosis of Mongolian gerbil. *World J Gastroenterol* 2003; **9**: 521-524

67 **Yang H**, Jeffrey PD, Miller J, Kinnucan E, Sun Y, Thoma NH, Zheng N, Chen PL, Lee WH, Pavletich NP. BRCA2 function in DNA binding and recombination from a BRCA2-DSS1-ssDNA structure. *Science* 2002; **297**: 1837-1848

68 **Churin Y**, Kardalinou E, Meyer TF, Naumann M. Pathogenicity island-dependent activation of Rho GTPases Rac1 and Cdc42 in *Helicobacter pylori* infection. *Mol Microbiol* 2001; **40**: 815-823

69 **Hotchin NA**, Cover TL, Akhtar N. Cell vacuolation induced by the VacA cytotoxin of *Helicobacter pylori* is regulated by the Rac1 GTPase. *J Biol Chem* 2000; **275**: 14009-14012

70 **van Belzen N**, Dinjens WN, Diesveld MP, Groen NA, van der Made AC, Nozawa Y, Vlietstra R, Trapman J, Bosman FT. A novel gene which is up-regulated during colon epithelial cell differentiation and down-regulated in colorectal neoplasms. *Lab Invest* 1997; **77**: 85-92

71 **Crabtree JE**, Xiang Z, Lindley IJ, Tompkins DS, Rappuoli R, Covacci A. Induction of interleukin-8 secretion from gastric epithelial cells by a cagA negative isogenic mutant of *Helicobacter pylori*. *J Clin Pathol* 1995; **48**: 967-969

72 **Sharma SA**, Tummuru MK, Miller GG, Blaser MJ. Interleukin-8 response of gastric epithelial cell lines to *Helicobacter pylori* stimulation *in vitro*. *Infect Immun* 1995; **63**: 1681-1687

73 **Tsuchiya N**, Kamei D, Takano A, Matsui T, Yamada M. Cloning and characterization of a cDNA encoding a novel hetero-

geneous nuclear ribonucleoprotein-like protein and its expression in myeloid leukemia cells. *J Biochem* 1998; **123**: 499-507

74 **Espinosa L**, Navarro E. Human serine/threonine protein kinase EMK1: genomic structure and cDNA cloning of isoforms produced by alternative splicing. *Cytogenet Cell Genet* 1998; **81**: 278-282

75 **Hirata Y**, Maeda S, Mitsuno Y, Akanuma M, Yamaji Y, Ogura K, Yoshida H, Shiratori Y, Omata M. *Helicobacter pylori* activates the cyclin D1 gene through mitogen-activated protein kinase pathway in gastric cancer cells. *Infect Immun* 2001; **69**: 3965-3971

76 **Mitsuno Y**, Yoshida H, Maeda S, Ogura K, Hirata Y, Kawabe T, Shiratori Y, Omata M. *Helicobacter pylori* induced transactivation of SRE and AP-1 through the ERK signalling pathway in gastric cancer cells. *Gut* 2001; **49**: 18-22

77 **Jawhari AU**, Noda M, Farthing MJ, Pignatelli M. Abnormal expression and function of the E-cadherin-catenin complex in gastric carcinoma cell lines. *Br J Cancer* 1999; **80**: 322-330

78 **Kuroda S**, Fukata M, Nakagawa M, Fujii K, Nakamura T, Ookubo T, Izawa I, Nagase T, Nomura N, Tani H, Shoji I, Matsuura Y, Yonehara S, Kaibuchi K. Role of IQGAP1, a target of the small GTPases Cdc42 and Rac1, in regulation of E-cadherin- mediated cell-cell adhesion. *Science* 1998; **281**: 832-835

79 **Cottet S**, Corthesy-Theulaz I, Spertini F, Corthesy B. Microaerophilic conditions permit to mimic in vitro events occurring during in vivo *Helicobacter pylori* infection and to identify Rho/Ras-associated proteins in cellular signaling. *J Biol Chem* 2002; **277**: 33978-33986

Science Editor Guo SY **Language Editor** Elsevier HK

PO Box 2345, Beijing 100023, China
www.wjgnet.com
wjg@wjgnet.com

ELSEVIER

World J Gastroenterol 2005;11(39):6144-6151
World Journal of Gastroenterology ISSN 1007-9327

• *BASIC RESEARCH* •

Endothelin-1 stimulates contraction and migration of rat pancreatic stellate cells

Atsushi Masamune, Masahiro Satoh, Kazuhiro Kikuta, Noriaki Suzuki, Kennichi Satoh, Tooru Shimosegawa

Atsushi Masamune, Masahiro Satoh, Kazuhiro Kikuta, Noriaki Suzuki, Kennichi Satoh, Tooru Shimosegawa, Division of Gastroenterology, Tohoku University Graduate School of Medicine, Sendai, Japan
Supported by Grant-in-Aid for Encouragement of Young Scientists from Japan Society for the Promotion of Science, No. 16590572 (to AM.), by Pancreas Research Foundation of Japan, No. 01-01 (to AM.), by the Kanae Foundation for Life and Socio-Medical Science (to AM), and by the Uehara Memorial Foundation (to AM)
Correspondence to: Dr. Atsushi Masamune, Division of Gastroenterology, Tohoku University Graduate School of Medicine, 1-1 Seiryo-machi, Aoba-ku, Sendai 980-8574, Japan. amasamune@int3.med.tohoku.ac.jp
Telephone: +81-22-717-7171 Fax: +81-22-717-7177
Received: 2004-12-19 Accepted: 2005-02-18

Abstract

AIM: To examine the ability of ET-1 to affect the cell functions of PSCs and the underlying molecular mechanisms.

METHODS: PSCs were isolated from the pancreas of male Wistar rats after perfusion with collagenase, and cells between passages two and five were used. Expression of ET-1 and ET receptors was assessed by reverse transcription-PCR and immunostaining. Phosphorylation of myosin regulatory light chain (MLC), extracellular-signal regulated kinase (ERK), and Akt was examined by Western blotting. Contraction of PSCs was assessed on hydrated collagen lattices. Cell migration was examined using modified Boyden chambers. Cell proliferation was assessed by measuring the incorporation of 5-bromo-2'-deoxyuridine.

RESULTS: Culture-activated PSCs expressed ET_A and ET_B receptors, and ET-1. ET-1 induced phosphorylation of MLC and ERK, but not Akt. ET-1 induced contraction and migration, but did not alter proliferation of PSCs. ET-1-induced contraction was inhibited by an ET_A receptor antagonist BQ-123 and an ET_B receptor antagonist BQ-788, whereas migration was inhibited by BQ-788 but not by BQ-123. A Rho kinase inhibitor Y-27632 abolished both contraction and migration.

CONCLUSION: ET-1 induced contraction and migration of PSCs through ET receptors and activation of Rho-Rho kinase. ET_A and ET_B receptors play different roles in the regulation of these cellular functions in response to ET-1.

Key words: Pancreatitis; Pancreatic fibrosis; Pancreatic stellate cells; Endothelin-1; Rho kinase

Masamune A, Satoh M, Kikuta K, Suzuki N, Satoh K, Shimosegawa T. Endothelin-1 stimulates contraction and migration of rat pancreatic stellate cells. *World J Gastroenterol* 2005; 11(39): 6144-6151
http://www.wjgnet.com/1007-9327/11/6144.asp

INTRODUCTION

In 1998, star-shaped cells in the pancreas, namely pancreatic stellate cells (PSCs), were identified and characterized[1,2]. In normal pancreas, stellate cells are quiescent and can be identified by the presence of vitamin A-containing lipid droplets in the cytoplasm. In response to pancreatic injury or inflammation, they are transformed ("activated") from their quiescent phenotype into myofibroblast-like cells, which actively proliferate, express the cytoskeletal protein α-smooth muscle actin, and produce extracellular matrix components. Many of the morphological and metabolic changes associated with the activation of PSCs in animal models of fibrosis also occur when these cells are grown in serum-containing medium in culture on plastic. There is accumulating evidence that activated PSCs play a pivotal role in the development of pancreatic fibrosis[1-4]. In addition, PSCs may participate in the pathogenesis of acute pancreatitis[3,5]. The activation of signal transduction pathways such as p38 mitogen-activated protein (MAP) kinase[6], Rho-Rho kinase[7], and c-Jun N-terminal kinase[8] is likely to play a role in PSC activation. But intracellular signal transduction pathways in PSCs remain largely unknown.

Endothelin-1 (ET-1), which acts through G-protein coupled ET_A and ET_B receptors, was initially described as a potent endothelial cell-derived vasoconstrictor isolated from the culture medium of porcine aortic endothelial cells[9]. Subsequent studies have shown that ET-1 is produced by a variety of cells and exhibits several biological activities such as vasoconstriction, regulation of peptide secretion, migration, and positive or negative effects on cell growth[10,11]. ET-1 has been implicated in the pathogenesis of cardiovascular, pulmonary, renal, and developmental disorders[11]. In addition, ET-1 plays a key role in the development of portal hypertension and hepatic fibrosis through its effects on hepatic stellate cells[12,13]. ET-1 has been shown to stimulate contraction via ET_A receptor[14], and inhibit proliferation via ET_B receptor[15] in hepatic stellate cells. But, the roles of ET-1 and ET receptors in the regulation of cell functions of PSCs remain largely unknown. In this study, we examined

the ability of ET-1 to affect the cell functions of PSCs and the underlying molecular mechanisms. We here report that ET-1 stimulated contraction and migration, but not proliferation, of PSCs through ET receptors and Rho-Rho kinase pathway.

MATERIALS AND METHODS

Materials

ET-1 was purchased from Peptide Institute (Osaka, Japan). Collagenase P was obtained from Roche Diagnostics (Mannheim, Germany). Rat recombinant platelet-derived growth factor (PDGF)-BB was purchased from R&D Systems (Minneapolis, MN). Rhodamine-labeled phalloidin was purchased from Molecular Probes (Eugene, OR). BQ-123, BQ-788, and U0126 were purchased from Calbiochem (La Jolla, CA). Y-27632 was a generous gift from Mitsubishi Pharma Co. (Osaka, Japan). Rabbit antibodies against extracellular-signal regulated kinase (ERK; phosphorylated and total), Akt (phosphorylated at Ser^{473} and total), and myosin regulatory light chain II (MLC; phosphorylated at Ser^{19} and total) were purchased from Cell Technologies, Inc. (Beverly, MA). Rabbit antibody against glyceraldehyde-3-phosphate dehydrogenase (GAPDH) was obtained from Trevigen (Gaithersburg, MD). All other reagents were purchased from Sigma-Aldrich (St. Louis, MO) unless specifically described.

Cell culture

All animal procedures were performed in accordance with the National Institutes of Health Animal Care and Use Guidelines. Rat PSCs were prepared from the pancreas tissues of male Wistar rats (Japan SLC Inc., Hamamatsu, Japan) weighing 200-250 g using the Nycodenz solution (Nycomed Pharma, Oslo, Norway) after perfusion with 0.3 g/L collagenase P as previously described[16]. The cells were resuspended in Ham's F-12 medium containing 100 mL/L heat-inactivated fetal bovine serum (MP Biomedicals, Irvine, CA), penicillin sodium, and streptomycin sulfate. Cell purity was always more than 90% as assessed by a typical star-like configuration and by detecting vitamin A autofluorescence. All experiments were performed using cells between passages two and five. We incubated PSCs in serum-free medium for 24 h before the addition of experimental reagents. For some experiments, BQ-123, BQ-788, U0126, or Y-27632 were added 30 min prior to the ET-1 treatment.

Reverse transcription-PCR

Total RNA was isolated using RNeasy total RNA preparation kit (Qiagen, Chatsworth, CA). Total RNA was reverse-transcribed, and the resultant cDNA was subjected to PCR as previously reported[17]. Specific primer sets were as follows (listed 5'-3'; forward and reverse, respectively). ET-1 precursor (preproET-1): TTGCTCCTGCTCCTC-CTTGAG and GGTCTTGATGCTGTTGCTGATG; ET_A: CGTCTTCTGCTTGGTTGTCA and TGGTTCT-GCTCCTGGTTCTT; ET_B CAAGACAGTATTCTGC CTGG and CAAGCAGGATTGCTTCTCCT. They were amplified using 30 cycles at 94 ℃ (for 1 min), at 50 ℃ (for 1 min), and at 72 ℃ (for 1 min). The products of PCR were separated by 15 g/L agarose gel electrophoresis and visualized under ultraviolet light after staining with ethidium bromide. The expected sizes of the PCR products were 382 bp for preproET-1, 321 bp for ET_A receptor, and 297 bp for ET_B receptor.

Immunostaining

PSCs were grown directly on slides, serum-starved for 24 h, and immunostaining for ET-1 was performed using a streptavidin-biotin peroxidase complex detection kit (Histofine Kit; Nichirei, Tokyo, Japan) as previously described[18]. Briefly, cells were fixed with 1 000 mL/L methanol at -20 ℃, and then endogenous peroxidase activity was blocked by incubation with hydrogen peroxide in methanol. After immersion in normal rabbit serum, the slides were incubated with mouse anti-ET-1 antibody (at 1:200 dilution) at 4 ℃ overnight. The slides were incubated with biotinylated anti-mouse immunoglobulin antibody, followed by peroxidase-conjugated streptavidin. Finally, color was developed by incubating the slides for several minutes with diaminobenzidine (Dojindo, Kumamoto, Japan). The expression of ET_A and ET_B was examined in a similar manner.

Western blotting

The level of activated, phosphorylated ERK was determined by Western blotting as previously described[19]. Cells were lysed in sodium dodecyl sulfate buffer. Cellular proteins (approximately 100 μg) were fractionated on a 100 g/L sodium dodecyl sulfate-polyacrylamide gel. They were transferred to a nitrocellulose membrane (Bio-Rad, Hercules, CA), and the membrane was incubated overnight at 4 ℃ with rabbit anti-phosphospecific ERK antibody. After incubation with peroxidase-conjugated goat anti-rabbit immunoglobulin G antibody for 1 h, proteins were visualized using an ECL kit (Amersham Biosciences, UK). The levels of total ERK, Akt (phosphorylated and total), and MLC (phosphorylated and total) were determined in a similar manner.

Fluorescence microscopy

Stress fibers were stained with rhodamine-labeled phalloidin as previously described[20]. After fixation with 40 g/L paraformaldehyde for 5 min, PSCs were permeablized with 1.5 mL/L Triton X-100 in PBS for 5 min. Cells were then incubated for 2 h at room temperature in a dark place with rhodamine-labeled phalloidin in blocking buffer (10 g/L bovine serum albumin in PBS). Cells were then washed thrice with PBS for 10 min each, and coverslipped with Fluoromount (Vector Laboratories, Burlingame, CA). Cells were observed with a Leica fluorescence microscope. Images were captured with a Leica QFISH system (Wetzlar, Germany).

Collagen gel contraction assay

Contraction of PSCs on collagen lattices was examined in six-well flat-bottom tissue culture plates (Becton Dickinson, Bedford, MA) as previously described[21]. Culture vessels were preincubated with PBS containing 10 g/L bovine serum albumin for 2 h at 37 ℃, washed, and air-dried. The gel mixture consisted of eight parts Vitrogen-100 (Collagen Corp., Palo Alto, CA), one part 10×minimal essential medium,

and one part 0.2 mol/L HEPES, pH 9.0, which resulted in a final collagen concentration of 2.4 g/L. It was prepared at 4 ℃, added to the culture vessel, and incubated at 37 ℃ for 2 h to allow gelation. PSCs were trypsinized, resuspended in serum-free medium (at 1×10^9 cells/L), plated on top of the gels (1 mL/well), and allowed to attach for 2 h. The collagen lattices were detached from the plate by gentle circumferential dislodgement using a fine needle, and ET-1 (at 100 nmol/L) was added to elicit contraction. After 24-h incubation, we measured the diameter of the collagen lattices, and calculated the "% of the original diameter (= 35 mm)". In addition, cell-free collagen lattices were incubated with 100 nmol/L ET-1 or serum-free medium alone.

Cell migration assay

Cell migration was assessed as previously described[16]. Serum-starved PSCs were trypsinized, and resuspended at the concentration of 3×10^8 cells/L in serum-free medium containing 10 g/L bovine serum albumin. For the assay, we used modified Boyden chambers with 8-μm pore filters (Iwaki Glass Co. Ltd., Funabashi, Japan) coated with rat-tail type I collagen. ET-1 was added to the lower chamber, and 250 μL of cell suspension was added to the upper chamber. The chambers were then incubated at 37 ℃ for 24 h. At the end of the incubation, the cell suspension in the upper chamber was aspirated, and the upper part of the filter was cleaned with cotton plugs. The cells migrated to the underside of the filter were stained with Difquick (Sysmex, Kobe, Japan), viewed, and counted at 200× magnification.

Cell proliferation assay

Serum-starved PSCs (approximately 80% density) were treated with ET-1 in the presence or absence of 100 mL/L fetal bovine serum or PDGF-BB (at 25 μg/L). Cell proliferation was assessed using a commercial kit (Cell proliferation ELISA, BrdU; Roche Diagnostics) according to the manufacturer's instruction. This is a colorimetric immunoassay based on the measurement of 5-bromo-2'-deoxyuridine (BrdU) incorporation during DNA synthesis. After 24-h incubation with experimental reagents, cells were labeled with BrdU for 3 h at 37 ℃. Cells were fixed, and incubated with peroxidase-conjugated anti-BrdU antibody. Then the peroxidase substrate 3,3',5,5'-tetramethylbenzidine was added, and BrdU incorporation was quantitated by $A_{370\text{-}492}$.

Statistical analysis

The results were expressed as mean±SD. Luminograms and autoradiograms are representative of at least three experiments. Differences between the groups were evaluated by ANOVA, followed by Fisher's test for post hoc analysis. A P value less than 0.05 was considered statistically significant.

RESULTS

Activated PSCs expressed ET-1 and ET receptors

We first examined whether culture-activated PSCs expressed ET-1 and ET receptors. ET-1 is a product of the gene coding for a large precursor protein (i.e. preproET-1)[9]. Culture-activated PSCs expressed ET_A and ET_B receptors, and ET-1, as assessed by reverse transcription-PCR and immunostaining (Figure 1).

ET-1 induced phosphorylation of ERK and MLC, but not Akt

In an attempt to elucidate the effect of ET-1 on cell functions of PSCs, we examined whether ET-1 activated intracellular signaling pathways. We examined the activation of ERK, Akt, and MLC, all of which are implicated in ET-1-induced cellular contraction and/or migration[22-24]. PSCs were treated with ET-1 at 100 nmol/L, and the activation of the signaling pathways by Western blotting using anti-phosphospecific antibodies. We chose this ET-1 concentration because previous studies have shown that ET-1 acts on ET receptors in a dose-dependent manner and ET-1 at this concentration effectively elicited effects in a variety of cell types[14,15,25,26]. PDGF-BB induced phosphorylation of ERK, Akt, and MLC whereas ET-1 induced phosphorylation of ERK and MLC but not Akt (Figure 2).

Y-27632 decreased stress fiber formation and MLC phosphorylation

It has been shown that RhoA, acting through its downstream effector Rho kinase, stimulates MLC phosphorylation, stress fiber formation, and contractile force generation[27,28]. The fact that ET-1 induced phosphorylation of MLC prompted us to examine the effect of Y-27632, a specific Rho kinase inhibitor[29], on the phosphorylation of MLC and stress fiber formation. Y-27632 decreased phosphorylation of MLC in a dose-dependent manner (Figure 3A). When cells were treated with Y-27632 at 25 μmol/L for 24 h, disassembly of stress fibers was observed (Figures 3B and 3C). In these experiments, Y-27632 up to 25 μmol/L did not affect the cell viability during the incubation as assessed by trypan blue exclusion test (data not shown). In addition, the effects of Y-27632 were reversible within 48 h after the removal of Y-27632 (Figures 3A and 3D). However, when PSCs were treated with Y-27632 at 50 μmol/L, cytotoxic effects were observed during the incubation (data not shown).

ET-1 induced contraction of PSCs

We examined whether ET-1 induced contraction of PSCs using collagen lattices. With no stellate cells, the size of the collagen lattices did not change in response to ET-1 (data not shown). When PSCs were plated on the lattices, and incubated with serum-free medium alone for 24 h, there was a slight reduction in the diameter of the lattices to 89±3% of their original size (Figure 4A). By incubation with 100 nmol/L ET-1, the diameter of the lattices decreased to 54±8% (Figure 4B). ET-1-induced contraction of PSCs was inhibited by an ET_A receptor antagonist BQ-123[30], an ET_B receptor antagonist BQ-788[31]. Y-27632 abolished ET-1-induced contraction, whereas a MAP kinase inhibitor U0126[32] was ineffective.

ET-1 induced migration, but did not alter proliferation of PSCs

ET-1 induced migration of PSCs, which was inhibited by BQ-788, Y-27632, and U0126, but not BQ-123 (Figure 5).

Previous studies have shown that ET-1 showed positive or negative effects on cell growth[15,25,26]. In agreement with the previous study[16], PDGF-BB and 100 mL/L fetal bovine serum increased proliferation of PSCs (Figure 6). ET-1 did not affect basal proliferation or proliferation in response to PDGF or serum.

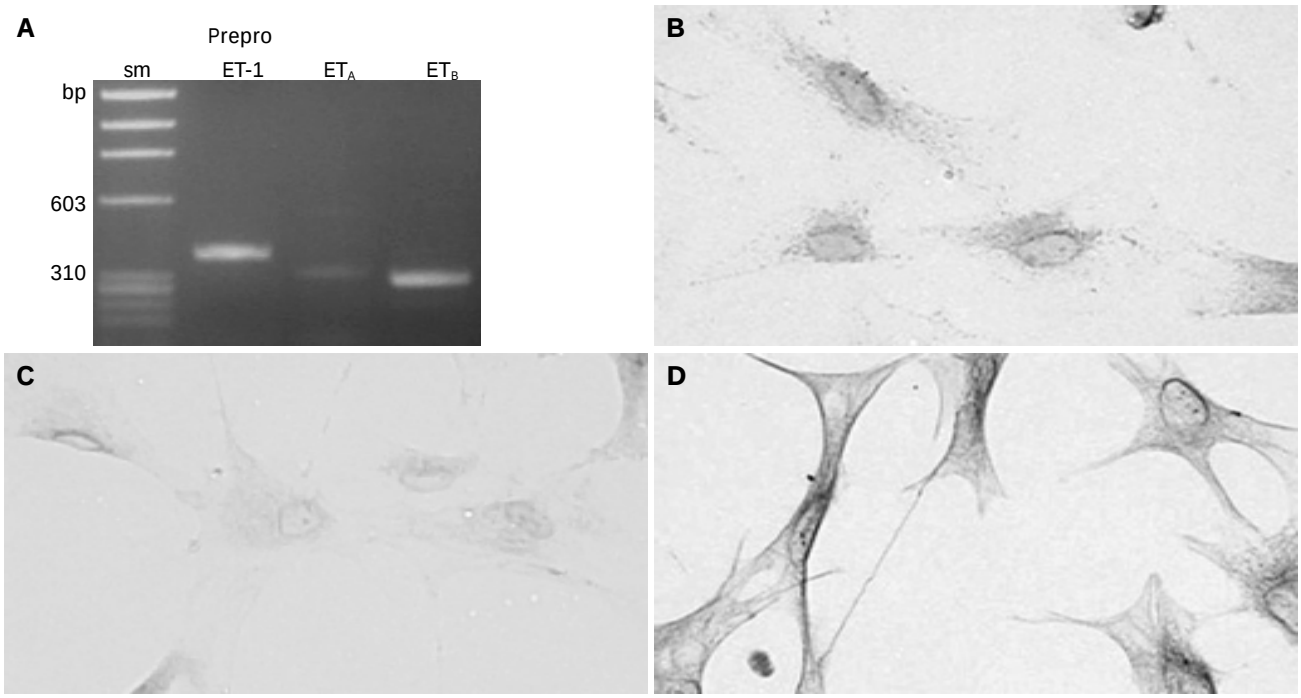

Figure 1 Culture-activated PSCs expressed ET and ET receptors. A: Total RNA was prepared from culture-activated, serum-starved PSCs. The expression of preproET-1, ET_A receptor and ET_B receptor was examined by reverse transcription-PCR. The expected sizes of the PCR products were 382 bp for preproET-1, 321 bp for ET_A receptor, and 297 bp for ET_B receptor. sm: size marker (ϕX174 *Hae*III digest). bp: bp; B-D: Serum-starved PSCs were grown directly on slides. Immunostaining for ET-1 (panel B), ET_A receptor (panel C), and ET_B receptor (panel D) was performed using a streptavidin-biotin peroxidase complex detection kit. Original magnification: ×20 objective.

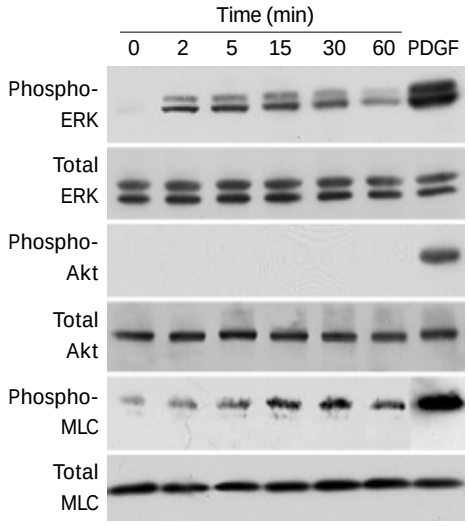

Figure 2 ET-1 induced phosphorylation of ERK and MLC, but not Akt. PSCs were treated with ET-1 (at 100 nmol/L) for the indicated time. Total cell lysates (approximately 100 μg) were prepared, and the levels of phosphorylated ERK, Akt, and MLC were determined by Western blotting. As positive controls, total cell lysates were prepared from PSCs treated with PDGF-BB (at 25 μg/L) for 5 min, and Western blotting was performed in a similar manner. Levels of total ERK, Akt, and MLC were also determined.

DISCUSSION

There is accumulating evidence that activated PSCs play a pivotal role in the pathogenesis of pancreatic fibrosis and inflammation[1-5]. We here showed that culture-activated PSCs expressed ET_A and ET_B receptors, and ET-1. ET-1 stimulated contraction and migration of PSCs, suggesting autocrine and paracrine mechanisms of ET-1-regulated cellular functions of PSCs. ET-1-induced contraction was inhibited by ET_A and ET_B receptor antagonists whereas ET-1-induced migration was inhibited by ET_B receptor antagonist but not by ET_A receptor antagonist. Thus, ET_A and ET_B receptors play different roles in the regulation of these cellular functions in response to ET-1.

Cellular migration and contraction are complex processes involving dynamic changes in the actin-myosin cytoskeleton, including generation of contractile forces[33]. It has been shown that contractile force is powered by myosin, which is activated by phosphorylation of MLC[33]. Phosphorylation of MLC is regulated by the balance of two enzymatic activities, i.e., MLC kinase(s) and myosin phosphatase. For example, MLC is phosphorylated by MLC kinase in a Ca^{2+}/calmodulin-dependent manner in smooth muscle cells[34]. RhoA, acting through its downstream effector Rho kinase, stimulates MLC phosphorylation and consequently contractile force generation through the inhibition of myosin phosphatase[27,28]. Activated Rho kinase promotes the contraction of isolated stress fibers and generates a long-lasting tensile activity by the maintained inhibition of myosin phosphatase[35]. On the other hand, contractile force generation by certain non-muscle cell types including fibroblasts may occur independently of myosin phosphorylation[36,37]. To clarify the role of myosin in ET-1-induced contraction and migration of PSCs, we examined the effect of ET-1 on the phosphorylation of MLC. We here showed that ET-1 induced the phosphorylation of MLC, supporting a role of myosin in contractile force generation in PSCs. In addition, an inhibitor of Rho kinase

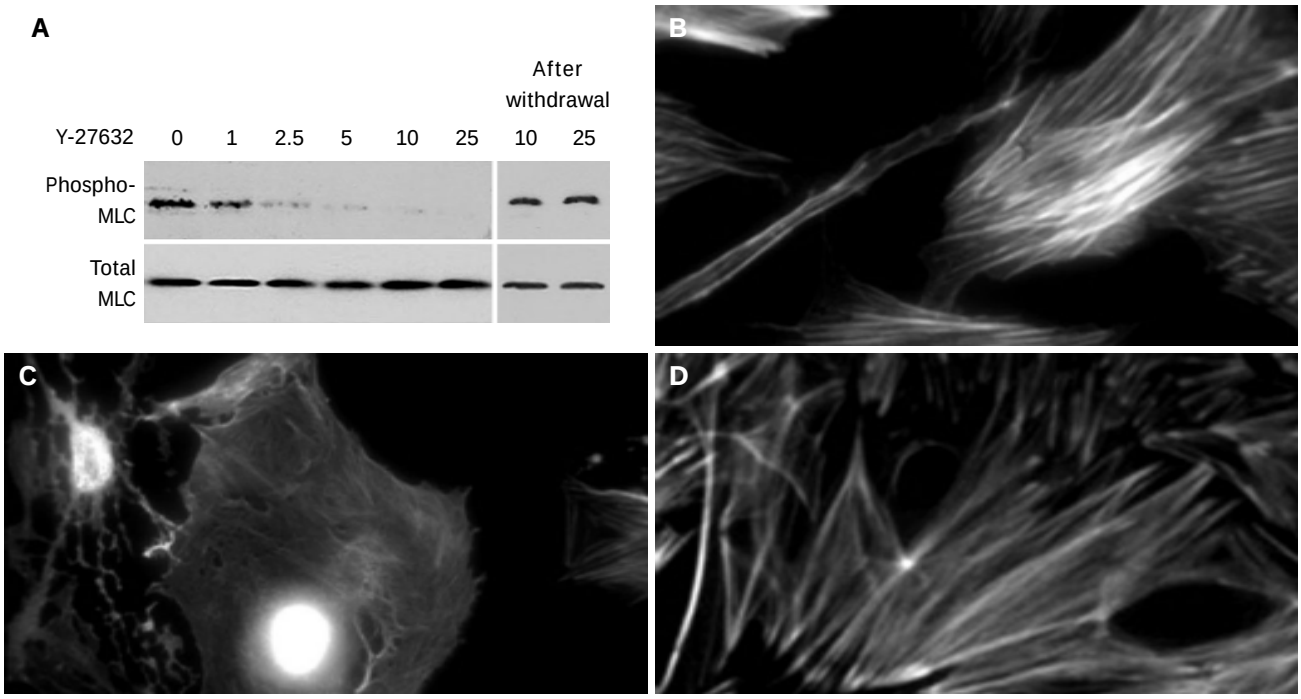

Figure 3 Y-27632 decreased stress fiber formation. A: PSCs were treated with ET-1 (at 100 nmol/L) in the presence of Y-27632 at the indicated concentrations (at μmol/L) for 30 min. Total cell lysates (approximately 100 μg) were prepared, and the levels of phosphorylated and total MLC were determined by Western blotting. In parallel experiments, Y-27632 was withdrawn after 30-min incubation, and replaced with 10% FBS. After 48-h incubation with 10% FBS, total cell lysates were prepared, and the levels of phosphorylated and total MLC were determined by Western blotting; B-D: PSCs were incubated with ET-1 (at 100 nmol/L) in the absence (B) or presence (C) of Y-27632 (at 25 μmol/L) for 24 h, and stained with rhodamine-labeled phalloidin. In parallel experiments, Y-27632 was withdrawn and replaced with 10% FBS. After 48-h incubation with 10% FBS, PSCs were stained with rhodamine-labeled phalloidin (D). Original magnification: ×60 objective.

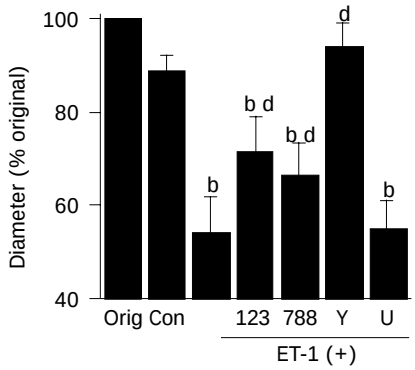

Figure 4 ET-1 induced contraction of PSCs. PSCs were plated on the surface of collagen lattices prepared in each well of a six-well plate and incubated for 2 h to allow adherence. The collagen lattices were then detached from the plate by gentle circumferential dislodgment. Serum-starved PSCs were left untreated ("Con") or were treated with ET-1 (at 100 nmol/L) in the absence or presence of BQ-123 ("123" at 10 μmol/L), BQ-788 ("788" at 10 μmol/L), Y-27632 ("Y" at 25 μmol/L), or U0126 ("U" at 5 μmol/L). Lattices were then detached from the plate, and incubated in serum-free medium (control, "Con") with or without 100 nmol/L ET-1. After 24-h incubation, we measured the diameter of the collagen lattices, and calculated the "% of the original diameter ("Orig" = 35 mm)". Data are shown as mean±SD (% of the original diameter, n = 8). ^{b}P<0.01 *vs* control (serum-free medium only), ^{d}P<0.01 *vs* ET-1 treatment only.

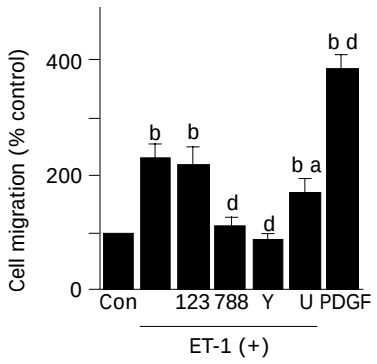

Figure 5 ET-1 induced migration of PSCs. Cell migration was assessed using modified Boyden chambers with 8-μm pore filters. Serum-starved PSCs were left untreated ("Con") or were treated with ET-1 (at 100 nmol/L) in the lower chamber in the absence or presence of BQ-123 ("123" at 10 μmol/L), BQ-788 ("788" at 10 μmol/L), Y-27632 ("Y" at 25 μmol/L), or U0126 ("U" at 5 μmol/L). After 24-h incubation, the cells migrated to the underside of the filter were stained, and counted under a light microscopy. As positive controls, cells were treated with PDGF-BB (at 25 μg/L) in the lower chamber, and cell migration was assessed in a similar manner. Data are shown as mean±SD (% of the control, n = 6). ^{b}P<0.01 *vs* control (serum-free medium only), ^{a}P<0.05, ^{d}P<0.01 *vs* ET-1 treatment only.

Y-27632 abolished the phosphorylation of MLC, stress fiber formation, contraction, and migration. These results agree with the idea that force generation by the myofibroblasts depends on the isometric contraction of stress fibers containing α-smooth muscle actin, and is mediated through Rho-Rho kinase[38]. Indeed, myosin mediates contractile force generation by hepatic stellate cells in response to ET-1[24]. We have previously shown that PDGF-BB induced migration of PSCs through the activation of phosphatidylinositol 3-kinase/Akt pathway[16]. Unlike PDGF-BB, ET-1 did not activate Akt but did induce migration of PSCs, excluding a role of phosphatidylinositol 3-kinase/Akt pathway in ET-

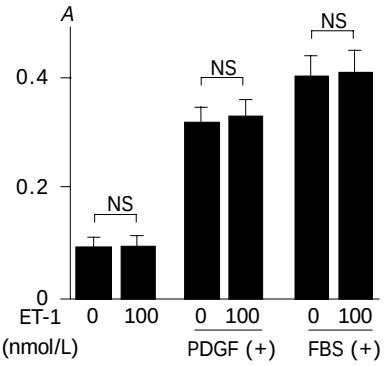

Figure 6 ET-1 did not alter basal or inducible proliferation of PSCs. Serum-starved PSCs were treated with ET-1 at 0 or 100 nmol/L in the absence or presence of PDGF-BB (at 25 μg/L) or 100 mL/L fetal bovine serum ("FBS"). After 24-h incubation, DNA synthesis was assessed by BrdU incorporation enzyme-linked immunosorbent assay. Data are shown as mean±SD (n = 6). NS: not significant, *A*: optical density.

1-mediated migration.

In this study, ET-1 induced contraction of PSCs through both ET_A and ET_B receptors as assessed by the contraction of collagen lattices. This is in agreement with the previous study showing that both ET_A and ET_B receptors play an important role in contraction of colonic myofibroblast cells[26], but disagrees with hepatic stellate cells where ET-1 induced contraction is through ET_A receptor[14]. Investigation of cellular contraction using collagen lattices (gels) was introduced by Bell *et al*.[39], and has been validated as a model of study of cellular contraction in a variety of cell types. Fibroblasts seeded on top of type I collagen gels bind and organize underlying collagen fibrils, both in close proximity and at a distance from cells[40]. After such reorganization, lattices are converted into a dense mass with the morphological appearance of dermal scar. Kawada *et al*.[41], reported a morphological study of ET-1-induced contraction of hepatic stellate cells on hydrated collagen gels. They demonstrated that contracted form of the stellate cells was morphologically characterized by the retraction of dendritic processes and the bending of the extended cell bodies that enfold the underlying collagen matrix. Because the cell body and processes are both closely attached to the collagen fibers, their contraction generates effective forces for the contraction of collagen gels.

ET-1 did not alter the proliferation of PSCs. The effect of ET-1 on growth and the underlying mechanisms depend on cell type. For example, ET-1 promotes the proliferation of human pulmonary artery smooth muscle cells through ET_A and ET_B receptors[25]. ET-1 did not affect the proliferation of human colonic myofibroblast cells[26]. In human hepatic stellate cells, ET-1 has been shown to inhibit the serum-induced proliferation through ET_B receptor, whereas ET-1 did not induce proliferation by itself[15]. Of note, Pinzani *et al*.[14], reported that ET-1 induced proliferation of early-passaged human hepatic stellate cells (passages 1 and 2), but the effect was less evident at a later stage of culture. This phenomenon is attributable at least in part to the progressive shift from a relative predominance of ET_A receptor to ET_B receptor during culture[14]. Because the effects of ET-1 on cell growth might be mediated by distinct ET receptors, the ratio between ET_A and ET_B receptors in the cells might constitute an additional factor that could affect the sensitivity of cells to the growth regulatory effects of ET-1. We and others have shown that ERK is a key mediator of PDGF-BB-induced mitogenic signals in PSCs[16,42]. In spite of the ability to activate ERK, ET-1 failed to alter the proliferation, suggesting that activation of ERK is required but not sufficient for the proliferation of PSCs. This is also in the case of stimulation by ethanol, acetaldehyde, and 4-hydroxy-2,3-nonenal in PSCs[43], and in agreement with the concept that activation of ERK, although necessary, may not be sufficient to justify the mitogenic properties of an agonist[44].

Klonowski-Stumpe *et al*.[45], reported that activated PSCs expressed ET_A receptor and ET-1, and that ET-1 increased cytosolic Ca^{2+} concentration[45]. Exogenous ET-1 did not induce contraction, and, even in the absence of exogenous addition of ET-1, PSCs reduced the area of hydrated collagen lattices to 75% of the original value within 6 h, which was significantly attenuated by BQ-123, but not by another ET_B receptor antagonist IRL-1 038. The reason for discrepancy of the results between our study and theirs remain unknown, but the different experimental systems (e.g., different cell passages, different ET-1 concentrations, different ET_B receptor antagonist, and different serum-starvation condition) employed may be one explanation. As the ET_A receptor antagonist inhibited basal contraction of PSCs in their study, the endogenous ET-1 from PSCs or ET-1 that remained in the culture supernatant appeared to be responsible for the basal contraction of PSCs. In addition to ET_A receptor, we here have shown for the first time that activated PSCs express ET_B receptor, and that exogenously added ET-1 induces migration of PSCs.

It has been accepted that hepatic stellate cell contraction in response to ET-1 plays an important role in the regulation of sinusoidal blood flow, and in the development of portal hypertension and hepatic fibrosis[12,13]. ET-1 is markedly overexpressed in different cellular elements in cirrhotic liver tissue, particularly in sinusoidal endothelial cells and activated hepatic stellate cells located in the sinusoids of the regenerating nodules at the edge of fibrous septa[16]. On the other hand, the pathophysiological implication of ET-1-induced contraction of PSCs remains obscure. Although PSCs are located predominantly in the periacinar regions in normal pancreas[1,2], perivascular and periductal localization has been also reported[46]. Ikejiri[46] showed that vitamin A-storing cells (now recognized as PSCs) were perivascularly localized in the pancreas of rats fed with vitamin A. Perivascular PSCs might participate in the regulation of blood flow and the development of microvascular ischemia during pancreatitis through ET-1 production[47]. Izumi *et al*.[48], reported that PSCs were found in the pancreatic duct wall of normal pancreas, and that the amount of such cells was excessively increased in patients with focal pancreatitis. They assumed that circular contraction of the ductal wall by proliferating PSCs might induce the stenosis of the main pancreatic duct and block the efflux of pancreatic juice from branch pancreatic ducts at the stenotic portion, leading to localized acinar atrophy and fibrosis[48]. In addition, PSCs might participate in control of the intraductal pressure, epithelial

cell reconstitution, and duct remodeling during the healing of ductal injury. Along this line, it is now well accepted that the contractile activity of myofibroblasts is responsible for connective tissue remodeling during wound healing[38]. Obviously, further studies are necessary to clarify the pathop-hysiological relevances of ET-1-mediated cell functions of PSCs.

ACKNOWLEDGMENTS

The authors thank Dr. Kenzo Kaneko for fluorescence microscopy, and Mitsubishi Pharma Co. for Y-27632.

REFERENCES

1 **Apte MV,** Haber PS, Applegate TL, Norton ID, McCaughan GW, Korsten MA, Pirola RC, Wilson JS. Periacinar stellate shaped cells in rat pancreas: identification, isolation and culture. *Gut* 1998; **43**: 128-133
2 **Bachem MG,** Schneider E, Gross H, Weidenbach H, Schmidt RM, Menke A, Siech M, Beger H, Grunert A, Adler G. Identification, culture, and characterization of pancreatic stellate cells in rats and humans. *Gastroenterology* 1998; **115**: 421-432
3 **Haber PS,** Keogh GW, Apte MV, Moran CS, Stewart NL, Crawford DH, Pirola RC, McCaughan GW, Ramm GA, Wilson JS. Activation of pancreatic stellate cells in human and experimental pancreatic fibrosis. *Am J Pathol* 1999; **155**: 1087-1095
4 **Masamune A,** Kikuta K, Satoh M, Sakai Y, Satoh A, Shimosegawa T. Ligands of peroxisome proliferator-activated receptor-gamma block activation of pancreatic stellate cells. *J Biol Chem* 2002; **277**: 141-147
5 **Masamune A,** Sakai Y, Kikuta K, Satoh M, Satoh A, Shimosegawa T. Activated rat pancreatic stellate cells express intercellular adhesion molecule-1 (ICAM-1) *in vitro*. *Pancreas* 2002; **25**: 78-85
6 **Masamune A,** Satoh M, Kikuta K, Sakai Y, Satoh A, Shimosegawa T. Inhibition of p38 mitogen-activated protein kinase blocks activation of rat pancreatic stellate cells. *J Pharmacol Exp Ther* 2003; **304**: 8-14
7 **Masamune A,** Kikuta K, Satoh M, Satoh K, Shimosegawa T. Rho kinase inhibitors block activation of pancreatic stellate cells. *Br J Pharmacol* 2003; **140**: 1292-1302
8 **Masamune A,** Kikuta K, Masamune A, Kikuta K, Suzuki N, Satoh M, Satoh K, Shimosegawa T. A c-Jun NH2-terminal kinase inhibitor SP600125 (anthra[1,9-cd]pyrazole-6 (2H)-one) blocks activation of pancreatic stellate cells. *J Pharmacol Exp Ther* 2004; **310**: 520-527
9 **Yanagisawa M,** Kurihara H, Kimura S, Tomobe Y, Kobayashi M, Mitsui Y, Yazaki Y, Goto K, Masaki T. A novel potent vasoconstrictor peptide produced by vascular endothelial cells. *Nature* 1988; **332**: 411-415
10 **Sakurai T,** Yanagisawa M, Masaki T. Molecular characterization of endothelin receptors. *Trends Pharmacol Sci* 1992; **13**: 103-108
11 **Levin ER.** Endothelins. *N Engl J Med* 1995; **333**: 356-363
12 **Friedman SL.** Molecular regulation of hepatic fibrosis, an integrated cellular response to tissue injury. *J Biol Chem* 2000; **275**: 2247-2250
13 **Rockey DC,** Chung JJ. Endothelin antagonism in experimental hepatic fibrosis. Implications for endothelin in the pathogenesis of wound healing. *J Clin Invest* 1996; **98**: 1381-1388
14 **Pinzani M,** Milani S, De Franco R, Grappone C, Caligiuri A, Gentilini A, Tosti-Guerra C, Maggi M, Failli P, Ruocco C, Gentilini P. Endothelin 1 is overexpressed in human cirrhotic liver and exerts multiple effects on activated hepatic stellate cells. *Gastroenterology* 1996; **110**: 534-538
15 **Mallat A,** Fouassier L, Preaux AM, Gal CS, Raufaste D, Rosenbaum J, Dhumeaux D, Jouneaux C, Mavier P, Lotersztajn S. Growth inhibitory properties of endothelin-1 in human hepatic myofibroblastic Ito cells. *J Clin Invest* 1995; **96**: 42-49
16 **Masamune A,** Kikuta K, Satoh M, Kume K, Shimosegawa T. Differential roles of signaling pathways for proliferation and migration of rat pancreatic stellate cells. *Tohoku J Exp Med* 2003; **199**: 69-84
17 **Wendel-Wellner M,** Noll T, Konig P, Schmeck J, Koch T, Kummer W. Cellular localization of the endothelin receptor subtypes ET_A and ET_B in the rat heart and their differential expression in coronary arteries, veins, and capillaries. *Histochem Cell Biol* 2002; **118**: 361-369
18 **Masamune A,** Satoh M, Kikuta K, Suzuki N, Shimosegawa T. Establishment and characterization of a rat pancreatic stellate cell line by spontaneous immortalization. *World J Gastroenterol* 2003; **9**: 2751-2758
19 **Masamune A,** Satoh K, Sakai Y, Yoshida M, Satoh A, Shimosegawa T. Ligands of peroxisome proliferator-activated receptor-gamma induce apoptosis in AR42J cells. *Pancreas* 2002; **24**: 130-138
20 **Kaneko K,** Satoh K, Masamune A, Satoh A, Shimosegawa T. Myosin light chain kinase inhibitors can block invasion and adhesion of human pancreatic cancer cell lines. *Pancreas* 2002; **24**: 34-41
21 **Rocky DC,** Housset CN, Friedman SL. Activation-dependent contractility of rat hepatic lipocytes in culture and *in vivo*. *J Clin Invest* 1993; **92**: 1795-1804
22 **Ishihata A,** Tasaki K, Katano Y. Involvement of p44/42 mitogen-activated protein kinases in regulating angiotensin II- and endothelin-1-induced contraction of rat thoracic aorta. *Eur J Pharmacol* 2002; **445**: 247-256
23 **Shi-Wen X,** Chen Y, Denton CP, Eastwood M, Renzoni EA, Bou-Gharios G, Pearson JD, Dashwood M, du Bois RM, Black CM, Leask A, Abraham DJ. Endothelin-1 promotes myofibroblast induction through the ETA receptor via a rac/phosphoinositide 3-kinase/Akt-dependent pathway and is essential for the enhanced contractile phenotype of fibrotic fibroblasts. *Mol Biol Cell* 2004; **15**: 2707-2719
24 **Saab S,** Tam SP, Tran BN, Melton AC, Tangkijvanich P, Wong H, Yee HF Jr. Myosin mediates contractile force generation by hepatic stellate cells in response to endothelin-1. *J Biomed Sci* 2002; **9**: 607-612
25 **Davie N,** Haleen SJ, Upton PD, Polak JM, Yacoub MH, Morrell NW, Wharton J. ETA and ETB receptors modulate the proliferation of human pulmonary artery smooth muscle cells. *Am J Respir Crit Care Med* 2002; **165**: 398-405
26 **Kernochan LE,** Tran BN, Tangkijvanich P, Melton AC, Tam SP, Yee HF Jr. Endothelin-1 stimulates human colonic myofibroblast contraction and migration. *Gut* 2002; **50**: 65-70
27 **Kimura K,** Ito M, Amano M, Chihara K, Fukata Y, Nakafuku M, Yamamori B, Feng J, Nakano T, Okawa K, Iwamatsu A, Kaibuchi K. Regulation of myosin phosphatase by Rho and Rho-associated kinase (Rho-kinase). *Science* 1996; **273**: 245-248
28 **Somlyo AP,** Somlyo AV. Signal transduction by G-proteins, rho-kinase and protein phosphatase to smooth muscle and non-muscle myosin II. *J Physiol* 2000; **522**: 177-185
29 **Uehata M,** Ishizaki T, Satoh H, Ono T, Kawahara T, Morishita T, Tamakawa H, Yamagami K, Inui J, Maekawa M, Narumiya S. Calcium sensitization of smooth muscle mediated by a Rho-associated protein kinase in hypertension. *Nature* 1997; **389**: 990-994
30 **Ihara M,** Noguchi K, Saeki T, Fukuroda T, Tsuchida S, Kimura S, Fukami T, Ishikawa K, Nishikibe M, Yano M. Biological profiles of highly potent novel endothelin antagonists selective for the ETA receptor. *Life Sci* 1992; **50**: 247-255
31 **Ishikawa K,** Ihara M, Noguchi K, Mase T, Mino N, Saeki T, Fukuroda T, Fukami T, Ozaki S, Nagase T, Nishikibr M, Yano M. Biochemical and pharmacological profile of a potent and selective endothelin B-receptor antagonist, BQ-788. *Proc Natl Acad Sci USA* 1994; **91**: 4892-4896
32 **Favata MF,** Horiuchi KY, Manos EJ, Daulerio AJ, Stradley DA, Feeser WS, Van Dyk DE, Pitts WJ, Earl RA, Hobbs F, Copeland RA, Magolda RL, Scherle PA, Trzaskos JM. Identification of a novel inhibitor of mitogen-activated protein kinase kinase. *J Biol Chem* 1998; **273**: 18623-18632

33 **Lauffenburger DA,** Horwitz AF. Cell migration: A physically integrated molecular process. *Cell* 1996; **84**: 359-369
34 **Somlyo AP,** Somlyo AV. Signal transduction and regulation in smooth muscle. *Nature* 1994; **372**: 231-236
35 **Katoh K,** Kano Y, Amano M, Onishi H, Kaibuchi K, Fujiwara K. Rho-kinase-mediated contraction of isolated stress fibers. *J Cell Biol* 2001; **153**: 569-584
36 **Obara K,** Nikcevic G, Pestic L, Nowak G, Lorimer DD, Guerriero V Jr, Elson EL, Paul RJ, de Lanerolle P. Fibroblast contractility without an increase in basal myosin light chain phosphorylation in wild type cells and cells expressing the catalytic domain of myosin light chain kinase. *J Biol Chem* 1995; **270**: 18734-18737
37 **Skuta G,** Ho CH, Grinnell F. Increased myosin light chain phosphorylation is not required for growth factor stimulation of collagen matrix contraction. *J Biol Chem* 1999; **274**: 30163-30168
38 **Hinz B,** Gabbiani G. Mechanisms of force generation and transmission by myofibroblasts. *Curr Opin Biotechnol* 2003; **14**: 538-546
39 **Bell E,** Ivarsson B, Merrill C. Production of a tissue-like structure by contraction of collagen lattices by human fibroblasts of different proliferative potential *in vitro*. *Proc Natl Acad Sci USA* 1979; **76**: 1274-1278
40 **Guidry C,** Grinnell F. Contraction of hydrated collagen gels by fibroblasts: evidence for two mechanisms by which collagen fibrils are stabilized. *Coll Relat Res* 1987; **6**: 515-529
41 **Kawada N,** Harada K, Ikeda K, Kaneda K. Morphological study of endothelin-1-induced contraction of cultured hepatic stellate cells on hydrated collagen gels. *Cell Tissue Res* 1996; **286**: 477-486
42 **Jaster R,** Sparmann G, Emmrich J, Liebe S. Extracellular signal regulated kinases are key mediators of mitogenic signals in rat pancreatic stellate cells. *Gut* 2002; **51**: 579-584
43 **Masamune A,** Kikuta K, Satoh M, Satoh A, Shimosegawa T. Alcohol activates activator protein-1 and mitogen-activated protein kinases in rat pancreatic stellate cells. *J Pharmacol Exp Ther* 2002; **302**: 36-42
44 **Blenis J.** Signal transduction via the MAP kinases: proceed at your own RSK. *Proc Natl Acad Sci USA* 1993; **90**: 5889-5892
45 **Klonowski-Stumpe H,** Reinehr R, Fischer R, Warskulat U, Luthen R, Haussinger D. Production and effects of endothelin-1 in rat pancreatic stellate cells. *Pancreas* 2003; **27**: 67-74
46 **Ikejiri N.** The vitamin A-storing cells in the human and rat pancreas. *Kurume Med J* 1990; **37**: 67-81
47 **Kakugawa Y,** Paraskevas S, Metrakos P, Giaid A, Qi SJ, Duguid WP, Rosenberg L. Alterations in pancreatic microcirculation and expression of endothelin-1 in a model of chronic pancreatitis. *Pancreas* 1996; **13**: 89-95
48 **Izumi M,** Suda K, Torii A, Inadama E. Pancreatic ductal myofibroblasts. Proliferative patterns in various pathologic situations. *Virchows Arch* 2001; **438**: 442-450

Science Editor Guo SY **Language Editor** Elsevier HK

PO Box 2345, Beijing 100023, China
www.wjgnet.com
wjg@wjgnet.com

ELSEVIER

World J Gastroenterol 2005;11(39):6152-6158
World Journal of Gastroenterology ISSN 1007-9327

• *BASIC RESEARCH* •

Identification of *anrF* gene, a homology of *admM* of andrimid biosynthetic gene cluster related to the antagonistic activity of *Enterobacter cloacae* B8

Xu-Ping Yu, Jun-Li Zhu, Xue-Ping Yao, Shi-Cheng He, Hai-Ning Huang, Wei-Liang Chen, Yong-Hao Hu, De-Bao Li

Xu-Ping Yu, Jun-Li Zhu, Xue-Ping Yao, Shi-Cheng He, Veterinary Medicine Department, Animal Science College, Zhejiang University, Hangzhou 310029, Zhejiang Province, China
Xu-Ping Yu, Hai-Ning Huang, Wei-Liang Chen, De-Bao Li, Institute of Biotechnology, Zhejiang University, Hangzhou 310029, Zhejiang Province, China
Jun-Li Zhu, College of Food Science, Biotechnology and Environmental Engineering, Zhejiang Gongshang University, Hangzhou 310035, Zhejiang Province, China
Xue-Ping Yao, Yong-Hao Hu, Veterinary Medicine Department, Animal Science College, Gansu Agricultural University, Lanzhou 730070, Gansu Province, China
Supported by the National Natural Science Foundation of China, No. 39870034; the National High Technology Research and Development Program of China, the 863 Program, No. 104-04-01-01; and the Major Project of Science and Technology Development of Zhejiang Province, No. 021102529
Co-first-authors: Xu-Ping Yu and Jun-Li Zhu
Co-correspondents: Xu-Ping Yu and De-Bao Li
Correspondence to: Dr. Xu-Ping Yu, Veterinary Medicine Department, Animal Science College, Zhejiang University, Hangzhou 310029, Zhejiang Province, China. xpyu@zju.edu.cn
Telephone: +86-571-86971096 Fax: +86-571-86971096
Received: 2005-01-24 Accepted: 2005-04-11

Abstract

AIM: To identify the gene (s) related to the antagonistic activity of *Enterobacter cloacae* B8 and to elucidate its antagonistic mechanism.

METHODS: Transposon-mediated mutagenesis and tagging method and cassette PCR-based chromosomal walking method were adopted to isolate the mutant strain (s) of B8 that lost the antagonistic activity and to clone DNA fragments around Tn5 insertion site. Sequence compiling and open reading frame (ORF) finding were done with DNAStar program and homologous sequence and conserved domain searches were performed with BlastN or BlastP programs at www.ncbi.nlm.nih.gov. To verify the gene involved in the antagonistic activity, complementation of a full-length clone of the *anrF* gene to the mutant B8F strain was used.

RESULTS: A 3 321 bp contig around the Tn5 insertion site was obtained and an ORF of 2 634 bp in length designated as *anrF* gene encoding for a 877 aa polyketide synthase-like protein was identified. It had a homology of 83% at the nucleotide level and 79% ID/87% SIM at the protein level, to the *admM* gene of *Pantoea agglomerans* andrimid biosynthetic gene cluster (AY192157). The Tn5 was inserted at 2 420 bp of the gene corresponding to the COG3319 (the thioesterase domain of type I polyketide synthase) coding region on B8F. The antagonistic activity against *Xanthomonas oryzae pv. oryzae* was resumed with complementation of the full-length *anrF* gene to the mutant B8F.

CONCLUSION: The *anrF* gene obtained is related to the antagonistic activity of B8, and the antagonistic substances produced by B8 are andrimid and/or its analogs.

Key words: *Enterobacter cloacae* B8; Antagonistic mechanism; *anrF* gene; Andrimid biosynthetic gene cluster

Yu XP, Zhu JL, Yao XP, He SC, Huang HN, Chen WL, Hu YH, Li DB. Identification of *anrF* gene, a homology of *admM* of andrimid biosynthetic gene cluster related to the antagonistic activity of *Enterobacter cloacae* B8. *World J Gastroenterol* 2005; 11(39): 6152-6158
http://www.wjgnet.com/1007-9327/11/6152.asp

INTRODUCTION

Enterobacter cloacae strain B8 isolated from rice leaves was first recognized as an antagonistic bacterium of *Xanthomonas oryzae pv. oryzae*[1]. Its biological characteristics, antagonistic activity, and substances have been reported[2,3]. Satisfactory results have been obtained on anti-rice bacterial leaf brilliant in net house and in field[4]. Additionally, *E. cloacae* B8 is also antagonistic to many other plant bacterial pathogens such as *Pseudomonas*, *Agrobacterium*[3]. It has been reported that substances purified from *E. cloacae* B8 inhibit human (animal) bacterial pathogens such as MRSA[5,6].

Few but an *E. cloacae* strain EcCT-501R3 was reported to have antagonistic activity, which inhibits *Pythium ultimum* sporangium germination[7,8]. A competitive exclusion mechanism, competitive utilization of long-chain fatty acids of seed exudates, has been discovered and verified with transposon-mediated mutagenesis and tagging[9]. Previous researches on *E. cloacae* B8, however, showed that it produces antagonistic substances and differs from EcCT-501R3[1,3].

To elucidate the antagonistic mechanism of *E. cloacae* B8, transposon tagging[9-12] strategy was employed to clone DNA fragment related to its antagonistic activity. After a DNA fragment was cloned, cassette PCR-based chromosomal

walking[13-15] was used to get the flanked unknown DNA. We have previously reported the cloning and analysis of an antagonistic-related DNA fragment[16,17] and the verification of loss of antagonistic activity of mutant strains, by Southern blotting analysis, as a result of the insertion of a single copy of Tn5[18]. Here, we report the cloning and identification of the full-length *anrF* gene and the verification of its participation in the antagonism of B8.

MATERIALS AND METHODS

Bacterial strains, plasmids and chemicals

E. cloacae B8 (rif^r) is the antagonistic bacterium isolated from rice leaves in our laboratory[3,19]. *X. oryzae pv. oryzae* strain Xcom3104 (rif^r kan^r) was used as an indicator bacterium of antagonistic activity. The suicide plasmid pZJ25 (cm^r kan^r mob::Tn5) and its host *E.coli* S17-1 (thi pro $hsdR^-$ $hsdM^+$ recA RP4)[20] were gifts from Professor Jin-Sheng Wang of Nanjing Agricultural University, China. The cloning vector pBluescript SK+ (pBS) and its host *E. coli* DH5a were purchased from Stratagene. pFastBac^{TM}HTA was purchased from Invitrogen. pMD18-T vector was a product of Takara. Restriction enzymes, T4 DNA ligase, CIAP, *Taq* DNA polymerase, dNTPs, DNA marker DL2000, marker 3 kb, PCR product purification kit, etc., were supplied by Promega, Takara, Sangon and/or Zeheng. Oligonucleotides and primers used in this research were synthesized in Bioasia Biotech.

Transposon-mediated mutagenesis

The transfer of suicide plasmid pZJ25 from *E. coli* host S17-1 (donor) to *E. cloacae* B8 (receptor, rif^r) was mediated with conjugation[21]. Tranposonated B8 clones (rif^r kan^r cm^s) were selected on plates with rifampicin and kanamycin. The antagonistic characteristics were then checked using Xcom 3104 (rif^r kan^r) as an indicator[19].

Cloning of F fragment from B8F with tagging method

Genomic DNA of B8F, an antagonistic mutant strain of B8, was isolated, cut with *Bam*HI and ligated to *Bam*HI cut and dephosphorylated pBS. Recombinant clones were selected on plates with both kanamycin and ampicillin. Only one DNA fragment on the left of the insertion site was obtained with this step, as *Bam*HI cut Tn5 into two fragments and the intact Kan^r gene was in the 2.7 kb left fragment. The F fragment was a DNA fragment on the left of inserted Tn5 on B8F genome (Figure 1).

Cloning of DNA on the right of insertion site with chromosomal walking

Two sets of cassettes and primers were adopted in our chromosomal walking experiments. The *Pst*I cassette and its related CP primer were synthesized as previously described[12]. The *Sau*3AI cassette and its related CS primer and FS2, F1815 and F2000, the specific primers corresponding to known sequences, were newly designed and synthesized. They were as follows:

*Pst*I cassette:
5' HO-AGATTCGGTGCGTGCTTGACTGCA-OH 3'
3' HO-TCTAAGCCACGCACGAACTG-OH 5'
*Sau*3AI cassette:
5' HO-CTGTGGTGGTTCCGATGTATG-OH 3'
3' HO-ACCACCAAGGCTACATACCTAG-OH 5'
Cassette primers:
CP primer: AGATTCGGTGCGTGCTTGAC
CS primer: CTGTGGTGGTTCCGATGTAT
Specific primers:
FS2: GTTTACTGGCCAGTTATTGTTG
F1815: CCACAGAACGTCTTGTCAT
F2000: CGGAATGAAGAGGGTAAGG

Genomic DNA was extracted from B8 and partially digested with *Sau*3AI or completely digested with *Pst*I. DNA of 2-10 kb in length was recovered from gel and ligated to *Sau*3AI or *Pst*I cassette to construct cassette genomic libraries. Related cassette primer (CS or CP) and specific primer were used to amplify target DNA of unknown region from the libraries. The PCR conditions were as follows: pre-denaturation for 5 min at 94 ℃, and denaturation at 94 ℃ for 30 s, annealing at 52 ℃ for 60 s and extension at 72 ℃ for 5 min for 30 cycles, and a final extension at 72 ℃ for 10 min. Three rounds of PCR-based chromosomal walking, using *Pst*I and *Sau*3AI cassettes and related primers by turns, were performed to cover the full length of *anrF* gene (Figure 1).The full-length *anrF* gene was shown on the top (gray single line). The direction of the gene (narrow horizontal arrow, at right) and the Tn5 insertion site (thick vertical arrow) were marked. The long double line underneath stood for the F contig obtained in this research. The dark part on

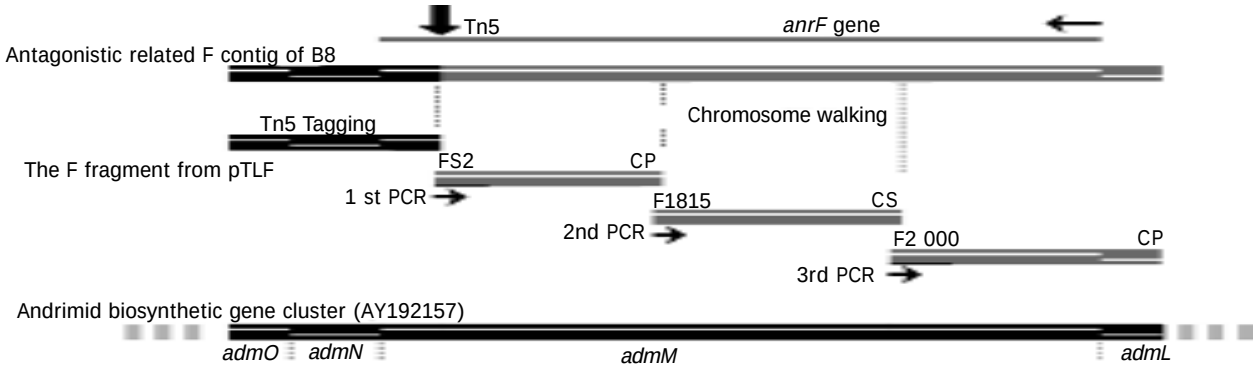

Figure 1 Framework of the cloning of full-length *anrF* gene with transposon tagging and chromosome walking.

the left of Tn5 insertion site (the F fragment) was obtained with transposon tagging. The gray part on the right was obtained with chromosomal walking. The four separate lines below were four steps (one tagging and three rounds of PCR) to get the contig. Primers were marked on top of the three gray lines. The black double line at the bottom showed the corresponding genes of *P. agglomerans* andrimid biosynthetic gene cluster (AY192157).

DNA sequencing and data analysis

The F fragment was sequenced, after subcloning of pTLF from M13 universal primer and P1 primer (CATGGAAG-TCAGATCCTGGA), a primer designed according to the sequence of the left edge of Tn5. PCR products of chromosomal walking were cloned into T-vector and sequenced using M13 universal primer. The DNA sequencing was done in Bioasia Biotech, Shanghai. DNA sequences obtained were edited, compiled, translated, and compared using DNAStar program. Homologous sequence and putative-conserved domain searches were done with BlastN and/or tBlastX and/or BlastP program at www.ncbi.nlm.nih.gov.

Continuity analysis of anrF gene in original B8 and its mutant B8F strain

Two primers were designed to amplify the full-length *anrF* gene. The upstream primer F21 (TTTTGTTGATGGAA-AGTCGCA) was located 144-126 bp up of the start codon. The downstream primer F2600 (CACCCAGCTGA-TGAAGTAAT) was located on opposite strand 73-56 bp down of the stop codon. The DNA fragments between the primers in the genomes of B8 and B8F were about 2 851 bp and 8.3 kb respectively. Genomic DNA of B8 or B8F was used as template. After 30 cycles of amplification, 6 μL of PCR products were applied to agarose gel electrophoresis to check the amplification. The amplified products were cloned and sequenced.

Verification of anrF gene participation in antagonism of B8

The full-length *anrF* gene amplified from B8 was cloned into pMD18-T vector and the resulting recombinant plasmid was designated as pMD-F. Gentamicin-resistance gene (*Gen*^{r}) was amplified with two primers (acc1-up: CGTGGAAACG-GATGAAG, acc1-down: ACCTGGCGGCGTTGTGACA) from pFastBac^{TM}HTA and cloned into pMD18-T too. The resulting recombinant plasmid was designated as pMD-G. The *Gen*^{r} gene was recovered from pMD-G with *Hin*dIII and *Bam*HI double cut and filled with klenow and inserted into *Xba*I cut and klenow filled pMD-F. The target plasmid with *Gen*^{r} and the full-length *anrF* gene was designated as pMD-FG.

Mutant *E. cloacae* B8F was cultured to an A_{600} about 0.6 in LB medium, and washed thrice in cold glycerol buffer. Plasmid pMD-FG was transformed into B8F with electroporation. The transformed bacteria were screened on plates with both ampicillin and gentamicin and verified by PCR amplification of *anrF* and *Gen*^{r} genes. The pMD-FG transformed strains were then inoculated on Wakimoto agar and cultured at 30 ℃ for 48 h, the resume of antagonistic characteristics was checked with the indication of *X. oryzae pv. oryzae* strain Xcom3104.

RESULTS

Transposon-mediated mutagenesis

The suicide plasmid pZJ25 was transferred into *E. cloacae* B8 by conjugation with the help of donor *E. coli* S17-1. The conjugation and transposition ratio was about 5×10^{-6}. A total of 1 500 transposed colonies (Rif^r Kan^r Cm^s) were obtained and two antagonistic mutant strains, one of which was designated as B8F, were selected.

Cloning of F fragment from B8F with tagging method

A recombinant plasmid designated as pTLF, a plasmid with intact *Kan*^{r} gene of Tn5 and a DNA fragment on the left of the insertion site (designated as F fragment), was isolated. The pTLF had two foreign *Bam*HI fragments, one of which was about 3.5 kb in length and contained the target F fragment and a fragment of Tn5 (with the *Kan*^{r} gene, about 2.7 kb in length). After subcloning, the 735 bp sequence of the F fragment was obtained with M13 universal sequencing primer and P1 primer.

Cloning of DNA fragments on the right of Tn5 insertion site with chromosomal walking

Only one DNA fragment on the left of insertion site was obtained with transposon tagging method. In order to know the full-length gene interrupted by Tn5 insertion, cassette PCR-based chromosomal walking method was adopted to clone DNA fragments on the right of insertion site. The framework of the cloning of the full-length *anrF* gene with transposon tagging and chromosomal walking was shown (Figure 1). With the use of specific primers (FS2, F1815, or F2000) and cassette primers (CP or CS) by turns, DNA fragments of unknown region were amplified from related cassette (*Pst*I or *Sau*3AI) libraries. The PCR products from three different rounds of chromosomal walking were obtained (Figure 2). They were about 1.2 kb in *Pst*I library (1st walking), about 950 bp in *Sau*3AI library (2nd walking), and about 900 bp in *Pst*I library (3rd walking), respectively. The total sequence obtained with chromosomal walking was 2 586 bp.

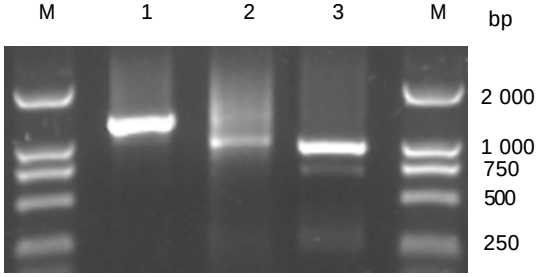

Figure 2 PCR products from three rounds of chromosomal walking. 1: PCR products, 1 209 bp in size, amplified from B8/*Pst*I-cassette library with FS2 and CP primers; 2: PCR products, 962 bp in size, amplified from B8/*Sau*3AI cassette library with F1815 and CS; 3: PCR products, mainly 900 bp in size, amplified from B8/*Pst*I cassette library with F2000 and CP; M: marker DL2000.

Sequence analysis of full-length anrF gene

A contig of 3 321 bp in length was obtained by transposon tagging and three rounds of chromosomal walking. Four ORFs, two complete and two partial were identified. One ORF, 2 634 bp in length, disrupted by the insertion of Tn5

in B8F was designated as *anrF* gene (accession no. AY633625) encoding for a 877 aa polyketide synthase-like protein. The Tn5 insertion site was at 2 420 bp of the *anrF* gene, and was at 214 bp before the stop codon.

BlastN search showed that the nucleotide sequence of *anrF* gene had a homology of 83% to that of *admM* gene of *P. agglomerans* andrimid biosynthetic gene cluster (AY192157). The alignment of *anrF* and *admM* genes is shown in Figure 3.

BlastP search showed that the deduced amino acid sequence encoded by the *anrF* gene was homologous to AdmM (79%

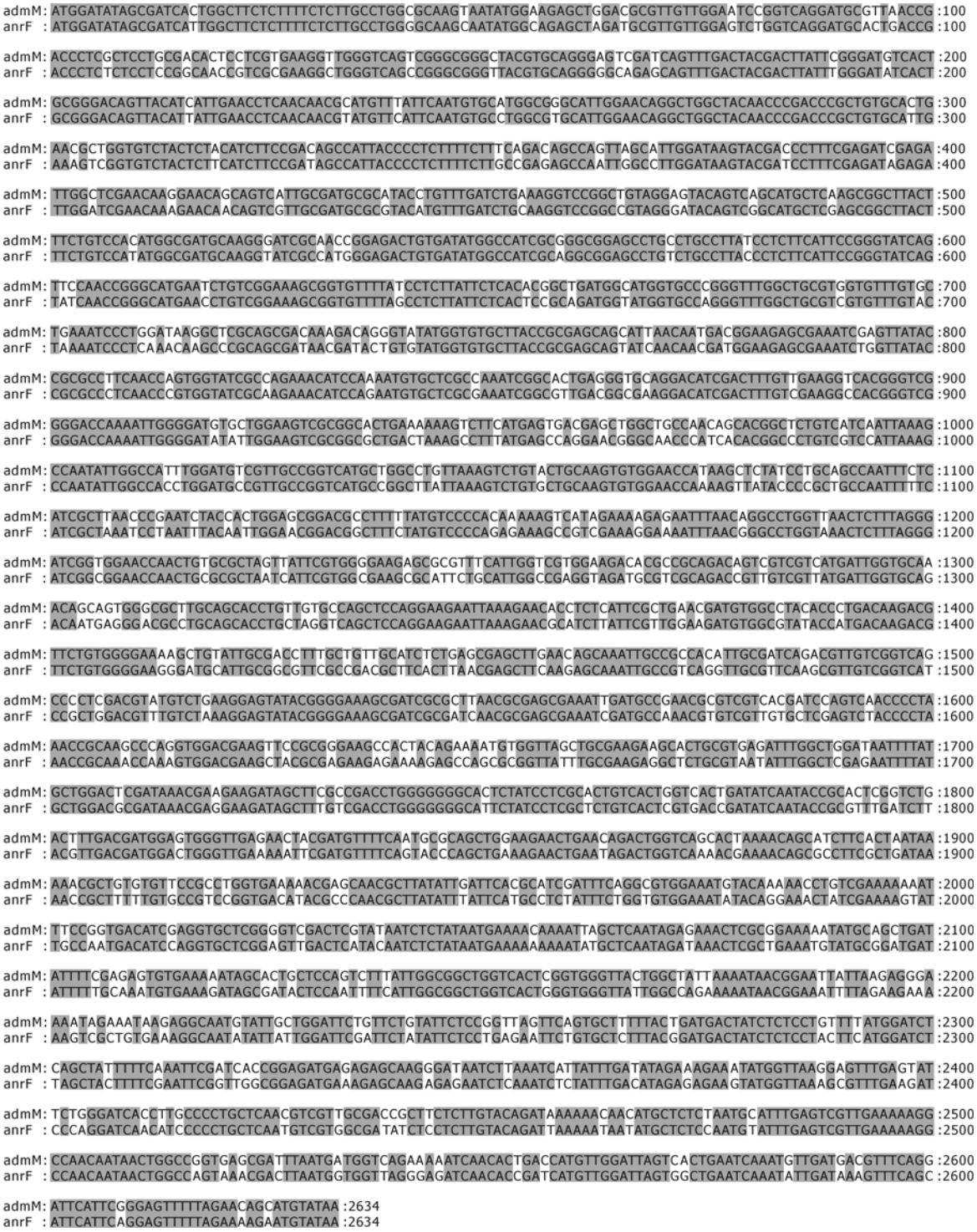

Figure 3 Alignment of nucleotide sequences of *anrF* gene and *admM* gene of *P. agglomerans* andrimid biosynthetic gene cluster (AY192157). The names of the genes are typed at the left and the number of nucleotides is at the right. The identical nucleotides between two genes are marked with gray background.

ID/87% SIM) and many other proteins of polyketide/non-ribosomal peptide synthetase or polyketide synthase (type I) modules (about 28-38% ID/45-58% SIM). Conserved domain search showed that the N-terminal of the protein (about 1-410 aa) encoded for a polyketide synthase module (COG3321) or animal-type fatty-acid synthase (KOG1202) or ketoacyl synthase (pfam00109 and pfam02801) or 3-oxoacyl-(acyl-carrier-protein) synthase (FabB or COG0304, and KOG1394)-like domain. The middle sequence (about 550-610 aa) encoded for a phosphopantetheine attachment site (pfam00550)-like domain. The C terminal (about 640-877 aa) encoded for a thioesterase of type I polyketide synthase (COG3319, pfam00975, and COG3208)-like domain, which was disrupted by the insertion of Tn5 in B8F.

Continuity analysis of anrF gene in original B8 and its mutant B8F strain

With F21 and F2600 as primers, no band was amplified in the reaction mixture using B8F genomic DNA as template, while a PCR product 2.8 kb in length, as expected, was observed in that of B8 (Figure 4). The 2.8 kb PCR product of B8 was further cloned and sequenced. The sequence result conformed the continuity of the *anrF* gene in B8.

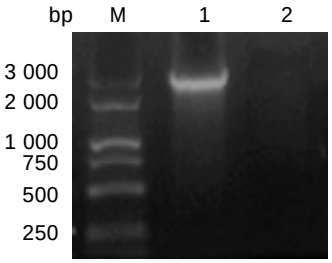

Figure 4 PCR amplification of full-length *anrF* gene. 1: PCR products amplified from B8; 2: PCR products amplified from B8F; M: marker 3 kb.

Verification of anrF gene participation in antagonism of B8

The pMD-FG, a plasmid with the full-length *anrF* and *Gen*^{r} genes, was constructed and transformed into the mutant *E. cloacae* B8F. The antagonistic activity of pMD-FG transformed B8F against *X. oryzae pv. oryzae* was then resumed, though the antagonistic ring was a little bit small and ambiguous (Figure 5).

DISCUSSION

E. cloacae B8 is an antagonistic bacterium isolated from rice leaves, using *X. oryzae pv. oryzae* Xcom3104 as an indicator[1]. It has a strong antagonistic activity against *X. oryzae pv. oryzae* and satisfactory results have been obtained on anti-rice bacterial leaf brilliant in net house and in field[4]. Further researches showed that *E. cloacae* B8 and its antagonistic substances are also antagonistic to many other plant bacterial pathogens such as *Pseudomonas*, *Agrobacterium*[3], and human (animal) bacterial pathogens such as MRSA[5,6]. *E. cloacae* B8 and its antagonistic substances can be potentially used for the control of the rice bacterial leaf brilliant and many other bacterial diseases of plants, animals and humans.

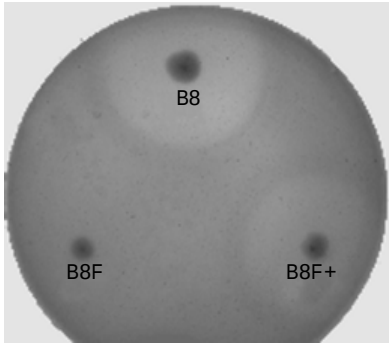

Figure 5 Antagonistic activity of B8, B8F and B8F/pMD-FG. B8F+: pMD-FG transformed B8F.

It was reported that *E. cloacae* EcCT-501R3 has an antagonistic activity[7,8]. Two antagonistic-related genes for linoleic acid utilization, *fadB* and *fadL*, have been cloned using transposon-mediated mutagenesis and tagging. Further researches have verified that *E. cloacae* EcCT-501R3 inhibits *Pythium ultimum* sporangium germination by a competitive exclusion mechanism, the competitive utilization of long-chain fatty acids of seed exudates[9].

Our previous work, however, showed that B8 has an antagonistic mechanism different from what has been reported[1,3]. To elucidate the antagonistic mechanism and to clarify the antagonistic substances of *E. cloacae* B8, transposon tagging strategy[9-12] was employed to clone genes related to its antagonistic activity. With suicide plasmid pZJ25 carrying Tn5, two antagonistic mutant strains, one of which was named B8F, were selected. Tagging with *Kan*^{r} gene of Tn5, the F fragment on the left of Tn5 insertion site was cloned in pTLF. Then, cassette PCR[13-15]-based chromosomal walking was applied to the amplification of unknown DNA fragments on the right of Tn5 insertion site. A contig of 3 321 bp in length was obtained after three rounds of chromosomal walking together with the F fragment from transposon tagging. One complete ORF of 2 634 bp in length, disrupted by the Tn5 insertion in B8F, was identified in the contig. It encoded for a 877 aa polyketide synthase-like protein and was designated as *anrF* gene. The Tn5 insertion site was at 2 420 bp of the *anrF* gene, and was at 214 bp before the stop codon, suggesting that the loss of antagonistic activity of mutant strain B8F was a result of the knock-out of *anrF* gene by Tn5.

To confirm this theory, the continuity of the *anrF* gene in the original B8 and its mutant B8F strains was checked. The complete *anrF* gene 2.8 kb in length was amplified from the B8 genome. The sequence result further confirmed the continuity of *anrF* gene in the original B8. The length of the DNA fragment between the primers in the genome of B8F was about 8.3 kb. However, no band was amplified from B8F. As the parameters set for amplification were suitable for amplification fragments 2.8 kb or less in length but not for fragments up to 8.3 kb.

In addition, plasmid pMD-FG with full-length *anrF* and *Gen*^{r} genes was constructed. After pMD-FG was transformed into B8F, a mutant strain of B8 knocked out by Tn5-mediated mutagenesis, the antagonistic

characteristics were resumed, indicating that the *anrF* gene participated in the production of the antagonistic activity of B8.

BlastN search showed that the nucleotide sequence of the *anrF* gene had a homology of 83% to that of the *admM* gene of *P. agglomerans* andrimid biosynthetic gene cluster (AY192157). BlastP search showed the deduced amino acid sequence encoded by the *anrF* gene was homologous to the AdmM (79% ID/87% SIM) and many other proteins of polyketide synthase/non-ribosomal peptide synthetase (about 28-38% ID/45-58% SIM). Domain search showed that the N-terminal of the protein encoded for a polyketide synthase module (COG3321) or animal-type fatty-acid synthase (KOG1202)-like domain. The middle sequence encoded for a phosphopantetheine attachment site (pfam00550)-like domain. And the C terminal encoded for a thioesterase of type I polyketide synthase (COG3319)-like domain, which was disrupted by the insertion of Tn5. It was this insertion that led to the loss of antagonistic activity of B8F, suggesting that the protein encoded by *anrF* gene is a polyketide synthase similar to AdmM of *P. agglomerans*, and that the antagonistic substances produced by B8 are andrimid and/or analogs of andrimid. This result is consistent with our early observations[1,3].

Andrimid and its analogs are antibiotic substances of the polyketide (pyrrolidinedione) family[22]. Only three different strains of bacteria, other than B8, have been reported to produce these substances so far. Frenenhagen *et al.*[23], first reported the identification of andrimid, a new peptide antibiotic produced by an intracellular bacterial symbiont isolated from a brown planthopper. It has been reported that andrimid exhibits a moderate activity against *Bacillus sp.* and a very good activity against *X. campestris*, an early name of the pathogen of bacterial blight in rice plants[23]. Needham *et al.*[24], reported that andrimid and Moiramides A-C are produced in culture by a marine isolate of *Pseudomonas fluorescens*. Singh *et al.*[25], further showed that andrimid secreted from this strain exhibits antibacterial activity against both Gram-positive and Gram-negative bacteria. Oclarit *et al.*[26], found that anti-*Bacillus* peptide antibiotic, an andrimid in the marine sponge, *Hyatella* species, is produced by an associated *Vibrio* species bacterium. Freiberg *et al.*[22], reported that andrimid and its analogs act as selective inhibitors of bacterial acetyl-CoA carboxylase.

However, no genes related to the production of andrimid are published so far, except for the andrimid biosynthetic gene cluster of *P. agglomerans* (AY192157). The complete genome of AY192157 is 28 485 bp in length and encodes for 21 genes, from *admA*, *admB* to *admU*. The *anrF* gene cloned in this research has a homology of 83% to *admM*. Furthermore, the arrangement and the sequences of other ORFs or non-coding regions around the *anrF* gene have shown that the F contig obtained in this research is an equivalent of a part of AY192157 (data not shown). *P. agglomerans* (formerly *Erwinia herbicola*) is a closely related but nonpathogenic bacterium of *E. amylovora*[27]. It usually accompanies *E. amylovora* in the wild and produces a family of antibiotics[28-30] to inhibit fire blight, a devastating disease of rosaceous plants such as apple and pear caused by the latter bacterium. *E. cloacae* B8 has been isolated from rice leaves as an antagonistic bacterium of *X. oryzae pv. oryzae*. However, both *E. cloacae* and *P. agglomerans* are members of the *Enterobacteriacea* family. Whether this is the reason why the *anrF* and *admM* genes have a high similarity, or whether the equivalents of andrimid biosynthetic genes are similar or identical in bacteria other than *Enterobacteriacea* family, including *Pseudomonas* and *Vibrio* remains to be studied.

REFERENCES

1 **Chen WL**, Ge WX, Li DB. A study on *Enterobacter cloacae* B8, *Bacillus subtillus* B826 and their antagonistic substance to *Xanthomonas campestris pv. oryzae*. *Zhejiang Nongye Daxue Xuebao* 1990; **16**(Suppl 2): 61-67

2 **Xu YP**, Zang RC, Chen WL, Lou YC. Promoting plant growth and IAA analysis of *Enterobacter cloacae* B8 fermentation liquid. *Zhejiang Daxue Xuebao* 2001; **27**: 282-284

3 **Chen WL**. Antagonistic substances produced by bacterial strains to *Xanthomonas oryzae pv. oryzae*. Ph. D. thesis. *Zhejiang Unviersity* 2001: 59-66

4 **Chen WL**, Xu P, Gong FH, Li DB. Study on coloninzation of *Enterobacter cloacae* B8x on rice leaves and its control of rice bacterial leaf blight (*Xanthomonas oryzae pv. oryzae*). *Nongye Shengwujishu Xuebao* 1994; **2**: 61-66

5 **Zhang R**, Chen WL, Zhu BR. The antagonistic activities of the extract of *Enterobacter clocae* B8 to methicillin-resistant *Staphylococcus aureus*. *Zhonghua Weishengwuxue He Mianyixue Zazhi* 2003; **23**: 172

6 **Ya-Ping J**, Wei-Liang C, Rong Z, Bai-Rong Z. The biological activity of antibacterial substance produced by *Enterobacter cloacae* B8. *Rinsho Biseibutshu Jinsoku Shindan Kenkyukai Shi* 2003; **13**: 115-120

7 **van Dijk K**, Nelson EB. Inactivation of seed exudates stimulants of *Pythium ultimum* sporangium germination by biocontrol strain of *Enterobacter cloacae* and other seed-associated bacteria. *Soil Biol Biochem* 1998; **29**: 351-355

8 **Kageyama K**, Nelson EB. Differential inactivation of seed exudate stimulation of *Pythium ultimum* sporangium germination by *Enterobacter cloacae* influences biological control efficacy on different plant species. *Appl Environ Microbiol* 2003; **69**: 1114-1120

9 **van Dijk K**, Nelson EB. Fatty acid competition as a mechanism by which *Enterobacter cloacae* suppresses *pythium ultimum* sporangium germination and damping-off. *Appl Environ Microbiol* 2000; **66**: 5340-5347

10 **Wei JF**, Zhang SG, Ma YC. Transposon Tn5-induced INA$^-$ Mutants in INA$^+$ Bacteria. *Yunan Nongye Daxue Xuebao* 2002; **17**: 1-4

11 **Mills D**. Transposon mutagenisis and its potential for studying virulence genes in plant pathogens. *Ann Rev Phytopathol* 1985; **23**: 297-320

12 **Kumar A**, des Etages SA, Coelho PS, Roeder GS, Snyder M. High-throughput methods for the large-scale analysis of gene function by transposon tagging. *Methods Enzymol* 2000; **328**: 550-574

13 **Kilstrup M**, Kristiansen KN. Rapid genome walking: a simplified oligo-cassette mediated polymerase chain reaction using a single genome-specific primer. *Nucleic Acids Res* 2000; **28**: E55-58

14 **Riley J**, Butler R, Ogilvie D, Finniear R, Jenner D, Powell S, Anand R, Smith JC, Markkham AF. A novel rapid method for the isolation of terminal sequences from yeast artificial chromosome (YAC) clones. *Nucleic Acids Res* 1990; **18**: 2887-2890

15 **Zhang Z**, Gurr SJ. Walking into the unknown: a 'step down' PCR-based technique leading to the direct sequence analysis of flanking genomic DNA. *Gene* 2000; **253**: 145-150

16 **Yu XP**, Zhu JL, Yao XP, He SC, Huang HN, Chen WL, Li DB.

Cloning and analysis of the antagonistic related genes of *Enterobacter cloacae* B8. *Chin Sci Bull* 2004; **49**: 1370-1375
17 **Yu XP**, Zhu JL, Yao XP, He SC, Huang HN, Chen WL, Li DB. Cloning and analysis of the antagonistic related genes of *Enterobacter cloacae* B8. *Kexue Tongbao* 2004; **49**: 1139-1144
18 **Huang HN**, Yu XP, Gong HF, Xu P, Chen WL, Li DB. Cloning and detecting of the antagonistic related genes of *Enterobacter cloacae* B8 with transposon tagging method. *Zhejiang Daxue Xuebao* 2005, in press
19 **Xu P**, Chen WL, Zhu WG, Li DB. A drug resisitant mutant of antagonistic bacterium *Eterobacter cloacae* B8. *Zhejiang Nongye Daxue Xuebao* 1992; **18**: 115-119
20 **Li P**, Long JY, Huang YC, Zhang Y, Wang JS. The avrXa3, a new member of avrBs3 family isolated from *Xanthomonas oryzae pv. oryzae* is an avirulent gene of double function. *Ziran Kexue Jinzhan* 2004; **14**: 767-781
21 **Wang JS**, He CY, Ye HY. Tn5-induced virulence gene mutants and their biochemical properties of *Xanthomonas campestris pv. oryzae*. *Zhiwu Bingli Xuebao* 1992; **22**: 217-223
22 **Freiberg C**, Brunner NA, Schiffer G, Lampe T, Pohlmann J, Brands M, Raabe M, Habich D, Ziegelbauer K. Identification and characterization of the first class of potent bacterial acetyl-CoA carboxylase inhibitors with antibacterial activity. *J Biol Chem* 2004; **279**: 26066-26073
23 **Frenenhagen A**, Tamura SY, Kenny PTM, Komura H, Naya Y, Nakanishi K. Andrimid, a new peptide antibiotic produced by an intracellular bacterial symbiont isolated from a brown planthopper. *J Am Chem Soc* 1987; **109**: 4409-4411
24 **Needham J**, Kelly MT, Ishige M, Andersen RJ. Andrimid and moiramides A-C, metabolites produced in culture by a marine isolate of the bacterium *Pseudomonas fluorescens*: structure elucidation and biosynthesis. *J Org Chem* 1994; **59**: 2058-2063
25 **Singh MP**, Mroczenski-Wildey MJ, Steinberg DA, Andersen RJ, Maiese WM, Greenstein M. Biological activity and mechanistic studies of andrimid. *J Antibiot* 1997; **50**: 270-273
26 **Oclarit JM**, Okada H, Ohta S, Kaminura K, Yamaoka Y, Iizuka T, Miyashiro S, Ikegami S. Anti-bacillus substance in the marine sponge, *Hyatella* species, produced by an associated *Vibrio* species bacterium. *Microbios* 1994; **78**: 7-16
27 **Gavini F**, Mergaert J, Beji A, Mielcarek C, Izard D, Kersters K, de Ley J. Transfer of *Enterobacter agglomerans* (Beijerinck 1988) Ewing and Fife 1972 to *Pantoea* gen. nov. as *Pantoea agglomerans* comb. nov. and description of *Pantoea dispersa* sp. nov. *Int J Syst Bacteriol* 1989; **39**: 337-345
28 **Wright SA**, Zumoff CH, Schneider L, Beer SV. *Pantoea agglomerans* strain EH318 produces two antibiotics that inhibit *Erwinia amylovora in vitro*. *Appl Environ Microbiol* 2001; **67**: 284-292
29 **Giddens SR**, Houliston GJ, Mahanty HK. The influence of antibiotic production and pre-emptive colonization on the population dynamics of *Pantoea agglomerans* (*Erwinia herbicola*) Eh1087 and *Erwinia amylovora* in planta. *Environ Microbiol* 2003; **5**: 1016-1021
30 **Wodzinski RS**, Paulin JP. Frequency and diversity of antibiotic production by putative *Erwinia herbicola* strains. *J Appl Bacteriol* 1994; **76**: 603-607

Science Editor Wang XL and Guo SY **Language Editor** Elsevier HK

PO Box 2345, Beijing 100023, China
www.wjgnet.com
wjg@wjgnet.com

ELSEVIER

World J Gastroenterol 2005;11(39):6159-6164
World Journal of Gastroenterology ISSN 1007-9327

• *BASIC RESEARCH* •

Receptor-binding domain of SARS-Cov spike protein: Soluble expression in *E.coli*, purification and functional characterization

Jing Chen, Lin Miao, Jia-Ming Li, Yan-Ying Li, Qing-Yu Zhu, Chang-Lin Zhou, Hong-Qing Fang, Hui-Peng Chen

Jing Chen, Lin Miao, Yan-Ying Li, Hong-Qing Fang, Hui-Peng Chen, Institute of Biotechnology, Academy of Military Medical Science, Beijing 100071, China
Jing Chen, Chang-Lin Zhou, The Pharmaceutical University of China, Nanjing 210009, Jiangsu Province, China
Jia-Ming Li, Qing-Yu Zhu, Institute of Microbiology and Epidemiology, Academy of Military Medical Sciences, Beijing 100071, China
Co-Correspondence: Hui-Peng Chen
Correspondence to: Hong-Qing Fang, Institute of Biotechnology, Academy of Military Medical Science, 20 Dongda Street, Fengtai District, Beijing 100071, China. fanghongqing@yahoo.com.cn
Telephone: +86-10-66948824
Received: 2005-03-22 Accepted: 2005-04-11

Abstract

AIM: To find a soluble and functional recombinant receptor-binding domain of severe acute respiratory syndrome-associated coronavirus (SARS-Cov), and to analyze its receptor binding ability.

METHODS: Three fusion tags (glutathione *S*-transferase, GST; thioredoxin, Trx; maltose-binding protein, MBP), which preferably contributes to increasing solubility and to facilitating the proper folding of heteroprotein, were used to acquire the soluble and functional expression of RBD protein in *Escherichia coli* (BL21(DE3) and Rosetta-gamiB (DE3) strains). The receptor binding ability of the purified soluble RBD protein was then detected by ELISA and flow cytometry assay.

RESULTS: RBD of SARS-Cov spike protein was expressed as inclusion body when fused as TrxA tag form in both BL21 (DE3) and Rosetta-gamiB (DE3) under many different cultures and induction conditions. And there was no visible expression band on SDS-PAGE when RBD was expressed as MBP tagged form. Only GST tagged RBD was soluble expressed in BL21(DE3), and the protein was purified by ÄKTA Prime Chromatography system. The ELISA data showed that GST•RBD antigen had positive reaction with anti-RBD mouse monoclonal antibody 1A5. Further flow cytometry assay demonstrated the high efficiency of RBD's binding ability to ACE2 (angiotensin-converting enzyme 2) positive Vero E6 cell. And ACE2 was proved as a cellular receptor that meditated an initial-affinity interaction with SARS-Cov spike protein. The geometrical mean of GST and GST•RBD binding to Vero E6 cells were 77.08 and 352.73 respectively.

CONCLUSION: In this paper, we get sufficient soluble N terminal GST tagged RBD protein expressed in *E.coli* BL21 (DE3); data from ELISA and flow cytometry assay demonstrate that the recombinant protein is functional and binding to ACE2 positive Vero E6 cell efficiently. And the recombinant RBD derived from *E.coli* can be used to developing subunit vaccine to block S protein binding with receptor and to neutralizing SARS-Cov infection.

Key words: Receptor-binding domain; SARS-Cov; Spike protein expression; *E.coli*

Chen J, Miao L, Li JM, Li YY, Zhu QY, Zhou CL, Fang HQ, Chen HP. Receptor-binding domain of SARS-Cov Spike protein: Soluble expression in *E.coli*, purification and functional characterization. *World J Gastroenterol* 2005; 11(39): 6159-6164

http://www.wjgnet.com/1007-9327/11/6159.asp

INTRODUCTION

Severe acute respiratory syndrome (SARS), a newly emerging infectious disease, is caused by a SARS-associated coronavirus (SARS-Cov)[1,2]. SARS-Cov can infect African green monkey kidney cells (Vero E6) and cause a similar disease in *Cynomolgus macaques* (*Macaca fascicularis*)[3,4]. The SARS viral genome comprises approximately 30 000 nucleotides, which are organized into approximately 13-15 open reading frames (ORFs), taking into consideration only those exceeding 50 amino acids in translational capacity[5,6]. Sequence comparison with corresponding ORFs of other known coronaviruses reveals a similar pattern of gene organization typical of coronaviruses[7]. SARS-Cov contains a single-strand plus-sense RNA genome about 30 kb in length and has a 5'-cap structure and a 3'-polyadenylation tract. And the genomic organization is typical of coronaviruses, having five major ORFs that encode the replicase polyproteins: the spike (S), envelope (E), and membrane (M) glycoproteins. The full-length genome sequence of SARS-Cov has been elucidated within few weeks after the identification of this novel pathogen[8-10].

When coronavirus enters the cells, the 50-region of viral genome is translated into a large poly-peptide that is cleaved by viral-encoded proteases to release RNA-dependent RNA polymerase and adenosine triphosphatase/helicase. These proteins, in turn, are responsible for replicating the viral genome as well as generating nested transcripts that are used in the synthesis of viral proteins. Viral membrane proteins, including S and M, are inserted into the endoplasmic reticulum (ER), while RNA genome assembles with the N

protein. This RNA-protein complex then associates with M proteins and buds into the lumen of the ER. The virus particles then migrate through the Golgi complex and exist in the cells by exocytosis[6,11]. The first step *in viral* infection is the binding of viral proteins to certain cellular receptors. So far, the S protein of coronavirus is considered as the site of viral attachment to the host cells. It has been shown that a cellular metallopeptidase, angiotensin-converting enzyme 2 (ACE2), could bind to S1 domain of SARS-Cov' S protein and support viral replication[12]. And a 193-amino-acid fragment of the S protein (residues 318-510) is a receptor binding domain (RBD) of SARS-Cov S protein[13]. Here we reported the soluble expression, purification, and functional characterization of RBD expressed in *Escherichia coli*.

MATERIALS AND METHODS

Materials

E.coli DH5α competent cells, *E.coli* BL21(DE3) competent cells, *E.coli* Rosetta-gamiB (DE3) competent cells, pET22b, TrxATag (Thioredoxin) expression vector pET32a were products of Novagen Inc. The genotype of Rosetta-gamiB (DE3): △*ara-leu 7697* △*lacX74* △*phoAPvuII pho*R *araD139 ahpC gale galK rspL* F'[*lac*+(*lacIq*)*pro*] *gor522*::Tn*10* (TcR) *trxB*:: kan (DE3) pRARE (CmR). GSTag (glutathione *S*-transferase) expression vector pGEX-4t-2 was purchased from Invitrogen Inc. Chromatography media Q Sepharose Fast Flow, Q Sepharose High Performance, Butyl Sepharose Fast Flow, Superdex 75, goat anti-GST polyclone antibody were purchased from Amersham Inc. FITC-labeled rabbit anti-goat IgG, goat anti-mouse IgG conjugated with HRP were products of Beijing Xin Jing Ke Biotechnology Co., Ltd. The primers with restriction enzyme sites *Bam*HI and *Xho*I to amplify RBD gene were synthesized by Beijing Bioasia Inc. pET-S plasmid containing the full length gene of S protein of SRAS-Cov (isolate BJ01, GenBank accession number AY278488) was kindly provided by Beijing Hua Da Gene Research Center. Anti-RBD of S protein mouse monoclonal antibody 1A5 was provided by the Institute of Microbiology and Epidemiology, Academy of Military Medical Sciences. pET-MBP was constructed by inserting maltose-binding protein (MBP) gene derived from *E.coli* JM109 strain into pET22b between *nde*I and *Bam*HI restriction enzyme sites, conserved by the Institute of Biotechnology, Academy of Military Medical Sciences.

Plasmids construction and engineering bacteria

A pair of primers was used in PCR reaction to amplify RBD gene (N terminal 318-510 amino acid fragments) of S protein from pET-S plasmid (EC1: 5'-CGGGATCCGACG-ATGACGATAAGAATATTACAAACTTGTGTCCT-3', EC2: 5'-CCG CTCGAGTTAAACCGTGGCCGGT-GGATTTAA-3'). The amplified RBD gene fragment was purified on a 10 g/L low-melting agarose gel, utilizing the PCR purification system (Q Biogene Inc.) The purified PCR products were directly ligated into expression vector pET32a, pETGEX-4t-2, and pET-MBP respectively. The progress of vector construction follows the example of pET32-RBD according to the clone strategy from TaKaRa Biotechnology Co., Ltd. (Figure 1). After transformation of the *E.coli* strain DH5α competent cells, the clone was selected on ampicillin containing (100 mg/L) plates for mini-preparation and insert evaluation was by enzyme digestion and DNA sequencing. Bacterial transformation for expressing RBD was carried out by incubating bacterial strain BL21(DE3) (Novagen) with pET32-RBD, pGEX-RBD, and pET-MBP-RBD plasmid DNAs on ice for 30 min and heat-shock treatment for 90 s as per the manufacturer's instruction, so did transforming pET32-RBD into bacterial strain Rosetta-gamiB(DE3) (Novagen) but ampicillin (100 mg/L), chloramphenicol (34 mg/L), kanamycin (12 mg/L), tetracycline (12.5 mg/L) selection. Hence expression of four engineering bacteria was performed (Table 1).

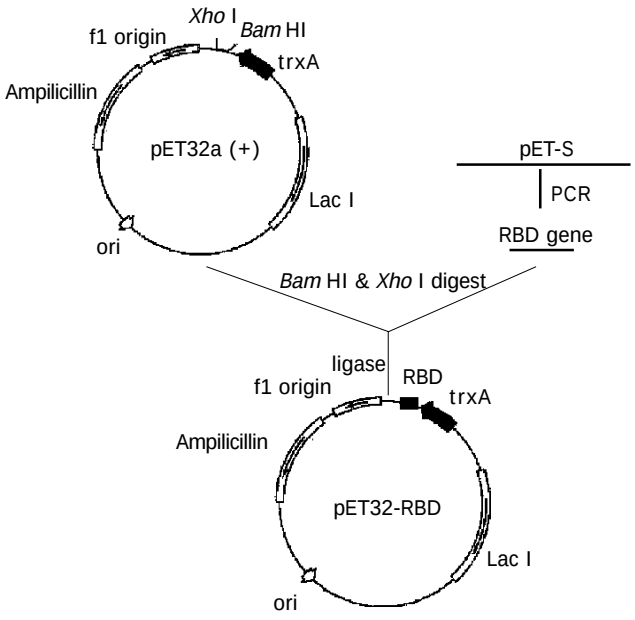

Figure 1 Schematic illustration of the constructs of expression vector pET32-RBD.

Optimization of protein expression and solubility analysis in E.coli

Each single colony on the LB plate was inoculated into

Table 1 Construction of recombinant plasmid and expression of engineering bacterium

Engineering bacterium	Recombinant plasmid	Expression host (*E.coli* strain)	Expression vector used	Fusion tag
E.coli BL-TB	pET32-RBD	BL21(DE3)	pET32a	TrxA·tag S·tag
E.coli R-TB	pET32-RBD	Rosetta-gamiB(DE3)	pET32a	TrxA·tag S·tag
E.coli BL-GB	pGEX-RBD	BL21(DE3)	pGEX-4t-2	GST·tag
E.coli BL-MB	pET-MBP-RBD	BL21(DE3)	pET-MBP	MBP·tag

5 mL of LB broth containing 100 μg/mL ampicillin (chloramphenicol (34 mg/L), kanamycin (12 mg/L), tetracycline (12.5 mg/L) additional for *E.coli* R-TB) and incubated overnight at 37 ℃ in a bacterial shaker. One hundred microliters of fresh engineering bacterium preparation was added to 20 mL of antibiotic containing LB broth. The bacteria were induced with 0.25-5 mmol/L IPTG when the optical density of the bacteria reached between 0.5 and 0.6 $A_{600\ nm}$, then shaked for an additional 1-8 h in a bacterial shaker at 20 or 37 ℃. One milliliter of the bacteria was taken out at 2, 4, 6, and 8 h, centrifuged, and lysed. Four microliters of cell lysate, after centrifuging the soluble and insoluble fragments, was electrophoresed on a 150 g/L SDS-PAGE for evaluation of protein expression. The expression of engineering bacteria derived from BL21(DE3) also performed by FML medium which is enriched in LB broth (7 g/L K_2HPO_4, 3 g/L NaH_2PO_4, 0.5 g/L $MgSO_4$, 2 g/L glucose, 2 mmol/L lactose) and target protein was induced by lactose. The protein expression has been evaluated after being cultured 9 h later as the same way.

Purification of the recombinant RBD protein

The *E.coli* BL-GB pellet from the 1 L culture was washed with 20 mmol/L Tris-HCl, pH 7.4, 5 mmol/L sodium EDTA, and 200 g/L sucrose. The pellet was resuspended with sonication buffer (20 mmol/L Tris-HCl, pH 8.0, 5 mmol/L EDTA) at the ratio of 1:40. The suspension was sonicated for lysing cells cooled in ice between sonication pulses. The lysate was centrifuged at 12 000 *g* for 30 min at 4 ℃ to separate out the debris. Then supernatant containing the recombinant RBD protein was purified by ÄKTA Prime Chromatography system using Q Sepharose FastFlow, Q Sepharose High Performance, Butyl Sepharose FastFlow, Superdex 75 gel exclusion Columns (Amersham-Pharmacia) respectively. The purified protein which conserved in 1×PBS was electrophoresed on a 150 g/L SDS-PAGE gel and stained with Coomassie blue. The gel was destained with 70 mL/L acetic acid and 50 mL/L methanol. The protein appeared to be induced quite well and purified to single band entities, demonstrating high purity of the protein products. The protein migrated at approximately 48 ku as expected.

ELISA

Purified GST·RBD protein was blocked to Maxisorp ELISA plate in 1×PBS at 1 μg/well. Anti-RBD of SARS-Cov spike protein mouse monoclonal antibody 1A5, then goat anti-mouse IgG conjugated with HRP was incubated with different ratios of dilution in each well at 37 ℃ for 2 h. Wells were washed with buffer then $A_{450\ nm}$ was measured.

Flow cytometry assay

A Becton Dickinson FACSCalibur cytofluorometer, which was in the Institute of Biotechnology, Academy of Military Medical Sciences, was used for flow cytometry. SARS-Cov susceptible Vero E6 cell was cultured in 12-well plate (5×10^6 cells/well). Cells were incubated at 37 ℃ for 3 h with 0.4 mg/mL purified GST protein and GST·RBD protein respectively, then washed thrice with fluorescence-activated cell sorting (FACS) buffer (PBS containing 20 g/L bovine serum)[14-16]. After being trypsinized, the cells were washed thrice with FACS buffer and then centrifuged at 2 000 r/min for 4 min in a 1.5 mL eppendorf tube for collecting cells. The prime antibody goat anti-GST polyclone antibody diluted in PBS containing 50 g/L bovine serum albumin at the ratio 1:2 000 were adsorbed to 5×10^6 cells in suspension for 1 h at room temperature. Then the secondary antibody was also adsorbed. Control, which was negative, was Vero E6 cells alone.

RESULTS

Soluble expression of recombinant RBD protein

TrxA tagged RBD protein expressed in two engineering bacteria (*E.coli* BL-TB and R-TB) were inclusion bodies. Under various cultures and induction conditions, *E.coli* BL-TB expressed RBD protein as inclusion body, including reduced IPTG induction concentration, shortened induction time and lowered induction temperature (data not shown). *E.coli* R-TB yielded high target protein expression, with level approaching approximately 40% of the total cellular protein but inclusion body. Especially, bacterial strain Rosetta-gamiB carries the thioredoxin reductase (*TrxB*) and glutathione reductase (*gor*) mutations which have the potential to enhance disulfide bond formation and ultimately solubility and activity, meanwhile it carries pRare plasmid which directs the rare tRNA genes synthesis that can enhance the expression of target protein. But the predominance of Rosetta-gamiB (DE3) for protein soluble expression was not clear. Maybe the overexpression of heteroprotein greatly counteract the helpfulness of host's *TrxB* and *gor* double mutations to the proper folding of the protein . Or the nature RBD folding form does not depend upon the disulfide bond formed by two cysteines (Figure 2A).

There was no visible expression in *E.coli* BL-MB in which RBD was MBP fused according to SDS-PAGE analysis. Some secondary structure might emerge at the upstream of ribosome binding domain of cloned gene in the pET-MBP-RBD. Or there was very little protein expressed and needed detection by Western blot. Among all four engineering bacteria, only *E.coli* BL-GB expressed soluble RBD protein GST tagged, and its expressional capacity was greater in FML medium than in LB broth. The protein migrated on SDS-GAGE at approximately 48 ku as expected (Figure 2B). So engineering bacterium BL-GB was selected to generate recombinant GST·RBD for further research (Figure 2C).

ELISA

Data from ELISA showed that the purified GST·RBD antigen had positive reaction with anti RBD mouse monoclonal antibody 1A5. Test result primarily indicated that the recombinant protein was by nature a three-dimensional structure (Figure 3).

Flow cytometry assay

To better detect the receptor binding ability of GST·RBD and then prove it was of dimensional structure and functional, flow cytometric analysis was performed (Figure 4). Because Vero E6 cell is SARS-Cov susceptible, the functional recombinant RBD should bind to ACE2 existing at the cell membrane of Vero E6 cell, after prime antibody and fluorescence-

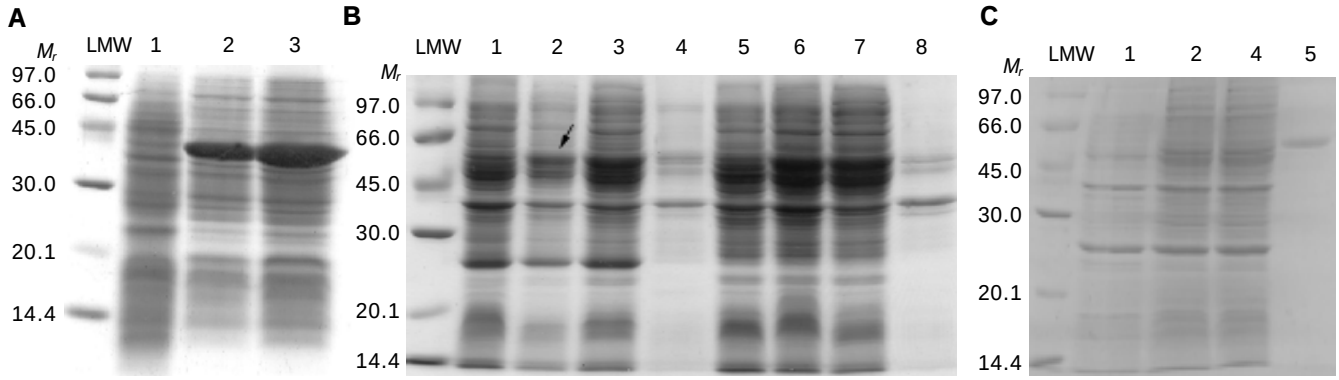

Figure 2 A: RBD expressed in *E.coli* R-TB as inclusion body form. LMW: protein low molecule weight marker (Amersham-Pharmacia); lane 1: *E.coli* BL21(DE3) negative control; lane 2: *E.coli* R-TB 5 mmol/L IPTG induced 4 h later; lane 3: *E.coli* R-TB 5 mmol/L IPTG induced 6 h later; B: *E.coli* BL-GB and BL-MB expression and solubility analysis. LMW: protein low molecule weight marker (Amersham-Pharmacia); lane 1: *E.coli* BL21(DE3) negative control; lane 2: *E.coli* BL-GB in FML medium; lane 3: soluble fraction; lane 4: insoluble fraction; lane 5: *E.coli* BL21(DE3) negative control; lane 6: *E.coli* BL-MB induced at 5 mmol/L IPTG 6 h later; lane 7: soluble fraction; lane 8: insoluble fraction; C: The purified recombinant RBD protein expressed in *E.coli* BL-GB. LMW: protein low molecule weight marker (Amersham-Pharmacia); lane 1: *E.coli* BL21(DE3) negative control; lane 2: IPTG induced *E.coli* BL-GB; lane 2: soluble fraction; lane 4: purified RBD protein.

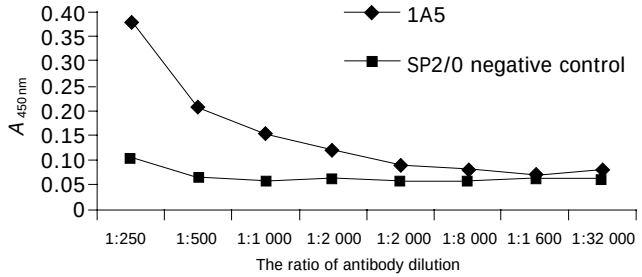

Figure 3 ELISA of GST·RBD antigen.

labeled secondary antibody was absorbed, it can be subjected to flow cytometry assay. Another negative control was set (Vero E6 cells with purified GST protein) to exclude the interference of GST tag and antibodies binding to cells. It has been seen that GST·RBD bound Vero E6 cells effectively. It also proved that the binding progress was decided by three-dimensional structure attachment because no side chain glycosylation was formed when heteroprotein expressed in *E.coli*.

DISCUSSION

During the pandemic outbreak of SARS in 2002/2003, despite the lack of effective and specific therapy, most SARS patients survived after the acute illness, and neutralizing antibodies were detectable in the sera of convalescent SARS patients[17,18]. Many researchers devoted themselves into developing anti SARS-Cov drugs. Currently, one candidate vaccine using inactivated SARS-Cov is in a phase I clinical trial in China. Although the inactivated SARS-Cov may be effective in protecting animals from challenge by the virus, its efficacy in human is unclear. There has been a serious safety concern since some antigens in the virions may elicit antibodies that did not neutralize, but rather infected. Some viral proteins may induce harmful immune and inflammatory response, a potential cause of SARS pathogenesis[19]. Now a number of vaccine candidates are of preclinical study, including inactivated vaccines, DNA vaccines, and attenuated viruses encoding SARS-Cov S protein[20-23]. Especially, vaccine blocking SARS-Cov entry into susceptible cell is a good way to fight against the virus[24].

The S proteins of coronaviruses are large type I membrane glycoprotein projections from viral envelope[25]. S proteins are responsible for both binding to receptors on host cells and for membrane fusion[11,12]. S proteins also contain important virus-neutralizing epitopes that elicit neutralizing

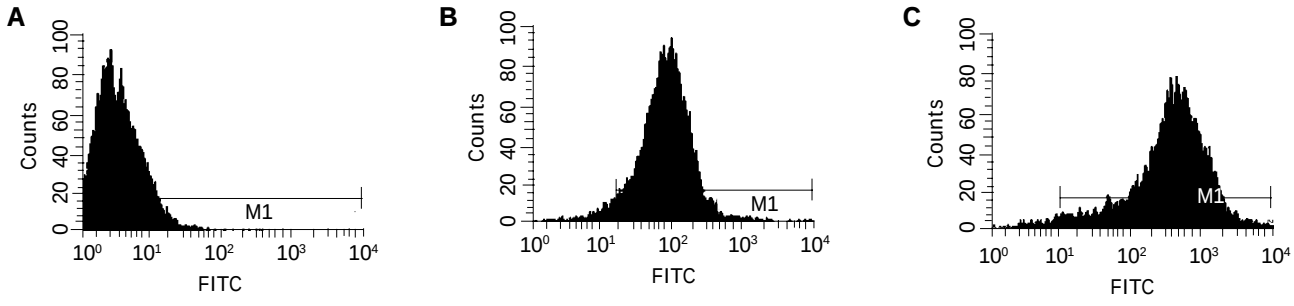

Figure 4 Cell binding test preformed by flow cytometry assay. A: Vero E6 cells alone, geometrical mean 3.3; B: Vero E6 cells+GST protein+two antibodies, geometrical mean 77.08; C: Vero E6 cells+GST·RBD+two antibodies, geometrical mean 352.73.

antibody in the host species. Furthermore, mutations in this gene dramatically affect the virulence, pathogenesis, and host cell tropism. The S1 domain of all characterized coronaviruses, including that of SARS-Cov, meditated an initial-affinity interaction with a cellular receptor[26-28]. In respect of that mutations in S protein' gene dramatically affect the virulence, pathogenesis, and host cell tropism, at the same time S proteins also contain important virus-neutralizing epitopes that elicit neutralizing antibody in the host species, so much work about antigenicity and receptor-binding ability of full length or fragments were done to discover the potent neutralization of SARS-Cov infection[29-32]. It has been proved that a cellular metallopeptidase, ACE2, could bind to S1 domain of SARS-Cov S protein and support viral replication[20]. Recent reports showed that a 193-amino-acid fragment of the S protein (residues 318-510) bound ACE2 more efficiently than did the full S1 domain and should be RBD of S protein of SARS-Cov, and rabbit antisera directed against RBD (cell expressed) were effective in binding to RBD on the S1 domain of SARS-Cov S protein and blocking RBD binding to soluble and cell-expressed ACE2. These data confirmed that the RBD of S protein has the potential to be developed as a subunit vaccine since it induces highly potent antibodies to block S protein binding to ACE2 and to neutralize SARS-Cov infection and has lower level of risk comparing with inactivated viruses. In these researches, the RBD protein was all expressed in mammalian cells and still in research pipeline.

These results suggested that RBD of S protein is a good candidate for vaccine because neutralizing antibodies are directed against S protein. Moreover, RBD of S protein is also a good target for antiviral therapies because blockade of binding of S protein to cellular receptor can prevent virus entry.

To research the receptor-binding ability of RBD, we chose *E.coli* as an expression host to get recombinant protein. According to the database from Internet there is 88.2% possibility of the recombinant RBD expressed in *E.coli* as inclusion body (www.biotech.ou.edu), at the same time, the gene of RBD contains lots of codon rarely used in *E.coli*, the expressional capacity should be little. In order to acquire soluble and functional recombinant protein, different fusion vectors, *E.coli* strain, culture, and induction conditions were considered. In this paper we adopted three fusion tags (GST, TrxA, MBP) which preferably contributes to increasing solubility and to the proper folding of heteroprotein when expressed in *E.coli*. At the same time we chose two *E.coli* strains: BL21 (DE3) and Rosetta-gamiB(DE3). Unexpectedly, TrxA tagged RBD protein expressed in Rosetta-gamiB(DE3) was inclusion body still, nature RBD folding form might not depend upon the disulfide bond formed by two cysteines. At last we got soluble expressed recombinant RBD protein as GST fusion form.

The recombinant GST·RBD protein was purified, and then proved positive reaction with anti RBD of S protein monoclonal antibody by ELISA and to have effective binding ability to ACE2 positive Vero E6 cell by flow cytometry assay. After removing the fusion tag, the recombinant protein can be directly used to develop subunit vaccine for blocking S protein binding with receptor and to neutralize SARS-Cov infection.

REFERENCES

1 **Lee N**, Hui D, Wu A, Chan P, Cameron P, Joynt GM, Ahuja A, Yung MY, Leung CB, To KF, Lui SF, Szeto CC, Chung S, Sung JJY. A major outbreak of severe acute respiratory syndrome in Hong Kong. *N Engl J Med* 2003; **348**: 1986-1994

2 **Peiris JS**, Lai ST, Poon LL, Guan Y, Yam LY, Lim W, Nicholls J, Yee WK, Yan WW, Cheung MT, Cheng VC, Chan KH, Tsang DN, Yung RW, Ng TK, Yuen KY. SARS study group. Coronavirus as a possible cause of severe acute respiratory syndrome. *Lancet* 2003, **361**: 1319-1325

3 **Fouchier RA**, Kuiken T, Schutten M, van Amerongen G, van Doornum GJ, van de Hoogen BG, Peiris M, Lim W, Stöhr K, Osterhaus AD. Aetiology: Koch's postulates fulfilled for SARS virus. *Nature* 2003; **423**: 240

4 **Ksiazek TG**, Erdman D, Goldsmith CS, Zaki SR, Peret T, Emery S, Tong S, Urbani C, Comer JA, Lim W, Rollin PE, Dowell SF, Ling AE, Humphrey CD, Shieh WJ, Guarner J, Paddock CD, Rota P, Fields B, DeRisi J, Yang JY, Cox N, Hughes JM, LeDuc JW, Bellini WJ, Anderson LJ. SARS Working Group. A novel coronavirus associated with severe acute respiratory syndrome. *N Engl J Med* 2003; **348**: 1953-1966

5 **Rota PA**, Oberste MS, Monroe SS, Nix WA, Campagnoli R, Icenogle JP, Penaranda S, Bankamp B, Maher K, Chen MH, Tong S, Tamin A, Lowe L, Frace M, DeRisi JL, Chen Q, Wang D, Erdman DD, Peret TC, Burns C, Ksiazek TG, Rollin PE, Sanchez A, Liffick S, Holloway B, Limor J, McCaustland K, Olsen-Rasmussen M, Fouchier R, Gunther S, Osterhaus AD, Drosten C, Pallansch MA, Anderson LJ, Bellini WJ. Characterization of a novel coronavirus associated with severe acute respiratory syndrome. *Science* 2003; **300**: 1394-1399

6 **Marra MA**, Jones SJ, Astell CR, Holt RA, Brooks-Wilson A, Butterfield YS, Khattra J, Asano JK, Barber SA, Chan SY, Cloutier A, Coughlin SM, Freeman D, Girn N, Griffith OL, Leach SR, Mayo M, McDonald H, Montgomery SB, Pandoh PK, Petrescu AS, Robertson AG, Schein JE, Siddiqui A, Smailus DE, Stott JM, Yang GS, Plummer F, Andonov A, Artsob H, Bastien N, Bernard K, Booth TF, Bowness D, Czub M, Drebot M, Fernando L, Flick R, Garbutt M, Gray M, Grolla A, Jones S, Feldmann H, Meyers A, Kabani A, Li Y, Normand S, Stroher U, Tipples GA, Tyler S, Vogrig R, Ward D, Watson B, Brunham RC, Krajden M, Petric M, Skowronski DM, Upton C, Roper RL. The Genome sequence of the SARS-associated coronavirus. *Science* 2003; **300**: 1399-1404

7 **Drosten C**, Günther S, Preiser W, Van der Werf S, Brodt HR, Becker S, Rabenau H, Panning M, Kolesnikova L, Fouchier RAM, Berger A, Burguière AM, Cinatl J, Eickmann M, Escriou N, Grywna K, Kramme S, Manuguerra JC, Müller S, Rickerts V, Stürmer M, Vieth S, Klenk HD, Osterhaus ADME, Schmitz H, Doerr HW. Identification of a Novel Coronavirus in patients with Severe Acute Respiratory Syndrome. *N Engl J Med* 2003; **348**: 1967-1976

8 **Holmes KV**. SARS-Associated Coronavirus. *N Engl J Med* 2003; **348**: 1948-1951

9 **Tsui SK**, Chim SS, Lo YM. Chinese university of Hong Kong molecular SARS Research Group. Coronavirus genomic-sequence variations and the epidemiology of the severe acute respiratory syndrome. *N Engl J Med* 2003; **349**: 187-188

10 **Ying W**, Hao Y, Zhang Y, Peng W, Qin E, Cai Y, Wei K, Wang J, Chang G, Sun W, Dai S, Li X, Zhu Y, Li J, Wu S, Guo L, Dai J, Wang J, Wan P, Chen T, Du C, Li D, Wan J, Kuai X, Li W, Shi R, Wei H, Cao C, Yu M, Liu H, Dong F, Wang D, Zhang X, Qian X, Zhu Q, He F. Proteomic analysis on structural proteins of Severe Acute Respiratory Syndrome coronavirus. *Proteomics* 2004; **4**: 492-504

11 **Simmons G**, Reeves JD, Rennekamp AJ, Amberg SM, Piefer AJ, Bates P. Characterization of severe acute respiratory syndrome-associated coronavirus (SARS-CoV) spike glycoprotein-mediated viral entry. *Proc Natl Acad Sci USA* 2004; **101**: 4240-4245

12 **Li W**, Moore MJ, Vasilieva N, Sui J, Wong SK, Berne MA, Somasundaran M, Sullivan JL, Luzuriaga K, Greenough TC, Choe H, Farzan M. Angiotensin- converting enzyme 2 is a functional receptor for the SARS coronavirus. *Nature* 2003; **426**: 450-454

13 **Wong SK**, Li W, Moore MJ, Choe H, Farzan M. A 193-amino-acid fragment of the SARS coronavirus S protein efficiently binds angiotensin- converting enzyme 2. *J Biol Chem* 2004; **279**: 3197-3201
14 **Jeffers SA**, Tusell SM, Gillim-Ross L, Hemmila EM, Achenbach JE, Babcock GJ, Thomas WD Jr, Thackray LB, Young MD, Mason RJ, Ambrosino DM, Wentworth DE, DeMartini JC, Holmes KV. CD209L (L-SIGN) is a receptor for severe acute respiratory syndrome coronavirus. *Proc Natl Acad Sci USA* 2004; **101**: 15748-15753
15 **Wang P**, Chen J, Zheng A, Nie Y, Shi X, Wang W, Wang G, Luo M, Liu H, Tan L, Song X, Wang Z, Yin X, Qu X, Wang X, Qing T, Ding M, Deng H. Expression cloning of functional receptor used by SARS coronavirus. *Biochem Biophys Res Commun* 2004; **315**: 439-444
16 **Chang MS**, Lu YT, Ho ST, Wu CC, Wei TY, Chen CJ, Hsu YT, Chu PC, Chen CH, Chu JM, Jan YL, Hung CC, Fan CC, Yanga YC. Antibody detection of SARS-CoV spike and nucleocapsid protein. *Biochem Biophys Res Commun* 2004; **314**: 931-936
17 **Zheng BJ**, Guan Y, Wong KH, Zhou J, Wong KL, Young BW, Lu LW, Lee SS. SARS-related virus predating SARS outbreak, Hong Kong. *Emerg Infec Dis* 2004; **10**: 176-178
18 **Nie QH**, Luo XD, Zhang JZ, Su Q. Current status of severe acute respiratory syndrome in China. *World J Gastroenterol* 2003; **9**: 1635-1645
19 **He Y**, Zhou Y, Liu S, Kou Z, Li W, Farzan M, Jiang S. Receptor-binding domain of SARS-CoV spike protein induces highly potent neutralizing antibodies: implication for developing subunit vaccine. *Biochem Biophys Res Commun* 2004; **324**: 773-781
20 **Zeng F**, Chow KY, Hon CC, Law KM, Yip CW, Chan KH, Peiris JS, Leung FC. Characterization of humoral responses in mice immunized with plasmid DNAs encoding SARS-CoV spike gene fragments. *Biochem Biophys Res Commun* 2004; **315**: 1134-1139
21 **Gao W**, Tamin A, Soloff A, D'Aiuto L, Nwanegbo E, Robbins PD, Bellini WJ, Barratt-Boyes S, Gambotto A. Effects of a SARS-associated coronavirus vaccine in monkeys. *Lancet* 2003; **362**: 1895-1896
22 **Sui J**, Li W, Murakami A, Tamin A, Matthews LJ, Wong SK, Moore MJ, Tallarico AS, Olurinde M, Choe H, Anderson LJ, Bellini WJ, Farzan M, Marasco WA. Potent neutralization of severe acute respiratory syndrome (SARS) coronavirus by a human mAb to S1 protein that blocks receptor association. *Proc Natl Acad Sci USA* 2004**; 101**: 2536-2541
23 **Bisht H**, Roberts A, Vogel L, Bukreyev A, Collins PL, Murphy BR, Subbarao K, Moss B. Severe acute respiratory syndrome coronavirus spike protein expressed by attenuated vaccinia virus protectively immunizes mice. *Proc Natl Acad Sci USA* 2004; **101**: 6641-6646
24 **Yang ZY**, Kong WP, Huang Y, Roberts A, Murphy BR, Subbarao K, Nabel GJ. A DNA vaccine induces SARS coronavirus neutralization and protective immunity in mice. *Nature* 2004; **428**: 561-564
25 **Ho Y**, Lin PH, Liu CY, Lee SP, Chao YC. Assembly of human severe acute respiratory syndrome coronavirus-like particles. *Biochem Biophys Res Commu* 2004; **318**: 833-838
26 **Liu S**, Xiao G, Chen Y, He Y, Niu J, Escalante CR, Xiong H, Farmar J, Debnath AK, Tien P, Jiang S. Interaction between heptad repeat 1 and 2 regions in spike protein of SARS-associated coronavirus: implications for virus fusogenic mechanism and identification of fusion inhibitors. *Lancet* 2004; **363**: 938-947
27 **Bosch BJ**, Martina BE, Van der Zee R, Lepault J, Haijema BJ, Versluis C, Heck AJ, Groot R, Osterhaus AD, Rottier PJ. Severe acute respiratory syndrome coronavirus (SARS-CoV) infection inhibition using spike protein heptad repeat-derived peptides. *Proc Natl Acad Sci USA* 2004; **101**: 8455-8460
28 **Spiga O**, Bernini A, Ciutti A, Chiellini S, Menciassi N, Finetti F, Causarono V, Anselmi F, Prischi F, Niccolaia N. Molecular modelling of S1 and S2 subunits of SARS coronavirus spike glycoprotein. *Biochem Biophys Res Commun* 2003; **310**: 78-83
29 **Ho TY**, Wu SL, Cheng SE, Wei YC, Huang SP, Hsiangc CY. Antigenicity and receptor-binding ability of recombinant SARS coronavirus spike protein. *Biochem Biophy Res Commun* 2004; **313**: 938-947
30 **Xiao X**, Chakraborti S, Dimitrov AS, Gramatikoff K, Dimitrov DS. The SARS-CoV S glycoprotein: expression and functional characterization. *Biochem Biophys Res Commun* 2003; **312**: 1159-1164
31 **Huang LR**, Chiu CM, Yeh SH, Huang WH, Hsueh PR, Yang WZ, Yang JY, Su IJ, Chang SC, Chen PJ. Evaluation of antibody responses against SARS coronaviral nucleocapsid or spike proteins by immunoblotting or ELISA. *J Med Viro* 2004; **73**: 338-346

Science Editor Guo SY **Language Editor** Elsevier HK

PO Box 2345, Beijing 100023, China
www.wjgnet.com
wjg@wjgnet.com

ELSEVIER

World J Gastroenterol 2005;11(39):6165-6169
World Journal of Gastroenterology ISSN 1007-9327

• *BRIEF REPORTS* •

Effects of *Saccharomyces boulardii* on fecal short-chain fatty acids and microflora in patients on long-term total enteral nutrition

Stéphane M Schneider, Fernand Girard-Pipau, Jérôme Filippi, Xavier Hébuterne, Dominique Moyse, Gustavo Calle Hinojosa, Anne Pompei, Patrick Rampal

Stéphane M Schneider, Jérôme Filippi, Xavier Hébuterne, Gustavo Calle Hinojosa, Patrick Rampal, Department of Hepato-Gastroenterology and Clinical Nutrition, Archet University Hospital, Nice, France
Fernand Girard-Pipau, Anne Pompei, Bacteriology Laboratory, Archet University Hospital, Nice, France
Dominique Moyse, Biostatistician, Paris, France
Gustavo Calle Hinojosa, Patrick Rampal, Department of Hepato-Gastroenterology, Princess Grace Hospital, Monte-Carlo, Monaco
Supported by a research grant from Laboratoires Biocodex, Montrouge, France, EU
Correspondence to: Dr. Stéphane M Schneider, Department of Gastroenterology and Clinical Nutrition, Archet University Hospital, BP 3079, F-06202 Nice Cedex 3, France. stephane.schneider@unice.fr
Telephone: +33-4-92-03-61-68 Fax: +33-4-92-03-65-75
Received: 2005-01-12 Accepted: 2005-06-02

Abstract

AIM: To assess the effects of *Sb* on fecal flora and short-chain fatty acids (SCFA) in patients on long-term TEN.

METHODS: Ten patients (3 females, 7 males, 59±5.5 years), on TEN for a median of 13 mo (1-125), and 15 healthy volunteers (4 females, 11 males, 32±2.0 years) received *Sb* (0.5 g bid PO) for 6 d. Two stool samples were taken before, on the last 2 d and 9-10 d after treatment, for SCFA measurement and for culture and bacterial identification. Values (mean±SE) were compared using sign tests and ANOVA.

RESULTS: Fecal butyrate levels were lower in patients (10.1±2.9 mmol/kg) than in controls (19.2±3.9, $P = 0.02$). Treatment with *Sb* increased total fecal SCFA levels in patients (150.2±27.2 *vs* 107.5±18.2 mmol/kg, $P = 0.02$) but not in controls (129.0±28.6 *vs* 113.0±15.2 mmol/kg, NS). At the end of treatment with *Sb*, patients had higher fecal butyrate (16.0±4.4 *vs* 10.1 [2.9] mmol/kg, $P = 0.004$). Total SCFAs remained high 9 d after treatment was discontinued. Before the treatment, the anaerobe to aerobe ratio was lower in patients compared to controls (2.4±2.3 *vs* 69.8±1.8, $P = 0.003$). There were no significant changes in the fecal flora of TEN patients.

CONCLUSION: *Sb*-induced increase of fecal SCFA concentrations (especially butyrate) may explain the preventive effects of this yeast on TEN-induced diarrhea.

Key words: Enteral nutrition; Diarrhea; *Saccharomyces boulardii*; Short-chain fatty acids; Intestinal microbiota

Schneider SM, Girard-Pipau F, Filippi J, Hébuterne X, Moyse D, Hinojosa GC, Pompei A, Rampal P. Effects of *Saccharomyces boulardii* on fecal short-chain fatty acids and microflora in patients on long-term total enteral nutrition. *World J Gastroenterol* 2005; 11(39): 6165-6169
http://www.wjgnet.com/1007-9327/11/6165.asp

INTRODUCTION

Diarrhea is the most frequent complication of enteral tube feeding, with an incidence as high as 63%[1]. Its consequences range from discomfort to life-threatening acidosis, increased morbidity and mortality, and higher financial costs for health providers[2]. One of the causes of diarrhea in tube-fed patients may be the consequences on colonic trophicity of a deficiency in luminal short-chain fatty acids (SCFAs). We have reported a major imbalance (namely a drop in the number of fecal anaerobic bacteria and an increase in the number of aerobic bacteria) in patients on long-term total enteral nutrition (TEN)[3]. The modifications of the intestinal microflora induced by a fiber-free polymeric enteral diet can be compared to those induced by broad-spectrum antibiotics such as ceftriaxone[4,5]. These effects may be synergic[6] and explain why antibiotics are a risk factor for enteral nutrition-induced diarrhea[7,8] and why enteral nutrition is a risk factor for antibiotic-induced diarrhea[9] and *Clostridium difficile* infection[10]. SCFAs, one of the most important by-products of anaerobes in the colon, are the main fuel for the colonocyte and they are involved in water and electrolyte absorption by the colonic mucosa. They have been shown to reverse fluid secretion in the ascending colon during enteral feeding[11], and may represent the link between diarrhea and the intestinal microflora during enteral nutrition.

Saccharomyces boulardii (*Sb*) is a probiotic yeast that has been successfully used for years in the prevention of antibiotic-associated diarrhea[12]. *Sb* has been proven to prevent the relapse of *Clostridium difficile* infection[13], and seems effective in preventing relapses in patients with Crohn's disease[14]. Three randomized controlled studies have reported its efficacy in the prevention of diarrhea in TEN patients from intensive care units, with a reduction in the number of patient-days with diarrhea by 25-83%[15-17]. However, these studies did not address the mechanisms of action of the probiotic. We therefore designed a prospective study to assess the effects of *Sb* on fecal SCFAs and intestinal microflora in TEN patients. Healthy volunteers (HVO) were

used as controls.

MATERIALS AND METHODS

Subjects

The TEN group consisted of 10 patients (3 females and 7 males), mean age 59±5.5 years (mean±SE), who had been on TEN for a median of 13 mo (range: 1-125 mo). The indication for TEN was dysphagia in six patients (three head and neck tumors, two strokes, and one resected neurinoma); three patients had upper gastro-intestinal surgery, and one patient had low oral intake due to severe depression. Two patients were receiving proton pump inhibitors. A commercially available polymeric diet, fiber-, lactose-, and gluten-free, with a concentration of 1.33 kcal/mL (Sondalis HP®, Nestlé Clinical Nutrition, Noisiel, France) was used to provide 20% protein (50% from casein and 50% from soy protein), 45% carbohydrate (maltodextrin), and 31% fat (24% from corn oil, 22% from colza oil, and 47% as medium-chain triglycerides). Nutrition was given through gastrostomy ($n = 7$), jejunostomy ($n = 2$), or naso-gastric ($n = 1$) tubes. Enteral nutrition was total, but patients who could drink water or tea were allowed to do so. Fifteen HVO (4 females and 11 males), mean age 32±2.0 years ($P<0.05$ *vs* TEN patients) were also studied. All HVO consumed a regular Western diet, and none of them had a history of gastrointestinal disease. At the time of the study, all experimental and normal subjects were in a stable condition, and none had diarrhea. Energy provided by the diet was covering their maintenance needs as calculated using the Harris and Benedict formulas, and the enteral feeds were stable throughout the study. No subject had undergone colectomy, and none had taken antibiotics or laxatives for at least 2 wk prior to the study. All subjects gave their written informed consent and the study was performed according to the Declaration of Helsinki and approved by the regional Ethics Committee.

Study design

Five hundred milligrams b.i.d. of *Sb* as lyophilized powder, provided by Laboratoires Biocodex (Montrouge, France), were administered orally (HVO) or via the feeding tube (TEN patients) for six consecutive days. Two fecal samples were collected at 1-d intervals from all subjects on the 2 d before treatment, on the last 2 d of treatment, and 9 and 10 d after treatment was discontinued. Antibiotic or laxative use during the study was an exclusion criterion.

Stool analysis

Stool samples were taken immediately after production, and analyzed within 2 h. SCFAs were studied as follows[18]: an aliquot of 200 mg of feces was weighed. This was suspended in sterile distilled water (1.6 mL) and hexanoic acid (0.2 mL) was added. 50% aqueous H_2SO_4 (0.4 mL) and diethyl ether (2 mL) were then added. The sample was mixed for 45 min with an orbital shaker, and centrifuged for 5 min at 3 000 r/min at room temperature. Anhydrous $CaCl_2$ was then added in order to remove residual water, and 2 μL of the extract was injected in the gas-liquid chromatograph (Hewlett-Packard 5890 Series II with a flame ionization detector). The standard solution was as follows: acetic, propionic, isobutyric, butyric, isovaleric, valeric, isocaproic, caproic, and hexanoic acids (10 meq/L each); it was assayed before each stool sample was analyzed. Sensitivity was 1 mmol. 500 mg of feces was taken from the center of the stool, weighed and submitted to serial dilutions up to 10^{-8} in BHI broth. Then, 0.1 mL of each dilution was spread on a range of selective and non-selective media. Whenever necessary, the media were pre-reduced to allow anaerobic growth. Media inoculated and incubated at 37 ℃ in aerobiosis were as follows: trypticase agar, Columbia agar supplemented with sheep blood, Columbia agar supplemented with nalidixic acid and colistin, and Drigalski medium (equivalent to Mac Conkey medium) at dilutions 10^{-2}, 10^{-4}, and 10^{-6}[19]. For anaerobic bacteria, media inoculated were as follows: Columbia agar supplemented with sheep blood spread with the dilutions 10^{-2}, 10^{-4}, and 10^{-8}, Columbia blood agar supplemented with kanamycin and vancomycin, *Bifidobacterium* agar, and *Bacteroides* agar (dilutions 10^{-2}, 10^{-4}, and 10^{-7}), rifampicin agar (10^{-1} and 10^{-7}), and CCFA (for isolation of *Clostridium difficile*), MRS agar (for isolation of lactobacilli), *Veillonella* agar, and crystal violet agar, all spread with dilutions 10^{-1} and 10^{-5}[19]. The differences between dilutions for each medium were based on the differences between the concentrations of concerned bacteria[20]. After 24-48 h of incubation in an anaerobic cabinet, the number of colonies of each colony type growing on each of the media used were counted. The absence of growth under 50 mL/L carbon dioxide was verified for anaerobic strains. Routine identification was performed with standard methods, then with microstrips (API 20 Enterobacteries or ID 32 Anaerobies, BioMerieux, Marcy L'Etoile, France). The ratio between anaerobes and aerobes was calculated as a marker of microbial imbalance[3,21].

Statistical analysis

Results are expressed as mean±SE. All fecal bacterial counts (colony-forming units [CFU] per gram of wet feces) were transformed to logarithms ($\log_{10}$ CFU) for statistical analysis. Values were compared at baseline using a non-parametric method. Comparisons within groups used a sign test; differences *vs* baseline are presented with distribution-free confidence intervals.

A two-way ANOVA was performed for quantitative parameters for exploratory purposes. The model included group (TEN or HVO), period of time (before, during or after treatment) and interaction group*period of time; all two by two differences between adjusted means were calculated and tested using *t*-tests. No adjustment was performed in this exploratory context. For SFCA assessments, two values were considered in the model at each time. Statistics were performed on SAS software from SAS Institute (Cary, NC, USA). Differences were considered as statistically significant for P lower than 0.05. A pilot study that reported a 40% increase of total SCFA concentration after treatment with *Sb* allowed us to calculate a number needed to treat ten subjects per group.

RESULTS

Fecal short-chain fatty acids

Acetate, propionate, and butyrate values are represented in Table 1. For all three main SCFAs, no significant change,

either during or after treatment, was observed in HVO. In TEN patients, butyrate concentrations were increased significantly (about 60%) during treatment. SCFA values 9 d after discontinuing *Sb* were not significantly different from baseline. The sum of all SCFAs was increased significantly in TEN patients under treatment, with an average increase of 42.8 mmol/kg (95%CI: 0.0-55.2, $P = 0.02$) during treatment and an average increase of 51.8 mmol/kg (95%CI: 14.4-110.6, $P = 0.02$) after treatment (Figure 1). There were no changes in HVO. Minor SCFAs did not change in either group.

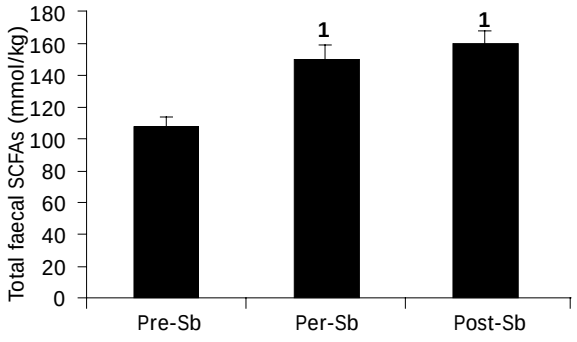

Figure 1 Fecal SCFAs in TEN patients. SCFA: short-chain fatty acids; *Sb*: *Saccharomyces boulardii*; [1]$P = 0.02$ *vs* pre-treatment values.

ANOVA showed an overall increase for acetate and SCFA sum after treatment on change from baseline values; significant interactions were noticed for propionate due to the increase in the TEN group opposed to a decrease in the HVO group, and for butyrate corresponding to differences in after-treatment concentrations higher in the HVO group in spite of higher baseline values in this group.

Fecal flora

Before treatment, there were significant differences in the fecal flora between HVO and TEN patients, as the latter had higher counts of aerobic bacteria and a lower anaerobes/aerobes ratio (Table 2). Among aerobes, the number of enterococci was higher in TEN patients (7.42±0.64 log CFU/g) than in HVO (6.1±0.46 log CFU/g, $P = 0.02$). Among anaerobes, peptostreptococci and *Bifidobacterium* spp., present in HVO, were absent in TEN patients. *Clostridium difficile* was not identified in any subject. There were no significant changes in the numbers of colony forming units of individual species or groups of bacteria in TEN patients during treatment with *Sb*, or after treatment. The only change observed in HVO was a decrease of Gram-positive anaerobes from 8.6±0.3 log CFU/g to 6.8±0.8 during treatment ($P = 0.035$).

Table 2 Fecal bacterial populations in TEN patients and HVO

		Before treatment concentration	During treatment concentration	After treatment concentration
Total bacteria	TEN	9.64 (0.31)	9.31 (0.41)	9.54 (0.36)
(log CFU/g)	HVO	9.53 (0.16)	9.56 (0.21)	9.20 (0.19)
Anaerobes	TEN	8.25 (1.01)	7.72 (0.76)	8.63 (0.62)
(log CFU/g)	HVO	9.47 (0.16)	8.73 (0.45)	8.97 (0.25)
Aerobes	TEN	8.84 (0.26)	8.83 (0.34)	8.71 (0.32)
(log CFU/g)	HVO	7.63 (0.22)	7.63 (0.24)	7.61 (0.26)
Anaerobes/				
aerobes ratio	TEN	2.42 (2.28)	0.51 (2.23)	2.89 (2.43)
	HVO	69.81 (1.81)	60.13 (2.47)	23.02 (2.01)

Mean (SE). TEN, total enteral nutrition; HVO, healthy volunteers. No significant difference.

Tolerance

There were no significant changes in the number of bowel movements and the consistency of stools during or after treatment in either HVO or TEN patients (data not shown). No fever or fungemia was reported. The only adverse effect attributed to *Sb* was a case of mild diarrhea in one patient which resolved without discontinuation of treatment.

Table 1 Fecal SCFAs in TEN patients and HVO

		Before treatment concentration (SEM)	During treatment			After treatment		
			Concentration (SEM)	Difference with pre-treatment value (95%CI)	P^1	Concentration (SEM)	Difference with pre-treatment value (95%CI)	P^1
Acetate	TEN	69.9 (12.3)	97.9 (25.2)	28.0 -6.1; 36.2	0.18	110.3 (24.1)	40.4 14.4; 71.4	0.02
	HVO	71.3 (10.3)	98.4 (29.8)	27.1 -13.1; 35.6	0.79	111.5 (17.5)	40.2 -7.0; 116.0	0.42
Propionate	TEN	20.9 (3.7)	26.2 (3.8)	5.3 -0.2; 12.6	0.18	26.0 (3.4)	5.1 -3.3; 14.3	0.18
	HVO	22.9 (3.0)	18.4 (2.4)	-4.5 -11.8; 4.5	0.30	23.0 (2.7)	0.1 -3.1; 6.9	0.12
Butyrate	TEN	10.1 (2.9)	16.0 (4.4)	5.8 0.1; 12.3	0.004	12.9 (2.5)	2.7 -3.9; 12.3	0.51
	HVO	19.2 (3.9)	16.4 (3.3)	-2.7 -9.7 ; 5.6	0.61	23.3 (3.1)	4.1 -1.4 ; 16.3	0.12

Values in mmol/kg of wet feces: mean (SE); TEN: total enteral nutrition, HVO: healthy volunteers. [1]Probability of sign test.

DISCUSSION

This study shows that both the fecal concentration of butyric acid and the anaerobe/aerobe ratio were lower in patients at high risk for diarrhea due to TEN than in HVO. Despite great inter-individual variations, treatment with *Sb* increased total SCFAs and butyrate fecal concentrations in TEN patients with a long-lasting increase of total SCFA concentrations when treatment was discontinued. Treatment with *Sb* did not affect the fecal flora in TEN patients, while it decreased Gram-positive anaerobes in HVO.

Sb is known to interact with the intestinal flora. Yeast proteins have been shown to neutralize cholera toxin[22] and to repress *Clostridium difficile* toxins A and B[23]; *Sb* also has an antagonistic effect on the growth of pathogenic micro-organisms in the intestine[24]. In our study, increased SCFA concentrations might explain the reported prevention by *Sb* of TEN-induced diarrhea by an increased water and electrolyte absorption and by a reduction in colonic pH, even though it was not measured in the stool samples from our subjects. A lower pH inhibits the growth of *Clostridium difficile*[25,26], a bacteria that can be acquired in up to 15% of hospitalized EN patients[10]. A viable mixed culture of *Lactobacillus acidophilus* and *Lactobacillus bulgaricus* (1 g t.i.d.) failed to prevent diarrhea in hospital inpatients receiving EN in a randomized controlled study[27]. Unlike *Sb*, lactobacilli taken orally do not increase SCFA fecal levels[28,29], which might explain these negative results. Prebiotics can also increase SCFAs in the colon; in a recently published study, administration for 2 wk of a soluble dietary fiber (galactomannans) in 20 elderly inpatients receiving EN was shown to decrease the water content of the feces and the frequency of daily bowel movements[30]. These results were associated with an increase of fecal SCFA levels, significant for total SCFAs, acetic and propionic acids. Although we confirmed the 40% increase in total SCFAs in the pilot phase of the study that was used to determine the number of subjects, a high variability prevented some important differences from reaching statistical significance. This variability did not seem to be time- or diet-dependent, as it was comparable in volunteers on a free diet and in patients who were on a stable controlled diet. *Sb* recovery in the stools after chronic administration is known to reach a plateau by the 3rd d and to disappear 5 d after treatment is discontinued[31]. The persistence of the effects on total SCFA concentrations 9-10 d after *Sb* discontinuation is suggestive of a prolonged action of the yeast and may indicate that daily treatment may not be necessary to sustain its effects on fecal SCFA concentrations.

known to be associated with a decrease of fecal anaerobes[35]; however, age does not influence fecal SCFA levels[36]; (2) Bacterial concentrations are known to differ depending on the intestinal segment in which samples are taken; nevertheless, analysis of feces is the most feasible technique and provides an accurate information on the intestinal microflora[37]; (3) Analysis of samples rather than 24 h-stools certainly deprives us of some information as TEN is known to modify the volume of daily stools. However, stool collection is often difficult in bed-ridden patients, especially those with neurological disorders. This is the main reason why we chose to perform this study in patients without diarrhea; (4) The correlation between SCFAs and bacterial counts in feces is reportedly poor[38]; (5) Lastly a standard bacterial count, however thorough, may miss some information. Molecular techniques[39] may help progressing in this field.

There is growing evidence regarding the health benefits of probiotics. In EN patients; besides prevention of diarrhea, a recent study reports less post-operative infections in patients receiving EN supplemented with fiber and *Lactobacillus plantarum* 299 than in those receiving parenteral nutrition of fiber-free TEN[40].

In conclusion, this study suggests one possible mechanism of action of the probiotic yeast *Sb*, especially for its preventive effects in enteral nutrition-induced diarrhea. It also supports its use, especially in patients who have other risk factors, such as antibiotic intake.

ACKNOWLEDGMENTS

The authors wish to thank Dr. Christine Alquier and Dr. Marie-Emmanuelle Le Guern for their invaluable help with study design and data handling, and Dr. Philippe Marteau and Dr. Ian Janssen for their advice.

REFERENCES

1 **Bliss DZ**, Guenter PA, Settle RG. Defining and reporting diarrhea in tube-fed patients - what a mess! *Am J Clin Nutr* 1992; **55**: 753-759
2 **Adam S**, Batson S. A study of problems associated with the delivery of enteral feed in critically ill patients in five ICUs in the UK. *Intensive Care Med* 1997; **23**: 261-266
3 **Schneider SM**, Le Gall P, Girard-Pipau F, Piche T, Pompei A, Nano JL. Total artificial nutrition is associated with major changes in the fecal flora. *Eur J Nutr* 2000; **39**: 248-255
4 **Welling GW**, Meijer-Severs GJ, Helmus G, van Santen E, Tonk RH, de Vries-Hospers HG. The effect of ceftriaxone on the anaerobic bacterial flora and the bacterial enzymatic activity in the intestinal tract. *Infection* 1991; **19**: 313-316
5 **Meijer-Severs GJ**, Van Santen E, Meijer BC. Short-chain fatty acid and organic acid concentrations in feces of healthy human volunteers and their correlations with anaerobe cultural counts during systemic ceftriaxone administration. *Scand J Gastroenterol* 1990; **25**: 698-704
6 **Hébuterne X**, Schneider SM. Impact of enteral nutrition on gastrointestinal functions. *Clin Nutr* 2001; **20**(Suppl 2): 57-61
7 **Keohane PP**, Attrill H, Love M, Frost P, Silk DB. Relation between osmolality of diet and gastrointestinal side effects in enteral nutrition. *Br Med J* 1984; **288**: 678-680
8 **Guenter PA**, Settle RG, Perlmutter S, Marino PL, DeSimone GA, Rolandelli RH. Tube feeding-related diarrhea in acutely ill patients. *J Parenter Enteral Nutr* 1991; **15**: 277-280
9 **Surawicz CM**, Elmer GW, Speelman P, McFarland LV, Chinn J, van Belle G. Prevention of antibiotic-associated diarrhea by *Saccharomyces boulardii*: a prospective study. *Gastroenterology* 1989; **96**: 981-988
10 **Bliss DZ**, Johnson S, Savik K, Clabots CR, Willard K, Gerding DN. Acquisition of *Clostridium difficile* and *Clostridium difficile*-associated diarrhea in hospitalized patients receiving tube feeding. *Ann Intern Med* 1998; **129**: 1012-1019
11 **Bowling TE**, Raimundo AH, Grimble GK, Silk DB. Reversal by short-chain fatty acids of colonic fluid secretion induced by enteral feeding. *Lancet* 1993; **342**: 1266-1268
12 **D'Souza AL**, Rajkumar C, Cooke J, Bulpitt CJ. Probiotics in prevention of antibiotic-associated diarrhea: meta-analysis. *BMJ* 2002; **324**: 1361-1366
13 **McFarland LV**, Surawicz CM, Greenberg RN, Fekety R, Elmer GW, Moyer KA, Melcher SA, Bowen KE, Cox JL, Noorani Z. A

randomized placebo-controlled trial of *Saccharomyces boulardii* in combination with standard antibiotics for *Clostridium difficile* disease. *JAMA* 1994; **271**: 1913-1918
14 **Guslandi M**, Mezzi G, Sorghi M, Testoni PA. *Saccharomyces boulardii* in maintenance treatment of Crohn's disease. *Dig Dis Sci* 2000; **45**: 1462-1464
15 **Bleichner G**, Bléhaut H, Mentec H, Moyse D. *Saccharomyces boulardii* prevents diarrhea in critically ill tube-fed patients. A multicenter, randomized, double-blind placebo-controlled trial. *Intensive Care Med* 1997; **23**: 517-523
16 **Schlotterer M**, Bernasconi P, Lebreton F, Wassermann D. Intérêt de *Saccharomyces boulardii* dans la tolérance digestive de la nutrition entérale à débit continu chez le brûlé. *Nutr Clin Metabol* 1987; **1**: 31-34
17 **Tempé JD**, Steidel AL, Bléhaut H, Hasselmann M, Lutun P, Maurier F. Prévention par *Saccharomyces boulardii* des diarrhées de l'alimentation entérale à débit continu. *Sem Hop Paris* 1983; **59**: 1409-1412
18 **Holdeman LV**, Cato EP, Moore WEC. Anaerobe laboratory manual, anaerobe laboratory. 4th edn ed. *Blacksburg VA Virginia Polytechnic Institute and State University* 1977
19 **Phillips E**, Nash P. Culture media. In: Lennette EH, Balows A, Hausler Jr WJ, Shadomy HJ, editors. Manual of Clinical Microbiology. 4th edition ed. *Washington DC American Society for Microbiology* 1985: 1051-1092
20 **Drasar BS**, Roberts AK. Methods for the study of anaerobic microflora. In: Levett PN, editor. Anaerobic microbiology. A practical approach. *Oxford Oxford University Press* 1991: 183-200
21 **Ruseler-van Embden JG**, Schouten WR, van Lieshout LM. Pouchitis: result of microbial imbalance? *Gut* 1994; **35**: 658-664
22 **Czerucka D**, Roux I, Rampal P. *Saccharomyces boulardii* inhibits secretagogue-mediated adenosine 3',5'- cyclic monophosphate induction in intestinal cells. *Gastroenterology* 1994; **106**: 65-72
23 **Castagliuolo I**, Riegler MF, Valenick L, LaMont JT, Pothoulakis C. *Saccharomyces boulardii* protease inhibits the effects of *Clostridium difficile* toxins A and B in human colonic mucosa. *Infect Immun* 1999; **67**: 302-307
24 **Ducluzeau R**, Bensaada M. Effet comparé de l'administration unique ou en continu de *Saccharomyces boulardii* sur l'établissement de diverses souches de *Candida* dans le tractus digestif de souris gnotoxéniques. *Ann Microbiol* 1982; **118B**: 491-501
25 **Rolfe RD**. Role of volatile fatty acids in colonization resistance to *Clostridium difficile*. *Infect Immun* 1984; **45**: 185-191
26 **Wang X**, Gibson GR. Effects of the *in vitro* fermentation of oligofructose and inulin by bacteria growing in the human large intestine. *J Appl Bacteriol* 1993; **75**: 373-380
27 **Heimburger DC**, Sockwell DG, Geels WJ. Diarrhea with enteral feeding: prospective reappraisal of putative causes. *Nutrition* 1994; **10**: 392-396
28 **Hove H**, Nordgaard-Andersen I, Mortensen PB. Effect of lactic acid bacteria on the intestinal production of lactate and short-chain fatty acids, and the absorption of lactose. *Am J Clin Nutr* 1994; **59**: 74-79
29 **Fukuda M**, Kanauchi O, Araki Y, Andoh A, Mitsuyama K, Takagi K. Prebiotic treatment of experimental colitis with germinated barley foodstuff: a comparison with probiotic or antibiotic treatment. *Int J Mol Med* 2002; **9**: 65-70
30 **Nakao M**, Ogura Y, Satake S, Ito I, Iguchi A, Takagi K. Usefulness of soluble dietary fiber for the treatment of diarrhea during enteral nutrition in elderly patients. *Nutrition* 2002; **18**: 35-39
31 **Bléhaut H**, Massot J, Elmer GW, Levy RH. Disposition kinetics of *Saccharomyces boulardii* in man and rat. *Biopharm Drug Dispos* 1989; **10**: 353-364
32 **Wells CL**, Maddaus MA, Reynolds CM, Jechorek RP, Simmons RL. Role of anaerobic flora in the translocation of aerobic and facultatively anaerobic intestinal bacteria. *Infect Immun* 1987; **55**: 2689-2694
33 **Cummings JH**, Macfarlane GT. Role of intestinal bacteria in nutrient metabolism. *Clin Nutr* 1997; **16**: 3-11
34 **Zimmaro DM**, Rolandelli RH, Koruda MJ, Settle RG, Stein TP, Rombeau JL. Isotonic tube feeding formula induces liquid stool in normal subjects: reversal by pectin. *J Parenter Enteral Nutr* 1989; **13**: 117-123
35 **Hopkins M**, Sharp R, Macfarlane G. Age and disease-related changes in intestinal bacterial populations assessed by cell culture, 16S-rRNA abundance, and community cellular fatty acid profiles. *Gut* 2001; **48**: 198-205
36 **Weaver GA**, Krause JA, Miller TL, Wolin MJ. Short chain fatty acid distributions of enema samples from a sigmoidoscopy population: an association of high acetate and low butyrate ratios with adenomatous polyps and colon cancer. *Gut* 1988; **29**: 1539-1543
37 **Whelan K**, Judd PA, Preedy VR, Taylor MA. Enteral feeding: the effect on faecal output, the faecal microflora and SCFA concentrations. *Proc Nutr Soc* 2004; **63**: 105-113
38 **Meijer-Severs GJ**, van Santen E. Short-chain fatty acid and organic acid concentrations in feces of 10 human volunteers and their correlation with anaerobe cultural counts over a 15-mo period. *Scand J Gastroenterol* 1989; **24**: 1276-1280
39 **Harmsen HJ**, Gibson GR, Elfferich P, Raangs GC, Wildeboer-Veloo AC, Argaiz A. Comparison of viable cell counts and fluorescence in situ hybridization using specific rRNA-based probes for the quantification of human fecal bacteria. *FEMS Microbiol Lett* 2000; **183**: 125-129
40 **Rayes N**, Hansen S, Seehofer D, Muller AR, Serke S, Bengmark S. Early enteral supply of fiber and Lactobacilli versus conventional nutrition: a controlled trial in patients with major abdominal surgery. *Nutrition* 2002; **18**: 609-615

Science Editor Guo SY **Language Editor** Elsevier HK

PO Box 2345, Beijing 100023, China
www.wjgnet.com
wjg@wjgnet.com

ELSEVIER

World J Gastroenterol 2005;11(39):6170-6175
World Journal of Gastroenterology ISSN 1007-9327

• *BRIEF REPORTS* •

Prevalence of cholelithiasis in patients with chronic inflammatory bowel disease

Wolfgang Kratzer, Mark M Haenle, Richard A Mason, Christian von Tirpitz, Volker Kaechele

Wolfgang Kratzer, Mark M Haenle, Richard A Mason, Christian von Tirpitz, Volker Kaechele, Department of Internal Medicine I, University Hospital Ulm, Robert-Koch-Str. 8, D-89081 Ulm, Germany
Correspondence to: PD Dr. med. Wolfgang Kratzer, University Hospital Ulm, Department of Internal Medicine I, Robert-Koch-Str. 8, 89081 Ulm, Germany. wolfgang.kratzer@medizin.uni-ulm.de
Telephone: +49-731-500-2-4538 Fax: +49-731-500-2-4867
Received: 2004-10-22 Accepted: 2005-01-05

Abstract

AIM: To investigate the effect of chronic inflammatory bowel disease (CIBD) specific risk factors for cholecystolithiasis, as duration and involvement pattern of the disease and prior surgery in patients with Crohn's disease (CD) and ulcerative colitis (UC).

METHODS: A total of 222 patients with CD (135 females, 87 males; average age, 35.8±11.8 years; range 17-81 years) and 88 patients with UC (39 females, 49 males; average age, 37.2±13.6 years; range 16-81 years) underwent clinical and ultrasound examinations. Besides age, sex and degree of obesity, patients' CIBD specific parameters, including duration and extent of disease and prior operations were documented and evaluated statistically using logistic regression.

RESULTS: The overall prevalence of gallbladder stone disease in patients with CD was 13% (n = 30). Only age could be shown to be an independent risk factor (P = 0.014). Compared to a collective representative for the general population in the same geographic region, the prevalence of cholecystolithiasis was higher in all corresponding age groups. Patients with UC showed an overall prevalence of gallbladder stone disease of only 4.6%.

CONCLUSION: Only age but not disease-specific factors such as duration and extent of disease, and prior surgery are independent risk factors for the development of cholecystolithiasis in patients with CIBD.

Key words: Crohn's disease, Ulcerative colitis, Gallstone disease, Ultrasonography, Ultrasound

Kratzer W, Haenle MM, Mason RA, von Tirpitz C, Kaechele V. Prevalence of cholelithiasis in patients with chronic inflammatory bowel disease. *World J Gastroenterol* 2005; 11(39): 6170-6175

http://www.wjgnet.com/1007-9327/11/6170.asp

INTRODUCTION

Besides the other extraintestinal complications[1], there is an increased rate of cholecystolithiasis in patients suffering from chronic inflammatory bowel disease (CIBD)[2-5]. The findings reported for ulcerative colitis (UC) are contradictory[6,7]. In the case of Crohn's disease (CD), the reports published to date are also inconsistent with regard to disease-specific factors, such as the duration of the disease[3,5,7,8], prior surgery (bowel resection)[2-4,7,8] and the pattern of disease involvement[2-6]. However, the incidence rate of gallbladder stone disease in patients with CIBD is often twice as high as in the general population, though the reason for this difference has yet to be satisfactorily explained[2-4].

In the majority of European and North American studies of the prevalence of cholecystolithiasis, there is a preponderance of cholesterol gallstones in the general population. The main identifiable risk factors for developing gallbladder stones include female sex, obesity and increasing age. In Asians, who show a high proportion of pigment gallstones, this predominance of females over males is not seen[9,10].

The pathophysiological explanation for the increased prevalence of gallbladder stones in patients with CD refers to the reduced absorption of bile acids in individuals with extensive involvement of the terminal ileum or following ileal resection[6,8]. The absolute number of bowel resections, the length of resected bowel and postoperative hypomotility of the gallbladder with subsequent formation of sludge and later, stones are currently under discussion as major risk factors for the higher prevalence of cholecystolithiasis in patients with CIBD[2-5].

The present study was to evaluate the importance of both the classical cholecystolithiasis risk factors, such as age, female sex and obesity and the effect of disease-specific parameters such as duration of the disease, pattern of involvement and prior surgery on the prevalence of gallbladder stones in patients with CD and UC.

MATERIALS AND METHODS

Patients

A total of 310 patients with CIBD presenting consecutive to our departmental section on Crohn's disease and ulcerative colitis over a period of approximately one year were screened for inclusion in the present study. The present study was conducted prospectively in accordance with the

principles of the Helsinki Declaration and approved by the Ethics Commission of the Medical Faculty.

Inclusion criteria included histologically confirmed CIBD and no history of cholecystolithiasis prior to first diagnosis of CIBD. Included in the study population were 222 patients with CD (135 females, 87 males; average age, 35.8±11.8 years; range 17-81 years) and 88 patients with UC (39 females, 49 males; average age, 37.2±13.6 years; range 16-81 years). The average period since the first diagnosis was 8.9±7.5 years (range: 0-34 years) in the group with CD and 6.8±5.8 years (range: 0-29 years) in the UC collective.

Risk factors

Besides the classical risk factors (age, female sex, obesity), disease-specific parameters such as time elapsed since the first diagnosis, pattern of disease involvement and prior surgical bowel resection in patients with CIBD were studied. Patients were subdivided into four age groups: ⩽30 years, 31-40 years, 41-50 years and 51 years and above.

For evaluation of obesity, patients were divided into three groups on the basis of their body-mass index (BMI):

Females:		Males:	
Ideal weight:	BMI < 21 kg/m²	Ideal weight:	BMI < 22 kg/m²
Normal weight:	BMI 21 -25 kg/m²	Normal weight:	BMI 22 -26 kg/m²
Overweight:	BMI > 25 kg/m²	Overweight:	BMI > 26 kg/m²

In order to study the effects of the duration of the disease (expressed as time elapsed since the first diagnosis with histological confirmation to the time of examination in the present study), patients were divided into four groups: up to 5 years, 6-10 years, 11-15 years and greater than 15 years. With regard to the parameter extent/pattern of disease, we differentiated in the CD group between patients who underwent or did not undergo surgical bowel resection. The group of patients who underwent resection was further subdivided into those who underwent ileocaecal resection and those who had undergone colectomy we did not further differentiate between partial and total colectomy (Figure 1). Type and number of bowel resections were obtained from the patient's chart. Patients with UC were divided into three subgroups: patients with no active disease, patients with disease involvement up to the left colic flexure, and patients with disease extending beyond the left colic flexure (Figure 2). Because only a few patients in the UC collective underwent either partial or total colectomy, a further differentiation between subcollectives with or without history of prior surgery was not done.

Examination

Patients presented in the morning for ultrasound examination in a fasting state.

The criteria for the diagnosis of cholecystolithiasis were defined as follows: one or more echogenic structures in the gallbladder with dorsal shadow; one or more echogenic structures in the gallbladder without dorsal shadow, which by means of multiplanar visualization or attempted mobilization could be differentiated with certainty from a gallbladder septum, Heister's valve or gallbladder polyps; a structure with significant echogenicity and dorsal shadow in the area of the gallbladder,

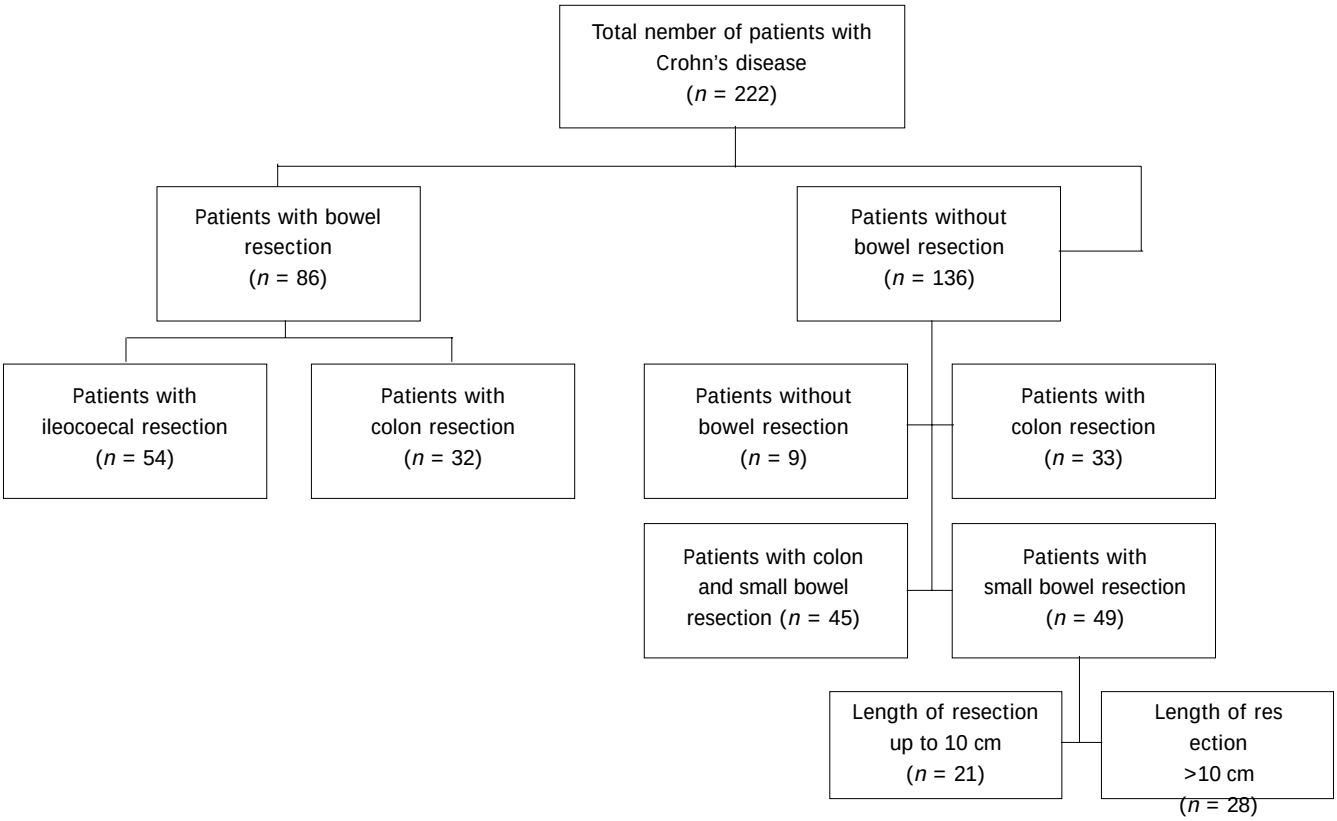

Figure 1 Pattern of involvement and bowel resections in patients with Crohn's disease.

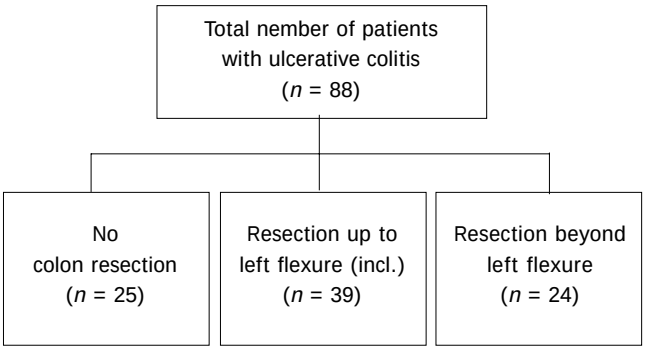

Figure 2 Pattern of involvement and bowel resections in patients with ulcerative colitis.

whose lumen was not definitely visualized; one or more echogenic structures in the gallbladder with or without dorsal shadow in the biliary tract; and no visualized gallbladder lumen in patients with history of prior cholecystectomy and corresponding incision(s) in the right upper abdominal quadrant.

Ultrasound examinations were performed using either the Ultramark 4 Plus or Ultramark 9 HDI with the 3.5- and 5.0-MHz transducer heads (ATL, Bothell, Washington, USA). Examination of the upper abdomen was conducted using the 3.5-MHz transducer head, while examination of the bowel was performed using the 5.0-MHz head. Ultrasound examinations were performed exclusively by two physicians experienced in diagnostic ultrasound of the abdomen. One-time visualization of concrements in the gallbladder based on the above criteria led to the patient's classification as suffering from cholecystolithiasis.

Evaluation of the pattern of disease involvement in the bowel was performed on the basis of sonographic criteria considering thickening of the intestinal wall. Wall thickness greater than 3 mm was considered pathologic. Bowel resection and time elapsed since the first diagnosis were established from the patient's history and chart.

Statistical treatment of the data

All data were first evaluated descriptively. For quantitative parameters, either mean with standard deviation or median with minimum and maximum was documented. While for qualitative parameters, relative and absolute frequencies were calculated.

The evaluation for prevalence in the subgroups and their confidence intervals was performed using a logistic regression model[11]. This model reproduces the influence of potential risk factors (independent variables) for the occurrence of a disease (dichotomous target parameter: here, cholecystolithiasis: yes/no). The importance of the potential risk factor was determined by the likelihood ratio test. By multiple application, several influence parameters could be simultaneously tested in one model and their respective influences were adjusted with regard to the other variables. The respective odds ratios, 95% confidence intervals and *P*-values served to quantify the change in risk of developing cholecystolithiasis due to the given factor. *P*-values between 0.05 and 0.1 were considered to represent trends or tendencies, while $P<0.05$ was considered statistically significant and the factor was classified as a "risk". The classical risk factors such as age, sex and BMI were included in the evaluation. Statistical calculation was performed using the SAS statistics software program (Institute Inc., Cary, NC).

RESULTS

Crohn's Disease

Patients with existing cholecystolithiasis and those with prior cholecystectomy were treated as a single group. Examination revealed gallbladder stones in 18 of the 222 patients with CD, while the other 12 underwent prior cholecystectomy, yielding a gallbladder stone prevalence of 13.5% ($n = 30$). The group of patients ⩽30 years of age numbered 101 subjects, representing nearly half of the collective. In these patients, gallbladder stone prevalence stood at 8% ($n = 8$). Prevalence of gallbladder stone disease increased with advancing age. The highest prevalence was found in the group of patients aged ⩾51 years, and stood at 37% in 10 of 27 subjects. No sex-specific differences were observed (Table 1).

Due to disease-specific implications, overweight patients with CD were rare. Thus, 45% of patients belonged to class I ($n = 100$), 37% to class II ($n = 83$) and only 18% to class III ($n = 39$). Assignment of patients to the various weight classes yielded a gallbladder stone prevalence of 14% ($n = 14$) for class I, 11% ($n = 9$) for class II and 13% ($n = 7$) for class III (Table 2).

Another parameter studied was the duration of CIBD. In the group of patients in whom elapsed time since the first diagnosis was 1-5 years, prevalence was the lowest. While in the other groups, the prevalence stood at 12%, 9%, and 28%, respectively (Table 2).

Isolated disease involvement affecting only the small bowel was observed in 49 patients. Isolated disease involvement affecting only the colon was seen in 33 patients, while the remaining 45 patients suffered from disease involving both the small bowel and colon. Patients who underwent surgical treatment were counted as a separate subgroup. The subgroup of patients with isolated disease affecting either the small intestine or colon only showed prevalence of 6%, each.

Table 1 Prevalence of cholecystolithiasis in relation to age and sex in Crohn's disease patients

Age(yr)	Males		Females		Total	
	n	prevalence (%)	*n*	prevalence (%)	*n*	prevalence (%)
⩽30	39	3	62	11	101	8
31-40	20	10	41	12	61	11
41-50	14	14	19	16	33	15
51⩾	14	36	13	38	27	37
Total	87	11	135	15	222	13.5

Table 2 Prevalence of cholecystolithiasis in relation to BMI, disease duration, pattern of involvement and bowel resections in Crohn's disease patients

BMI-classes	Patients (*n*)	Prevalence (%)
Ideal weight (males:< 22; females:< 21)	100	14
Normal weight (males: 22-26; females: 21-25)	97	11
Overweight (males: > 26; females: > 25)	26	13
Total	222	13.5
Disease duration in years		
1-5 yr	86	8
6-10 yr	57	12
11-15 yr	32	9
16-34 yr	47	28
Total	222	13.5
Pattern of disease involvement or prior surgery		
No visualized involvement	9	22
Isolated to small bowel	49	6
Isolated to colon	33	6
Both small bowel and colon involved	45	13
Ileocaecal-/ileal resection	54	22
Partial or total colectomy	32	16
Total	222	13.5

Patients with disease affecting both the small and large bowel, gallbladder stone prevalence stood at 13% (Table 2).

Evaluating for length of affected bowel segments, prevalence of gallbladder stones in a group of 21 patients with segment length up to 10 cm stood at 5% (n = 1) and at 7% in 28 patients with segment length exceeding of 10 cm (n = 2).

Eighty-six of all the patients in the CD group, underwent surgical bowel resection. Fifty-four patients underwent ileocaecal and/or ileum resection, while four other patients underwent ileotransversostomy or ileoascendostomy in addition to ileocaecal resection. Seventeen patients had a history of right hemicolectomy, while the other 10 underwent segmental colectomy. Only one patient underwent total colectomy. The groups with ileocaecal resection and ileum resection were combined in the univariate statistical analysis and compared to the group with colon resections.

In the group of patients who underwent partial resection of the small bowel, prevalence of gallbladder stone disease stood at 22% (12 of 54) and at 16% (5 of 32) in the colectomized group.

A logistic regression model considering patients' age, sex and BMI identified only age as a risk factor for developing gallbladder stone disease. No correlation with the prevalence of gallbladder stones was observed for the parameters such as sex, BMI, disease pattern, duration of the disease and prior intestinal resections (Table 3).

Ulcerative Colitis

Criteria used in the evaluation of the collective of patients with UC corresponded to those applied to CD patients. The overall prevalence of gallbladder stones in the UC group was lower than the comparable prevalence in the CD group. In the smaller subcollective of the UC group, gallbladder stones were observed only in female subjects. Using the same BMI-based weight classes applied to the CD collective, the following distribution according to weight was found in the UC group: 42% (n = 37), ideal weight; 34% (n = 30), normal weight; and 24% (n = 21), overweight. In the group of UC patients at ideal body weight, 5% (n = 2) had gallbladder stones, compared to 7% (n = 2) in those at normal weight and in none of the 21 overweight patients

Table 3 Risk factors for gallbladder stone disease at multiple logistic regression in patients with Crohn's disease

Risk factors	Odds ratio (OR)	95% CI	*P*
Age (yr)	1.048	1.010-1.089	[1]0.0143
Female Sex	1.732	0.704-4.263	0.2321
BMI (kg/m²)	0.937	0.822-1.069	0.3357
Duration of disease	1.045	0.983-1.111	0.1627
Pattern of involvement / bowel resections	0.236	0.025-4.611	0.4970

[1]statistically significant.

Univariate analysis yielded a gallbladder stone prevalence of 2% in patients who had elapsed 1-5 years since the first diagnosis of UC, 10% in the 6-10 year group and 6% in the 11-15 year group. In the group of patients who had passed 16-34 years since the first diagnosis, no disease was complicated by the development of cholecystolithiasis.

In 39 patients, disease did not extend the left colic flexure, while areas of bowel involvement beyond the left colic flexure were observed in 24 patients. Failure to visualize thickening of the intestinal at the time of examination was documented in 25 patients. Prevalence of gallbladder stone disease stood at 3% (n = 1) in patients with disease not extending the left colic flexure, but in 12.5% (n = 3) in those with disease involvement beyond the left colic flexure. We did not find evidence of gallbladder stone disease in any of the patients without documented bowel wall thickening at the time of examination. Unlike the group of patients with CD, the number of patients in the UC group with a history of prior bowel resections was too small for meaningful statistical analysis.

Because of the small number of gallstones (n = 4) identified in the UC group, no subgroup analyses were conducted.

DISCUSSION

The prevalence of gallbladder stones in patients with Crohn's disease in our collective was 13.5%, which is almost twice as high as that (7-8%) for age-matched groups of the general population in the same geographic area[12]. Comparable findings have also been reported from Italy and Sweden[2-4]. On the other hand, patients with ulcerative colitis have a prevalence of 4.6% and are not more frequently affected by cholecystolithiasis. Only Lorusso *et al.*[6], and Jones *et al.*[13], have reported that the prevalence of cholecystolithiasis is higher in UC patients than in the general population. Recent prospective sonographic surveys of larger CD and UC populations have studied the prevalence of cholecystolithiasis in these groups in comparison to a general population and used a multivariate logistic regression model to estimate the relative risk associated with the respective parameters[2-6].

Many, mostly earlier studies are unsuitable for comparison because of selection bias in the reference group, non-correspondence of the survey period or survey in another geographic region[14-17]. Other researchers have not drawn a comparison[7,18].

In the group of patients with CD, the prevalence increased with age from 8% in the group of subjects under 30 years of age to 37% in the 51-and-over age group. The multivariate analysis identified only age as an independent risk factor (OR: 1.048; CI: 1.010-1.089; $P = 0.0143$). It was reported that the prevalence of gallbladder stone increases in higher age groups[5,6] . In our own collective of patients with UC, we were not able to identify any correlation between advancing age and increased prevalence of cholecystolithiasis.

In our initial evaluation, sex was also identified as a univariate risk factor in CD and UC patients, though this did not hold true when the multiple logistic regression model was applied. The actual influence of female sex as a risk factor in the etiology of gallbladder stones is controversial[2,3,6,7,14]. Because of the small number of subjects in most studies, the results should be interpreted with caution.

Multiple analysis failed to demonstrate an increased prevalence of cholecystolithiasis in relation to the degree of obesity in either the CD ($P = 0.3357$) or UC ($P = 0.8397$) groups in our population. Most studies, especially the newer ones, have not included BMI as a risk factor in studies of UC patients[14-16,19]. Lorusso *et al*.[6], and Schölmerich *et al*.[7], have also failed to identify evidence supporting patients' degree of obesity as an independent risk factor contributing to the development of cholecystolithiasis.

Univariate analysis of disease duration suggested a correlation between the increasing length of time elapsed since the first diagnosis of CIBD and the prevalence of gallbladder stone disease. This was not confirmed by multiple logistic regression analysis ($P = 0.1627$) as it has been previously[2,3]. Findings in the literature are contradictory[17,20,21]. Reasons for the divergent findings are to be sought in the characteristics of the disease and in individual disease history of patients. In order to arrive at a relevant and objective evaluation of disease duration as an independent risk factor contributing to increased prevalence of cholecystolithiasis, analysis must include other factors, such as inflammatory activity, pattern of disease involvement, number and type of bowel resections, number and duration of remission phases, as well as type and success of other therapeutic measures. Because of the small number of cases in this subgroup, further statistical evaluation of these influence parameters was not meaningful. Gallstone prevalence was at 22% in patients with partial resection of the small bowel ($n = 12$) and 16% in the group that underwent resection of the colon ($n = 12$). Partial resection of the small bowel could not be identified as an independent risk factor in the multivariate analysis ($P = 0.4970$). Our data contradict those of previous[2,3]. A possible reason for the failure to identify the extent and number of bowel resections as independent risk factors at multivariate analysis may be the smaller number of patients in our collective who underwent ileocecal resection.

Because a separate evaluation of pattern of disease involvement and bowel resection is difficult, we defined these as a single parameter in our multiple logistic regression. The retrospective evaluation of surgical findings further limits the strength of our results. Multiple analysis failed to reveal any correlation between cholecystolithiasis, pattern of disease involvement and prior surgical bowel resection in CD patients ($P = 0.4970$). Earlier radiologic studies have shown an increase in gallbladder stone prevalence in relation to the length of resected bowel segments[4,8,9,16,18]. The disadvantages of these studies, however, refer primarily to the absence of multivariate analysis and a small number of subjects.

Studies showed that the bile acid pool reduces in patients with Crohn's disease[22]. Lapidus *et al*.[23,24], showed that the risk for pigment gallstones increases in patients with ileocoecal resections accompanied with manifestly elevated bilirubin and deoxycholic acid fractions in the bile suggesting that an increased risk for cholesterol gallstones in these patients does not exist.

Recently published data show that patients with Crohn's disease after colectomy or patients with small bowel Crohn's disease have an increased risk for cholesterol stones, and that patients with ileitis are prone to develop mixed, pigment-rich gallstones[25]. These changes after colectomy have not been detected in patients with ulcerative colitis[26].

In conclusion, the findings of the present study have identified only "age" as an independent risk factor for increased prevalence of gallbladder stones. Neither disease duration, pattern of disease involvement nor number or total length of resected bowel segments appear to be risk factors contributing to the development of gallbladder stones in these patients. Prospective multicenter studies should be conducted to assess all potential risk factors including therapy intervals between disease flares, phases of parenteral nutrition and prospective documentation of surgical data.

REFERENCES

1 **Lakatos L**, Pandur T, David G, Balogh Z, Kuronya P, Tollas A, Lakatos PL. Association of extraintestinal manifestations of inflammatory bowel disease in a province of western Hungary with disease phenotype: Results of a 25-year follow-up study. *World J Gastroenterol* 2003; **9**: 2300-2307

2 **Bargiggia S**, Maconi G, Elli M, Molteni P, Ardizzone S. Sonographic prevalence of liver steatosis and biliary tract stones in patients with inflammatory bowel disease: study of 511 subjects at a single center. *J Clin Gastroenterol* 2003; **36**: 417-420

3 **Fraquelli M**, Losco A, Visentin S, Cesana BM, Pometta R, Colli A. Gallstone disease and related risk factors in patients with Crohn disease: analysis of 330 consecutive cases. *Arch Intern Med* 2001; **8**: 2201-2204

4 **Lapidus A**, Bangstad M, Astrom M, Muhrbeck O. The prevalence of gallstone disease in a defined cohort of patients with Crohn's disease. *Am J Gastroenterol* 1999; **94**: 1261-1266

5 **Hutchinson R**, Tyrrell PN, Kumar D, Dunn JA, Li JK, Allan RN. Pathogenesis of gall stones in Crohn's disease: an alternative explanation. *Gut* 1994; **35**: 94-97

6 **Lorusso D**, Leo S, Mossa A, Misciagna G, Guerra V. Cholelithiasis in inflammatory bowel disease. A case-control study. *Dis Colon Rectum* 1990; **33**: 791-794

7 **Schölmerich J**, Braun G, Volk BA, Spamer C, Hoppe-Seyler P, Gerok W. Detection of extraintestinal and intestinal abnormalities in inflammatory bowel disease by ultrasound. *Dig Surg* 1987; **4**: 82-87

8 **Kangas E**, Lehmusto P, Matikainen M. Gallstones in Crohn's

disease. *Hepatogastroenterology* 1990; **37**: 83-84
9 **Brett M**, Barker DJ. The world distribution of gallstones. *Int J Epidemiol* 1976; **5**: 335-341
10 **Kratzer W**, Mason RA, Kachele V. Prevalence of gallstones in sonographic surveys worldwide. *J Clin Ultrasound* 1999; **27**: 1-7
11 **Hosmer DW Jr**, Lemeshow S. Applied logistic regression. *New York Wiley* 1989
12 **Kratzer W**, Kron M, Hay B, Pfeiffer MM, Kachele V. Prevalence of cholecystolithiasis in South Germany-an ultrasound study of 2 498 persons of a rural population. *Z Gastroenterol* 1999; **37**: 1157-1162
13 **Jones MR**, Gregory D, Evans KT, Rhodes J. The prevalence of gallbladder disease in patients with ileostomy. *Clin Radiol* 1976; **27**: 561-562
14 **Kurchin A**, Ray JE, Bluth EI, Merritt CR, Gathright JB, Pehrsson BF. Cholelithiasis in ileostomy patients. *Dis Colon Rectum* 1984; **27**: 585-588
15 **Baker AL**, Kaplan MM, Norton RA, Patterson JF. Gallstones in inflammatory bowel disease. *Am J Dig Dis* 1974; **19**: 109-112
16 **Hill GL**, Mair WS, Goligher JC. Gallstones after ileostomy and ilealresection. *Gut* 1975; **16**: 932-936
17 **Heaton KW**, Read AE. Gall stones in patients with disorders of the terminal ileum and disturbed bile salt metabolism. *Br Med J* 1969; **3**: 494-496
18 **Andersson H**, Bosaeus I, Fasth S, Hellberg R, Hulten L. Cholelithiasis and urolithiasis in Crohn's disease. *Scand J Gastroenterol* 1987; **22**: 253-256
19 **Bluth EI**. Ultrasound evaluation of small bowel abnormalities. *Am J Gastroenterol* 1983; **78**: 788-793
20 **Heaton KW**. Disturbances of bile acid metabolism in intestinal disease. *Clin Gastroenterol* 1977; **6**: 69-89
21 **Marks JW**, Conley DR, Capretta TL, Bonorris GG, Chung A, Coyne MJ. Gallstone prevalence and biliary lipid composition in inflammatory bowel disease. *Am J Dig Dis* 1977; **22**: 1097-1100
22 **Vantrappen G**, Ghoos Y, Rutgeerts P, Janssens J. Bile acid studies in uncomplicated Crohn's disease. *Gut* 1977; **18**: 730-735
23 **Lapidus A**, Einarsson K. Effects of ileal resection on biliary lipids and bile acid composition in patients with Crohn's disease. *Gut* 1991; **32**: 1488-1491
24 **Lapidus A**, Einarsson C. Bile composition in patients with ileal resection due to Crohn's disease. *Inflamm Bowel Dis* 1998; **4**: 89-94
25 **Pereira SP**, Bain IM, Kumar D, Dowling RH. Bile composition in inflammatory bowel disease: ileal disease and colectomy, but not colitis, induce lithogenic bile. *Aliment Pharmacol Ther* 2003; **17**: 923-933
26 **Akerlund JE**, Einarsson C. Effects of colectomy on bile composition, cholesterol saturation and cholesterol crystal formation in humans. *Int J Colorectal Dis* 2000; **15**: 248-252

Science Editor Wang XL and Guo SY **Language Editor** Elsevier HK

PO Box 2345, Beijing 100023, China
www.wjgnet.com
wjg@wjgnet.com

ELSEVIER

World J Gastroenterol 2005;11(39):6176-6181
World Journal of Gastroenterology ISSN 1007-9327

• *BRIEF REPORTS* •

Quantitative evaluation of long-term liver repopulation and the reconstitution of bile ductules after hepatocellular transplantation

Yun-Wen Zheng, Nobuhiro Ohkohchi, Hideki Taniguchi

Yun-Wen Zheng, Hideki Taniguchi, Department of Regenerative Medicine, Graduate School of Medical Science, Yokohama City University, Yokohama 236-0004, Japan
Nobuhiro Ohkohchi, Yun-Wen Zheng, Department of Surgery, Institute of Clinical Medicine, University of Tsukuba, Tsukuba 305-8575, Japan
Hideki Taniguchi, Research Unit for Organ Regeneration, Center for Developmental Biology, RIKEN, Kobe 650-0047, Japan
Supported by the National Project for Realization of 'Regenerative Medicine' and Grants-in-Aid (14207046, 12557096) for Scientific Research from the Ministry of Education, Culture, Sports, Science and Technology, Japan and a grant from MITSUBISHI Foundation
Correspondence to: Professor Hideki Taniguchi, MD, PhD, Department of Regenerative Medicine, Graduate School of Medical Science, Yokohama City University, Fukuura 3-9, Kanazawa-Ku, Yokohama 236-0004, Japan. rtanigu@med.yokohama-cu.ac.jp
Telephone: +81-45-787-8963 Fax: +81-45-787-8963
Received: 2004-12-22 Accepted: 2005-03-21

Abstract

AIM: The treatment of liver disease is severely limited by a shortage of donor livers. In trying to address this growing problem, hepatocellular transplantation (HTx) has received much attention as an alternative to whole organ transplant. However, the expansion of transplanted cells is at low level, and the reconstitution of functional liver tissue is limited by this cellular property. We set up an animal model to better understand cell dose effect and the kinetics of liver repopulation following HTx.

METHODS: Dipeptidyl peptidase IV (DPPIV)-deficient rats treated with retrorsine and subjected to partial hepatectomy were infused with DPPIV-positive hepatocytes. Rats were injected with varying numbers of donor hepatocytes down to 100 cells low, and liver repopulation was examined at different time points up to 20 mo long. Repopulation was assessed by computer-aided quantitative detection.

RESULTS: Transplanted hepatocytes underwent multiple rounds of proliferation and stably repopulated the injured livers after 20 mo and at all cell doses. Transplanted cells divided 14 times within the 3-mo time period following infusion, and the liver repopulation reached a plateau between 3 and 20 mo. Approximately 90% replacement occurred. Donor-derived cells also reconstituted the bile ductules of the recipients.

CONCLUSION: The ability of transplanted hepatocytes to fully reconstitute injured livers strongly supports further investigation into the clinical potential of HTx. Additionally, the observation that transplanted hepatocytes also form components of the biliary system suggests that these cells may have bi-potential property of the stem cells.

Key words: Hepatocellular transplantation; Hepatic stem cell; Kinetics; Cell dose; Long-term repopulation; Bile ductules; Quantification; *In vivo*; Therapeutic potential

Zheng YW, Ohkohchi N, Taniguchi H. Quantitative evaluation of long-term liver repopulation and the reconstitution of bile ductules after hepatocellular transplantation. *World J Gastroenterol* 2005; 11(39): 6176-6181
http://www.wjgnet.com/1007-9327/11/6176.asp

INTRODUCTION

In patients with end-stage liver disease, liver transplantation is the only effective treatment, but this is limited by the shortage of potential organs. Cell transplantation (Tx) has the potential to overcome this shortage as well as the high cost and morbidity associated with the whole organ transplant. Isolated hepatocellular transplantation (HTx) was investigated several decades ago as one of the earliest forms of cell transplantation[1] and has come to the stage of clinical therapies in recent years[2,3]. However, transplanted hepatocytes do not seem to proliferate well and reconstitution of liver function is not sufficient in the models used thus far[3,4]. Endogenous hepatocytes greatly outnumbered the transplanted cells and it is conceivable that, if both populations respond equally well to proliferative stimuli, donor cells would never achieve sufficient numbers[5]. Some models allowing for the selective proliferation of transplanted cells have made progress in addressing this problem[6-9]. Disruption of the proliferative capacity of endogenous hepatocytes followed by transplantation is an alternative strategy to achieve these goals. Retrorsine[7,10] or irradiation[9] has been used to inhibit the proliferation of endogenous hepatocytes and allow transplanted hepatocytes to fully repopulate the liver, making the clinical application of HTx more feasible. Application of the prospective therapy may become a reality if answers to the following questions are obtained. How long can donor-derived hepatocytes continue to repopulate the damaged recipient liver? What is the relationship between repopulation efficiency and cell dose of HTx? Will transplanted hepatocytes be able to repopulate other tissues in addition to the liver parenchyma? Moreover, the capability of long-term tissue repopulation[5] should also be addressed in the animal model, with a longer post-transplant period than the life span of liver cells.

We used dipeptidyl peptidase IV (DPPIV) as a genetic marker of transplanted cells in rats treated with retrorsine and subjected to partial hepatectomy (PH). Retrorsine, a DNA-alkylating agent that disrupts cell-cycle progression in hepatocytes, prevented the recipient hepatocytes from proliferating, and, following PH, only transplanted cells proliferated and repopulated the liver[7]. Using this model, we addressed the above questions and discussed the prospects of HTx in clinical application, and also the heterogeneity and the stem cell property of hepatocytes.

MATERIALS AND METHODS

Animals

Male Fischer 344 DPPIV wild-type ($DPPIV^+$) rats used as hepatocyte donors for Tx were purchased from SLC of Japan and female Fischer 344/DuCrj DPPIV-deficient ($DPPIV^-$) recipient rats were purchased from Charles River of Japan. Animals were maintained in daily 12-h cycles of alternating light and darkness. All studies were conducted under protocols approved by the Laboratory Animal Resource Center of University of Tsukuba, Japan.

Retrorsine treatment and partial hepatectomy

Recipients, 4-wk-old Fischer 344 rats, were treated with retrorsine similar to previous descriptions with some modifications[7,11]. Briefly, a retrorsine (Sigma) working solution was prepared in acidified saline with 1 mol/L HCl; this was neutralized with 1 N NaOH and adjusted to a final concentration of 6 mg/mL. The animals received two intraperitoneal injections with 30 mg/kg body weight 2 wk apart. Donor cells were infused either 1 mo or 2 wk following retrorsine treatment. All recipients were subjected to two-thirds surgical PH.

Cell isolation and transplantation

Parenchymal hepatocytes were isolated from normal adult rats (8-10-wk old) using a standard two-step collagenase perfusion method described by Seglen[12]. After perfusion, the cells were centrifuged at 50 g for 1 min and filtered with a nylon mesh to remove aggregated cells and residual tissue. Cell viability was between 80% and 90% as determined by trypan blue dye exclusion. Limiting dilution of the freshly isolated cells was performed from 2×10^6, 1×10^6, 1×10^5, 1×10^4, and 1×10^3 to 1×10^2. Hepatocytes in 0.2 mL Dulbecco's modified Eagle's medium were infused through the portal vein. Two to three animals were used for each time point, and experiments were repeated at least twice. After 1-3 mo, and up to 20 mo following Tx, animals were killed and the livers were sampled.

Histochemical staining

DPPIV histochemical staining was performed as described[7,13]. Sampled rat livers were embedded in optimum cutting temperature compound, frozen in liquid nitrogen and stored at -80 ℃. DPPIV activity was visualized in tissues fixed with chloroform–acetone (1:1, v/v) for 10 min, followed by incubation with glycyl-L-proline-4-methoxy-2-naphthyl-amide (Sigma) substrate for 30 min at room temperature. The counterstaining was performed with hematoxylin.

Quantitative detection

DPPIV-positive areas were captured by Photograb-2500, v1.0 (Fujifilm) through a Nikon Eclipse E800 microscope and analyzed by computer program, WinROOF v3.2 (Mitani Corp.).

To determine the number of hepatocytes per repopulated colony, we considered a colony as a large sphere and a single hepatocyte as a small sphere. If the average radius of one colony in cross-sectional analysis on slide is expressed as R, the overall volume of the colony is $2\pi R^3\sqrt{1.5}$. The number of hepatocytes estimated per colony sphere was calculated by $\text{volume}_{\text{colony-sphere}}/\text{volume}_{\text{hepatocyte}}$. Cell division during Tx for a colony sphere was calculated by $\log_{10}(1.5(R/r)^3\sqrt{1.5})/\log_{10}2$ ($r\approx10$ μm, radius of one hepatocyte).

RESULTS

Kinetics of liver repopulation

The canaliculi enzyme DPPIV is highly expressed in epithelial cells (including hepatocytes) of many organs in rats except in one substrain of inbred Fischer rats. It is a stable and easily distinguishable marker for use in enzyme histochemistry in models of HTx[7,14]. After transplantation, DPPIV-positive cells constituted 14.8±4.2%, 50.7±13.9% and 70.4±9.0% of the total hepatocyte number at 1, 2, and, 3 mo of follow-up, respectively (Figures 1A-C). Twenty months after transplantation, a repopulation rate as high as 95% was observed, with an average rate of 89.8±4.7% (Figure 1D). Histochemical analysis also clearly showed that donor cells proliferated and expanded through recipient liver tissue (Figure 2A and Table 1), and, at the latest time point, occupied nearly the full volume of the recipient liver (Figure

Table 1 Effect of transplant cell dose and time on the efficiency of liver repopulation *in vivo* after HTx

Time of Tx (mo)	Kinetics of repopulation				Effect of cell dose on repopulation				
	1	2	3	20	3	3	3	3	3
Infused cell number Post Tx	2×10^6	2×10^6	2×10^6	1×10^6	1×10^6	1×10^5	1×10^4	1×10^3	1×10^2
Liver repopulation (%)	14.8±4.2	50.7±13.9	70.4±9.0	89.8±4.7	51.0±4.7	28.9±7.2	13.8±15.0	1.1±1.2	0.6±0.6
Colony number/mm^2	5.48±1.10	5.1±1.40	NA	NA	2.64±0.16	0.91±0.05	0.37±0.39	0.09±0.07	0.01±0.01
Diameter of colony (μm)	149.4±110.5	280.1±219.4	NA	NA	425.2±278.8	376.7±64.8	476.5±54.5	354.5±108.9	698.7±39.2
Number of animals	6	6	3	4	3	3	4	4	4
Area examined (mm^2)	365.0	402.0	66.6	2386.5	77.6	284.1	464.8	458.0	470.5

Donor cells were derived from $DPPIV^+$ rats. Recipients were DPPIV-deficient rats treated with retrorsine and two-thirds PH; $DPPIV^+$ cells were visualized by their enzymatic activity after histochemical staining of cryostat sections. The characteristics of repopulation, colony number and colony diameter were analyzed based on $DPPIV^+$ cells. Computer-aided area analysis was used for quantitative detection of repopulation. All of the data presented as mean±SD from three to six individuals in two or three independent experiments. HTx: hepatocellular transplantation; Tx: transplantation; NA: not applicable.

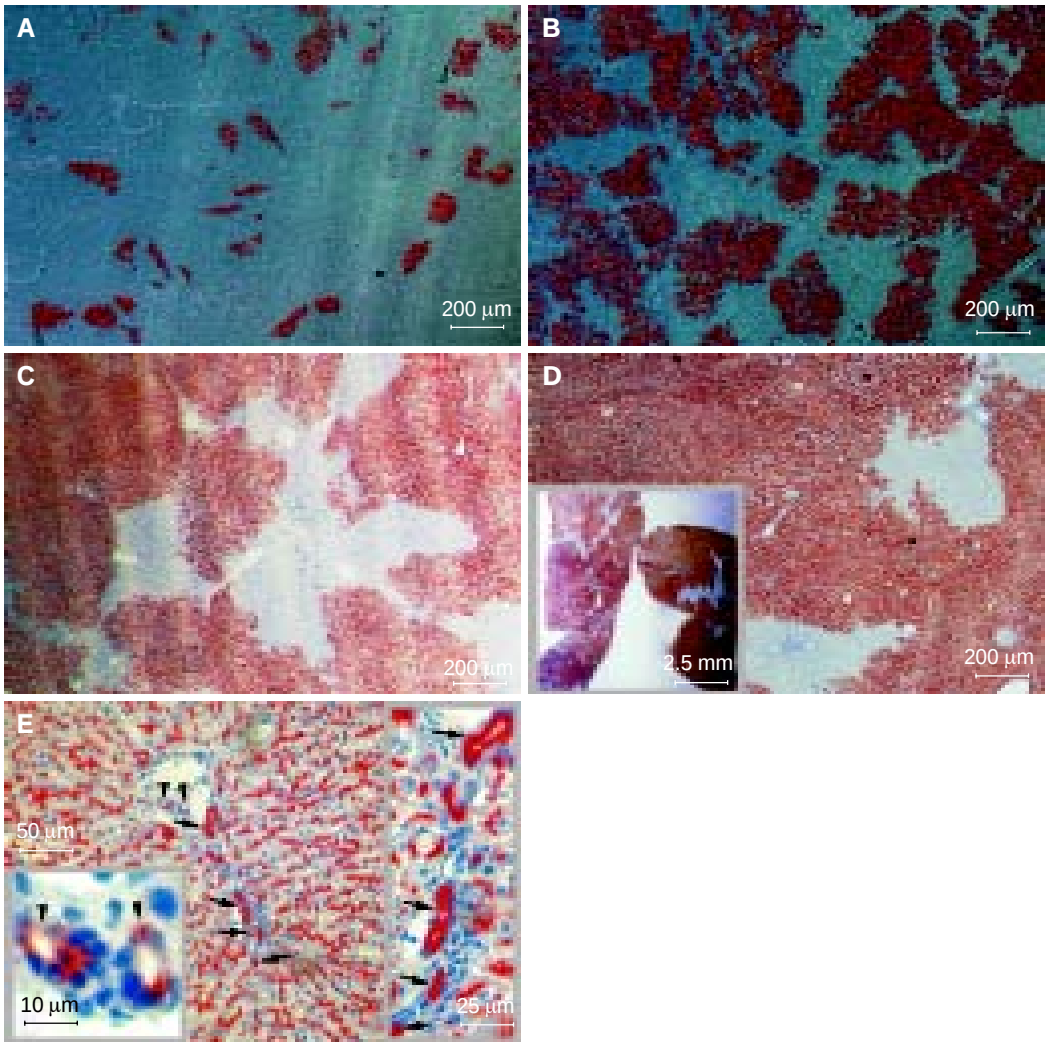

Figure 1 Long-term liver repopulation 1-20 mo after hepatocellular Tx and hepatic epithelial reconstitution from donor hepatocytes. Recipient DPPIV-deficient Fischer rats were treated with retrorsine and subjected to two-thirds PH. DPPIV-positive donor hepatocytes were infused through the portal vein. 2×10^6 donor cells per recipient in A-C and 1×10^6 in D and E. Cryostat sections show DPPIV-positive cells as red-brown after histochemical staining. Data presented as mean±SD from three to six individuals in two or three independent experiments. Tx: transplantation; DPPIV: dipeptidyl peptidase IV. A: 1-mo repopulation: 14.8±4.2%; polarization contrast image; B: 2-mo repopulation: 50.7±13.9%; polarization contrast image; C: 3-mo repopulation: 70.4±9.0% with hematoxylin counterstaining; D: 20-mo repopulation: 89.8±4.7% with hematoxylin counterstaining. The inset box displays the cross-sections of hepatic lobes under stereomicroscopy and E: DPPIV-positive cells not only were expressed in parenchyma but also were found in Hering's canal-like structures (arrow) and interlobular bile duct-like structure (arrowhead) in recipient liver; hematoxylin counterstaining.

1D, inset). Between 3 and 20 mo, the repopulation rate increased by only 20%, suggesting that the phenomena had reached a plateau. Using a similar model, Laconi *et al.*[15], observed a repopulation rate of 81% at 8 mo in female recipients; this is consistent with our results.

The lobular architecture and overall histological appearance of the livers were normal following HTx, and hepatocyte morphology, hepatic plate structure, and the appearance of cells lining the sinuses were normal compared to untreated livers (data not shown). Despite extensive hepatocyte proliferation and the appearance of "nodules" of transplanted cells, no tumors were observed in the liver up to 20 mo after Tx. Additionally, the survival of all four recipients up to 20 mo indicates that no abnormalities incompatible with life develop following transplant.

Colony size and cell replication

Colony size analyses more clearly defined the magnitude of transplanted cell proliferation in recipient animals. Table 1 presents the characteristics and distribution of donor cells following transplantation with varied cell numbers and at different time points after Tx. $DPPIV^+$ colonies expanded linearly between 1 and 3 mo after Tx from 150 to 425 μm in diameter (Figure 2B). The area of recipient livers occupied by donor cells similarly increased over 3 mo.

Hepatocytes are thought to be symmetric, 8 or 12-sided cells[16], but, in order to simplify calculations, we considered a hepatocyte as a sphere and assumed that one colony arose from one hepatocyte. Additionally, we made the assumption that repopulated colonies assumed a grossly spherical shape, and the number of cells occupying these colonies could be calculated by comparing the volume of one cell with the volume of a colony. Based on these assumptions and analyses, transplanted hepatocytes underwent about nine rounds of cell replication after the 1st mo and another three and two rounds in 2nd and 3rd mo, respectively. Donor cell

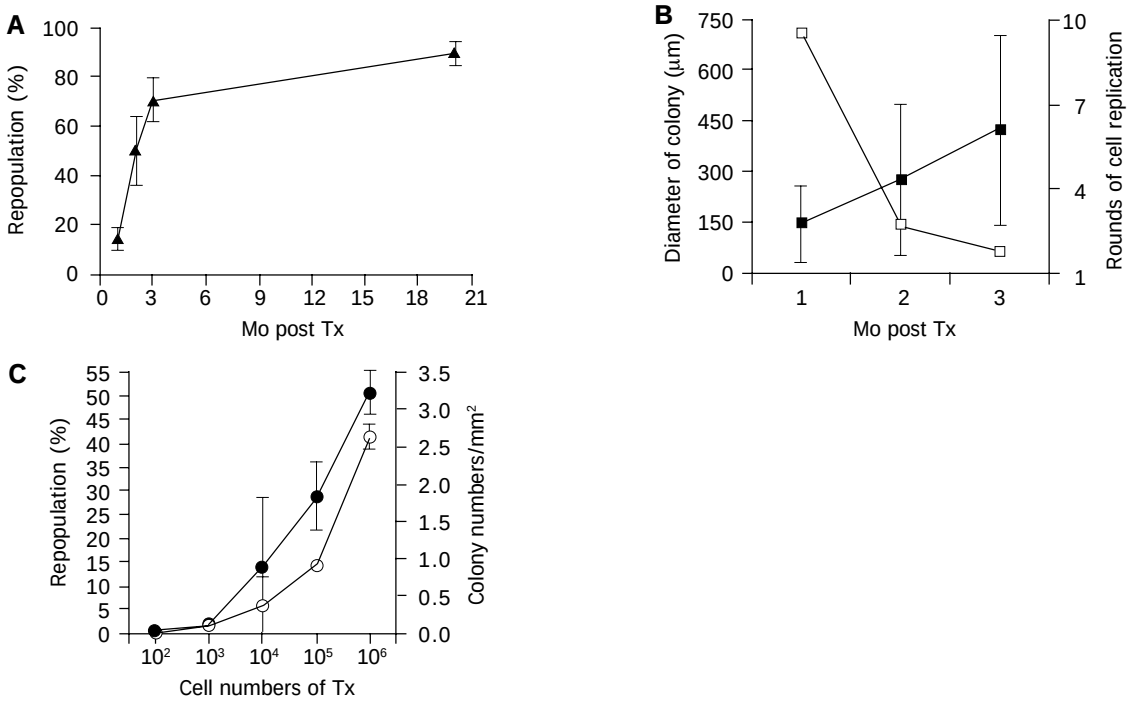

Figure 2 Repopulation kinetics of hepatocellular Tx. DPPIV$^+$ donor hepatocytes were isolated and infused into DPPIV-deficient rats through the portal vein. The visualized DPPIV$^+$ cells in recipient were processed by a computer-aided analysis. Data are presented as mean±SD from three to six individuals in two or three independent experiments. Tx: transplantation; DPPIV: dipeptidyl peptidase IV. A: Kinetics of liver repopulation. Transplanted cell numbers into 1-3 mo and 20 mo were 2×10^6 and 1×10^6, respectively. The repopulation rate increased dramatically over 3 mo and reached a plateau at 20 mo; B: Kinetics of colony size and cell replication. Transplanted cell numbers into 1-2 mo and 3 mo were 2×10^6 and 1×10^6, respectively. The estimation technique of cell replication rounds is explained in Results. The average colony size from donor hepatocytes in the 3 mo after Tx are filled squares and the estimated number of rounds of cell replication are open squares and C: Cell-dose effect on liver repopulation and colony numbers. All samples collected at 3 mo after Tx and the repopulation rate (filled circles) and colony numbers (open circles) showed a similar trend.

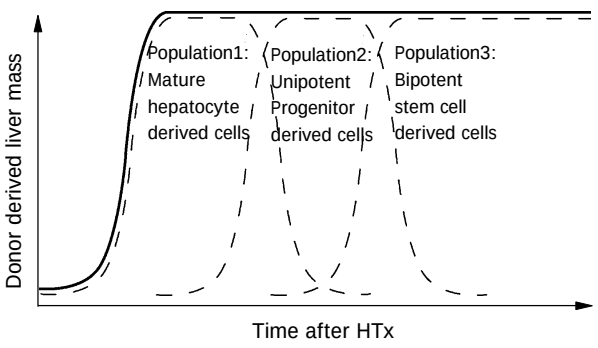

Figure 3 Schematic diagram of long-term repopulation after HTx. Different cell populations may be required for different phases of liver regeneration/repopulation. The solid lines express the repopulation of donor-derived cells in the liver and the broken lines are the repopulation from the possible contributors. This assumes a heterogeneous population of transplanted hepatocytes. HTx: hepatocellular transplantation.

division was high only in the 1st mo, and it dramatically decreased over the following period (Figure 2B), but replication never stopped although it slowed down to very low level.

Effect of cell dose on liver repopulation

The ability of different numbers of transplanted cells to repopulate the liver is unknown, despite the importance of this information for stem cell biology and the clinical application of HTx. As seen in Table 1 and Figure 2C, transplantation of 10^2-10^6 led to liver repopulation rates from 0.6% up to 51% 3 mo after transplant, and the repopulated colonies reached 0.01-2.64/mm^2 in recipient livers. Effective repopulation occurred even in the 100-cell group. Therefore, liver repopulation for no more than 3 mo does not seem to depend on an infrequent cell fraction, but hepatocytes in general are able to form colonies following transplantation.

DPPIV-positive cholangiocytes in recipient livers

DPPIV is expressed in both hepatocytes and bile duct epithelial cells, in a characteristic bile canalicular distribution and a diffuse cytoplasmic pattern, respectively[7,17,18]. Twenty months after transplant with one million hepatocytes, interlobular bile duct-like cells and Hering's canal-like cells also expressed the donor-derived genetic marker, DPPIV (Figure 1E). To our knowledge, this is the first report of bile duct differentiation of transplanted hepatocytes. This finding contrasts with the widely accepted view that hepatocytes are uni-potential following transplant[19].

DISCUSSION

In contrast to fully differentiated cells in adult mammalian tissues, hepatocytes possess an enormous proliferative capacity and are capable of replacing the entire liver mass under some circumstances. In the normal resting liver, the hepatocyte turnover rate at any given time is about 1 in 20 000-40 000 cells, and normal liver tissue is replaced over the course of 1 year[20]. If transplanted hepatocytes did not undergo cell

division or the division did not last for a sufficient duration of time, few donor cells would have remained at the 20-mo time point. However, recipient livers were almost exclusively comprised of donor cells at 20 mo after transplant (Figure 1D, inset). The tissue renewal by donor-derived hepatocytes occurs multiple times in the recipient liver in more than 1-year long-term repopulation. The present findings demonstrate that the 'long-term tissue repopulation' characteristics defined for stem cells[5] are expressed by adult hepatocytes as well. The present study markedly differs from previous reports[7,14,15] in having the post-transplantation period longer than the life span of liver cells, and it also takes into account the cell-dose effect. The extremely long period of observation was necessary because it facilitated analysis of cell kinetics of long-lived cells to trace the transplanted cells and to show whether they possess the stem cell properties or not.

To differentiate and colonize, a wide range of tissues to reconstitute them *in vivo* is another important property of stem cells. In the present study, bi-potential capability of donor-derived cells displayed an interesting aspect of tissue reconstitution. Hepatocytes are thought to be "functional" or "committed" progenitors[19], but 20 mo after transplant, cholangiocytes (interlobular bile duct-like cells and Hering's canal-like cells) expressed the donor cell marker (Figure 1E). It indicates that the bi-potential stem cells, however, existed in donor-derived cells. We had not previously observed donor-derived cholangiocytes in other no longer than 6-mo old Tx groups. Why is the regeneration of biliary system so rare to be observed? One possible answer is that a minor proportion of donor-derived bi-potential cells spend a long time to differentiate and competitively reconstitute the system in the recipient. The low frequent appearance may predict and represent an important inherent nature of hepatic stem cells.

Hepatocytes may be capable of only one or two rounds of cell division when responding to cell loss under normal physiological conditions[21,22], but we observed at least 14 rounds of replication in the 3-mo time period following transplantation. Various physiological needs may stimulate a variety of responses from different populations of hepatocytes. It is possible that the transplanted cells were not a homogenous population of hepatocytes. This could explain the ability of the donor cells to proliferate to a greater extent than previously thought as well as the generation of cholangiocytes. Indeed, adult hepatocytes exhibit heterogeneous proliferative potential *in vitro*[23]. The potential complexity of the liver cells populations is outlined in Figure 3. Liver tissue may be comprised of a large number of mature hepatocytes that rapidly respond to physiological cell loss and tissue injury (population 1) for a short time, a small number of uni-potential progenitors that rapidly replicate in response to liver injury for a limited time period (population 2), and rare bi-potential stem cells capable of self-renewal that slowly respond to severe liver injury for a long time (population 3). Further studies with some other approaches, such as, flow-cytometric cell sorting and *in vitro* colony assay[24,25] are clearly needed to investigate this hypothesis.

While the biological phenomena underlying our observations are not very clear, the therapeutic potential of hepatocyte transplant is very clear. A small number of transplanted cells efficiently and stably repopulated injured rat livers. With the expansion of waiting lists for orthotopic liver transplant growing, the availability of donor cells makes HTx even more attractive. Among the potential applications of HTx, supply metabolic support in acute or chronic liver failure and definitive treatment of inherited metabolic disorders are included. At the very least, HTx could be used as a bridge therapy to prolong the lives and function of patients awaiting transplants. It is reasonable to assume that mechanism that controls regeneration may be fairly similar among various species, and the knowledge obtained from researches of liver regeneration in the animal model is applicable to the human liver. Our study may be a guide for initial investigations of HTx in human. For example, in our animal model, the cell infusion ratio of donor cells to recipient liver cells was about 1/200 ($2\times10^6/4\times10^8$), and we achieved 50% and 70% repopulation rates 2 and 3 mo after Tx. Human liver tissue is thought to weigh 1 500 *g* with 2.5×10^{11} parenchymal cells. Extrapolating from our data, approximately 1.25×10^9 cells would be used for human HTx, and if 10% of isolated hepatocytes could be collected from a liver (2.5×10^{10}cells), a single liver could be used for 20 HTx. The low cost, high preservability and availability of sources could make HTx an extremely promising treatment for end-stage liver disease.

Taken together, the long-term repopulation potential, high replacement rate and full tissue reconstitution following HTx in our model further strengthens the therapeutic potential of this technique. Additionally, our observations raise interesting possibilities as to the composition and proliferation of hepatocyte populations as well as the hepatic stem cell nature.

ACKNOWLEDGMENTS

Authors thank Dr. Mei Gu, Dr. Pei Gan, Dr. Hirotoshi Miyoshi, Dr. Kennichi Yanagi and Dr. Chika Miyoshi for expert technical assistances on liver perfusion and surgical operation.

REFERENCES

1 **Matas AJ,** Sutherland DE, Steffes MW, Mauer SM, Sowe A, Simmons RL, Najarian JS. Hepatocellular transplantation for metabolic deficiencies: decrease of plasms bilirubin in Gunn rats. *Science* 1976; **192**: 892-894

2 **Grossman M,** Raper SE, Kozarsky K, Stein EA, Engelhardt JF, Muller D, Lupien PJ, Wilson JM. Successful *ex vivo* gene therapy directed to liver in a patient with familial hypercholesterolaemia. *Nat Genet* 1994; **6**: 335-341

3 **Fox IJ,** Chowdhury JR, Kaufman SS, Goertzen TC, Chowdhury NR, Warkentin PI, Dorko K, Sauter BV, Strom SC. Treatment of the Crigler-Najjar syndrome type I with hepatocyte transplantation. *N Engl J Med* 1998; **338**: 1422-1426

4 **Grossman M,** Rader DJ, Muller DW, Kolansky DM, Kozarsky K, Clark BJ 3rd, Stein EA, Lupien PJ, Brewer HB Jr, Raper SE, Wilson JM. A pilot study of *ex vivo* gene therapy for homozygous familial hypercholesterolaemia. *Nat Med* 1995; **1**: 1148-1154

5 **Shafritz DA,** Dabeva MD. Liver stem cells and model systems for liver repopulation. *J Hepatol* 2002; **36**: 552-564

6 **Rhim JA,** Sandgren EP, Degen JL, Palmiter RD, Brinster RL. Replacement of diseased mouse liver by hepatic cell transplantation. *Science* 1994; **263**: 1149-1152

7 **Laconi E,** Oren R, Mukhopadhyay DK, Hurston E, Laconi S, Pani P, Dabeva MD, Shafritz DA. Long-term, near-total liver replacement by transplantation of isolated hepatocytes in rats treated with retrorsine. *Am J Pathol* 1998; **153**: 319-329

8 **Overturf K,** Al-Dhalimy M, Tanguay R, Brantly M, Ou CN, Finegold M, Grompe M. Hepatocytes corrected by gene therapy are selected *in vivo* in a murine model of hereditary tyrosinaemia type I. *Nat Genet* 1996; **12**: 266-273

9 **Guha C,** Sharma A, Gupta S, Alfieri A, Gorla GR, Gagandeep S, Sokhi R, Roy-Chowdhury N, Tanaka KE, Vikram B, Roy-Chowdhury J. Amelioration of radiation-induced liver damage in partially hepatectomized rats by hepatocyte transplantation. *Cancer Res* 1999; **59**: 5871-5874

10 **Gordon GJ,** Coleman WB, Grisham JW. Bax-mediated apoptosis in the livers of rats after partial hepatectomy in the retrorsine model of hepatocellular injury. *Hepatology* 2000; **32**: 312-320

11 **Gordon GJ,** Coleman WB, Grisham JW. Temporal analysis of hepatocyte differentiation by small hepatocyte-like progenitor cells during liver regeneration in retrorsine-exposed rats. *Am J Pathol* 2000; **157**: 771-786

12 **Seglen PO.** Preparation of isolated rat liver cells. *Methods Cell Biol* 1976; **13**: 29-83

13 **Lojda Z,** Gossrau R, Schiebler TH. Peptidase. In: Enzyme Histochemistry: A laboratory manual. *Berlin Springer Verlag* 1979: 199-203

14 **Coleman WB,** McCullough KD, Esch GL, Faris RA, Hixson DC, Smith GJ, Grisham JW. Evaluation of the differentiation potential of WB-F344 rat liver epithelial stem-like cells *in vivo*. Differentiation to hepatocytes after transplantation into dipeptidylpeptidase-IV-deficient rat liver. *Am J Pathol* 1997; **151**: 353-359

15 **Laconi S,** Pillai S, Porcu PP, Shafritz DA, Pani P, Laconi E. Massive liver replacement by transplanted hepatocytes in the absence of exogenous growth stimuli in rats treated with retrorsine. *Am J Pathol* 2001; **158**: 771-777

16 **Elias H,** Sherrick JC. Morphology of the liver. *New York Academic Press* 1969: 5-74

17 **Hubbard AL,** Bartles JR, Braiterman LT. Identification of rat hepatocyte plasma membrane proteins using monoclonal antibodies. *J Cell Biol* 1985; **100**: 1115-1125

18 **Walborg EF Jr,** Tsuchida S, Weeden DS, Thomas MW, Barrick A, McEntire KD, Allison JP, Hixson DC. Identification of dipeptidyl peptidase IV as a protein shared by the plasma membrane of hepatocytes and liver biomatrix. *Exp Cell Res* 1985; **158**: 509-518

19 **Zheng YW,** Taniguchi H. Diversity of hepatic stem cells in the fetal and adult liver. *Semin Liver Dis* 2003; **23**: 337-348

20 **Zimmermann A.** Liver regeneration: the emergence of new pathways. *Med Sci Monit* 2002; **8**: RA53-63

21 **Sell S.** Heterogeneity and plasticity of hepatocyte lineage cells. *Hepatology* 2001; **33**: 738-750

22 **Magami Y,** Azuma T, Inokuchi H, Kokuno S, Moriyasu F, Kawai K, Hattori T. Cell proliferation and renewal of normal hepatocytes and bile duct cells in adult mouse liver. *Liver* 2002; **22**: 419-425

23 **Tateno C,** Takai-Kajihara K, Yamasaki C, Sato H, Yoshizato K. Heterogeneity of growth potential of adult rat hepatocytes *in vitro*. *Hepatology* 2000; **31**: 65-74

24 **Suzuki A,** Zheng YW, Kondo R, Kusakabe M, Takada Y, Fukao K, Nakauchi H, Taniguchi H. Flow-cytometric separation and enrichment of hepatic progenitor cells in the developing mouse liver. *Hepatology* 2000; **32**: 1230-1239

25 **Suzuki A,** Zheng YW, Kaneko S, Onodera M, Fukao K, Nakauchi H, Taniguchi H. Clonal identification and characterization of self-renewing pluripotent stem cells in the developing liver. *J Cell Biol* 2002; **156**: 173-184

Science Editor Guo SY **Language Editor** Elsevier HK

PO Box 2345, Beijing 100023, China
www.wjgnet.com
wjg@wjgnet.com

ELSEVIER

World J Gastroenterol 2005;11(39):6182-6187
World Journal of Gastroenterology ISSN 1007-9327

• *BRIEF REPORTS* •

Serum leptin levels and insulin resistance are associated with gallstone disease in overweight subjects

Nahum Méndez-Sánchez, Luisa B Bermejo-Martínez, Yolanda Viñals, Norberto C Chavez-Tapia, Irina Vander Graff, Guadalupe Ponciano-Rodríguez, Martha H Ramos, Misael Uribe

Nahum Méndez-Sánchez, Yolanda Viñals, Norberto C Chavez-Tapia, Irina Vander Graff, Martha H Ramos, Misael Uribe, Departments of Biomedical Research and Gastroenterology and Liver Unit, Medica Sur Clinic and Foundation, Mexico City, Mexico
Luisa B Bermejo-Martínez,Clinical Research Center, National Institute of Perinatology. Mexico City, Mexico
Guadalupe Ponciano-Rodríguez,Faculty of Medicine, National Autonomous University of Mexico (UNAM). Mexico City, Mexico
Supported by the National Council of Science and Technology of Mexico (CONACYT) and The Ministry of Health (SSA), Mexico project No. M0059-M9602 (NM-S and MU)
Correspondence to: Nahum Méndez-Sánchez, MD, PhD, Departments of Biomedical Research, Gastroenterology and Liver Unit, Medica Sur Clinic and Foundation, Puente de Piedra 150, Col. Toriello Guerra, Mexico City, Mexico. nmendez@medicasur.org.mx
Telephone: +52-55-5606-6222-4215 Fax: +52-55-5666-4031
Received: 2005-01-05 Accepted: 2005-06-02

Abstract

AIM: To establish an association between the serum leptin levels and the development of gallstone disease (GD).

METHODS: We carried out a non-matched case-controlled study in a university hospital in Mexico City. Two hundred and eighty-seven subjects were included: 97 cases with gallstones and 190 controls. Body mass index (BMI), fasting plasma leptin, insulin, serum lipid, and lipoprotein levels were measured. Insulin resistance was calculated by homeostasis model assessment (HOMA-IR). Unconditional logistic regression analysis (univariate and multivariate) stratified by BMI was used to calculate the risk of GD.

RESULTS: The multivariate conditional regression analysis revealed a model for those patients with BMI <30. The selected variables in the model were HOMA-IR index with OR = 1.31, P = 0.02 and leptin higher than median with OR = 2.11, P = 0.05. In the stratum of BMI ⩾30, we did not find a useful model.

CONCLUSION: We concluded that insulin resistance and the development of GD appears to be associated with serum leptin levels in subjects with overweight, but not in obese subjects with similar metabolic profiles.

Key words: Obesity; Leptin; Gallstones; Cholesterol; Insulin resistance

Méndez-Sánchez N, Bermejo-Martínez LB, Viñals Y, Chavez-Tapia NC, Graff IV, Ponciano-Rodríguez G, Ramos MH, Uribe M. Serum leptin levels and insulin resistance are associated with gallstone disease in overweight subjects. *World J Gastroenterol* 2005; 11(39): 6182-6187
http://www.wjgnet.com/1007-9327/11/6182.asp

INTRODUCTION

The prevalence of obesity has been increasing progressively worldwide, and is closely associated with the increased morbidity caused by several of the most common diseases in the Western world, including diabetes, hypertension, cardiovascular disease, cancer, and gallstone disease (GD)[1]. Obesity is one of the main risk factors for cholesterol gallstone formation and has been associated with the supersaturation of bile with cholesterol as a result of the increased hepatic secretion of this sterol[2-5].

On the other hand, leptin, the product of the *ob* gene, is an adipose-tissue-derived hormone considered to regulate the limitation of food intake and increased energy expenditure, and thus adiposity[6]. These findings are similar in human beings mainly failure to produce adequate amounts of leptin, or resistance to its central action, which may result in the development of obesity[7].

To identify a link between leptin and the effects of obesity on gallstone formation, Duggirala *et al*.[8], in a previous study explored the role of leptin as an indicator of adiposity and its relation to GD in a Mexican-American population. They reported that leptin levels correlated significantly with the incidence of GD in both sexes, especially in women. Ruhl and Everhart[9] evaluated the possibility that serum leptin levels are better predictors of GD than the body mass index (BMI). They found that leptin concentrations were associated with GD in both sexes (P<0.001), but this association disappeared after controlling BMI and waist-to-hip circumference in both women (P = 0.29) and men (P = 0.65). They concluded that serum leptin concentrations are not better predictors of GD than anthropometry.

Mendez-Sanchez *et al*.[10], demonstrated a significant and positive correlation between plasma leptin levels and biliary cholesterol saturation in a group of obese subjects. This correlation emerged following a modest degree of weight loss. We believe that one additional mechanism with obesity and high risk for GD is serum leptin level and insulin resistance. The aim of the present study was to find whether there is an association between serum leptin levels and the development of GD.

MATERIALS AND METHODS

Populations and sample

This study was carried out at the check-up unit of the Diagnostic Clinic at the Medica Sur Clinic and Foundation. This hospital provides care mainly for middle- and high-income individuals from Mexico City and other metropolitan Mexican areas. The study was approved by the Human Subjects Committee at The Medica Sur Clinic and Foundation as conforming to the ethical guidelines of the 1975 Declaration of Helsinki, and written informed consent was obtained from all participants before entry. A total of 287 subjects were included in this study: 97 cases with gallstones (42 women and 55 men) and 190 controls (79 women and 111 men). Ages were similar in both groups (52.9±11.8 and 52.7±11.7 years). GD cases and controls were a series of consecutive asymptomatic subjects who were referred to the unit by their companies as an annual requirement, but not for symptomatic disease. Abdominal ultrasound was performed on all subjects using a Sonoline Elegra instrument (Siemens Medical System, Germany) with a 3.5 MHz transducer. Ultrasound diagnosis of GD was assessed by the presence of strong intraluminal echoes that were gravity-dependent or attenuated ultrasound transmission (acoustic shadowing). At the completion of each patient's participation in the study, all ultrasonographic studies were evaluated by the same radiologist. No discrepancies were found between the results of the first and second evaluations ($\kappa = 0.93$).

Physical examination

Body weight was measured, in light clothing and without shoes, to the nearest 0.10 kg. Height was measured to the nearest 0.5 cm. BMI was calculated as weight in kilograms divided by height in square meters.

Analytical techniques

Plasma leptin levels were determined by radioimmunoassay using a human leptin RIA kit (Linco Research, St. Charles, MO, USA). Both the intra- and inter-assay coefficients of variation were less than 5%. Insulin levels were measured using an immunoenzymometric assay (MEIA; Abbott Diagnostics), with inter- and intra-assay coefficients of variation less than 3%. Plasma glucose in the fasting state was measured in duplicate with an automated analyzer. The coefficient of variation for a single determination was 1.5%. Cholesterol, HDL-cholesterol, and triglycerides were measured by enzymatic colorimetric methods, using CHOL, HDL-C plus (second generation) and TG assays (Roche Diagnostics Co., Indianapolis, IN, USA). Low-density lipoprotein (LDL) cholesterol concentrations were calculated using the Friedewald formula[11]. Non-HDL cholesterol was calculated as total cholesterol minus HDL cholesterol, as surrogate in cases where LDL cholesterol was inaccurate[12]. Insulin resistance was calculated by means of the homeostasis model assessment (HOMA-IR). HOMA-IR = [fasting insulin (μU/mL) ·fasting glucose (mmol/L)]/22.5, high index of insulin resistance a value >2.5[13].

Statistical analysis

We examined the relationship between anthropometric measures and serum leptin and concentrations by first comparing means of these variables in persons with and without GD. To further study these relations while controlling the effects of covariates related to GD, we used logistic regression for the univariated and multivariated analysis stratifying by BMI (EGRET: Epidemiological Graphics, Estimation, and Testing Package v 1.02.10. Cytel Software Corporation, USA, 1997). Multivariate analyses excluded persons with missing values for any factor were included in the model. The comparison of single frequencies and crossing variables, χ^2 test, *F* exact test, and Mann-Whitney U, and clustering by using SPSS/PC 10.0 program (Chicago, IL, USA, 1999). $P<0.05$ was considered to indicate statistical significance.

RESULTS

We collected information from 97 cases and 190 matched controls (control/patient ratio of 1.96). Cases and their respective controls did not differ in age or lipid values (Table 1). Patients and controls tended to differ in BMI values (28.2 *vs* 27, $P = 0.12$). The index for resistance to insulin (HOMA-IR) was higher among patients than controls (2.9 *vs* 2.4, $P = 0.04$, Table 1).

We stratified subjects according to overweight or obesity, with a BMI value of 30 as the cut-off point, according to World Health Organization[14]. We observed a statistically

Table 1 Comparison of variables between cases and controls

Variable	Cases *n* = 97					Controls *n* = 190					*P*[1]
	Mean	SD	Median	Min	Max	Mean	SD	Median	Min	Max	
Age (yr)	52.1	12.1	51.0	19.0	85.0	50.5	11.7	50.0	18.0	85.0	0.25
BMI (kg/m^2)	28.2	5.5	27.7	18.6	54.9	27.0	3.9	26.9	19.0	40.1	0.12
Leptin (ng/mL)	18.2	44.7	10.2	1.9	431.0	11.0	6.5	9.5	1.3	40.7	0.11
Insulin (μU/mL)	11.1	7.4	9.1	1.8	35.7	9.4	6.3	7.6	2.0	43.7	0.07
T-chol (mmol/L)	5.43	1.09	5.46	2.48	8.38	5.38	1.03	5.4	3.36	9.44	0.95
LDL (mmol/L)	3.44	0.85	3.36	1.11	5.61	3.49	0.85	3.41	1.60	6.13	0.73
HDL (mmol/L)	1.19	0.36	1.14	0.47	2.72	1.22	0.36	1.14	0.52	2.56	0.42
NHDL (mmol/L)	4.27	1.03	4.34	1.78	7.34	4.27	0.98	4.24	2.40	8.53	0.90
TGC (mmol/L)	1.89	1.15	1.70	0.43	6.78	1.71	0.96	1.46	0.06	7.38	0.18
HOMA-IR	2.9	2.2	2.3	0.4	11.7	2.4	1.8	1.8	0.4	13.2	0.04

[1]Mann-Whitney *U* test. BMI, body mass index; T-chol, total cholesterol; LDL, low-density cholesterol; HDL, high-density cholesterol; NHDL, non-HDL cholesterol; TGC, triglycerides.

significant difference in rate between cases and controls according to the tercile distribution in those patients who were not obese (34.7% *vs* 22.9%, $P = 0.04$, Table 2). In the same stratum (BMI<30), cases had a higher prevalence of insulin resistance, according to HOMA-IR, than controls, with borderline statistical significance (40.3% *vs* 27.5%, $P = 0.07$, Table 2). In a multivariate model, adjusted for BMI and insulin levels did not change the association related with leptin levels (data not shown). In the stratum of obese patients (BMI≥30), we observed no statistical differences between control and patient variables, except for hypertriglyceridemia, which had a higher incidence among cases than among controls.

Because of the matched design of the investigation, we analyzed the data under conditional logistic regression analyses. With univariate conditional logistic regression, we observed a higher probability of GD in those patients with BMI <30 according to HOMA-IR index value (OR = 1.33; 95%CI 1.06-1.68, $P = 0.02$) and to both leptin levels (by median or tercile distribution with an OR=2.25; 95%CI 1.08-4.69, $P = 0.03$ and OR = 1.67; 95%CI 1.03-2.69, $P = 0.04$, respectively; Table 3). In the stratum of obese patients, we identified a lower probability of GD associated with high levels of leptin, with both median and tercile distributions (OR = 0.12; 95%CI 0.01-1.0, $P = 0.05$ and OR = 0.14; 95%CI 0.02-0.98, $P = 0.05$, respectively; Table 3). Other variables were not significantly associated.

Multivariate conditional regression analysis (92 cases and 188 controls) identified a correlation for those patients with BMI <30. The selected variables in the model were HOMA-IR with OR = 1.31; 95%CI 1.04-1.66, $P = 0.02$ and

Table 2 Comparison of variables between cases and controls, stratified by BMI

Variable	BMI <30				P^1	BMI ≥30				P^1
	Cases $n = 72$		Controls $n = 153$			Cases $n = 25$		Controls $n = 37$		
	No	%	No	%		No	%	No	%	
Gender (male)	42	58.3	89	58.2	1.0	13	52.0	22	59.5	0.61
Age >50 yr	38	52.8	69	45.1	0.32	13	52.0	21	56.8	0.80
Leptin ≥9.78 ng/mL	37	51.4	61	39.9	0.11	16	64.0	30	81.1	0.15
Leptin					0.04[2]					0.25[2]
$Tercile_1$<7.67 ng/mL	22	30.6	64	41.8		5	20.0	4	10.8	
$Tercile_2$7.6–12.4 ng/mL	25	34.7	54		35.3		7	28.0	9	24.3
$Tercile_3$>12.4 ng/mL	25	34.7	35	22.9		13	52.0	24	64.9	
Insulin≥20 μU/mL	9	12.5	0	0	<0.0001	4	16.0	12	32.4	0.24
HOMA-IR (>2.5)	29	40.3	42	27.5	0.07	15	60.0	24	64.9	0.79
T-chol≥6.21 mmol/L	19	26.4	45	29.4	0.75	6	24.0	6	16.2	0.52
LDL≥4.14 mmol/L[3]	19	27.1	40	26.7	1.0	5	21.7	7	18.9	1.0
HDL<1.03 mmol/L	27	37.5	50	32.7	0.55	8	32.0	13	35.1	1.0
NHDL ≥4.91 mmol/L	20	27.8	43	28.1	1.0	5	20.0	7	18.9	1.0
TGC ≥1.70 mmol/L	32	44.4	62	40.5	0.66	17	68.0	14	37.8	0.04

[1]*F* exact test. [2]χ^2 for linear trend. [3]Five missing values for cases and 2 for controls. BMI, body mass index; T-chol, total cholesterol; LDL, low-density cholesterol; HDL, high density cholesterol; NHDL, non-HDL cholesterol; TGC, triglycerides.

Table 3 Univariated analysis of conditional logistic regression, stratified by BMI

Variable	BMI <30			BMI ≥30		
	OR	95%CI	*P*	OR	95%CI	*P*
Age (yr)	1.20	0.97–1.49	0.09	0.93	0.68–1.26	0.62
Leptin (ng/mL)	1.06	0.99–1.13	0.09	0.91	0.81–1.03	0.15
Insulin (μU/mL)	1.09	1.02–1.16	0.01	0.94	0.86–1.03	0.17
HOMA-IR	1.33	1.06–1.68	0.02	0.85	0.61–1.17	0.32
T-chol (mmol/L)	1.0	0.99–1.00	0.32	1.02	0.99–1.05	0.27
LDL (mmol/L)	1.0	0.99–1.01	0.51	1.01	0.98–1.05	0.39
HDL (mmol/L)	0.99	0.97–1.01	0.44	1.02	0.95–1.09	0.66
NHDL (mmol/L)	1.0	0.99–1.01	0.44	1.02	0.99–1.05	0.30
TGC (mmol/L)	1.0	1.0–1.0	0.86	1.0	1.0–1.01	0.30
Leptin ≥9.78 ng/mL	2.25	1.08–4.69	0.03	0.12	0.01–1.0	0.05
Leptin terciles (ng/mL)	1.67	1.03–2.69	0.04	0.14	0.02–0.98	0.05
Insulin ≥20 μU/mL		Non convergence		0.47	0.12–1.88	0.29
HOMA-IR >2.5	1.46	0.75–2.83	0.27	0.44	0.11–1.84	0.26
T-chol ≥6.21 mmol/L	0.86	0.42–1.74	0.67	3.88	0.38–39.5	0.25
LDL ≥4.14 mmol/L	1.06	0.55–2.04	0.87	1.50	0.36–6.30	0.58
HDL <1.03 mmol/L	1.26	0.66–2.41	0.49		Non convergence	
NHDL ≥4.91mmol/L	1.07	0.54–2.13	0.84	0.78	0.07–8.88	0.84
TGC ≥1.7 mmol/L	1.09	0.60–1.99	0.77	3.03	0.76–12.1	0.12

OR, odds ratio; 95%CI, 95% confidence intervals; BMI, body mass index; T-chol, total cholesterol; LDL, low-density cholesterol; HDL, high density cholesterol; NHDL, non-HDL cholesterol; TGC, triglycerides.

leptin levels higher than the median value, with OR = 2.11; 95%CI 0.99-4.53, $P = 0.05$ (Table 4). In the stratum with BMI ⩾30, we did not identify any useful correlation.

Table 4 Multivariated analysis of conditional logistic regression, stratified by BMI

Variables	BMI <30			BMI ⩾30		
	OR	95%CI	*P*	OR	95%CI	*P*
HOMA-IR	1.31	1.04–1.66	0.02	No model founded		
Leptin ⩾9.78 ng/mL	2.11	0.99–4.53	0.05			

OR, odds ratio; 95%CI, 95% confidence intervals.

DISCUSSION

This study was designed to examine the role of serum leptin levels as a risk factor for developing GD. We observed that plasma leptin levels and the HOMA-IR are highly associated in the group of subjects with BMI <30, because they increase the probability of GD, but that the same plasma leptin levels are associated with a lower probability of GD in the group of subjects with BMI >30.

How can we explain these findings? Bile is the route by which cholesterol is eliminated from the body, and reverse cholesterol transport is the metabolic pathway by which cholesterol is moved from peripheral tissues to the liver for biliary secretion[15,16]. Van Patten *et al.*[17], reported that obesity in leptin-receptor-defective Zucker (*fa/fa*) rats is associated with decreased biliary cholesterol secretion due to the uncoupling of cholesterol and phospholipid from bile-salt secretion. High-dose leptin partially normalized cholesterol secretion in these obese rats without altering lipid composition, implying that both the chronic effects of obesity and a relative resistance to leptin contributed to the impaired biliary cholesterol elimination. From these data, it is clear that leptin plays a role in the elimination of cholesterol from the body.

In the present study, the question arises: Why is BMI important in the association between serum leptin levels and GD, especially in subjects with BMI <30. It has been suggested that in human obesity, leptin levels adapt to changes in energy balance. During fasting[17] or weight loss[18], leptin concentrations decrease, whereas they increase during overfeeding or weight gain. Obese human beings have high leptin concentrations[18]. Leptin mRNA expression in fat cells correlates significantly with body fat mass[18]. Hyperleptinemia is thought to be indicative of "leptin resistance", and may play a role in the pathogenesis of obesity[18,19]. We believe that leptin levels are important risk factors for GD, before "leptin resistance" is apparent, i.e., when the leptin levels are not as high as those observed in obese subjects. In accordance with this hypothesis, Hyogo *et al.*[20], showed that weight loss in chow-fed C57BL/6J *ob/ob* mice induced by chronic intraperitoneal administration of high-dose leptin (10 μg/g per d) is associated with cholesterol gallstone formation.

A 25% reduction in body weight over a 28-d period was sufficient to produce cholesterol crystals and gallstones in the gallbladder bile of all lithogenic-diet-fed mice treated with low-dose leptin. Nevertheless, neither cholesterol crystals nor stones were observed in any chow-fed mouse. These findings indicate that, whereas leptin replacement is required for cholesterol cholelithiasis in *ob/ob* mice, a lithogenic diet accelerates this process[21].

The other variable associated with GD in the present study was the HOMA-IR. Recently, we have found a strong relationship between GD and metabolic syndrome, of which the cardinal feature is hyperinsulinemia[22]. In fact, hyperinsulinemia has been proposed as a risk factor for GD, and some studies support this hypothesis. For example, Scragg *et al.*[23], found that mean fasting insulin levels to be higher in patients of both sexes with GD, independent of age and triglyceride levels. Laakso *et al.*[24], also found that subjects with GD had significantly higher levels of insulin than controls. Haffner *et al.*[25], in the San Antonio Heart Study, observed increasing hyperinsulinemia and a high incidence of GD in both Mexican-Americans and non-Hispanic whites. In Mexico, Gonzalez Villalpando *et al.*[26], found higher fasting insulin levels in women with GD than in controls, but no such relationship was observed in men. Ruhl and Everhart[27], in an well-presented study, have confirmed this association of GD with higher fasting serum insulin and C-peptide levels in women. The association was independent of fasting glucose levels and other covariates related to GD.

Increasing cholesterol saturation of the bile and decreasing gallbladder motility are two possible mechanisms by which insulin plays a role in gallstone formation. At present, these are considered very important in the pathogenesis of gallstones. It has also been suggested that high concentrations of insulin increase the activity of 3-hydroxy-3-methylglutaryl coenzyme A reductase[28,29], the rate-limiting enzyme in hepatic synthesis of new cholesterol, or by activating LDL receptors, resulting in greater hepatic uptake of LDL cholesterol[30]. By inhibiting basal and cholecystokinin-stimulated gallbladder motility, insulin might also increase the risk of developing gallstones through an effect on motility[31].

There are several unresolved issues concerning the biological effects of leptin and its relationship to GD about the importance of motility[32], secretion or both. Tran *et al.*[33,34], included other factors in the link between obesity and gallstone formation, particularly an impaired response to neurotransmitters (mainly neuropeptide Y). The present work shows that there is probably a threshold to the biological activity of leptin, and the differences between our experimental groups indicate that leptin has a "lithogenic effect" in selected overweight subjects. Wauters *et al.*[35], analyzed how polymorphisms in the leptin-receptor gene influence fat topography and levels of abdominal fat in human beings, providing further evidence for the wide response spectrum to several grades of obesity and several grades of leptin-resistance. Similar data on the effects of leptin on lipid metabolism demonstrate differences between sexes and grades of obesity[36], including evidence for the independent effects of leptin on lipid metabolism[37]. These complex data were observed in both healthy subjects and disease models[38,39]. Recently, it was observed that besides fat mass and gender, which are the main determinants of leptin levels in type 2 diabetic and healthy subjects, insulin

secretion and the degree of insulin resistance also contribute significantly to leptin levels[40]. In the present study, there were more insulin-resistant subjects in the BMI >30 group, and these data indicate a correspondence between greater obesity, higher resistance, and a lack of biological effects (in this case GD). This study contribute to show one side of a wide clinical response of a metabolic disturbance, in subjects with similar grade of insulin resistance, but different phenotype (BMI) we observe an unexpected response of leptin effect. However, this is only a hypothesis drawn from the data on the relationship between leptin and insulin resistance[41].

Due to the sample analyzed (mainly employees) we loose randomization effect, and could not reflect general population behavior. By otherwise a lack of metabolic difference between cases and controls (HOMA-IR), could explain contradictory data in obese group; however, this unexpected finding could represent similar leptin response even do differences in body composition.

In conclusion, the results of the present study show that, as with insulin resistance, the development of GD appears to be associated with serum leptin levels in overweight subjects.

ACKOWLEDGEMENTS

The authors thank to Dr. Antonio R. Villa for his kind assistance in the statistical analysis.

REFERENCES

1 **Mantzoros CS.** The role of leptin in human obesity and disease: a review of current evidence. *Ann Intern Med* 1999; **130**: 671-680
2 **Mabee TM,** Meyer P, DenBesten L, Mason EE. The mechanism of increased gallstone formation in obese human subjects. *Surgery* 1976; **79**: 460-468
3 **Reuben A,** Maton PN, Murphy GM, Dowling RH. Bile lipid secretion in obese and non-obese individuals with and without gallstones. *Clin Sci* 1985; **69**: 71-79
4 **Stahlberg D,** Rudling M, Angelin B, Bjorkhem I, Forsell P, Nilsell K, Einarsson K. Hepatic cholesterol metabolism in human obesity. *Hepatology* 1997; **25**: 1447-1450
5 **Bennion LJ,** Grundy SM. Effects of obesity and caloric intake on biliary lipid metabolism in man. *J Clin Invest* 1975; **56**: 996-1011
6 **Rohner-Jeanrenaud F,** Jeanrenaud B. Obesity, leptin, and the brain. *N Engl J Med* 1996; **334**: 324-325
7 **Hickey MS,** Israel RG, Gardiner SN, Considine RV, McCammon MR, Tyndall GL, Houmard JA, Marks RH, Caro JF. Gender differences in serum leptin levels in humans. *Biochem Mol Med* 1996; **59**: 1-6
8 **Duggirala R,** Mitchell BD, Blangero J, Stern MP. Genetic determinants of variation in gallbladder disease in the Mexican-American population. *Genet Epidemiol* 1999; **16**: 191-204
9 **Ruhl CE,** Everhart JE. Relationship of serum leptin concentration and other measures of adiposity with gallbladder disease. *Hepatology* 2001; **34**: 877-883
10 **Mendez-Sanchez N,** Gonzalez V, King-Martinez AC, Sanchez H, Uribe M. Plasma leptin and the cholesterol saturation of bile are correlated in obese women after weight loss. *J Nutr* 2002; **132**: 2195-2198
11 **Friedewald WT,** Levy RI, Fredrickson DS. Estimation of the concentration of low-density lipoprotein cholesterol in plasma, without use of the preparative ultracentrifuge. *Clin Chem* 1972; **18**: 499-502
12 **Packard CJ,** Saito Y. Non-HDL cholesterol as a measure of atherosclerotic risk. *J Atheroscler Thromb* 2004; **11**: 6-14
13 **Matthews DR,** Hosker JP, Rudenski AS, Naylor BA, Treacher DF, Turner RC. Homeostasis model assessment: insulin resistance and beta-cell function from fasting plasma glucose and insulin concentrations in man. *Diabetologia* 1985; **28**: 412-419
14 Obesity : preventing and managing the global epidemic : report of a WHO consultation. Technical report series / World Health Organization, 894. 2000, Geneva: World Health Organization. 253
15 **Fredenrich A,** Bayer P. Reverse cholesterol transport, high density lipoproteins and HDL cholesterol: recent data. *Diabetes Metab* 2003; **29**: 201-205
16 **Rader DJ.** Regulation of reverse cholesterol transport and clinical implications. *Am J Cardiol* 2003; **92**: 42J-49J
17 **Van Patten S,** Ranginani N, Shefer S, Nguyen LB, Rossetti L, Cohen DE. Impaired biliary lipid secretion in obese Zucker rats: leptin promotes hepatic cholesterol clearance. *Am J Physiol Gastrointest Liver Physiol* 2001; **281**: G393-404
18 **Considine RV,** Sinha MK, Heiman ML, Kriauciunas A, Stephens TW, Nyce MR, Ohannesian JP, Marco CC, McKee LJ, Bauer TL, Caro JF. Serum immunoreactive-leptin concentrations in normal-weight and obese humans. *N Engl J Med* 1996; **334**: 292-295
19 **Maffei M,** Halaas J, Ravussin E, Pratley RE, Lee GH, Zhang Y, Fei H, Kim S, Lallone R, Ranganathan S, Kern PA, Friedman JM. Leptin levels in human and rodent: measurement of plasma leptin and ob RNA in obese and weight-reduced subjects. *Nat Med* 1995; **1**: 1155-1161
20 **Hyogo H,** Roy S, Paigen B, Cohen DE. Leptin promotes biliary cholesterol elimination during weight loss in ob/ob mice by regulating the enterohepatic circulation of bile salts. *J Biol Chem* 2002; **277**: 34117-34124
21 **Hyogo H,** Roy S, Cohen DE. Restoration of gallstone susceptibility by leptin in C57BL/6J ob/ob mice. *J Lipid Res* 2003; **44**: 1232-1240
22 **Mendez-Sanchez N,** Chavez-Tapia NC, Motola-Kuba D, Sanchez-Lara K, González V, Ponciano-Rodríguez G, Baptista H, Ramos MH, Uribe M. Metabolic syndrome as a risk factor for gallstone disease. *World J Gastroenterol* 2005; **11**: 1653-1657
23 **Scragg RK,** Calvert GD, Oliver JR. Plasma lipids and insulin in gall stone disease: a case-control study. *Br Med J* 1984; **289**: 521-525
24 **Laakso M,** Suhonen M, Julkunen R, Pyorala K. Plasma insulin, serum lipids and lipoproteins in gall stone disease in non-insulin dependent diabetic subjects: a case control study. *Gut* 1990; **31**: 344-347
25 **Haffner SM,** Diehl AK, Mitchell BD, Stern MP, Hazuda HP. Increased prevalence of clinical gallbladder disease in subjects with non-insulin-dependent diabetes mellitus. *Am J Epidemiol* 1990; **132**: 327-335
26 **Gonzalez Villalpando C,** Rivera Martinez D, Arredondo Perez B, Martinez Diaz S, Gonzalez Villalpando ME, Haffner SM, Stern MP. High prevalence of cholelithiasis in a low income Mexican population: an ultrasonographic survey. *Arch Med Res* 1997; **28**: 543-547
27 **Ruhl CE,** Everhart JE. Association of diabetes, serum insulin, and C-peptide with gallbladder disease. *Hepatology* 2000; **31**: 299-303
28 **Nepokroeff CM,** Lakshmanan MR, Ness GC, Dugan RE, Porter JW. Regulation of the diurnal rhythm of rat liver beta-hydroxy-beta-methylglutaryl coenzmye A reductase activity by insulin, glucagon, cyclic AMP and hydrocortisone. *Arch Biochem Biophys* 1974; **160**: 387-396
29 **Osborne AR,** Pollock VV, Lagor WR, Ness GC. Identification of insulin-responsive regions in the HMG-CoA reductase promoter. *Biochem Biophys Res Commun* 2004; **318**: 814-818
30 **Chait A,** Bierman EL, Albers JJ. Low-density lipoprotein receptor activity in cultured human skin fibroblasts. Mechanism of insulin-induced stimulation. *J Clin Invest* 1979; **64**: 1309-1319
31 **Gielkens HA,** Lam WF, Coenraad M, Frolich M, van Oostayen JA, Lamers CB, Masclee AA. Effect of insulin on basal and

cholecystokinin-stimulated gallbladder motility in humans. *J Hepatol* 1998; **28**: 595-602

32 **Goldblatt MI,** Swartz-Basile DA, Svatek CL, Nakeeb A, Pitt HA. Decreased gallbladder response in leptin-deficient obese mice. *J Gastrointest Surg* 2002; **6**: 438-442

33 **Tran KQ,** Goldblatt MI, Swartz-Basile DA, Svatek C, Nakeeb A, Pitt HA. Diabetes and hyperlipidemia correlate with gallbladder contractility in leptin-related murine obesity. *J Gastrointest Surg* 2003; **7**: 857-862

34 **Tran KQ,** Swartz-Basile DA, Nakeeb A, Pitt HA. Gallbladder motility in agouti-yellow and leptin-resistant obese mice. *J Surg Res* 2003; **113**: 56-61

35 **Wauters M,** Mertens I, Chagnon M, Rankinen T, Considine RV, Chagnon YC, Van Gaal LF, Bouchard C. Polymorphisms in the leptin receptor gene, body composition and fat distribution in overweight and obese women. *Int J Obes Relat Metab Disord* 2001; **25**: 714-720

36 **Tungtrongchitr R,** Pongpaew P, Phonrat B, Tribunyatkul S, Viroonudomphol D, Supawan V, Jintaridhi P, Lertchavanakul A, Vudhivai N, Schelp FP. Serum leptin and lipid profiles in Thai obese and overweight subjects. *Int J Vitam Nutr Res* 2001; **71**: 74-81

37 **Marinari GM,** Scopinaro N, Adami GF. Leptin and HDL-cholesterol in non-diabetic normotensive subjects. *Obes Surg* 2001; **11**: 252-253

38 **Remsberg KE,** Talbott EO, Zborowski JV, Evans RW, McHugh-Pemu K. Evidence for competing effects of body mass, hyperinsulinemia, insulin resistance, and androgens on leptin levels among lean, overweight, and obese women with polycystic ovary syndrome. *Fertil Steril* 2002; **78**: 479-486

39 **Silha JV,** Krsek M, Hana V, Marek J, Jezkova J, Weiss V, Murphy LJ. Perturbations in adiponectin, leptin and resistin levels in acromegaly: lack of correlation with insulin resistance. *Clin Endocrinol* 2003; **58**: 736-742

40 **Wauters M,** Considine RV, Yudkin JS, Peiffer F, De Leeuw I, Van Gaal LF. Leptin levels in type 2 diabetes: associations with measures of insulin resistance and insulin secretion. *Horm Metab Res* 2003; **35**: 92-96

41 **Ceddia RB,** Koistinen HA, Zierath JR, Sweeney G. Analysis of paradoxical observations on the association between leptin and insulin resistance. *Faseb J* 2002; **16**: 1163-1176

Science Editor Guo SY **Language Editor** Elsevier HK

PO Box 2345, Beijing 100023, China
www.wjgnet.com
wjg@wjgnet.com

ELSEVIER

World J Gastroenterol 2005;11(39):6188-6192
World Journal of Gastroenterology ISSN 1007-9327

• *BRIEF REPORTS* •

Treatment of genotype 2 and 3 chronic hepatitis C virus-infected patients

Perdita Wietzke-Braun, Volker Meier, Katrin Neubauer-Saile, Sabine Mihm, Giuliano Ramadori

Perdita Wietzke-Braun, Volker Meier, Katrin Neubauer-Saile, Sabine Mihm, Giuliano Ramadori, Abteilung für Gastroenterologie und Endokrinologie, Georg-August-Universität, Göttingen, Germany
Correspondence to: Professor Dr. Giuliano. Ramadori, Abteilung für Gastroenterologie und Endokrinologie, Georg-August-Universität, Robert-Koch-Strasse 40, 37075 Göttingen, Germany. gramado@med.uni-goettingen.de
Telephone: +49-551-39-6301 Fax: +49-551-39-8596
Received: 2004-12-30 Accepted: 2005-03-21

Abstract

AIM: Before pegylated interferon alpha (IFN) was introduced for the therapy of chronic hepatitis C virus (HCV)-induced hepatitis, conventional thrice weekly IFN therapy was supplemented by ribavirin. Also, at that time, higher and more frequent doses of IFN were expected to be more effective than the standard regimen of 3 MU thrice weekly. As ribavirin significantly increases side effects and negatively influences the quality of life particularly in young patients, we started a prospective non-randomized study with a daily IFN-2a monotherapy as an initial treatment for chronic hepatitis C.

METHODS: Forty-six consecutive chronic HCV-infected patients received 3 MU IFN-2a per day as an initial treatment. Patients with genotype 2 or 3 (n = 12) were treated for 24 wk, and patients with genotypes other than 2 or 3 (n = 34) for 48 wk. Treatment outcome was followed up for 48 wk after the end of treatment (EOT). Virological response was defined as the absence of detectable serum HCV-RNA. Patients without virological response at 12 wk after the start of treatment received low-dose ribavirin (10 mg(kg • d)) additionally.

RESULTS: During treatment, three genotype 3 patients were excluded from the study due to incompliance. The remaining patients (n = 9) infected with genotype 2 or 3 showed an initial virological response rate of 100%. Six patients (66.7%) were still found to be virus-free at the end of follow-up period. In these patients, initial virological response was evident already after 2 wk of treatment. In contrast, initial virological response occurred first after 4 wk of treatment in the three patients who relapsed (33.3%). In comparison, patients infected with genotypes other than 2 or 3 (n = 34) showed an initial virological response rate of only 23.5% (n = 8), and even in combination with ribavirin a sustained virological response (SVR) rate of only 11.8% (n = 4) could be achieved.

CONCLUSION: In chronic HCV-infected patients with genotype 2 or 3, a SVR can be expected after 24 wk of daily dose IFN-2a treatment without ribavirin, if initial virological response develops early. This finding is worth to be confirmed in a prospective randomized study with pegylated IFN.

Key words: Chronic hepatitis C virus infection; Genotype 2 and 3; Alpha interferon; Daily dose interferon therapy

Wietzke-Braun P, Meier V, Neubauer-Saile K, Mihm S, Ramadori G. Treatment of genotype 2 and 3 chronic hepatitis C virus-infected patients. *World J Gastroenterol* 2005; 11 (39): 6188-6192
http://www.wjgnet.com/1007-9327/11/6188.asp

INTRODUCTION

The hepatitis C virus (HCV) is the most common infectious agent associated with post-transfusion and community-acquired non-A-non-B hepatitis as well as cryptogenic cirrhosis[1,2]. Most of the patients with acute HCV infection will develop chronic liver disease[2]. In studies with 10-20 years of follow-up, cirrhosis secondary to chronic HCV infection develops in 20-30%[2,3] and is the most common indication for liver transplantation worldwide[4]. Also, patients with HCV-associated cirrhosis have an increased risk for the development of hepatocellular carcinoma, which is estimated to be between 1% and 4% per year [5].

Even before the discovery of HCV, introduction of interferon alpha (IFN) for the treatment of non-A-non-B hepatitis was an outstanding revolution in antiviral therapy in 1986[6]. Initial therapeutic regimen consisted of 3 MU IFN thrice weekly (TIW) for 6 mo. The response rate at the end of treatment (EOT) resulted in 29-32%[7,8], but the sustained virological response (SVR) rate was only about 6-18%[7-10]. Apart from extending the duration of IFN monotherapy to 12 or 18 mo, higher doses of IFN TIW failed to significantly increase virologic response rates at EOT and SVR rates (range 13-20%) in most studies[7,11,12]. Combination of IFN 3 MU TIW and ribavirin 1 000-1 200 mg/d for 6 mo was shown to increase the response rate at EOT up to 53-57% and SVR rates up to 31-35%[7,12]. With the combination of IFN 3 MU TIW and ribavirin 1 000-1 200 mg/d for 12 mo, the response rates at EOT of 50-54% and SVR rates of 38-47% could be obtained[7,12-14]. However, ribavirin can increase side effects (e.g., hemolysis and renal dysfunction) and has been shown to have teratogenic

and/or embryocidal effects[15]. Many HCV-infected patients are either women at child bearing age or fertile men. Thus, addition of ribavirin to IFN should be avoided when possible. One of the reasons for marginal response to IFN is its short half-life of approximately 8 h[16], which leads to wide fluctuations in IFN plasma concentrations during treatment. Among patients treated with IFN TIW, an intermittent increase in viral load can be observed on treatment-free days[17]. Daily dose IFN therapy might sustain more stable IFN plasma concentrations, thus maintaining a better antiviral effect on HCV. Viral kinetic studies suggest that higher and more frequent doses of IFN may improve the initial response rate and may be more effective in HCV clearance[18,19]. Therefore, we evaluated the efficacy, safety, and tolerability of initial daily IFN monotherapy in naive patients with chronic HCV-infection. This monocentric non-randomized study was started before pegylated IFN was introduced into the market.

MATERIALS AND METHODS

Selection of patients

Patients who were 18 years or older, with compensated chronic HCV infection, not previously treated with IFN or ribavirin were eligible for the study. Eligible patients had persistent elevations of serum alanine aminotransferase (ALT) and/or aspartate aminotransferase (AST) activities for at least 6 mo before the start of treatment, a positive third-generation anti-HCV test using an immunoblot procedure (CHIRON RIBA HCV 3.0 SIA, Ortho Diagnostic Systems Inc., Raritan, USA), and positive serum HCV RNA by reverse transcriptase-polymerase chain reaction (RT-PCR). Patients with decompensated liver disease, serum elevated alpha-fetoprotein concentration, previous organ transplantation, severe cardiac or chronic pulmonary disease, neoplastic disease, seizure disease, hemoglobinopathies, poorly controlled diabetes, severe retinopathy, autoimmune disorders, thyroid gland alterations, active alcohol or injection drug abuse, history of major psychiatric disease, pregnancy, unwillingness to practice contraception, significant anemia (hemoglobin <120 g/L), leukocytopenia (<3 000/μL) or thrombocytopenia (<50 000/μL) were not included. Active hepatitis A virus, human immunodeficiency virus, hepatitis B virus, cytomegalovirus or Ebstein-Barr virus infections were excluded by conventional laboratory tests. Findings consistent with a diagnosis of chronic hepatitis C were shown on liver biopsy during the preceding year, as determined by a single pathologist. The study was approved by the local ethics committee and conformed to the ethical guidelines of the 1975 Declaration of Helsinki. Informed consent was obtained from all treated patients.

Detection of serum HCV-specific RNA by RT-PCR

RNA was extracted from serum samples (140 μL) using the QIAamp Viral RNA Kit (Qiagen, Hilden, Germany) according to the manufacturer's protocol. One-fifth of the extracted material from serum was subjected to a nested RT-PCR procedure essentially as described[20].

Quantification of serum HCV-specific RNA

The amount of serum HCV-RNA was determined by using the AmpliSensor System according to the instruction of the manufacturer (AmpliSensor System, BAG, Lich, Germany).

Determination of HCV genotypes

HCV genotyping was performed using the Innolipa HCV II line probe assay (Innogenetics, Ghent, Belgium).

Treatment

Patients received subcutaneously 3 MU IFN-2a (Roferon-A, F.Hoffmann-La Roche, Basel, Switzerland) daily. Patients with genotype 2 or 3 were treated for 24 wk, and patients with genotypes other than 2 or 3 for 48 wk. Follow-up period was 48 wk after EOT. Virological response was defined as non-detectability of serum HCV-RNA. Patients who had no virological response after 12 wk of treatment received ribavirin (10 mg/kg BW/day) additionally as described previously[21].

Monitoring

All patients were assessed in an outpatient setting for safety, tolerance, and efficacy at the end of weeks 2, 4, 6, 8, and every further 4th wk during treatment. When treatment was completed, patients were assessed at wk 4, 12, and 24, 36 and 48. Clinical examination, total blood cell counts and routine biochemical tests were conducted at that time. Serum was analyzed for the presence of HCV-RNA by RT-PCR before treatment, and at wk 2, 4, 12, 24, 36, and 48 during treatment for patients treated for 48 weeks and at wk 2, 4, 12, and 24 for patients treated 24 wk. During follow-up period, serum was tested for the presence of HCV-RNA at wk 4, 12, 24, 36 and 48.

RESULTS

Characteristics of the patients

Forty-six consecutive chronic HCV-infected patients (16 female, 30 male, mean age 42 years, ranging from 21 to 67 years) were enrolled. The cause for HCV transmission could be identified as blood transfusions in 17.4% (n = 8) and injection drug use in 39.1% (n = 18). Twenty patients (43.5%) had other or unknown transmission of HCV infection. Before treatment, AST levels were elevated with a mean of 27.9 U/L ranging from 12 to 67 U/L, ALT levels with a mean of 51.5 U/L ranging from 16 to 142 U/L, and gamma glutamyl transpeptidase (gamma-GT) levels with a mean of 34.5 U/L ranging from 5 to 288 U/L. HCV genotypes were classified in 12 patients (26%) as 1a, in 20 (43.5%) as 1b, in 1 (2.2%) as 1a and 1b, in 1 (2.2%) as 2a and 2c, in 4 (8.7%) as 3a, in one (2.2%) as 3a and 3c, in 6 (13%) as 3c, and in 1 (2.2%) as 5a. Before treatment, the mean serum HCV-RNA level was 4.87×10^5 copies/mL ranging from 1×10^3 to 6.5×10^6 (SD 1.02×10^6). Patients showed histological diagnosis of mild chronic hepatitis (39.1%, n = 18), moderate chronic hepatitis (37%, n = 17), severe chronic hepatitis (8.7%, n = 4), cirrhosis (8.7%, n = 4), or unknown histology in 6.5% (n = 3). All patients received daily dose IFN-2a therapy as initial treatment.

Outcome of patients with genotype 2 or 3

Patients with genotype 2 or 3 (n = 12) showed an initial

virological response rate of 100% under daily dose IFN-2a treatment. During treatment, however, three genotype 3 patients were excluded from the study due to incompliance. Thus, at that time (two patients after 4 wk and one patient after 12 wk of treatment) the drop outs were virological responders. All patients who completed therapy (n = 9) had a complete biochemical and virological response at the end of 24-wk treatment. During follow-up, after EOT three of nine patients (33.3%) developed a relapse. In these patients, initial virological response first occurred after 4 wk of treatment. The remaining six patients (66.7%) sustainingly eradicated the virus, i.e. serum viral RNA was non-detectable for at least a 48-wk period after EOT. Data of treatment response and follow-up are shown in Figure 1.

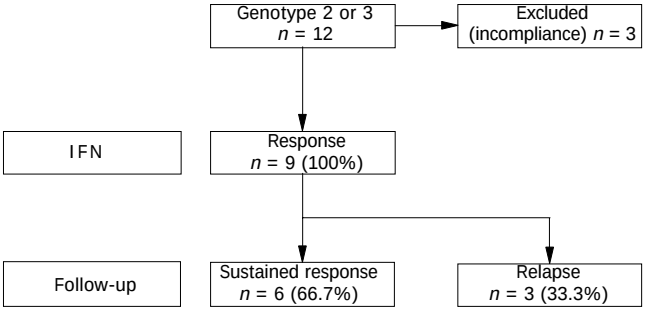

Figure 1 Outcome of 12 HCV-infected patients with genotype 2 or 3 after *the* end of treatment and follow-up. Abbreviations: EOT (end of treatment), IFN (interferon al*pha*).

Outcome of patients with genotypes other than 2 or 3

Patients with genotypes other than 2 or 3 (n = 34) showed an initial virological response rate of 23.5% (8/34) under daily dose IFN-2a treatment. These 8/34 patients (23.5%) were still virological responders at the end of 48 wk daily dose IFN-2a treatment. Two of thirty-four patients (5.9%) stopped IFN therapy due to alopecia (n = 1) and loss of weight (n = 1). During follow-up, five patients (14.7%) who had eliminated the virus at EOT relapsed, and three (8.8%) had a SVR, 48 weeks after EOT.

Twenty-four of thirty-four patients (70.6%) failed to develop an initial virological response under IFN-2a monotherapy and were treated with ribavirin (10 mg/kg BW/day) in combination as described previously[22]. Ten patients (29.4%) showed a response and 13 (38.2%) a non-response at the end of 48-wk treatment. One patient (2.9%) stopped combination therapy due to hemolysis. During follow-up, 9 (26.5%) patients with a response at EOT relapsed and only one (2.9%) patient showed a SVR, 48 weeks after EOT.

Overall outcome

During treatment, three patients with genotype 3 had to be excluded from the study due to incompliance. At the completion of 24- and 48-wk treatment, 27 of 43 patients (62.8%) showed a virological response and 13 of 43 patients (30.2%) showed a virological non-response. In 3 of 43 patients (7%), treatment was discontinued due to alopecia (n = 1) and loss of weight (n = 1) under IFN-2a monotherapy, and due to hemolysis (n = 1) under combination therapy. Forty-eight weeks after the end of 24- and 48-wk treatment, 17 of 27 patients with a response at the end of 24- and 48-wk treatment relapsed (63%). In summary, the overall SVR rate was 23.3% (10 of 43 patients) 48 wk after EOT.

Side effects

Beside the 3/43 (7%) drop outs, daily dose IFN-2a therapy (3 MU) was well tolerated. Monitoring of side effects by questioning and clinical examination revealed flu-like symptoms (e.g. pyrexia, myalgia and rigors) in one quart of cases. Mild leukocytopenia (minimum 1 800/μL) and thrombocytopenia (minimum 70 000/μL in a patient without cirrhosis and 59 000/μL in a patient with cirrhosis) was generally seen.

Side effects of additional ribavirin therapy were thyroid gland alterations (two patients with hypothyroidism and one with hyperthyroidism) and loss of weight (n = 1). Beside the one drop out due to hemolysis (minimum hemoglobin 86 g/L), decrease in hemoglobin was generally seen to a minimum of 98 g/L. There was no need of transfusion or drug dose reduction. All side effects were completely reversible within 1 mo after EOT.

DISCUSSION

In chronic HCV-infected patients, SVR rates range from 6-15% after a 6-mo course of IFN TIW to 13-25% after 12 mo of therapy[11]. One of the reasons for marginal response to IFN is its short half-life of approximately 8 h[16], which leads to wide fluctuations in the plasma concentrations of the drug during treatment period. Among patients treated with IFN TIW, an intermittent increase in viral load can be observed on treatment-free days[17]. In this prospective monocentric non-randomized study, we report our experience on 46 consecutive chronic HCV-infected patients who received 3 MU IFN-2a daily as initial regimen. Patients with genotype 2 or 3 were treated for 24 wk, and patients with genotypes other than 2 and 3 for 48 wk. Three patients with genotype 3 were excluded from the study due to incompliance. At the end of 24-wk treatment, 17/43 (39.5%) of our patients including 9/9 (100%) with genotype 2 or 3 and 8/34 (23.5%) with genotypes other than 2 or 3 eliminated the virus below the limit of detectability. In comparison, IFN 3 MU TIW for 24 wk resulted in virological response rates of 29-32% at EOT[7,8]. The rate of complete responders (23.5%) was unchanged after 48 wk of treatment in our patients with genotypes other than 2 or 3. IFN 3 MU TIW for 48 wk can induce virological response at EOT in 24-33%[7,12] of patients including different genotypes. Also, a dose of IFN 6 MIU TIW for 12 wk followed by IFN 3 MIU TIW for the remaining 36 wk resulted in a complete response rate of 25% at EOT in patients including different genotypes[22].

SVR, 48 wk after EOT resulted in 6/9 (66.7%) of our patients with genotype 2 or 3 after 24 wk 3 MU IFN daily therapy and 3/34 (8.8%) with genotypes other than 2 or 3

after 48 wk 3 MU IFN daily therapy. Compared to our results, IFN 3 MU TIW for 24 wk resulted in SVR in 2% of patients with genotype 1 and in 16% with other genotypes[7]. IFN 3 MU TIW for 48 wk resulted in SVR in 7% of patients with genotype 1 and in 29% with other genotypes[7]. In the trial of Poynard *et al.*[12], a SVR after IFN 3 MU TIW for 48 wk was observed in 33% of patients with genotype 2 and 3 and in 11% with genotype 1, 4, 5, and 6.

Combination of IFN 3 MU TIW with ribavirin at a dosage of 1 000-1 200 mg/d for 24 wk is able to induce response rates at EOT in 53-57%[7,12]. SVR was observed in 18% of patients with genotype 1, 4, 5, or 6[12] and in 16% of patients with genotype 1[7]. Our results are difficult to compare with these results, because we added ribavirin in a lower dose (10 mg/kg BW/day) after 12 wk of daily dose IFN-2a therapy in patients with genotype other than 2 or 3 who were virological non-responders at that time. However, addition of low-dose ribavirin (10 mg/kg BW/day) is able to induce a response at 48-wk EOT in 10/24 (41.7%) initial virological non-responders to a daily dose IFN-2a monotherapy. But SVR 48 wk after EOT is low (1/10 patients), because relapse occurred in the other 9 patients. Therefore, for patients with genotypes other than 2 or 3, this regimen appears not to be sufficient. They need a combination therapy from the beginning on for a longer time or in higher dose.

Nowadays, data on pegylated IFN for treatment of HCV-infected patients are available in the literature[13,14,22]. Interestingly, pegylated IFN-2a monotherapy at a dosage of 180 μg once a week for 48 wk can induce SVR rates of 45% in patients with genotype 2 and 3[22]. Compared to these results, daily dose IFN 3 MU for 24 wk is able to induce 66.7% SVR rates in patients with genotype 2 and 3. These patients with a SVR 48 wk after EOT showed an initial virological response already after 2 wk daily dose IFN-2a monotherapy, whereas patients who relapsed after EOT showed the initial virological response first after 4 wk daily dose IFN-2a treatment. Thus, avoidance of ribavirin in a subgroup of patients with genotype 2 and 3 who showed an initial virological response early after 2 wk of IFN treatment might prevent drug associated adverse events and potential teratogenic effect in patients at child bearing age[15]. This is of particular interest, because the majority of treated patients in our study had a mean age of 42 years and 41-44 years in studies using IFN TIW monotherapy, pegylated IFN monotherapy, and combination with ribavirin[7,12-14,22]. During and 6 mo after the administration of ribavirin, at least two forms of effective contraception are advised[15]. An additional economic fact is the increased cost of ribavirin treatment in HCV patients.

Side effects are comparable with those reported for 3-6 MU TIW IFN therapy[7,12,22]. None of our patients needed dose modification due to adverse event or laboratory abnormality, but in 7% of our patients IFN therapy was discontinued due to alopecia (n = 1) and loss of weight (n = 1), and ribavirin associated hemolysis (n = 1). For comparison of our results, meta-analysis of individual patient data from European centers revealed approximately 10% withdrawal of patients during treatment[23]. In studies with 3-6 MU IFN TIW, discontinuation from therapy ranges from 10% to 14% of patients[7,12,22]. Daily dose IFN therapy does not increase the discontinuation rate in comparison to TIW IFN therapy.

In conclusion, the use of daily dose IFN-2a 3 MU for HCV-infected patients is safe and well tolerated, but is able to induce only similar SVR rates 48 wk after EOT compared to IFN TIW for patients with genotypes other than 2 or 3. Addition of low-dose ribavirin after 12 wk daily dose IFN-2a monotherapy in virological non-responders at that time can increase the initial response at EOT, but relapse rate is high during follow-up. However, in patients with genotype 2 or 3, SVR rates of 66.7% can be achieved (48 wk after EOT with 3 MU IFN-2a monotherapy daily for 24 wk). Thus, our regimen appears to be at least as effective as pegylated IFN-2a for 48 wk[22]. Noteworthy is the finding that the development of a SVR seems to be related to the time of the initial virological response. In all cases, an early initial virological response after 2 wk of IFN treatment was followed by a SVR after 24 wk daily IFN monotherapy without ribavirin. A later initial virological response after 4 wk was associated with a relapse after EOT. In accordance with our results, Bekkering *et al.*[24], retreated 11 non-responders to previous TIW IFN therapy with daily dose IFN and found that all three sustained responders (genotype 3 in two cases and genotype 1a in one case) had undetectable plasma HCV RNA at d 14.

Recently, promising results in patients with genotype 2 and 3 treated with pegylated IFN and ribavirin combination therapy have been published[25,26]. Cornberg *et al.*[25], reduced the duration of combination therapy with standard weight-based dose of ribavirin (1 000-1 200 mg/d) from 48- to 24-wk treatment in patients with genotype 2 and 3. This regimen resulted in a SVR of approximately 85%[25]. In March 2004, Hadziyannis *et al.*[26], published the results of 1 311 patients treated with different regimens of short- and long-term pegylated IFN-2a (24 or 48 wk) in combination with low-dose ribavirin (800 mg/d) or standard weight-based dose of ribavirin (1 000 or 1 200 mg/d). Patients with genotype 2 or 3 were shown to be adequately treated with low-dose ribavirin in combination with pegylated IFN-2a for 24 wk[26]. Furthermore, our data suggest that there is a subgroup of patients with genotype 2 or 3 that can clear the virus with IFN-2a alone. As a result of the introduction of pegylated IFN, daily dosing of IFN has become outdated and in patients with genotype 2 or 3 HCV-infection pegylated IFN should be used as primary treatment for 24 wk with secondary addition of low-dose ribavirin (after 2 wk) only in case of failure of initial virological response 2 wk after initiation of therapy.

REFERENCES

1 **Choo QL,** Kuo G, Weiner AJ, Overby LR, Bradley DW, Houghton M. Isolation of a cDNA clone derived from bloodborne non-A, non-B viral hepatitis genome. *Science* 1989; **244**: 359-362

2 **Hoofnagle JH.** Course and Outcome of hepatitis C. *Hepatology* 2002; **36**: S21-S29

3 **Cohen J.** The Scientific Challenge of Hepatitis C. *Science* 1999; **285**: 26-30

4 **Wietzke-Braun P,** Braun F, Sattler B, Ramadori G, Ringe B. Initial steroid-free immunosuppression after liver transplantation in recipients with hepatitis C virus related cirrhosis. *World J Gastroenterol* 2004; **10**: 2213-2217

5 **Di Bisceglie AM.** Hepatitis C and Hepatocellular Carcinoma. *Hepatology* 1997; **26**: 34S-38S

6 **Hoofnagle JH,** Mullen KD, Jones DB, Rustgi VK, Di Bisceglie A, Hellahan C, Park Y, Meschievitz C, Jones EA. Treatment of chronic non-A, non-B hepatitis with recombinant human alpha interferon: a preliminary report. *N Engl J Med* 1986; **315**: 1575-1578

7 **McHutchison JG,** Gordon S, Schiff ER, Shiffman ML, Lee WM, Rustgi VK, Goodman Z, Ling MH, Cort S, Albrecht JK. Interferon alfa-2b alone or in combination with ribavirin as initial treatment for chronic hepatitis C. *N Engl J Med* 1998; **339**: 1485-1492

8 **Lai MY,** Kao JH, Yang PM, Wang JT, Chen PJ, Chan KW, Chu JS, Chen DS. Long term efficacy of ribavirin plus interferon alfa in the treatment of chronic hepatitis C. *Gastroenterology* 1996; **111**: 1307-1312

9 **Chemello L,** Cavalletto L, Bernardinello E, Guido M, Pontisso P, Alberti A. The effect of interferon alfa and ribavirin combination therapy in naive patients with chronic hepatitis C. *J Hepatology* 1995; **23**: 8-12

10 **Reichard O,** Norkrans G, Fryden A, Braconier JH, Sonnerborg A, Weiland O. Randomized, double-blind, placebo-controlled trial of interferon alpha-2b with and without ribavirin for chronic hepatitis C. *Lancet* 1998; **351**: 83-87

11 **Poynard T,** Leroy V, Cohard M, Thevenot T, Mathurin P, Opolon P, Zarski PJ. Meta-analysis of interferon randomized trials in the treatment of viral hepatitis C: effects of dose and duration. *Hepatology* 1996; **24**: 778-789

12 **Poynard T,** Marcellin P, Lee SS, Niederau C, Minuk GS, Ideo G, Bain V, Heathcote J, Zeuzem S, Trepo C, Albrecht J. Randomized trial of interferon alpha2b plus ribavirin for 48 wk or for 24 wk versus interferon alpha2b plus placebo for 48 wk for treatment of chronic infection with hepatitis C virus. *Lancet* 1998; **352**: 1426-1432

13 **Manns MP,** McHutchison JG, Gordon SC, Rustgi VK, Shiffman M, Reindollar R, Goodman ZD, Konry K, Ling M, Albrecht JK. Peginterferon alfa-2b plus ribavirin compared with interferon alfa-2b plus ribavirin for initial treatment of chronic hepatitis C: a randomised trial. *Lancet* 2001; **358**: 958-965

14 **Fried MW,** Shiffman ML, Reddy KR, Smith C, Marinos G, Goncales FL Jr, Haussinger D, Diago M, Carosi G, Dhumeaux D, Craxi A, Lin A, Hoffman J, Yu J. Peginterferon alfa-2a plus ribavirin for chronic hepatitis C virus infection. *N Engl J Med* 2002; **347**: 975-982

15 **Keating GM,** Curran MP. Peginterferon-α-2a (40 kD) plus ribavirin. A review of its use in the management of chronic hepatitis C. *Drugs* 2003; **63**: 1-29

16 **Wills RJ.** Clinical pharmacokinetics of interferons. *Clin Pharmacokinet* 1990; **19**: 390-399

17 **Lam NP,** Neumann AU, Gretch DR, Wiley TE, Perelson AS, Layden TJ. Dose-dependent acute clearance of hepatitis C genotype 1 virus with interferon alfa. *Hepatology* 1997; **26**: 226-231

18 **Neumann AU,** Lam NP, Dahari H, Gretch DR, Wiley TE, Layden TJ, Perelson AS. Hepatitis C viral dynamics *in vivo* and the antiviral efficacy of interferon alfa therapy. *Science* 1998; **282**: 103-107

19 **Zeuzem S,** Schmidt JM, Lee JH, von Wagner M, Teuber G, Roth WK. Hepatitis C virus dynamics *in vivo*: effect of ribavirin and interferon alfa on viral turnover. *Hepatology* 1998; **29**: 245-252

20 **Mihm S,** Hartmann H, Fayyazi A, Ramadori G. Preferential virological response to interferon-alpha 2a in patients with chronic hepatitis C infected by virus genotype 3a and exhibiting a low gamma-GT/ALT ratio. *Dig Dis Sci* 1996; **41**: 1256-1264

21 **Wietzke-Braun P,** Meier V, Braun F, Ramadori G. Combination of ‚low-dose' ribavirin and interferon alfa-2a therapy followed by interferon alfa-2a monotherapy in chronic HCV-infected non-responders and relapsers after interferon alfa-2a monotherapy. *World J Gastroenterol* 2001; **7**: 222-227

22 **Zeuzem S,** Feinman SV, Rasenack J, Heathcote EJ, Lai MY, Gane E, O'Grady J, Reichen J, Diago M, Lin A, Hoffman J, Brunda MJ. Peginterferon alfa-2a in patients with chronic hepatitis C. *N Engl J Med* 2000; **343**: 1666-1672

23 **Schalm SW,** Hansen BE, Chemello L, Bellobuono A, Brouwer JT, Weiland O, Cavalletto L, Schvarcz R, Ideo G, Alberti A. Ribavirin enhances the efficacy but not the adverse effects of interferon in chronic hepatitis C. *J Hepatol* 1997; **26**: 961-966

24 **Bekkering FC,** Brouwer JT, Leroux-Roels G, van Vlierberghe H, Elewaut A, Schalm SW. Ultrarapid hepatitis C virus clearance by daily high-dose interferon in non-responders to standard therapy. *J Hepatol* 1998; **28**: 960-964

25 **Cornberg M,** Hüppe D, Wiegand J, Felten G, Wedemeyer H, Manns MP. Treatment of chronic Hepatitis C with Peg-Interferon alpha-2b and ribavirin: 24 wk of therapy are sufficient for HCV genotype 2 and 3. *Z Gastroenterol* 2003; **41**: 517-522

26 **Hadziyannis SJ,** Sette H, Morgan TR, Balan V, Diago M, Marcellin P, Ramadori G, Bodenheimer H Jr, Bernstein D, Rizzetto M, Zeuzem S, Pockros PJ, Lin A, Ackrill AM. Peginterferon alpha-2a and ribavirin combination therapy in chronic hepatitis C: a randomized study of treatment duration and ribavirin dose. *Ann Intern Med* 2004; **140**: 346-355

Science Editor Guo SY **Language Editor** Elsevier HK

PO Box 2345, Beijing 100023, China
www.wjgnet.com
wjg@wjgnet.com

ELSEVIER

World J Gastroenterol 2005;11(39):6193-6196
World Journal of Gastroenterology ISSN 1007-9327

• *BRIEF REPORTS* •

Quantitative analysis of plasma HBV DNA for early evaluation of the response to transcatheter arterial embolization for HBV-related hepatocellular carcinoma

Ying-Wen Su, Yu-Wen Huang, Sheng-Hsuan Chen, Chin-Yuan Tzen

Ying-Wen Su, Division of Hematology-Oncology, Department of Internal Medicine, Mackay Memorial Hospital, Taipei, Taiwan, China
Yu-Wen Huang, Department of Medical Research, Mackay Memorial Hospital, Taipei, Taiwan, China
Sheng-Hsuan Chen, Department of Gastroenterology, Taipei Medical University Hospital, Taipei, Taiwan, China
Chin-Yuan Tzen, Department of Medical Research, Department of Pathology, Mackay Memorial Hospital, Taipei, Taiwan, China
Supported by the grant NSC91-2314-B-195-026 from National Science Council, Taiwan, China
Co-first-authors: Ying-Wen Su
Correspondence to: Dr. Chin-Yuan Tzen, MD, PhD, Department of Pathology, Mackay Memorial Hospital, 45 Minsheng Road, Tamshui, Taipei, Taiwan, China. jeffrey@ms2.mmh.org.tw
Telephone: +886-2-28094661-2491 Fax: +886-2-28093385
Received: 2005-03-24 Accepted: 2005-06-02

Abstract

AIM: To assesse changes in plasma HBV DNA after TAE in HBV-related HCC and correlate the levels with the pattern of lipiodol accumulation on CT.

METHODS: Between April and June 2001, 14 patients with HBV-associated HCC who underwent TAE for inoperable or recurrent tumor were studied. Levels of plasma HBV DNA were measured by real-time quantitative PCR daily for five consecutive days after TAE. More than twofold elevation of circulating HBV DNA was considered as a definite elevation. Abdominal CT was performed 1-2 mo after TAE for the measurement of lipiodol retention.

RESULTS: Circulating HBV DNA in 10 out of 13 patients was elevated after TAE, except for one patient whose plasma HBV DNA was undetectable before and after TAE. In group I patients (n = 6), the HBV DNA elevation persisted for more than 2 d, while in group II (n = 7), the HBV DNA elevation only appeared for 1 d or did not reach a definite elevation. There were no significant differences in age or tumor size between the two groups. Patients in group I had significantly better lipiodol retention (79.31±28.79%) on subsequent abdominal CT than group II (18.43±10.61%) (P = 0.02).

CONCLUSION: Patients with durable HBV DNA elevation for more than 2 d correlated with good lipiodol retention measured 1 mo later, while others associated with poor lipiodol retention. Thus, circulating HBV DNA may be an early indicator of the success or failure of TAE.

Key words: Hepatocellular carcinoma; Transcatheter arterial embolization; HBV DNA

Su YW, Huang YW, Chen SH, Tzen CY. Quantitative analysis of plasma HBV DNA for early evaluation of the response to transcatheter arterial embolization for HBV-related hepatocellular carcinoma. *World J Gastroenterol* 2005; 11 (39): 6193-6196

http://www.wjgnet.com/1007-9327/11/6193.asp

INTRODUCTION

In patients with advanced hepatocellular carcinoma (HCC), transcatheter arterial embolization (TAE) has been widely used in Asian countries[1,2]. After TAE, tumor necrosis appears to be complete by 2 d[3]. Circulating plasma DNA is increased after traumatic injury and has been postulated as a prognostic marker for such condition[4]. We wondered if there were other circulating markers that would allow an earlier assessment of response to treatment. Although HCC lacks universal oncogene, HBV is closely linked to HCC. Integrated HBV fragments are frequently detected in the tumors of patients with positive hepatitis B surface antigen (HBsAg)[5]. We therefore studied patients with HBV-related HCC to determine how their circulating plasma and HBV DNA changed after TAE and how those measurements correlated with lipiodol retention on computed tomography (CT).

MATERIALS AND METHODS

Patients

HBsAg-positive patients with advanced HCC between April and June 2001 at the Mackay Memorial Hospital, Taipei, Taiwan were considered for enrollment. Only those who had inoperable tumors that were also not suitable for percutaneous ethanol injection were included. Diagnosis of HCC was made by cytology or by elevated α-fetoprotein (AFP) and typical imaging results (CT and celiac angiography). Patients with contraindications for TAE (such as uncorrectable bleeding disorder, severe thrombocytopenia [platelet count <50 000], a history of radiocontrast allergy, Child's grade C liver cirrhosis, elevated serum creatinine [>2.0 mg/dL], or tumor thrombus in the main portal trunk) were excluded. All patients studied gave informed consent. Patients who could not complete five consecutive days of study were excluded from the final analysis.

TAE through selective hepatic arterial catheterization

was performed via a femoral artery by radiologists at Mackay Memorial Hospital. Under fluoroscopic guidance, 3-10 mL of iodized oil (Laboratoire Guerbet, France) was injected slowly followed by gelatin-sponge pieces (Gelfoam, Johnson and Johnson Med Ltd) and 1 g of cephazolin. Gelfoam was used to activate intravascular thrombosis and cephazolin was used to prevent bacterial infection. After embolization, angiography was performed to determine the extent of vascular occlusion and to assess blood flow in other arteries. After the procedure, patients received intravenous hydration, antiemetic medication, and acetaminophen for pain control. They were discharged from the hospital when oral intake was adequate.

Blood tests and follow-up studies

Blood samples for HBV DNA were taken before TAE and after the procedure every 18-24 h for five consecutive days. Liver function was evaluated before and at 1 wk and 1 mo after TAE to assess the degree of toxicity. Enhanced CT scans of the abdomen using a 10-mm thick slice were performed on a GE HiSpeed scanner (GE Medical Systems) 1-2 mo after TAE. The tumor volume and volume of tumor retaining lipiodol were calculated with GE HiSpeed CT/i system software by reconstructing and viewing the data on a GE Advantage Windows Workstation. The morphologic therapeutic response was assessed by calculation of lipiodol-retaining tumor volume as a percentage whole tumor volume: Percentage of lipiodol retention = (lipiodol-retained lesion volume)/(whole tumor volume)×100%.

Real-time quantitative PCR for HBV DNA

Real-time quantitative PCR analysis was performed on an ABI Prism 7700 Sequence detection system (PE Applied Biosystems) by using SYBR green I as a double-strand DNA-specific binding dye. Briefly, DNA was extracted from a 400 μL plasma sample by using a QIAamp Blood kit (Qiagen Ltd) according to the manufacturer's instruction. The primers for HBV DNA were 184F 5'-GGA CCC CTG CTC GTG TTA CA-3' and 273R 5'-GAG AGA AGT CCA CCM CGA GTC TAG A-3' according to Pas *et al*.[6]. A product of 89 bp from a region of the HBV pre-S gene was amplified. The region was chosen because the pre-S to S open reading frame is generally conserved whereas the core gene is frequently deleted and the X ORF is often truncated[7]. Each reaction mixture contained 5 μL of 10× SYBR Green PCR buffer, 25 mmol/L $MgCl_2$, 200 nmol/L of each deoxynucleoside triphosphate (dATP, dCTP, dTTP, and dGTP), Taq Gold DNA polymerase 0.25 μL, AmpErase uracil *N*-glycosylase (UNG) 0.5 μL, 100 nmol/L of forward and reverse primers and 5 μL of the DNA extract from the plasma sample. The final volume of each PCR reaction mixture was 50 μL. Each sample was assayed in triplicate. Multiple negative water blanks were included in each run as a negative control. Thermal cycling was performed under the following conditions: stage I: at 50 ℃ 2 min, during which UNG could inactivate possible contaminating amplicons, and at 95 ℃ for 10 min, to allow Taq Gold polymerase to activate and inactivate the UNG; stage II: 40 cycles at 95 ℃ for 15 s and 60 ℃ for 1 min, and then stage III: 95 ℃ for 15 s, followed by 60 ℃ for 2 min. After real-time PCR, the amplified products were gradually heated to 95 ℃ for about 20 min. The instrument automatically measured the changing level of fluorescence continuously. This analysis gave the melting temperature. HBV standards were prepared from the serum of two patients with recently reactivated hepatitis B. Amplified PCR products were cloned into pGEM®-T easy vector (Promega Co.) and transformed into JM 109 competent cells. Plasmid DNA was isolated using a plasmid DNA miniprep system (Viogene, USA). Plasmid preparations were quantified spectrophotometrically and standards were prepared by serial dilution from 4×10^1 to 4×10^8 copies/mL.

Data analysis

After amplification, data were captured onto a Macintosh computer, analysis was done with Sequence Detection software (PE Applied Biosystems). Data were collected at the annealing step (60 ℃) of every cycle, and the threshold cycle (Ct) for each sample was calculated by determining the point at which the fluorescence exceeded the threshold limit. A standard curve was calculated automatically by plotting the Ct values against standards of known concentration and calculation of the linear regression line of this curve. Calculation of the correlation coefficient (r^2) was done for each run, using a minimal value of 0.95. Sample copy numbers were calculated by interpolation of the experimentally determined standard curve. In this study, the percent coefficient of variation (%CV) of threshold cycle was 1.25% (range: 0-4.73%) for HBV DNA, similar to that of a previous report 19.

Changes in plasma HBV DNA and statistical analysis

Patient's plasma HBV DNA with twofold elevation was considered as a definite elevation. We classified the changes in plasma HBV DNA into two groups. Group I patients had an elevated HBV DNA level post-TAE for more than 2 d. In group II patients, the HBV DNA elevation only appeared for 1 d or did not reach the definite elevation before d 5. Data were reported as the mean±SD. Clinical characteristics and lipiodol retention of the two groups were compared by using Student *t* test and Fisher test. A P value <0.05 was considered statistically significant.

RESULTS

Fourteen HBsAg seropositive patients with HCC (12 men and 2 women) were studied. The average age was 62 years, ranging between 39 and 81 years. Thirteen had Child Class A and one had Child Class B cirrhosis. Five patients received TAE for the first time and the others were being treated again for recurrent disease. The post-embolization symptoms (fever, abdominal pain, and vomiting) in all patients were mild and subsided within one week. Liver function recovered completely in all patients within one week, and no subsequent liver dysfunction was noted over the course of the study.

Plasma HBV DNA changes after TAE

Except for one patient with undetectable plasma HBV DNA before and after TAE, 10 out of 13 patients had increased plasma HBV DNA after embolization. Six patients had HBV DNA rising for more than 2 d (group I). Among seven

patients in group II, three patients did not reach definite HBV elevation and the other four had temporal HBV DNA elevation within 3 d after TAE. The mean diameter of the embolized tumor in group I was 5.92±3.98 and 5.00±2.20 cm in group II, a non-significant difference (P = 0.61). The lipiodol retention in the embolized tumors in group I was 79.31±28.79% and in group II, 18.43±10.61%, a statistically significant difference (P = 0.02). No significant differences were observed between the two groups regarding age or tumor size (Table 1).

Table 1 Basic characteristics before TAE and lipiodol retention percentage after TAE of group I and group II patients

	Group I (n = 6)	Group II (n = 7)	P
Age, yr (range)	57.6 (39-79)	65.6 (38-81)	0.34
Gender (male/female)	6/0	5/2	-
Pretreatment AFP (ng/mL)	707±1 536	3 024±5 307	0.32
Tumor size (cm)	5.92±3.98	5.00±2.20	0.61
Disease status at entry			-
For the first time TAE (n)	3	2	
For recurrence (n)	3	5	
Lipiodol retention (%)	79.31±28.79	18.43±10.61	0.02[a]

n: patient number. Statistical data are expressed as mean±SD. [a]P<0.05, with statistical significance.

DISCUSSION

Our study showed a significant correlation between durable elevation of plasma HBV DNA concentration after TAE and lipiodol retention one month later. Group I patients with an persistently elevated HBV DNA level apparently sustained more tumor damage after TAE as evidenced by good lipiodol retention, while group II patients with temporary or no elevation in HBV DNA probably had unsuccessful TAE, as indicated by poor lipiodol retention.

The anticancer effects caused by TAE are due to selective blockade of the tumor blood supply. Integrated HBV DNA can be detected in both tumor and nontumor liver tissues of HBV carriers[8]; so the immediate elevation of plasma HBV DNA after TAE might come from damages to the two parts of the same arterial territory. Both integrated HBV DNA and non-integrated episomal HBV DNA are included. Although it has been recently published that HBV may be reactivated by transarterial chemoembolization (TACE), the reported time to reactivation after the last TACE was more than 25 d[9]. In our study, none of our patients had persistently abnormal or deteriorating liver dysfunction after TAE, suggesting that HBV reactivation was not likely to occur within the short period.

With gelfoam embolization, it can produce temporary or permanent occlusion of the targeted artery[10]. From our results, plasma HBV DNA elevated within short-term follow-ups in 10 out of 13 patients. They can be considered as consequences of ischemic injury to liver although the effects may be temporary or persistent. Persistence of HBV DNA in our patients indicates that the occlusion of tumor feeding artery by TAE was complete. It correlated with good lipiodol retention, a factor known to predict a good response. Among patients without persistent elevation of circulating DNA (group II), they tend to have less successful TAE, which may be due to technical or tumor factors (such as incomplete arterial occlusion, presence of collateral blood supply, or tumors with resistance to reperfusion injury)[11-15]. In such patients, other treatment modalities should be considered early to achieve better tumor control.

Monitoring the outcome of TAE is important because it is an important prognostic factor influencing management decisions, such as retreating, incorporation of various non-surgical procedures (e.g., percutaneous ethanol injection, intra-arterial chemotherapy, or local ablation techniques), or deciding to withhold further anti-tumor therapy[16]. In order to evaluate response to TAE, clinicians commonly use tumor regression, AFP levels, and the degree of lipiodol accumulation on CT. All these methods have limitations. Tumor regression is seldom recognized before 4 wks after TAE, and some tumors fail to shrink despite complete necrosis found on pathology of resected lesions[17,18]. Although a good correlation has been found between histologically proven tumor necrosis and reduction in AFP, this correlation has only been demonstrated in patients with a pre-TAE AFP level $\geqslant$200 ng/mL[19]. This marker is therefore of little use in patients who do not have markedly elevated AFP before TAE. The degree of lipiodol retention also correlates well with the degree of necrosis[18]. Compact lipiodol uptake has also been correlated with a better chance of survival than less compact uptake, indicating its usefulness as a post treatment prognostic marker. However, the need to wait 4 wk after treatment for the agent to be cleared from the uninvolved hepatic parenchyma[20] limits its usefulness. In some cases, hepatic washout is particularly slow, making interpretation of the CT image difficult[21].

Recent data indicate that human plasma DNA possesses a short half-life in the circulation[22]. The rapid kinetics suggests that circulating DNA analysis may be useful in monitoring clinical progress. One potential limitation of its clinical application is that serial blood sampling after TAE may be inconvenient for patients. If, as implied by this preliminary study, circulating plasma DNA persistently correlates with lipiodol retention, it may prove to be a useful tool for early evaluation of the response to TAE. If further studies support our findings, circulating levels of HBV DNA after TAE may be an early indicator for which patients require additional treatment.

REFERENCES

1 **Liu CL**, Fan ST. Nonresectional therapies for hepatocellular carcinoma. *Am J Surg* 1997; **173**: 358-365
2 **Acunas B**, Rozanes I. Hepatocellular carcinoma: treatment with transcatheter arterial chemoembolization. *Eur J Radiol* 1999; **32**: 86-89
3 **Yoshida T**, Sakon M, Umeshita K, Kanai T, Miyamoto A, Takeda T, Gotoh M, Nakamura H, Wakasa K, Monden M. Appraisal of transarterial immunoembolization for hepatocellular carcinoma: a clinicopathologic study. *J Clin Gastroenterol* 2001; **32**: 59-65
4 **Lo YM**, Rainer TH, Chan LY, Hjelm NM, Cocks RA. Plasma DNA as a prognostic marker in trauma patients. *Clin Chem* 2000; **46**: 319-323
5 **Lai MY**, Chen DS, Chen PJ, Lee SC, Sheu JC, Huang GT, Wei TC, Lee CS, Yu SC, Hsu HC. Status of hepatitis B virus DNA

in hepatocellular carcinoma: a study based on paired tumor and nontumor liver tissues. *J Med Virol* 1988; **25**: 249-258

6 **Pas SD**, Fries E, De Man RA, Osterhaus AD, Niesters HG. Development of a quantitative real-time detection assay for hepatitis B virus DNA and comparison with two commercial assays. *J Clin Microbiol* 2000; **38**: 2897-2901

7 **Brechot C**. Pathogenesis of hepatitis B virus-related hepatocellular carcinoma: old and new paradigms. *Gastroenterology* 2004; **127**(5 Suppl 1): S56-S61

8 **Shafritz DA**, Shouval D, Sherman HI, Hadziyannis SJ, Kew MC. Integration of hepatitis B virus DNA into the genome of liver cells in chronic liver disease and hepatocellular carcinoma. Studies in percutaneous liver biopsies and post-mortem tissue specimens. *N Engl J Med* 1981; **305**: 1067-1073

9 **Jang JW**, Choi JY, Bae SH, Kim CW, Yoon SK, Cho SH, Yang JM, Ahn BM, Lee CD, LeeYS, Chung KW, Sun HS. Transarterial chemo-lipiodolization can reactivate hepatitis B virus replication in patients with hepatocellular carcinoma. *J Hepatol* 2004; **41**: 427-435

10 **Huang MS**, Lin Q, Jiang ZB, Zhu KS, Guan SH, Li ZR, Shan H. Comparison of long-term effects between intra-arterially delivered ethanol and Gelfoam for the treatment of severe arterioportal shunt in patients with hepatocellular carcinoma. *World J Gastroenterol* 2004; **10**: 825-829

11 **Liou TC**, Shih SC, Kao CR, Chou SY, Lin SC, Wang HY. Pulmonary metastasis of hepatocellular carcinoma associated with transarterial chemoembolization. *J Hepatol* **23**: 563-568

12 **Savastano S**, Miotto D, Casarrubea G, Teso S, Chiesura-Corona M, Feltrin GP. Transcatheter arterial chemoembolization for hepatocellular carcinoma in patients with Child's grade A or B cirrhosis: a multivariate analysis of prognostic factors. *J Clin Gastroenterol* 1999; **28**: 334-340

13 **Sonomura T**, Yamada R, Kishi K, Nishida N, Yang RJ, Sato M. Dependency of tissue necrosis on gelatin sponge particle size after canine hepatic artery embolization. *Cardiovasc Intervent Radiol* 1997; **20**: 50-53

14 **Yamakado K**, Nakatsuka A, Tanaka N, Matsumura K, Takase K, Takeda K. Long-term follow-up arterial chemoembolization combined with transportal ethanol injection used to treat hepatocellular carcinoma. *J Vasc Interv Radiol* 1999; **10**: 641-647

15 **Selzner M**, Rudiger HA, Selzner N, Thomas DW, Clavien PA. Transgenic mice overexpressing human Bcl-2 are resistant to hepatic ischemia and reperfusion. *J Hepatol* 2002; **36**: 218-225

16 **Catalano O**, Esposito M, Lobianco R, Cusati B, Altei F, Siani A. Hepatocellular carcinoma treated with chemoembolization: assessment with contrast-enhanced doppler ultrasonography. *Cardiovasc Intervent Radiol* 1999; **22**: 486-492

17 **Solomon B**, Soulen MC, Baum RA, Haskal ZJ, Shlansky-Goldberg RD, Cope C. Chemoembolization of hepatocellular carcinoma with cisplatin, doxorubicin, mitomycin-C, ethiodol, and polyvinyl alcohol: prospective evaluation of response and survival in a U.S. population. *J Vasc Interv Radiol* 1999; **10**: 793-798

18 **Takayasu K**, Arii S, Matsuo N, Yoshikawa M, Ryu M, Takasaki K, Sato M, Yamanaka N, Shimamura Y, Ohto M. Comparison of CT findings with resected specimens after chemoembolization with iodized oil for hepatocellular carcinoma. *Am J Roentgenol* 2000; **175**: 699-704

19 **Okusaka T**, Okada S, Ueno H, Ikeda M, Yoshimori M, Shimada K, Yamamoto J, Kosuge T, Yamasaki S, Iwata R, Furukawa H, Moriyama N, Sakamoto M, Hirohashi S. Evaluation of the therapeutic effect of transcatheter arterial embolization for hepatocellular carcinoma. *Oncology* 2000; **58**: 293-299

20 **Choi BI**, Kim HC, Han JK, Park JH, Kim YI, Kim ST, Lee HS, Kim CY, Han MC. Therapeutic effect of transcatheter oily chemoembolization therapy for encapsulated nodular hepatocellular carcinoma: CT and pathologic findings. *Radiology* 1992; **182**: 709-713

21 **Lencioni R**, Pinto F, Armillotta N, Di Giulio M, Gaeta P, Di Candio G, Marchi S, Bartolozzi C. Intrahepatic metastatic nodules of hepatocellular carcinoma detected at lipiodol-CT: imaging-pathologic correlation. *Abdom Imaging* 1997; **22**: 253-258

22 **Lo YM**, Zhang J, Leung TN, Lau TK, Chang AM, Hjelm NM. Rapid clearance of fetal DNA from maternal plasma. *Am J Hum Genet* 1999; **64**: 218-224

Science Editor Guo SY **Language Editor** Elsevier HK

PO Box 2345, Beijing 100023, China
www.wjgnet.com
wjg@wjgnet.com

ELSEVIER

World J Gastroenterol 2005;11(39):6197-6201
World Journal of Gastroenterology ISSN 1007-9327

• *BRIEF REPORTS* •

Glutamine-supplemented total parenteral nutrition attenuates plasma interleukin-6 in surgical patients with lower disease severity

Ming-Tsan Lin, Sung-Pao Kung, Sung-Ling Yeh, Koung-Yi Liaw, Ming-Yang Wang, Ming-Liang Kuo, Po-Houng Lee, Wei-Jao Chen

Ming-Tsan Lin, Department of Surgery and Primary Care Medicine, National Taiwan University Hospital and National Taiwan University College of Medicine, Taipei, Taiwan, China
Sung-Pao Kung, Department of Surgery, School of Medicine, National Yang-Ming University, Taipei, Taiwan, China
Sung-Ling Yeh, Institute of Nutrition and Health Sciences, Taipei Medical University, Taipei, Taiwan, China
Koung-Yi Liaw, Ming-Yang Wang, Po-Houng Lee, Wei-Jao Chen, Department of Surgery, National Taiwan University Hospital and National Taiwan University College of Medicine, Taipei, Taiwan, China
Ming-Liang Kuo, Laboratory of Molecular and Cellular Toxicology, Institute of Toxicology, National Taiwan University College of Medicine, Taipei, Taiwan, China
Supported by a Research Grant from the National Science Council, Taipei, Taiwan, No. NSC91-2314-B002-245
Co-correspondents: Sung-Pao Kung
Correspondence to: Wei-Jao Chen, MD, PhD, Department of Surgery, National Taiwan University Hospital, 7 Chung-Shan S. Road, Taipei, Taiwan, China. chenwj@ha.mc.ntu.edu.tw
Telephone: +886-2-23123456-2122 Fax: +886-2-23412969
Received: 2005-02-15 Accepted: 2005-06-09

Abstract

AIM: To evaluate whether the effect of Gln dipeptide-enriched total parenteral nutrition (TPN) on postoperative cytokine alteration depended on the disease severity of surgical patients.

METHODS: Forty-eight patients with major abdominal surgery were allocated to two groups to receive isonitrogenous (0.228 g nitrogen/kg per d) and isocaloric (30 kcal/kg per d) TPN for 6 d. Control group (Conv) using conventional TPN solution received 1.5 g amino acids/kg per day, whereas the test group received 0.972 g amino acids/kg per day and 0.417 g L-alanyl-L-glutamine (Ala-Gln)/kg per day. Blood samples were collected on d 1 and d 6 postoperatively for plasma interleukin (IL)-2, IL-6, IL-8, and interferon (IFN)-γ analysis.

RESULTS: Plasma IL-2 and IFN-γ were not detectable. IL-6 concentrations were significantly lower on the 6th postoperative day in the Ala-Gln group than those in the Conv group in patients with APACHE II≤6, whereas no difference was noted in patients with APACHE II>6. There was no difference in IL-8 levels between the two groups. No difference in cumulative nitrogen balance was observed on d 2-5 after the operation between the two groups (Ala-Gln -3.2±1.6 g *vs* Conv -6.5±2.7 g). A significant inverse correlation was noted between plasma IL-6 levels and cumulative nitrogen balance postoperatively in the Ala-Gln group, whereas no such correlation was observed in the Conv group.

CONCLUSION: TPN supplemented with Gln dipeptide had no effect on plasma IL-8 levels after surgery. However, Gln supplementation had a beneficial effect on decreasing systemic IL-6 production after surgery in patients with low admission illness severity, and lower plasma IL-6 may improve nitrogen balance in patients with abdominal surgery when Gln was administered.

Key words: Glutamine; Total parenteral nutrition; Interleukin-6; Abdominal surgery

Lin MT, Kung SP, Yeh SL, Liaw KY, Wang MY, Kuo ML, Lee PH, Chen WJ. Glutamine-supplemented total parenteral nutrition attenuates plasma interleukin-6 in surgical patients with lower disease severity. *World J Gastroenterol* 2005; 11(39): 6197-6201
http://www.wjgnet.com/1007-9327/11/6197.asp

INTRODUCTION

Glutamine (Gln) is the most abundant amino acid in plasma and in the intracellular free amino acid pool[1]. It is essential for a wide variety of physiologic process, in particular, the growth and function of immune cells including lymphocytes and macrophages[2]. Gln has traditionally been thought as a nonessential amino acid; however, previous reports have shown that Gln depletion occurs in critically injured patients. The extent and duration of Gln depletion are proportional to the severity of illness[3,4]. Laboratory and clinical data suggest that Gln is essential during certain catabolic conditions, such as burns, major surgery, and infection[5-8]. Total parenteral nutrition (TPN) is widely used in the treatment of critically ill patients. Conventional TPN solution does not contain Gln, because Gln is relatively unstable in solution during heat sterilization and long-term storage. Exogenous Gln may be required to satisfy the body's Gln requirement under stressed conditions. Previous studies have shown that TPN supplemented with Gln improved nitrogen balance, enhanced immune response and shortened hospital stay in surgical patients[9-12].

Surgery is known to impair the immune response, and may consequently increase risk of postoperative infection and sepsis[13]. The decrease in the plasma Gln

level following major surgery may contribute to the state of immunosuppression[12,14]. Studies have shown that depressed Gln concentrations were associated with reduced proliferation of lymphocyte in healthy volunteers[14], and Gln depletion may be partly responsible for T cell suppression seen in severely stressed patients[15,16]. In addition to its role in lymphocyte function, Gln may have an indirect effect to mediate a reduction in proinflammatory cytokine release. Parry-Billings *et al*.[3], demonstrated that plasma Gln level was negatively correlated with the production of interleukin (IL)-6 under major surgery. De Beaux *et al*.[17], showed that Gln-supplemented TPN significantly reduced blood mononuclear cell IL-8 release in severe acute pancreatitis patients. A previous report by our laboratory have shown that the effect of Gln administration on improving nitrogen economy was only observed in patients with low, but not high Chronic Health Evaluation (APACHE II) scores[11]. This result indicates that the effect of Gln on attenuating catabolic response may depend on the characteristics and severity of the diseases. We hypothesized that the effect of synthetic Gln supplementation on proinflammatory cytokine release was also associated with the severity of diseases. In this study, we administered a Gln-dipeptide containing TPN to patients postoperatively to investigate the effect of synthetic Gln-dipeptide on cytokine production after surgery. Also, the Gln effect on the severity of stress and cytokine production was evaluated.

MATERIALS AND METHODS

Patients

This was a randomized, double-blind, parallel multicenter clinical trial carried out in National Taiwan University Hospital and Veterans General Hospital, Taipei, Taiwan. This study was performed from August 1999 to May 2000, and was approved by the ethical committee of the two centers. Patients with major metabolic, circulatory, and renal diseases were excluded, and no emergency cases were included. Only major gastrointestinal surgery patients who needed TPN for nutritional support were enrolled. APACHE II score and Therapeutic Intervention Scoring system (TISS) were evaluated after admission[18]. Patients with APACHE II between 2-10 and TISS>10 were included. The informed consent was obtained from each patient before the experiment was performed. A total of 48 patients (28 males and 20 females, age range 40-82 years, mean 66 years) were included. These patients were randomly allocated to either a test group or a control group. The separation of patients into low and high APACHE II groups was post hoc. Since patients with APACHE II score between 2 and 10 were enrolled, we chose the midpoint 6 as the cut-off point to differentiate low- and high-disease severity in this study. Demographic for all patients is summarized in Table 1.

Feeding regimen

The two groups were isonitrogenous and isocaloric. Nitrogen intake was 0.228 g/kg body weight per ds. Caloric intake was 30 kcal/kg per ds. The nonprotein calories were given as dextrose and fat in a ratio of 70:30. Patients of the control group (Conv group, n = 23) were administered a commercially available amino acid solution (Moriamin-SN 10%, Chinese Pharmaceuticals, Taipei, Taiwan). The Conv group received 1.5 g amino acid/kg per day. Patients of the test group (L-alanyl-L-glutamine (Ala-Gln) group, n = 25) received 0.972 g amino acid/kg per day supplemented with 0.417 g/kg per ds Ala-Gln, which provide 0.28 g Gln/kg per day (Dipeptiven, Fresenius Kabi, Bad Homburg, Germany). The Gln containing solutions were prepared by the clinical pharmacist under aseptic condition and adjusted to the weight of each individual patient. The amino acids and dextrose mixture with electrolytes, vitamins, and trace elements were administered through a central venous catheter. Fat emulsion (Lipovenos 20%, Fresenius AG, Germany) was given through a separate canal in the central venous line. Half strength was administered on the 1st d, and full strength was given thereafter for the remaining days. During the experimental period, no enteral nutrition was administered. Neither the patients nor the investigator knew that the applied TPN regimens were with or without Ala-Gln.

Measurements of the plasma parameters and cumulative nitrogen balance

Routine clinical chemistry was measured before and after the surgery. The blood samples were also obtained on postoperative d 1 and on d 6 after TPN administration for analysis of plasma cytokine concentrations. Cytokines including IL-2, IL-6, IL-8, and interferon (IFN)-γ were measured using a commercially available ELISA in microtiter

Table 1 Demographic data of the patients

	Ala-Gln group			Conv group		
	All patients	APACHE ≤6	APACHE >6	All patients	APACHE ≤6	APACHE >6
Age (yr)	66.7±9.0	61.7±11.2	70.1±6.0	67.6±8.4	64.5±7.6	70.6±8.7
Weight (kg)	56.9±9.1	57.7±8.6	56.3±10.1	57.6±10.3	55.3±8.6	59.8±12.0
Height (cm)	157.8±6.4	160.4±6.7	156.0±6.1	160.1±8.3	158.8±8.0	161.3±9.0
Male/female	14/11	4/6	10/5	14/9	6/5	8/4
Diagnosis:						
Gastric Ca	18	6	12	14	6	8
Pancreas Ca	4	3	1	4	2	2
Colon Ca	1	0	1	3	2	1
Hepatoma	1	1	0	1	1	0
Duodenal Ca	0	0	0	1	0	1
Rectal Ca	1	0	1	0	0	0

plates (BioSource International, Camarillo, CA, USA). Antibody specific for human IL-2, IL-6, IL-8, and IFN-γ were coated onto the wells of microtiter stripes provided. Urine and drainage was collected throughout the study, and cumulative nitrogen balance was calculated from postoperative d 2-5 as previously described[11].

Statistics

The data are expressed as mean±SD, repeated measure analysis of variance were used to compare the treatment differences at each day, and *t*-test was used for the difference between the two groups. Pearson's correlation coefficients were used to calculate the linear relationship between plasma IL-6 and cumulative nitrogen balance of the patients. A *P* value <0.05 was considered significant.

RESULTS

Most of the patients had laboratory values within normal range at baseline and on d 6 after the operation despite the patients being administered with Conv or Ala-Gln solution (data not shown). No adverse reactions were found after the Gln-dipeptide containing solution was administered.

Plasma IL-2 and IFN-γ levels were not detectable. Plasma IL-6 concentrations were significantly lower after TPN administration for 6 d, regardless whether the patients were in Conv group or Ala-Gln group. In patients with APACHE II≤6, plasma IL-6 concentrations on the postoperative d 6 in the Ala-Gln group were significantly lower than those in the Conv group. However, there were no differences in IL-6 concentrations between the two groups after infusing TPN for 6 d in patients with APACHE II>6 (Table 2). No significant difference in plasma IL-8 concentrations were observed between the postoperative d 6 and d 1, regardless whether the patients were infused with Ala-Gln or Conv solution. Also, there were no differences in IL-8 levels between the two groups on d 6 and 1 postoperatively (Table 3).

There was no difference in cumulative nitrogen balance on days 2-5 after the operation between the two groups (Ala-Gln -3.2±1.6 g *vs* Conv -6.5±2.7 g). A significant inverse correlation was observed between plasma IL-6 levels on d 6 and cumulative nitrogen balance postoperatively in the Ala-Gln group ($P = 0.027$), whereas no such correlation was noted in the Conv group ($P = 0.919$) (Table 4).

Table 2 Plasma IL-6 concentrations on d 1 postoperatively and on d 6 after TPN administration

	Conv (pg/mL)	Ala-Gln (pg/mL)
All patients	(23)	(25)
D 1[1]	38.8±31.5	52.5±48.7
D 6	12.4±12.1[a]	7.9±5.9[a]
APACHE II≤6	(11)	(10)
D 1	31.2±21.8	37.1±35.4
D 6	11.9±10.5[a]	3.2±1.9[a,b]
APACHE II>6	(12)	(15)
D 1	45.1±41.7	59.8±53.4
D 6	12.9±14.8[a]	16.1±17.2[a]

[1]D 1 represents the data obtained after TPN administration. Figures in parentheses indicate number of patients. [a]P<0.05 *vs* d 1 after Surgery. [b]$P = 0.029$ from Conv group D 6 in APACHE II ≤ 6.

Table 3 Plasma IL-8 concentrations on d 1 postoperatively and on d 6 after TPN administration

	Conv (pg/mL)	Ala-Gln (pg/mL)
All patients	(23)	(25)
D 1[1]	18.9±8.4	37.6±46.1
D 6	28.3±22.4	64.6±62.8
APACHE II≤6	(11)	(10)
D 1	19.4±9.9	15.6±9.0
D 6	36.9±45.9	24.5±8.9
APACHE II>6	(12)	(15)
D 1	18.5±7.3	48.4±52.3
D 6	31.0±30.4	81.3±67.9

[1]D 1 represents the data obtained before TPN administration. Figures in parentheses indicate number of patients.

Table 4 Correlation between plasma IL-6 concentrations and cumulative nitrogen balance postoperatively

	r	*P*
Total patients (38)	–0.2092	0.249
Ala-Gln group (20)	–0.6608	0.027[a]
Conv group (18)	0.033	0.919

[a]P<0.05 using pearson's correlation.

DISCUSSION

In this study, we analyzed plasma IL-2, IL-6, IL-8, and IFN-γ concentrations on postoperative days, because these cytokines are involved in the response to tissue injury[19,20]. IL-2 is produced by mitogen-stimulated T lymphocyte, and was originally isolated as a T-cell growth factor. IFN-γ promotes production of proinflammatory mediator such as IL-1 and TNF-α[19,20]. IL-1β, TNF-α, and IL-6 are major mediators of inflammation and acute phase response. We only measured IL-6 levels, because TNF-α and IL-1 have rarely been detected in the plasma of injured patients[20,21]. In this study, plasma IL-2 and IFN-γ were not detectable either. It is possible that the cytokines are bioactive in biologic fluid at levels well below the range of detectability by current immunoassays[20]. The effect of Gln supplementation on plasma IL-2 and IFN-γ cannot be found in this study.

IL-8 is a chemotactic and activating factor for immune response. Previous reports had shown that plasma IL-8 concentration were much higher in patients with sepsis compared with noninfectious shock, and associated with a fatal outcome[19]. Study by De Beaux *et al*.[17], showed that Gln-supplemented TPN reduces *in vitro* blood mononuclear cell IL-8 release in acute pancreatitis. In this study, no significant differences in plasma IL-8 concentrations were observed between the postoperative d 1 and 6. Also, there were no differences in IL-8 levels between the two groups on postoperative days. This result indicated that Gln administration did not influence the changes of IL-8 in surgical patients. Since IL-8 is associated with clinical,

biochemical, and inflammatory markers of sepsis[22,23], it is compatible to the fact that patients in this study were not complicated with infection, as shown in our previous report[11].

IL-6 is a multifunctional cytokine expressed by a variety of cells. Cruickshank *et al.*[21], reported that systemic response of IL-6 to surgical trauma increased with the severity of surgical insult. Elevation of IL-6 after trauma and elective surgery has been associated with infectious morbidity as well as mortality[24]. Foex and Shelly[25] suggest that IL-6 is a sensitive marker of tissue damage after surgery. In this study, we observed that plasma IL-6 concentrations significantly reduced after TPN administration for 6 d, regardless whether the patients were in Conv group or Ala-Gln group. This result might mean that TPN formula administration attenuated the inflammatory response of the surgical insult. The result also showed that plasma IL-6 levels on postoperative d 6 in the Ala-Gln group were significantly lower than the Conv group in patients with APACHE II$\leqslant$6, but not in patients with higher APACHE II scores. This finding suggests that in patients with lower disease severity, TPN supplemented with Gln had a significant favorable effect on reducing inflammatory response postoperatively. Studies have shown that after operation and trauma, Gln deprivation is observed and the severity of Gln deprivation is proportional to the severity of diseases[3,4]. It is possible that in patients with lower APACHE II score, the demand of Gln is much less than the patients with higher score, and Gln supplementation provides adequate substrate for the function of immune system, and thus reduced the inflammatory response of the surgical insult. Palmer *et al.*[4], showed that TPN supplemented with Gln had no effect on muscle and plasma biochemical changes in critically ill patients. Since this study was a post hoc investigation, whether higher dose of Gln may have beneficial effect on reducing IL-6 concentrations in patients with higher disease severity needs to be clarified.

In this study, we observed a negative correlation between plasma IL-6 and cumulative nitrogen balance postoperatively in the Ala-Gln group, whereas such correlation was not found when data of all patients were pooled and in the Conv group. This finding may indicate that the severity of protein catabolism cannot be predicted by plasma IL-6 level, possibly because the variation of nitrogen loss and plasma IL-6 levels was wide among individual surgical patient. However, Gln administration may consistently improve nitrogen balance and reduced plasma IL-6, and thereby a negative correlation between cumulative nitrogen balance and plasma IL-6 was found. Since nitrogen balance represents a complicated net result of protein catabolism and synthesis in the body, whether Gln play roles in modulating the relationship between IL-6 and protein metabolism required further investigation.

In summary, this study showed that TPN supplemented with Gln dipeptide had no significant influence on plasma IL-8 levels after surgery. However, Gln supplementation had a beneficial effect on decreasing systemic IL-6 production after surgery in patients with low admission illness severity, and lower plasma IL-6 may improve nitrogen balance in patients with abdominal surgery when Gln was administered.

ACKNOWLEDGMENTS

The authors thank Ms. Irene Cheng and Ms. Hui-Jen Huang for their help in collecting data and blood samples. We thank Frensenius AG (Bad Homburg, Germany) for supporting and supplying Gln dipeptide.

REFERENCES

1 **Bergstrom J,** Furst P, Noree LO, Vinnars E. Intracellular free amino acid concentration in human muscle tissue. *J Appl Physiol* 1974; **36**: 693-697
2 **Smith RJ,** Willmore DW. Glutamine nutrition and requirements. *J Parenter Enter Nutr* 1990; **14**: 94S-99S
3 **Parry-Billings M,** Baigrie RJ, Lamont PM, Morris P, Newsholme EA. Effects of major and minor surgery on plasma glutamine and cytokine levels. *Arch Surg* 1992; **127**: 1237-1240
4 **Palmer TEA,** Griffiths RD, Jones C. Effect of parenteral L-glutamine on muscle in the very severely ill. *Nutrition* 1996; **12**: 316-320
5 **Willmore DW,** Shabert JK. Role of glutamine in immunologic responses. *Nutrition* 1998; **14**: 618-626
6 **De-Souza DA,** Greene LJ. Phamacological nutrition after burn injury. *J Nutr* 1998; **128**: 797-803
7 **Quan ZF,** Yang C, Li N, Li JS. Effect of glutamine on change in early postoperative intestinal permeability and its relation to systemic inflammatory response. *World J Gastroenterol* 2004; **10**: 1992-1994
8 **Li JY,** Lu Y, Hu S, Sun D, Yao YM. Preventive effect of glutamine on intestinal barrier dysfunction induced by severe trauma. *World J Gastroenterol* 2002; **8**: 168-171
9 **Jiang ZM,** Cao JD, Zhu XG, Zhao WX, Yu JC, Ma EL, Wang XR, Zhu MW, Shu H, Liu YW. The impact of alanyl-glutamine on clinical safety, nitrogen balance, intestinal permeability, and clinical outcome in postoperative patients: a randomized, double-blind, controlled study of 120 patients. *J Parenter Enter Nutr* 1999; **23**: S62-S66
10 **Morlion BJ,** Stehle P, Wachtler P, Siedhoff HP, Koller M, Konig W, Furst P, Puchstein C. Total parenteral nutrition with glutamine dipeptide after major abdominal surgery. *Ann Surg* 1998; **227**: 302-308
11 **Lin MT,** Kung SP, Yeh SL, Lin C, Lin TH, Chen KH, Liaw KY, Lee PH, Chang KJ, Chen WJ. Glutamine-supplemented total parenteral nutrition on nitrogen economy depends on severity of diseases in surgical patients. *Clin Nutr* 2002; **21**: 213-218
12 **Heberer M,** Babst R, Juretic A, Gross T, Horig H, Harder F, Spagnoli GC. Role of glutamine in the immune response in critical illness. *Nutrition* 1996; **12**: S71-S72
13 **Lennard TW,** Shenton BK, Borzotta A, Donnelly PK, White M, Gerrie LM, Proud G, Taylor RM. The influence of surgical operations on components of human immune system. *Br J Surg* 1985; **72**: 771-776
14 **Parry-Billings M,** Evans J, Calder PC, Newsholme EA. Does glutamine contribute to immunosuppression after major burns? *Lancet* 1990; **336**: 523-525
15 **Rohde T,** Maclean DA, Klarlund Pedersen B. Glutamine, lymphocyte proliferation and cytokine production. *Scand J Immunol* 1996; **44**: 648-650
16 **Yaqoob P,** Calder PC. Glutamine requirement of proliferating T lymphocytes. *Nutrition* 1997; **13**: 646-651
17 **De Beaux AC,** O'riordain MG, Ross JA, Jodozi L, Carter DC, Fearon KC. Glutamine-supplemented total parenteral nutrition reduces blood mononuclear cell interleukin-8 release in severe acute pancreatitis. *Nutrition* 1998; **14**: 261-265
18 **Dellinger EP.** Use of scoring systems to assess patients with surgical sepsis. *Surg Clin North Am* 1988; **68**: 123-145
19 **Ertel W,** Morrison MH, Wang P, Zheng F, Ayala A, Chaudry IH. The complex of cytokines in sepsis. *Ann Surg* 1991; **214**: 141-148

20 **Fong Y,** Moldawer LL, Shires GT, Lowry SF. The biologic characteristics of cytokines and their implication in surgical patients. *Surg Gynecol Obstet* 1990; **170**: 363-378
21 **Cruickshank AM,** Fraser WD, Burns HJG, Van Dame J, Shenkin A. Response of serum interkeulin-6 in patients undergoing elective surgery in varing intensity. *Clin Sci* 1990; **79**: 161-165
22 **Marty C,** Misset B, Tamion F, Fitting C, Carlet J, Cavaillon JM. Circulating interleukin-8 concentrations in patients with multiple organ failure of septic and nonseptic origin. *Crit Care Med* 1994; **22**: 673-679
23 **Baigrie RJ,** Lamont PM, Kwiatkowski D, Dallman MJ, Morris PJ. Systemic cytokine response after major surgery. *Br J Surg* 1992; **79**: 757-760
24 **Biffl WL,** Moore EE, Moore FA, Peterson VM. Interleukin-6 in the injured patient: marker of injury or mediator of inflammation? *Ann Surg* 1996; **224**: 647-664
25 **Foex BA,** Shelly MP. The cytokine response to critical illness. *J Accid Emerg Med* 1996; **13**: 154-162

Science Editor Guo SY **Language Editor** Elsevier HK

PO Box 2345, Beijing 100023, China
www.wjgnet.com
wjg@wjgnet.com

ELSEVIER

World J Gastroenterol 2005;11(39):6202-6207
World Journal of Gastroenterology ISSN 1007-9327

• *BRIEF REPORTS* •

Expression of serine protease SNC19/matriptase and its inhibitor hepatocyte growth factor activator inhibitor type 1 in normal and malignant tissues of gastrointestinal tract

Lei Zeng, Jiang Cao, Xing Zhang

Lei Zeng, First Affiliated Hospital, College of Medicine, Zhejiang University, Hangzhou 310003, Zhejiang Province, China
Jiang Cao, Xing Zhang, Clinical Research Institute, Sir Run Run Shaw Hospital, Zhejiang University, Hangzhou 310016, Zhejiang Province, China
Supported by the National Natural Science Foundation of China, No. 30271450; the Natural Science Foundation of Zhejiang Province, No. 300466
Correspondence to: Dr. Jiang Cao, Clinical Research Institute, Sir Run Run Shaw Hospital, Zhejiang University, 3 East Qingchun Road, Hangzhou 310016, Zhejiang Province, China. caoj@zju.edu.cn
Telephone: +86-571-86006336 Fax: +86-571-86960497
Received: 2005-03-01 Accepted: 2005-04-18

Abstract

AIM: To provide the expression profile of serine protease SNC19/matriptase and its inhibitor hepatocyte growth factor activator inhibitor type 1 (HAI-1) in normal and malignant tissues of gastrointestinal tract at mRNA level for further study on their correlations with tumor progression and metastasis.

METHODS: Total RNAs were prepared from 37 samples of colorectal cancer tissues, 40 samples of gastric cancer tissues, and their adjacent normal tissues. The expression of SNC19/matriptase and HAI-1 in these samples was detected by real-time fluorescent quantitative PCR using glyceraldehyde-3-phosphate dehydrogenase as internal standard, and the clinical significance for the correlation with clinicopathological parameters was evaluated.

RESULTS: In gastric cancer tissues the expression of HAI-1 and SNC19/matriptase was significantly lower than that in the corresponding adjacent normal tissues (Z = -3.280, P = 0.006; Z = -4.651, P = 0.000). HAI-1:SNC19/matriptase ratio showed no difference between normal and malignant tissues (P>0.05). Analysis of clinicopathological parameters showed decreased expression of HAI-1 and HAI-1:SNC19/matriptase ratio associated with stage III/IV gastric tumors as compared to stage I/II ones (Z = -2.140, P = 0.031; Z = -2.155, P = 0.031), and with lymph node-positive gastric cancer tissues as compared to lymph node-negative ones (Z = -2.081, P = 0.036; Z = -2.686, P = 0.006). The expression of SNC19/matriptase had no relationship with stages and lymph node metastasis (P>0.05). The expression of HAI-1 and HAI-1:SNC19/matriptase ratio increased in well-differentiated gastric cancer tissues, but there was no statistical significance (P>0.05). The difference of SNC19/matriptase expression was not significant in gastric cancer tissues of different histological differentiation status (P>0.05). In colorectal cancer tissues, the expression of HAI-1 and SNC19/matriptase was also markedly lower than that in their adjacent normal tissues (Z = -3.100, P = 0.002; Z = -2.731, P = 0.006), whereas HAI-1:SNC19/matriptase ratio showed no difference. Decreased expression of HAI-1 was associated with increased invasive depth and lymph node metastasis, but there was no statistical significance (P>0.05). The difference of SNC19/matriptase expression and HAI-1:SNC19/matriptase ratio was not significant in different stages and different lymph node metastasis status (P>0.05). The expression of SNC19/matriptase, HAI-1 or HAI-1:SNC19/matriptase ratio showed no difference in colorectal cancer tissues of different histological differentiation status (P>0.05).

CONCLUSION: The expressions of SNC19/matriptase and its inhibitor HAI-1 are decreased in gastrointestinal cancer tissues compared to their normal counterparts, and the decreased expression of HAI-1 may correlate with invasion and lymph node metastasis. The possible mechanisms involved need to be further investigated.

Key words: Matriptase; Hepatocyte growth factor activator inhibitor type 1; Expression; Metastasis

Zeng L, Cao J, Zhang X. Expression of serine protease SNC19/matriptase and its inhibitor hepatocyte growth factor activator inhibitor type 1 in normal and malignant tissues of gastrointestinal tract. *World J Gastroenterol* 2005; 11(39): 6202-6207
http://www.wjgnet.com/1007-9327/11/6202.asp

INTRODUCTION

Hepatocyte growth factor (HGF), also known as scatter factor (SF)[1], is a pleiotropic factor which functions as a mitogen, a morphogen, and a motogen for a variety of cells bearing Met receptor tyrosine kinase, particularly for epithelial cells and vascular endothelial cells[2-4]. To date, a significant body of evidence is accumulating in favor of the notion that HGF/SF and Met play an important role in tumorigenesis, invasiveness, differentiation and angiogenesis of tumor cells[5,6]. HGF/SF is secreted by mesenchymal cells as an inactive precursor form, which lacks biological activity. The proteolytic activation of a single-chain precursor

form to a two-chain heterodimeric active form is a critical limiting step in the HGF/SF-induced Met signaling pathway[7]. Five proteases have been supposed to be responsible for the activation of HGF/SF: hepatocyte growth factor activator (HGFA), which exhibits the most potent activity, urokinase-type plasminogen activator (uPA), tissue-type plasminogen activator, blood coagulation factor XIIa[8,9], and SNC19/matriptase[10,11]. SNC19 initially identified from subtractive hybridization screening[12], has been confirmed to be indistinguishable from serine protease matriptase, which was first found in T47-D human breast cancer cells[13]. In addition to activation of HGF/SF, SNC19/matriptase can also degrade extracellular matrix (ECM), and activate another ECM-degrading protease uPA which is involved in tumor invasion[13-15]. SNC19/matriptase contributes to ECM degradation, cellular motility, epithelial migration and turnover, tissue remodeling, and it is supposed to be involved in tumor cell invasion and metastasis[14,16].

Hepatocyte growth factor activator inhibitor type 1 (HAI-1) is a Kunitz-type serine protease inhibitor which was initially purified from the conditioned medium of a human MKN45 stomach carcinoma cell line in 1997[17]. HAI-1 can specifically inhibit serine proteases HGFA and SNC19/matriptase, and they both are activators of HGF/SF[17-19]. Although it is supposed that HAI-1 and SNC19/matriptase may be involved in tumorigenesis, progression, and metastasis[16,20-22], more evidence is needed to draw a definite conclusion. This paper presents new evidence for the expression of HAI-1 and SNC19/matriptase in normal and malignant tissues of gastrointestinal tract at mRNA level, and their correlations with tumor progression and metastasis.

MATERIALS AND METHODS

Patients and tissues

A total of 40 samples from gastric cancer patients (median age, 58.95±12.43 years; range, 29-82 years; 28 men and 12 women) and 37 samples from colorectal cancer patients (median age, 61.64±13.54 years; range, 32-89 years; 13 men and 24 women), after surgical treatment in Second Affiliated Hospital, Zhejiang University College of Medicine, were studied retrospectively. The stage of gastric cancer was classified according to UICC guidelines (1985). Dukes' stage of colorectal cancer was classified according to the diagnosis and treatment criteria for common malignancy in China (1990). Tumor location, tumor histology, and histological grade were determined by pathological examination.

Specimens and RNA preparation

Cancer tissues and their adjacent normal tissues at least 15 cm away from cancer were collected immediately after excision, snap-frozen in liquid nitrogen, and stored at -80 ℃ for RNA extraction. Total RNAs were extracted from the tissue samples by TRIzol reagent (Gibco BRL Co., USA) according to the manufacturer's instructions in 0.1% RNase-free DEPC H_2O. RNA samples were quantified by ultraviolet spectrophotometry (Hewlett-Packard Co., USA).

Primers and probes

Primers and probes used for real-time fluorescent quantitative PCR were designed with the software PrimerExpress (Applied Biosystems Inc., USA). To avoid possible amplification of contaminating genomic DNA, primers were designed, so that each PCR product covered at least one intron. The sequences of primers and probes are listed in Table 1.

Table 1 Sequences of primers and probes

Target gene (amplicon size)		Sequence (5′–3′)
HAI-1	Upstream primer	TGA GGA AGA GCA GCA GTG CC
(151 bp)	Downstream primer	GGC TAC CAC CAC CAC AAT GC
	Probe	*FAM*-CCA GCA CAG GCT CTG TGG AGA TGG C -*TAMRA*
SNC19/ matriptase	Upstream primer	GGG ACA CAC CCA GTA TGG AGG
(168 bp)	Downstream primer	CCG GAA TCA CCC TGG CAG GA
	Probe	*FAM*-TCC TGC AAA AGG GTG AGA TCC GCG -*TAMRA*
GAPDH	Upstream primer	CTT AGC ACC CCT GGC CAA G
(151 bp)	Downstream primer	GAT GTT CTG GAG AGC CCC G
	Probe	*FAM*-CAT GCC ATC ACT GCC ACC CAG AAG A -*TAMRA*

PCR standards

Plasmids containing HAI-1, SNC19/matriptase or glyceraldehyde-3-phosphate dehydrogenase (GAPDH) cDNAs were constructed and maintained in our laboratory. Purified plasmid DNAs were quantified by absorbance at 260 nm and serially diluted as PCR standards.

Real-time RT-PCR

Two micrograms of total RNA was used in a 25 μL reverse transcription reaction system containing oligo $(dT)_{15}$ and M-MLV reverse transcriptase (Promega Co., USA). For real-time PCR, the cDNA samples were brought to a final concentration of 50 mmol/L KCl, 10 mmol/L Tris-HCl (pH 9.0), 1.5 mmol/L $MgCl_2$, 0.1% Triton-X 100, 200 μmol/L dNTPs, 0.2 μmol/L each primer, 0.1 μmol/L probe, and 5 U/μL Taq DNA polymerase (Promega Co., USA). The reactions were carried out under pre-optimized conditions. Samples were amplified with a hold at 95 ℃ for 5 min, followed by 40 cycles of denaturation at 95 ℃ for 20 s, annealing at 60 ℃ for 20 s and extension at 72 ℃ for 20 s in the ABI Prism 7700 sequence detector (Perkin Elmer Co., USA). Serially diluted standard specimens with the concentration of 10^6-10^{10} copies/mL were used to plot the standard curve. No template control and no reverse transcription control were included; 2% agarose gel electrophoresis was used in optimizing procedure.

Statistical analysis

All statistical analyses were done by the SPSS 11.0 software package. Non-parametric data were analyzed with Wilcoxon, Mann-Whitney, and Kruskal-Wallis rank sum tests to evaluate the association between SNC19/matriptase and HAI-1 mRNA expression and clinicopathological parameters. $M(Q_R)$ was computed as summary statistics.

RESULTS

Real-time RT-PCR of SNC19/matriptase and HAI-1

Real-time fluorescent quantitative RT-PCR was performed to determine the expression of SNC19/matriptase and HAI-1 at mRNA level using GAPDH as internal control. Figure 1 shows the detection and plotting of the GAPDH standard curve. The PCR products were subjected to 2% agarose gel electrophoresis in optimized procedure, as shown in Figure 2. The products were specific, with anticipated sizes confirmed by DNA sequencing.

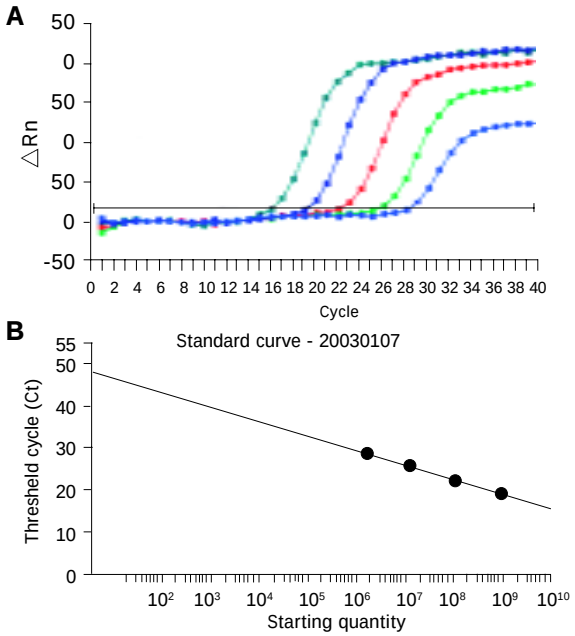

Figure 1 Representative real-time RT-PCR analysis for GAPDH mRNA copy levels. A: Amplification plots of pGEM-T Easy/GAPDH cDNA; B: standard curve plotted against pGEM-T Easy/GAPDH cDNA copy number.

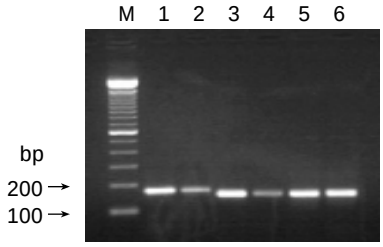

Figure 2 Expression of SNC19/matriptase and HAI-1 in gastric cancer tissue and its corresponding normal tissue (real-time RT-PCR products assay). M: Marker (100-bp DNA ladder); lanes 1 and 2: SNC19/matriptase (168 bp); lanes 3 and 4: HAI-1 (151 bp); lanes 5 and 6: GAPDH (151 bp); lanes 1, 3 and 5: gastric normal tissues; lanes 2, 4, and 6: gastric cancer tissues. Figures in brackets indicate the sizes of real-time RT-PCR products.

Expression of HAI-1 and SNC19/matriptase in normal and malignant tissues of gastrointestinal tract and correlation with clinicopathological parameters

The mRNA copy numbers of HAI-1, SNC19/matriptase and internal control GAPDH in each of normal and malignant tissues of gastrointestinal tract were detected by real-time fluorescent quantitative RT-PCR technique. The ratios of HAI-1:GAPDH and SNC19/matriptase: GAPDH were used as the relative expression level of HAI-1 and SNC19/matriptase, respectively. As shown in Table 2, the expression of HAI-1 and SNC19/matriptase in both gastric and colorectal cancer tissues was markedly lower than that in their adjacent normal tissues ($P<0.01$), while HAI-1:SNC19/matriptase ratio showed no significant difference between normal and malignant tissues of gastrointestinal tract ($P>0.05$).

The correlations between the expression of HAI-1 and SNC19/matriptase and clinicopathological parameters were evaluated (Tables 3 and 4). In gastric cancer tissues (Table 3), decreased expression of HAI-1 and HAI-1: SNC19/matriptase ratio were associated with stage III/IV cancer tissues compared to stage I/II ones ($Z = -2.140$, $P = 0.031$; $Z = -2.155$, $P = 0.031$). The expression of SNC19/matriptase had no relationship with clinical stages ($P>0.05$). The expression of HAI-1 and HAI-1:SNC19/matriptase ratio in lymph node-positive cancer tissues were lower than those in lymph node-negative ones ($Z = -2.081$, $P = 0.036$; $Z = -2.686$, $P = 0.006$). The expression of HAI-1 and HAI-1:SNC19/matriptase ratio increased in well-differentiated gastric cancer tissues, but there was no statistical significance ($P>0.05$). The differences of SNC19/matriptase were not significant in gastric cancer tissues with different histological differentiation status ($P>0.05$). In colorectal cancer tissues, the expression of HAI-1 was lower in Dukes' C/D cancer tissues than in Dukes' B ones. HAI-1 expression in lymph node-positive cancer tissues was lower than that in lymph node-negative ones. Decreased expression of HAI-1 was associated with increased invasive depth and lymph node metastasis, although there was no statistical significance ($P>0.05$). However, the differences of SNC19/matriptase expression and HAI-1:SNC19/matriptase ratio were not significant in different stages and different lymph node metastasis status ($P>0.05$). All the expression of HAI-1 and SNC19/matriptase and their ratio showed no statistical significance in different histological differentiation status ($P>0.05$). In gastrointestinal cancers, the expression of HAI-1 and SNC19/matriptase and HAI-1:SNC19/matriptase ratio showed no difference in patients of different ages, genders, location of tumors, and histological types ($P>0.05$).

Table 2 Expression of HAI-1 and SNC19/matriptase in normal and malignant tissues of gastrointestinal tract [$M(Q_R)$]

	Gastric tissues			Colorectal tissues		
	HAI-1	SNC19	HAI-1:SNC19	HAI-1	SNC19	HAI-1:SNC19
Normal tissues	0.012 (0.021)	0.010 (0.014)	1.420 (1.662)	0.014 (0.022)	0.010 (0.014)	0.971 (1.415)
Malignant tissues	0.005 (0.013)	0.004 (0.005)	1.365 (1.820)	0.009 (0.007)	0.005 (0.005)	1.520 (1.215)
Z	-3.280	-4.651	-0.121	-3.100	-2.731	-0.999
P	0.001	0.000	0.904	0.002	0.006	0.318

Table 3 Correlation between HAI-1 and SNC19/matriptase expression and clinicopathology in gastric cancer tissues [$M(Q_R)$]

	Patients	HAI-1	SNC19	HAI-1:SNC19
Age (yr)				
<40 yr	3	0.005 (0.011)	0.003 (0.002)	1.415 (1.416)
40–60 yr	17	0.005 (0.016)	0.005 (0.006)	1.680 (2.022)
>60 yr	20	0.005 (0.001)	0.003 (0.003)	0.882 (0.144)
Gender				
Men	28	0.005 (0.013)	0.004 (0.004)	1.220 (1.631)
Women	12	0.005 (0.020)	0.003 (0.005)	1.680 (1.571)
Location				
Cardia	7	0.005 (0.004)	0.003 (0.002)	1.430 (0.210)
Body	7	0.007 (0.023)	0.004 (0.005)	2.620 (2.846)
Pylorus	17	0.005 (0.015)	0.005 (0.005)	1.080 (1.631)
Unknown	9	0.005 (0.110)	0.003 (0.004)	1.220 (1.219)
Tumor histology				
Adenocarcinoma	18	0.005 (0.008)	0.004 (0.004)	1.365 (1.442)
Mucoid carcinoma	7	0.005 (0.021)	0.003 (0.008)	1.740 (1.626)
Poorly differentiated carcinoma	11	0.003 (0.016)	0.003 (0.004)	0.882 (2.377)
Unknown	4	0.005 (0.114)	0.005 (0.004)	1.555 (1.386)
N factor				
N0	12	0.017 (0.032)[a]	0.004 (0.005)	2.280 (3.148)[e]
N1/N2	28	0.004 (0.005)	0.004 (0.005)	1.080 (1.489)
UICC stage				
I/II	10	0.017 (0.020)[c]	0.004 (0.005)	2.280 (2.718)[g]
III/IV	30	0.004 (0.007)	0.003 (0.004)	1.245 (1.541)
Histological grade				
Well	3	0.011 (0.008)	0.003 (0.002)	2.870 (1.753)
Moderate	15	0.005 (0.004)	0.004 (0.004)	1.400 (1.121)
Poor	22	0.004 (0.017)	0.003 (0.007)	1.150 (0.470)

[a]P<0.05, [c]P <0.05 *vs* lymph node-positive group (N1/N2); [e]P <0.05, [g]P<0.05 *vs* stage III/IV group.

Table 4 Correlation between HAI-1 and SNC19/matriptase expression and clinicopathology in colorectal cancer tissues [$M(Q_R)$]

	Patients	HAI-1	SNC19	HAI-1:SNC19
Age (yr)				
<40 yr	3	0.004 (0.003)	0.005 (0.002)	0.778 (0.349)
40–60 yr	10	0.007 (0.102)	0.003 (0.003)	0.798 (1.096)
>60 yr	23	0.009 (0.104)	0.005 (0.005)	0.677 (0.459)
Unknown	1			
Gender				
Men	13	0.005 (0.109)	0.005 (0.006)	0.944 (0.728)
Women	24	0.009 (0.100)	0.005 (0.004)	0.667 (0.592)
Location				
Cecum/ascending colon	9	0.009 (0.101)	0.005 (0.006)	0.660 (0.482)
Transverse colon	2	0.003 (0.003)	0.002 (0.002)	0.862 (0.377)
Descending/ sigmoid colon	6	0.010 (0.004)	0.006 (0.002)	0.663 (0.715)
Rectum	19	0.005 (0.009)	0.004 (0.005)	0.778 (1.158)
Unknown	1			
Tumor histology				
Adenocarcinoma	32	0.005 (0.009)	0.004 (0.005)	0.734 (0.788)
Mucoid carcinoma	4	0.009 (0.012)	0.005 (0.004)	0.511 (0.194)
Poorly differentiated carcinoma	1			
N factor				
N0	18	0.010 (0.015)	0.005 (0.009)	1.470 (0.699)
N1/N2	19	0.007 (0.005)	0.005 (0.004)	1.480 (0.980)
Dukes' stage				
A	7	0.011 (0.015)	0.004 (0.008)	1.790 (3.860)
B	10	0.010 (0.016)	0.006 (0.015)	1.290 (1.243)
C/D	20	0.006 (0.006)	0.005 (0.005)	1.385 (0.955)
Histological grade				
Well	8	0.005 (0.010)	0.006 (0.024)	0.891 (1.482)
Moderately	24	0.009 (0.009)	0.004 (0.005)	1.485 (1.250)
Poorly	5	0.009 (0.012)	0.005 (0.005)	1.790 (1.000)

DISCUSSION

The inhibitors of serine proteases are important regulators of enzyme activities. They are classified into at least 10 families[23]. Among them, serpins (serine protease inhibitor) such as Kunitz-type inhibitors are correlated with suppression of tumor invasion[24].

Serine protease SNC19/matriptase is a newly characterized ECM-degrading protease, which may also function as an activator for HGF/SF and other proteases. HAI-1, the cognate Kunitz type inhibitor of SNC19/matriptase, was first found in the stomach carcinoma cell line. Although the expression of HAI-1 has been studied in some types of cancer, the expression profile in normal and malignant gastric tissues is still absent.

As was found in epithelial ovarian cancers that all HAI-1-positive tumors are also SNC19/matriptase positive[16], the imbalance between the protease and the inhibitor may play an important role in the development of tumors. In this study, HAI-1 and SNC19/matriptase showed a remarkable decrease in cancer tissues compared to their adjacent normal tissues in gastrointestinal tract, but the ratio of HAI-1: SNC19/matriptase showed no significant difference between normal and malignant gastrointestinal tissues. Whether the ratio is critical to tumor development or progression needs to be further investigated. Since a novel function of the integral membrane Kunitz-type inhibitor in the regulation of pericellular protease activity has been suggested, HAI-1 may act not only as an inhibitor but also as a reservoir of this enzyme on cell surface[25,26]. With this possibility and other lines of evidence, the situation in cancer may be more complicated. HAI-1 has a strong affinity for both HGFA and SNC19/matriptase to form a protease/inhibitor complex and its specific Kunitz domains are responsible for the inhibitory activity[27]. It was reported that HAI-1 may participate in the activation of SNC19/matriptase through their low-density lipoprotein receptor class A domains interacting with each other, and HAI-1-mediated activation and inhibition of SNC19/ matriptase occur in human mammary epithelial cells[28]. At the same time, HAI-1 not only inhibits the activity of SNC19/matriptase but also prevents it from being hydrolyzed by other proteases[29]. It was reported that decreased immunoreactivity of membrane-form HAI-1 and enhanced ectodomain shedding of HAI-1 are found in colorectal adenocarcinoma cells[30]. There might be a more complicated interaction between HAI-1 and SNC19/matriptase rather than simple activity inhibition. In breast cancer cells, SNC19/matriptase is detected mainly as an uncomplexed form, whereas in human milk a complex containing matriptase and HAI-1 is detectable[18]. The active form of SNC19/matriptase may release from HAI-1 fragment into extracellular milieu, thus playing a role in tumor cells as ectodomain shedding of HAI-1 enhances, which may provide SNC19/matriptase opportunities to actively down-stream biological factors.

HAI-1 expression and HAI-1: SNC19/matriptase ratio decrease in gastric cancer tissues where invasion and lymph node metastasis occur. HAI-1 may play a role in progression and metastasis of gastric cancer by inhibiting HGF. SNC19/ matriptase showed no significant difference in invasive tumors in this study. Lower ratio of HAI-1:SNC19/

matriptase in stage III/IV cancers compared to stage I/II ones may be due to the down-regulated expression of HAI-1. The expression of HAI-1 tends to increase in well-differentiated gastric cancer tissues. It was reported that the expression of HAI-1 increases as the histological grade decreases in hepatocellular carcinoma [31], and decreases in poorly differentiated breast tumors [32]. HAI-1 displays different patterns of expression in different tissues[33].

In colorectal cancer tissues, HAI-1 expression is inverse correlated tumor invasion and lymph node metastasis. In our study, the expression of HAI-1, SNC19/matriptase and their ratio did not show differences in colorectal cancer tissues with different differentiation status, but the expression of HAI-1 seemed to be related to histological grades. Further analysis regarding the patients' age, gender, location, and histological type of tumor showed no correlation with HAI-1 expression.

In conclusion, both SNC19/matriptase and HAI-1 are downregulated in gastrointestinal cancer tissues, and the underlying mechanisms need to be extensively investigated. A larger scale study both in case number and disease spectrum needs to be carried out to elucidate the exact role of SNC19/matriptase and HAI-1 in tumor development and progression.

REFERENCES

1 **Weidner KM,** Arakaki N, Hartmann G, Vandekerckhove J, Weingart S, Rieder H, Fonatsch C, Tsubouchi H, Hishida T, Daikuhara Y. Evidence for the identity of human scatter factor and human hepatocyte growth factor. *Proc Natl Acad Sci USA* 1991; **88**: 7001-7005

2 **Naldini L,** Weidner KM, Vigna E, Gaudino G, Bardelli A, Ponzetto C, Narsimhan RP, Hartmann G, Zarnegar R, Michalopoulos GK. Scatter factor and hepatocyte growth factor are indistinguishable ligands for the MET receptor. *Embo J* 1991; **10**: 2867-2878

3 **Boros P,** Miller CM. Hepatocyte growth factor: a multifunctional cytokine. *Lancet* 1995; **345**: 293-295

4 **Matsumoto K,** Nakamura T. Emerging multipotent aspects of hepatocyte growth factor. *J Biochem* 1996; **119**: 591-600

5 **Bellusci S,** Moens G, Gaudino G, Comoglio P, Nakamura T, Thiery JP, Jouanneau J. Creation of an hepatocyte growth factor/scatter factor autocrine loop in carcinoma cells induces invasive properties associated with increased tumorigenicity. *Oncogene* 1994; **9**: 1091-1099

6 **Nakamura T,** Matsumoto K, Kiritoshi A, Tano Y. Induction of hepatocyte growth factor in fibroblasts by tumor-derived factors affects invasive growth of tumor cells: *in vitro* analysis of tumor-stromal interactions. *Cancer Res* 1997; **57**: 3305-3313

7 **Gak E,** Taylor WG, Chan AM, Rubin JS. Processing of hepatocyte growth factor to the heterodimeric form is required for biological activity. *FEBS Lett* 1992; **311**: 17-21

8 **Shimomura T,** Miyazawa K, Komiyama Y, Hiraoka H, Naka D, Morimoto Y, Kitamura N. Activation of hepatocyte growth factor by two homologous proteases, blood-coagulation factor XIIa and hepatocyte growth factor activator. *Eur J Biochem* 1995; **229**: 257-261

9 **Mars WM,** Zarnegar R, Michalopoulos GK. Activation of hepatocyte growth factor by the plasminogen activators uPA and tPA. *Am J Pathol* 1993; **143**: 949-958

10 **Cao J,** Zheng S, Zheng L, Cai X, Zhang Y, Geng L, Fang Y. A novel serine protease SNC19 associated with human colorectal cancer. *Chin Med J* 2001; **114**: 726-730

11 **Lee SL,** Dickson RB, Lin CY. Activation of hepatocyte growth factor and urokinase/plasminogen activator by matriptase, an epithelial membrane serine protease. *J Biol Chem* 2000; **275**: 36720-36725

12 **Cao J,** Cai X, Zheng L, Geng L, Shi Z, Pao CC, Zheng S. Characterization of colorectal-cancer-related cDNA clones obtained by subtractive hybridization screening. *J Cancer Res Clin Oncol* 1997; **123**: 447-451

13 **Lin CY,** Anders J, Johnson M, Sang QA, Dickson RB. Molecular cloning of cDNA for matriptase, a matrix-degrading serine protease with trypsin-like activity. *J Biol Chem* 1999; **274**: 18231-18236

14 **Satomi S,** Yamasaki Y, Tsuzuki S, Hitomi Y, Iwanaga T, Fushiki T. A role for membrane-type serine protease (MT-SP1) in intestinal epithelial turnover. *Biochem Biophys Res Commun* 2001; **287**: 995-1002

15 **Mignatti P,** Rifkin DB. Biology and biochemistry of proteinases in tumor invasion. *Physiol Rev* 1993; **73**: 161-195

16 **Oberst MD,** Johnson MD, Dickson RB, Lin CY, Singh B, Stewart M, Williams A, al-Nafussi A, Smyth JF, Gabra H, Sellar GC. Expression of the serine protease matriptase and its inhibitor HAI-1 in epithelial ovarian cancer: correlation with clinical outcome and tumor clinicopathological parameters. *Clin Cancer Res* 2002; **8**: 1101-1107

17 **Shimomura T,** Denda K, Kitamura A, Kawaguchi T, Kito M, Kondo J, Kagaya S, Qin L, Takata H, Miyazawa K, Kitamura N. Hepatocyte growth factor activator inhibitor, a novel Kunitz-type serine protease inhibitor. *J Biol Chem* 1997; **272**: 6370-6376

18 **Lin CY,** Anders J, Johnson M, Dickson RB. Purification and characterization of a complex containing matriptase and a Kunitz-type serine protease inhibitor from human milk. *J Biol Chem* 1999; **274**: 18237-18242

19 **Kataoka H,** Miyata S, Uchinokura S, Itoh H. Roles of hepatocyte growth factor (HGF) activator and HGF activator inhibitor in the pericellular activation of HGF/scatter factor. *Cancer Metastasis Rev* 2003; **22**: 223-236

20 **Oberst M,** Anders J, Xie B, Singh B, Ossandon M, Johnson M, Dickson RB, Lin CY. Matriptase and HAI-1 are expressed by normal and malignant epithelial cells *in vitro* and *in vivo*. *Am J Pathol* 2001; **158**: 1301-1311

21 **Johnson MD,** Oberst MD, Lin CY, Dickson RB. Possible role of matriptase in the diagnosis of ovarian cancer. *Expert Rev Mol Diagn* 2003; **3**: 331-338

22 **Kang JY,** Dolled-Filhart M, Ocal IT, Singh B, Lin CY, Dickson RB, Rimm DL, Camp RL. Tissue microarray analysis of hepatocyte growth factor/Met pathway components reveals a role for Met, matriptase, and hepatocyte growth factor activator inhibitor 1 in the progression of node-negative breast cancer. *Cancer Res* 2003; **63**: 1101-1105

23 **Laskowski M Jr,** Kato I. Protein inhibitors of proteinases. *Annu Rev Biochem* 1980; **49**: 593-626

24 **Kobayashi H,** Shinohara H, Takeuchi K, Itoh M, Fujie M, Saitoh M, Terao T. Inhibition of the soluble and the tumor cell receptor-bound plasmin by urinary trypsin inhibitor and subsequent effects on tumor cell invasion and metastasis. *Cancer Res* 1994; **54**: 844-849

25 **Kataoka H,** Shimomura T, Kawaguchi T, Hamasuna R, Itoh H, Kitamura N, Miyazawa K, Koono M. Hepatocyte growth factor activator inhibitor type 1 is a specific cell surface binding protein of hepatocyte growth factor activator (HGFA) and regulates HGFA activity in the pericellular microenvironment. *J Biol Chem* 2000; **275**: 40453-40462

26 **Kataoka H,** Itoh H, Hamasuna R, Meng JY, Koono M. Pericellular activation of hepatocyte growth factor/scatter factor (HGF/SF) in colorectal carcinomas: roles of HGF activator (HGFA) and HGFA inhibitor type 1 (HAI-1). *Hum Cell* 2001; **14**: 83-93

27 **Denda K,** Shimomura T, Kawaguchi T, Miyazawa K, Kitamura N. Functional characterization of Kunitz domains in hepatocyte growth factor activator inhibitor type 1. *J Biol Chem* 2002; **277**: 14053-14059

28 **Lee MS,** Kiyomiya KI, Benaud C, Dickson RB, Lin CY. Simultaneous activation and HAI-1-mediated inhibition of matriptase induced at activation foci in human mammary epithelial cells. *Am J Physiol Cell Physiol* 2004; **288**: C932-C941
29 **Oberst MD,** Williams CA, Dickson RB, Johnson MD, Lin CY. The activation of matriptase requires its noncatalytic domains, serine protease domain, and its cognate inhibitor. *J Biol Chem* 2003; **278**: 26773-26779
30 **Nagaike K,** Kohama K, Uchiyama S, Tanaka H, Chijiiwa K, Itoh H, Kataoka H. Paradoxically enhanced immunoreactivity of hepatocyte growth factor activator inhibitor type 1 (HAI-1) in cancer cells at the invasion front. *Cancer Sci* 2004; **95**: 728-735
31 **Nagata K,** Hirono S, Ido A, Kataoka H, Moriuchi A, Shimomura T, Hori T, Hayashi K, Koono M, Kitamura N, Tsubouchi H. Expression of hepatocyte growth factor activator and hepatocyte growth factor activator inhibitor type 1 in human hepatocellular carcinoma. *Biochem Biophys Res Commun* 2001; **289**: 205-211
32 **Parr C,** Watkins G, Mansel RE, Jiang WG. The hepatocyte growth factor regulatory factors in human breast cancer. *Clin Cancer Res* 2004; **10**: 202-211
33 **Parr C,** Jiang WG. Expression of hepatocyte growth factor/scatter factor, its activator, inhibitors and the c-Met receptor in human cancer cells. *Int J Oncol* 2001; **19**: 857-863

Science Editor Wang XL and Guo SY **Language Editor** Elsevier HK

PO Box 2345, Beijing 100023, China
www.wjgnet.com
wjg@wjgnet.com

ELSEVIER

World J Gastroenterol 2005;11(39):6208-6211
World Journal of Gastroenterology ISSN 1007-9327

• *BRIEF REPORTS* •

Microcirculation disturbance affects rats with acute severe pancreatitis following lung injury

Xue-Min Liu, Qing-Guang Liu, Jun Xu, Cheng-En Pan

Xue-Min Liu, Qing-Guang Liu, Jun Xu, Cheng-En Pan, Department of Hepatobiliary Surgery, Xi'an Jiaotong University First Hospital, Xi'an 710061, Shaanxi Province, China
Supported by the National Natural Science Foundation of China, No. 30371398
Correspondence to: Dr. Xue-Min Liu, Department of Hepatobiliary Surgery, Xi'an Jiaotong University First Hospital, Xi'an 710061, Shaanxi Province, China. a1090224@pub.xaonline.com
Telephone: +86-29-85324009
Received: 2004-02-28 Accepted: 2004-04-05

Abstract

AIM: To study the effects of microcirculation disturbance (MD) on rats with acute severe pancreatitis (ASP).

METHODS: We developed ASP rat models, and anatomized separately after 1, 3, 5, 7, and 9 h. We took out blood and did hemorrheologic examination and erythrocyte osmotic fragility test, checked up the water content, capillary permeability, and genetic expression of intercellular adhesion molecule-1 (ICAM-1) in lung tissues, examined the apoptosis degree of blood vessel endothelium while we tested related gene expression of Bax and Bcl-2 in lung tissues. We did the same examination in control group.

RESULTS: The viscosity of total blood and plasma, the hematocrit, and the erythrocyte osmotic fragility were all increased. Fibrinogen was decreased. The water content in lung tissues and capillary permeability were increased. Apoptosis degree of blood vessel endothelium was increased too. ICAM-1 genetic expression moved up after 1 h and reached its peak value after 9 h.

CONCLUSION: MD plays an important role in ASP following acute lung injury (ALI). The functional damage of blood vessel endothelium, the apoptosis of capillary vessel endothelium, WBC edging-concentration and the increasing of erythrocyte fragility are the main reasons of ALI.

Key words: Microcirculation; Acute pancreatitis; Lung injury

Liu XM, Liu QG, Xu J, Pan CE. Microcirculation disturbance affects rats with acute severe pancreatitis following lung injury. *World J Gastroenterol* 2005; 11(39): 6208-6211
http://www.wjgnet.com/1007-9327/11/6208.asp

INTRODUCTION

Microcirculation change has a great effect on causing diseases and acute severe pancreatitis (ASP) process. The lung can be damaged easily[1]. About 70% of deaths are due to acute respiratory distress syndrome[2,3]. In this study, we observed the microcirculation in rats and the changes in lung. The relationship between acute lung injury (ALI) and microcirculation change in rats with ASP was studied.

MATERIALS AND METHODS

Experimental animals and grouping

Rats were provided by the Experimental Animal Center of Medical School of Xi'an Jiaotong University. Experiment group (40 rats) was injected with 4% sodium taurocholate 1 mL/kg by puncturing pancreatic duct to make ASP models. Control group (eight rats) was only turned over duodenum. Experiment group was divided into five subgroups, eight rats in each group. They were anatomized after 1, 3, 5, 7, and 9 h, respectively.

Hemorrheologic examination and erythrocyte osmotic fragility test

Blood sedimentation (BS) was done with 0.2 mL venous blood. After centrifugation, hematocrit was read. The content of fibrinogens (CB) was recorded after water bath and centrifugation. The viscosity of total blood (VTB) and plasma (VP) was checked up in another 1-2 mL venous blood. The resistance of RBC to different concentrations of hypo-osmotic saline was examined. The permeability fragility of RBC was detected.

TUNEL examination

Lung tissues were fixed and sliced. Apoptosis staining experiment was done. We observed the change of lung capillary vessel endothelium apoptosis under a light microscope. The cells with brown-blue nuclei were considered as apoptosis cells.

Lung Bcl-2 and Bax protein examination with immunohistochemical method

The cells stained brown or brown-yellow were positively stained cells. To account the positive staining, we counted four high-power fields according to the formula: positive rate = the number of positive cells/total number of cells×100%. It was determined as negative staining (-) when the positive rate was <15%, and as positive staining when the positive rate was 15-50% (+), 50-75% (++), and >75% (+++), respectively.

Lung capillary permeability

The change of lung capillary permeability was detected by injecting Evan's blue into veins. Using a 625-nm spectrophotometer, the concentration of Evan's blue represented the milligrams of the dyes per gram of wet weight lung.

Water content in lung tissue

First, we weighed the wet weight of lung tissues, and after being parched for 72 h at 70 ℃, we weighed the dry weight. The water content (%) = (wet weight-dry weight)/wet weight.

RT-PCR examination of ICAM-1

We took β-actin as an inner contrast gene. Lung RNA was isolated by TRIzol. Oligo(dT)$_{15}$ was used as a primer. The reaction conditions were at 42 ℃ for 15 min, at 99 ℃ for 5 min, at 4 ℃ for 4 min, and then we got the first chain of cDNA. PCR was done for 1 min at 94 ℃, for 1 min at 55 ℃, for 2 min at 72 ℃, 35 circles in all. Finally, it was expanded for 10 min at 72 ℃. After electrophoresis, we confirmed the quantity with a white/ultraviolet transilluminator. The expanding quantity of targeted genes/the expanding quantity of inner contrast genes expressed the quantity of detected genes.

Statistical analysis

The data were expressed as mean±SD. Kruskal-Wallis method and Mann-Whitney method were adopted to compare the two indexes.

RESULTS

Pathological observation of lung tissues

We observed the pathological change of lung tissues and found that interstitial pulmonary edema, focal and congestive pulmonary atelectasis were present at the forepart of ASP. PMNs were present in capillaries, and thrombosis was visible in capillaries (Figure 1). The changes aggravated gradually.

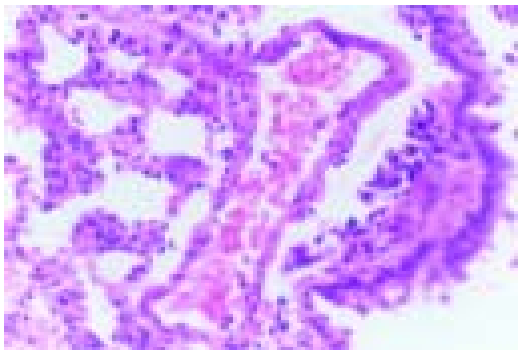

Figure 1 Interstitial pulmonary edema, infiltration of PMNs, and thrombosis in capillaries in lung, HE staining, ×20.

Apoptosis of capillary endothelium in lung

Apoptosis endothelium could be examined in lungs of control group. After the models were made, the number of apoptosis endothelial cells was increased. When we compared the number of apoptosis cells at 3 h with that at 9 h, we found that the number of apoptosis endothelial cells at 9 h was greater than that at 3 h. This trend was related to the grade of ALI.

Lung Bcl-2 and Bax protein expression

Bcl-2 and Bax protein were less expressed in normal lung tissues. After ASP models were made, we found that Bcl-2 and Bax protein expression was obvious. Bax protein expression accorded with the changes of cell apoptosis, and reached its peak in 7-9 h. Bcl-2 expression was inversely correlated with the changes of cell apoptosis, and declined gradually after 3 h (Table 1).

Table 1 Positive staining rate of Bcl-2 and Bax in each period of time (%, mean±SD, n = 8)

	1 h	3 h	5 h	7 h	9 h
Bcl-2[a]	37.3±4.3	84.6±4.3	67.4±2.1	70.3±4.2	52.3±5.3
Bax[a]	42.3±4.4	62.6±4.8	68.2±3.3	77.6±4.2	79.3±5.7

[a]P<0.05 *vs* each period of time.

ICMA-1 and RT-PCR examination

The genetic expression of intercellular adhesion molecule-1 (ICAM-1) in lung tissues was increased after 1 h and reached its peak after 9 h. The gene expressions of ICAM-1 were significantly different in each period of time (P<0.05, Figure 2).

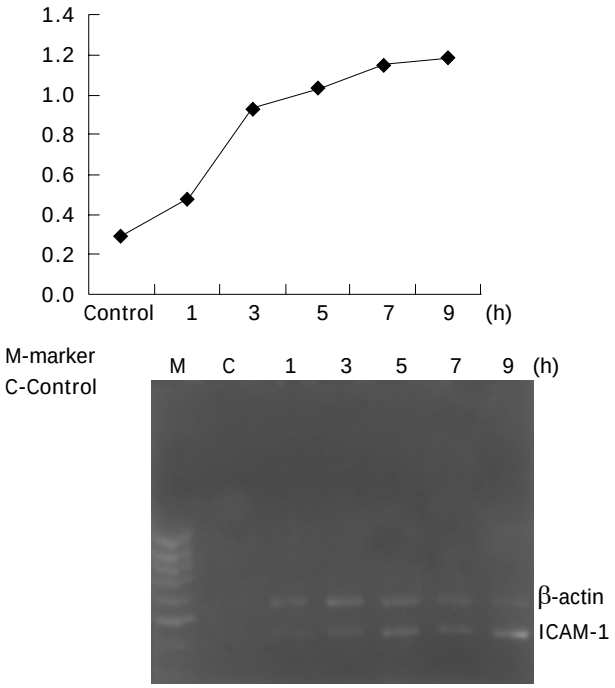

Figure 2 ICAM-1 genetic expression in different periods of time. The genetic expression of ICAM-1 in lung tissues was increased after 1 h and reached its peak after 9 h (n = 8).

Water content and capillary permeability in lung

Compared with control group, the water content and capillary permeability in lung tissues in ASP group were both increased

Table 2 Water content and capillary permeability in lung tissues in each period of time (mg/g, mean±SD, n = 8)

	Control	1 h	3 h	5 h	7 h	9 h
Water content[b]	0.69±0.03	0.72±0.02	0.74±0.02	0.75±0.02	0.76±0.02	0.77±0.03
Capillary permeability[b]	0.048±0.005	0.068±0.005	0.086±0.010	0.106±0.009	0.113±0.012	0.112±0.004

[b]P<0.01 *vs* control group.

Table 3 Hemorrheology in ASP in each period of time (mean±SD, n = 8)

	Control	1 h	3 h	5 h	7 h	9 h
High VTB (mPa·s)[b]	5.65±1.04	7.66±0.90	7.81±0.41	7.79±0.32	8.32±0.46	9.49±1.34
Low VTB (mPa·s)[b]	14.57±4.00	22.72±2.26	23.77±3.13	22.80±1.61	29.46±4.81	30.91±7.28
VP (mPa·s)[b]	3.57±0.49	5.10±0.87	4.56±1.08	5.76±0.88	6.25±1.00	8.00±1.34
BS (mm/h)[b]	9.33±0.82	0.90±0.11	0.59±0.31	0.33±0.15	0.12±0.11	0.03±0.03
Hematocrit (%)[b]	44.92±2.73	56.00±2.59	57.17±2.88	57.67±1.86	59.17±2.96	62.17±3.39
CB (g/L)[b]	452.3±29.9	145.0±45.4	142.0±14.6	88.3±20.8	67.4±17.7	51.3±19.1
Original hemolysis[b]	0.45±0.02	0.47±0.02	0.47±0.02	0.47±0.02	0.47±0.02	0.49±0.02
Complete hemolysis[b]	0.36±0.00	0.38±0.02	0.39±0.02	0.40±0.03	0.41±0.02	0.43±0.02

[b]P<0.01 *vs* control group.

obviously in each period of time (Table 2).

Hemorrheologic examination

Compared with control group, each items of hemorrheology were diverse in each period of time (Table 3).

DISCUSSION

The main characteristic of acute pancreatitis is the change in blood circulation of pancreas and the whole body[4-6]. Blood volume declined obviously in early period of ASP. Hemoperfusion could exacerbate ASP. In this experiment, sodium taurocholate was injected through the pancreatic duct to make ASP models. We observed various indexes of ASP at different time points. Significant hemorrheology changes could be observed in rats with ASP. The blood viscosity and the erythrocyte osmotic fragility were increased. The capillary permeability in lung tissues was also increased. Interstitial pulmonary and microthrombosis were found. Obvious microcirculation disturbance (MD) could be observed in lung tissues and the whole body of rats with ASP. After the models were made, the number of apoptosis endothelial cells and the genetic expression of ICAM-1 in lung tissues were significantly increased, suggesting that ASP can cause MD in many ways and plays an important role in causing and exacerbating ALI.

WBCs adhered to the blood vessel endothelium could cause inflammation[7-9]. Adhesion molecule could play an important role in adhesion process, and its expression could reflect the change of blood vessel endothelium[10-17]. After ASP models were made, ICAM-1 gene expression was increased and became easier for WBCs to adhere to blood vessel endothelium. Therefore, it made WBCs to invade the lung tissues more easily.

For vein wall permeability, blood vessel endothelium is the main barrier. In this study, the number of apoptosis cells increased and apoptosis was accorded with the increasing of lung tissues, vessel permeability and water content. We think that the increasing of apoptosis cells in lung tissues could alter the structure integrality of capillary endothelium. Because the endothelial cells could not renew rapidly by themselves, apoptosis could lead to decrease of blood vessel endothelial cell storage. This kind of change results in the increase of blood vessel endothelium gap and its permeability[18,19].

Our study found that hemorrheology changed obviously in blood of ASP rats, thus leading to more serious MD of pancreas and other organs. This is the main reason for pancreas necrosis and ARDS representation[20,21]. The primary presentations are the decline of RBC aggregation capacity, increase of VTB and VP as well as WBC edging-concentration. The later is the primal step of WBCs swimming outside of blood vessel, leading to grievous inflammation and ALI[22]. WBC edging-concentration in rats with ASP was affected not only by inflammation medium and chemotatic factor but also by other factors, such as tiny vein, blood viscosity, and RBC aggregation[23].

The erythrocyte fragility was increased after ASP presentation, and became more serious following the progress of the disease. The increase of erythrocyte fragility could reflect the defective capacity of RBC distortion. RBCs break up easily, and release adenosine diphosphate, thus causing the activation of coagulation system and disseminated intravascular coagulation, leading to the decrease of fibrinogen.

In conclusion, MD plays an important role in the process of ASP with lung injury. Ameliorating MD could not only reduce local damages in pancreas, but also protect the lung and other organs in the body. Therefore, ameliorating MD is an effective therapy in treating ASP.

REFERENCES

1 **Zhu AJ**, Shi JS, Sun XJ. Organ failure associated with severe acute pancreatitis. *World J Gastroenterol* 2003; **9**: 2570-2573
2 **Liu XM**, Pan CE, Liu QG, Wang ZF. The diagnosis and treatment of lung injury following severe acute pancreatitis. *Zhonghua Gandan Waike Zazhi* 2002; **8**: 116-117
3 **Zhao M**, Chen RF. The pathogenesis of lung injury following acute necrotizing pancreatitis. *Shijie Huaren Xiaohua Zazhi* 2001; **9**: 954-957

4 **Foitzik T**, Eibl G, Hotz B, Hotz H, Kahrau S, Kasten C, Schneider P, Buhr HJ. Persistent multiple organ microcirculatory disorders in severe acute pancreatitis: experimental findings and clinical implications. *Dig Dis Sci* 2002; **47**: 130-138
5 **Zhou ZG**, Zhang ZD, Yan LN, Shu Y, Cheng Z, Zhao JC, Lan P, Feng XM, Wang R. The feature of pancreatic microcirculatory impairment in caerulein induced acute pancreatitis. *Zhonghua Waike Zazhi* 1999; **37**: 138-140
6 **Xia SH**, Zhao XY, Guo P, Da SP. Hemocirculatory disorder in dogs with severe acute pancreatitis and intervention of platelet activating factor antagonist. *Shijie Huaren Xiaohua Zazhi* 2001; **9**: 550-554
7 **Chen H**, Li F, Cheng YF, Sun JB. Pathogenic role of neutrophils in evolution of acute pancreatitis in rats. *Shijie Huaren Xiaohua Zazhi* 2001; **9**: 776-779
8 **Gukovskaya AS**, Vaquero E, Zaninovic V, Gorelick FS, Lusis AJ, Brennan ML, Holland S, Pandol SJ. Neutrophils and NADPH oxidase mediate intrapancreatic trypsin activation in murine experimental acute pancreatitis. *Gastroenterology* 2002; **122**: 974-984
9 **Kyriakides C**, Jasleen J, Wang Y, Moore FD Jr, Ashley SW, Hechtman HB. Neutrophils, not complement, mediate the mortality of experimental hemorrhagic pancreatitis. *Pancreas* 2001; **22**: 40-46
10 **Sun W**, Zhang JD, Zhao Y, Zhao Y, Wang Q. Expression of IL-6 and integrin family cell adhesion molecules in acute necrotizing pancreatitis complicated with multiple organ injury in rats. *Shijie Huaren Xiaohua Zazhi* 2003; **11**: 753-755
11 **Shi L**, Tian FZ, Huang DR, Li X, Zhao B, Gu DY, Tang XD, Wang Y. Effect of hepatic NF-κB on ICAM-1 expression in rats with acute pancreatitis. *Shijie Huaren Xiaohua Zazhi* 2003; **11**: 1505-1507
12 **Yi Y**, Gao NR. The celluliar adhering elements and acute pancreatitis. *Shijie Huaren Xiaohua Zazhi* 2001; **9**: 70-71
13 **Lundberg AH**, Fukatsu K, Gaber L, Callicutt S, Kotb M, Wilcox H, Kudsk K, Gaber AO. Blocking pulmonary ICAM-1 expression ameliorates lung injury in established diet-induced pancreatitis. *Ann Surg* 2001; **233**: 213-220
14 **Nakae H**, Endo S, Sato N, Wakabayashi G, Inada K, Sato S. Involvement of soluble adhesion molecules in acute pancreatitis. *Eur Surg Res* 2001; **33**: 377-382
15 **Powell JJ**, Siriwardena AK, Fearon KC, Ross JA. Endothelial-derived selectins in the development of organ dysfunction in acute pancreatitis. *Crit Care Med* 2001; **29**: 567-572
16 **Telek G**, Ducroc R, Scoazec JY, Pasquier C, Feldmann G, Roze C. Differential upregulation of cellular adhesion molecules at the sites of oxidative stress in experimental acute pancreatitis. *J Surg Res* 2001; **96**: 56-67
17 **Frossard JL**, Saluja A, Bhagat L, Lee HS, Bhatia M, Hofbauer B, Steer ML. The role of intercellular adhesion molecule 1 and neutrophils in acute pancreatitis and pancreatitis-associated lung injury. *Gastroenterology* 1999; **116**: 694-701
18 **Liu XM**, Liu QG, Pan CE, Xu GF, Zhang T, Huang JY, Zhang M. Influence of apoptosis of endothelial cell on lung injury following severe acute pancreatitis in rats. *Disi Junyi Daxue Xuebao* 2003; **24**: 1677-1679
19 **Wu RQ**, Song XH, Xu YX, Meng XJ. Apoptosis of endothelial cells in alteration of microvascular permeability in lung during sepsis. *Zhonghua Waike Zazhi* 2000; **38**: 385-387
20 **Wang ZF**, Pan CE, Liu SG, Liang GG, Zhang M. The significance of hemorrheologic alternation in acute necrotizing pancreatitis. *Zhongguo Putong Waike Zazhi* 2000; **9**: 225-227
21 **Wang ZF**, Pan CE, Liang GG, Liu SG, Zhang M. The treatment of acute necrotizing pancreatitis by modifying hemorrheologic alternation. *Zhonghua Gandan Waike Zazhi* 2000; **6**: 89
22 **Zhou YK**, Wu Y. The correlation between blood rheology and multiple organic injury in acute pancreatitis. *Shijie Huaren Xiaohua Zazhi* 2000; **8**: 1055-1057
23 **Liang GG**. The study of the relationship between apparent vislosity and the aggregation of erythrocytes when the blood performs a tubular steady laminal flow with small pressure difference. *Xi'an Yike Daxue Xuebao* 2000; **21**: 259-262

Science Editor Wang XL and Li WZ **Language Editor** Elsevier HK

PO Box 2345, Beijing 100023, China
www.wjgnet.com
wjg@wjgnet.com

ELSEVIER

World J Gastroenterol 2005;11(39):6212-6215
World Journal of Gastroenterology ISSN 1007-9327

• *BRIEF REPORTS* •

Effects of hepatitis B virus on p53 expression in hepatoma cell line SMMU-7721

Jian-Hui Qu, Ming-Hua Zhu, Jing Lin, Can-Rong Ni, Fang-Mei Li, Zhi Zhu, Guan-Zhen Yu

Jian-Hui Qu, Ming-Hua Zhu, Jing Lin, Can-Rong Ni, Fang-Mei Li, Zhi Zhu, Guan-Zhen Yu, Department of Pathology, the Second Military Medical University, Shanghai 200433, China
Supported by the National Natural Science Foundation of China, No. 30070344
Co-first-authors: Jian-Hui Qu and Ming-Hua Zhu
Correspondence to: Ming-Hua Zhu, Department of Pathology, the Second Military Medical University, Shanghai 200433, China. mhzhu2000@hotmail.com
Telephone: +86-21-25074604
Received: 2004-10-18 Accepted: 2005-03-28

Abstract

AIM: To investigate the contribution of HBV in the development of hepatocarcinoma by examining the effects of HBV on p53 function in SMMU-7721 cell line.

METHODS: Plasmid pCMVp53 was transfected or cotransfected with pCMVHBVa (wild-type HBV) or PCMVHBVb (mutation type HBV) into the hepatoma cell line SMMU-7721 by lipofectamine. Apoptosis cells were labeled with annexin V-FITC and confirmed by flow cytometry. Reporter plasmid PG13-CAT or p21-luc was cotransfected, respectively, into each group to determine the transactivation activity of p53 and its effect on p21 promoter. Western blot was performed to observe p53 expression in hepatoma cell line of each group.

RESULTS: The group transfected with pCMVp53 alone exhibited higher luciferase activity and higher apoptosis rate, otherwise, the p53 expression and reporter activity of PG13-CAT or P21-luc as well as cell apoptosis rate were obviously higher in the group cotransfected of pCMVp53 with pCMVHBVa, but not in the other cotransfected group.

CONCLUSION: Transient transfection of HBV into the SMMU-7721 cell line can enhance p53 expression and its effects on development of hepatocarcinoma.

Key words: Hepatitis B virus; p53; p21; Hepatoma

Qu JH, Zhu MH, Lin J, Ni CR, Li FM, Zhu Z, Yu GZ. Effects of hepatitis B virus on p53 expression in hepatoma cell line SMMU-7721. *World J Gastroenterol* 2005; 11(39): 6212-6215
http://www.wjgnet.com/1007-9327/11/6212.asp

INTRODUCTION

HBV is a major etiological factor associated with hepatocarcinogenesis, but its role in the transformation process remains unknown. p53 is an important tumor suppressor and its mutation or inactivation is thought to be involved in the development of various types of cancers, including primary hepatocellular carcinoma (PHC)[1]. It has been reported that the p53 protein could bind with HBx antigen to form the complexes, which led to p53 inactivation[2,3]. Genetic alterations in the cellular genome in HBV-transfected HepG2 cells were also detected, which could indicate HBV replication[4]. In view of the intimate relationship between HBV infection and hepatoma, relationship between HBV and p53 is always a research spot. In this experiment, we observed the effect of HBV on p53 expression and activity in SMMU-7721 cell line.

MATERIALS AND METHODS

Materials

Plasmids and cell Human hepatoma cell line, SMMU-7721, was constructed in our laboratory, which can express wild type p53, but without HBV replication. The plasmids of pCMVHBVa (wild type HBV), pCMVHBVb (mutant type HBV, C-T substitution at 1 653 bp) and pCMVp53 (containing wild type p53 1.8 kb cDNA) were supplied by the Center for Human Virology of Thomas Jefferson University. PG13-CAT was kindly provided by Dr. Vogelstein, which contains 13 consecutive p53 recognition sites, making the expression of chloramphenicol acetyltransferase (CAT) regulated by p53 protein in the cells, and its inner control plasmid was pSVβ-gal (Promega, USA). p21-luc (kindly provided by Dr. Vogelstein) contains p53 binding site with p21 promoter and luciferase reporter gene. The inner control plasmid PRL-SV40 (Promega) was cotransfected into cells to eliminate the difference caused by transfection efficiency or cell counts.

Chemicals and reagents Lipofectamine™ transfection reagent was purchased from Gibco BRL (Gaithersburg, MD, USA). Dual Luciferase Assay System was purchased from Promega (USA). Annexin-V-FITC reagent was from Bender MedSystems (Vienna, Austria), CAT-ELISA kit was purchased from Roche (Mannheim, Germany). BCA protein detection kit was from Tian-Cheng Company (Shanghai, China). Protein prestained marker was provided by BioLabs (Australasia). Western blotting luminal reagent was from Santa Cruz (USA). Mouse mAb P53-DO7 was from Antibody Diagnostica Incorporation (USA). Internal control β-actin antibody was from Sigma (USA). Goat-anti-mouse horseradish peroxidase antibody and PVDF were from Hua-Mei Biological Company (Shanghai, China).

Methods

Cell culture and transient transfection with plasmid DNA SMMU-7721 cells were cultured in DMEM media supplemented with 100 mL/L fetal calf serum (FCS) and antibiotics, and incubated at 37 ℃ in a humidified atmosphere containing 50 mL/L CO_2. The experiment was divided into four groups: pCMVp53 was transfected alone or cotransfected with pCMVHBVa or pCMVHBVb into the SMMU-7721 cell; and the control group was transfected by sperm DNA. The total of 2 μg DNA was transfected into the cells in each group. DNA amount was held constant in all experiments by adjusting with sperm DNA. Plasmid DNAs were introduced into SMMU-7721 by lipofectamine™ following the manufacturer's instructions. Briefly, cells were seeded into 35-mm culture dishes for 24 h and the medium was refreshed 4 h before transfection. The DNA mixed with 12 μL of lipofectamine™ was added to each plate and incubated in serum-free medium at 37 ℃ for 6.5 h, and then the medium was replaced with RPMI containing 100 mL/L FCS. Sixty hours after transfection, cells were observed under microscope. Cells were harvested to detect the apoptotic rate by flow cytometry or p53 expression by Western blot.

CAT ELISA Cells were prepared and transfected as aforementioned. Total amount (2.0 μg) of DNAs were kept constant by adding PG13-CAT. SV40-driven β-gal internal control plasmid and the respective test plasmids were as follows: pCMVHBVa, pCMVHBVb, pCMVp53, or the control sperm DNA. Before harvesting, the cells were washed thrice with PBS and extracted following the manufacturer's instructions. β-Galactosidase activity was determined in 96-well plates. A total of 200 μL aliquot of the clear lysates was tested for CAT concentration in the CAT ELISA according to the manufacturer's instructions (Roche Molecular Biochemicals). The CAT concentration of each sample was normalized with respect to β-gal activity.

Luciferase assays Transfections were carried in triplicate. Exponentially growing cells were plated at a density of 5×10^4/well in 0.5 mL medium into 24-well plates. Cells were cultured overnight before transfection. Then 300 ng of luciferase reporter constructs were cotransfected with 300 ng of constructs expressing wild-type p53 proteins or pCMVHBVa or pCMVHBVb. Renilla luciferase expression vector (3 ng) was regarded as an internal control. DNA amount was held constant in all experiments by adjusting with sperm DNA. The cells were harvested 60 h after transfection by lysis with passive lysis buffer (Promega). Firefly and Renilla luciferase activities were assayed using Dual Luciferase Assay System (Promega) according to the manufacturer's instructions. The firefly luciferase activity was normalized to Renilla luciferase activity to compensate for variability in transfection efficiencies.

Flow cytometric analysis of apoptotic cells The cells were stained with FITC-labeled annexin V (Bender MedSystems) and propidium. FITC-labeled annexin V has been used to detect apoptotic cells because annexin binds PS exposed to the outer membrane in apoptotic cells[5-7]. Flow cytometric analysis was performed with a Becton Dickinson flow cytometer (FACScan), and the results were analyzed with the CELLQUEST program (Becton Dickinson).

Western blot analysis Cell pellets were lysed in lysis buffer containing protease inhibitors. The protein concentration of each cell lysate was determined with the BCA assay kit. Eighty micrograms of total protein was separated in a 100 g/L SDS-polyacrylamide gel and transferred to a polyvinylidene difluoride transfer membrane according to standard procedures. Western blotting using anti-p53 mouse mAb DO-7 (1:1 000 dilution) was performed. ECL internal control protein β-actin detection was performed simultaneously.

Statistical analysis

The results were expressed as mean±SD. Differences between experimental groups were evaluated by Student's *t*-test. *P* value <0.05 was considered statistically significant.

RESULTS

The promoter activity of p21 in each transient transfection group

Expression of p53 has an influence on the p21 promoter. As a control, we first tested whether wild-type p53 protein could activate transcription from a p21 promoter. Wild-type p53 triggered an increase in transcription from the p21 promoter and the luciferase values increased significantly when pCMVHBVa was cotransfected, but not in the pCMVHBVb-cotransfected group (Table 1).

Table 1 Luciferase activity in each group (mean±SD)

Groups	p21-luc
pCMVp53	1.218±0.041[a]
pCMVp53+pCMVHBVa	2.197±0.522[a,c]
pCMVp53+pCMVHBVb	0.937±0.210[e]
Control	0.764±0.274

[a]*P*<0.05 *vs* control group; [c]*P*<0.05 *vs* pCMVp53 group; [e]*P*<0.05 *vs* pCMVp53+pCMVHBVa group.

Effect of HBV on transcription activity of p53

To determine the effect of HBV on the transcriptional activities of p53, p53 plasmid was transfected transiently alone or cotransfected with HBVa or HBVb, along with the PG13-CAT reporter construct (the CAT reporter gene under the control of a p53-responsive element). Even in the group transfected with PG13-CAT plasmid alone, a weak expression of CAT enzyme (1.272±0.253) was observed, which suggested that there was an underlying transcription effect of p53 in SMMU-7721. However, in the group with pCMVp53 transfection-induced overexpression of p53, CAT activity was found to be greatly increased (3.585±0.869). Moreover, the group cotransfecting HBVa with PG13-CAT also had a significantly increased CAT activity than that of the group transfected with PG13-CAT alone (2.559±0.231), while cotransfection of HBVb had no marked influence on CAT activity of PG13-CAT (Table 2).

Western blot for p53 expression

It was found that an increase in p53 transcription activity was associated with HBV replication, then it was interesting to examine whether it was caused by the upregulation of p53 protein expression. Our results showed that p53 had a weak expression in the normal SMMU-7721 cells. However,

Table 2 CAT activity in each group

Groups	CAT activity
PG13-CAT	1.272±0.253
HBVa+PG13-CAT	2.559±0.231[a]
HBVb+PG13-CAT	1.585±0.347
pCMVp53+PG13-CAT	3.585±0.869[a]

[a]$P<0.05$ *vs* PG13-CAT group.

p53 expression was markedly increased after transfection with the pCMVp53 plasmid. Furthermore, cotransfection of pCMVp53 with pCMVHBVa showed an even higher p53 expression, while the change was not remarkable when pCMVHBVb was cotransfected with p53 (Figure 1).

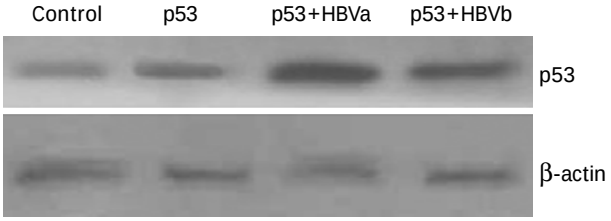

Figure 1 Western blot analysis of p53 expression in each group. Cell lysates (80 μg) were electrophoresed on SDS-PAGE gels and proteins were transferred to PVDF membranes.

Detection of apoptosis by FITC-annexin V/PI double staining

One of the important effects of p53 was its apoptosis-promoting effect. Thus, we observed the apoptosis rate which, in some sense, could indicate p53 activity. We observed that pCMVp53-transfected group had a significantly higher apoptosis rate than the control group (12.32% *vs* 6.91%). There was a much higher apoptosis rate in the pCMVp53 and pCMVHBVa cotransfected group (23.08%), but not in the pCMVp53 and pCMVHBVb cotransfected group (12.20%, Figure 2).

DISCUSSION

Although several data have suggested that the transformation process and tumorigenesis result from activation of oncogenes and inactivation of tumor suppressor genes of the DNA repair system, the question remains of what applies to PHC development. Despite the long-standing association between HBV and PHC development, the role of HBV in the transformation process is still unknown.

The long list of loci with frequent mutations associated with PHC suggests that the mechanism generating these genetic changes might be important in PHC development and needs to be identified. Mutation or inactivation of tumor suppressor gene p53 and its downstream gene p21WAF1 may have an implication in the PHC development [8]. Under normal conditions, p53 is most probably latent. Exposure of cells to p53-activating signals can lead, within a relatively short time, to a marked elevation of p53 protein.

In this experiment, HBV and p53 were transiently transfected into SMMU-7721 cell in order to investigate the apoptosis of the cells, p53 expression, and activity of p53 downstream gene-p21WAF1 promoter and the replication of HBV. Our results showed that the transfection of p53

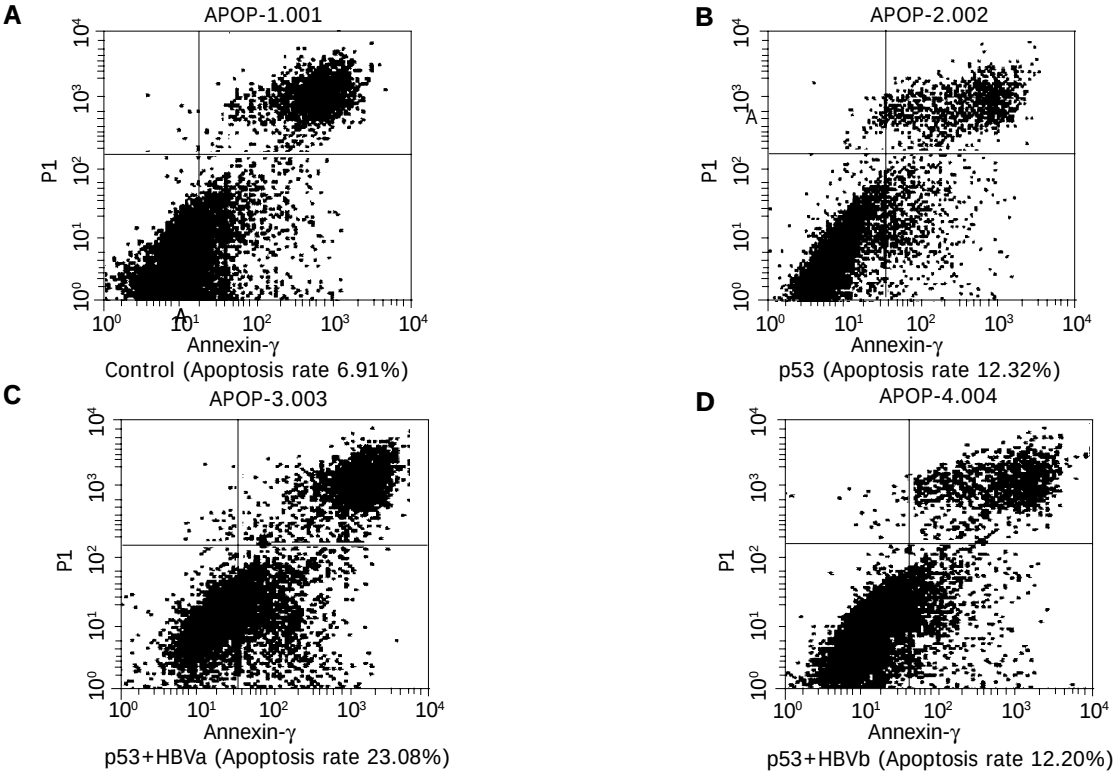

Figure 2 Flow cytometric analysis of cell apoptosis. SMMU-7721 cells were transfected with p53, p53+HBVa, p53+HBVb. The cells were stained by FITC-labeled annexin V and propidium (A-D).

alone in SMMU-7721 cells could increase p21-promoter activity and the apoptosis rate of the cells, suggesting that p53 could promote p21 transcription and contribute to the apoptosis process of the cells. While cotransfection of wild-type HBV markedly increased both p53 protein expression and its transcription activity, and simultaneously, the cell apoptosis rate was significantly increased. In contrast, cotransfection of mutant HBV did not show any effect.

As we know, wild-type p53 is usually a very labile protein, turning over with a half-life sometimes as short as few minutes[9]. On contrary, mutant p53 has a longer half-life, which makes its accumulation in cells. It is generally accepted that the accumulation of active p53 in response to stress occurs mainly through post-translational mechanism, which stabilizes the p53 and increases the ability of nucleolus location[10]. The current results showed that HBV may contribute to promote the stability and activity of p53.

Shi *et al*.[11], showed that p21 (WAF1/CIP1) expression was inversely correlated with p53 expression in hepatitis C virus (HCV)-related hepatocellular carcinomas (HCCs), but not with HBV-related HCCs and HCCs without viral infection, suggesting that different modes of p21 (WAF1/CIP1) regulation are involved in HCCs, differing from their hepatitis viral infection status, and p21 (WAF1/CIP1) expression appears to be predominantly related to altered p53 in HCV-related HCCs. Livezey *et al*.[12], analyzed the p21/Waf1 protein expression in several different kinds of cells by Western blot and indicated that p21/Waf1 protein was upregulated in cells that replicate HBV, but there was still no reasonable interpretation about this phenomenon. Since p21WAF1/CIP1 (p21) is a universal inhibitor of cyclin-dependent kinases and is regulated transcriptionally by p53, which is activated by DNA stress, its expression reflects DNA stress in chronic hepatitis. We observed the correlationship of HBV with p53 and p21, raising the possibility that HBV may have an effect on p21 expression through p53 upregulation, thereby leading to the cell apoptosis.

It has been reported that expression of p21WAF1 in the hepatic disease may be correlated with the disease progression. p21 expression has been reported to be upregulated by the stress of inflammation and fibrosis, and might be influenced by viral proteins in human chronic liver disease. Once the liver develops HCC, the p21 mRNA expression decreases to prominently low levels[13]. In hepatocarcinogenesis induced by HBV and aflatoxin B in tree shrews, the immunopositivity for p21 was found before HCC development, which suggested that p21 protein might be an early marker in the development of HCC[14]. The upregulated p21 expression may play a role as a guard to prevent hepatocytes from tumorgenicity in hepatitis.

Most of the previous reports deemed that apoptosis could not happen to the carcinogenesis cells and/or such cells had no response to the death signal, which lead to unlimited cell growth. But recent research indicates that tumor cells not only exhibited excessive proliferation, but also underwent apoptosis at rates that far exceed those in normal tissue. Proliferation and apoptosis of the tumor cells coexist at all stages and the rates of cell replication are higher than that of apoptosis, allowing a preferential net gain of pre-neoplastic cells[15]. Though HBV chronic infection is an important risk factor of HCC development, HBV-related hepatocarcinoma often happens after dozens of years of infection. In this study, we found that transient transfection of HBV induced apoptosis of SMMU-7721 cells and inactively proliferation. Thus, it is considered that there may be a balance between proliferation and apoptosis in HBV-infected hepatic cells. Hence, disruption of this balance, that is, predominance of proliferation over apoptosis, leads to tumorigenesis.

REFERENCES

1 **Harris CC**. p53: at the crossroads of molecular carcinogenesis and risk assessment. *Science* 1993; **262**: 1980-1981
2 **Zhu MH**. Department of Pathology, Fourth Military Medical University, Xi'an. *Zhonghua Yixue Zazhi* 1993; **73**: 325-328
3 **Feitelson MA**, Zhu M, Duan LX, London WT. Hepatitis B x antigen and p53 are associated *in vitro* and in liver tissues from patients with primary hepatocellular carcinoma. *Oncogene* 1993; **8**: 1109-1117
4 **Livezey KW**, Negorev D, Simon D. Hepatitis B virus-transfected Hep G2 cells demonstrate genetic alterations and de novo viral integration in cells replicating HBV. *Mutat Res* 2000; **452**: 163-178
5 **Martin SJ**, Reutelingsperger CP, McGahon AJ, Rader JA, van Schie RC, LaFace DM, Green DR. Early redistribution of plasma membrane phosphatidylserine is a general feature of apoptosis regardless of the initiating stimulus: inhibition by overexpression of Bcl-2 and Abl. *J Exp Med* 1995; **82**: 1545-1556
6 **Koopman G**, Reutelingsperger CP, Kuijten GA, Keehnen RM, Pals ST, van Oers MH. Annexin V for flow cytometric detection of phosphatidylserine expression on B cells undergoing apoptosis. *Blood* 1994; **84**: 1415-1420
7 **Vermes I**, Haanen C, Steffens-Nakken H, Reutelingsperger C. A novel assay for apoptosis. Flow cytometric detection of phosphatidylserine expression on early apoptotic cells using fluorescein labelled Annexin V. *J Immunol Methods* 1995; **184**: 39-51
8 **Hussain SP**, Hollstein MH, Harris CC. p53 tumor suppressor gene: at the crossroads of molecular carcinogenesis, molecular epidemiology, and human risk assessment. *Ann N Y Acad Sci* 2000; **919**: 79-85
9 **Rogel A**, Popliker M, Webb CG, Oren M. p53 cellular tumor antigen: analysis of mRNA levels in normal adult tissues, embryos, and tumors. *Mol Cell Biol* 1985; **5**: 2851-2855
10 **Meek DW**. Mechanisms of swithing on p53: a role for covalent modification. *Oncogene* 1999; **18**: 7666-7675
11 **Shi YZ**, Hui AM, Takayama T, Li X, Cui X, Makuuchi M. Reduced p21(WAF1/CIP1) protein expression is predominantly related to altered p53 in hepatocellular carcinomas. *Br J Cancer* 2000; **83**: 50-55
12 **Livezey KW**, Negorev D, Simon D. Hepatitis B virus-transfected Hep G2 cells demonstrate genetic alterations and de novo viral integration in cells replicating HBV. *Mutat Res* 2000; **452**: 163-178
13 **Wagayama H**, Shiraki K, Yamanaka T, Sugimoto K, Ito T, Fujikawa K, Takase K, Nakano T. P21WAF1/CTP1 expression and hepatitis virus type. *Dig Dis Sci* 2001; **46**: 2074-2079
14 **Su JJ**, Ban KC, Li Y, Qin LL, Wang HY, Yang C, Ou C, Duan XX, Lee YL, Yang RQ. Alteration of *p53* and *p21* during hepatocarcinogenesis in tree shrews. *World J Gastroenterol* 2004; **10**: 3559-3563
15 **Grasl KB**, Ruttkay NB, Mullauer L, Taper H, Huber W, Bursch W, Schulte-Hermann R. Inherent increase of apoptosis in liver tumors: implications for carcinogenesis and tumor regression. *Hepatology* 1997; **25**: 906-912

Science Editor Kumar M and Guo SY **Language Editor** Elsevier HK

PO Box 2345, Beijing 100023, China
www.wjgnet.com
wjg@wjgnet.com

ELSEVIER

World J Gastroenterol 2005;11(39):6216-6218
World Journal of Gastroenterology ISSN 1007-9327

• *BRIEF REPORTS* •

Alterations of intestinal immune function and regulatory effects of L-arginine in experimental severe acute pancreatitis rats

Shi-Feng Qiao, Tian-Jing Lü, Jia-Bang Sun, Fei Li

Shi-Feng Qiao, Department of General Surgery, Beijing Shijitan Hospital, Beijing 100038, China
Tian-Jing Lü, Department of Immunology, Institute of Urology, Peking University, Beijing 100034, China
Jia-Bang Sun, Fei Li, Department of General Surgery, Xuanwu Hospital of Capital University of Medical Sciences, Beijing 100053, China
Correspondence to: Shi-Feng Qiao, Department of General Surgery, Beijing Shijitan Hospital, Yangfangdian District, Beijing 100038, China. qiaoshf@tom.com
Received: 2004-12-08 Accepted: 2005-01-05

Abstract

AIM: To discuss the changes of intestinal mucosal immune function in rats with experimental severe acute pancreatitis (SAP) and the regulatory effect of L-arginine.

METHODS: Male adult Wistar rats were randomly divided into pancreatitis group, sham-operation group, and L-arginine treatment group. Animals were killed at 24, 48, and 72 h after SAP models were developed and specimens were harvested. Endotoxin concentration in portal vein was determined by limulus endotoxin analysis kit. CD3+, CD4+, CD8+ T lymphocytes in intestinal mucosal lamina propria were examined by immunohistochemistry. Secretory immunoglobulin A (SIgA) in cecum feces was examined by radioimmunoassay.

RESULTS: Compared to the control group, plasma endotoxin concentration in the portal vein increased, percentage of CD3+ and CD4+ T lymphocyte subsets in the end of intestinal mucosal lamina propria reduced significantly, CD4+/CD8+ ratio decreased, and SIgA concentrations in cecum feces reduced at 24, 48, and 72 h after SAP developed. Compared to SAP group, the L-arginine treatment group had a lower level of plasma endotoxin concentration in the portal vein, a higher CD3+ and CD4+ T lymphocyte percentage in the end of intestinal mucosal lamina propria, an increased ratio of CD4+/CD8+ and a higher SIgA concentration in cecum feces.

CONCLUSION: Intestinal immune suppression occurs in the early stage of SAP rats, which may be the main reason for bacterial and endotoxin translocation. L-arginine can improve the intestinal immunity and reduce bacterial and endotoxin translocation in SAP rats.

Key words: Acute pancreatitis; Immunity; Intestinal mucosa; L-arginine

Qiao SF, Lü TJ, Sun JB, Li F. Alterations of intestinal immune function and regulatory effects of L-arginine in experimental severe acute pancreatitis rats. *World J Gastroenterol* 2005; 11(39): 6216-6218
http://www.wjgnet.com/1007-9327/11/6216.asp

INTRODUCTION

Infection is a common and usually lethal complication during severe acute pancreatitis (SAP). In previous studies, the prevalence of infection in SAP varies between 40% and 70%, and most of the deaths of patients are related with infection. The gastrointestinal tract may be the origin of bacterial translocation during SAP, and SAP may influence the gut barrier function, leading to the occurrence of gut origin sepsis. In this study, we discussed the changes of intestinal immunity in SAP rats.

MATERIALS AND METHODS

Animals and materials

Male Wistar rats weighing 250-300 g; L-arginine (Sigma Chemical Co.); sodium taurocholate (Sigma Chemical Co.); mouse anti-rat anti-CD3, CD4, CD8 mAb (Santa Cruz Co.); SIgA radioimmunoassay kit (Institute of Atomic Energy Physics Chinese Academy of Sciences, Beijing); limulus endotoxin analysis kit (Shanghai Medical Laboratory) were used in the study.

SAP model and experimental groups

Rats were fasted for 14 h before the experiment. Animals were anesthetized by intraperitoneal injection of 10% chloral (3 mL/kg) and then SAP models were developed as previously described[1]. Under sterile conditions, a middle laparotomy was performed. The SAP rat model was developed by pumping 3% sodium taurocholate (TCA) into the pancreatic tract at a rate of 18 mL/h (1 mL/kg). Fifty-four rats were randomly divided into SAP group (n = 18), sham group (n = 18), and L-arginine treatment group (n = 18). The rats were allowed to drink 1% L-arginine water for 5 d before SAP model was developed. At 24, 48, and 72 h after the model was developed, animals from each experimental group were killed and specimens were harvested.

Analysis of serum endotoxin in portal vein by limulus methods

The serum endotoxin concentration in portal vein was assayed by chromogenic limulus analysis kit according to the manufacturer's protocol.

Immunohistochemistry

Intestinal tissue fragment (3 cm from cecum) was cut and fixed by immersing in 4% paraformaldehyde immediately. The specimens were embedded in regular paraffin wax and cut into 4-μm-thick sections. Tissue sections were deparaffinized and rehydrated in PBS. Endogenous peroxidase activity was blocked by incubation with 3% H_2O_2/PBS for 10 min. After being immersed in 1% BSA/PBS at 37 ℃ for 1 h, the sections were incubated with mouse anti-rat anti-CD3, CD4, CD8 mAb at 4 ℃ overnight. The specimens were incubated with peroxidase-conjugated goat anti-rat secondary antibody for 2 h at room temperature. Finally, the specimens were immersed in DAB for 10 min. Brown staining cells were defined as positive cells and counted in four high microscope view, the percentage of positive cells and CD4+/CD8+ ratio were calculated.

Analysis of SIgA content by radioimmunoassay methods

Cecum feces were diluted with water to double volumes. Samples were shaken at 4 ℃ overnight and then examined by SIgA radioimmunoassay test kit.

Statistical analysis

Data were analyzed by *t* test and expressed as mean±SD. $P<0.05$ was considered statistically significant.

RESULTS

Changes of serum endotoxin in portal vein of rats

Compared to the control group, plasma endotoxin concentration in the portal vein increased significantly 24, 48, and 72 h after SAP model was developed ($P<0.01$). The L-arginine treatment group had a lower level of endotoxin concentration than SAP group ($P<0.01$, Table 1).

Table 1 Changes of serum endotoxin in rat portal vein (U: Eu/mL)

Group	24 h	48 h	72 h
NS	0.041±0.011	0.039±0.007	0.042±0.015
SAP	0.157±0.024[b]	0.150±0.018[b]	0.146±0.014[b]
L-Arg	0.087±0.011[d]	0.079±0.016[d]	0.082±0.013[d]

[b]$P<0.01$ *vs* NS; [d]$P<0.01$ *vs* SAP.

Percentage of CD3+, CD4+, CD8+ T lymphocytes in intestinal mucosal lamina propria Percentage of CD3+, CD4+ T lymphocytes subsets in the end of intestinal mucosal lamina propria in SAP group reduced significantly and the CD4+/CD8+ ratio decreased. Compared to the SAP group, the L-arginine treatment group had a higher CD3+, CD4+ T lymphocyte percentage and a higher ratio of CD4+/CD8+ (Table 2).

Changes of SIgA content in cecum feces SIgA concentrations in cecum feces reduced significantly 24, 48, and 72 h after SAP was developed. SIgA concentrations in cecum feces increased in the L-arginine treatment group (Table 3).

Table 2 Percentage of CD3+, CD4+, CD8+ T lymphocytes in intestinal mucosal lamina propria (mean±SD)

Group		24 h	48 h	72 h
CD3+	NS	20.54±3.46	22.32±4.78	21.24±5.32
	SAP	11.24±3.06[b]	12.07±4.24[b]	11.07±3.16[b]
	L-Arg	14.36±2.12[c]	17.45±3.52[c]	15.42±4.18[c]
CD4+	NS	12.78±3.39	11.56±3.14	12.47±2.53
	SAP	7.23±1.46[a]	8.34±1.69[a]	9.06±2.94[a]
	L-Arg	9.85±2.51	9.22±2.75	9.42±2.72
CD8+	NS	9.69±1.65	8.89±1.95	9.41±2.57
	SAP	9.73±2.75	9.12±2.47	8.12±3.59
	L-Arg	8.72±2.63	9.05±3.95	7.87±1.79
CD4+/CD8+	NS	1.32	1.30	1.35
	SAP	0.74	0.91	0.96
	L-Arg	1.13	1.02	1.07

[a]$P<0.05$ *vs* NS; [b]$P<0.01$ *vs* NS; [c]$P<0.05$ *vs* SAP.

Table 3 Changes of SIgA content in cecum feces (mean±SD, μg/mL)

Group	24 h	48 h	72 h
NS	8.70±2.69	8.52±1.84	9.24±1.73
SAP	4.75±1.07[a]	4.45±0.94[a]	4.69±1.28[a]
L-Arg	7.57±1.69[c]	7.55±1.45[c]	8.42±2.17[c]

[a]$P<0.05$ *vs* NS; [c]$P<0.05$ *vs* SAP.

DISCUSSION

SAP is a very common disease in clinical surgery. Though the diagnosis and therapy have been improved, its mortality is 10-20%. Secondary pancreatic infection and multiple organ dysfunction syndrome (MODS) are major causes of death in patients with SAP. Infection is the most common clinical syndrome at present and the morbidity in SAP patients is about 40-70%[2]. Infection is also an important factor for SAP followed by MODS[3]. Bacterial infection is devastative for the pancreas and other tissues, and increases the mortality of acute pancreatitis patients. Clinical data and animal experimental studies have shown that most bacteria-associated pancreatic and peripancreatic infection are of enteric origin[4], and the gut seems to be the principal source of the infection[5]. The gastrointestinal tract is regarded as the largest immune organ in the body containing diverse immunocytes to prevent bacterial and endotoxin translocation from indigenous gut flora. Viable enteric bacteria must pass through the intestinal mucosal barrier to extraintestinal sites, leading to gut-associated infection. During the course of SAP, gastrointestinal tract may be attacked and gut-barrier function is damaged, allowing a large amount of bacteria and endotoxin to enter into the systemic circulation, leading to bacteremia and endotoxemia that may cause more severe complications. Prevention of gut bacterial translocation is most important in avoiding extraintestinal infection and improving the prognosis of SAP patients.

SIgA plays an important role in intestinal mucosal defense and is the first line of defense on intestinal and extra-intestinal mucosal surfaces. SIgA can prevent bacterial adherence and subsequent invasion of the mucosal surface, which is considered crucial in initiating mucosal invasion and infection. SIgA deficiency results in bacterial overgrowth, adherence and translocation[6]. Our results showed that SIgA concentration in cecum feces of the SAP group reduced significantly, indicating that SIgA secretion from intestinal mucosa to the intestinal tract was decreased in SAP rats. SIgA deficiency may increase dissociative bacteria and

endotoxin concentration in the intestinal tract, and their migration through the intestinal mucosa and entry into the portal vein blood[7].

CD3 molecules are expressed on the surface of all mature T lymphocytes and can be used to measure the total number of mature T lymphocytes. In our study, the number of CD3+, CD4+ T lymphocytes in intestinal mucosal lamina propria reduced significantly in SAP rats and remained at the lower level at 72 h. The ratio of CD4+/CD8+ T lymphocytes markedly decreased, indicating that mature T lymphocytes are decreased in intestinal mucosa and immune function is suppressed in SAP rats, while CD8+ T lymphocytes do not change significantly. Because the majority of T lymphocytes in intestinal mucosal lamina propria are CD4+ T lymphocytes, change of CD8+ T lymphocytes is not the main trend[8]. Further experiments are needed to validate the results. Since the number of CD4+ T lymphocytes reduces, cytokines including IL-2, IL-4, IL-6, IL-7, IL-12, IFN-γ are secreted by CD4+ T helper (T_H) lymphocytes and the number of active effector Tc cells reduces accordingly. Thus, the intestinal immune function decreases significantly in SAP rats.

L-arginine is important for the proliferation and maturation of CD3+ T lymphocytes. Dietary arginine may increase the number of CD4+ and CD8+ T lymphocytes as well as the IgG and IgA content[9-11]. Our results have confirmed that oral supplement of L-arginine increases the number of CD3+ and CD4+ T lymphocytes as well as the ratio of CD4+/CD8+ T lymphocytes in intestinal mucosal lamina propria and SIgA concentration in cecum feces in SAP rats, suggesting that L-arginine can improve the immune responsibility of intestinal mucosa and decrease the bacterial and endotoxin translocation in SAP rats.

REFERENCES

1 **Aho HJ**, Koskensalo SM, Nevalainen TJ. Experimental pancreatitis in the rat sodiumtaurocholate-induced acute hemorrhagic pancreatitis. *Scand J Gastroenterol* 1980; **15**: 411-416

2 **Bassi C**, Mangiante G, Falconi M, Salvia R, Frigerio I, Pederzoli P. Prophylaxis for septic complications in acute necrotizing pancreatitis. *J Hepatobiliary Pancreat Surg* 2001; **8**: 211-215

3 **Isenmann R**, Rau B, Beger HG. Bacterial infection and extend of necrosis are determinants of organ failure in patients with acute necrotizing pancreatitis. *Br J Surg* 1999; **86**: 1020-1024

4 **McNaught CE**, Woodcock NP, Mitchell CJ, Rowley G, Johnstone D, MacFie J. Gastric colonisation, intestinal permeability and septic morbidity in acute pancreatitis. *Pancreatology* 2002; **2**: 463-468

5 **Samel S**, Lanig S, Lux A, Keese M, Gretz N, Nichterlein T, Sturm J, Lohr M, Post S. The gut origin of bacterial pancreatic infection during acute experimental pancreatitis in rats. *Pancreatology* 2002; **2**: 449-455

6 **Langkamp-Henken B**, Glezer JA, Kudsk KA. Immunological structure and function of the gastrointestinal tract. *Nutr Clin Pract* 1992; **7**: 100-108

7 **Qin HL**, Su ZD, Gao Q, Lin QT. Early intrajejunal nutrition: bacterial translocation and gut barrier function of severe acute pancreatitis in dogs. *Hepatobiliary Pancreat Dis Int* 2002; **1**: 150-154

8 **Gautreaux MD**, Deitch EA, Berg RD. T lymphocytes in host defense against bacterial translocation from the gastrointestinal tract. *Infect Immun* 1994; **62**: 2874-2884

9 **Ochoa JB**, Strange J, Kearney P, Gellin G, Endean E, Fitzpatrick E. Effects of L-arginine on the proliferation of T lymphocyte subpopulations. *J Parenter Enteral Nutr* 2001; **25**: 23-29

10 **Kung SP**, Wu CW, Lui WY. Arginine modulated cyclosporine-induced immune suppression in rats transplanted with gastric cancer cells. *In Vivo* 2001; **15**: 39-44

11 **Kobayashi T**, Yamamoto M, Hiroi T, McGhee J, Takeshita Y, Kiyono H. Arginine enhances induction of T helper 1 and T helper 2 cytokine synthesis by Peyer's patch alpha beta T cells and antigen-specific mucosal immune response. *Biosci Biotechnol Biochem* 1998; **62**: 2334-2340

Science Editor Wang XL and Guo SY **Language Editor** Elsevier HK

PO Box 2345, Beijing 100023, China
www.wjgnet.com
wjg@wjgnet.com

ELSEVIER

World J Gastroenterol 2005;11(39):6219-6220
World Journal of Gastroenterology ISSN 1007-9327

• *CASE REPORT* •

Primary biliary cirrhosis after aortoiliac reconstruction surgery using a Y-graft: A case report

Tomoko Inoue, Katsuya Shiraki, Hiroyuki Fuke, Yutaka Yamanaka, Kazumi Miyashita, Keiichi Ito, Masahiro Suzuki, Kazushi Sugimoto, Kazumoto Murata, Takeshi Nakano

Tomoko Inoue, Katsuya Shiraki, Hiroyuki Fuke, Yutaka Yamanaka, Kazumi Miyashita, Keiichi Ito, Masahiro Suzuki, Kazushi Sugimoto, Kazumoto Murata, Takeshi Nakano, First Department of Internal Medicine, Mie University School of Medicine, 2-174 Edobashi, Tsu, Mie 514-8507, Japan
Correspondence to: Katsuya Shiraki, MD, PhD, First Department of Internal Medicine, Mie University School of Medicine, 2-174 Edobashi, Tsu, Mie 514-8507, Japan. katsuyas@clin.medic.mie-u.ac.jp
Telephone: +81-59-231-5015
Received: 2004-08-14 Accepted: 2004-09-30

Abstract

Primary biliary cirrhosis (PBC) is an autoimmune disease characterized by anti-mitochondrial antibodies and destruction of intra-hepatic bile ducts. Though little is known about the etiology of PBC, some reports suggest that xenobiotics and viral infections may induce PBC. We describe a case of PBC after the aortoiliac reconstruction surgery using a Y-graft.

Key words: Gall bladder cancer; Metastasis; Metastatic cardiac tumor

Inoue T, Shiraki K, Fuke H, Yamanaka Y, Miyashita K, Ito K, Suzuki M, Sugimoto K, Murata K, Nakano T. Primary biliary cirrhosis after aortoiliac reconstruction surgery using a Y-graft: A case report. *World J Gastroenterol* 2005; 11(39): 6219-6220
http://www.wjgnet.com/1007-9327/11/6219.asp

INTRODUCTION

Primary biliary cirrhosis (PBC) is a chronic inflammatory process primarily affecting the medium-sized intra-hepatic bile ducts, leading to chronic cholestasis and often progressing to cirrhosis and liver failure, which requires liver transplantation. PBC is thought of as an autoimmune disease because it is closely associated with various immunological abnormalities, the hallmark being the presence of anti-mitochondrial antibodies in over 95% of patients.

CASE REPORT

A 61-year-old male was admitted to our hospital in September 1995 with biochemical cholestasis and abnormal liver function tests. He had taken anti-hypertensive agents (amlodipine and betaxolol) since February 1995. His blood examination sometimes presented very mild biochemical cholestasis without any symptoms. Viral hepatitis was denied, but autoantibody was not checked at that time. Earlier in March 1995, he had an abdominal aortic aneurysm and underwent aortoiliac reconstruction using a Y-graft. Ten days after the surgery, his chemistry showed marked cholestasis, including alkaline phosphatase levels 5-10 times the upper limit of normal and gamma glutamyltransferase levels 5-15 times higher than the upper limit of normal. At first, drug-induced cholestasis was suspected and he started other anti-hypertensive medications (nifedipine and imidapril). Cholestasis improved after changing these medications for a while, but it worsened in August 1995. On admission to our hospital in September 1995, he denied any preceding or on-going fever, flu-like illness, pruritus, abdominal pain, anorexia, vomiting, joint pain, dry eyes, or skin rashes. He denied previous blood transfusion, iv drug abuse, or alcohol abuse. There was no family history of liver disease or malignancy.

Physical examination revealed mild hepatomegaly, but no ascites or mass. The laboratory data showed an alkaline phosphatase level of 572 IU/L, a gamma glutamyltransferase level of 726 IU/L, an AST of 43 IU/L, an ALT of 30 IU/L, a total bilirubin of 0.5 g/dL, a direct bilirubin of 0.2 g/dL, an IgG level of 2 180, an IgM level of 384, and a total cholesterol level of 204 mg/dL. Antinuclear antibody titer was 1 280-fold beyond the upper normal limit, anti-smooth muscle antibody was 80-fold, and anti-mitochondrial antibody was 80-fold higher. A hepatitis profile for hepatitis B and C was negative. An abdominal ultrasound revealed a slightly atrophic liver with dull edge, dilated common bile duct (12 mm), and a gallbladder stone. His liver biopsy showed inflammatory destruction of the intrahepatic septal and interlobular bile ducts within the portal space, and expanded portal tracts by lymphocytes with sparse neutrophils or eosinophils, suggesting PBC (stage I by Scheuer staging) (Figure 1).

A diagnosis of asymptomatic PBC was established on the basis of cholestasis, a positive AMA, and the histological findings. The patient was started on ursodeoxycholic acid 600 mg thrice a day, with a positive response to the cholestasis.

DISCUSSION

PBC is a chronic cholestatic liver disease of unknown cause. Progressive bile duct injury from portal and periportal inflammation could result in progressive fibrosis and eventually cirrhosis. Evidence to date suggests that

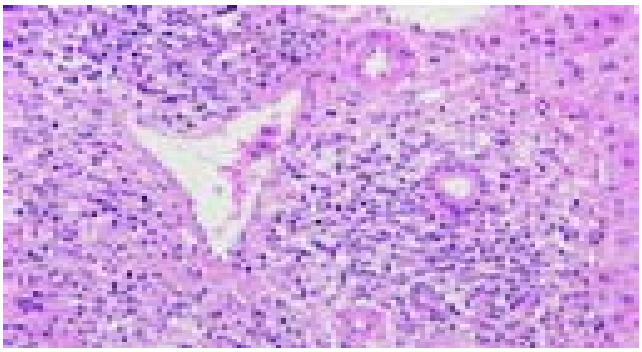

Figure 1 The liver biopsy showed inflammatory destruction of the intrahepatic septal and interlobular bile ducts within the portal space, and expanded portal tracts by lymphocytes with sparse neutrophils or eosinophils.

immunological and genetic factors might cause the disease. Evidence for an immunologic cause of PBC includes immunohistochemical data showing the presence of activated T cells in areas of bile duct destruction and the presence of highly specific autoantibodies reactive with antigens on the surface of biliary epithelial cells. Environmental factors[1] and infectious agents[2-4] also may trigger an autoimmune attack. Other reports suggest that the disease may be induced by xenobiotics and that halogenated compounds will bind to the PDC-E2 autoantigen, breaking tolerance and leading to an intense mucosal response[5]

Our patient had mild cholestasis before the operation and developed marked biochemical cholestasis after the aortoiliac reconstruction using a Y-graft. This suggests that he may have been in the very early stages of PBC before the surgery and the graft implantation might have exacerbated the autoimmune response, leading to further bile duct injury. The trigger might be the graft itself or the drugs used in the perioperative period. There is only one case report of PBC after graft replacement for abdominal aortic aneurysm[6], in which the graft itself was considered to induce the autoimmune response, resulting in liver injury. Some reports suggest that xenobiotics are metabolized in the liver, thereby increasing the potential for liver-specific alteration of proteins, and that a liver-specific autoimmune disease can be observed in some patients exposed to anesthetics[5]

We report a rare case of PBC after aortoiliac reconstruction using a Y-graft, suggesting that the graft itself or medications in the perioperative period might induce or exacerbate an autoimmune response, leading to bile duct injury. In the view of the risk to trigger onset of PBC, it becomes worthwhile to carefully evaluate past surgeries and medications carefully.

REFERENCES

1 **Parikh-Patel A,** Gold EB, Worman H, Krivy KE, Gershwin ME. Risk factors for primary biliary cirrhosis in a cohort of patients from the United States. *Hepatology* 2001; **33**: 16-21

2 **Roesler KW,** Schmider W, Kist M, Batsford S, Schiltz E, Oelke M, Tuczek A, Derrenborn T, Beringer D, Kreisei W. Identification of beta-subunit of bacterial RNA-polymerase-a non-species-specific bacterial protein-as a target of antibodies in primary biliary cirrhosis. *Dig Dis Sci* 2003; **48**: 561-569

3 **Poupon R,** Poupon RE. Retrovirus infection as a trigger for primary biliary cirrhosis? *Lancet* 2004; **363**: 260-261

4 **Xu L,** Shen Z, Guo L, Federa B, Keogh A, Joplin R, O'Donnell B, Aitken J, Carman W, Neuberger J, Mason A. Does a betaretrovirus infection trigger primary biliary cirrhosis? *Proc Natl Acad Sci USA* 2003; **100**: 8454-8459

5 **Long SA,** Water JV, Gershwin ME. Antimitochondrial antibodyies in primary biliary cirrhosis: the role of xenobiotics. *Autoimmunity Reviews* 2002; **1**: 37-42

6 **Ohmori S,** Itoh K, Kuniyoshi M, Shimizu A, Takase K, Nakano T, Tameda Y, Kosaka Y. An elder man's case of primary biliary cirrhosis with autoimmune hepatitis after the graft replacement of abdominal aortic aneurysma. *Acta Hepatol Japonica* 1999; **40**: 409-413

Science Editor Zhu LH and Guo SY **Language Editor** Elsevier HK

PO Box 2345, Beijing 100023, China
www.wjgnet.com
wjg@wjgnet.com

ELSEVIER

World J Gastroenterol 2005;11(39):6221-6224
World Journal of Gastroenterology ISSN 1007-9327

• *CASE REPORT* •

Primary pancreatic anaplastic large cell lymphoma, ALK negative: A case report

Christos G Savopoulos, NE Tsesmeli, GD Kaiafa, AT Zantidis, MT Bobos, AI Hatzitolios, ST Papavramidis, IS Kostopoulos

Christos G Savopoulos, NE Tsesmeli, GD Kaiafa, AT Zantidis, AI Hatzitolios, 1st Medical Propedeutic Department, AHEPA Hospital, Aristotle University of Thessaloniki, St. Kyriakidi 1, Thessaloniki 54636, Greece
MT Bobos, IS Kostopoulos, Department of Pathology, Aristotle University Medical School, Thessaloniki 54006, Greece
ST Papavramidis, 3rd Department of Surgery, AHEPA Hospital, Aristotle University of Thessaloniki, St. Kyriakidi 1, Thessaloniki 54636, Greece
Correspondence to: Dr. Christos G Savopoulos, 1st Medical Propedeutic Department, AHEPA Hospital, Aristotle University of Thessaloniki, St. Kyriakidi 1, Thessaloniki 54636, Greece. chrsavop@med.auth.gr
Telephone: +30-2310-994783 Fax: +30-2310-285128
Received: 2005-04-13 Accepted: 2005-05-12

Abstract

We present the fourth case of a primary pancreatic anaplastic large cell lymphoma (ALCL), ALK-. An 80-year-old man was admitted to our clinic for further investigation of a fever of unknown origin. He noted anorexia, weight loss and fatigue. His laboratory tests showed anemia and a great elevation of ESR, LDH, and β_2 microglobulin. In CT and MRI scan, a soft tissue mass in the pancreas was observed. A repeated endoscopy after his admission revealed an ulcerated mass-like deformity of the duodenal bulb. Explorative laparotomy confirmed a diffuse spread of an unresectable malignant pancreatic mass extending to the adjacent organs. Duodenal and surgical biopsies identified an ALCL of T-cell lineage, ALK-. The patient died in the Intensive Care Unit due to hemodynamic instability. Our case is the first one indicating that primary pancreatic lymphoma should be suspected in a patient with pancreatic mass and elevated serum LDH and β_2 microglobulin.

Key words: Anaplastic large cell lymphoma; Primary pancreatic lymphoma; Lactate dehydrogenase; β_2 microglobulin

Savopoulos CG, Tsesmeli NE, Kaiafa GD, Zantidis AT, Bobos MT, Hatzitolios AI, Papavramidis ST, Kostopoulos IS. Primary pancreatic anaplastic large cell lymphoma, ALK negative: A case report. *World J Gastroenterol* 2005; 11(39): 6221-6224
http://www.wjgnet.com/1007-9327/11/6221.asp

INTRODUCTION

Malignant tumors of the pancreas constitute about 15% of cancer patients and the most frequent of them is the adenocarcinoma of the pancreas[1]. Primary pancreatic lymphoma (PPL) is a very rare disease constituting less than 0.5% of all pancreatic malignancies and less than 2% of extranodal lymphomas[2]. Primary pancreatic anaplastic large cell lymphomas (PPALCL) are extremely rare. Only three cases of PPALCL have been reported in the literature[1,3,4]. Herein we report the fourth case of PPALCL which was diagnosed by duodenal and surgical biopsies.

CASE REPORT

An 80-year-old man, who was under evaluation of a fever of unknown origin in a Private Health Center, was admitted to our clinic for further investigation. He was complaining of an intermittent fever of 2 mo duration which stabilized during the last 3 wk. Anorexia, weight loss of about 10 kg in the last 6 mo and fatigue were also reported. Physical examination was unremarkable except for a leg edema. His hematological profile was as follows: Hct: 31%, Hb: 9.9 g/L, MCV: 92 fl, MCH: 30 pg/cell, reticulocytes: 1.6%, WBC: 10.6×10^9 cells/L (neutrophils 80% -lymphocytes 11% -monocytes 6% -eosinophils 2.5% -basophils 0.5%), PLT: 389×10^9/L, ESR: 110 mm, CRP: 13 mg/dL (normal range: 0-0.8 mg/dL). Serum biochemistry showed a great elevation of LDH: 1 880 U/L (normal range: 313-618 U/L) and hypoalbuminemia: 2.1 g/L (normal range: 3.4-4.8 g/L), with normal total proteins: 7.1 g/L (normal range: 6.6-8.7 g/L) though. Elevated b_2 microglobulin: 4.19 mg/L (normal range: 1.42-3.21 mg/L) was also found. Other biochemical, serologic and immunologic investigations were normal. Laboratory studies performed after the onset of the symptoms, with values similar to our findings, were available from the patient's file. A chest and abdominal CT scan, also available to us, had demonstrated that the uncinate process and partially the head of the pancreas were blurred (Figure 1A); enlarged peripancreatic, mesenteric, para-aortic and inferior vena cava lymph nodes were found. At that time, he had undergone a gastrointesinal endoscopy without pathologic findings. In further imaging study with MRI scan, a soft tissue mass located in the head of the pancreas and especially the uncinate process had appeared (Figure 1B). A slow flow signal of inferior vena cava had been observed due to the mass compression. After his admission in our clinic, a new endoscopy of the upper gastrointestinal tract revealed an ulcerated mass-like deformity of the duodenal bulb with a friable surface (Figure 2). Gastric and duodenal mucosal biopsy specimens were taken. Bone marrow biopsy was also performed. Glucocorticoids were administrated

as a second choice therapy after antibiotics treatment, based on FUO treatment's protocol and on the high indication of a lympho-proliferative disorder. Temporary clinical and laboratory improvement was noticed (ESR declination: 55 mm). Explorative laparotomy confirmed a diffuse spread of a malignant mass of the pancreas extending to the adjacent organs. Because of the brittle consistency and necrotic surface of the pancreatic mass, the biopsy specimen was taken from the adhesion of pancreatic surface with gastric serosa. Hematoxylin-and-eosin-stained sections of the duodenal biopsy revealed a diffuse dense infiltration of duodenal mucosa by large pleomorphic cells with abundant eosinophilic cytoplasm, ovoidal or irregular nuclei with one or prominent nucleoli (Figure 3A). Rare cells with embryo-like, horseshoe-shaped nuclei or cells with multiple nuclei resembling Reed-Sternberg cells were found. The mitotic activity was intermediate and several atypical mitoses were observed. Scanty neoplastic cells infiltrated the epithelium of intestinal glands as well as the surface epithelium. Histologic sections from the second biopsy material showed loose connective tissue with numerous dilated vessels and lymphatics, most of them having tumor cell emboli with morphology similar to the neoplastic population of the duodenal mucosa (Figure 3B). The intravascular presence of neoplastic cells was confirmed by immunohistochemistry using the endothelial cell marker CD34 (Novocastra, Newcastle, UK). Immunohistochemical stains of both biopsies showed the following tumor-cell immunophenotype: CD45+, CD45RO+, EMA+, CD43+ (DakoCytomation, Glostrup, Denmark), CD30+ (Figure 4), Muc1+, Fascin+ (Novocastra, Newcastle, UK), CD20-, CD45RA-, CAM 5.2-, Anaplastic Lymphoma Kinase (ALK)1-(DakoCytomation, Glostrup, Denmark) and CD3- (Novocastra, Newcastle, UK). Cellular phenotype and immunophenotype support

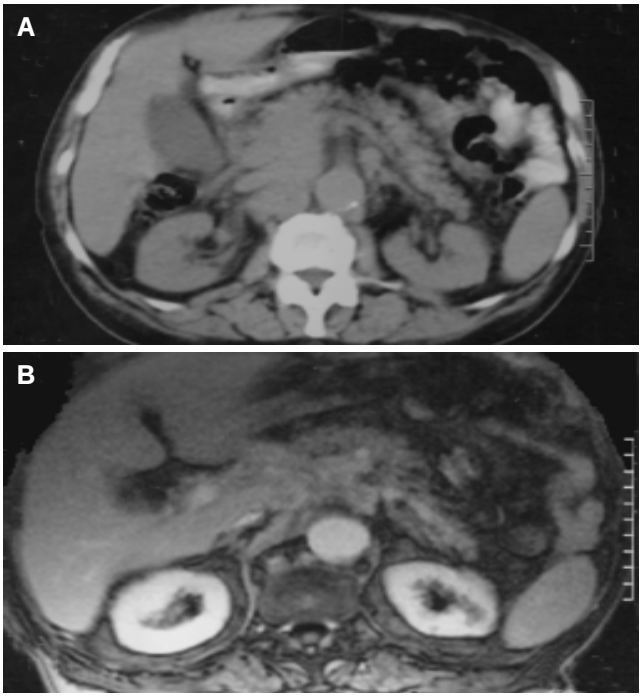

Figure 1 A: Abdominal CT scan showing the head of the pancreas and the uncinate process blurred. B: The mass in the pancreatic head and especially the uncinate process in MRI scan.

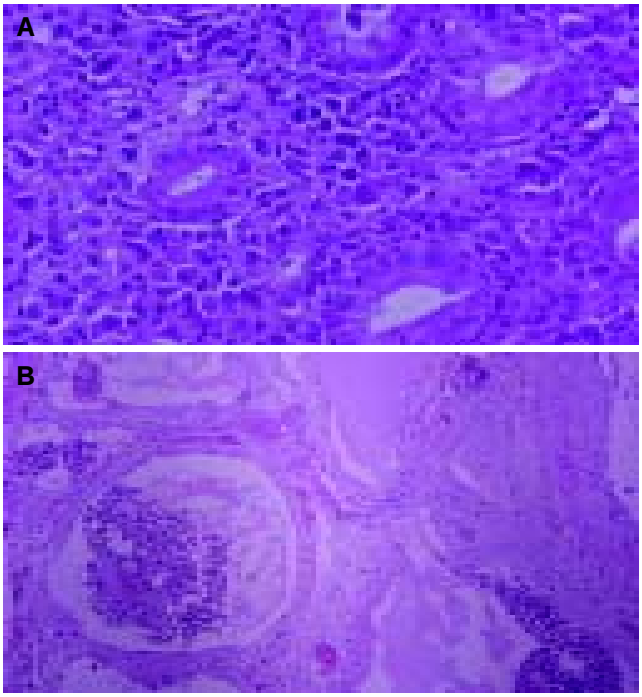

Figure 3 A: Duodenal mucosa infiltrated by polymorphous neoplastic lymphoid cells with eosinophilic cytoplasm and large nuclei. Small numbers of acute inflammatory cells are also present (hematoxylin-eosin ×400). B: Connective tissue and vascular lumens with neoplastic emboli with similar morphologic features as in the duodenal biopsy (hematoxylin-eosin ×200).

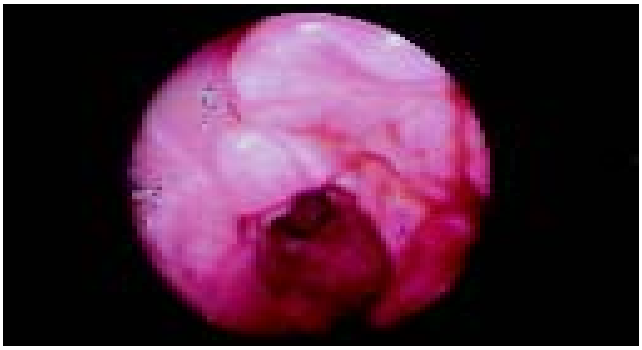

Figure 2 Endoscopic view of the ulcerated mass-like deformity of the duodenal bulb with a friable surface.

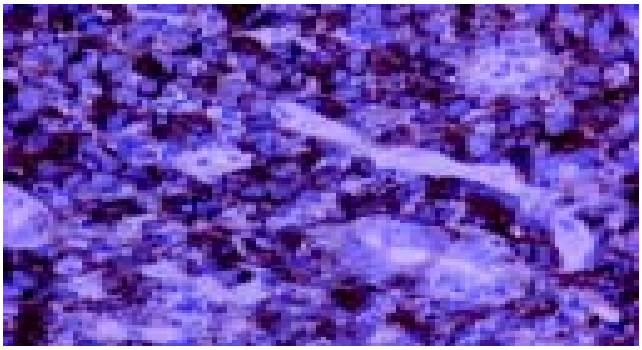

Figure 4 Strong CD30 immunohistochemical expression of lymphoma cells in the duodenal mucosa (×400).

the diagnosis of anaplastic large cell lymphoma (ALCL), of T-cell lineage, ALK negative. Fluorescent *in situ* hybridization (FISH) using LSI ALK dual color, break apart rearrangement probe (Abbott GmbH and Company, KG, Wiesbaden-Delkenheim, Germany) was performed in paraffin-embedded tissue sections from both specimens. Presence of two fused yellow signals or two adjacent (one orange and one green signals) in 200 non-overlapping tumor-cell nuclei showed lack of ALK gene rearrangement at 2p23 region. Bone marrow biopsy showed no evidence of lymphoma involvement. The patient died in the Intensive Care Unit 2 d later due to hemodynamic instability.

DISCUSSION

PPL is an extremely rare neoplasm that may be confused with the most common pancreatic adenocarcinoma. The majority of PPL reported to date in literature have been classified as B-cell type, but several cases of T-cell pancreatic lymphomas have also been described[2]. Most cases are intermediate or high grade NHL with diffuse large B-cell lymphoma being the predominant type. Presenting symptoms are nonspecific, including abdominal pain, weight loss, nausea, vomiting. Systemic-B symptoms such as fever, chills and night sweats are uncommon. Imagining techniques such as CT, percutaneous U/S and recently endoscopic U/S are the most useful procedures to evaluate the staging of pancreatic masses, although they cannot identify their neoplastic nature. A cytohistological diagnosis can be performed by U/S and CT guided techniques, endoscopy and explorative laparotomy[2]. Chemotherapy treatment with CHOP (cyclophosphamide, adriamycin, vincristine, and prednisolone) is usually administrated in patients with lymphomas[1,2]. The accurate distinction of ALCL from non-lymphoid malignancies is critical from the standpoint of patient's management because primary ALCL responds to radically different chemotherapy than adenocarcinoma[5,6].

ALCL is an uncommon type of NHL, first described by Stein *et al.*, in 1985 as a pleomorphic large cell lymphoma with strong membrane and Golgi associated CD30/Ki-1 antigen expression in a very high percentage of neoplastic lymphoid cells, with the involvement of paracortical region and sinuses of lymph nodes[7]. In the latest World Health's Organization (WHO) classification of NHLs, ALCL is a distinctive nature T-cell lymphoma subtype[5]. Clinical presentations of ALCL include a systemic form with nodal and/or extranodal involvement, primary cutaneous ALCL, HIV-related ALCL and ALCL occurring as a secondary event in patients with lymphomatoid papulosis, mycosis fungoides and rarely Hodgkin disease. The main histologic patterns accepted by WHO are the common variant, the lymphohistiocytic and the small cell variant[5]. In these lymphomas, the most frequent genetic alteration is the translocation t (2; 5) (p23; q35) between the ALK gene on chromosome 2 and the nucleophosmin (NPM) gene on chromosome 5. As a result of this translocation, the hybrid (NPM-ALK) gene promotes the production of chimeric NPM-ALK protein. The NPM-ALK fusion chimeric protein can be detected immunohistochemically using monoclonal or polyclonal antibodies, by RT-PCR and FISH[5,8]. ALK immunohistochemical expression is detected in 60-85% of ALCL cases[5]. ALK+ ALCL is most frequent in the first decades of life, shows a male predominance and often has advanced stage disease with frequent B-symptoms and extranodal involvement. It also tends to respond better to chemotherapy than ALK-systemic ALCL[5,8].

Our patient was considered to be affected by PPL according to Dawson *et al.*, clinical criteria which include: (1) the absence of superficial lymphadenopathy or enlargement of mediastinal lymph nodes on chest radiography, (2) a normal leukocyte count in peripheral blood, (3) main mass in the pancreas with lymph-nodal involvement confined to the peripancreatic region, and (4) the absence of hepatic or splenic involvement[9]. The elevated values of LDH and β_2 microglobulin in addition to the clinical characteristics of our patient, such as intermittent fever, anorexia, weight loss and fatigue, also suggested the lymphoproliferative nature of the mass. Moreover, the presence of the mass in the pancreas at imaging techniques while the duodenum was normal in the first endoscopy, proved that it originated in the pancreas and not in the duodenum which is an extremely rare location also.

Only three patients with primary pancreatic ALCL are reported in the literature. The first case described in 1997 in Japan by Maruyama *et al.*, was diagnosed by both duodenal and surgical pancreatic biopsies[3]. The second case was published in 2003 in Israel by Cohen *et al.*, and was diagnosed by operative pancreatic biopsy[1]. Chim *et al.*, recently reported the third case and they supported the diagnosis on operative mesenteric lymph node material biopsy because the tumor resection was not possible[4]. In our case a pancreaticoduodenectomy, the "Whipple procedure" was not performed, as in the case of Chim *et al.*, because of a friable tissue consistency and patient's hemodynamic instability during surgery. Therefore, the diagnosis of our PPALCL was based on the biopsy material taken from duodenal mucosa (three small pieces) and the adhesion of pancreatic surface with gastric serosa.

LDH and β_2 microglobulin are considered to be tumor markers in lymphoproliferative disorders and have an important prognostic value[10,11]. According to the textbook of Sleisenger and Fordtran's, whenever a large mass is identified in the pancreas without biliary obstruction or pain the diagnosis of pancreatic lymphoma should be contemplated, particularly in the presence of an elevated serum LDH level[12]. A high LDH level was found in our patient in contrast to the three previously reported cases of PPALCL. The LDH values were normal in the cases of Chim *et al.*, and Cohen *et al.*, and non-recorded in the case of Maruyama *et al.* In addition, an elevated β_2 microglobulin level was noticed in our case such as reported in ALCL either ALK+ or ALK-in the study of Rassidakis *et al.*[11].

After chemotherapy administration, a remission of disease for 30 mo in the case reported by Cohen *et al.*, and for 18 mo in the case reported by Maruyama *et al.*, were achieved respectively, whereas in the recently reported case by Chim *et al.*, a partial remission of 6 mo duration was noticed because the patient died of disease progression. Our patient did not receive a postoperative chemotherapy because unfortunately he died 2 d after the explorative

Table 1 Clinical and pathologic data of primary pancreatic ALCL reported cases in chronological order

	Maruyama *et al*.[3]	Cohen *et al*.[1]	Chim *et al*.[4]	Present study
A/G	46/F	22/M	27/F	80/M
Clinical symptoms	Back pain, anorexia	Upper abdominal pain, upper GI bleeding	Upper abdominal pain, weight loss	FUO, anorexia, weight loss, fatigue
Physical examination	Icteric conjunctivae, flat and soft abdomen with mild tenderness	Pallor, epigastric mass	Epigastric mass	Leg edema
Radiological findings	CT: mass in pancreatic head, ERP: without pathologic changes in MPD	CT: mass in pancreatic head	CT: mass in pancreatic head	CT: mass in pancreatic head and uncinate process, MRI: CT findings+IVC compression
Endoscopy	Submucosal protrusion with erosion of the second portion of the duodenum	Duodenal bleeding near to Vater's papilla	Bleeding ulceration of the first portion of the duodenum	Ulcerated mass-like deformity of the duodenal bulb
Laboratory findings	ALT, AST, ALP, total, and direct bilirubin elevated, serum amylase decreased, LDH: ND	Peripheral eosinophilia, LDH: in normal range	LDH: in normal range	LDH: elevated, β_2 microglobulin: elevated
Surgical operation	Whipple's	Whipple's	Not performed	Not performed
Pathologic (IHC) findings	CD30+, CD45+, CD45RO+, EMA-, ALK:ND	CD30+, CD45RO+, CD3+, EMA+, ALK-	CD30+, CD45–, CD45RO+, ALK:ND	CD30+, CD45+, CD45RO+, EMA+, CD3-, ALK-
Treatment	MACOP-P	CHOP	CHOP	Glucocorticoids (symptomatic)
Follow up	NED at 18 mo	NED at 30 mo	6 mo, died of disease progression	Died due to hemodynamic instability 2 d after explorative laparotomy

A/G: age/gender, ALK: anaplastic lymphoma kinase, ALP: alkaline phosphatase, ALT: alanine aminotransferase, AST: aspartate aminotransferase, CHOP: chemotherapy regimen consisting of cyclophosphamide, adriamycin, vincristine and prednisolone, EMA: epithelial membrane antigen, ERP: endoscopic retrograde pancreatography, F: female, FUO: fever of unknown origin, GI: gastrointestinal, IHC: immunohistochemistry, IVC: inferior vena cava, LDH: lactate dehydrogenase, M: male, MACOP-P: chemotherapy regimen consisting of methotrexate, adriamycin, cyclophosphamide, vincristine, prednisolone and peplomycin, MPD: main pancreatic duct, ND: no data available, NED: no evidence of disease.

laparotomy.

The clinical information, laboratory and pathologic findings of the present case and the previously reported ones, are summarized in Table 1.

In conclusion, our case - added to the three published cases - is the fourth one of primary pancreatic ALCL, ALK-. From the clinical point of view, since most clinicians do not consider PPL in the differential diagnosis of a pancreatic mass, our case indicates that PPL should be suspected in a patient with pancreatic mass and elevated serum markers, particularly LDH and β_2 microglobulin. Biopsy specimens' results from either the mass or the adjacent infiltrated organs, such as the duodenum in our case, confirm the diagnosis and identify the lymphoma. Thus, an earlier diagnosis leads to an appropriate and timeable treatment and finally, a better prognosis.

REFERENCES

1 **Cohen Y**, Libster D, Amir G, Hiller N, Da'as N, Ben Yehuda D, Polliack A. Primary ALK positive anaplastic large cell lymphoma of the pancreas. *Leuk Lymphoma* 2003; **44**: 205-207

2 **Arcari A**, Anselmi E, Bernuzzi P, Berte R, Lazzaro A, Moroni CF, Trabacchi E, Valisa D, Vercelli A, Cavanna L. Primary pancreatic lymphoma. Report of five cases. *Haematologica* 2005; **90**: ECR09

3 **Maruyama H**, Nakatsuji N, Sugihara S, Atsumi M, Shimamoto K, Hayashi K, Tsutsumi M, Konishi Y. Anaplastic Ki-1-positive large cell lymphoma of the pancreas: a case report and review of the literature. *Jpn J Clin Oncol* 1997; **27**: 51-57

4 **Chim CS**, Ho J, Ooi GC, Choy C, Liang R. Primary anaplastic large cell lymphoma of the pancreas. *Leuk Lymphoma* 2005; **46**: 457-459

5 **Delsol G**, Ralfkiaer E, Stein H, Wright D, Jaffe ES. Anaplastic large cell lymphoma. In: Jaffe ES, Harris NL, Stein H, Vardiman JW, eds. Pathology & Genetics. Tumors of Haematopoetic and Lymphoid Tissues. *Lyon IARC Press* 2001: 230-235

6 **Yoshikawa I**, Murata I, Tanaka Y, Kanagawa K, Tabaru A, Itoh H, Otsuki M. Primary CD30 (Ki-1)-positive anaplastic large cell lymphoma of the duodenum. *Dig Dis Sci* 1996; **41**: 2343-2347

7 **Stein H**, Mason DY, Gerdes J, O'Connor N, Wainscoat J, Pallesen G, Gatter K, Falini B, Delsol G, Lemke H. The expression of the Hodgkin's disease associated antigen Ki-1 in reactive and neoplastic lymphoid tissue: evidence that Reed-Sternberg cells and histiocytic malignancies are derived from activated lymphoid cells. *Blood* 1985; **66**: 848-858

8 **Greer JP**, Kinney MC, Loughran TP Jr. T Cell and NK cell lymphoproliferative disorders. *Hematology* 2001; **72**: 259-281

9 **Dawson IM**, Cornes JS, Morson BC. Primary malignant lymphoid tumours of the intestinal Tract: Report of 37 cases with a study of factors influencing prognosis. *Br J Surg* 1961; **49**: 80-89

10 **Cooper D**. Tumor Markers. In: Goldman L, Ausiello D, eds. Cecil Textbook of Medicine, 22nd edition. *Philadelphia SAUNDERS* 2004: 1131-1134

11 **Rassidakis GZ**, Goy A, Medeiros JL, Jiang Y, Thomaides A, Remache Y, Cabanillas F, Sarris AH, Gilles F. Prognostic significance of Muc-1 expression in systemic anaplastic large cell lymphoma. *Clin Cancer Res* 2003; **9**: 2213-2220

12 **Fernandez-del Castillo C**, Jimenez RE. Pancreatic cancer, cystic pancreatic neoplasms, and other nonendocrine pancreatic tumors. In: Sleisenger & Fordtran's, eds. Gastrointestinal and Liver Disease, 7th edition. *Philadelphia SAUNDERS* 2002: 970-987

Science Editor Guo SY **Language Editor** Elsevier HK

PO Box 2345, Beijing 100023, China
www.wjgnet.com
wjg@wjgnet.com

ELSEVIER

World J Gastroenterol 2005;11(39):6225-6227
World Journal of Gastroenterology ISSN 1007-9327

• *CASE REPORT* •

Adenosquamous carcinoma arising within a retrorectal tailgut cyst: Report of a case

Zoran Krivokapic, Ivan Dimitrijevic, Goran Barisic, Velimir Markovic, Miodrag Krstic

Zoran Krivokapic, Ivan Dimitrijevic, Goran Barisic, Velimir Markovic, Miodrag Krstic, Institute for Digestive Diseases, Clinical Center of Serbia, Belgrade, Serbia and Montenegro
Correspondence to: Zoran Krivokapic, MD, FRCS, First Surgical Clinic, Koste Todorovica 6, Belgrade 11000, Serbia and Montenegro. scpy@beotel.yu
Telephone: +381-11-3031-830 Fax: +381-11-3031-830
Received: 2005-03-07 Accepted: 2005-04-02

Abstract

Retrorectal, developmental tail gut cysts, include dermoid cysts, rectal duplication cysts and retrorectal cyst-hamartomas. Retrorectal cyst-hamartomas (RCH) are derived from remnants of the tail gut, the most caudal part of the embryonic hind gut, which normally involutes by the 8th wk of embryonic development (3-8 mm stage). They have specific radiological and histopathological features that distinguish them from other similar formations (dermoid cysts, enteric duplication cysts and teratomas). We report a patient with adenosquamous carcinoma arising within RCH, who underwent complete resection of the cyst through anterior laparotomy, and reached complete (recurrence-free for 14 mo, so far) functional recovery. The cyst was incidentally discovered during hysterectomy 12 years ago. Diagnostic, therapeutic and histopathological aspects of this rare case are discussed. The mentioned period between diagnosis and surgical treatment suggests that RCH, given enough time, can develop malignant degeneration, and should be resected at the time of diagnosis.

Key words: Tailgut cyst; Malignant transformation

Krivokapic Z, Dimitrijevic I, Barisic G, Markovic V, Krstic M. Adenosquamous carcinoma arising within a retrorectal tailgut cyst: Report of a case. *World J Gastroenterol* 2005; 11 (39): 6225-6227
http://www.wjgnet.com/1007-9327/11/6225.asp

CASE REPORT

The report was about a 47-year-old woman with a family history, where both her mother and daughter underwent surgery for presacral cysts in other institutions. Both of these cysts were benign in nature. The patient also had a positive history of obstructional bronchitis. The presacral cyst was discovered 11 years ago during hysterectomy because of myomatous uterus. Physical examination showed a fistulous opening on the perianal skin near posterior commissure with no apparent communication with the cyst. Proctoscopic examination showed posterior extrinsic compression of the rectum. Aside from these findings, there were no other abnormalities. Laboratory studies showed anemia and hypoproteinemia (RBC 2, 40×10E12/L; HGB 79 g/L; total proteins 45 g/L). Abdominal ultrasound showed no abnormalities. Transrectal ultrasound showed the tailgut cyst posterior to and causing deformity of rectal wall. The scan identifies five layers of the rectal wall of which the outer hypoechoic layer represents the muscularis propria (Figure 1). There was no radiological evidence of extrapelvic disease. After preoperative immunological testing, because of hypersensitivity to a number of drugs, she underwent complete resection of the mass through anterior laparotomy. The cystic mass was loosely connected to the lower sacrum through fibrous attachments. Communication with the opening was not established. After removal of the intact cyst, the opening on perianal skin was sutured. The patient soon reached a complete functional recovery.

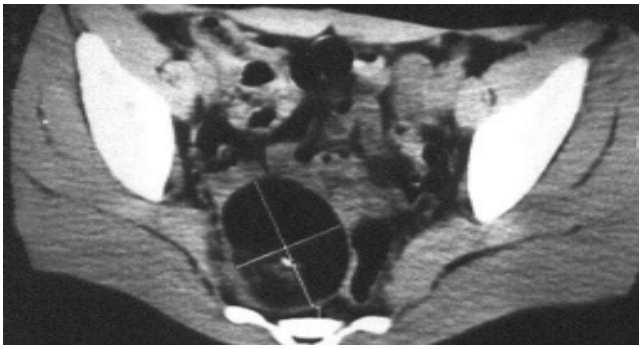

Figure 1 CT scan of the pelvis showing solitary cystic, retrorectal tumor.

PATHOLOGIC FINDINGS

Gross examination revealed irregularly shaped ovoid multiloculated cystic formation measuring 85 mm in greatest diameter (Figure 2). On cut surface, there was a large dominant cyst surrounded by number of small irregular cysts with diameter up to 15 mm, all of them showing mucopurulent content. Microscopically, a wide range of epithelial covering were represented, commonly found in gastrointestinal tract, focally eroded or displaced by respiratory-type epithelium in some areas. Ulcerated areas were surrounded with strong histiocyte infiltrate.

Figure 2 Showing irregularly shaped ovoid formation measuring 85 mm in greatest diameter.

Malignant alteration of the cyst was presented as ill-defined nodular thickening (7 mm), histologically presenting adenosquamous carcinoma, mostly well-differentiated adenocarcinoma admixed with foci of squamous differentiation or poorly differentiated areas and clear resection margins (Figures 3A and B).

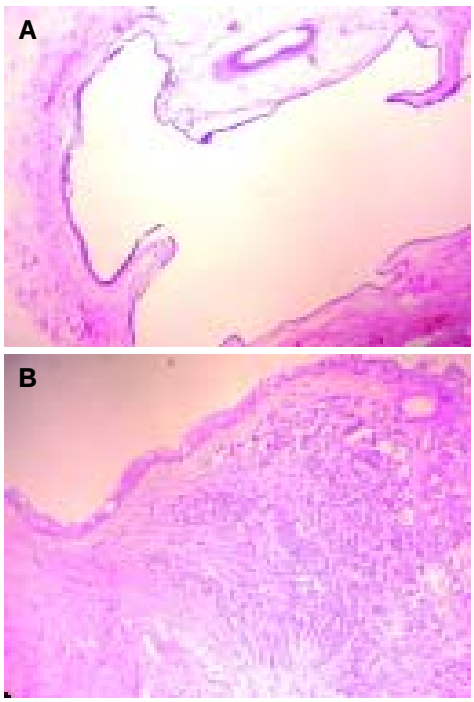

Figure 3 A and B Showing malignant alteration of the cyst histologically presenting adenosquamous carcinoma, mostly well differentiated adenocarcinoma admixed with foci of squamous differentiation or poorly differentiated areas and clear resection margins.

DISCUSSION

Retrorectal cyst-hamartomas (RCH) are reasonably rare, and they are always localized within the retrorectal space, which is bordered by rectum anteriorly, posteriorly by the sacrum, superiorly by the peritoneal reflection, inferiorly by the levator ani and coccygeus muscle, and laterally by the ureters and iliac vessels[1].

They can be found in all age groups including infancy, but they are more commonly reported in middle-aged females, and as mentioned, they are thought to arise from postnatal primitive gut remnants[2,3].

The clinical presentation of the cyst is non-specific, and it is most frequently related to a compressive effect of a growing mass within the pelvis (e.g. rectal fullness, urinary frequency, change in stool caliber, rectal bleeding)[4].

Around 50% of the cysts are discovered incidentally on routine physical examination[1]. Symptoms due to infection are also possible, and fistulous communication with the rectum or with the perianal skin can develop, often after inappropriate surgery. Recurring retrorectal abscess or recidivant perianal fistula can in fact be the infected tail gut cyst[1].

Plain radiography may show a soft tissue mass without destruction of the bone. Irigography can only confirm extramural compression of the rectum[1]. Computed tomography (CT) shows a well marginated retrorectal mass with CT numbers varying from water to soft tissue density.

Transrectal ultrasound is used to asses rectal and perirectal masses[1]. Its good sides are that it is simple, accurate and inexpensive. A diagnostic biopsy for cystic masses is not advised[4]. It may fail to confirm potential malignant diagnosis, and it carries a significant hazard of spillage of malignant cells, or may lead to the infection of the cyst.

Malignant transformation of RCH is very rare. Prasad *et al*.[5], identified 10 cases of malignancy in the literature. The outcome of the treatment of these malignancies varies from case to case. The most important factors for the prognosis are the time of the diagnosis, radicality of surgical resection and histopathological diagnosis; much better prognosis is with neuroendocrine cases, than with adenocarcinomas.

Complete excision of the cyst along with the margin of normal tissue followed by careful examination of the specimen is recommended. Anterior approach, as mentioned, was used in this case. Posterior approach is used for resection of the cyst localized below the level of S4, higher lesions are addressed through anterior approach, and smaller lesions can be reached through transvaginal approach. Combined anterior and posterior pelvic approach is advised by some authors[4] in cases of malignant transformation of the cyst.

Although this case demonstrates how malignant cyst can be successfully removed, with complete functional and oncological recovery, other experiences[4] show rapid and diffuse systemic failure and it is strongly recommended to aggressively address all RCHs as early as identifiable. For the same reason, adjuvant chemotherapy should be considered in some cases at least. Other interesting aspect of this case is the possible hereditary component, which certainly needs additional investigation.

REFERENCES

1 **Hutton KAR,** Benson EA. Case Report: Tailgut Cyst-Assesment with Transrectal Ultrasound. *Clin Radiol* 1992; **45**: 288-289
2 **Hjermstad BM,** Helwing EB. Tailgut cysts: report of 53 cases. *Am J Clin Pathol* 1988; **89**: 139-147
3 **Mourra N,** Caplin S, Parc R, Flejou JF. Presacral Neuroendo-

crine carcinoma Developed in a Tailgut Cyst: report of a case. *Dis Colon Rectum* 2003; **46**: 411-413
4 **Schwarz RE,** Lyda M, Lew M, Paz IB. A carcinoembryonic antigen-secreting adenocarcinoma arising within a retrorectal tailgut cyst: clinicopathological consideratinos. *Am J Gastroenterol* 2000; **95**: 1344-1347
5 **Prasad AR,** Amin MB, Randolph TL, Lee CS, Ma CK. Retrorectal cyst-hamartoma. Report of 5 cases with malignancy arising in 2. *Arch Pathol Lab Med* 2000; **124**: 725-729
6 **Bohm B,** Milsom JW, Fazio VW, Lavery IC, Church JM, Oakley JR. Our approach to the management of congenital presacral tumors in adults. *Int J Colorectal Dis* 1993; **8**: 134-138
7 **Madanes AE,** Kennison RD, Mitchhell G Jr. Removal of a presacral tumor via a Schuchatdt incision. *Obstet Gynecol* 1981; **57**: 945-965
8 **Freirer DT,** Stanley JC, Tompson NW. Retrorectal tumors in adults. *Surg Gynec Obstet* 1971; 681-686
9 **Abel ME,** Nelson R, Prasad ML, Pearl RK, Orsay CP, Abcarian H. Parasacrococcygeal approach for the resection of retrorectal developmental cysts. *Dis Colon Rectum* 1985; **28**: 855-858
10 **Spencer RJ,** Jackman RJ. Surgical management of precoccygeal cysts. *Surg Gynec Obstet* 1962; 449-452

Science Editor Guo SY **Language Editor** Elsevier HK

PO Box 2345, Beijing 100023, China
www.wjgnet.com
wjg@wjgnet.com

ELSEVIER

World J Gastroenterol 2005;11(39):6228-6231
World Journal of Gastroenterology ISSN 1007-9327

• *CASE REPORT* •

Agenesis of the gallbladder: A dangerously misdiagnosed malformation

Nicolas Peloponissios, Michel Gillet, René Cavin, Nermin Halkic

Nicolas Peloponissios, Michel Gillet, Nermin Halkic, Department of Surgery, Centre Hospitalier Universitaire Vaudois, Lausanne 1011, Switzerland
René Cavin, Department of Surgery, Centre Hospitalier de la Riviera, Montreux 1820, Switzerland
Correspondence to: Dr. Nermin Halkic, Department of Surgery/ CHUV/BH 15, Lausanne 1011,
Switzerland. nermin.halkic@chuv.hospvd.ch
Telephone: +41-21-314-22-48 Fax: +41-27-314-23-60
Received: 2003-08-02 Accepted: 2004-04-29

Abstract

Isolated agenesis of the gallbladder is a rare anomaly, often asymptomatic. However, one patient out of four presented with right upper abdominal pain, nausea, and fatty food intolerance. The condition is frequently mistaken with an excluded or sclero-atrophic gallbladder, regardless of the imaging modality used. Consequently, AG often leads to unnecessary and potentially dangerous laparoscopic surgery as described in a few case reports over the last 10 years. The aim of this study is to clarify the diagnostic and therapeutic approach of this unusual pathology. Two cases seen in our institutions were retrospectively reviewed, together with a review of the American and European literature. During laparoscopy, the absence of normal anatomical structures and the impossibility of pulling on the gallbladder to expose and dissect the triangle of Callot increases the risk of iatrogenic injury to biliary or portal structures. Depending on the experiment of the surgeon in laparoscopic procedure, this has to be taken into account to decide a conversion to laparotomy. A high index of suspicion is necessary when interpreting the radiological images. In case of doubt, a MRI-cholangiography is mandatory. Because of possible inherited transmission, relatives with a history of biliary symptoms should be investigated.

Key words: Gallbladder; Laparoscopy; Pathology

Peloponissios N, Gillet M, Cavin R, Halkic N. Agenesis of the gallbladder: A dangerously misdiagnosed malformation. *World J Gastroenterol* 2005; 11(39): 6228-6231
http://www.wjgnet.com/1007-9327/11/6228.asp

INTRODUCTION

In animals, the absence of a gallbladder has been a subject of research since the Aristotelian era[1]. Present in 1/6 of cases of biliary atresia[2], the isolated absence of the gallbladder and cystic duct is rare. Patients become symptomatic in 23% of cases[3,4], and agenesis of the gallbladder (AG) will almost always be misinterpreted as cholecystitis with cystic duct obstruction or as a sclero-atrophic gallbladder, therefore leading to unnecessary surgery. Reported for the first time in human beings by Bergman in 1702[5], it has since been described several times in case reports. During laparoscopic surgery, it represents a pitfall for the surgeon[6,7]: the biliary or portal structures can easily be injured during dissection as one searches for a gallbladder that does not exist. The absence of normal anatomical structures and the inability to pull on the gallbladder to dissect the triangle of Callot represent a risk of iatrogenic injury.

This review is based on a Medline and PubMed search from 1960 to 2003. Keywords used were agenesis of the gallbladder, absence of gallbladder, congenital syndromes, ultrasound, cholangiography, hepatobiliary scintigraphy, endoscopic retrograde cholangiopancreatography, magnetic resonance cholangiography, biliary dyskinesia, postcholecystectomy syndrome, laparoscopic surgery. Relevant literature was selected from the abstracts and cross-references of the retrieved literature were used to complete the search.

Between 1992 and 1999, two cases of AG were reported in our two institutions (Centre Hospitalier Universitaire Vaudois and Centre Hospitalier Cantonal de Fribourg), which are briefly described.

CASE REPORT

Case one

A 34-year-old man was admitted for right upper abdominal pain and bloating after meals for the last 9 years. The ultrasonography showed a scleroatrophic gallbladder and the intravenous cholangiogram revealed a very narrow biliary tree without opacification of the gallbladder. Total bilirubin was slightly elevated, and the direct fraction was twice the normal value. Other laboratory results were within normal limits. During the laparoscopic procedure, no gallbladder could be identified. A branch of the right hepatic duct was injured. Laparoscopy was converted to a median laparotomy. Initial dissection was carried out on the vena portis thought to be an ectopic gallbladder. Neither the intraoperative cholangiogram performed through the accidentally divided segmental duct nor the surgical exploration could demonstrate a gallbladder. The segmental biliary duct was ligated and the area drained.

Case two

A 76-year-old asymptomatic man went to his physician for

a check-up. Ultrasonography revealed a tumor of the right kidney, which was confirmed by a CT scan. Both failed to identify the gallbladder, but showed an increased size of the common bile duct. A median laparotomy was decided in order to deal with both pathologies. In place of the gallbladder, a small fibrous structure (1.5 cm×1 cm) was found and excised. The intraoperative cholangiogram did not show an ectopic gallbladder. A choledocotomy with the extraction of two gallstones was realized and an abdominal right nephrectomy performed. The histopathological analysis did not demonstrate any gallbladder tissue.

DISCUSSION

AG can be observed in both children and adults, with a median age of 46 at the time of diagnosis[8]. It is almost always a fortuitous finding during abdominal surgery or at autopsy. The prevalence range is 0.007-0.13%. The incidence of this malformation is slightly lower in surgical cholecystectomy series (0.007-0.027%)[9,10] than that in autopsy reports (0.04-0.13%)[5,11-13]. The male to female ratio is equal in autopsy reports[11,14] but seems to reach the same ratio (2-3 women for 1 man) in the clinical group as other biliary tract diseases[15,16]. AG occurs in association with other malformations in 40-65% of cases[8,11,17]. It is then found above all in children[8,11,13], leading in most cases to death in the first year of life[8,13,18,19]. Two congenital syndromes with multiple anomalies including gallbladder agenesis have been described: cerebrotendinous xanthomatosis[20] and the G syndrome[18]. AG has been occasionally mentioned with trisomy 18 and the Klippel-Feil syndrome[8,21,22]. Some authors[23-25] reported this anomaly in children with congenital malformations caused by thalidomide (up to 10% in Männl's series)[24].

This anomaly is explained by an embryological disturbance occurring during the 3rd wk of gestation and concerning the caudal portion of the anterior diverticulum of the primitive gut. It is an anomaly of the development of vessels located on each side of the gallbladder bud (sinus venosus cordis, omphaloenteric, and umbilical veins)[26]. This may explain the association of this anomaly with cardiac, vascular, gastro-intestinal, and abdominal wall malformations observed in the multiple fetal anomaly group[18]. AG may be inherited, with several familial cases observed, including across two generations[4,15,19,27-29]. These series suggest a non-sex-linked heredity with variable penetration.

Patients with AG will become symptomatic in about 23% of cases[4,19,30,31]. In 1988, Bennion *et al*.[8], found 208 symptomatic cases of AG in the literature. 90.1% presented with right upper abdominal pain, 66.3% with nausea or vomiting and 37.5% with fatty food intolerance. Thirty-two percent of these patients presented with a common bile duct dilatation whereas only 27% had gallstones. In the literature, AG is associated with a dilatation of the common duct or gallstones in 25-50% of cases[15,31,32]. The symptomatology and the increased frequency of gallstones has been attributed, by some authors, to biliary dyskinesia[16,30-34] and compared by others to a postcholecystectomy syndrome[8]. According to Toouli *et al*.[35], and Meshkinpour *et al*.[36], the biliary dyskinesia may be due to a hypertonic muscular retrograde contraction of the Oddi sphincter leading to a common duct dilatation, biliary stasis and gallstone formation[35,37]. Tanaka *et al*.[38], showed in 1983 that induction of a spasm of the Oddi sphincter reproduced the same painful symptomatology as biliary dyskinesia, and was associated with increased pressure in the common bile duct. However, it does not explain why the majority of patients become asymptomatic postoperatively (94% of cases in Bennion's series)[8]. Furthermore, the presence and development of a sphincter regulating the bile flow seems to be related to the presence or absence of the gallbladder. Indeed in animals without a gallbladder, the sphincter is poorly developed[39]. According to Lindskog[40], common bile duct dilatation without stones may simply indicate that the calculi have passed. Nevertheless, when we compare the frequency of common duct stones after cholecystectomy (5%) with the frequency of stones in AG (23%), we must recognize that this condition predisposes to calculus formation. Ahlberg *et al*.[9], did not show any changes in the bile lipid composition of patients with AG. However, the small number of patients in this study does not allow any conclusions to be drawn. Similar studies were realized in postcholecystectomy patients with conflicting results due to differences in methodology and patient selection[9,41-44].

When reviewing the literature, with the exception of two cases of AG[27,33], the preoperative investigations carried out on symptomatic patients failed to demonstrate the diagnosis. Whatever the method was used, cholangiography, hepatobiliary scintigraphy, ultrasound (US) or even endoscopic retrograde cholangiopancreatography (ERCP), the diagnosis proposed was almost always cystic duct obstruction or a small contracted gallbladder[3,6,7,45-47].

Ultrasonography is actually the investigation method of choice for the diagnosis of common bile duct stones, with a sensitivity of 95-98%. Crade *et al*.[48], defined three categories of abnormal ultrasounds of the gallbladder. The only case of AG in this study came from the second category (as also seen in other numerous cases described in the literature[7,30,46,47,49]): (1) shadowy gravity-dependent opacities within the gallbladder, (2) nonvisualization of the gallbladder lumen, and (3) nonshadowy opacities within the gallbladder lumen. The accuracy of US in these three different categories is 100%, 96%, and 61%, respectively[48]. The great difficulty in visualizing a contracted gallbladder on stones is well known[48,50]. According to Hammond[51], there is always either a recognizable segment of wall or a thin rim of bile identifying the gallbladder. He bases his assertion on MacDonald's *et al*.[52], and Raptopoulos's *et al*.[53], reports, which described the WES triad (demonstration of the gallbladder wall, the echo of the stone, and the acoustic shadow) or the double arc shadow (two parallel arcuate echogenic lines separated by a thin anechoic space with distal acoustic shadowing). However, the examination conditions as well as the examiner's experience does not always permit such accurate appreciation. Shadowy opacities misdiagnosed as stones can be due to intestinal gas artefacts or to other structures in close proximity, such as a calcified hepatic lesion or a surgical clip[46,51].

The hepatobiliary scintigraphy with new ^{99m}Tc-IDA agents and quantification of function is increasingly giving results,

especially in the detection of gallbladder anomalies[54]. Nevertheless, the nonvisualization of the gallbladder remains typical of cystic duct obstruction, as well as AG[54].

ERCP has been used in addition to other diagnostic methods[6,27,33,55,56]. Again, the nonvisualization of the gallbladder was interpreted as an occlusion of the cystic duct.

Magnetic resonance cholangiography is a noninvasive and well demonstrated imaging method in the evaluation of the biliary tract[57–59]. As it does not require contrast administration to visualize the bile, it is not compromised by biliary stasis. It can then demonstrate an excluded and/or ectopic gallbladder. However, this technique is not readily available. It may not yet replace ultrasound as the gold standard of acute gallbladder imaging but it is an ideal complementary study to inconclusive sonographic studies[60].

Selective arteriography of the hepatic artery has been proposed to prove gallbladder agenesis[6,61], but remains a very invasive procedure.

Reviewing the recent literature[62-65] concerning the AG, we noticed that symptomatic patients are still unnecessarily operated. In only two cases, AG was demonstrated by nonoperative means[27,33]. It was the evocation of this disorder in the initial assessment (US and cholangiography), which led to diagnosis. An ERCP increased the suspicion and AG was confirmed in each case by repeated US and cholangioscintigraphy during follow-up in asymptomatic patients.

In conclusion, AG is an unusual anomaly, mimicking a biliary stone disease in 23% of cases. This condition must be kept in mind in the differential diagnosis of ultrasonographically undetected or scleroatrophic gallbladder. When the WES triad or double arc shadow are not present, this congenital malformation should be suspected. An ectopic location of the gallbladder should be excluded. In case of doubt a conservative approach involving repeat investigations, in asymptomatic patients or after the acute phase, will avoid unnecessary surgery.

When AG is a laparoscopical discovery, the possibility of iatrogenic injury, by dissecting the portal structures without normal anatomical landmarks, has to be taken into account to decide a conversion to laparotomy. An intraoperative cholangiography should be realized through the common duct. Intraoperative ultrasound can demonstrate an ectopic gallbladder but is not always available. The lesser omentum, the falciform ligament, and the liver must be palpated. The exploration will also include a Kocher maneuver to explore the posterior wall of the duodenum as well as the head of the pancreas. The scar tissue in the gallbladder bed and the portal area must be carefully explored.

Associated malformations need not be systematically sought in adults, but family heredity has to be taken into account. Relatives with past or repetitive biliary symptomatology should have at least an ultrasonography when asymptomatic.

REFERENCES

1 **Vanderpool D,** Klingensmith W, Oles P. Congenital absence of the gallbladder. *Am J Surg* 1964; **30**: 324-330
2 **Rabinovitch J,** Rabinovitch P, Rosenblatt P, Pines B. Rare anomalies of the gallbladder. *Ann Surg* 1958; **148**: 161-168
3 **Serour F,** Klin B, Strauss S, Vinograd I. False-positive ultrasonography in agenesis of the gallbladder: a pitfall in the laparoscopic cholecystectomy approach. *Surg Laparosc Endosc* 1993; **3**: 144-146
4 **Nadeau LA,** Cloutier WA, Konecki JT, Morin G, Taylor RW. Hereditary gallbladder agenesis: twelve cases in the same family. *J Maine Med Assoc* 1972; **63**: 1-4
5 **Latimer EO,** Mendez FL, Hage W. Congenital absence of gallbladder. Report of three cases. *Ann Surg* 1947; **126**: 229-242
6 **Cabajo CM,** Martin del Olmo JC, Blanco AJ, Atienza SR. Gallbladder and cystic duct absence. An infrequent malformation in laparoscopic surgery. *Surg Endosc* 1997; **11**: 483-484
7 **Amaral JF,** Ferland R. Agenesis of the gallbladder: laparoscopic diagnosis. *Surg Laparosc Endosc* 1993; **3**: 337-341
8 **Bennion RS,** Thompson JEJ, Tompkins RK. Agenesis of the gallbladder without extrahepatic biliary atresia [see comments]. *Arch Surg* 1988; **123**: 1257-1260
9 **Ahlberg J,** Angelin B, Einarsson K, Leijd B. Biliary lipid composition and bile acid kinetics in patients with agenesis of the gallbladder with a note on the frequency of this anomaly. *Acta Chir Scand* 1978; **482**: 15-20
10 **Ferris DO,** Glazer IM. Congenital absence of gallbladder. Four surgical cases. *Arch Surg* 1965; **91**: 359-361
11 **Monroe SE,** Ragen FJ. Congenital absence of the gallbladder. *California Medicine* 1956; **85**: 422-423
12 **Mouzas G,** Wilson AK. Congenital absence of the gall-bladder with stone in the common bile-duct. *Lancet* 1953; **1**: 628-629
13 **Tallmage GK.** Congenital absence of the gallbladder. *Arch Pathol* 1938; **26**: 1060-1062
14 **Heffernon EW,** Weber CM. Congenital absence of the gallbladder. *JAMA* 1960; **174**: 844-895
15 **Wilson JE,** Deitrick JE. Agenesis of the gallbladder: case report and familial investigation. *Surgery* 1986; **99**: 106-109
16 **Sanders GB,** Flores T, Arriola P. Congenital absence of the gallbladder and cystic duct: a review of the literature and report of a case. *Am Surg* 1968; **34**: 750-754
17 **Haughton V,** Lewicki AW. Agenesis of the gallbladder. Is preoperative diagnosis possible? *Radiology* 1973; **106**: 305-306
18 **Turkel SB,** Swanson V, Chandrasoma P. Malformations associated with congenital absence of the gall bladder. *J Med Genet* 1983; **20**: 445-449
19 **Sterchi JM,** Baine RW, Myers RT. Agenesis of the gallbladder-an inherited defect? *South Med J* 1977; **70**: 498-499
20 **Winter RB,** Baraitser M. Multiple congenital anomalies. a diagnostic compendium. First edition ed. Cambridge: *Chapman and Hall Medical* 1991: 109
21 **Gajic SI.** Gallbladder agenesis in a patient with Klippel-Feil syndrome [letter]. *Arch Pathol Lab Med* 1981; **105**: 682-683
22 **Warkany J,** Passarge E, Smith LB. Congenital malformations in autosomal trisomy syndromes. *Am J Dis Child* 1966; **112**: 502-517
23 **Schinzel A.** Phocomelia and additional anomalies in two sisters. *Hum Genet* 1990; **84**: 539-541
24 **Mannl HF.** Gallbladder agenesis. *Med Welt* 1978; **29**: 1969-1974
25 **Kreipe U.** Abnormalities of internal organs in thalidomide embryopathy. A contribution to the determination of the sensitivity phase in thalidomide administration during early pregnancy. *Arch Kinderheilkd* 1967; **176**: 33-61
26 **Blechschmidt CM.** Agenesis of the gallbladder-borderline-case of normality? *Anat Anz* 1982; **151**: 281-285
27 **Venuta A,** Laudizi L, Miceli F, Pantusa M, Laudizi Z. Agenesis of the gallbladder. Description of 2 cases in 2 siblings. *Pediatr Med Chir* 1989; **11**: 465-466
28 **Becker IW,** Mastroni PP. Congenital absence of the gallbladder with a family history. *Am Surg* 1979; **45**: 541-542
29 **Kobacker JL.** Congenital absence of the galbladder: a possible hereditary defect. *Ann Int Med* 1950; **25**: 1008-1012
30 **Jackson RJ,** McClellan D. Agenesis of the gallbladder. A cause of false-positive ultrasonography. *Am Surg* 1989; **55**: 36-40
31 **Dickinson CZ,** Powers TA, Sandler MP, Partain CL. Congenital absence of the gallbladder: another cause of false-

positive hepatobiliary image. *J Nucl Med* 1984; **25**: 70-72
32 **Langley JR,** Hull DC. Congenital absence of the gallbladder: Review of the literature and report of a new case. *Am Surg* 1974; **40**: 548-551
33 **O'Sullivan J,** O'Brien PA, MacFeely L, Whelton MJ. Congenital absence of the gallbladder and cystic duct: nonoperative diagnosis. *Am J Gastroenterol* 1987; **82**: 1190-1192
34 **Frey C,** Bizer L, Ernst C. Agenesis of the gallbladder. *Am J Surg* 1967; **114**: 917-926
35 **Toouli J,** Geenen JE, Hogan WJ, Dodds WJ, Arndorfer RC. Sphincter of Oddi motor activity: a comparison between patients with common bile duct stones and controls. *Gastroenterology* 1982; **82**: 111-117
36 **Meshkinpour H,** Mollot M, Eckerling GB, Bookman L. Bile duct dyskinesia. Clinical and manometric study. *Gastroenterology* 1984; **87**: 759-762
37 **Madden JL.** Common duct stones. Their origin and surgical management. *Surg Clin North Am* 1973; **53**: 1095-1113
38 **Tanaka M,** Ikeda S, Nakayama F. Continuous measurement of common bile duct pressure with an indwelling microtransducer catheter introduced by duodenoscopy: new diagnostic aid for postcholecystectomy dyskinesia-a preliminary report. *Gastrointest Endosc* 1983; **29**: 83-88
39 **Gilloteaux J.** Introduction to the biliary tract, the gallbladder, and gallstones. *Microsc Res Tech* 1997; **38**: 547-551
40 **Lindskog BI.** Congenital absence of the gallbladder. *Acta Chir Scand* 1973; **139**: 208-209
41 **Almond HR,** Vlahcevic ZR, Bell CCJ, Gregory DH, Swell L. Bile acid pools, kinetics and biliary lipid composition before and after cholecystectomy. *N Engl J Med* 1973; **289**: 1213-1216
42 **Pomare EW,** Heaton KW. The effect of cholecystectomy on bile salt metabolism. *Gut* 1973; **14**: 753-762
43 **Kimball A,** Pertsemlidis D, Panveliwalla D. Composition of biliary lipids and kinetics of bile acids after cholecystectomy in man. *Am J Dig Dis* 1976; **21**: 776-781
44 **Shaffer EA,** Small DM. Biliary lipid secretion in cholesterol gallstone disease. The effect of cholecystectomy and obesity. *J Clin Invest* 1977; **59**: 828-840
45 **Belli G,** D'Agostino A, Iannelli A, Rotondano G, Ceccarelli P. Isolated agenesis of the gallbladder. An intraoperative problem. *Minerva Chir* 1997; **52**: 1119-1121
46 **Kestenholz PB,** von FM, Harder F. Agenesis of the gallbladder in adults: a laparoscopic diagnosis. *Chirurg* 1997; **68**: 643-645
47 **Azmat N,** Francis KR, Mandava N, Pizzi WF. Agenesis of the gallbladder revisited laparoscopically. *Am J Gastroenterol* 1993; **88**: 1269-1270
48 **Crade M,** Taylor KJ, Rosenfield AT, de GC, Minihan P. Surgical and pathologic correlation of cholecystosonography and cholecystography. *Am J Roentgenol* 1978; **131**: 227-229
49 **Hershman MJ,** Southern SJ, Rosin RD. Gallbladder agenesis diagnosed at laparoscopy. *J R Soc Med* 1992; **85**: 702-703
50 **Vas W,** Salem S. Cholecystosonography in diagnosis of cholelithiasis-pathologic and radiographic correlation. *J Can Assoc Radiol* 1980; **31**: 116-119
51 **Hammond DI.** Unusual causes of sonographic nonvisualization or nonrecognition of the gallbladder: a review. *J Clin Ultrasound* 1988; **16**: 77-85
52 **MacDonald FR,** Cooperberg PL, Cohen MM. The WES triad-a specific sonographic sign of gallstones in the contracted gallbladder. *Gastrointest Radiol* 1981; **6**: 39-41
53 **Raptopoulos V,** D'Orsi C, Smith E, Reuter K, Moss L, Kleinman P. Dynamic cholecystosonography of the contracted gallbladder: the double- arc-shadow sign. *Am J Roentgenol* 1982; **138**: 275-278
54 **Gad MA,** Krishnamurthy GT, Glowniak JV. Identification and differentiation of congenital gallbladder abnormality by quantitative technetium-99m IDA cholescintigraphy. *J Nucl Med* 1992; **33**: 431-434
55 **Lotz G,** Stahlschmidt M. Agenesis of the gallbladder. *Chirurg* 1986; **57**: 37-39
56 **Kennard GK.** Congenital agenesis of the gallbladder. A diagnostic problem. Report of a case. *Mil Med* 1985; **150**: 283-285
57 **Chan FL,** Chan JK, Leong LL. Modern imaging in the evaluation of hepatolithiasis. *Hepatogastroenterology* 1997; **44**: 358-369
58 **Vanbeckevoort D,** Van HL, Ponette E, Marchal G, Bosmans H, De CB. Imaging of gallbladder and biliary tract before laparoscopic cholecystectomy: comparison of intravenous cholangiography and the combined use of HASTE and single-shot RARE MR imaging. *J Belge Radiol* 1997; **80**: 6-8
59 **Schuster DM,** Pedrosa MC, Robbins AH. Magnetic resonance cholangiography. *Abdom Imaging* 1995; **20**: 353-356
60 **Adusumilli S,** Siegelman ES. MR imaging of the gallbladder. Magn Reson Imaging. *Clin N Am* 2002; **10**: 165-184
61 **di Natale I.** Agenesis of the gallbladder (diagnostic considerations). Apropos of a case. *Chir Ital* 1985; **37**: 618-623
62 **Gotohda N,** Itano S, Horiki S, Endo A, Nakao A, Terada N, Tanaka N. Gallbladder agenesis with no other biliary tract abnormality: report of a case and review of the literature. *J hepatobiliary Pancreat Surg* 2000; **7**: 327-330
63 **Fisichella PM,** Di Stefano A, Di Carlo I, La Greca G, Russello D, Latteri F. Isolated agenesis of the gallbladder: report of a case. *Surg Today* 2002; **32**: 78-80
64 **Sarli L,** Violi V, Gobbi S. Laparoscopic diagnosis of gallbladder agenesis. *Surg Endosc* 2000; **14**: 373
65 **Dell'Abate P,** Iosca A, Galimberti A, Faraci R, Soliani P, Foggi E. Agenesis of the gallbladder found at laparoscopy in an adult patient with cardiac malformation. *Dig Surg* 2000; **17**: 284-286

Science Editor Zhang JZ **Language Editor** Elsevier HK

PO Box 2345, Beijing 100023, China
www.wjgnet.com
wjg@wjgnet.com

ELSEVIER

World J Gastroenterol 2005;11(39):6232-6234
World Journal of Gastroenterology ISSN 1007-9327

• *CASE REPORT* •

Treatment of a duodenal perforation secondary to an endoscopic sphincterotomy with clips

Panagiotis Katsinelos, George Paroutoglou, Basilios Papaziogas, Athanasios Beltsis, Stavros Dimiropoulos, Konstantinos Atmatzidis

Panagiotis Katsinelos, George Paroutoglou, Athanasios Beltsis, Stavros Dimiropoulos, Department of Endoscopy and Motility Unit, "G.Gennimatas" Hospital, Ethnikis Aminis 41, 54635 Thessaloniki, Greece
Basilios Papaziogas, Konstantinos Atmatzidis, 2nd Surgical Clinic, "G.Gennimatas" Hospital, Aristotle University of Thessaloniki, Ethnikis Aminis 41, 54635 Thessaloniki, Greece
Correspondence to: Dr. Panagiotis Katsinelos, Department of Endoscopy and Motility Unit, "G.Gennimatas" Hospital, Ethnikis Aminis 41, 54635 Thessaloniki, Greece. pantso@the.forthnet.gr
Telephone: +30-2310-211221 Fax: +30-2310-210401
Received: 2004-11-29 Accepted: 2005-02-18

Abstract

Perforation is one of the most serious complications of endoscopic sphincterotomy (ES) necessitating immediate surgical intervention. We present a case of successful management of such a complication with endoclipping. A 85-year-old woman developed duodenal perforation after ES. The perforation was identified early and its closure was achieved using three metallic clips in a single session. There was no procedure-related morbidity or complications and our patient was discharged from hospital 10 d later. Endoclipping of duodenal perforation induced by ES is a safe, effective and alternative to surgery treatment.

Key words: Endoclipping; Duodenal perforation; Endoscopic sphincterotomy

Katsinelos P, Paroutoglou G, Papaziogas B, Beltsis A, Dimiropoulos S, Atmatzidis K. Treatment of a duodenal perforation secondary to an endoscopic sphincterotomy with clips. *World J Gastroenterol* 2005; 11(39): 6232-6234
http://www.wjgnet.com/1007-9327/11/6232.asp

INTRODUCTION

The most serious complications of endoscopic sphincterotomy (ES) are pancreatitis, hemorrhage and perforation[1]. Although perforation is uncommon, occurring in less than 1% of patients undergoing ES, it is associated with high morbidity and mortality[2].

Applications of endoscopic metallic clips other than the treatment of bleeding lesions have been reported, such as sealing of iatrogenic endoscopic perforations[3].

We describe a 85-year-old woman who developed symptomatic post-ES perforation and was successfully treated by endoscopic clip placement. To our knowledge, this is the second reported case of post-ES perforation that was treated endoscopically with clip placement.

CASE REPORT

A 85-year-old woman was admitted because of recurrent episodes of abdominal pain, fever, and jaundice over a period of 1 mo. Her past medical history revealed a cholecystectomy 10 years ago, mild heart failure and hypertension. Laboratory tests showed cholestasis. US demonstrated intra- and extra-hepatic biliary dilatation. Magnetic resonance imaging cholangiography showed a large stone (diameter 18 mm) in the lower part of the common bile duct.

Endoscopic biliary sphincterotomy was performed using an electrosurgical unit with standard pull sphincterotome without the use of guidewire. The length of sphincterotomy was large, according to the size of the common bile duct stone. The extraction of the stone was impossible. We performed a successful mechanical lithotripsy and the fragments were extracted with a basket.

Twelve hours later, the patient complained of moderate pain in the upper abdomen, which diminished after analgesics administration. Physical examination disclosed fever of 37.8 ℃ but no signs of peritoneal irritation. A chest X-ray was normal. Laboratory studies revealed an elevated ESR (75 mm/h) and C-reactive protein concentration (3.62 mg/dL, normal <0.5 mg/dL). The WBC count was 11 888/μL (normal 4 000-8 000/μL) and the percentage of neutrophils was high (86%).

An abdominal CT demonstrated free retroperitoneal air and a small amount of dirty fluid around the duodenum as well as enhancement of choledochal duct with gastrografin (Figure 1).

We decided to try endoscopic repair of the duodenal perforation, after an extensive discussion about the type of therapy with her relatives, and an informed consent was signed. With a rotating colon clipping device (HX-6UR-1, Olympus), five clips were carefully placed in the upper part of sphincterotomy. Although two were misclipped, the other three were well fitted (Figure 2). A standard 0.035-inch biliary super-stiff guidewire (Jagwire, Microvasive) was then passed endoscopically and fluoroscopically into the jejunum and a nasogastric tube with the tip removed was passed into the duodenum and centered over the perforation site.

Intravenous hyperalimentation and treatment with antibiotics (ciprofloxacin 1 g/d and metronidazole 1.5 g/d)

were administered. Clinically, the patient did well and the abdominal pain that was initially present decreased, no signs of peritonitis developed and the fever subsided. Three days later, a water-soluble contrast was instilled via the nasogastric tube and on radiography no leakage of contrast was found. She began to eat 7 d after the clipping procedure and was discharged on d 10. A second abdominal CT performed 20 d later demonstrated resolution of the retroperitoneal air and inflammation.

No further problems occurred after 5 mo of follow-up.

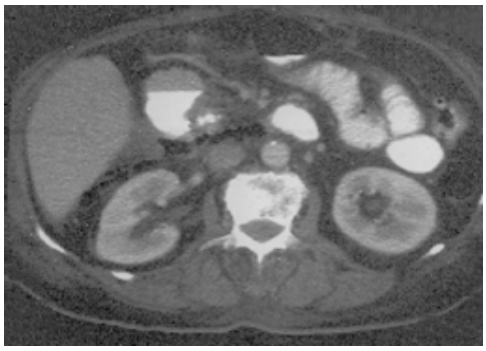

Figure 1 Free retroperitoneal air and a small amount of dirty fluid around the duodenum.

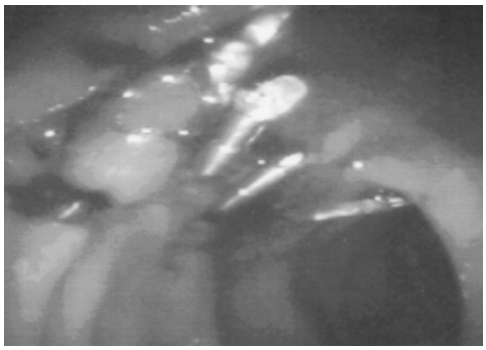

Figure 2 Three clips placed on the upper part of sphincterotomy.

DISCUSSION

The approach to management of duodenal perforation after ES is controversial. Some investigators advocate conservative management based on clinical course, while others advocate surgical repair in all cases because of the complications associated with delayed operative intervention[4-6].

Dunham *et al*.[4], have reported about the outcome after conservative treatment in seven patients when free air was recognized immediately. Two of these patients died after the development of toxic shock despite delayed surgery. In a recent prospective study by Freeman *et al*.[1], five of the eight ES perforations were severe and one resulted in death.

In recent years, endoscopic clip placement, developed as a hemostatic procedure, has been used for closure of iatrogenic perforations[3]. Binmoeller *et al*.[7], described the first successful endoscopic closure of an iatrogenic perforation by using a clip-application device in 1993. Subsequently, the use of this method in the esophagus[8,9], duodenum[10], and colon[11,12] has been described. Baron *et al*.[13], described the first case of a 39-year-old man with familial adenomatous polyposis who presented duodenal perforation after a papillectomy and ES. They identified immediately free air in the retroperitoneum and the perforation was closed by the use of a clipping device and the placement of five clips.

The decision about the treatment after an iatrogenic perforation must be made very carefully, because conservative treatment may surely be used when perforation is small and retroperitoneal, non-operative management failed but with delayed laparotomy results in greater contamination necessitating major surgery. In our patient, the perforation was small, well defined, and detected without delay, thus meeting all the criteria for a conservative approach. Therefore, we decided to try to close the perforation immediately with metallic clips. After successful endoscopic clipping, our patient recovered quickly without any complication and was discharged early from hospital. The immediate closure of the perforation prevented any further abdominal contamination and contributed to the good outcome of the patient. Although this complication could be resolved with the conservative management strategy of nasogastric suction and antibiotics, we believe that our patient with the size of the duodenal wall defect may require prolonged hospitalization and/or surgical management.

It must be emphasized that the endoclipping device has been designed for use through the end-viewing endoscope. Therefore, the deployment of clips is more difficult when a side-viewing endoscope is used and damage to the endoclipping device may occur. The deployment of the clips requires significant experience from the endoscopist when a duodenoscope is used, especially in a limited space as is the major papilla area. The placement of the clips should be made carefully on the upper part of the sphincterotomy to avoid closure of pancreatic or common bile duct orifice.

In cases of iatrogenic perforation, if the defect is closed early with metallic clips, contamination of the peritoneal cavity or retroperitoneal space can be minimized. Although the difference in outcome between conservative management and clipping is unknown, clipping therapy is more certain to prevent contamination.

In conclusion, when perforation is caused by ES, endoscopic closure using metallic clips without laparotomy might be the first choice of treatment, although it is essential to monitor the patient closely, with particular attention to signs of transition from localized to generalized peritonitis.

REFERENCES

1 **Freeman ML,** Nelson DB, Sherman S, Haber GB, Herman ME, Dorsher PJ, Dorsher PJ, Moore JP, Fennerty MB, Ryan ME, Shaw MJ, Lande JD, Pheley AM. Complications of endoscopic sphincterotomy. *N Engl J Med* 1996; **335**: 909-918

2 **Cotton PB,** Lehman G, Vennes J, Geenen JE, Russell RC, Meyers WC, Liguory C, Nickl N. Endoscopic sphincterotomy complications and their management: a attempt at consensus. *Gastrointest Endosc* 1991; **37**: 383-393

3 **Raju GS,** Gajula L. Endoclips for GI endoscopy. *Gastrointest Endosc* 2004; **59**: 267-279

4 **Dunham F,** Bourgeois N, Gelin M, Jeanmart J, Toussaint J, Cremer M. Retroperitoneal perforations following endoscopic

sphincterotomy: clinical course and management. *Endoscopy* 1982; **14**: 92-96

5 **Chung RS,** Sivak MV, Ferguson DR. Surgical decision in the management of duodenal perforation complicating endoscopic sphincterotomy. *Am J Surg* 1993; **165**: 700-703

6 **Chaudhary A,** Aranya RC. Surgery in perforation after endoscopic ephincterotomy: sonner, later, or not at al? *Ann R Coll Surg* 1996; **78**: 206-208

7 **Binmoeller KF,** Grimm H, Soehendra N. Endoscopic closure of a perforation using metallic clips after snare excision of a gastric leiomyoma. *Gastrointest Endosc* 1993; **39**: 172-174

8 **Wewalka FW,** Clodi PH, Haidinger D. Endoscopic clipping of esophageal perforation after pneumatic dilatation for achalasia. *Endoscopy* 1995; **27**: 608-611

9 **Cipolletta L,** Bianco MA, Torindano G, Marmo R, Piscopo R, Meucc C. Endoscopic clipping of perforation following pneumatic dilation of esophagojejunal anastomotic strictures. *Endoscopy* 2000; **32**: 720-722

10 **Roses LL,** Ramirez AG, Seco AL, Blanco ES, Alonso DL, Avila S, Lopez BU. Clip closure of a duodenal perforation secondary to a biliary stent. *Gastrointest Endosc* 2000; **51**: 487-489

11 **Mana F,** Vogelaere KD, Urban D. Iatrogenic perforation of the colon during diagnostic colonoscopy: endoscopic treatment with clips. *Gastrointest Endosc* 2001; **54**: 258-259

12 **Yoshikane H,** Hidano H, Sakakibara A, Ayakawa T, Mori S, Kawashima H, Goto H, Niwa Y. Endoscopic repair by clipping of iatrogenic colonic perforation. *Gastrointest Endosc* 1997; **46**: 464-466

13 **Baron TH,** Gostout CJ, Herman L. Hemoclip repair of a sphincterotomy-induced duodenal perforation. *Gastrointest Endosc* 2000; **52**: 566-568

Science Editor Wang XL and Guo SY **Language Editor** Elsevier HK

PO Box 2345, Beijing 100023, China
www.wjgnet.com
wjg@wjgnet.com

ELSEVIER

World J Gastroenterol 2005;11(39):6235-6237
World Journal of Gastroenterology ISSN 1007-9327

• *CASE REPORT* •

Ruptured hepatoblastoma with massive internal bleeding in an adult

Hung-Yen Ke, Jia-Hui Chen, Yee-Min Jen, Jyh-Cherng Yu, Chung-Bao Hsieh, Cheng-Jueng Chen, Yao-Chi Liu, Teng-Wei Chen, De-Chuan Chan

Hung-Yen Ke, Jia-Hui Chen, Yee-Min Jen, Jyh-Cherng Yu, Chung-Bao Hsieh, Cheng-Jueng Chen, Yao-Chi Liu, Teng-Wei Chen, De-Chuan Chan, Division of General Surgery, Department of Surgery, Department of Radio-Oncology, Tri-Service General Hospital, National Defense Medical Center, Taipei, Taiwan, China
Correspondence to: Dr. De-Chuan Chan, Division of General Surgery, Tri-Service General Hospital, 325, Sec. 2, Chen-Kung Road, Neihu 114, Taipei, Taiwan, China. drkehy@yahoo.com.tw
Telephone: +886-2-8792-7191 Fax: +886-2-8792-7273
Received: 2005-04-18 Accepted: 2005-05-24

Abstract

Hepatoblastoma is the most common primary hepatic tumor of children. However, only a very few cases have been reported in adults. Most studies support treatment with chemotherapy followed by surgical resection. We present the first reported case of adult hepatoblastoma in Taiwan. A 52-year-old female suffered from sudden onset of abdominal pain and general weakness for days. Internal bleeding with hemorrhagic shock was suspected and two massive lesions in both lobes of the liver with hemoperitoneum were noted from imaging studies. Surgical resection of the larger left lobe tumor and radio-frequency ablation of the right smaller one were performed. The histopathology diagnosis was of a hepatoblastoma.

Key words: Adult hepatoblastoma; Hepatoblastoma rupture; Internal bleeding; Hepatoblastoma; Mixed type hepatoblastoma

Ke HY, Chen JH, Jen YM, Yu JC, Hsieh CB, Chen CJ, Liu YC, Chen TW, Chan DC. Ruptured hepatoblastoma with massive internal bleeding in an adult. *World J Gastroenterol* 2005; 11(39): 6235-6237
http://www.wjgnet.com/1007-9327/11/6235.asp

INTRODUCTION

Hepatoblastoma is the most common tumor of the liver for children under the age of 2 years[1]. Reports of adult cases are extremely rare. Most of these tumors arise in the embryo during the development of the liver and contain embryonic features such as numerous mitoses. They sometimes show ribbon-like, rosette-like, or papillary formations[2]. We present the first case of adult hepatoblastoma that was reported in Taiwan.

CASE REPORT

The patient was a 52-year-old female, who suffered from abdominal discomfort and called into a regional hospital for help. Abdominal computed tomography (CT) revealed two large hepatic masses with intra-abdominal fluid accumulation. Hepatic tumor with rupture was suspected, and she was referred to our hospital for further evaluation. She had been relatively healthy in the past. There was no significant past history or family history. Laboratory studies showed the following values: AST 58 U/L; ALT 44 U/L; hemoglobin 74 g/L; platelet count 101 000/UL; hepatitis B antigen negative; anti-hepatitis B antibody positive; anti-hepatitis C antibody positive. CT scans of the abdomen (Figure 1) showed massive accumulation of intra-abdominal fluid and one large heterogeneous mass (c. 11.4 cm×18.8 cm×22 cm) with cystic and solid components in the left lobe of the liver. Another homogeneous well-enhanced lesion about 3 cm wide in segment 8 of the liver was also noted. Catheter angiography (Figure 2) showed a huge hepatic tumor with faint tumor blush in the left lobe and a 2.5 cm large hypervascular tumor in the right lobe. These were presumed to be hepatocellular carcinomas. Further intra-arterial embolization was not performed because of technical problems and lack of cooperation by the patient. We diagnosed a ruptured and bleeding hepatocellular carcinoma. Exploratory laparotomy with a left lateral hepatectomy was performed to resect the tumor. Intraoperative radio-frequency ablation (RFA) was also applied to the smaller tumor in the right lobe of the liver.

The specimen recovered consisted of an encapsulated mass measuring 22 cm×16 cm×15 cm in size with extensive necrosis and hemorrhage. Grossly, it was friable and soft in consistency (Figure 3). Microscopically, histopathology sections showed pictures of immature hepatocytic epithelial elements intermixed with prominent vessels and extramedullary hematopoiesis including all three lineages (Figure 4A). There was extensive tumor necrosis and hemorrhage. Immunohistochemical stains showed the following: vimentin positive (Figure 4B); myeloperoxidase (MPO) positive for the extramedullary hematopoietic myeloid series (Figure 4C); factor 8 positive for extramedullary hematopoietic megakaryocytes (Figure 4D); CD34 positive for vascular endothelium and hematoprogenitor cells; alpha fetoprotein negative; S100 positive. These pathology results were consistent with the diagnosis of a hepatoblastoma. The patient was discharged 10 d after the operation.

Figure 1 CT scans of the abdomen showed massive accumulation of intra-abdominal fluid and one large heterogeneous mass (c 11.4 cm×18.8 cm×22 cm) with cystic and solid components in the left lobe of the liver.

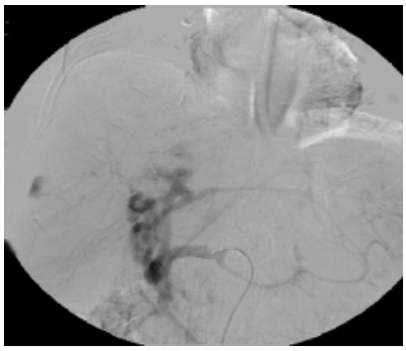

Figure 2 Catheter angiography showed a huge hepatic tumor with faint tumor blush in the left lobe and a 2.5 cm large hypervascular tumor in the right lobe. These were presumed to be hepatocellular carcinomas.

Figure 3 The specimen recovered consisted of an encapsulated mass measuring 22 cm×16 cm×15 cm in size with extensive necrosis and hemorrhage. Grossly, it was friable and soft in consistency.

DISCUSSION

Hepatoblastoma is a highly malignant tumor occurring in infants, and reports of adult cases are extremely rare. A review search in the literature revealed only 23 adult cases of hepatoblastoma including the present one. This case is also the first adult hepatoblastoma that was reported in Taiwan.

Ishank and Glunz classified hepatoblastomas into two groups in 1967: epithelial type and mixed epithelial and mesenchymal type[3]. The tumor type from this patient was distinguished from a hepatocellular carcinoma by the presence of angiodysplasia and also by the peculiar arrangement of bright and dark epithelial cells in sheets or ribbons[3-5]. This patient, therefore, had a tumor of the mixed epithelial and mesenchymal type according to this

Table 1 Summary of reported hepatoblastoma in adults

Case	Reporter	Sex/Age (yr)	Pathology type	Diagnosis	Survival time
1	Barnett[6] (1958)	M/35	Mixed	Embryonic tumor	Died 1 mo after surgery
2	Alexander[7] (1961)	F/68	Mixed	Primary mixed tumor	Postmortem
3	Ojima[8] (1964)	M/48	Mixed	Malignant mixed tumor	Postmortem
4	Kerr[5] (1966)	M/56	Mixed	Hepatic embryonic mixed tumor	Sudden death
5	Blanding[9] (1968)	M/84	Mixed	Malignant tumor	Died after biopsy
6	Cater[10] (1969)	M/78	Mixed	Hepatoblastoma	1 mo after surgery
7	Goldman[11] (1969)	F/65	Mixed	Rhabdomyosarco-hepatoma	Sudden death
8	Meyer[12] (1974)	F/19	Mixed	Hepatoblastoma	Not described
9	Ludwig[13] (1975, case 1)	F/53	Mixed	Mixed malignant tumor	Died after surgery
10	Ludwig[13] (1975, case 2)	M/40	Mixed	Mixed malignant tumor	Postmortem
11	Jameson[14] (1978)	F/51	Mixed	Hepatoblastoma	Postmortem
12	Yoshida[15] (1979)	M/60	Mixed	Hepatoblastoma	Died 2 mo after surgery
13	Honan[16] (1980)	F/27	Mixed	Mixed hepatoblastoma	Postmortem
14	Kishimoto[17] (1984)	M/60	Mixed	Malignant mixed tumor	Died 2 d after surgery
15	Kawarada[18] (1985, case 1)	M/43	Mixed	Nonhepatocytic malignant mixed tumor	Alive for 32 mo after surgery
16	Kawarada[18] (1985, case 2)	M/49	Mixed	Hepatocytic malignant mixed tumor	Postmortem
17	Sugino[2] (1989)	M/22	Epithelial	Hepatoblastoma	Died 9 mo after surgery
18	Altmann[19] (1992, case 1)	M/73	Mixed	Hepatoblastoma	Not described
19	Altmann[19] (1992, case 2)	F/35	Epithelial	Hepatoblastoma	Not described
20	Harada[20] (1995)	M/24	Mixed	Hepatoblastoma	Died 16 mo after surgery
21	Sugino[2] (1995)	F/22	Mixed	Hepatoblastoma	Alive for 38 mo after surgery
22	Ahn[1] (1997)	F/51	Mixed	Hepatoblastoma	Died 2 mo after surgery
23	Present case (2005)	F/52	Mixed	Hepatoblastoma	Alive 6 mo after surgery

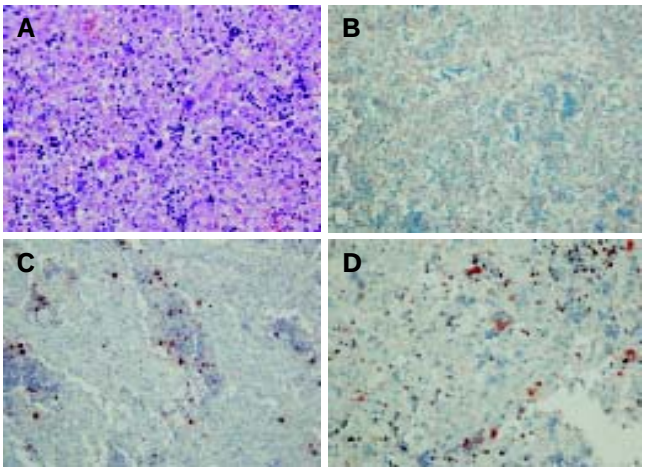

Figure 4 Immature hepatocytic epithelial elements intermixed with prominent vessels and extramedullary hematopoiesis including all three lineages (A). Vimentin positive (B); MPO positive for the extramedullary hematopoietic myeloid series (C); factor 8 positive for extramedullary hematopoietic megakaryocytes (D).

classification. Most cases in the literature are of the mixed type.

The precise mechanism to cause the tumor has been elusive; present investigations of the cytogenetic and molecular genetic aberrations in hepatoblastomas revealed involvement of chromosomal loci on 1q, 2 (or 2q), 4q, 8 (or 8q), and 20[21]. Loss of heterozygosity imprinting at locus 11p 15.5 also suggest a common genetic basis for hepatoblastoma[21]. Shin-ichi *et al*., found that abnormalities in Wnt signaling pathway seen in frequent mutation of the β-catenin gene may play a role in the genesis of hepatoblastoma[22]. They also found that the patients with hepatoblastoma with high expression of polo-like kinase 1 (PLK1) represented significantly poorer outcome[22]. Therefore, PLK1 may become a useful tool to develop new diagnostic as well as therapeutic strategies of hepatoblastoma.

Otherwise, only one of the previously reported cases was a 12-year-old boy who presented with a ruptured tumor with massive bleeding as we saw in this patient[23]. We successfully resected the larger hepatic tumor and treated the smaller one with RFA, although most adult cases of hepatoblastoma have been unresectable[4]. The clinical and pathological findings of previously reported cases and the present one are summarized in Table 1. The mean age of the 23 patients was 48.5 years and there were more males (13) than females (10). Eleven patients received surgery. Twenty one of these tumors were of the mixed type. Survival time ranged from 1 to 38 mo after surgery with a mean survival time of 9.7 mo. The prognosis for patients with this disease is very poor. Current treatments for the tumor include surgery and chemotherapy. Combination chemotherapy with adriamycin and cisplatin has been considered effective for hepatoblastoma[2]. Our patient has just been discharged and will be followed up.

REFERENCES

1 **Ahn HJ.** Mixed hepatoblastoma in an adult – A case report and literature review. *JKMS* 1997; **12**: 369–373
2 **Sugino K,** Dohi K, Matsuyama T, Asahara T, Tamamoto M. A case of hepatoblastoma occurring in an adult. *Jpn J Surg* 1989; **19**: 489–493
3 **Ishank KG,** Glunz PR. Hepatoblastoma and hepatocarcinoma in infancy and childhood: report of 47 cases. *Cancer* 1967; **20**: 396–422
4 **Inoue S,** Nagao T, Ishida Y, Wada C, Beck Y, Uchida H, Okudaira M. Successful resection of a large hepatoblastoma in a young adult: report of a case. *Surg Today* 1995; **25**: 974–977
5 **Kerr JFR.** Hepatic embryonic mixed tumor in an adult. *J Pathol Bacter* 1966; **92**: 238–240
6 **Barnett W,** Erickson E, halpert B. Embryonic tumor of the liver in an adult. *Cancer* 1958; **11**: 306-309
7 **Alexander M.** A mixed tumor of the liver in an adult. *J Pathol* 1961; **82**: 217-219
8 **Ojima MA,** Sugiyama T, Takeda T, Hazama F, Nakakuki F, Uesugi Y, Miyazaki A, Suzuki Y, Fukushima M. Six cases of rare malignant tumors of the liver. *Acta Pathol pn* 1964; **14**: 95-102
9 **Blanding J.** Mixed malignant tumors in the liver of adults. Case report and review of some features. *Arch Pathol Lab Med* 1968; **86**: 108-110
10 **Cater R.** Hepatoblastoma in an adult. *Cancer* 1969; **23**: 191-197
11 **Goldman R,** Friedman N. Rhabdomyosarcohepatoma in an adult and embryonal hepatoma in a child. *Am J Clin Pathol* 1969; **51**: 137-143
12 **Meyer P,** Livolsi V, Cornog J. Hepatoblastoma associated with oral contraceptive. *Lancet* 1974; **2**: 1387
13 **Ludwig J,** Grier MW, Hoffman HN, McGill DB. Calcified mixed alignant tumor of the liver. *Arch Pathol Lab Med* 1975; **99**: 162-166
14 **Jameson CP.** Hepatoblastoma in a middle aged South African woman. *SA Med J* 1978; **53**: 143-144
15 **Yoshida T,** Okazaki N, Yoshino M, Shimamura Y, Miyazawa N, Miyamoto K, Kishi K. A case of hepatoblastoma in adult. *Jpn J Clin Oncol* 1979; **9**: 163-168
16 **Honan RP,** Haqqani MT. Mixed hepatoblastoma in the adult: case report and review of the literature. *J Clin Pathol* 1988; **3**: 1058-1063
17 **Kishimoto Y,** Hijiya S, Nagasaki R. Malignant mixed tumor of the liver in adults. *Am J Gastroenterol* 1984; **79**: 229-235
18 **Kawarada Y,** Uehara S, Noda M, Yatani R, Mizumoto R. Nonhepatocytic malignant mixed tumor primary in the liver. *Cancer* 1985; **55**: 1790-1798
19 **Altmann HW.** Epithelial and mixed hepatoblastoma in the adult – Histological observation and general considerations. *Path Res Pract* 1992; **188**: 16-26
20 **Harada T,** Matsuo K, Kodama S, Higashihara H, Nakayama Y, Ikeda S. Adult hepatoblastoma: case report and review of the literature. *Aust New Zeal J Surg* 1995; **65**: 686-688
21 **Toshihito N,** Masanori N, Hiroyuki S, Motoaki C, Kiminobu S, Taro I, Tsugumichi K, Masahiro F, Mitsuru I, Hideo M. Cytogenetic abnormalities in hepatoblastoma: report of two new cases and review of the literature suggesting imbalance of chromosomal regions on chromosome 1, 4, and 12. *Cancer Genet Cytogenet* 2005; **156**: 8-13
22 **Yamada S,** Ohira M, Horie H, Ando K, Takayasu H, Suzuki Y, Sugano S, Hirata T, Goto T, Matsunaga T, Hiyama E, Hayashi Y, Ando H, Suita S, Kaneko M, Sasaki F, Hashizume K, Ohnuma N, Nakagawara A. Expression profiling and differential screening between hepatoblastomas and the corresponding normal livers: identification of high expression of the PLK1 oncogen as a poor-prognostic indicator of hepatoblastomas. *Oncogene* 2004; **23**: 5901-5911
23 **Toshio I,** Masahiro S, Yuki T, Toru K, Jyunichi T, Takaya M, Hiroharu T, Hisahiro N, Shinji H, Koaki O. Successful resection of a ruptured hepatoblastoma prior to chemotherapy: report of a case. *Surg Today* 2004; **34**: 710-714

Science Editor Guo SY **Language Editor** Elsevier HK

PO Box 2345, Beijing 100023, China
www.wjgnet.com
wjg@wjgnet.com

ELSEVIER

World J Gastroenterol 2005;11(39):6238
World Journal of Gastroenterology ISSN 1007-9327

Acknowledgments to Reviewers of *World Journal of Gastroenterology*

Many reviewers have contributed their expertise and time to the peer review, a critical process to ensure the quality of *World Journal of Gastroenterology*. The editors and authors of the articles submitted to the journal are grateful to the following reviewers for evaluating the articles (including those were published and those were rejected in this issue) during the last editing period of time.

Trond Berg, Professor
Department of Molecular Biosciences, University of Oslo, PO Box 1041 Blindern, Oslo 0316, Norway

Bruno Clement, Professor
INSERM U-620, University of Rennes I, Faculty of Medicine, 2 ave. L. Bernard, Rennes 35043, France

Xue-Gong Fan, Professor
Xiangya Hospital, Changsha 410008, China

Edoardo G Giannini, Assistant Professor
Department of Internal Medicine, Gastroenterology Unit, Viale Benedetto XV, no. 6, Genoa, 16132, Italy

Hans Gregersen, Professor
The Research Administration, Aalborg Hospital, Hobrovej 42 A, Aalborg 9000, Denmark

Anna S Gukovskaya, Professor
Department of Medicine, UCLA, 11301 Wilshire Blvd, Los Angeles 91301, United States

Werner Hohenberger, Professor
Chirurgische Klinik und Poliklinik, Krankenhausstrasse 12, Erlangen D-91054, Germany

Masayoshi Ito, M.D.
Department of Endoscopy, Yotsuya Medical Cube, 5-5-27-701 Kitashinagawa, Shinagawa-ku, Tokyo 1410001, Japan

Hiroaki Itoh, M.D.
First Department of Internal Medicine, Akita University Scool of Medicine, 1-1-1, Hondou, Akita City 010-8543, Japan

Tsuneo Kitamura, Associate Professor
Department of Gastroenterology, Juntendo University Urayasu Hospital, Juntendo University School of Medicine, 2-1-1 Tomioka, Urayasu-shi, Chiba 279-0021, Japan

Zahariy Krastev, Professor
Department of Gastroneterology, Universiti Hospital "St. Ivan Rilski", #15, blvd "Acad. Ivan Geshov", Sofia 1431, Bulgaria

Shoji Kubo, M.D.
Hepato-Billiary-Pancreatic Surgery, Osaka City University Graduate School of Medicine, 1-4-3 Asahimachi, Abeno-ku, Osaka 545-8585, Japan

Fin Stolze Larsen, Associate Professor
Hepatology A-2121, Rigshospitalet Univ. Hospital of Copenhagen, Blegdamsvej 9, Copenhagen 2100, Denmark

James Neuberger, Professor
Liver Unit, Queen Elizabeth Hospital, Birmingham B15 2TH, United Kingdom

Mikio Nishioka, M.D.
Ehime Rosai Hospital, 13-27 Minami Komatsubara, Niihama 792-8550, Japan

Gustav Paumgartner, Professor
University of Munich, Klinikum Grosshadern, Marchioninistr. 15, Munich D-81377, Germany

Zhiheng Pei, Assistant Professor
Department of Pathology and Medicine, New York University School of Medicine, Department of Veterans Affairs, New York Harbor Healthcare System, 6001W, 423 East 23rd street, New York NY 10010, United States

Lun-Xiu Qin, Professor
Liver Cancer Institute and Zhongshan Hospital, Fudan University, 180 Feng Lin Road, Shanghai 200032, China

Manfred Stolte, Professor
Institute of Pathology, Klinikum Bayreuth, Preuschwitzer Str. 101, Bayreuth 95445, Germany

Michael Trauner, Professor
Medical University Graz, Auenbruggerplatz 15, Graz A-8036, Austria

Takato Ueno, Professor
Research Center for Innovative Cancer Therapy, Kurume University, 67 Asahi-machi, Kurume 830-0011, Japan

Toshio Watanabe, Associate Professor
Department of Gastroenterology, Osaka City University, Graduate School of Medicine, 1-4-3 Asahimachi, Abenoku-ku, Osaka 545-8585, Japan

Harry H-X Xia, M.D.
Department of Medicine, The University of Hong Kong, Pokfulam Road, Hong Kong, China